SHAPE THEORY AND MATHEMATICAL DESIGN OF A GENERAL GEOMETRIC KERNEL THROUGH REGULAR STRATIFIED OBJECTS

A thesis submitted for the degree of Doctor of Philosophy

by

Abel João Padrão Gomes

Department of Information Systems and Computing

Brunel University

September 2000

PAGE NUMBERING AS ORIGINAL

Abstract

This dissertation focuses on the mathematical design of a unified shape kernel for geometric computing, with possible applications to computer aided design (CAM) and manufacturing (CAM), solid geometric modelling, free-form modelling of curves and surfaces, feature-based modelling, finite element meshing, computer animation, etc.

The generality of such a unified shape kernel grounds on a shape theory for objects in some Euclidean space. Shape does not mean herein only geometry as usual in geometric modelling, but has been extended to other contexts, e.g. topology, homotopy, convexity theory, etc. This shape theory has enabled to make a shape analysis of the current geometric kernels. Significant deficiencies have been then identified in how these geometric kernels represent shapes from different applications.

This thesis concludes that it is possible to construct a general shape kernel capable of representing and manipulating general specifications of shape for objects even in higher-dimensional Euclidean spaces, regardless whether such objects are implicitly or parametrically defined, they have 'incomplete boundaries' or not, they are structured with more or less detail or subcomplexes, which design sequence has been followed in a modelling session, etc. For this end, the basic constituents of such a general geometric kernel, say a combinatorial data structure and respective Euler operators for n-dimensional regular stratified objects, have been introduced and discussed.

Preface

The author began the work described in this thesis in 1989 (University of Coimbra, Portugal) leading to the following papers:

- A. Gomes and J. Teixeira. Form feature modelling in an hybrid CSG/Brep scheme. *Computers & Graphics*, Vol.15, No.2, pp.217-229, 1991.
- A. Gomes, R. Bidarra, and J. Teixeira. A cellular approach for feature-based modelling. In M. Göbel and J. Teixeira (eds.), *Proceedings of the Workshop on Graphics Modeling and Visualization in Science and Technology*, Springer-Verlag, 1992.
- A. Gomes and J. Teixeira. A mathematical framework for set-theoretic solid models. In A. Middleditch and A. Requicha (eds.), Proceedings of the Conference CSG'94, *Set-Theoretic Solid Modelling: Techniques and Applications*, Information Geometers Ltd., 1994.
- A. Gomes and J. Teixeira. Cellta: a kernel for feature-based modeling. *Computer Graphik Topics*, Vol.6, No.4, 1994.
- A. Gomes and J. Teixeira. Modeling shape through a cellular representation scheme. In J. Teixeira and J. Rix (eds.), *Proceedings of the Workshop on Graphics and Modeling in Graphics & Technology*, Springer-Verlag, 1996.

This work was carried out at the University of Coimbra, Portugal, where the author was Assistant Lecturer on Computer Graphics and Geometric Modelling. It is primarily author's own work.

In 1996 he joined Brunel University to work on the development of the Σ-geometric kernel under the supervision of Professor Alan Middleditch. During the period April 1997 to October 1998, Professor Alan Middleditch and Dr Chris Reade were working on refinements to the Djinn API to a geometric modelling kernel. Although, we collaborated closely on the intimate relationships between subanalytic sets and their stratifications, the two projects remained distinct. Djinn is a universal interface that does not define techniques for their implementation, whilst Σ-geometric kernel is a geometric modeller. Although Djinn influenced Σ-kernel, there are differences of viewpoint, e.g. the definitions for point set frontier and boundary are different.

This dissertation contains some material which has already been presented in the form of the following publications:

- A. Gomes and A. Middleditch. Synthesis of a unified approach to shape modelling. In W. Strasser, R. Klein, and R. Rau (eds.), *Geometric Modeling: Theory and Practice*, Springer-Verlag, 1997.
- A. Gomes, A. Middleditch, and C. Reade. Issues and solutions in feature-based modelling: re-designing the shape kernel of CAD systems. In G. Jacucci (ed.), *Proceedings of the 10th International Conference IFIP TC5 WG 5.2/5.3 Conference, PROLAMAT'98*, Kluwer Publishers, September, 1998.
- A. Gomes, A. Middleditch, and C. Reade. A mathematical model for boundary representations of n-dimensional geometric objects. In W. Bronsvoort and D. Anderson (eds.), *Fifth Symposium on Solid Modeling and Applications*, ACM Press, 1999, pp.270–277.
- A. Middleditch, C. Reade and A. Gomes. Set combinations of the mixed-dimension cellular objects of the Djinn API. *Computer-Aided Design*, Vol.31, No.11, September 1999.
- A. Middleditch, C. Reade and A. Gomes. A representation-independent geometric modelling kernel. *Proceedings of the First Conference on Geometric Modeling and Processing*, Hong-Kong, April 10-12, IEEE Press, 2000.
- A. Middleditch, C. Reade and A. Gomes. Point sets and cell structures relevant to computer aided design. *International Journal of Shape Modeling*, Vol.6, No.2, pp.175–205, 2000.

Although some of the material in Chapter 1 is extracted from the first two papers (Brunel stage), it is primarily the author's own work. In contrast, the last four papers are not primarily the author's work. This material is presented in Chapter 3 together with the author's work on Thom-Boardman stratifications. The remaining chapters of the dissertation are entirely the author's contribution.

Acknowledgements

I am profoundly grateful to my supervisors Professor Alan Middleditch and Dr. Chris Reade for enhancing my knowledge in geometric computing and mathematics with frequent meetings around the Djinn project. And, obviously, for their friendship. I reserve for myself the way they —Alan, in particular— gave me room and freedom to undertake my project successfully, with confidence and respect by my self-minded personality. I also remember with joy the wonderful summertime at Alan and Judy's home cutting the grass and put it into the compost boxes, carrying out oak branches on a barrow, watering the garden, etc. Thanks Judy!

I should say that I was very well received at Brunel, either in the Centre for Geometric Modelling and Design (located on the second floor of the Manufacturing and Engineering Systems Department) and in my own Department of Information Systems and Computing. I remember particularly well the encouragement and supportive words of Professor Ray Paul in our first talk. My thanks to Professor Bob O'Keefe too.

I would also like to thank to Prof. Dr. Rosália Rodrigues, head of Computer Science Group at the Mathematics Department, University of Coimbra, and Dr. Jivka Ovtcharova, project manager in feature-based CAD systems, Department of Industrial Applications, Fraunhofer-Institut für Graphische Datenverarbeitung, Darmstadt (Germany) who recommended me for a doctoral programme at Brunel. Since then Prof. Dr. Rosália Rodrigues has backed me in the University of Coimbra, what I have appreciated for many reasons. On the other hand, my expertise in feature-based modelling is is part due to the collaboration with Jivka when I spent a few months in Zentrum für Graphische Datenverarbeitung (ZGDV), Darmstadt (Germany), 1990. Since then we have hold our friendship, even after she has moved to Tecmath GmbH, Kaiserslautern (Germany).

I have also to thank to my colleagues and friends in the Mathematics Department of the University of Coimbra, and now Mathèmatics and Informatics Department of the University of Beira Interior, for sharing their knowledge and lecturing experiences.

A few words of acknowledgement for my friends at Brunel too, Ali Mousavi, Belen Dominguez-Ballesteros, Kai Strunz, Wattanapong Kurdthongmee (Lek), Rui Sousa, and Adriano Marques.

Finally, I am deeply indebted to my lady and wife Eduarda who tempered my rationalist mind with humanism, tolerance, and wisdom all over these years.

Contents

Introduction

This dissertation reflects much of the author's interdisciplinary view of what should be the modern geometric modelling, a synergetic engineering science research area which integrates mathematics, computer science and engineering. The title of this dissertation mirrors my concerns and aims in defining a theoretical and unified basis to deal with the shape of engineering artifacts, encompassing those of solid modelling, free-form modelling and feature-based modelling.

Its major aims are the following:

- To find a general-purpose *geometric* model suited to interactive design, engineering analysis, and manufacturing.
- To find a general-purpose *geometric* model that incorporates the strengths and eliminates the weaknesses of current geometric solid models, CSG-rep (Constructive Solid Geometry representation) and B-rep (Boundary representation), without hybrid solutions.
- To find a general-purpose *geometric* model whose geometry encompasses the solid and free-form geometries.
- To find a general-purpose *geometric* model with arbitrary regular structure or stratifiability. This is the key not only to unify CSG and B-rep models, but also to integrate solid models and feature models. It allows us to relegate all the geometric interactions between subobjects (e.g. form features) to the geometric model itself, relieving applications (e.g. feature modellers) of unnecessary overheads.
- To find a general-purpose *shape* model capable of processing in a unified way the conventional shapes of geometric modellers and the shapes associated with feature modellers.

This thesis assumes that current geometric modellers are just particular shape modellers that implement parts or submodels of a more general mathematical model. In this respect, regular stratifications (e.g. Whitney stratifications) constitute a mathematical and unified model for the family of all B-rep models, while the association of subanalytic geometry with regular stratified objects enables us to extend the theoretical unification to the family of CSG models, because the Booleans are then theoretically allowed. Subanalyticity is also crucial to a possible integration of solid and

free-form geometries. The integration of feature shapes is assured by in-built covering of Whitney subobjects or subcomplexes, but requires the development of a shape theory beyond the analytic and subanalytic geometries. Such a shape theory relates geometric shapes to fundamental topological shapes (manifolds), differential shapes and singularities (submanifolds), convex shapes (depressions and protrusions) and homotopic shapes (e.g. components, holes and voids in $\mathbb{R}^3$). This general shape taxonomy has been synthesised over the last few years analysing and studying the shape of engineering artifacts, the fundamentals of the (topological) shape theory of Borsuk, relationships between topology and geometry, differential topology and geometry, the deficiencies of solid modellers to process form features, the theory of convexity, etc. Also, the reformulation of the Djinn mathematical model accomplished by Alan, Chris and myself during the last years determined a few but important improvements in my own model. For example, it was useful to better understand the theoretical relationship between Euler operators and standard/stratified Boolean operators.

This thesis is organised as follows. Chapter 1 develops a mathematical shape theory that covers most shape aspects involved in shape modelling, i.e. geometric solid modelling, geometric free-form modelling and geometric feature modelling. Significant effort has been made to understand and to explain (for an engineering audience) how mathematicians perceive the concept of shape in different mathematical branches such as point-set topology, homotopy theory, differential topology, geometry, and theory of convexity. The main conclusions are that each of these mathematical areas focus on specific maps between spaces with the objective to infer specific properties of such spaces up to equivalence. It is then possible to classify spaces by the action of a particular map; for example, two spaces are topologically equivalent if and only if there is a homeomorphism between them. A particular useful part of this chapter is that the author shows that the concept of C^r manifold smoothness in differential geometry is exactly what is called G^r geometric continuity in geometric design, and, more importantly, it is independent of the representation form, explicit, implicit or parametric. Moreover, the notion of C^r continuity in differential topology and geometry is a particular case of the notion of continuity used in general topology, seeing that a diffeomorphism is a homeomorphism. Another particularly useful part of Chapter 1 concerns the proposal of the theory of convexity as the mathematical theory behind form feature modelling based on the assumption that shape aspects should be separated from functional and engineering aspects of design and manufacturing. It is —to the best of my knowledge— the first mathematical shape theory for feature-based modelling. As will be shown there is a clear hierarchy of shape maps between subspaces in $\mathbb{R}^n$ which leads to a hierarchical taxonomy of shapes. These shape maps and classification of shapes are of great importance to expose the

deficiencies of current geometric modellers in shape processing. Chapter 1 ends with an overview of a general-purpose shape modeller.

Chapter 2 deals with the mathematical theory of smoothness —or the lack of it—, which shows the relationships between smoothness of mappings and smoothness of manifolds. It is shown that the mathematical notion of C^r smoothness or continuity generalises the various concepts of geometric continuity used in computer-aided geometric design. But, more importantly, we end up to understand that the definition of manifolds, varieties, and more general point sets follow the same mathematical theory, whether they are defined explicitly, implicitly, or parametrically. This allows us to say that solid modelling and free-form modelling of curves and surfaces are no longer separate research areas in geometric modelling.

Chapter 3 introduces the mathematics behind our general geometric model, the subanalytic regular stratifications. The generality of this geometric model comes from the following facts:

- Subanalytic geometry provides a large class of geometric objects, covering practically all engineering artefacts. Subanalytic sets need not be relatively open or closed.
- Subanalytic sets are invariant under projections which is essential in interactive design based on computer graphics systems.
- Subanalytic sets are closed under Boolean operations. They generalise the semianalytic sets used by *constructive solid geometry* representations (CSG-reps). Booleans are useful as high-level design operators.
- Subanalytic sets are regularly stratifiable. For example, they admit Whitney stratifications, which are generalisations of the manifold structures used by boundary representations (B-reps).
- Regularly stratified subanalytic sets are combinatorial Euler-invariant. Thus, Euler operators can be used to construct engineering artefacts, as usual in B-reps.
- Regularly stratified subanalytic sets or complexes admit coverings of subcomplexes. This enables the *internal* representation of geometric subobjects such as, for example, form features.

Chapter 4 details the data structure of the Σ-geometric kernel for regular stratified objects. The data structure represents geometric objects independently of its dimension, local and global compactness, and clusters or subcomplexes. Its underlying representation, called *subcomplex-tuple representation* is a generalisation of the cell-tuple representation of Brisson. The view of an object as

a covering of subobjects or subcomplexes enables the internal representation of, for example, form features, which avoids known problems in integrating solid modellers and feature modellers.

Chapter 5 describes Euler operators to construct geometric objects in $\mathbb{R}^n$, which constitutes a generalisation to previous Euler operators in $\mathbb{R}^3$. They make use of the shape theory introduced in Chapter 1. They were designed after achieving a general Euler formula for regular stratified objects in $\mathbb{R}^n$. Also, stratified Boolean operators are concisely described. The relationships between standard Boolean operators, stratified Boolean operators and Euler operators are then clarified.

Finally, conclusions are drawn in the end of the thesis.

CHAPTER 1

Shape theory

The existence of analogies between central figures of various theories implies the existence of a general theory which underlies the particular theories and unifies them with respect to those central features.

E. Moore, New Haven Colloquium Lectures, 1906

What is shape? To say that two objects have the same shape has an intuitively obvious, but sometimes very imprecise meaning in design, and engineering in general. This is because engineering design involves distinct levels of detail; an engineering artefact usually consists of an assembly of components —and this agrees with the mathematical notion of a topological space with a number of connected components—, a component may contain various through holes, each hole with a specific geometric pattern (cylindrical, square, etc.) determined by functional requirements performance, life time, cost, and so forth.

Analogously, in mathematics, there are various levels of detail in analysis and synthesis of the shape of more abstract spaces. (In fact, hierarchical constructions of the human mind seems to be spread over all knowledge areas.) But, in contrast, the concept of shape can be now rigorously defined, theoretically developed and refined. For example, a cube and a sphere are topologically indistinguishable, but we know they are geometrically distinct. In other words, a cube and a sphere have the same topological type, but distinct geometric types. This is so because the level of shape detail in topology is coarser than in Euclidean geometry. To see that two distinct figures or point sets have the same shape type, we use a particular kind of mapping for shape matching. This suggests that we can define a *shape taxonomy* for point sets in $\mathbb{R}^n$ by setting shape equivalence classes for each kind of mapping, each mapping corresponding to a particular level of shape detail.

A major purpose of this thesis is precisely to show how the various research areas in *geometric modelling* or *shape modelling* —i.e. geometric solid modelling, geometric free-form modelling, and geometric feature modelling— are related to distinct levels of shape detail or shape types. This allows us to describe the shape of engineering artefacts from different settings and points of view. This is not new in mathematics, where each view of more abstract artefacts corresponds to a mapping between

them. For example, topologists make use of homeomorphisms to capture the global shape properties of a space, whereas differential geometers use diffeomorphisms to evaluate its smoothness properties. Roughly speaking, we can then say that each branch of mathematics is developed and established around a particular kind of mapping.

Thus, we intend to know which shape mappings (and, ultimately, which mathematical theories) are associated with the various research branches of geometric modelling. In fact, a distinct shape type is defined for each kind of shape mapping. The fact that distinct shape mappings imply distinct shape types makes us to think of relating these shape types by relating their corresponding shape mappings. The result is a general hierarchical shape taxonomy in the context of geometric modelling. This is of paramount importance for those interested in to find a general mathematical basis to an effective *shape integration* in computer aided engineering environments. This is also important to comprehend the shape deficiencies and incompabilities of current geometric modellers, and the technical difficulties of current standard formats in the transference of data between distinct CAD/CAM systems.

1. Shape mappings, groups and geometries

In mathematics, the unification of diverse disciplines is achieved by abstraction [**13**, p.7]. The existence of particular theories with common essential characteristics implies the existence of a general theory for all them. A general theory corresponds to a higher level of abstraction that its particular theories. For example, the *projective geometry* used in computer graphics or, better, in the design and implementation of computer graphical systems such as GKS (Graphical Kernel System), PHIGS (Programmer Hierarchical Interactive Graphical System), GL (Graphical Library), etc., generalises the *affine geometry*, which in turn is a generalisation of the *Euclidean geomety*. These three geometries are all examples or instances of Klein geometries. According to Klein, a geometry $(X, \mathcal{G})$ consists of a space X, some properties possessed by figures (or subsets) in that space, and a group $\mathcal{G}$ of mappings or transformations of the space that preserve these properties. More formally, a *Klein geometry* is the ordered pair $(X, \mathcal{G})$, where X is a space and $\mathcal{G}$ is a group of mappings of X onto itself. Note that X and $\mathcal{G}$ are left unspecified, i.e. the nature of the elements of X and mappings of $\mathcal{G}$ (the operation associated with $\mathcal{G}$ is the composition of mappings) are not specified or instanciated.

The view of geometry as a space and a group acting on it is called the *Kleinian view of geometry*, after the 19th-century German mathematician Felix Klein who proposed it first. It has the virtue of enabling us to generate many geometries, while seeing how they are related. The bigger the abstraction, the smaller the detail. A Klein geometry uses two important abstract devices by means of which many areas of mathematics are unified. The first is the concept of *space*. A space is basically a

set with some kind of structure. For example, as explained later, a set with a topological structure gives rise to a topological space. A space is rather abstract because neither the elements of its underlying set nor the structure type is specified. The second abstract device is the concept of a group. A group is basically a set and a binary operation associated with it.

DEFINITION 1.1. Let G be a set and $\circ$ be a binary operation defined on G. Then $(G,\circ)$ is a **group** if the following axioms hold.

(i) *Closure Axiom.* For all $g_1, g_2 \in G$, $g_1 \circ g_2 \in G$.

(ii) *Identity Axiom.* There exists an *identity element* $i \in G$ such that, for all $g \in G$, $g \circ i = g = i \circ g$.

(iii) *Inverse Axiom.* For each $g \in G$, there exists an *inverse element* $g^{-1} \in G$ such that $g \circ g^{-1} = i = g^{-1} \circ g$.

(iv) *Associativity Axiom.* For all $g_1, g_2, g_3 \in G$, $g_1 \circ (g_2 \circ g_3) = (g_1 \circ g_2) \circ g_3$.

In a Klein geometry, the elements of the set underlying the group are maps. Although these maps are a specialisation for the elements of such a set, their nature is still left unspecified. Klein geometry is a typical example of unification by abstraction in mathematics. By not specifying, or by ignoring, the nature of a space and the nature of the maps defined on it, a general theory for geometry follows, and many geometries can be generated.

EXAMPLE 1.1. (**Euclidean geometry**). The set $\mathbb{R}^n$ is then made into a metric space by defining the distance $\mathrm{d}(p,q) = (\sum_{i=1}^{n}(p_i - q_i)^2)^{1/2}$ between the n-tuples $p = (p_1,\ldots,p_n)$ and $q = (q_1,\ldots,q_n)$. This metric space is called *Euclidean n-space* and is denoted by $\mathbb{E}^n$. ($\mathbb{E}^n$ is often identified with $\mathbb{R}^n$ for brevity.) n-dimensional Euclidean geometry $(\mathbb{E}^n, I(n))$ is precisely the Euclidean n-space $\mathbb{E}^n$ together with the group $I(n)$ of *isometries* (translation, rotation, and reflection) of $\mathbb{E}^n$. By definition, an isometry is a homeomorphism (and, thus, a map) f of $\mathbb{E}^n$ onto itself which *preserves distances*, that is, for which $d(f(p), f(q)) = d(p,q)$ [**5**, p.1]. For obvious reasons, isometries are also called *rigid motions*. Properties, such as lengths, areas, volumes, angles, that remain unchanged by the group of isometries are called *metric invariants*.

EXAMPLE 1.2. (**Affine geometry**). It is the geometry of parallelism. If in $\mathbb{E}^n$ we retain the topology, the notion of straight line, and the notion of parallelism among straight lines but discard the metric structure, we obtain *affine n-space*, which we denote by $\mathbb{A}^n$ [**5**, p.2]. In $\mathbb{A}^n$ we do not care about distance between points. The *affine geometry* $(\mathbb{A}^n, A(n))$ is an extension of Euclidean geometry, where $A(n)$ is the group of transformations, called *affinities* (or *affine transformations*). The group of affinities includes the group of isometries in addition to scalings and shearings. Affinities are

homeomorphisms that preserve parallelism, not distances. Properties, such as the parallelism of lines and collinearity of points, that are unchanged by the group of affinities are called *affine invariants.* Note that the metric or Euclidean invariants are not generally affine invariants because the invariable properties of the Euclidean geometry are not in general invariable properties of the affine geometry. For example, squares can be transformed into parallelograms and circles into ellipses.

EXAMPLE 1.3. (**Projective geometry**). Consider the set of all points of $\mathbb{R}^{n+1}$ except $(0,\ldots,0)$. The exclusion of $(0,\ldots,0)$ is a technical convenience. Two points $p = (p_1,\ldots,p_{n+1})$ and $q = (q_1,\ldots,\ldots,q_{n+1})$ are said to be equivalent if there is a number c such that $q_1 = cp_1,\ldots,q_{n+1} = cp_{n+1}$. This relation of equivalence partitions $\mathbb{R}^{n+1}$ into mutually disjoint equivalence classes. Let $\mathbb{P}^n$ denote the set of those equivalence classes of $\mathbb{R}^{n+1}$. $\mathbb{P}^n$ is called *projective n-space* [**5**, p.60]. The *projective geometry* is a generalisation of the affine geometry. The new important sort of maps which are possible in the projective geometry are the perspective transformations. The maps allowed in projective geometry form a group, called group of *projectivities* (or *projective transformations*), which includes the group of affinities. The properties preserved by projectivities are concurrence of lines and collinearity of points. It is clear that the invariable properties of the projective geometry are not in general invariable properties of the affine geometry. For example, a square can change to any quadrilateral and a circle to any non-degenerate conic section (ellipse, parabola, hyperbola).

The set $\mathbb{R}^n$ may be then endowed with various mathematical structures, each one for a specific geometry. Thus, a geometry defined on $\mathbb{R}^n$ is characterised by its group of mappings. As suggested above, there is a hierarchy of geometries based on the generalisation of mappings. One of the purposes of this chapter is to expose the different geometries and shape mappings used in geometric modelling, namely geometric solid modelling, geometric free-form modelling, geometric feature modelling. This leads us to a general shape taxonomy for geometric modelling. More importantly, this allows us to anticipate a general theory for geometric modelling, where we can see the relationships between the seemingly distinct branches of geometric modelling. The idea behind this possible theory is to achieve a unified shape model capable of unifying and integrating the extant models in geometric modelling.

2. Shape, shape equivalence

Initially, Klein's definition was considered very general. It encompassed all of the known geometries of his time, and furthermore it was extensible to non-mathematical applications [**13**, p.26]. Remarkbly, Klein wrote in 1912, "What the modern physicists call relativity theory is the theory of

invariants of a four-dimensional space-time continuum (Minkowski's world) with respect to a given group of collineations (the Lorentz group), and hence is a geometry."

However, it was understood that Klein's definition of a geometry had two drawbacks. First, it is not absolutely general. Second, it is not 'purely' geometrical. The Klein's definition relates a geometry to a group (an algebraic concept) of mappings which are usually given by expressions relating the coordinates (another nongeometrical concept) of a point in terms of the coordinates of the transformed point, or vice-versa. It was then realised that the concept of a group imposed a serious restriction on a geometry.

A more general concept of *geometry* or *shape* can be achieved by removing the group condition on the mappings of a geometry. Doing so one comes to the essential concept underlying any geometry: *equivalence* of subsets or figures of a space X. Such an essential concept of shape equivalence was introduced in geometric modelling literature by Gomes and Middleditch [**45**]. Their paper constitutes the first attempt to achieve a unified shape theory in geometric modelling. In particular, it outlines a first mathematical theory for geometric feature modelling.

To understand that the essence of any geometry lies in the *choice of equivalent subsets* rather than in the mechanisms (algebraic or whatever) by means of which the choice is defined, consider again the Klein geometry. The Klein geometry $(X, \mathcal{G})$ studies those and only those properties of a subset (or figure) that are *invariant* under every mapping (transformation) of the group $\mathcal{G}$. Thus, a property of a subset A of X is an object of study in the Klein geometry if and only if it is a property of each subset $g(A)$ for every $g \in \mathcal{G}$, where $g(A)$ stands for the subset into which A is mapped by the mapping g of X onto itself.

It is now apparent that an *equivalence relation* is established in the class of all subsets of X by defining two subsets $A, B \in X$ to be equivalent (symbolically, $A \approx B$) provided there exists an element g of $\mathcal{G}$ such that $B = g(A)$. Because $\mathcal{G}$ contains an identity element, it follows that $A \approx A$, and since $\mathcal{G}$ contains the inverse of each of its elements, the relation $A \approx B$ implies that $B \approx A$. At last, if A, B, C are subsets of X such that $A \approx B$ and $B \approx C$, then $B = g_1(A)$, $C = g_2(B)$, and $C = g_2 \circ g_1(A) = g_3(A)$, where g_3 is the element of $\mathcal{G}$ that is the group product of g_1, g_2 in the order indicated. Hence, $A \approx C$, and thus the transitive property of the equivalence is also established.

In seeking the geometric essence of Klein's definition suggests the following general definition for a geometry or shape.

DEFINITION 1.2. The pair $(X, \mathcal{E})$ is a **geometry** (or **shape**) over a set X, where $\mathcal{E}$ is an equivalence relation defined in the set of all subsets (or figures) of X. The geometry $(X, \mathcal{E})$ studies those and only

those properties of a subset A of X that it has in common with all subsets equivalent to A; these are the invariant properties.

Observe that a geometry is defined in terms of a *set* rather than a space. This also widens the applicability of the notion, although this fact is irrelevant in geometric modelling because X is usually the Euclidean space. Obviously, every Klein geometry is also a geometry according to Definition 1.2. Nevertheless, there are geometries in mathematics which are not Klein geometries. For example, the Riemann geometry is not a Klein geometry. Both Riemann geometry and Klein geometries are generalisations of the Euclidean geometry. All them are particular cases of Cartan geometries (see Sharpe [**103**] for further details).

In geometric modelling, there is a particular interest in to know which geometries are involved in its various branches of research, and, if possible, to relate them somehow. The set associated with all the geometries used in geometric modelling is the n-dimensional Euclidean space $\mathbb{R}^n$ (and sometimes the projective space $\mathbb{P}^{n-1}$). Therefore, these geometries defined over the same space Euclidean space are in principle only distinguishable from each other by means of their shape mappings and, ultimately, shape equivalence relations. They arise from different definitions of equivalent subsets. As shown in the next sections, a hierarchy of geometries can be established by hierarchically relating their corresponding shape equivalences. Furthermore, a classification or taxonomy of shapes involved in geometric modelling can be defined. This is extremely important not only to expose the shape deficiencies of current geometric modellers, but also to propose an alternative architecture for a shape-complete geometric modeller.

3. Geometry: Euclidean shape mappings

The n-dimensional Euclidean geometry $(\mathbb{R}^n, \mathrm{I}(n))$ is a Klein geometry. This geometry is particularly useful in computer graphics systems since the group the isometries $\mathrm{I}(n)$ are used to move geometric objects in the ambient space that is usually $\mathbb{R}^3$.

But the leading idea here is to classify subspaces of $\mathbb{R}^n$ against mappings. In this respect, isometries are particularly useful because they lead us to the concept of *Euclidean geometric equivalence* or *Euclidean congruence.* Two subsets X, Y of $\mathbb{R}^n$ are *Euclidean-congruent,* or $X \cong Y$, if X can be *rigidly moved* such that it is exactly superimposed on Y; that is, if there is an isometry between them. It is a well-know fact that *Euclidean congruence* is an equivalence relation [**40**, p.152]. Thus, by Definition 1.2, $(\mathbb{R}^n, \cong)$ is a geometry or shape, called *n-dimensional Euclidean geometry.* (Note that the Euclidean geometry is identified by either its group of isometries or its Euclidean congruence.)

It studies properties which are left unchanged by isometries (congruencies or rigid motions), which are *distance-preserving mappings.* This means that *isometries preserve the size and shape of every geometric figure.*

EXAMPLE 1.4. Let us consider the 2-dimensional Euclidean geometry $(\mathbb{R}^2, I(2))$ and $A = \{(x,y) \in \mathbb{R}^2 : 0 \leq x \leq 1.5 \text{ and } 0 \leq y \leq 1\}$ a rectangle in $\mathbb{R}^2$ (Figure 1). The action of the mapping $g : \mathbb{R}^2 \to \mathbb{R}^2$ given by $(x,y) \mapsto (x+1, y+0.5)$ on A is a translation of A along the x-axis and y-axis by $\delta x = 1$ and $\delta y = 0.5$, respectively. The result is a rectangle A^* that is Euclidean-congruent to A. The original rectangle A and the transformed rectangle A^* are said to be in the same Euclidean geometric equivalence class, or, alternatively, they have the same Euclidean geometric type.

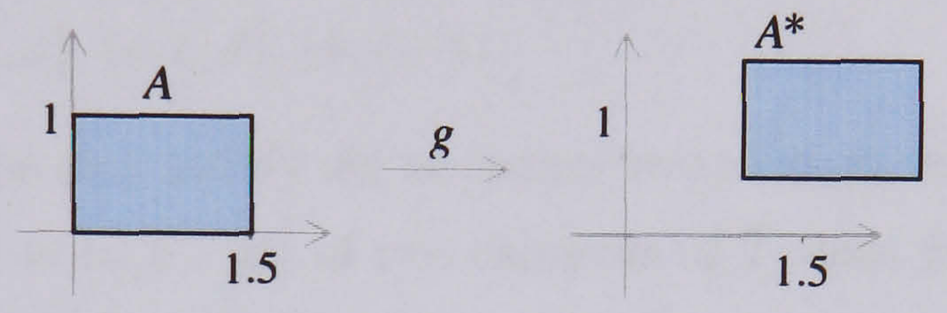

FIGURE 1. The action of a translation on a rectangle.

4. Topology: topological shape mappings

The general topology is built upon the theory of sets. The study in topology starts with the idea of associating some kind of structure, usually called *topology* or *topological structure*, to a set. As shown below, this fact leads to the concept of *continuity*, which is one of most fundamental concepts in mathematics.

4.1. Topologies and topological spaces.

DEFINITION 1.3. A **topology** is a collection $\mathcal{T}$ of sets which satisfies the following two axioms.

(i) The union of any (may be infinite) number of sets in $\mathcal{T}$ belongs to $\mathcal{T}$.

(ii) The intersection of a *finite* number of sets in $\mathcal{T}$ belongs to $\mathcal{T}$.

That is, the union of the sets in any subcollection of $\mathcal{T} = \{U_i : i \in I\}$ is a set in $\mathcal{T}$; and, the intersection of the sets in any finite subcollection of $\mathcal{T} = \{U_i : i \in I\}$ is a set in $\mathcal{T}$. From the set theory, we know that the empty set $\varnothing$ is subset of every other set; hence, it is an element of $\mathcal{T}$. Furthermore, the axiom (i) above implies that the set $X = \cup\{U_i \in \mathcal{T} : i \in I\}$ is necessarily in $\mathcal{T}$ because $\mathcal{T}$ is a subcollection of itself, and every set U_i of $\mathcal{T}$ is a subset of X. The set X is called the *space* of the

topology $\mathcal{T}$ and $\mathcal{T}$ is a *topology* for X. Besides, the pair $(X,\mathcal{T})$ is a *topological space* if an additional axiom is satisfied: (iii) $\varnothing, X \in \mathcal{T}$. $\mathcal{T}$ is a topology on X iff $(X,\mathcal{T})$ is a *topological space*. The elements U_i of the topology $\mathcal{T}$ are called *open* relative to $\mathcal{T}$, or $\mathcal{T}$-open, or if only one topology $\mathcal{T}$ is under consideration, simply open sets. The simplest topology, called *trivial or indiscrete topology*, is the family of two open sets, empty set and X itself, respectively, while the largest, called *discrete topology*, is the family of all subsets of X.

EXAMPLE 1.5. Consider the following families of subsets of $X = \{a,b,c,d,e\}$:

(a) $\mathcal{T}_1 = \{X, \varnothing, \{a\}, \{c,d\}, \{a,c,d\}, \{b,\ c,d,e\}\}$;
(b) $\mathcal{T}_2 = \{\varnothing, \{a\}, \{a,b\}, \{a,b,c\}\}$;
(c) $\mathcal{T}_3 = \{X, \varnothing, \{a\}, \{c,d\}, \{a,c,d\}, \{b,c,d\}\}$.

$\mathcal{T}_1$ and $\mathcal{T}_2$ are topologies since they satisfy the necessary two axioms, but $\mathcal{T}_3$ is not a topology since the union $\{a,c,d\} \cup \{b,c,d\} = \{a,b,c,d\}$ of two elements of $\mathcal{T}_3$ does not belong to $\mathcal{T}_3$, i.e. $\mathcal{T}_3$ does not satisfy the first axiom. Consequently, $\mathcal{T}_3$ is not a topology on any set, and X in particular. On the other hand, yet $\mathcal{T}_2$ is a topology, it is not a topology on X, because X is not in $\mathcal{T}_2$. Only $\mathcal{T}_1$ is a topology on X since the three axioms of a topological space are satisfied; hence, $(X,\mathcal{T}_1)$ is a topological space. These examples clearly show that the concept of topology is independent of the concept of topological space; the converse is not true. For 'independence' we mean that the notion of topology preceeds the notion of topological space, as the notion of set comes before the notion of topology.

EXAMPLE 1.6. (a) Let X be the real line $\mathbb{R}$. All open intervals (a,b) and their unions define a topology called the *usual topology* in $\mathbb{R}$; a and b may be $-\infty$ and ∞, respectively. Similarly, the usual topology in $\mathbb{R}^n$ can be defined by taking a product $(a_1,b_1) \times \ldots \times (a_n,b_n)$ and their unions. Thus, in $\mathbb{R}^n$, the open sets of the usual topology agree with our 'intuitive open sets' used in geometric modelling.
(b) The same is not applicable to the upper-limit topology $\mathcal{U}$ on $\mathbb{R}^n$. For example, in $\mathbb{R}$, $\mathcal{U}$ is generated by the open-closed intervals $(a,b]$. This example shows that the open sets of a topology do not necessarily correspond to our 'intuitive open sets'.

Let $(X,\mathcal{T})$ be a topological space and A be any subset of X. Then $\mathcal{T} = \{U_i\}$ induces the *relative topology* in A by $\mathcal{T}' = \{U_i \cap A : U_i \in \mathcal{T}\}$. The concept of *relative* or *induced* topology is relevant to geometric modelling of dimensionally nonhomogeneous objects, as will be apparent throughout this thesis.

EXAMPLE 1.7. Let $X = \mathbb{R}^3$ and take the 2-sphere $\mathbb{S}^2 = \{(x,y,z) \in \mathbb{R}^3 : x^2+y^2+z^2 = 1\}$. A topology in $\mathbb{S}^2$ may be given by the relative topology induced by the usual topology on $\mathbb{R}^3$. Each open set in $\mathbb{S}^2$ results from the intersection of an open set in $\mathbb{R}^3$ with $\mathbb{S}^2$.

4.2. Closed sets, closure. As for open sets of a topological space, its closed sets do not coincide necessarily with our 'intuitive closed sets'. Let $(X,\mathcal{T})$ be a topological space. A subset A of X is *closed* if its complement in X is an open set, i.e. $X \setminus A \in \mathcal{T}$.

EXAMPLE 1.8. As seen in Example 1.5, the collection of sets $\mathcal{T}_1 = \{X, \varnothing, \{a\}, \{c,d\}, \{a,c,d\}, \{b, c,d,e\}\}$, defines a topology on $X = \{a,b,c,d,e\}$. The closed subsets of X are $\varnothing$, X, $\{b,c,d,e\}$, $\{a,b,e\}$, $\{b,e\}$ and $\{a\}$, i.e. the complements of the open subsets of X. Observe that there are subsets of X, such as $\{b,c,d,e\}$, which are both open and closed, and there are subsets of X, such as $\{a,b\}$, which are not neither open nor closed.

Besides, by the definition of closed set and the axiom (iii) of a topological space $(X,\mathcal{T})$, X and $\varnothing$ are both open *and* closed. Going a little further, by the definition of closed set, the axioms of a topological space and DeMorgan's Laws give an alternative and equivalent definition of topological space in terms of closed subsets of X, with the difference that, unlike the union axiom, the intersection axiom is not required to involve a finite collection of closed sets.

Let A be a subset of a topological space X. The *closure* of A, denoted by $\mathrm{Cl}(A)$, is the intersection of all closed sets that contain A. Note that $\mathrm{Cl}(A)$ is a closed set since it is the intersection of closed sets. Furthermore, $\mathrm{Cl}(A)$ is the smallest closed set which contains A. Accordingly, a set A is *closed* iff $A = \mathrm{Cl}(A)$.

4.3. Interior, exterior, boundary, frontier. It is remarkable that there are four types of subsets in a topological space; they are *open*, *closed*, *open and closed* simultaneouly, and *neither open nor closed.* Therefore, in a general setting, the concepts of closure, exterior, interior, boundary, and frontier of a subset A in a topological space X must be applicable to any kind of subset.

Let A be a subset of a topological space X. A point $\mathbf{x} \in A$ is called an *interior point* of A if $\mathbf{x}$ belongs to an open set contained in A. The set of interior points of A, denoted by $\mathrm{Int}(A)$, is called the *interior* of A. Thus, A is open iff $A = \mathrm{Int}(A)$.

From the concept of interior of a subset A of a topological space X, $\mathrm{Ext}(A)$ (the *exterior* of A), $\mathrm{Bd}(A)$ (the *boundary* of A) and $\mathrm{Fr}(A)$ (the *frontier* of A), and even $\mathrm{Cl}(A)$ (the *closure* of A) can be defined as follows:

$$
\begin{aligned}
&\mathrm{Ext}(A) = \mathrm{Int}(X \setminus A) \\
(1) \qquad &\mathrm{Bd}(A) = A \setminus \mathrm{Int}(A) \\
&\mathrm{Fr}(A) = \mathrm{Bd}(A) \cup \mathrm{Bd}(X \setminus A)
\end{aligned}
$$

$$\mathrm{Cl}(A) = \mathrm{Int}(A) \cup \mathrm{Fr}(A) = A \cup \mathrm{Fr}(A) = A \cup \mathrm{Bd}(X \setminus A)$$

The necessity to distinguish between boundary and frontier of A comes from the fact that A may be neither open nor closed; in geometric modelling, A is said to have 'incomplete' boundary, what is mathematically non-sense. However, intuitively, 'incomplete' boundary means that it lacks part of the frontier, or that the boundary $\mathrm{Bd}(A)$ is a proper subset of $\mathrm{Fr}(A)$.

EXAMPLE 1.9. In Figure 2, a table of fundamental topological shapes in $\mathbb{R}^2$ is depicted. The most essential topological shapes are the disc (or closed ball) $\mathbb{D}^n = \{\mathbf{x} \in \mathbb{R}^n : \|\mathbf{x}\| \leq 1\}$, the (open) ball $\mathbb{B}^n = \{\mathbf{x} \in \mathbb{R}^n : \|\mathbf{x}\| < 1\}$, and the sphere $\mathbb{S}^{n-1} = \{\mathbf{x} \in \mathbb{R}^n : \|\mathbf{x}\| = 1\}$, respectively. For $n = 0$, this yields $\mathbb{D}^0 = \mathbb{B}^0 = \{0\}$, $\mathbb{S}^{n-1} = \varnothing$. This table shows that: (i) open spaces have no boundary; (ii) boundary and frontier of a closed space coincide; (iii) the distinction between boundary and frontier is necessary to keep the axiomatic consistency for clopen (closed and open) and nclopen (not closed and not open) spaces.

The topological operators (1) may induce a certain ambiguity in our minds. Recall that they have been derived from the notion of *open set*, what depends on the topology used to topologise a point set A. For example, let us take the interval $(-1, 1)$. This interval is open in $\mathbb{R}$, but it is not open when considered as a subset of $\mathbb{R}^2$, since any open set of $\mathbb{R}^2$ about a point of $(-1, 1)$ overlaps with the upper and lower half-planes of $\mathbb{R}^2$. Similarly, the real line $\mathbb{R}$ itself is both open and closed, but when it is considered as a subset of $\mathbb{R}^2$, it is no longer open. It is closed in $\mathbb{R}^2$. This means that the openness or closedness of a subset A depends on its ambient space X (or, to be more precise, on the topology of its ambient space X). Thus, the point sets resulting from the topological operators (1) applied to a subset $A \subseteq X$ depend on the ambient space X. To remedy this problem, or, equivalently, to obtain the same sets from (1) regardless of the dimension of the ambient space X, we make use of the notion of *relatively open set.*

DEFINITION 1.4. (see Kinsey [**66**, pp.16-18]) Let $A \subseteq X$. A *relatively open subset* of A is a set of the form $N \cap A$, for some open subset N of X.

$X \in \mathbb{R}^2$	$\mathrm{Int}(X)$	$\mathrm{Ext}(X)$	$\mathrm{Bd}(X)$	$\mathrm{Fr}(X)$	$\mathrm{Cl}(X)$
$\mathbb{D}^0$ x	$\varnothing$	$\mathbb{R}^2 \setminus \mathbb{D}^0$	$\mathbb{D}^0$	$\mathbb{D}^0$	$\mathbb{D}^0$
$\mathbb{S}^0$ x y	$\varnothing$	$\mathbb{R}^2 \setminus \mathbb{S}^0$	$\mathbb{S}^0$	$\mathbb{S}^0$	$\mathbb{S}^0$
$\mathbb{D}^1$ x y	$\varnothing$	$\mathbb{R}^2 \setminus \mathbb{D}^1$	$\mathbb{D}^1$	$\mathbb{D}^1$	$\mathbb{D}^1$
x	$\varnothing$	$\mathbb{R}^2 \setminus (\mathbb{D}^0 \cup \mathbb{B}^1)$	$\mathbb{D}^0 \cup \mathbb{B}^1$	$\mathbb{D}^0 \cup \mathbb{B}^1$	$\mathbb{D}^0 \cup \mathbb{B}^1$
$\mathbb{B}^1$	$\varnothing$	$\mathbb{R}^2 \setminus \mathbb{B}^1$	$\mathbb{B}^1$	$\mathbb{B}^1$	$\mathbb{B}^1$
$\mathbb{D}^2$	$\mathbb{B}^2$	$\mathbb{R}^2 \setminus \mathbb{D}^2$	$\mathbb{S}^1$	$\mathbb{S}^1$	$\mathbb{D}^2$
x	$\mathbb{B}^2$	$\mathbb{R}^2 \setminus (\mathbb{D}^0 \cup \mathbb{B}^1 \cup \mathbb{B}^2)$	$\mathbb{D}^0 \cup \mathbb{B}^1$	$\mathbb{S}^1$	$\mathbb{D}^2$
$\mathbb{B}^2$	$\mathbb{B}^2$	$\mathbb{R}^2 \setminus \mathbb{B}^2$	$\varnothing$	$\mathbb{S}^1$	$\mathbb{D}^2$

FIGURE 2. Basic topological shapes in $\mathbb{R}^2$.

This is so because the topology $\mathcal{T} = \{U_i\}$ of X induces a relative topology $\mathcal{T}' = \{U_i \cap A : U_i \in \mathcal{T}\}$ in A. Thus, in the relative topology, the point set returned by any topological operator (1) applied to A is always the same independently of the dimension of the ambient space X. The Definition 1.4 is then the starting point to define the relative versions of $\mathrm{Int}(A)$, and, subsequently, $\mathrm{Ext}(A)$, $\mathrm{Bd}(A)$, $\mathrm{Fr}(A)$, and $\mathrm{Cl}(A)$.

4.4. Continuity. Continuity is not a topological property of a topological space. Instead, it is a property of a function defined between two topological spaces.

DEFINITION 1.5. Let X and Y be topological spaces. A function $f : X \to Y$ is **continuous** if the inverse image of an open set in Y is an open set in X.

This definition is very deep in many respects. Let us mention a few:

- First, it shows that continuity depends on the topologies of X and Y, i.e. it does not make sense to define continuity for a function if the domain X and the range Y are not topological spaces.
- Second, it is general since the nature of X and Y, and their topologies are left unspecified. Therefore, definitions of continuity as found in, for example, in analysis, theory of manifolds

or even free-form curves and surfaces in geometric design are certainly particular cases of it.

- Third, it leads to the concepts of homeomorphism and topological equivalence, and consequently to the shape classification of spaces under homeomorphisms. This is particularly useful to shape theory developed here, and mathematical theory for geometric feature modelling in particular.

EXAMPLE 1.10. Let $f : \mathbb{R} \to \mathbb{R}$ be a function defined by

$$f(x) = \begin{cases} x-1 & \text{if } x \leq 3 \\ \frac{1}{2}(x+5) & \text{if } x > 3 \end{cases}$$

whose graph in $\mathbb{R}^2$ is depicted in Figure 3(a). Note that the inverse of the open interval $(1,3)$ is the open-closed interval $(2,3]$ which is not an open set. Hence f is not continuous.

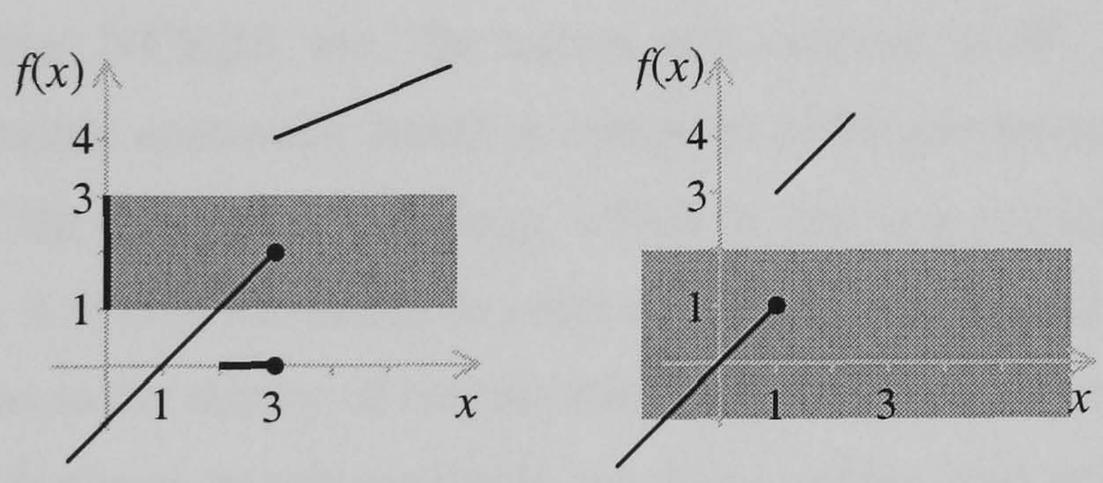

FIGURE 3

EXAMPLE 1.11. Let $\mathcal{T}$ be the usual topology on the real line $\mathbb{R}$ and let $\mathcal{U}$ be the upper-limit topology on $\mathbb{R}$ which is generated by the open-closed intervals $(a,b]$. Furthermore, let $f : \mathbb{R} \to \mathbb{R}$ defined by

$$f(x) = \begin{cases} x & \text{if } x \leq 1 \\ x+2 & \text{if } x > 1 \end{cases}$$

whose graph in $\mathbb{R}^2$ is depicted in Figure 3(b).

(i) Let $A = (-1,2) \in \mathcal{T}$. Then $f^{-1}(A) = (-1,1]$. That is, $A \in \mathcal{T}$ but $f^{-1}(A) \notin \mathcal{T}$. Hence f is not continuous relative to $\mathcal{T}$.

(ii) Let $A = (a,b] \in \mathcal{U}$. Then

$$f^{-1}(A) = \begin{cases} (a,b] & \text{if } a < b \leq 1 \\ (a,1] & \text{if } a < 1 < b \leq 3 \\ (a,b-2] & \text{if } a < 1 < 3 < b \\ \varnothing & \text{if } 1 \leq a < b \leq 3 \\ (1,b-2] & \text{if } 1 \leq a < 3 < b \\ (a-2,b-2] & \text{if } 3 \leq a < b \end{cases}$$

In each case, $f^{-1}(A)$ is an open set in $\mathcal{U}$. Hence f is continuous with respect to $\mathcal{U}$.

4.5. Homeomorphism, topological equivalence. The concept of topological space provides the most essential and natural manner for dealing with continuity. Specialised notions of continuity can be found in calculus, theory of functions, theory of manifolds, and mathematics in general. A kind of continuity of particular interest in geometric design of free-form curves and surfaces is the geometric continuity or visual continuity. It underpinnes the mathematical theory behind the parametric formulations of Bézier, B-splines, NURBS, etc., for curves and surfaces in $\mathbb{R}^3$. As shown in Chapter 2, the various kinds of geometric continuity found in computer aided geometric design are all particular cases of C^r continuity of the differential topology, which in turn is a particular case of (topological) continuity. Furthermore, it is also important in solid modelling, but here the focus is on the lack of smoothness, what leads us to the theory of singularities and, consequently, to the partition of the surface of a solid into smooth pieces or submanifolds, say faces, edges, and vertices. Edges and vertices are altogether the singularities of such a surface, that is, the point subsets of the surface where it is not smooth. This suggests that the notion of smoothness may work as a natural interplay between two important and 'separate' branches of geometric modelling: computer aided geometric design and solid modelling.

Now, we are much more interested in the general notion of continuity as provided by topology. It leads to the concept of homeomorphism, and, consequently, the notion of topological equivalence between topological spaces. That is, our idea is to distinguish two topological spaces from each other, and ultimately to achieve a taxonomy of topological shapes. In topology, two topological spaces are said to be equivalent if it is possible to transform one to the other by *continuous deformation.* Intuitively speaking, these topological spaces are seen as made out of ideal rubber which can be deformed somehow. However, such a continuous deformation is constrained by the fact that the dimension is unchanged. This kind of transformation is mathematically called homeomorphism.

DEFINITION 1.6. Let X and Y be topological spaces. A function $f : X \to Y$ is a **homeomorphism** if it is continuous and has an inverse $f^{-1} : Y \to X$ which is also continuous. If there is a homeomorphism between X and Y, X is said to be **homeomorphic** to Y and vice-versa. X and Y are then also said to be **topologically equivalent**.

Equivalently, X is homeomorphic to Y if there exist mappings $f : X \to Y$ and $f^{-1} : Y \to X$ such that $f \circ f^{-1} = \mathrm{id}_X$ and $f^{-1} \circ f = \mathrm{id}_Y$.

EXAMPLE 1.12. An interval without end points is homeomorphic to a line $\mathbb{R}$. In fact, let $f : X \to Y$ be $f(x) = \tan x$, with $X = (-\pi/2, \pi/2)$ and $Y = \mathbb{R}$. Since $\tan x$ is one-to-one on X and has an inverse, $\tan^{-1} x$, which is one-to-one on $\mathbb{R}$, f is indeed an homeomorphism.

EXAMPLE 1.13. An (open) unit ball $\mathbb{B}^2 = \{(x,y) \in \mathbb{R}^2 : x^2 + y^2 < 1\}$ is homeomorphic to $\mathbb{R}^2$. A homeomorphism $f : \mathbb{B}^2 \to \mathbb{R}^2$ may be

$$f(x,y) = \left(\frac{x}{(1-x^2-y^2)^{1/2}}, \frac{y}{(1-x^2-y^2)^{1/2}}\right)$$

while the inverse $f^{-1} : \mathbb{R}^2 \to \mathbb{B}^2$ is

$$f^{-1}(x,y) = \left(\frac{x}{(1+x^2+y^2)^{1/2}}, \frac{y}{(1+x^2+y^2)^{1/2}}\right)$$

It is easy to check that $f \circ f^{-1} = \mathrm{id}_{\mathbb{R}^2}$, and $f^{-1} \circ f = \mathrm{id}_{\mathbb{B}^2}$.

Example 1.13 can be even generalised to any dimension: an open ball $\mathbb{B}^n$ is homeomorphic to $\mathbb{R}^n$. This may be found a little surprising in that a bounded space, $\mathbb{B}^n$, is topologically equivalent to an unbounded space, $\mathbb{R}^n$; hence, *boundedness* cannot be a topological invariant. [Boundedness corresponds to the notion of 'finite extension' in solid modelling. Note the boundedness has nothing to do with boundary of a set. By definition, a subset of $\mathbb{R}^n$ is *bounded* if it is contained in an open n-ball; a n-ball centred on point $\mathbf{p} \in \mathbb{R}^n$ is the set of points $\{\mathbf{q} \in \mathbb{R}^n : \|\mathbf{p} - \mathbf{q}\| < r\}$ for some $r \in \mathbb{R}^+$.]

EXAMPLE 1.14. A square $I^2 = \{(x,y) \in \mathbb{R}^2 : (|x| = 1, |y| \leq 1), (|x| \leq 1, |y| = 1)\}$ is homeomorphic to a circle $\mathbb{S}^1 = \{(x,y) \in \mathbb{R}^2 : x^2 + y^2 = 1\}$ (Figure 4). A homeomorphism $f : I^2 \to \mathbb{S}^1$ may be given by

$$f(x,y) = \left(\frac{x}{r}, \frac{y}{r}\right) \text{ with } r = (x^2+y^2)^{1/2}.$$

Since r cannot vanish, f is invertible, being its inverse $f^{-1} : S^1 \to I^2$ given by

$$f^{-1} = (rx, ry).$$

This result is easily generalised to the n-dimensional cube: I^n is homeomorphic to n-dimensional sphere $\mathbb{S}^n$.

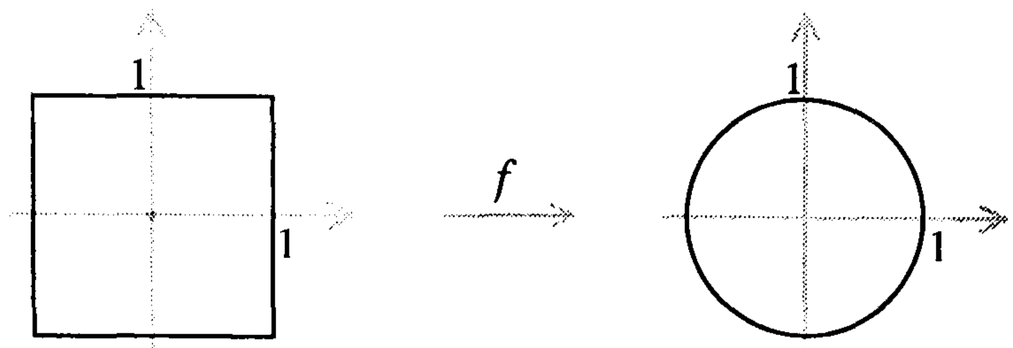

FIGURE 4. A homeomorphism between a circle and a square.

EXAMPLE 1.15. A circle $\mathbb{S}^1 = \{(x,y) \in \mathbb{R}^2 : x^2 + y^2 = 1\}$ is homeomorphic to an ellipse $E = \{(x,y) \in \mathbb{R}^2 : (x/a)^2 + (y/b)^2 = 1\}$. A homeomorphism $f : \mathbb{S}^1 \to E$ may be given by

$$f(x,y) = (ax, by).$$

It is easy to see that isometries are particular homeomorphisms [**5**, p.1]. In contrast, homeomorphisms are not isometries. Homeomorphisms do not preserve distances. Thus, unlike isometries, homeomorphisms do not preserve size and shape in the Euclidean geometric sense. But, by Brouwer's Dimension Invariance Theorem (see [**23**, p.53]), we know that homeomorphisms are dimension-invariant, that is, they are dimension-preserving. For example, the homeomorphim in Figure 4 transforms a square into a circle, with an apparent change in the geometric shape, but without changing the dimension that is 1. Sometimes, one says that isometries are too-rigid shape mappings, while homeomorphisms to too-relaxed or deformable shape mappings. Homeomorphisms form a group of mappings on the Euclidean space [**122**, p.51]; hence $(\mathbb{R}^n, \text{Homeo}(n))$ is a Klein geometry.

Homeomorphims behave like *elastic transformations* of subsets made of perfectly elastic rubber. However, we must be careful to ensure that distinct points remain distinct. We are not allowed to force two different points to coalesce into one point. For example, a line cannot be topologically deformed into one of its points because that would change its dimension. Therefore, two subsets are topologically equivalent if and only if one subset can be made to coincide with the other by an elastic transformation or homeomorphism. For example, a solid sphere can be elastically deformed into a solid cube, a cube with a depression, or even a cube with a protrusion; they are said to be homeomorphic or of the same topological type. See [**66**, p.24] for a proof that *topological equivalence* $\simeq$ is an equivalence relation. So, by Definition 1.2, the pair $(\mathbb{R}^n, \simeq)$ is a geometry or shape that only recognises the continuity properties of subsets of $\mathbb{R}^n$, where $\simeq$ is the topological equivalence relation

in that establishes equivalence classes of homeomorphic subsets in $\mathbb{R}^n$. This geometry $(\mathbb{R}^n, \simeq)$ is here called *topology*. It studies properties which are left unchanged by homeomorphisms. Obviously, the *topology* $(\mathbb{R}^n, \simeq)$ as a kind of geometry or shape should not be mistaken by a *topology* or *topological structure* $\mathcal{T}$ *on a set*, say $\mathbb{R}^n$.

5. Homotopy: homotopic shape mappings

Above we drew an analogy between homeomorphic spaces in topology and Euclidean-congruent figures in geometry. By relaxing the Euclidean-congruence in such a way that only the distance ratios instead of distances themselves are kept, we have the *similarity geometry*. This geometry is then a relative of Euclidean geometry since it is conformal, i.e. it preserves angles [**103**, p.141], and thus a subgeometry of the affine geometry. For example, any two cubes are similar, but not necessarily Euclidean-congruent.

Analogously, by relaxing point non-coalescence condition in topology, we obtain a more general geometry, called *homotopy*. However, it is *not* a Klein geometry, because the mappings used in homotopy, called *homotopies* or *homotopy mappings* do not form a group under composition, as explained further ahead. The coalescence of points is admissible in homotopy, but not completely. Such coalescence is restricted by the concept of *deformation retract* as shown below. Making an analogy, the property of being a deformation retract is analogous to similarity in geometry. As with similar figures in geometry, if X is a deformation retract of Y in homotopy, then there are obvious ways that X and Y differ, but there are also some essential characteristics in which they are the same [**66**, p.187].

We assume, for convenience, that all spaces are at least Hausdorff. A Hausdorff space X (e.g. any Euclidean space) enjoys the property that distinct points are separated by disjoint neighbourhoods, i.e. given any $\mathbf{x}, \mathbf{y} \in X$ with $\mathbf{x} \neq \mathbf{y}$, it is impossible to find points arbitrarily close both to $\mathbf{x}$ and to $\mathbf{y}$ [**23**, p.143]. This rids a space of weird pathologies.

DEFINITION 1.7. Let $f, g : X \to Y$ be continuous mappings. Then, f is **homotopic** to g, denoted by $f \sim g$, if there is a continuous mapping $H : X \times I \to Y$ such that $H(x,0) = f(x)$ and $H(x,1) = g(x)$. The mapping H is called a **homotopy** between f and g.

Equivalently, we can say that there is a continuous family of continuous mappings from X to Y between f and g, which are determined by varying t in the unit interval $I = [0,1]$. Thus, a homotopy between f and g in Y is defined by $(x,t) \mapsto (1-t)f(x) + tg(x)$ [**22**, p.109]. Therefore, a homotopy is

a parametric shape interpolation between images of two mappings. Shape interpolation is particularly useful to animation systems based on morphing techniques.

For an illustration of homotopic functions, let us take $X = I$ such that $f, g : I \to Y$ are two mappings from the interval to a topological space Y, as depicted in Figure 5(a). A homotopy from f to g is pictured in Figure 5(b).

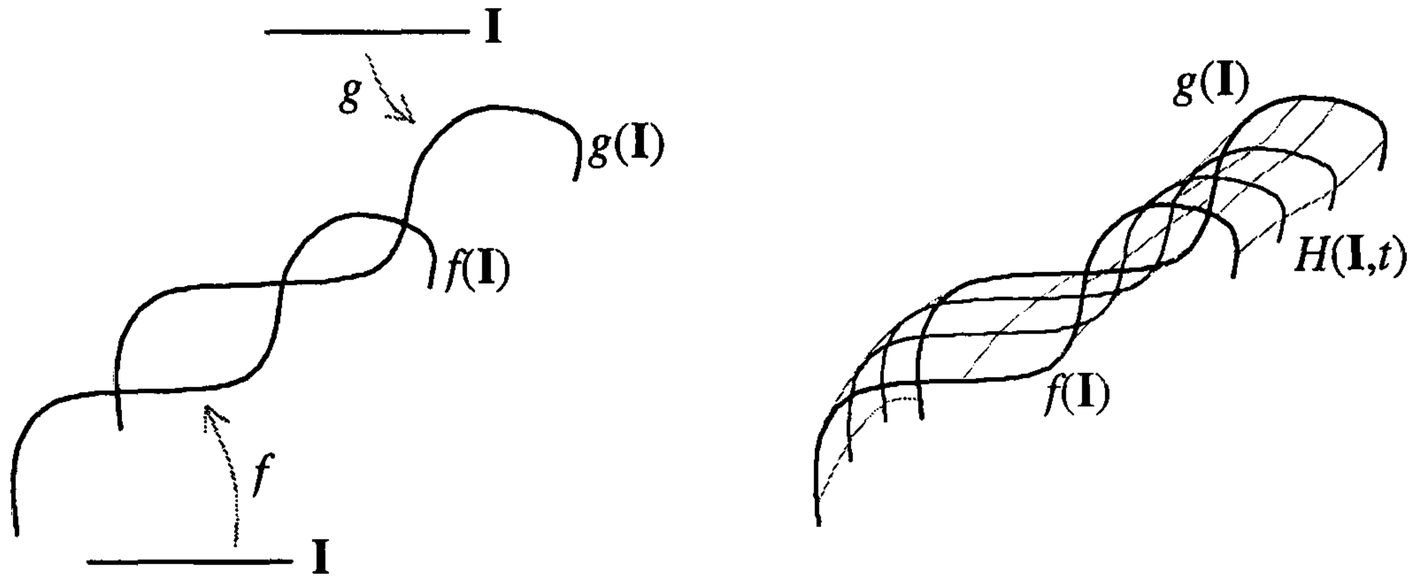

(a) f,g:I→X, with X=$\mathbf{R}^3$ (b) A homotopy from f to g

FIGURE 5

One real-life example of a homotopy is the human aging process, by taking t as a time variable. In fact, the human topological shape of a youngster is related to the shape of a wrinkled person 80 years old by a homotopy describing the shape at every age between [**66**, p.184]. Another example is a waving flag, topologically equivalent to a rectangle at any time t, but whose embedding in $\mathbb{R}^3$ varies with t. An analytic example of an homotopy is as follows.

EXAMPLE 1.16. Define $f : \mathbb{S}^1 \to \mathbb{S}^1$ by

$$f(\cos(2\pi u), \sin(2\pi u)) = (\cos(2\pi u + \frac{\pi}{2}), \sin(2\pi u + \frac{\pi}{2}))$$

for $0 \leq u \leq 1$. Consider that f rotates the circle $\mathbb{S}^1$ by 90° counterclockwise. A homotopy of f is defined by

$$H((\cos(2\pi u), \sin(2\pi u)), t) = (\cos(2\pi u + \frac{\pi}{2}t), \sin(2\pi u + \frac{\pi}{2}t))$$

for $0 \leq t \leq 1$. So, for each value of t, H is a function from the circle to the circle.

$$H((\cos(2\pi u), \sin(2\pi u)), 0) = (\cos(2\pi u), \sin(2\pi u))$$

$$H((\cos(2\pi u), \sin(2\pi u)), 1) = (\cos(2\pi u + \frac{\pi}{2}), \sin(2\pi u + \frac{\pi}{2}))$$

Thus, $H((\cos(2\pi u), \sin(2\pi u)), 0)$ is the identity function on $\mathbb{S}^1$, denoted by $\mathrm{id}_{\mathbb{S}^1}$, and

$$H((\cos(2\pi u), \sin(2\pi u)), 1) = f$$

i.e. the function f is homotopic to the identity function, $f \sim \mathrm{id}_{\mathbb{S}^1}$.

The previous examples may suggest that the topological shape is preserved by homotopies. But this is not true. Let us see a counterexample of a homotopy that do not preserve topological shape.

EXAMPLE 1.17. Consider $X = [0,2]$ and $Y = \{0\}$ and let $f, g : X \to Y$, $f(x) = x$ and $g(x) = 0$. A homotopy between f and g is given by $H(x,t) = (1-t)x$. In fact, $f(x) = H(x,0) = x$ and $g(x) = H(x,1) = 0$. Thus, despite f and g are homotopic, the image $f(X) = X$ is not homeomorphic to the image $g(X) = \{0\}$ since they have different dimensions. The effect of H here is to shrink a 1-dimensional space $X = [0,2]$ onto its a 0-dimensional subspace $Y = \{0\}$. Putting it in other way, X and Y are homotopic, but not homeomorphic.

DEFINITION 1.8. Let X and Y be topological spaces. X and Y are of the same **homotopy type** (or **homotopic**), written as $X \sim Y$, if there is continuous mappings $f : X \to Y$ and $g : Y \to X$ such that $f \circ g \sim \mathrm{id}_Y$ and $g \circ f \sim \mathrm{id}_X$. f is called the **homotopy equivalence** and g, its **homotopy inverse**.

This generalises the Definition 1.6 of topological equivalence. Therefore, two homeomorphic spaces are of the same homotopy type, but the converse is not necessarily true. The Example 1.17 clearly illustrates this situation. What is more, 'of the same homotopy type' is an equivalence relation in the set of topological spaces (see [**91**, p.96] for a proof), the equivalence class of which is called the *homotopy class*. An homotopy class is somewhat coarser than homeomorphism [**91**, p.55]. Basically, we relax the conditions in Definition 1.6 so that the continuous functions f and g need not have inverses. Consequently, homotopies do not form a group, and *homotopy* is a geometry by the Definition 1.2, but not in the sense of Klein. The next example illustrates this situation.

EXAMPLE 1.18. From the Example 1.17 we know that the spaces $X = [0,2]$ and $Y = \{0\}$ are of the same homotopic shape, but not homeomorphic. Let $f : X \to Y$, $f(x) = 0$ and $g : Y \to X$, $g(0) = 1$ two continuous functions. Then $f \circ g = \mathrm{id}_Y$, while $g \circ f \neq \mathrm{id}_X$, although $f \circ g \sim \mathrm{id}_Y$ and $g \circ f \sim \mathrm{id}_X$.

The concept of homotopy defined above is also called *homotopy of length 1* because it uses the unit interval I. But, it can be even extended to intervals of any length. The next example illustrates an homotopy of infinite length, where I is replaced by $\mathbb{R}$.

EXAMPLE 1.19. $\mathbb{S}^1$ is of the same homotopy type as a cylinder because a cylinder is a direct product $\mathbb{S}^1 \times \mathbb{R}$ and we can shrink $\mathbb{R}$ to a point at each point of $\mathbb{S}^1$. Analogously, the Möbius strip is of the same homotopy type as $\mathbb{S}^1$, yet they are not homeomorphic.

EXAMPLE 1.20. A 2-ball $\mathbb{B}^2 = \{(x,y) \in \mathbb{R}^2 : x^2 + y^2 < 1\}$ is of the same homotopy type as a point. $\mathbb{B}^2 - \{(0,0)\}$ is of the same homotopy type as $\mathbb{S}^1$. Also, $\mathbb{R}^2 - \{(0,0)\}$ is of the same homotopy type as $\mathbb{S}^1$ and $\mathbb{R}^3 - \{(0,0,0)\}$ as $\mathbb{S}^2$.

The continuous deformation of spaces in homotopy theory is then stronger than in topology, because the coalescence of points is allowed. This enables us to say that, for example, the essential homotopic shape of an interval in $\mathbb{R}$ is a point. We are actually interested in to know how such coalescence captures the essential homotopic shape of any subspace in $\mathbb{R}^n$. This is useful to compare two subspaces in $\mathbb{R}^n$ from the homotopy point of view, and is important for the design of a shape-complete geometric kernel, as the Σ-geometric kernel proposed in this thesis.

Therefore, we intend to capture the homotopic shape of a space X by *continuously deformation* of it onto a subspace $Y \subseteq X$, that is $X \sim Y$.

DEFINITION 1.9. Let Y ($\neq \varnothing$) be a subspace of X. If there is a continuous mapping $f : X \to Y$ such that $f|_Y = \mathrm{id}_Y$, Y is called a **retract** of X and f a **retraction**.

Equivalently, we say that the entire X is mapped onto Y *keeping points in Y fixed.* [By 'keeping points in Y fixed' we mean $f(x) = x$ for all $x \in Y$.] Putting it differently, f collapses X onto its subspace Y. With $Y \subseteq X$, let the inclusion function $i : Y \to X$ be defined by $i(x) = x$. Note that i does not move any points. So, f is a retraction iff $f(i(x)) = x$, that is, $f \circ i = \mathrm{id}_Y$. We should not expect that $i \circ f : X \to X$ be id_X, since $i \circ f$ first shrinks the bigger space X onto Y, and then stretches out Y back into X without changing it.

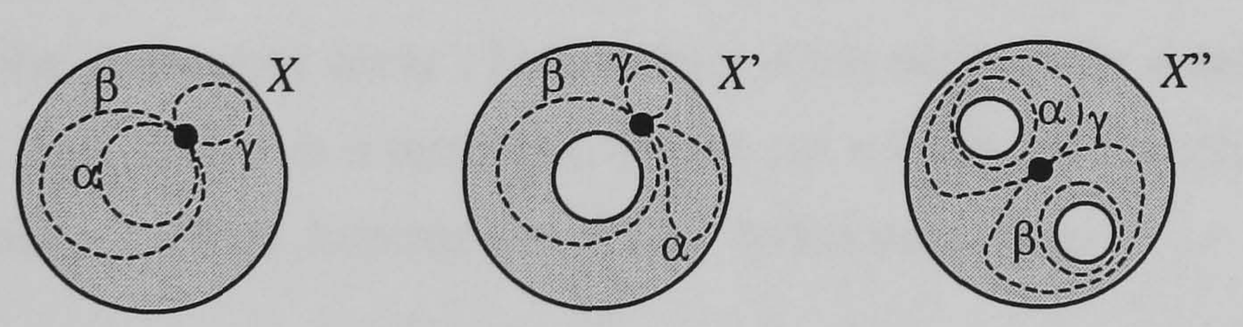

(a) Examples of retracts

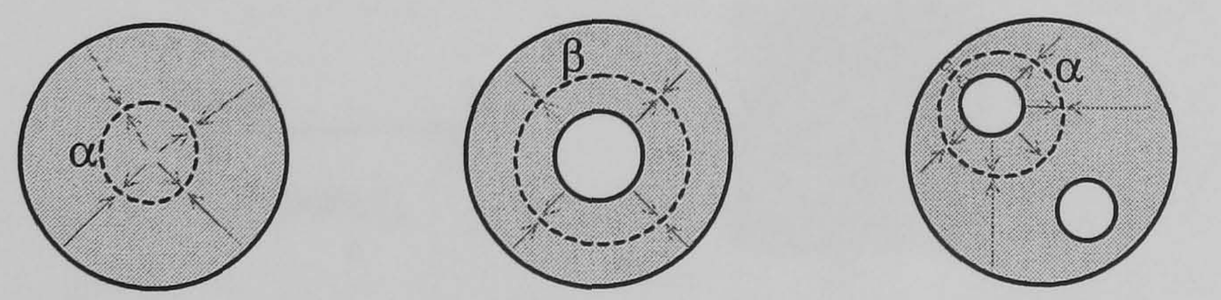

(b) Actions of retractions

FIGURE 6

EXAMPLE 1.21. Let us look at Figure 6(a), where three retracts for each space X, X', and X'' are shown. Such retracts are the circles or loops α, β, γ. Note that X does not include any through hole, while X' possesses one hole and X'' two holes. In Figure 6(b), the arrows illustrate the retraction effects of X, X', and X'' onto the circles α, β, and γ, respectively.

As suggested in Figure 6, there are many retracts of a space, but not all capture its essential homotopic shape. For example, since X is homotopic to a point, all the circles might be collapsed onto a point in X. Thus, no circle in X captures the essential homotopic shape of X. On the other hand, the annulus X' has a hole that is an obstruction to continuous deformation of the circle β into a point. However, this hole do not prevent the continuous deformation of the circles α, γ into a point in X'. It is then said that X' and β (but not α or γ) are of the same homotopy type or the same homotopic shape. Analogously, unlike the double circle γ in X'', the circles α and β (or even its union) do not have the same homotopy type as X''.

In homotopy theory, a retract Y of a set X with the same homotopy type as X is called a *deformation retract* of X. Thus,

DEFINITION 1.10. A subset $Y \subseteq X$ is a **deformation retract** of X if there is a retraction $f : X \to Y$ such that $i \circ f \sim \mathrm{id}_X$, with i is the inclusion function.

This is equivalent to say that there is a homotopy $H : X \times I \to X$ between id_X and a retraction $f : X \to Y$ such that $H(x,0) = x$ and $H(x,1) \in Y$ for any $x \in X$, and $H(x,t) = x$ for any $x \in Y$ and any $t \in I$ (see [**91**, p.97] for this equivalent definition).

Thus the difference between a retract and a deformation retract is that a deformation retract is basically a retract in 'the homotopic sense', but a retract is not necessarily a deformation retract. For example, in Figure 6, the circle α is a retract of X'' but not a deformation retract, since the second hole in X'' prevents the continuous deformation of $\mathrm{id}_{X''}$ to the retraction.

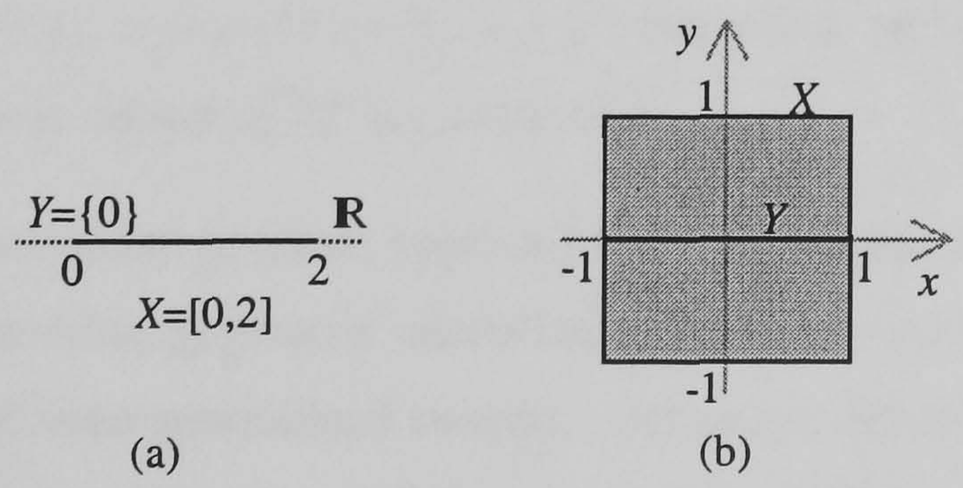

FIGURE 7. Deformation retracts of (a) an interval and (b) a square.

EXAMPLE 1.22. Let $X = [0,2]$ and $Y = \{0\}$ a subset of X. A retraction $f : X \to Y$ is defined by $f(x) = 0$ for each $x \in X$. Note that $i \circ f(x) = i(f(x)) = i(0) = 0$ considered as a point in X. Let us define $H(x,t) = tx$, $t \in I$ and $x \in X$. Thus, for each $x \in X$, $H(x,1) = x$ and $H(x,0) = 0.x = 0 = i \circ f(x)$. Thus $i \circ f \sim \mathrm{id}_X$ so $Y = \{0\}$ is a deformation retract of Y, Figure 7(a).

EXAMPLE 1.23. Let X and Y be the square of points (x,y) where $-1 \leq x \leq 1$, $-1 \leq y \leq 1$ and the center line segment $y = 0$, $-1 \leq x \leq 1$, respectively. A deformation retract takes X to Y by defining the retraction $f(x,y) = (x,0)$. The homotopy is given by $H[(x,y),t] = (x,ty)$, $t \in I$, and is depicted in Figure 7(b).

EXAMPLE 1.24. Let $Y = \{e^{i\theta} : 0 \leq \theta \leq 2\pi\}$ be the unit circle and $X' = \{re^{i\theta} : 0 \leq \theta \leq 2\pi, \frac{1}{2} \leq r \leq \frac{3}{2}\}$ be an annulus (see Figure 6(b)). Let $f : X' \to Y$ be a retraction be defined by $f(re^{i\theta}) = e^{i\theta}$ and $i : Y \to X'$ be the inclusion function defined by $i(e^{i\theta}) = e^{i\theta}$. Then $i \circ f : re^{i\theta} \mapsto e^{i\theta}$ and $f \circ i : e^{i\theta} \mapsto e^{i\theta}$. Note that $i \circ f \sim \mathrm{id}_{X'}$ and $f \circ i = \mathrm{id}_Y \sim \mathrm{id}_Y$. In fact, there exists a homotopy $H(re^{i\theta},t) = (1-t)re^{i\theta} + te^{i\theta} = [1+(r-1)(1-t)]e^{i\theta}$ which interpolates between $i \circ f$ and id_Y, keeping the points on Y fixed. Hence Y is a deformation retract of X'.

EXAMPLE 1.25. Using the same technique as in previous example, it is not difficult to show that the unit circle $\mathbb{S}^1$ is a deformation retract of $\mathbb{D}^2 - \{0\}$, with $\mathbb{D}^2 = \{(x,y) : x^2 + y^2 \leq 1\}$. Besides, it can be shown that the unit sphere $\mathbb{S}^n$ is a deformation retract of $\mathbb{D}^{n+1} - \{0\}$.

DEFINITION 1.11. If a point $p \in X$ is a deformation retract of X, X is said to be **contractible**.

Let $c : X \to \{p\}$ be a constant mapping. If X is contractible, there exists a homotopy $H : X \times I \to X$ such that $H(x,0) = c(x) = p$ and $H(x,1) = \mathrm{id}_X(x) = x$ for any $x \in X$ and, moreover, $H(p,t) = p$ for any $t \in I$. The homotopy H is called a *contraction*.

EXAMPLE 1.26. $X = \mathbb{R}^n$ is contractible to the origin 0. In fact, if we define $H : \mathbb{R}^n \times I \to \mathbb{R}^n$ by $H(x,t) = tx$, we have (i) $H(x,0) = 0$ and $H(x,1) = x$ for any $x \in X$ and (ii) $H(0,t) = 0$ for any $t \in I$. Now it is clear that any convex subset of $\mathbb{R}^n$ is contractible.

The homotopy theory has many possible applications in geometric modelling. For example, homotopies can be used to describe geometric modelling operations such as *sweeps* (either they are translational or rotational, or even generalised sweeps, with shape deformation or not) and *offsets*, as well as operations of dimension reduction in finite-element modelling. Also, some of the Euler operators used by B-rep geometric modellers implement homotopy operations such as *expansions* (e.g. *mev*, the shorthand of *make edge and vertex*) and collapses (e.g. *kev*, the shorthand of *kill edge and*

vertex). This suggests that homotopy theory may work as a mathematical setting for many important geometric operations. This is so because homotopies are basically mappings of shape interpolation such that the image of a mapping f is continuously deformed to the image of another mapping g.

Nevertheless, for the present time, we are primarily concerned to show how the classification of shape mappings allows us to classify spaces, that is, to achieve a shape classification of spaces in $\mathbb{R}^n$. This is important in the design and construction of any n-dimensional geometric kernel, in particular stratified geometric kernels (e.g. boundary-representation geometric kernels). In fact, for a geometric kernel that is able to model objects in higher dimensions, we have to be aware of the homotopic shape of the frontier of each manifold in a stratified point set. (Roughly speaking, a stratified point set is a point set partitioned into manifolds or strata such as, for example, vertices, edges and faces.) Otherwise, it would be rather difficult to have Euler operators carrying out reasoning queries of homotopic shape nature, not just topological queries such as incidence (or connectedness) and adjacency of manifolds. For example, to add a connected open edge (a 1-manifold) between two vertices (or 0-manifolds) of a stratified object, the corresponding Euler operator has to determine first whether or not such vertices belong to distinct object components, regardless of the shape complexity of such components. Clearly, this shows that a geometric kernel of stratified objects is more than a geometric and topological shape engine. Above all, it is a homotopic shape kernel for basically two reasons. First, we should take into account that geometric and topological shapes are particular homotopic shapes, what results from the fact that isometries are particular homeomorphisms, and in turn homeomorphisms are particular homotopies. Second, shape reasoning about the global shape properties of point sets has inherently a homotopic nature as explained later on.

6. Differential topology: smooth shape mappings

If one thinks of topology as the natural area of mathematics within which *continuity* is studied, then differential topology is the natural area of mathematics within which one studies *smoothness* [**92**, p.25]. Of course, all differentiable mappings are also continuous, but not vice-versa. The differentiable mappings are for continuous mappings as diffeomorphisms are for homeomorphisms. So, while a homeomorphism is a continuous mapping that has continuous inverse, a diffeomorphism is a differentiable mapping that has differentiable inverse. Thus, diffeomorphisms form a subgroup of the group of homeomorphisms. Analogously, as homeomorphisms are central to topology, diffeomorphisms are central to differential topology. As Sharpe notes in [**103**, p.12], differential topology is the study of the properties of smooth manifolds that are preserved by diffeomorphism.

As their relative mappings, diffeomorphisms allow us to distinguish a geometric object from another somehow. Diffeomorphisms are finer shape filters than homeomorphisms. However, they are coarser shape filters than isometries. For example, consider two 1-dimensional manifolds, a square and a circle, depicted in Figure 4. The mapping f in Figure 4 represents a continuous deformation of the square into the circle, i.e. it is a homeomorphism. But because of the right-angled bends at the corners of the square, we do not expect f to be differentiable at those corners. This leads us to reject a square as a candidate for a 1-dimensional smooth manifold. We do not reject though, a smooth curve such as a circle. Thus, a square and a circle are homeomorphic but not diffeomorphic, and the mapping f in Figure 4 is not a diffeomorphism.

Obviously, by specialising from continuous mappings to differentiable mappings, and even further to analytic mappings, we are able to cross areas of mathematics where shape of spaces is studied, namely topology, differential topology and geometry, respectively. This section deals with such differentiable shape mappings and how they are related to differentiable or smooth shapes as usual in geometric modelling. Surprisingly, or may be not, the concept of C^r smoothness as defined by differential topology is basically a specialisation of the notion of continuity defined in topology. C^r smoothness is for parametric formulations of curves and surfaces what we call geometric continuity G^r (visual smoothness) in CAGD. Moreover, the notion of C^r smoothness was developed in mathematics to be independent of any formulations, regardless of whether they are parametric or implicit, or even explicit. Besides, the theory of smoothness in differential topology underpinnes the theory of singularities and the theory of stratifications, two of the essential theories to support the development of an integrated geometric model for solid modelling and parametric formulations of curves and surfaces as usual in CAGD.

6.1. Topological structure of a manifold. Manifolds are generalisations of curves and surfaces to arbitrary dimensional objects. This subsection deals with the *topological structure* underlying the differential structure of a manifold. The *differential structure* of a manifold is introduced in the next subsection.

As a preliminary to the definition of a differentiable manifold, we recall the definition of a topological manifold (or just manifold). A manifold M of dimension n is a Hausdorff space with a countable basis of *open sets* and with the further property that each point has a neighbourhood homeomorphic to an *open* subset of $\mathbb{R}^n$ [**15**, p.52]. Obviously, the open sets of M form a topology or topological structure on M. Therefore, a topological manifold M can be covered with a family of open subsets, each one can be assigned coordinates in $\mathbb{R}^n$ by a homeomorphism from it onto an open subset of $\mathbb{R}^n$.

Let U one of those open subsets in M and f a *homeomorphism* from U onto an open subset of $\mathbb{R}^n$, Figure 8. To $\mathbf{x} \in U$ we assign the n *coordinates* $f_1(\mathbf{x}), \ldots, f_n(\mathbf{x})$ of its image $f(\mathbf{x})$ in $\mathbb{R}^n$. Each component function $f_i(\mathbf{x})$ of f is a real-valued function on U, the i-th *coordinate function.* Each pair (U, f) is called a *chart* (or *local coordinate system* or *coordinate neighbourhood*); U is called a *chart domain* or *patch.* Obviously, if $\mathbf{x}$ lies also in a second chart (V, g) (more specifically, in a patch V), then it has also coordinates $g_1(\mathbf{x}), \ldots, g_n(\mathbf{x})$ in this neighbourhood. Since f and g are homeomorphisms, this defines a homeomorphism $h = g \circ f^{-1} : f(U \cap V) \to g(U \cap V)$, the domain and range being the two open subsets of $\mathbb{R}^n$ which correspond to the points of $U \cap V$ by the two coordinate mappings f, g, respectively [**15**, p.52], Figure 8. Similarly, by definition, $h^{-1} = f \circ g^{-1}$ is also a homeomorphism. These homeomorphisms $h = g \circ f^{-1}$ and $h^{-1} = f \circ g^{-1}$ are called *transition mappings* (or *overlap mappings* or *coordinate change mappings*). For 'geography' reasons, a collection of charts that cover a manifold is called an *atlas.*

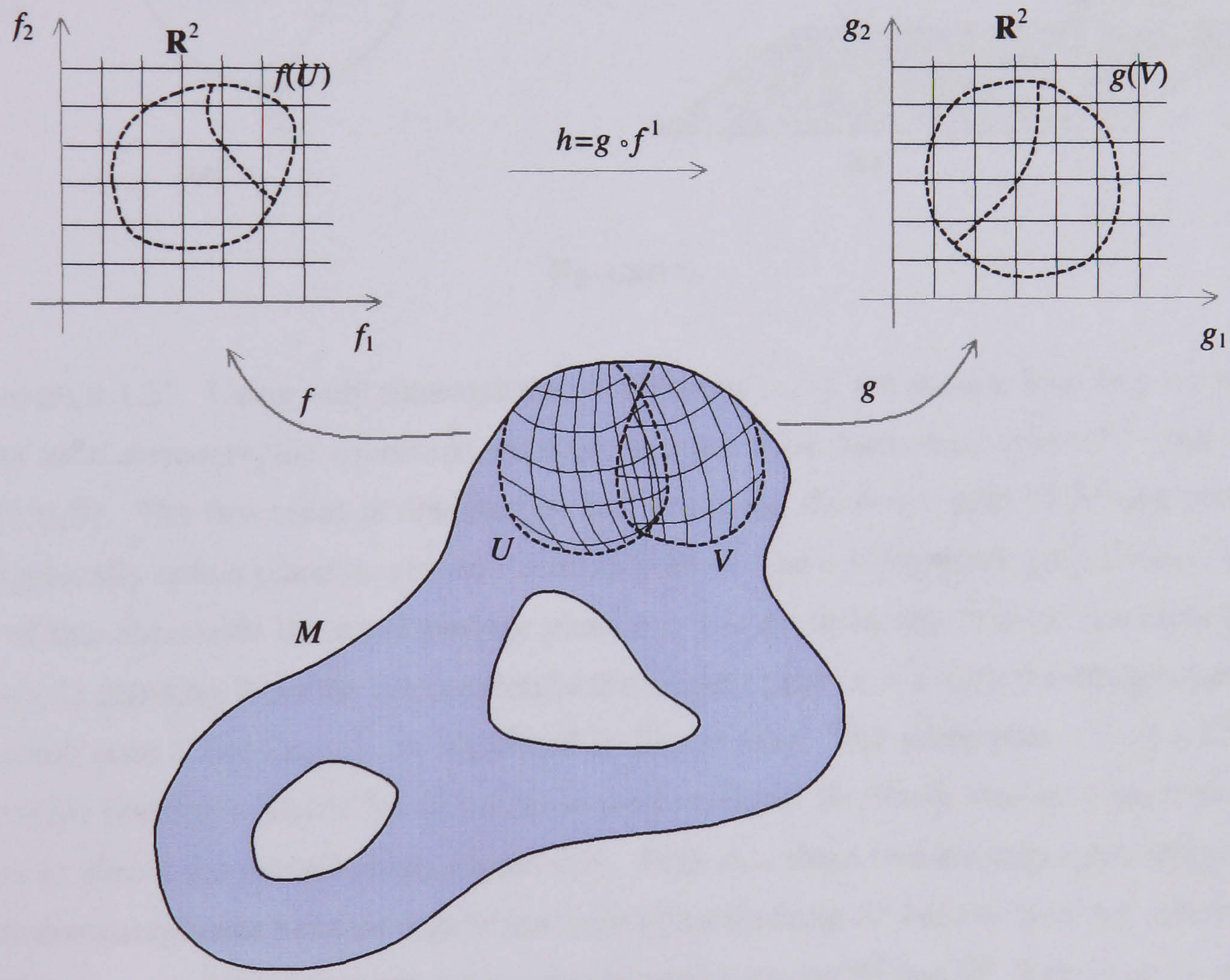

FIGURE 8

When a n-manifold is *globally* homeomorphic to $\mathbb{R}^n$, only one chart is necessary; otherwise, more charts are required. In fact, because of the *local* homeomorphism between a n-manifold and $\mathbb{R}^n$,

each point in a manifold is given a chart associated with its neighbourhood. [By definition, a local homeomorphism of $\mathbb{R}^n$ is a homeomorphism of some open subset of $\mathbb{R}^n$ onto another [**44**, p.2]. This means that the domain of a local homeomorphism need not be all of $\mathbb{R}^n$.] If a manifold is (globally) homeomorphic to $\mathbb{R}^n$, then it is a neighbourhood of all its points, and $\mathbb{R}^n$ can be considered as the only coordinate system for all its points. Therefore, the charts on a manifold are defined by local, bijective, continuous mappings called homeomorphisms from a n-manifold to $\mathbb{R}^n$. Of course, there are usually several ways (i.e. atlases) to cover a manifold with charts.

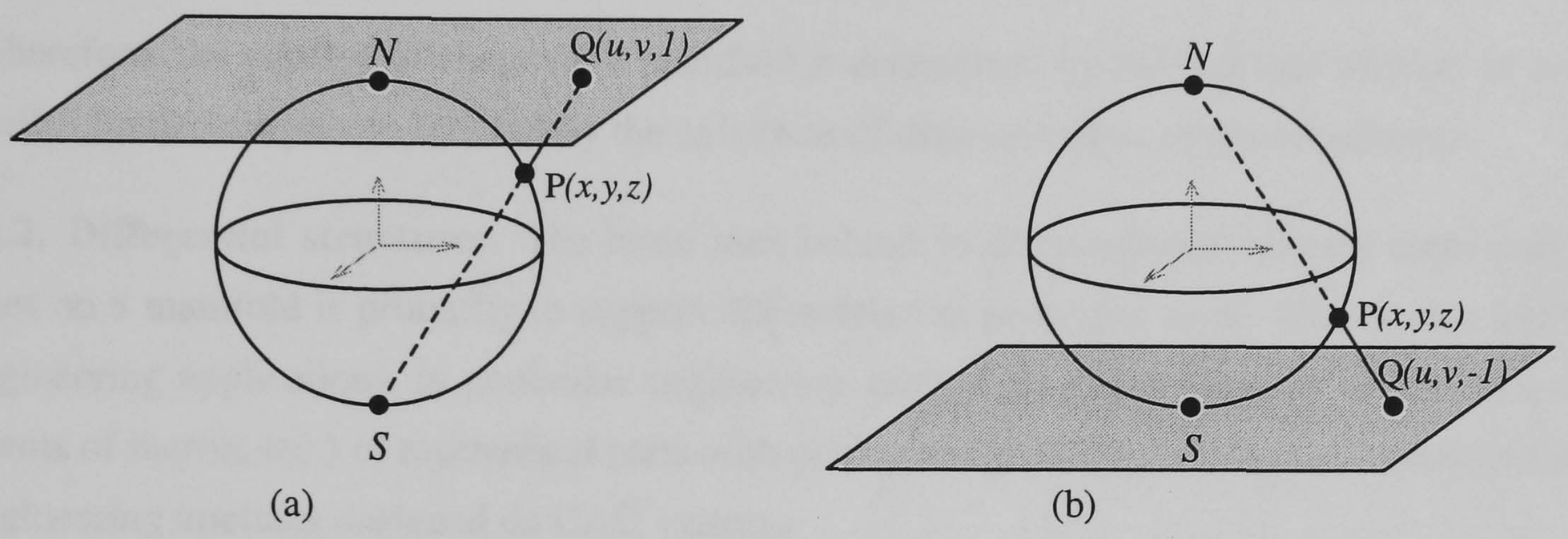

FIGURE 9

EXAMPLE 1.27. Using only stereographic coordinates (u,v), we need at least two stereographic charts (or local stereographic coordinate systems) to cover a 2-dimensional sphere $\mathbb{S}^2$ centered at the origin $(0,0,0)$. The first chart is obtained by first removing the south pole of $\mathbb{S}^2$ and then project stereographically onto a plane tangent to the north pole N. The stereographic projection of any point (x,y,z) of this chart onto the north tangent plane $z=1$ is given by the first two coordinates of the point $(u,v,1)$ resulting from the intersection of the tangent plane $z=1$ with the straight line defined by the south pole S and (x,y,z), as illustrated in Figure 9(a). The south pole S works here as the stereographic projection centre for all points in the first chart. Similarly, we can change the roles of the poles to obtain the second chart, Figure 9(b). Note that these two stereographic projections are in fact homeomorphisms because a pole has been removed from $\mathbb{S}^2$ before each projection onto the plane. However, no single homeomorphism can be used between $\mathbb{S}^2$ and $\mathbb{R}^2$. This example illustrates a *topological impossibility* to cover $\mathbb{S}^2$ with just one chart.

EXAMPLE 1.28. The surface of $\mathbb{S}^2$ in $\mathbb{R}^3$ can be also parametrised by polar coordinates (θ,ϕ). They can be obtained from the cartesian coordinates $x=\sin\theta\cos\phi$, $y=\sin\theta\sin\phi$, and $z=\cos\theta$, with $\phi\in[0,2\pi]$ and $\theta\in[0,\pi]$ by inversion to yield $\theta=\tan^{-1}(\frac{(x^2+y^2)^{1/2}}{z})$ and $\phi=\tan^{-1}(y/x)$. Note that

the θ-coordinate has a discontinuity at $z = 0$, what means that the polar coordinates are not defined on the equator of $\mathbb{S}^2$. Similarly, the ϕ-coordinate is not defined at the poles since $x = y = 0$. This suggests that we have to use various polar parametrisations to cover completely $\mathbb{S}^2$ with polar charts. This example illustrates a *analytic impossibility* to cover $\mathbb{S}^2$ with just one chart. Obviously, other coordinate systems, either stereographic projections from different points (other than poles) on $\mathbb{S}^2$ or polar coordinate systems, or even distinct kinds of local coordinate systems on the same manifold could be used to cover $\mathbb{S}^2$.

Therefore, the number of charts on a manifold is determined by the fact that whether or not it is (globally) homeomorphic to $\mathbb{R}^n$, and by the existence of discontinuities in the coordinates.

6.2. Differential structures. The basic idea behind local coordinate systems associated with patches on a manifold is primarily to support differentiation processes on it. This is very important to engineering applications, in particular engineering analysis (e.g. computation of volumes, areas, moments of inertia, etc.) of mechanical parts with parametric geometry and finite-element modelling of engineering artefacts designed on CAD systems.

The coordinates on a manifold may be kept arbitrary until some specific calculation is to be carried out. Then, because coordinate systems or charts of an atlas usually overlap, we have to introduce a certain compatibility condition to guarantee that the charts fit together nicely, say in a sufficiently *smooth* way. It is then necessary to ensure that the transition from a coordinate system to another is *smooth*. Without this compatibility condition, a differentiable function in one chart may be not differentiable in the other chart. As shown below this enables us to develop calculus on a manifold. This is exactly the essence of the differential topology, a combination of manifolds (from topology) with the differential calculus of mappings (from function theory) between manifolds.

Now we are ready to construct differentiable and analytic structures on a manifold. To this end, recall that every point of a topological manifold M lies in a very large collection of charts, but whenever two chart patches overlap we have formulas just given for change of coordinates. The basic idea that leads to differentiable manifolds is to try to select a subfamily or subcollection of charts (i.e. an atlas) so that the change of coordinates is always given by differentiable mappings; that is, the homeomorphisms associated with the charts of an atlas must be differentiable mappings.

Let us then review some important notions from (real) function theory (see [**56**, p.2] for more details). Let $\mathbb{R}^m$ and $\mathbb{R}^n$ denote two Euclidean spaces of m and n dimensions, respectively. Let X, Y be open subsets of $\mathbb{R}^m, \mathbb{R}^n$, respectively, and $f : X \to Y$ be a mapping of X into Y. If $n = 1$, we say that the function f is C^r (or C^r *differentiable* or *differentiable of class* C^r, or C^r *smooth* or *smooth of class*

C^r) on X, for $r \in \mathbb{N}$, if the partial derivatives of f exist and are continuous on X, that is, at each point $\mathbf{x} \in X$. In particular, f is C^0 if f is continuous. If $n > 1$, the mapping f is C^r if each of the *component functions* f_i $(1 \leq i \leq n)$ of f is C^r. We say that f is C^∞ (or just *differentiable* or *smooth*) if it is C^r for all $r \geq 0$. [In the case when $n = 1$ it is customary to replace the term "mapping" (or "map") by the term "function".] Moreover, f is called a C^r *diffeomorphism* if: (i) f is a homeomorphism and (ii) both f and f^{-1} are C^r differentiable, $r \geq 1$ (when $r = \infty$ we simply say *diffeomorphism*).

DEFINITION 1.12. Any two charts (U, f) and (V, g) are C^r **compatible** if $U \cap V$ nonempty implies that the mappings $h = g \circ f^{-1}$ and $h^{-1} = f \circ g^{-1}$ giving the change of coordinates are C^r. This is equivalent to requiring h and h^{-1} to be C^r diffeomorphisms of the open subsets $f(U \cap V)$ and $g(U \cap V)$ of $\mathbb{R}^n$, as illustrated in Figure 8 with $m = n = 2$.

The condition of compatibility has then to do with the differentiability of transition mappings. Thus,

DEFINITION 1.13. A C^r **atlas** on a manifold M of dimension m is a collection of charts $\{(U_i, f_i)\}$, $i \in I$, on M where $f_i(U_i)$ is an open subset of $\mathbb{R}^m$ such that the following conditions are satisfied:

(i) $M = \cup U_i$;

(ii) for each pair $i, j \in I$ the charts (U_i, f_i) and (U_j, f_j) are C^r compatible.

Therefore, for differentiable manifolds, all transition mappings must be homeomorphims (or C^0) and C^r $(1 \leq r < \infty)$, and so an atlas is said to be a C^r *atlas* (or C^r *differentiable atlas* or *atlas of class* C^r). A *differential* or *smooth atlas* is just a C^∞ atlas.

REMARK 1. The condition (i) is here called *atlas condition* and concerns a topological structure of a manifold. In fact, the open sets in a manifold define a topology [**1**, p.125]; for a proof, take as basis of the topology the family of finite intersections of charts domains or patches. Furthermore, given such an atlas, there is a unique topology on M making it a C^r atlas on M [**60**, p.14]. The condition (ii), here called *differential compatibility condition*, has to do with the differential compatibility of the transition mappings.

Obviously, every manifold has many possible atlases. Two C^r atlases are equivalent if the union of them is also a C^r atlas. If the union of two C^r atlases is again a C^r atlas, they are said to be C^r *compatible*. The C^r compatibility of atlases is an equivalence relation, the equivalence class of which is called the C^r *structure*. It is also said that mutually C^r compatible atlases define the same C^r structure on M [**91**, p.134]. The union of the atlases in a C^r structure is called the *maximal* C^r

atlas. Of course, if $r = \infty$, we have a C^∞ *structure* (also called a *differential* or *smooth structure*) on a manifold M.

In order to specify a differentiable structure on a manifold, it suffices to specify a differentiable atlas and, in general, one preferably chooses one as small as possible.

EXAMPLE 1.29. The Euclidean space $\mathbb{R}^m$ is the most trivial example, where a single chart covers the whole space and f is the identity mapping. This is true even if we let $\mathbb{R}^m$ mean a single point for $m = 0$. The manifolds of dimension 0 are then the discrete topological spaces. Every discrete topological space X is a 0-manifold, the charts being given by $(\{x\}, f)$, $f : x \mapsto 0$, $x \in X$.

EXAMPLE 1.30. Let M be a connected 1-dimensional manifold. There are only two manifolds possible: a real line $\mathbb{R}$ and the circle $\mathbb{S}^1$. All the others are homeomorphic to either $\mathbb{R}$ or $\mathbb{S}^1$. Let us construct an atlas on $\mathbb{S}^1$. Specifically, take the circle $x^2 + y^2 = 1$ in $\mathbb{R}^2$. At least two charts are necessary, as pictured in Figure 10. Let $f_1^{-1} : (0, 2\pi) \to \mathbb{S}^1$ be defined by $f_1^{-1} : \theta \mapsto (\cos\theta, \sin\theta)$ whose image is $\mathbb{S}^1 - \{(1,0)\}$. In addition, let $f_2^{-1} : (-\pi, +\pi) \to \mathbb{S}^1$ be defined by $f_2^{-1} : \theta \mapsto (\cos\theta, \sin\theta)$ whose image is $\mathbb{S}^1 - \{(-1,0)\}$. Clearly, f_1^{-1} and f_2^{-1} are invertible and all the mappings f_1, f_2, f_1^{-1} and f_2^{-1} are continuous. Thus f_1 and f_2 are homeomorphisms. It is not difficult to check that the mappings $f_{21} = f_1 \circ f_2^{-1}$ and $f_{12} = f_2 \circ f_1^{-1}$ are smooth.

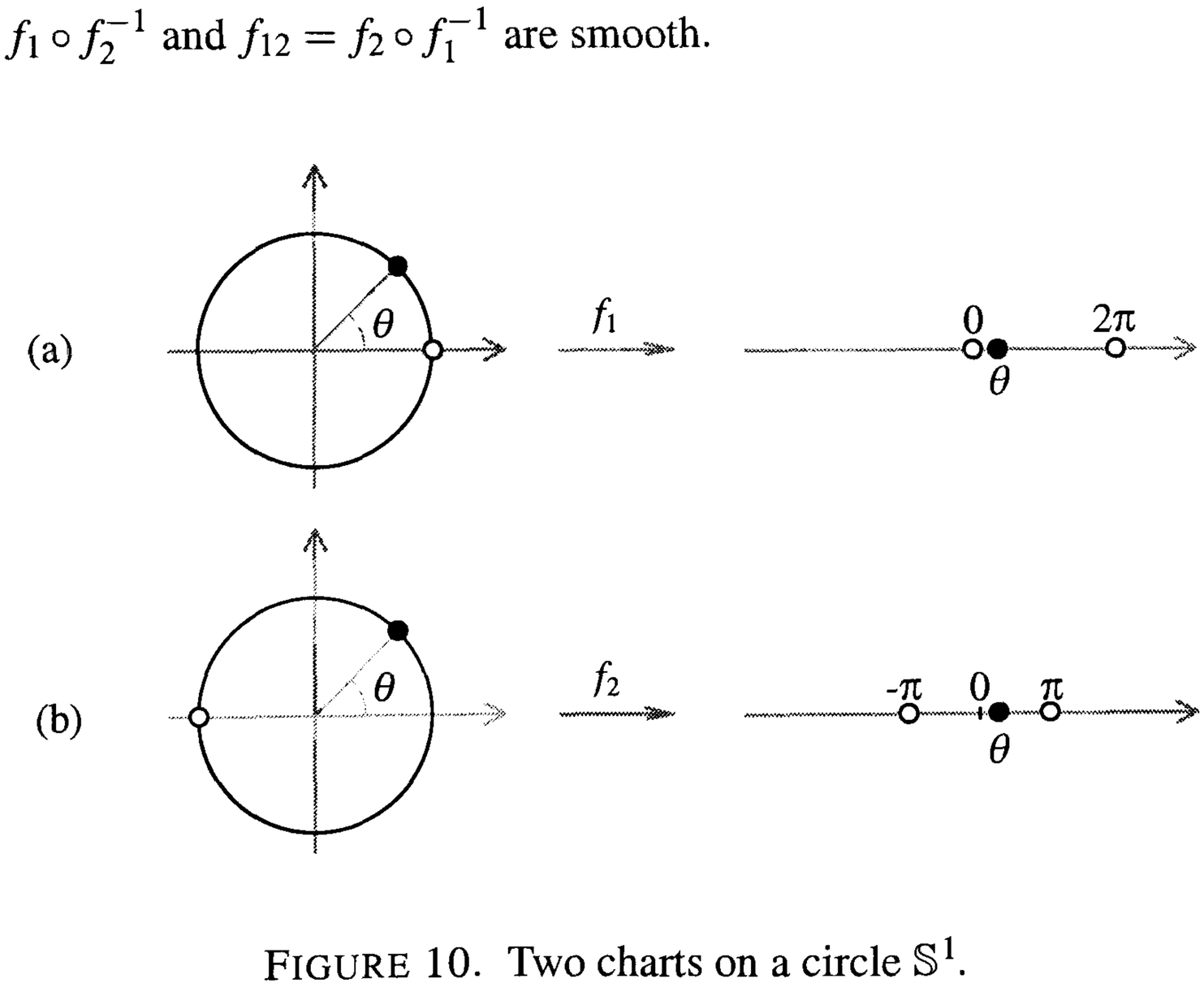

FIGURE 10. Two charts on a circle $\mathbb{S}^1$.

EXAMPLE 1.31. The n-dimensional sphere $\mathbb{S}^n$ is a differentiable manifold (see [**91**, p.136] for a proof).

DEFINITION 1.14. A C^r **manifold** M of dimension m is a topological manifold with a C^r structure of dimension m. Of course, if $r = \infty$, M is called a C^∞ **manifold** (or **differential manifold** or **smooth manifold**).

REMARK 2. Note that no assumption on the connectedness has been made for a manifold. In fact, in many mathematical applications the manifolds are disconnected.

REMARK 3. The transition mappings of a C^r structure of a manifold are diffeomorphisms. This is of paramount importance in geometric design, because as seen later it means that differential manifolds are in fact *visually* smooth. That is, a C^r manifold (e.g. a curve or a surface) is what in geometric design is called a G^r manifold, or a manifold with geometric continuity G^r. Moreover, because the definition of a C^r manifold does not depend on the representation, whether it is parametric, explicit or implicit, the concept of geometric continuity seems to be redundant from a mathematical point of view.

6.3. Analytic structures. An *analytic structure* on a manifold M is defined in a similar way to a differentiable structure. We just replace "differentiable" by "analytic" transition mappings. In this case M is called an *analytic manifold.* It is clear that we can always regard an analytic manifold as a differentiable manifold. It is often convenient to do so because it is known that the class of differentiable functions is much richer than the class of analytic functions in $\mathbb{R}^n$. In fact, analyticity is subsumed under differentiability. In other words, every analytic manifold is a differentiable manifold, but not vice-versa.

Let us make clear the relationship between analyticity and differentiability in $\mathbb{R}^n$. Let $f(\mathbf{x})$ ($\mathbf{x} = x_1, \ldots, x_n$) be a real-valued function defined on an open subset U of $\mathbb{R}^n$. The function f is *analytic* at the point $\mathbf{p}$ in U if there is a neighbourhood of $\mathbf{p}$ on which f can be represented by means of its Taylor expansion in the variables $\mathbf{x} = x_1, \ldots, x_n$ [**5**, p.115]. Obviously, f is analytic on U if it is analytic at each point of U [**106**, p.56]. From the theory of power series, we know that such a function has partial derivatives of all orders and is thus differentiable [**98**, p.181]. On the contrary, a differential function need not be analytic. To make the distinction between differentiable and analytic functions concrete, let us take the following classical example in mathematical literature.

EXAMPLE 1.32. Let

$$f(x) = \begin{cases} e^{-1/x^2} & \text{for } x \neq 0 \\ 0 & \text{for } x = 0 \end{cases}$$

Then f is differentiable even at the point $x = 0$. But all derivatives of f are equal to zero at $t = 0$, that is, all Taylor coefficients of f vanish at $x = 0$. The only real analytic function with this property

is the function which is identically zero. Thus, because of the correspondence 1-1 between analytic functions and their Taylor series, f cannot be real analytic at $t = 0$. Besides, note that for any analytic function there is a vast horde of differential (or smooth) but nonanalytic functions with the same Taylor series expansion [**43**, p.588].

This implies that engineering artefacts, or at least their frontiers, must be analytic. Otherwise, one cannot avoid the mathematical horror of pathologies like that in Example 1.32. Analyticity guarantees the uniqueness of Taylor series for a function. We conclude that analytic spaces constitute a first approximation to an appropriate geometric coverage or domain in geometric modelling.

By generalisation of functions to mappings, we say that a mapping of an open subset of $\mathbb{R}^n$ into $\mathbb{R}^n$ is called analytic if the real-valued functions which describe this mapping are all analytic. Thus, a differentiable manifold is called (real) analytic if it may be covered by a family of charts among which the coordinate transformations are (real) analytic mappings. It follows that the product $M \times N$ of two (real) analytic manifolds M, N is (real) analytic (e.g. $\mathbb{R}^3 = \mathbb{R}^1 \times \mathbb{R}^2$) and that a submanifold of a (real) analytic manifold is (real) analytic [**5**, p.118].

7. Convexity theory: convex shape mappings

The notion of *convex hull* $H(X)$ of a point set X is central to theory of convexity. (See, for example, the book entitled *Convexity* due to R. Webster [**114**] for a good reference about convexity theory.) The convexities of a point set X in $\mathbb{R}^n$ concerns to the convex subsets $\{X_i\}$ definable in X. The concavities of X are the convexities of the complement of X in $H(X)$, say $H(X) - X$. On the other hand, a mapping $f : X \to Y$ is *convex* or *convexity-preserving* if the image under f of each convex set in X is a convex set in Y [**114**, p.343]. That is, a convex mapping transforms every convex subset of a point set X into a convex subset of the corresponding image point set Y. The most familiar type of a convexity-preserving mapping is the affine mapping. But, not every convexity-preserving mapping is affine [**114**, p.343]. In fact, Meyer and Kay [**82**] proved in 1973 that, if $f : \mathbb{R}^m \to \mathbb{R}^n$ $(m \geq 2)$ is an injective convexity-preserving mapping, then f is an affine transformation. Affine mappings are collinearity-preserving, i.e. they map parallel lines onto parallel lines [**114**, p.343–350]. For example, the uniform scaling is an affine mapping —and therefore a convexity-preserving mapping— that preserve the ratio of the distances between any three points, not the distances themselves. So, the uniform scaling of a cube has as image a bigger cube. But, under a convexity-preserving mapping, a cube can be transformed into a parallelipipedic block —preserving so the collinearity—, or into a pyramid —not preserving the collinearity.

Apart of the preliminary work due to Gomes and Middleditch [**45**], no mathematical theory has been devised so far for geometric feature modelling, but the convexity theory seems to be able to fill the gap. Let us then concentrate on convex mappings. A convex mapping induces a convex decomposition in both (not necessarily convex) X and Y such that each convex subset of X corresponds to a convex subset of Y. We are particularly interested in convex homomorphisms, i.e. mappings that map convex subsets of X onto convex subsets of Y, preserving the interrelationships or adjacencies between them. Doing so, we can determine whether X and Y have the same *convex type*, or, equivalently, to say that they are convex-equivalent. The number of convex subsets is not necessarily finite, though the finite case is easier to deal with on computers.

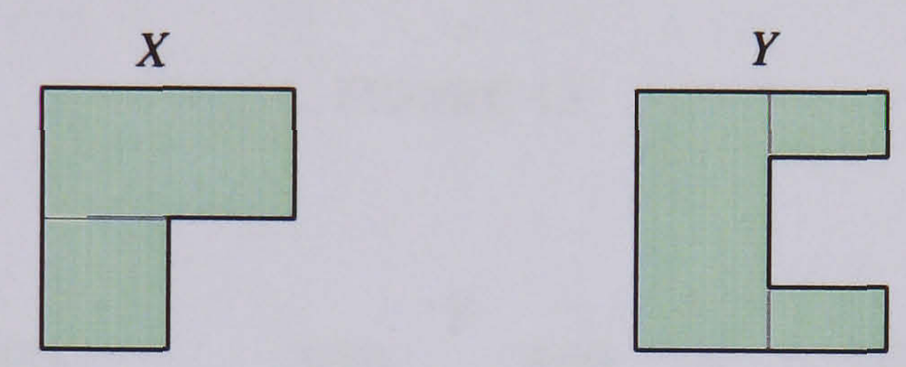

FIGURE 11

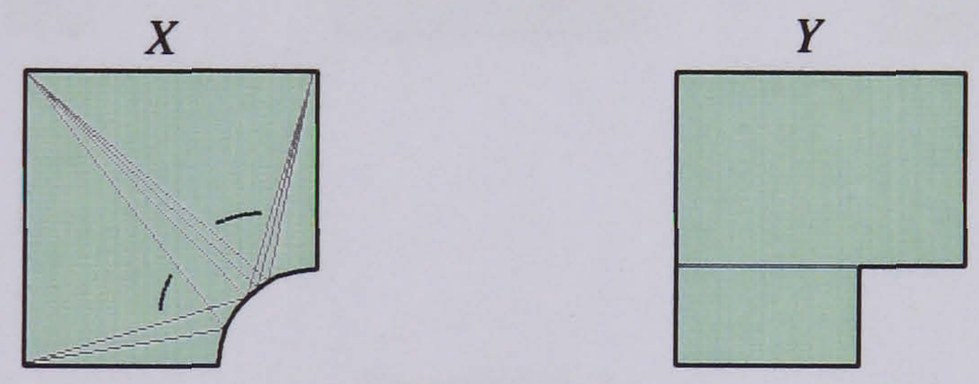

FIGURE 12

EXAMPLE 1.33. In Figure 11, X has two irreducible convex subsets, while Y has three irreducible convex subsets. Therefore, X and Y have different convex types, or, equivalently, they are convex inequivalent.

Recall that, by definition, an *irreducible convex subset* of a set X cannot be a subset of another convex subset of X.

EXAMPLE 1.34. In Figure 12, X is not finitely decomposable into convex subsets. It only admits an infinite convex decomposition into triangles, each of which has a vertex at each point of the arc in the boundary of X. But, the point set Y admits a finite convex decomposition into two irreducible convex subsets. Thus, X and Y have distinct convex types.

Examples 1.33 and 1.34 suggest that the number of irreducible convex subsets is a shape invariant. Let us call it *convexity number*, which is denoted by ξ. As usual for shape invariants, the fact that two point sets have identical convexity numbers does not mean that they have the same convex type. However, if they have the same convex type, they necessarily have identical convexity numbers.

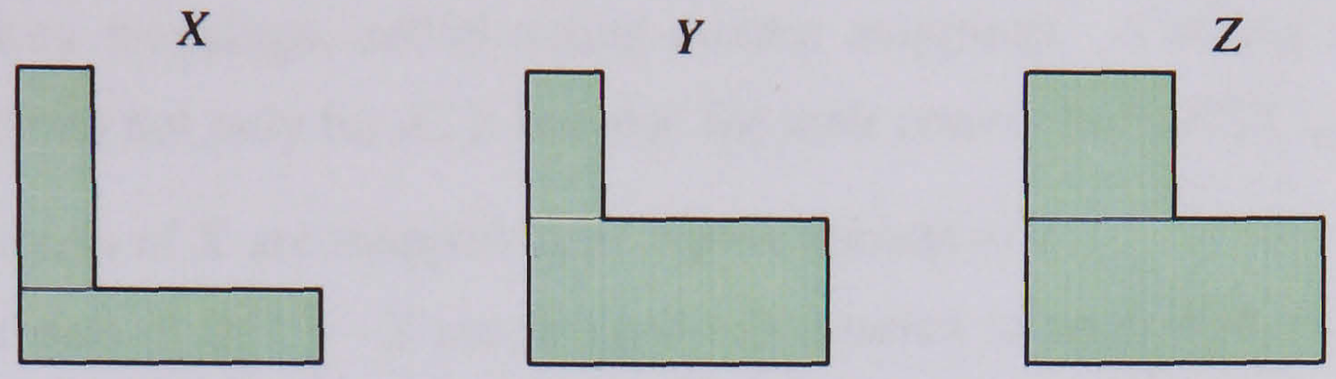

FIGURE 13

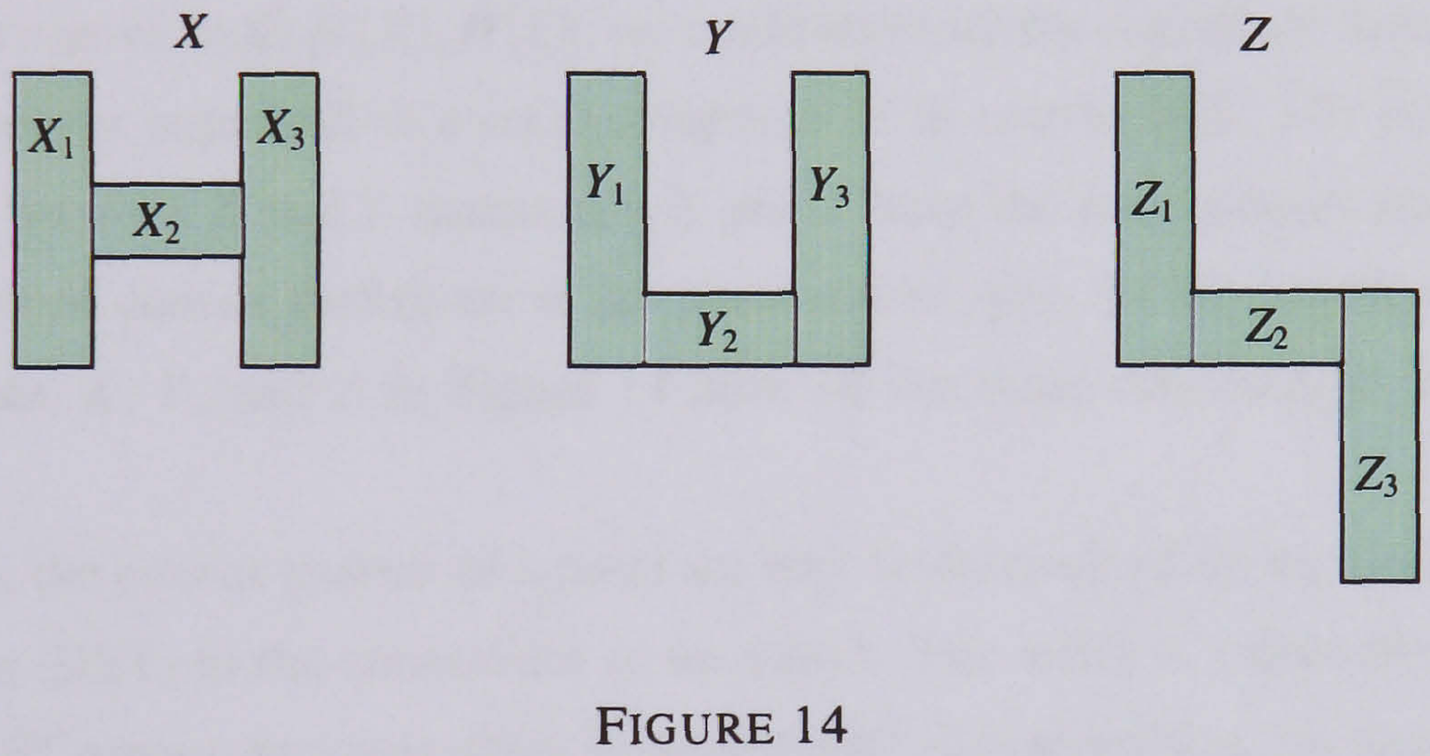

FIGURE 14

EXAMPLE 1.35. Let us look at Figure 13. The L-shaped objects X, Y, Z have all the same convexity number $\xi = 2$. Besides, they have analogous adjacency relationships. Thus, they have the same convex type. Note that, the convex type of a point set does not change by varying the sizes of its convex subsets.

EXAMPLE 1.36. Let us look at Figure 14. X is a H-shaped object, Y is a U-shaped object, and Z is a $\llcorner$-shaped object. They have identical convex types since their convexity numbers, as well as the adjacency relationships between the corresponding convex subsets, are equal. Intuitively, they have the same convex type because Y can be obtained from X by moving down the convex subset X_2, and Z can be determined from Y by moving down the convex subset Y_3. Note that these translations of convex subsets do not change the adjacency relationships between analogous convex subsets.

However, the objects X, Y, Z depicted in Figure 14 have distinct convex patterns somehow. X has the convex pattern of a H-object, Y has the convex pattern of an U-object, and Z is a $\llcorner\urcorner$-shaped object. In fact, in terms of convexity, they differ from each other somehow since X possesses two concavities, Y has only one concavity, and Z has also two concavities. To distinguish between them , we have to use more strict convex mappings, called strong convex mappings. A *strong convex mapping* is a convex mapping defined not only for X, Y but also for their convex hulls $H(X), H(Y)$ such that:

- Convex subsets of X are mapped onto convex subsets of Y.
- Convex subsets of $H(X) - X$ are mapped onto convex subsets of $H(Y) - Y$.
- Adjacency relationships are preserved between analogous convex subsets of $H(X)$ and $H(Y)$.
- The convex type is preserved between analogous unions of (two) adjacent convex subsets of $H(X)$ and $H(Y)$.

Instead of the convex hulls $H(X), H(Y)$, we could alternatively use two of their convex superhulls $\aleph(X)$, $\aleph(Y)$. A convex superhull of a set is a superset of its convex hull. The existence of a strong convex mapping between X and Y means that X and Y have the same *convex pattern.* Clearly, two objects with the same convex pattern are of the same convex type, but the converse is not necessarily true. For example, X, Y, and Z in Figure 14 have all the same convex type, but distinct convex patterns.

Alternatively, the convex pattern of a point set may be determined by applying the *boundary extension technique* (BET) to the concavities of an object. The result is a decomposition into convex subsets, called *BET convex decomposition*, or simply *BET decomposition.* (A similar convex decomposition has been proposed in [**45**].) It is illustrated in Figure 15. Basically, the BET decomposition of a 2-dimensional object is obtained by extending edges incident at concave vertices. For 3-dimensional objects, we extend faces incident to concave edges instead. It is here assumed that an object admits a finite convex decomposition (see X in Figure 12 for a counterexample). The main advantages of the BET decomposition of a point set are:

- The adjacency pattern is explicitly represented through intersection convex subsets.
- It is adequate as a general convex decomposition for geometric feature modelling, independently of the design sequence of an engineeering artefact.
- It enables the construction of the convex pattern. The resulting convex pattern is similar to that one obtained by the medial-axis transformation [**12**].

In fact, convex pattern of a set X can be obtained by combining the adjacency relationships between convex subsets of X with suplementary geometric information. This geometric information

concerns the 1-dimensional object formed by connecting the geometric centers of adjacent convex subsets of X through line segments.

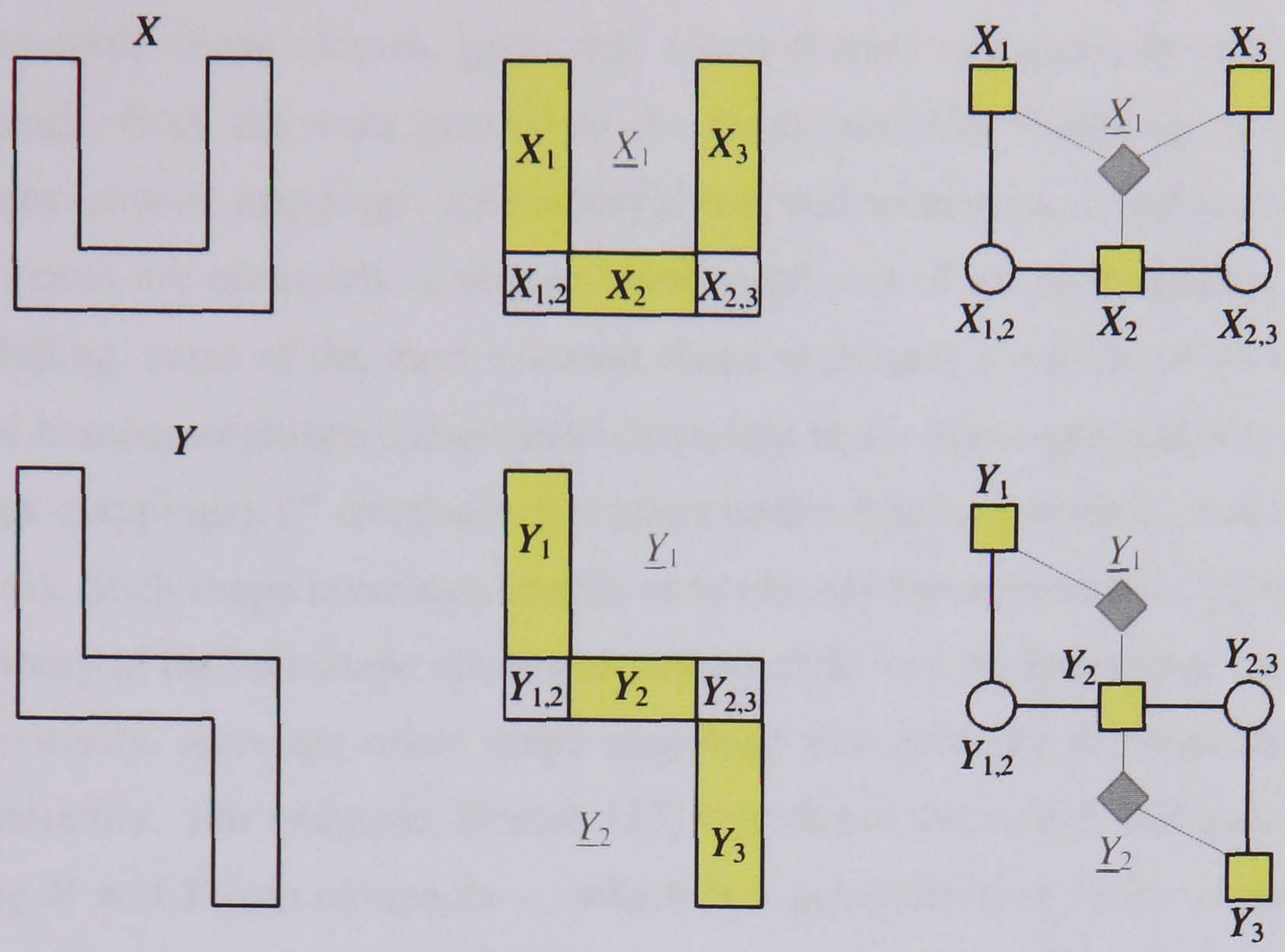

FIGURE 15

EXAMPLE 1.37. In Figure 15, the U-shaped object X, its BET decomposition, and its corresponding convex pattern, respectively, are depicted. X consists of three convex subsets X_1, X_2, X_3. The convex subsets $X_{1,2}$ and $X_{2,3}$ are intersection subsets of X_1, X_2, and X_2, X_3, respectively. These intersection subsets explicitly represent the adjacency relationships between convex subsets, what facilitates the construction of the convex pattern of X. $\underline{X}_1$ denotes the convex set of $H(X) - X$. Similarly, Figure 15 also illustrates the $\llcorner\urcorner$-shaped object Y, as well as its BET decomposition and convex pattern. $\underline{Y}_1$ and $\underline{Y}_2$ are the convex subsets of $H(Y) - Y$. As shown, X and Y have distinct convex patterns, though their convex types are equal.

The discussion above suggests that the convexity theory is relevant as a mathematical theory for geometric feature modelling.

8. Shape invariants, shape taxonomy

From the discussion above follows that there is a close relationship between a shape mapping between two sets and their shapes. Basically, every kind of shape mapping allows us to get a different way of looking at the shape of a figure or subset of $\mathbb{R}^n$. A particular shape mapping induces a

new view or perception of the shape of a particular figure. That is, there are as many shape classes as shape mappings. So, we have homotopy shape classes, topological shape classes, convex shape classes, diffeomorphic shape classes, geometric shape classes hierarchicaly related by a hierarchy of shape mappings, from the most general to the more particular mapping, namely: homotopies, homeomorphisms, convex mappings, diffeomorphisms, and isometries, respectively.

Shape invariants are obviously associated with each sort of shape mapping. In the context of geometric modelling, some of the more relevant shape invariants are *Betti numbers* (invariant under homotopies and homeomorphisms), *dimension* (invariant under homeomorphisms), *convexity* (invariant under convex mappings), C^r *continuity* (invariant under diffeomorphisms), and *distance* (invariant under isometries). Such shape invariants enable us to classify the admissible shapes of subsets in $\mathbb{R}^n$. That is, a taxonomy of distinct shape classes of subsets of $\mathbb{R}^n$ can be determined by using these shape invariants. Obviously, there are other shape mappings that give rise to other shape classes in the mathematics literature. For example, Borsuk [**17**] introduced the notion of fundamental class from X to Y —being X and Y two compacta—, which is a generalisation of the classical notion of the homotopy class of a mapping X to Y. However, in geometric modelling, we are interested only in spaces with 'well-behaved' local properties, that is Hausdorff spaces. This avoids certain pathological spaces which have the local disc-like property but are not Hausdorff. The aim of this section is then to establish a shape taxonomy for figures or subsets of $\mathbb{R}^n$ that are relevant in geometric modelling.

8.1. Geometric shape classes. Geometric design of engineering artefacts make use of computer graphics systems to visualise geometric objects on a computer display. One of the main properties that such geometric objects should possess is that they should keep their Euclidean-congruence under isometries. This fact allows the user or designer to move, rotate, and mirror a geometric object on display screen without any kind of shape deformation.

The Euclidean-congruence requirement of geometric modellers is critical in setting up their *geometric coverage*. The most common geometric class of objects used in geometric modelling is the class of *semi-algebraic sets*, i.e. point sets defined by polynomial equalities and inequalities (see Chapter 3 for further details). They form a geometry called *semialgebraic geometry* which is invariant under rational mappings [**58**, p.453]. Since every isometry is a particular rational mapping, we conclude that applying an isometry to a semialgebraic set has as a result another semialgebraic set that is Euclidean-congruent with the former set. Thus, the Euclidean congruence leads to the definition shape subclasses in a geometry such as, for example, the semialgebraic geometry, each subclass identifying a particular geometric shape.

EXAMPLE 1.38. In Figure 16, the rectangles $A = (x \geq 0) \cap (x \leq 1) \cap (y \geq 0) \cap (y \leq 1)$, $B = (x \geq 0) \cap (x \leq 2) \cap (y \geq 0) \cap (y \leq 1)$, $C = (x \geq 0) \cap (x \leq 3) \cap (y \geq 0) \cap (y \leq 1)$ belong to distinct semialgebraic subclasses because they are not congruent, i.e. they cannot be exactly superimposed on each other by a rigid motion (translations, rotations, and reflections). In fact, their areas —recall that the area of a geometric figure is an Euclidean geometric invariant— are distinct.

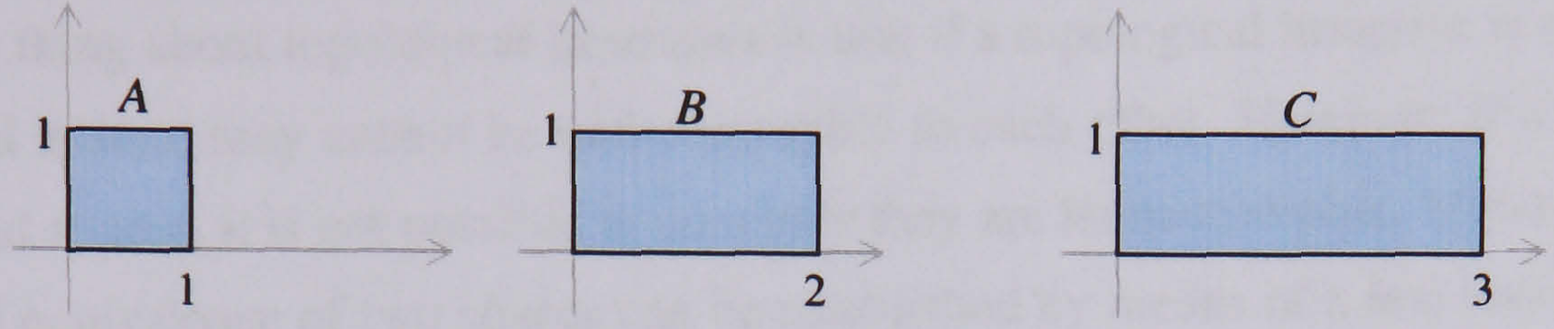

FIGURE 16. Semialgebraic rectangles with distinct geometric shapes.

Obviously, each semialgebraic subclass defined by congruence is an equivalence class.

EXAMPLE 1.39. In Figure 17, the point sets $A = (x^2 + y^2 \leq 4) \setminus [(x > -1) \cap (x < 1) \cap (y > 0)]$, $B = (x^2 + y^2 \leq 4) \setminus [(y > -1) \cap (y < 1) \cap (x > 0)]$, $C = [(x-4)^2 + y^2 \leq 4] \setminus [(y > -1) \cap (y < 1) \cap (x > 4)]$ are Euclidean-congruent. They are in the same Euclidean geometric shape class, i.e. they are Euclidean-geometrically equivalent. In geometric modelling, they are called *instances* of the same geometric primitive or point set. Applying a clockwise rotation of 90 degrees about the origin to A results in B, and B is transformed into C by a translation $\delta x = 4$.

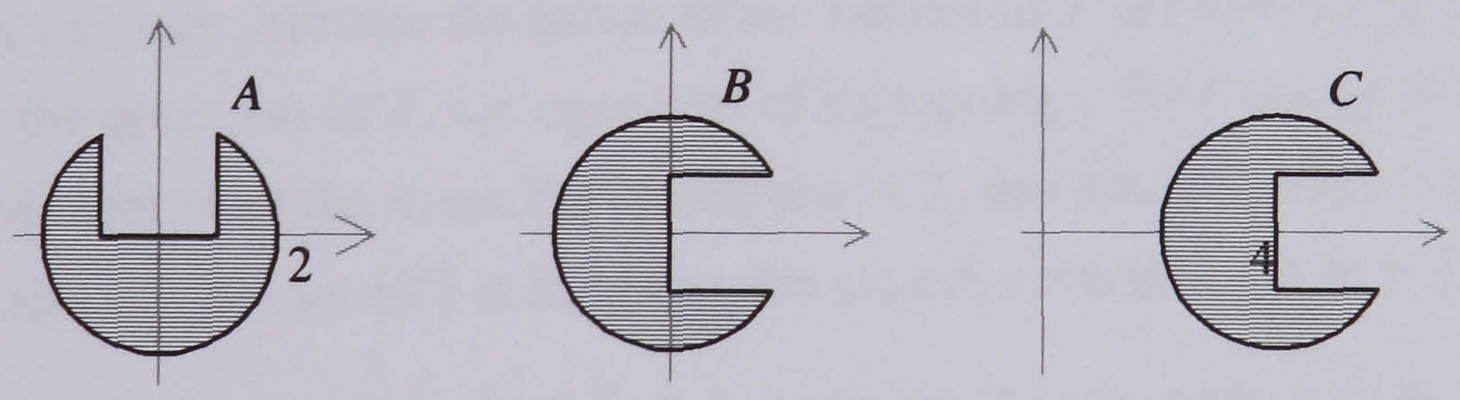

FIGURE 17. Distinct semialgebraic slotted discs that are Euclidean-geometrically equivalent.

The number of distinct semialgebraic subsets in $\mathbb{R}^n$ is certainly infinite, each belonging to a semialgebriac subclass. This means that, given a particular geometry (semialgebraic or else), it is not possible to finitely enumerate all of its geometric shapes. It is up to designers and constructors of geometric kernels an CAD systems to define basic geometric primitives and constructive algorithms to generate more complex geometric shapes that embody engineering components, assemblies, or any other artefacts.

8.2. Topological shape classes. Often it is not easy to find a homeomorphism between two subspaces of $\mathbb{R}^n$; for example, between a doughnut and a torus. This is troublesome because leads to difficulties in characterising classes of topological equivalence for subspaces in $\mathbb{R}^n$. In this respect, topological invariants are quite useful. They are properties (e.g. compactness, orientability, etc.) or quantities (e.g. Euler characteristic, Betti numbers, etc.) which are preserved under homeomorphisms. The interesting thing about topological invariants is that if a topological invariant is not the same for two topological spaces, they cannot be homeomorphic to each other. However, if it is the same for both topological spaces, it is not possible to conclude they are homeomorphic. However, sometimes, the topological equivalence of two spaces can be established by means of a few invariants; the well-known Surface Classification Theorem (see [**3**, p.18]) is an example of it.

8.2.1. *Compactness.* Although boundedness fails to be a topological property, a related notion does qualify, say compactness. As mentioned before, boundedness is a mathematical notion for what in geometric computing is called 'finite extension". As far as compactness is concerned, it is related to the concept of "finite describability" in geometric computing. This is one of the major requirements to represent geometric objects on computers; for example, a solid cube may be described by the union of a finite family of subsets homeomorphic to closed balls $\mathbb{D}^n$, $1 \leq n \leq 3$, respectively, 12 closed edges, 6 closed faces, and one closed solid.

Let X be a topological space. A *covering* of X is a family $\{A_i\}$ of subsets of X such that $\cup_{i\in I} A_i = X$. If a subset of a covering of X still covers X, it is said to be a *subcovering*. Note that a covering is not necessarily a topology, because the nature of the subsets of X are left unspecified. But, if all the A_i happen to be the open sets in X, i.e. open sets of its topology, the covering is said to be an *open covering*. Analogously, if all the A_i are the closed sets in X, one has a *closed covering*. Note that for any topological space X, the set $\{X\}$ is an open (also closed) covering of X as is $\{X, \varnothing\}$.

DEFINITION 1.15. A topological space X is **compact** if every open covering of X has a finite subcovering.

EXAMPLE 1.40. A point is compact.

EXAMPLE 1.41. An infinite discrete space X is not compact, since the set of singletons $\{x\}$ for each $x \in X$ is an open covering of X without finite subcovering.

EXAMPLE 1.42. Any finite space X is compact, since any open covering of X is a finite set.

EXAMPLE 1.43. Let $\{]1/n, 1]\}$, $n \in \mathbb{N}$, be an open covering of $]0, 1]$. The interval $]0, 1]$ is not compact because no finite subcovering of $\{]1/n, 1]\}$ covers $]0, 1]$.

As this latter example shows, boundedness is not enough for a set to be compact. Another condition, say *covering finiteness*, is required.

THEOREM 1.1. *Let X be a subset of $\mathbb{R}^n$. X is compact iff it is closed and bounded.*

Since compactness is an topological invariant, it can be used to classify topological shapes. Here they are some examples in $\mathbb{R}^n$, the space of interest in geometric modelling.

EXAMPLE 1.44. A closed line $[-1,1]$ is not homeomorphic to an open line $(-1,1)$, since $[-1,1]$ is compact while $(-1,1)$ is not. However, $(-1,1)$ and $(-1,1]$ are not distinguishable via compactness, because none of them is compact.

EXAMPLE 1.45. A circle $\mathbb{S}^1$ is not homeomorphic to $\mathbb{R}$, since $\mathbb{S}^1$ is compact in $\mathbb{R}^2$ while $\mathbb{R}$ is not.

Compactness is not only significant for distinguishing topological shapes, but also in compactification operations in geometric computing. If X is a compact space, then removing points from X is liable to produce a non-compact space. The idea of *compactification* is the reverse procedure —given a space X, can points be added to X to produce a compact space?

DEFINITION 1.16. A **compactification** of a space X is a compact space $\hat{X}$ and a homeomorphism f from X onto the subset $f(X)$ of $\hat{X}$ such that $f(X)$ is dense in $\hat{X}$, i.e. $\mathrm{Cl}(f(X)) = \hat{X}$.

There are several types of compactifications. The simplest compactification is the *Alexandroff one-point compactification.* This compactification requires only one point to become a space compact. For example, the one-point compactification of $\mathbb{R}^n$ is homeomorphic to the n-sphere $\mathbb{S}^n$; in particular, $\mathbb{R}^2$ which is homeomorphic to $\mathbb{S}^2$ with a point removed can be compactified into $\mathbb{S}^2$ by adding a point.

A more general compactification is the *Freundenthal compactification.* The intuitive idea is that the open interval $]0,1[$ should be compactified by adding two *ends*, for example by adding 0 and 1 to yield the closed interval $[0,1]$. With a Freundenthal compactification $\hat{X} \setminus X$ is 0-dimensional, but the number of ends may be infinite.

In geometric computing, more general compactifications are necessary as $\hat{X} \setminus X$ is possibly n-dimensional; a classical example is the compactification of the set difference of two closed solids with two faces partially overlapping. Compactifications are then particular 'regularisation' operations in geometric modelling. However, the 'regularisation' operation of eliminating 'dangling' or remanescent subspaces from a dimensionally non-homogeneous space is not a compactification operation. It is worth noting that even the Euler operators that subdivide a closed surface can be viewed as a two-stage operation of de-compactification (e.g. remove a point $\mathbf{x}$ from $\mathbb{S}^2$ yielding $\mathbb{S}^2 \setminus \mathbf{x}$) followed by its compactification (i.e. union of $\mathbf{x}$ to $\mathbb{S}^2 \setminus \mathbf{x}$).

8.2.2. *Connectedness.* The examples in Section 4 show that the continuity of a function depends on the topologies of X and Y, and it does not correspond to our intuitive notion of a graph without 'gaps' since the graph of a continuous function may have gaps, as illustrated above. The relationship between continuity of a function and the inexistence of 'gaps' in its graph is, however, valid with the usual topology in $\mathbb{R}^n$. The existence or not of 'gaps' in a set is characterised by a topological property called connectedness, which is distinct from continuity of a function.

Connectedness, like compactness, is a topological invariant. That is, if X is homeomorphic to Y, then X is connected iff Y is connected. Therefore, compactness of a topological space X can be also described in terms of the open sets of its topology.

THEOREM 1.2. *A topological space X is* connected *iff X is not the union of two non-empty disjoint open sets; or, equivalently, X and $\varnothing$ are the only subsets of X which are both open and closed.*

EXAMPLE 1.46. Let $X = \{a,b,c,d,e\}$ be a set and $\mathcal{T} = \{X, \varnothing, \{a\}, \{c,d\}, \{a,c,d\}, \{b,c,d,e\}\}$ a topology on X. X is disconnected or separated since $\{a\}$ and $\{b,c,d,e\}$ are complements and hence both open and closed. In other words, is the disjoint union of $\{a\}$ and $\{b,c,d,e\}$, i.e. $X = \{a\} \cup \{b,c,d,e\}$.

EXAMPLE 1.47.

1. A discrete space with more than one point is disconnected, while $\varnothing$ and $\{a\}$ are connected spaces.
2. The real line $\mathbb{R}$ with the usual topology is a connected space since $\mathbb{R}$ and $\varnothing$ are the only subsets of $\mathbb{R}$ which are both open and closed. Analogously, $\mathbb{R}^n$ is connected.
3. Any open interval of $\mathbb{R}$ is homeomorphic to $\mathbb{R}$ and hence is connected.

The connectedness of a topological space X can also be described in terms of the closure operator in X. A topological space X is *connected* if for any non-empty subsets A and B such that $X = A \cup B$, either $A \cap \mathrm{Cl}(B) \neq \varnothing$ or $B \cap \mathrm{Cl}(A) \neq \varnothing$.

EXAMPLE 1.48. Let $A =]0,1[$, $B =]1,2[$ and $C = [2,3[$ be intervals on $\mathbb{R}$. Now A and B are separated since $\mathrm{Cl}(A) = [0,1]$ and $\mathrm{Cl}(B) = [1,2]$, and so $A \cap \mathrm{Cl}(B)$ and $\mathrm{Cl}(A) \cap B$ are empty. But B and C are separated since $2 \in C$ is a limit point of B; hence, $\mathrm{Cl}(B) \cap C = [1,2] \cap [2,3[= \{2\} \neq \varnothing$.

EXAMPLE 1.49. Let $A = \{(x,0) \in \mathbb{R}^2 : x \leq 0\}$ and $B = \{(x,y) \in \mathbb{R}^2 : y = \sin(1/x), 0 < x \leq 1\}$ be two subsets of $\mathbb{R}^2$, Figure 18. Now $(0,0)$ in A is a limit point of B; hence A and B are connected.

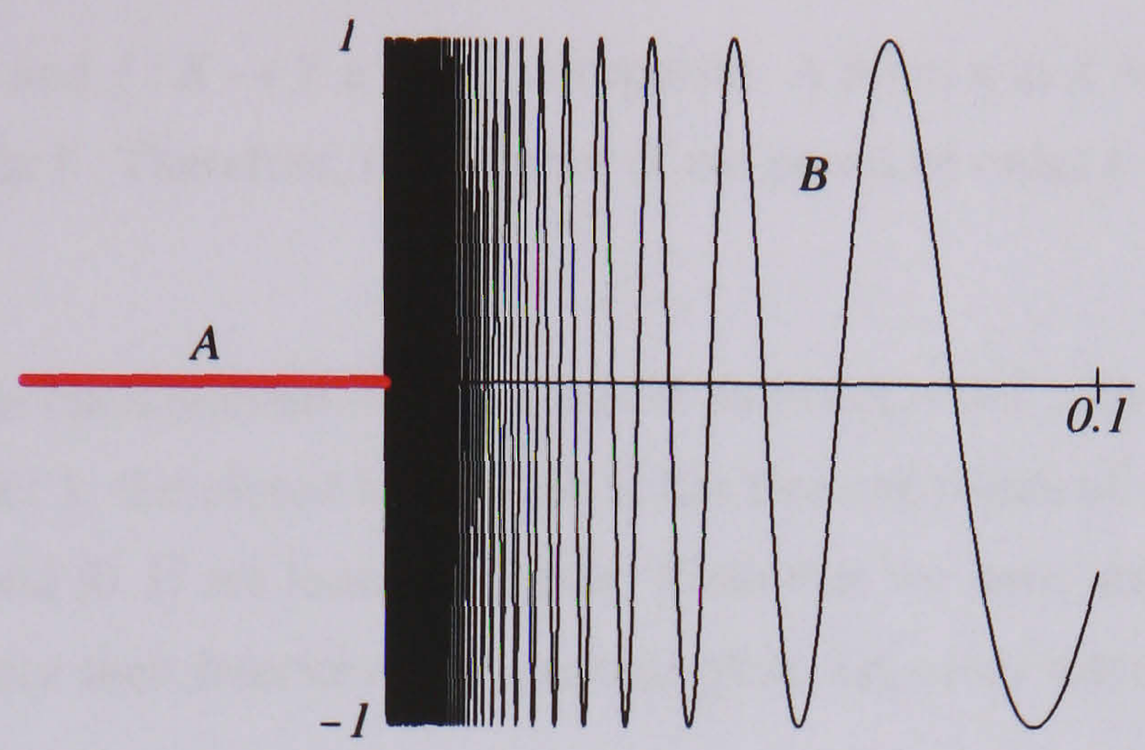

FIGURE 18

If a space is not itself connected, then the next best thing is to be able to decompose it into a disjoint family of maximal (or largest) connected subspaces.

DEFINITION 1.17. A **component** C of a topological space X is a maximal connected subspace of X, that is, a connected subspace which is not a proper subset of any connected subset of X.

Clearly, C is non-empty. Also, a connected space clearly has only one component, namely, the space itself. In a discrete space, it is easy to see that each point is a component.

Connectedness is related to a numerical topological invariant: the 0th Betti number β_0. It stands for the number of disjoint 'pieces', called components, of a topological space. Because of the maximality of the components, β_0 captures then the largest shape of a topological space. Still in the present chapter, we will see that the Betti numbers capture the shape in large of a topological space, called *global shape*. They are also important in the design of combinatorial geometric data structures such as, for example, B-Reps and in shape data structure proposed in this thesis.

8.2.3. *Cut-Pointedness.* Let $f : X \to Y$ be a homeomorphism. If C is a component of a point $x \in X$, then $f(C)$ is a component of $f(x)$ in Y. (This follows from the fact that $A \subseteq X$ is connected iff $f(A)$ is connected.) Consequently, f induces a bijection of the components of X to the components of Y. Thus, the number of components of X is a topological invariant of X; it is known as the 0th Betti number, β_0. Despite the usefulness of this invariant to describe the global shape of a geometric object, and design and construction of shape data structures (e.g. B-Reps), it fails to distinguish different connected spaces.

DEFINITION 1.18. Let X be a connected space, and $k \in \mathbb{N}$. A point $\mathbf{x} \in X$ is a **cut point of order k** if $X \setminus \{\mathbf{x}\}$ has k components.

Let X be connected, and $f : X \to Y$ a homeomorphism. A point $\mathbf{x}$ in X is a cut point of order k in X iff $f(\mathbf{x})$ is a cut point in Y. Therefore, the number of cut points of order k is a topological invariant in X.

EXAMPLE 1.50. The open interval $]0,1[$ has no cut points of order 1; the half-open interval $[0,1[$ has one cut point of order 1; the closed interval $[0,1]$ has two cut points of order 1. Thus, no two of the spaces $]0,1[$, $[0,1[$ and $[0,1]$ are homeomorphic. Note that we have not considered any interior point of the intervals, since their interiors are homeomorphic, i.e. every interior point is a cut point of order 2.

EXAMPLE 1.51. Let $f : [0,1[\to \mathbb{R}^2$ be defined by $f(t) = (\cos 2\pi t, \sin 2\pi t)$, i.e. f is one-to-one and continuous function which maps $[0,1[$ onto the unit circle, Figure 19. Following the cut point invariant, one concludes that $[0,1[$ and unit circle are not homeomorphic; for example, removing the point $t = 1/2$ from $[0,1[$ yields two components, but removing any point from the circle, the number of components holds at 1.

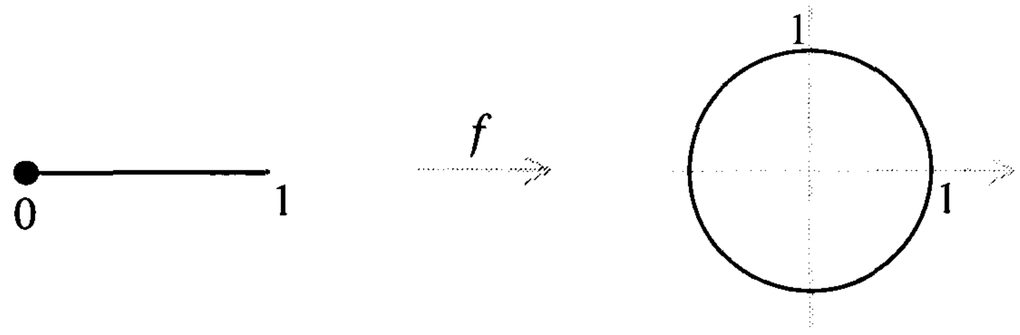

FIGURE 19. The half-open interval is not homeomorphic to the circle.

EXAMPLE 1.52. In Figure 20, no two of the following 1-dimensional spaces are homeomorphic since they can be distinguished by the numbers of cut points of various orders. Every point of the triangle (a) is a cut point of order 1; in (b), $\mathbf{r}$ is a cut point of order 2; in (c), the point $\mathbf{r}$ is the only cut point of order 3; analogously, in (d), the points $\mathbf{r}$ and $\mathbf{s}$ are the only cut points of order 3.

However, the cut point invariant fails to distinguish between the spaces depicted in Figure 21. Nevertheless, they can be distinguished from each other by means of a stronger invariant, called *local cut point invariant.*

DEFINITION 1.19. A point $\mathbf{x} \in X$ is a **local cut point of order** k if each neighbourhood N of $\mathbf{x}$ contains a connected neighbourhood M of $\mathbf{x}$ such that $M \setminus \{\mathbf{x}\}$ has k components.

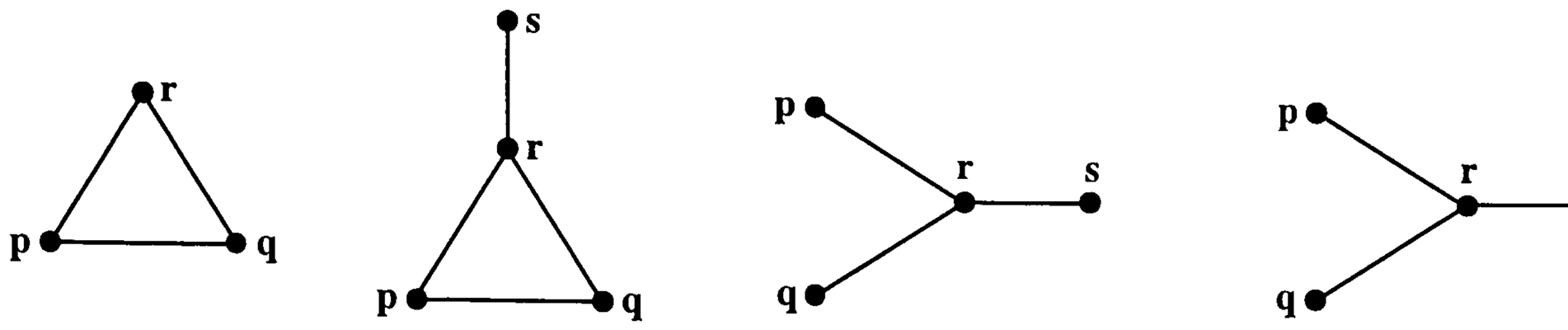

FIGURE 20

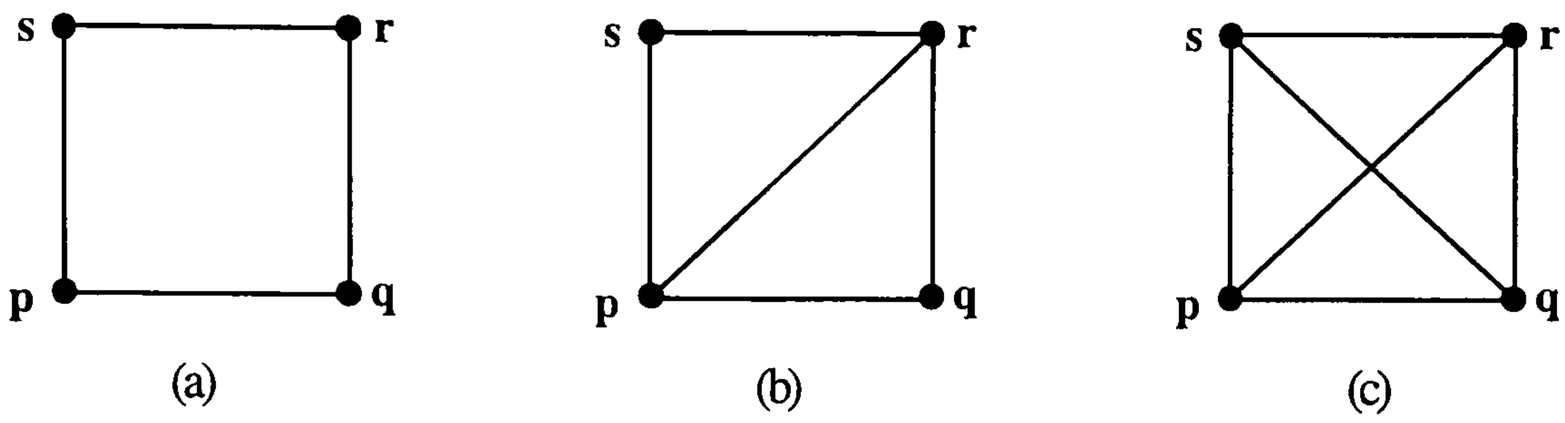

FIGURE 21

Therefore, if X is homeomorphic to Y, then X and Y must possess the same number of local points of order $k \in \mathbb{N}$. The spaces of Figure 21 are distinguished by the fact that the first (a) has no local cut points of order 3, the second (b) has two local cut points of order 3, and the other (c) possesses a local point of order 4.

Obviously, the representation of local cut points is an important requirement in the design of modern dimensionally non-homogeneous shape data structures, in particular those which are combinatorial. Unfortunately, because of the lack of a general mathematical theory underpinning the design and construction of current geometric data structures, cut points are absent or poorly represented. Even vertex-based combinatorial B-Rep data structures fail to represent arbitrary shapes at a vertex (or cut point), i.e. they are not capable of representing a bouquet of arbitrary shapes at a vertex; this is apparent whenever at least a bouquet petal is multiply incident at a vertex, what requires a complete control of the data structure on connectedness at a cut point.

8.2.4. *Dimension.* Dimension is perhaps the most important topological invariant. It allows at a first glance to distinguish between two spaces of distinct dimensions. This means that not all 'deformations' are allowed; for example, a line cannot be coalesced to a point (or, conversely, a point cannot be pulled out to a line), a cylinder cannot be contracted into a disk (or, conversely, a disk

cannot be expanded into a cylinder), and so forth. That is, the so-called 'elastic deformations' or homeomorphisms are dimension-invariant.

In fact, by the Theorem of the *Invariance of Dimension*, if $\mathbb{R}^m$ is homeomorphic to $\mathbb{R}^n$, then $m = n$. Thus, two points, two open intervals, etc., and, in general, spaces homeomorphic to the unit open ball $\mathbb{B}^n$ have the same dimension. These spaces homeomorphic to $\mathbb{B}^n$ or $\mathbb{R}^n$ are called n-*cells* in the theory of cell complexes, and more generally in the homology theory. Cells are particular manifolds. Manifolds are locally-defined topological shapes or *local topological shapes.* In fact, a *n*-manifold is a topological space *locally* homeomorphic to $\mathbb{R}^n$. "Locally' means in the neighbourhood of each point of the manifold. That is, each point in a *n*-manifold has an open neighbourhood that is homeomorphic to $\mathbb{R}^n$. In this case the homeomorphism is said to be *local* (see [**75**, p.122] for further details). The 'locality' of manifolds is reinforced by the fact that they often appear as 'building blocks' or 'bricks' of stratified objects. This is the case of stratified objects represented and manipulated by B-rep geometric kernels. Therefore, dimension allows us to distinguish points, lines, surfaces, solids and, in general, *n*-dimensional manifolds (or simply *n*-manifolds) from each other. Manifolds are then the basic (topological) shapes used in geometric modelling. All manifolds of the same dimension constitute a topological shape class. For example, all points are in the class of 0-manifolds, all the open line segments belong to the class of 1-manifolds, all the open surfaces belong to the class of 2-manifolds, all the open solids are part of the class of the 3-manifolds, and so on.

However, topological spaces with the same dimension are not necessarily homeomorphic. For example, a closed cell $\mathbb{D}^n = \mathrm{Cl}(\mathbb{B}^n)$ is not homeomorphic to an open cell $\mathbb{B}^n$, and a non-closed, non-open cell is not homeomorphic to neither a closed cell nor a open cell. These facts agree with the following theorem: if $f : \mathbb{D}^n \to \mathbb{D}^n$ is a homeomorphism, then $f|\mathbb{B}^n, \mathbb{B}^n$ and $f|\mathbb{S}^{n-1}, \mathbb{S}^{n-1}$ are defined and are homeomorphisms. In other words, the homeomorphism between two subsets X,Y of $\mathbb{R}^n$ implies the existence of homeomorphisms between their interiors and their boundaries. This is relevant because makes possible to distinguish between two non-closed, non-open subsets in $\mathbb{R}^n$, what has not been possible so far. For example, in Figure 22, three non-closed, non-open subsets of $\mathbb{R}^2$ are depicted. None of them is homeomorphic to any other two. The boundary of the first (a) is 0-dimensional, while it is 1-dimensional for the other two, (b) and (c); the boundary of the second subspace (b) has only one component, while the third has two components.

8.2.5. *Betti numbers, homology groups.* Topological equivalence does not preserve geometric properties such as distances, angles, convexity, etc. A geometric mapping (rigid motion or isometry) is a particular homeomorphism with null elasticity. However, the elasticity of a homeomorphism is constrained by the fact that two distinct points of a space are not allowed to coaslesce into one point.

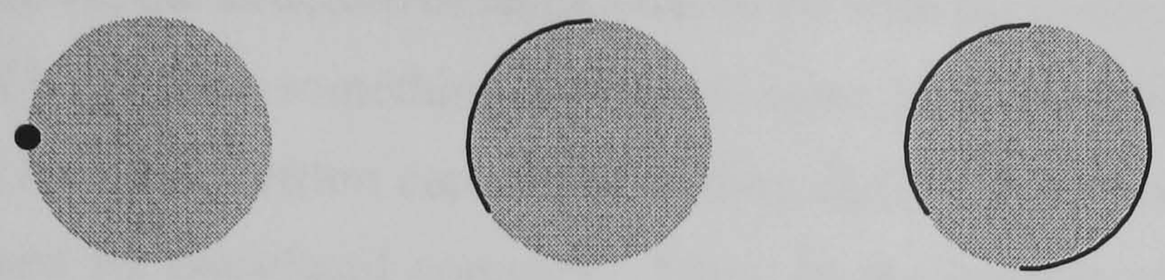

FIGURE 22

For example, a solid cylinder is not topologically deformable into a disc, nor a disc into a point. As seen in Section 5, these two more general shape deformation mappings are called homotopies. In fact, since a solid cylinder, a disc, and a point are all contractible, they are said to have the same homotopy type. However, they do not possess the same topological type because they have distinct dimensions.

Even equidimensional objects are not necessarily homeomorphic. This is the case for manifolds. In fact, local homeomorphisms do not distinguish between two manifolds of the same dimension. For example, a plane, a spherical surface and a toroidal surface are all 2-manifolds, but it is known that they are *not* of the same topological type. To see that two n-manifolds are topologically distinct, we make use of other topological invariants such as the homology groups H_n or Betti numbers β_n $(n = 0,1,2,\ldots)$. These topological invariants capture the *global topological shape* of a space up to topological equivalence.

By definition, the n-th Betti number β_n of a space X is the rank of the n-dimensional homology group $H_n(X)$, that is, $\beta_n = \text{rank}\, H_n(X)$ [**66**, p.143]. (Recall that the rank of a group on a set X is the cardinal number of X [**75**, p.69].) Homology theory assigns to any topological space X a sequence of Abelian or commutative groups $H_0(X), H_1(X), H_2(X), \ldots$, and to any continuous mapping $f : X \to Y$ a sequence of homomorphisms $f^* : H_n(X) \to H_n(Y)$ $(n = 0,1,2,\ldots)$. Informally speaking, the n-dimensional homology group $H_n(X)$ stands for a set of n-cycles of (the complex associated with) a space X that are *essential* to characterise the shape of X. For example, many 1-cycles are definable on a torus $\mathbb{T}^2$, but only two are essential to capture the topological shape of X; in fact, $\mathbb{T}^2 = \mathbb{S}^1 \times \mathbb{S}^1$. Thus, the 1st Betti number of $\mathbb{T}^2$ is $\beta_1 = 2$. The purpose of all of this is to come up with something that allows us to determine the essential topological shape of a space. Important characteristics of topological shape include the ability to make a loop by identifying two vertices of an edge, or enclose a cavity, as in the sphere or torus. Recall that 1-cycles are edges which form loops, and 2-cycles are faces that are gathered together to form a hollow cavity [**66**, p.128].

Let X be a topological space. The rank of the group $H_0(X)$ is equal to the number of connected components of X [**75**, p.148]. That is, $H_0(X)$ has a basis in 1-1 correspondence with the set of

components of X. Therefore, the structure of $H_0(X)$ has to do with the connectedness of X. Similarly, the groups $H_1(X)$, $H_2(X)$, ..., have something to do with some kind of higher connectivity of X [**75**, p.148]. See [**66**, p.131] for an algorithm capable of finding $H_n(X)$. By abuse of language, X is here taken as both a space and its associated complex. Thus, in the context of homology theory, X is a 'subdivided' space as in [**21**], or a stratified space as in this doctoral work. A stratified space is basically a space partitioned into manifolds (see Chapter 3 for more details.)

Since the clear relationship between the homology groups and Betti numbers associated to a stratified space X, one says that Betti numbers are topological invariants containing a lot of information about the global shape of a space. A k-th Betti number β_k denotes the number of essential k-cycles in X.

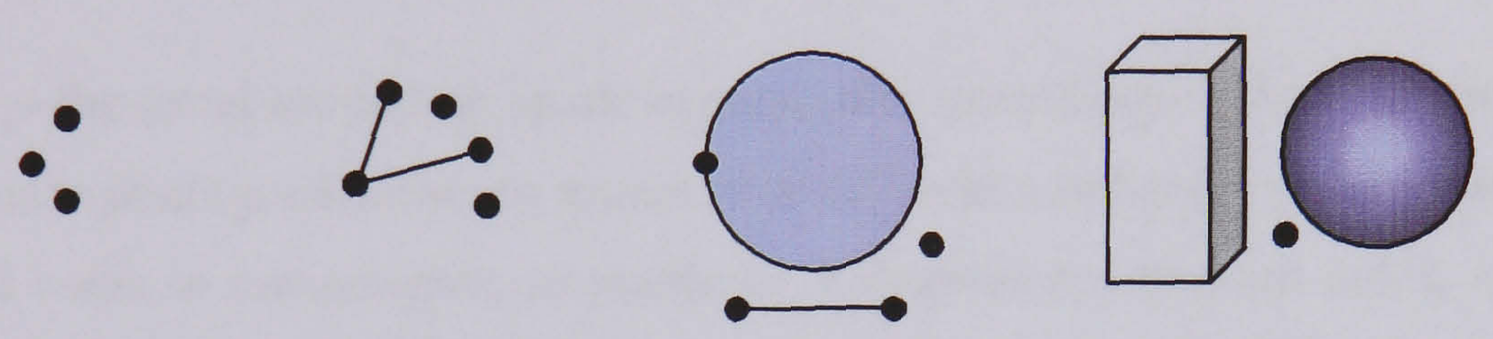

FIGURE 23. Spaces with the same $\beta_0 = 3$.

EXAMPLE 1.53. Consider the four topological spaces in $\mathbb{R}^3$, Figure 23. Each has three essential 0-cycles corresponding to three components; hence $\beta_0 = 3$. There are not essential higher dimensional cycles, so $\beta_i = 0$ $(i \geq 1)$. However, there are edges in 1-cycles as, for example, the 1-cycle bounding the disc (Figure 23(c)), and faces in 2-cycles as, for example, the box bounding an open solid (Figure 23(d)), but they are not essential. These two cycles bound an open disc and an open solid, respectively. They are said to be 'filled', and then not essential. To be essential, these cycles cannot bound any 'filling' manifold, they must form a loop with a through hole or a box with a hollow cavity.

EXAMPLE 1.54. Consider the three topological spaces in $\mathbb{R}^3$, Figure 24. Each has two essential 1-cycles corresponding to their through holes; hence $\beta_1 = 2$. The squared space (a) is of dimension 1. The diagonal edge subdivides one through hole into two. The first hole corresponds to the 1-cycle α, and the second hole is identified by the 1-cycle β. Each 1-cycle consists of two edges of the square and the diagonal edge, as well as their bounding vertices. The object (b) possesses two essential 1-cycles α, β which are inner boundaries of the back to back moon-shaped 2-manifolds. Analogously,

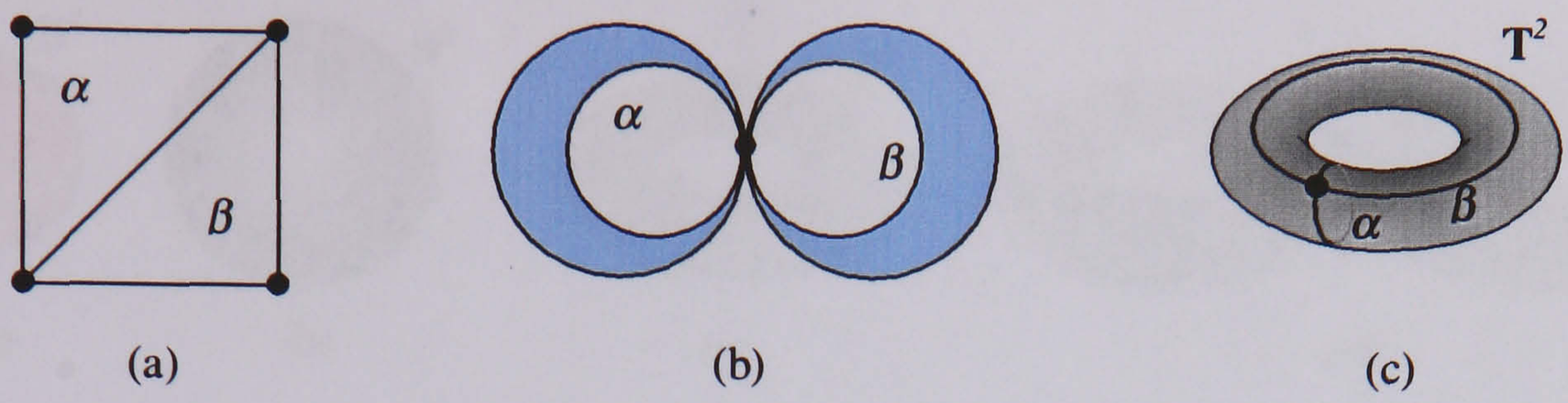

(a) (b) (c)

FIGURE 24. Spaces with the same $\beta_1 = 2$.

the 2-dimensional torus (c) includes two 1-cycles α and β. Besides, this torus encloses a cavity, so their constituents, namely one vertex, two edges and a face, form a 2-cycle; hence, $\beta_2 = 1$ for such a torus.

Thus, in $\mathbb{R}^3$ —the usual modelling space in geometric modeliing—, the first three Betti numbers $\beta_0, \beta_1, \beta_2$ allow us to distinguish between spaces with different numbers of *components*, *holes through components*, and *voids in components*, respectively. Components, through holes, and voids are the *global topological shapes* in $\mathbb{R}^3$. Betti numbers can be combined to form the Euler characteristic of a space X in $\mathbb{R}^n$.

THEOREM 1.3. (Kinsey [**66**, p.142]) *Let X be a n-dimensional space. Then*

$$\chi(X) = \beta_0 - \beta_1 + \beta_2 - + \cdots + (-1)^n \beta_n$$

As shape invariants, Betti numbers allow us to classify each d-dimensional subclass of manifolds. Starting with the lower dimension manifolds, it is clear that stratified 0-manifolds do not have neither 1-cycles (or through holes) nor 2-cycles (or voids). In fact, they are only distinguishable from each other by the number of components. For example, a 0-manifold with just one point-component (a component with a single point) is topologically distinct from a 0-manifold with two point-components provided that their 0th Betti numbers are distinct, $\beta_0 = 1$ and $\beta_0 = 2$, respectively. Obviously, a discrete topological space with an infinite number of points is a 0-manifold with an infinite number of point-components.

The topological type of any 1-manifold is characterised by the first two Betti numbers. The third Betti number β_2 is always zero for 1-manifolds, that is, they cannot possess essential 2-cycles (or internal voids). Therefore, any component of a 1-manifold is homeomorphic to either $\mathbb{B}^1$ (no through holes) or $\mathbb{S}^1$ (just one through hole).

Similarly, 2-manifolds are classified by the first three Betti numbers. The novelty here is that now the essential 2-cycles may be part of 2-manifolds. However, any component of a 2-manifold at

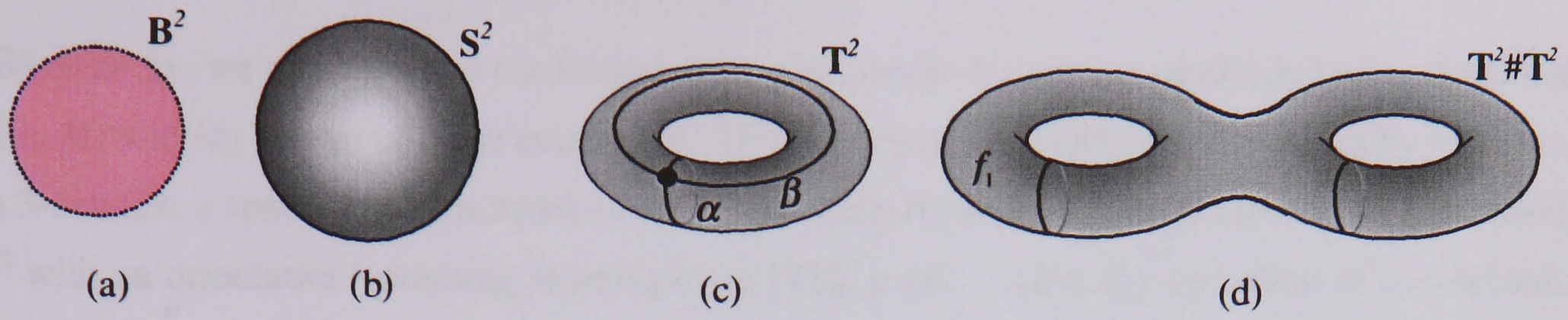

FIGURE 25. Taxonomy of 2-manifolds.

most possesses one 2-cycle (or void). Any component of a 2-manifold is homeomorphic to either an open 2-ball $\mathbb{B}^2$, a 2-sphere $\mathbb{S}^2$, or a 2-sphere $\mathbb{S}^2$ with a number of handles as illustrated in Figure 25(a),(b), and (c,d), respectively. In particular, the well-known Theorem of Surface Classification asserts that every orientable, compact, connected surface without boundary[1] is topologically equivalent or homeomorphic to a 2-sphere or a *connected sum* of tori [**57**, p.122]. (Non-orientable surfaces are not considered here.) The connected sum (#) of two surfaces is defined as follows: remove an arbitrary disc from each surface and connect the two resulting boundary circles by an arbitrary general cylinder. This suggests a method of construction for every surface without boundary: take the 2-sphere $\mathbb{S}^2$ (Fig.25(b)), remove two disjoint discs and then add a cylinder by sewing its two boundary circles to the boundaries of the holes in the sphere. The result is a 2-sphere $\mathbb{S}^2$ with a handle, which is nothing more than (is homeomorphic to) the 1-fold torus $\mathbb{T}^2$, Fig.25(c). By repetition, we are able to construct a sphere with two, three, or any finite number k of handles, or, equivalently, a 2-fold torus $\mathbb{T}^2\#\mathbb{T}^2$ (Figure 25(d)), or in general a k-fold torus $\mathbb{T}^2\#\mathbb{T}^2\#\ldots\#\mathbb{T}^2$, respectively. It is clear that the connected sum is a commutative, associative operation on the set of topological types of compact surfaces. Besides, the sphere $\mathbb{S}^2$ works as a unit or neutral element for this operation. However, there are not inverses. Thus, the set of topological types of compact surfaces does not form a group under the operation of connected sum. It only forms a semigroup [**75**, p.9].

---

[1]A topological space M is an n-dimensional *manifold with boundary* if each of its points has either a neighbourhood homeomorphic to $\mathbb{R}^n$, or else an open neighbourhood homeomorphic to an open set in the upper half-space $\mathbb{R}^n_+ = \{\mathbf{x} \in \mathbb{R}^n : x_n \geq 0\}$ of $\mathbb{R}^n$ [**35**, p.209]. Examples of manifolds with boundary are: (i) an n-dimensional manifold, (ii) the disc $\mathbb{D}^n$, (iii) the cylinder $\mathbb{S}^1 \times \mathbb{I}$, where $\mathbb{I} = [0,1]$, and (iv) a closed halfspace in $\mathbb{R}^n$. The *boundary* of M, denoted by ∂M, is the set of points in M which have neighbourhoods homeomorphic to $\mathbb{R}^n_+$ but which have no neighbourhoods homeomorphic to $\mathbb{R}^n$. Note that it is possible for a manifold with boundary to have an empty boundary [**22**, p.131]. It is then said to be a *manifold without boundary*. If M is a manifold with boundary and $\partial M = \varnothing$, then $M = M - \partial M$ is of course a manifold. Therefore, any manifold without boundary is, by definition, a manifold. It is standard terminology to refer to compact manifolds without boundary as 'closed' manifolds [**19**, p.359]; for example, a 2-sphere $\mathbb{S}^2$ and a torus $\mathbb{T}^2$ are two closed surfaces or 2-manifolds.

By analogy, we can form the connected sum of connected, compact, and oriented 3-manifolds in $\mathbb{R}^4$. Let M_1 and M_2 be two of these manifolds. Their connected sum $M_1 \# M_2$ is formed by removing an open 3-cell (i.e. a space homeomorphic to an open 3-ball) from each and then identifying the resulting of $\mathbb{S}^2$ with an orientation-reversing isomorphism [**111**, p.36]. Under the operation of connected sum the set of connected, compact, and oriented 3-manifolds becomes also a commutative semigroup with unit the 3-sphere $\mathbb{S}^3$ [**111**, p.37]. By the unique decomposition theorem for 3-manifolds due to Milnor [**88**], *any* connected, compact, and oriented 3-manifold can be regarded as the unique connected sum of irreducible manifolds with perhaps one or more handles attached. [A 3-manifold M is *irreducible* if every embedded 2-sphere bounds a 3-cell. A 3-manifold M is *prime* if in any decomposition $M = M_1 \# M_2$ either M_1 or M_2 is a 3-sphere $\mathbb{S}^3$ (see [**111**, p.37]).] For example, it is clear that $\mathbb{S}^2 \times \mathbb{S}^1$ is prime but not irreducible. It can be thought of as a 'handle' in the sense that it results from $\mathbb{S}^3$ by excising two 3-cells and identifying their boundaries. The Milnor Theorem shows that the Poincaré Conjecture (see Subsection 8.4) does not prevent us to construct and manipulate 3-manifolds in $\mathbb{R}^4$ or higher dimensions. Thus, the 3-manifolds are characterised or classified by the first four Betti numbers. Obviously, they may include essential k-cycles ($0 \leq k \leq 2$) in $\mathbb{R}^3$. Besides, they may contain essential 3-cycles in $\mathbb{R}^n$ ($n \geq 4$). The number of these 3-cycles in a 3-dimensional or higher manifolds is the 3th Betti number β_3.

This process of classification of manifolds can be generalised to higher dimensions by induction on dimension (and connected sum). The classification of manifolds in $\mathbb{R}^n$ is very important in geometric modelling, because —as shown in next chapters— it facilitates the design and implementation of data structures for n-dimensional stratified geometric objects.

8.3. Diffeomorphic shape classes. We have seen that homeomorphisms classify spaces according to whether it is possible to deform one space to the other *continuously*. We have also seen that the topological equivalence relation on the Euclidean space produces equivalence classes of subsets in it. The most important topological equivalence classes were shown to be the classes of n-dimensional topological manifolds. Likewise, diffeomorphisms classify spaces into equivalence classes of spaces according to whether it is possible to deform one space to the other *smoothly*. Two diffeomorphic spaces are essentially the same in so far as their differential topology is concerned. Therefore, smoothness imposes an additional constraint on the manifolds; consequently, a class of manifolds of the same dimension is further divided into subclasses of manifolds of distinct smoothness. These equidimensional manifolds with the same smoothness are said to be *diffeomorphic* manifolds. Thus, applying the notion of diffeomorphism given in Subsection 6.2 to equidimensional manifolds, we have:

DEFINITION 1.20. Let M and N be manifolds of the same dimension. A C^r mapping $f : M \to N$ is called a C^r **diffeomorphism** of M onto N if $f(M) = N$, f is one-to-one, and the inverse mapping f^{-1} is also C^r. If a C^r diffeomorphism exists between two manifolds, they are called C^r **diffeomorphic**; in case of $r = \infty$, they are said to be just **diffeomorphic**.

Clearly, by this definition, a diffeomorphism is a homeomorphism. But the converse is not true. However, a homeomorphism need not to be a diffeomorphism. Even a *differentiable* homeomorphism need not to be a diffeomorphism (see Example 1.57). In a word, diffeomorphisms are mappings that fall between isometries and homeomorphisms.

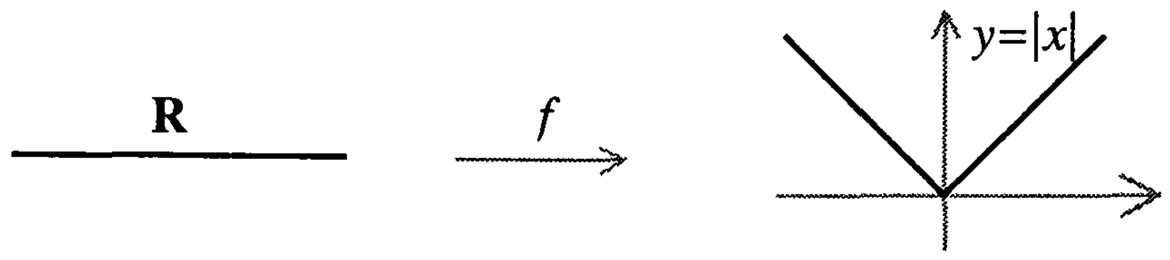

FIGURE 26

EXAMPLE 1.55. Consider the mapping $f : \mathbb{R} \to \mathbb{R}^2$ defined by $t \mapsto (t, |t|)$, Figure 26. Its image is a 1-manifold, the curve $y = |x|$ in $\mathbb{R}^2$. f is then a parametrisation of this curve in $\mathbb{R}^2$. It is not C^1 (and, then not differentiable) at $t = 0$, because its second component function is not C^1. Thus, f is not a diffeomorphism, and $\mathbb{R}$ and $y = |x|$ in $\mathbb{R}^2$ are not diffeomorphic 1-manifolds.

For the study of the differential geometry of manifolds it is essential that there exists tangent spaces (tangent lines for 1-manifolds, tangent planes for 2-manifolds, and so on) at every point. A point of a n-manifold where a n-dimensional tangent space is not defined is called a *singularity.* This suggests that two manifolds with different number of singularities cannot be diffeomorphic. In fact, the following theorem confirms our intuition.

THEOREM 1.4. (See Hirsch [**60**] on p.32) *Diffeomorphic manifolds have diffeomorphic boundaries.*

As a consequence, a cube cannot be diffeomorphic to a pyramid. Let us see a more formal example.

EXAMPLE 1.56. The curve $y = |x|$ in $\mathbb{R}^2$ in the previous example can be given a C^1 parametrisation $g : \mathbb{R} \to \mathbb{R}^2$ where $g(t) = (t|t|, t^2)$, $t \in \mathbb{R}$. The coordinate functions of g are given by

$$g_1(t) = \begin{cases} t^2 & \text{when } t \geq 0 \\ -t^2 & \text{when } t < 0 \end{cases} \quad \text{and} \quad g_2(t) = t^2, \quad t \in \mathbb{R}.$$

Both g_1 and g_2 are C^1 at 0. Therefore, g is C^1 at 0 and has a tangent vector there despite the fact that its image has a corner at $g(0) = (0,0)$. Since the tangent vector at 0 is $g'(0) = (0,0)$, there is no associated tangent line. However, g is not C^2 because its derivative $g'(t) = (2|t|, 2t)$ is not C^1. In fact, the right-hand and left-hand derivatives of g' are different, 2 and -2 , respectively. (Note that g_1 and g_1' have two patches each, so we have to check the equality of their lateral derivatives at the junction point.) This suggests that it is possible to find a parametrisation C^r for a non-C^r mapping by increasing (squaring) the exponent of the parameter t. Nevertheless, this does not eliminate any singularities; it just promotes a C^r singularity to a $C^{>r}$ singularity. That is, singularities possess an intrinsic nature, regardless the parametrisation used for a curve.

EXAMPLE 1.57. Let $f : \mathbb{R} \to \mathbb{R}$ given by $f(t) = t^2$, $t \in \mathbb{R}$, has as image the line $\mathbb{R}$ itself, which is known to be smooth. The function f is C^1 (and also differentiable or C^∞) everywhere; it is also analytic. However, $f^{-1}(u) = u^{1/2}$ is not C^1 since it has no derivative at $u = 0$. Thus, despite the smoothness of $\mathbb{R}$, f is not a diffeomorphism.

These two examples suggest that:

- A C^r mapping between manifolds does not imply that its image manifold is C^r (see Example 1.56).
- The C^r manifold can be image of a mapping which is not a C^r diffeomorphism (see Example 1.57).

Thus, it is necessary to distinguish between C^r smoothness on manifolds and C^r smoothness for mappings. However, in next chapter, it is shown that a C^r diffeormorphism ensures that its image of a smooth manifold is also smooth. Moreover, the idea of G^r smoothness (or geometric continuity) used in computer aided geometric design (CAGD) is nothing more than C^r smoothness in differential geometry. In fact, the pre-condition $f' \neq 0$ is used in CAGD in order to guarantee the invertibility of f, what is the same to say that f is a diffeomorphism. Thus, the essential concept behind a C^r smooth manifold is that of C^r diffeomorphism. The singularities of a mapping are related to the singularities of its component functions. Recall that a mapping is only a C^r mapping if their components are C^r. More difficult it seems to be to check that a mapping is a C^r diffeomorphism. Fortunately, the following theorem comes up to help us in this respect.

THEOREM 1.5. (see Hirsch [**60**, p.20]) *A C^r mapping which is a C^1 diffeomorphism is a C^r diffeomorphism.*

It is also known that if $f : M \to N$ and $g : N \to P$ are C^r mappings of manifolds, then so is $g \circ f$ [**1**, p.132]. It follows from the previous definition that the set $\mathrm{Diff}^r(M)$ of C^r diffeomorphisms of M to M forms a group under composition [**5**, p.36], i.e. a Klein geometry. $\mathrm{Diff}^r(M)$ also denotes the group of reparametrisations of M [**91**, p.142].

Diffeomorphisms are then the essential mappings studied in differential geometry. They are behind the idea of C^r smoothness on manifolds. C^r smoothness is independent on the representation, either it is parametric or implicit. In computer aided geometric design (CAGD), *visual smoothness*, also called *geometric continuity* G^r, is concerned with how parametric curves and surfaces should be joined in a smooth way. This concern might surprise differential geometers, who are used to dealing with the concept of a C^r curve or surface as one of the basic facts of life, as explained by Gregory in [**47**, p.353]. But, in geometric design practice, a complicated curve or surface is composed by glueing several patches together. So, the resulting curve or surface is C^r everywhere if and only if their constituent patches are C^r and any two patches join with geometric continuity C^r along their matching vertices or edges, respectively [**52**, p.56]. This is equivalent to the existence of a C^r (regular) reparameterisation of the curve or surface. This agrees with the definition of a C^r curve or surface in differential geometry and its use is now well established in CAGD [**47**, p.354].

Besides, diffeomorphisms do not only allow us to develop a mathematical theory for the free-form objects in CAGD, but also to understand the close relationships between the *geometry* of objects (not necessarily parametric free-form objects used in geometric design and modelling) and their *structure* (roughly, their critical points and singularities). In fact, more than that, diffeomorphisms and C^r smoothness are also behind the theory of stratifications. The leading idea of a stratification is to subdivide a n-dimensional point set into subsets such that all singularities of the original object are contained in subsets of dimension less than n. Thus, the stratification of an object or point set is driven up by lack of smoothness. This is the traditional use of stratifications. But, we use it for other purposes in solid modelling. For example, cube surface can be constructed by first attaching eight vertices (or singularities of dimension 0) to an initial empty point set, and subsequently its twelve edges (or singularities of dimension 1) and six faces. This allows us to antecipate a unified view of the free-form geometric objects usual in CAGD and other geometric objects usually used in solid modelling.

8.4. Homotopic shape classes. An equivalence class which is somewhat coarser than homeomorphism is 'of the same homotopy type'. The classical notion of the homotopy type was introduced

by Hurewicz in a series of four papers, in 1935-36, which appeared in the *Proceedings of the Koninklijke Nederlandse Akademie van Wetenschapen* [**63**]. It allows to classify the spaces from the point of view of their most important *global topological properties*, called homotopy properties [**16**, p.77], and neglect the local ones. This makes us to think of a possible relationship between homotopic shape of an arbitrary topological space (manifold or else) and the associated Betti numbers, which are topological invariants.

Let us now concentrate on the homotopic shape classes. In Section 5, we have already found some homotopic shape classes. For example, the homotopic shapes of the disc X, the annulus Y, an double-annulus Z in Figure 6 are a point, a circle (or loop), and the one-point union of two circles, respectively. In fact, X is contractible, so it deformation retracts to a point. And, in general, if we take a number k of non-intersecting disks, we obtain a deformation retract consisting of k points. In other words, the 0-dimensional homotopic class is a discrete space, i.e. a family of isolated points. The homotopic shapes of Y and Z are given by a 1-bouquet and a 2-bouquet of 1-circles, respectively. A *k-bouquet* is defined as the one-point union (also called the *wedge product*[2]) of k circles [**91**, p.107]. A 1-circle is homeomorphic to a 1-sphere $\mathbb{S}^1$. Therefore, a 1-dimensional homotopic class is a bouquet of 1-circles. Using the language of group theory, a k-bouquet of 1-circles is nothing more than the wedge product of a number k of 1-circles. In fact, the set of homotopy classes of 1-circles (or 1-loops) form a group under wedge product, called *first homotopy group* or (*fundamental homotopy group*) [**91**, p.93], and denoted by π_1. Moreover, the 1st homotopy group is invariant under homeomorphisms, and hence is a topological invariant [**91**, p.97].

Higher dimensional homotopy groups may be assigned to a topological space X. The *n-th homotopy group* ($n \geq 1$) is the set of homotopy classes of n-circles (or n-loops), and is denoted by $\pi_n(X)$. It is also a group under the wedge product. However, the 0-th homology group $\pi_0(X)$ is not a group [**91**, p.116]; it denotes the number of connected components of X. The higher dimensional homotopic classes are then k-bouquets of n-circles (or n-loops). A n-circle is homeomorphic to a n-sphere $\mathbb{S}^n$. Thus, in general, the homotopic shape of a topological space is given by a family of bouquets of circles.

From the above discussion, we see that the homotopic shape classes are n-loops ($n \geq 0$) or bouquets of loops (not necessarily of the same homotopic type).

---

[2]Let us define first the notion of 'pointed space'. A *pointed space* (X, x_0) is a topological space X and a point x_0 of X, called the *base point* such that $\{x_0\}$ is closed in X. Let (X, x_0), (Y, y_0) be pointed spaces. The *wedge product* of X and Y is the space $X \vee Y$ obtained from X and Y by identifying x_0 with y_0 [**23**, p.116]. For example, $\mathbb{S}^1 \vee \mathbb{S}^1$, $\mathbb{S}^1 \vee \mathbb{S}^2$, and $\mathbb{S}^2 \vee \mathbb{S}^2$ (for some choice of base points) are one-point unions of tangential spheres.

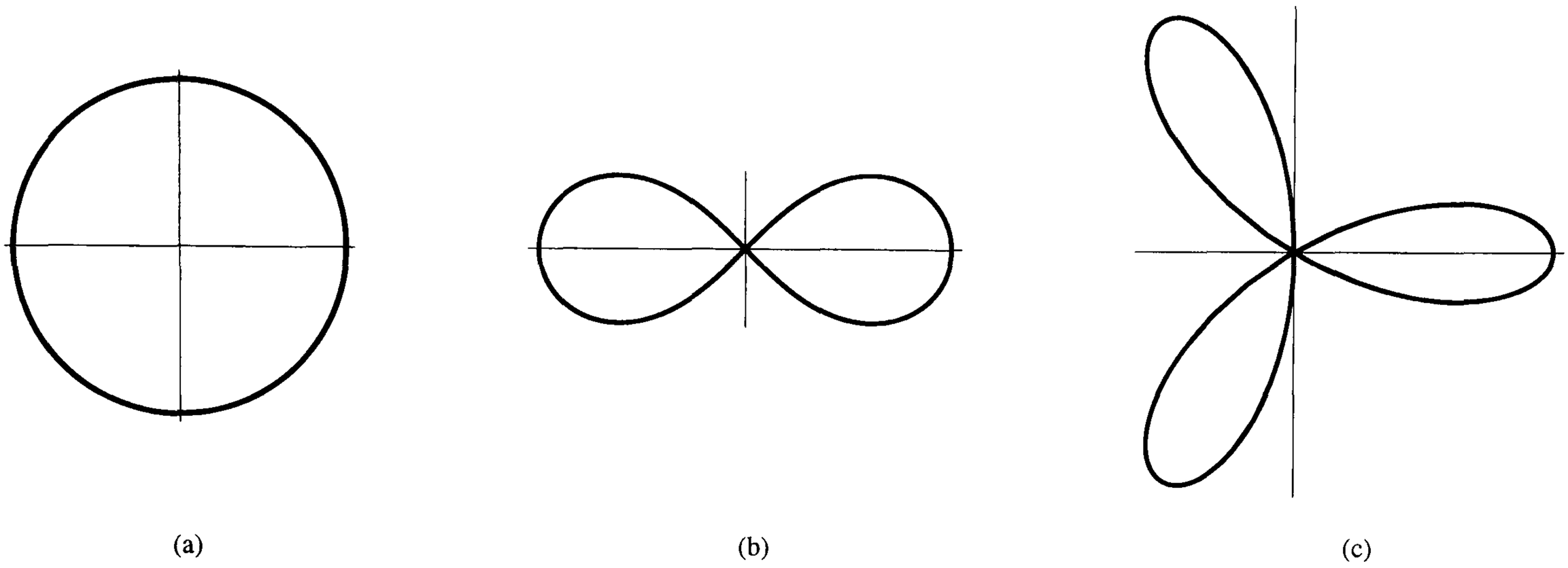

(a) (b) (c)

FIGURE 27. Bouquets of 1-dimensional loops.

EXAMPLE 1.58. In $\mathbb{R}^2$, only bouquets of 1-loops are allowed. Examples are depicted in Figure 27. The circle $x^2+y^2=1$ (Figure 27(a)), the lemminiscate of Bernoulli $(x^2+y^2+a^2)^2-4a^2x^2=a^4$ (Figure 27(b)) and the clover leaf $x^3-3xy^2-(x^2+y^2)^3=0$ (Figure 27(c)) are bouquets of one, two, three 1-loops in $\mathbb{R}^2$, *respectively*. These bouquets belong to distinct 1-dimensional homotopic classes, but they are all in the first homotopy group π_1.

EXAMPLE 1.59. The homopotic shape of the lemminiscate of Bernoulli pictured in Figure 27(b) is distinct from the homotopic shape of a 2-dimensional torus $\mathbb{T}^2$. Nevertheless, their 1-dimensional homotopic shapes are identical because the lemminiscate of Bernoulli is homotopy equivalent to $\mathbb{S}^1 \vee \mathbb{S}^1$, which is a subset of $\mathbb{T}^2 = \mathbb{S}^1 \times \mathbb{S}^1$.

EXAMPLE 1.60. The homotopy shape of the subspace of $\mathbb{R}^3$ depicted in Figure 28(a) includes four components. The first component is a point-component $\mathbb{D}^0$, so its homotopic image is also a point. The second component is a relatively closed line $\mathbb{D}^1$, which is contractible to a point. So, its homotopic image is also a point-component $\mathbb{D}^0$. The third component is a triangle, and therefore homotopically deformable to $\mathbb{S}^1$. The last component is a union of six bouquets containing seven petals: two ballons topologically equivalent to two 2-spheres $\mathbb{S}^2$, one spherical solid object topologically equivalent to a 3-disc $\mathbb{D}^3$, two relatively closed curved segments, one filled triangle, and one 2-torus $\mathbb{T}^2 = \mathbb{S}^1 \times \mathbb{S}^1$. The ballons remain the same provided that each is not homotopy deformable to a point or a line. However, the relatively closed curved segments are homotopy deformable to a point. The dangling curved segment is homotopy deformable to a point in the bigger $\mathbb{S}^2$. Analogously, the second curved segment is contractible such that the resulting point is shared by the bigger 2-sphere

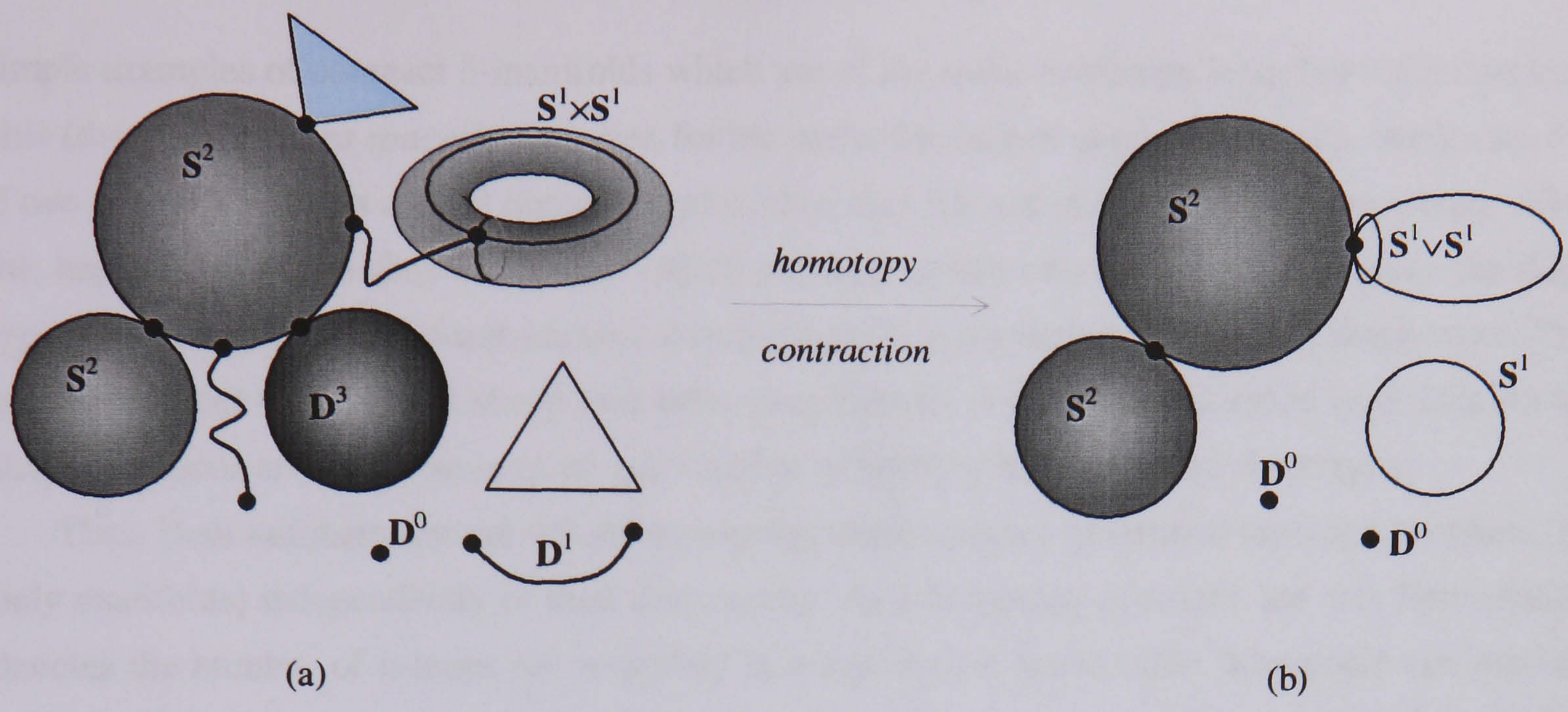

FIGURE 28. Bouquets of variable-dimensional loops.

and the torus. Also, the solid sphere is contractible to a point in the bigger 2-sphere, as well as the filled triangle. Finally, it is known that the homotopy type of a 2-torus is wedge product $\mathbb{S}^1 \vee \mathbb{S}^1$ of two 1-circles.

This suggests that there is a clear correspondence between the homology groups $H_n(X)$ (or, equivalently, Betti numbers) and homotopy groups $\pi_n(X)$ defined on a set. This is useful to determine shape equivalence between two topological spaces from both topological and homotopic points of view. In fact, as known in algebraic topology, if $f : X \to Y$ is a homeomorphism of X onto Y, then the induced homomorphism $f^* : H_n(X) \to H_n(Y)$ is a isomorphism for all n. This means that the algebraic structure of the groups $H_n(X)$ $(n = 0, 1, 2, \ldots)$ depends only on the topological type of X [**75**, p.148]. Equivalently, if X and Y possess the same topological type, their corresponding Betti numbers are identical. Remarkably, in homotopy theory, an even stronger statement holds: if f is a homotopy equivalence, then f^* is an isomorphism. Therefore, the structure of $H_n(Y)$ only depends on the homotopy type of X [**75**, p.148]. The conclusion is that two spaces possessing the same homotopy type have isomorphic homology groups. This means that Betti numbers are also homotopy invariants, and thus they are independent of the dimension.

For example, in spite of a 1-circle and an annulus are not of the same topological type, they are of the same homotopy type; consequently, their corresponding Betti numbers are identical. Moreover, there are spaces with identical dimensions that are of the same homotopy type —what implies that their Betti numbers are the same—, but not homeomorphic. As written on [**75**, p.114], there are fairly

simple examples of compact 3-manifolds which are of the same homotopy type, but not homeomorphic (the so-called *lens spaces*). However, for the particular case of compact surfaces, one knows that if two compact surfaces are not homeomorphic, then they are not of the same homotopy type. All of this happens because a shape invariant —Betti numbers in this case— may not determine the shape type of a space. Shape invariants are useful to distinguish two spaces with different shape types. That is, if two spaces have distinct shape invariants, then they are not of the same shape type. But, if their shape invariants are equal, no one can say whether or not they have the same shape type.

Thus, Betti numbers capture the global topological invariance of general topological spaces (not only manifolds) independently of their dimensions. As a homotopy invariant, the n-th Betti number denotes the number of n-loops (or n-circles) in a topological space (after homotopic contraction). Note that n-cycles in homology theory are precisely stratified n-loops. Thus, a n-loop determines a *n-dimensional hole*; hence, the n-th Betti number is said to determine the n-dimensional connectivity.

Note that each n-dimensional Euclidean space is associated with the $(n-1)$-th Betti number, i.e. with $(n-1)$-loops which determine $(n-1)$-dimensional holes. For example, consider the closed ball or disc $\mathbb{D}^3 = \mathrm{Cl}(\mathbb{B}^3)$ in $\mathbb{R}^3$. Then, $\mathbb{S}^2 = \mathrm{Fr}(\mathbb{D}^3)$ is the simplest 2-loop in $\mathbb{R}^3$. It encloses a hollow cavity or void, so it determines a 2-hole. Recall that torus-shaped 2-holes are also possible in $\mathbb{R}^3$. Likewise, $\mathbb{S}^1 = \mathrm{Fr}(\mathbb{D}^2)$ is the simplest 1-loop in $\mathbb{R}^2$; it is a 1-bouquet with a single 1-loop. It is not contractible in $\mathbb{R}^2$, so it determines a 1-hole. Also, $\mathbb{S}^0 = \mathrm{Fr}(\mathbb{B}^1) = \{-1, 1\}$ determines the simplest 0-hole in $\mathbb{R}^1$; it consists of two point-components or 0-loops. A 0-hole denotes the absence of a path between two components. Therefore, the number of 0-holes is equal to the number of components less one. In general, a n-sphere $\mathbb{S}^n$ is the frontier of a closed ball or disc $\mathbb{D}^{n+1} = \mathrm{Cl}(\mathbb{B}^{n+1}) = \{\mathbf{x} \in \mathbb{R}^{n+1} : |\mathbf{x}| \leq 1\}$, that is, $\mathbb{S}^n = \mathrm{Fr}(\mathbb{D}^{n+1}) = \{\mathbf{x} \in \mathbb{R}^{n+1} : |\mathbf{x}| = 1\}$ (see [**66**, pp.133-134]). In fact, we know that the sphere $\mathbb{S}^{n-1}$ is called the frontier of $\mathbb{D}^n$. Furthermore, a famous theorem says that there does not exist any retraction of the closed $(n+1)$-ball $\mathbb{D}^{n+1}$ onto its boundary sphere $\mathbb{S}^n = \mathrm{Bd}(\mathbb{D}^{n+1})$ (see [**66**, p.199] for a proof). Note that $\mathbb{B}^n$ is homeomorphic to $\mathbb{R}^n$, and that it is contractible. Thus, $\mathbb{S}^n$ possesses a n-hole in $\mathbb{R}^{n+1}$. But, it is clear that there are more complicated n-holes in $\mathbb{R}^{n+1}$ that are not of the same homotopy type as $\mathbb{S}^n$. Any n-hole is the union of manifolds that form a n-cycle. This allows us to say that a n-cycle determines a 'stratified' n-hole. All this gives us a dimension-based inductive perception of the shape of things, say subsets, in $\mathbb{R}^n$, what enables us to build up structured models of them on a computer.

An important point here is that we have assumed that a compact n-manifold that has the homotopy type of an n-sphere is homeomorphic to $\mathbb{S}^n$. But this remains a conjecture for $n = 3$, the so-called *Poincaré Conjecture*. In fact, from the Theorem of Surface Classification, we know that any

simply-connected (i.e. connected without 1-holes or $\pi_1(M) = 0$), compact surface without boundary is homeomorphic to the 2-sphere $\mathbb{S}^2$. Poincaré conjectured that an analogous statement for $n = 3$, that is, that a simply-connected, compact 3-manifold without boundary is homeomorphic to the 3-sphere $\mathbb{S}^3$. However, this is still unknown whether or not it is true. Nevertheless, there are examples of simply-connected, compact 4-manifolds which are not homeomorphic to $\mathbb{S}^4$ (for example, $\mathbb{S}^2 \times \mathbb{S}^2$) [**75**, p.114]. Oddly enough, an analogous statement of the Poincaré Conjecture for higher dimensions ($n > 3$) has been proven, namely, that a compact, connected n-manifold without boundary M, and $\pi_1(M) = 0$, is homeomorphic to $\mathbb{S}^n$, the n-sphere. This generalised Poincaré Conjecture was proved for $n > 4$ by Smale in 1960. In 1982, Freedman proved this conjecture for $n = 4$.

This means that the *topological classification* of 3-manifolds remains unsolved. Note that this conjecture involves only the 3-manifolds without boundary with $\pi_1 = 0$, those which are embedded in $\mathbb{R}^4$ or higher. Nevertheless, the *homotopy classification* of 3-manifolds is known (see [**111**] and [**88**]). Thus, the Poincaré Conjecture is not a problem to model computational geometric objects in higher dimensions. In fact, boundary-representation geometric objects, also called B-rep geometric objects, concilliates local topological shapes with (global) homotopic shapes by means a a Euler-Poincaré formula that relates the alternate sum of manifolds of distinct dimensions to the alternate sum of corresponding Betti numbers. This shows how homotopic shapes are crucial in the design and implementation of boundary-based geometric modellers, also called B-rep (boundary representation) modellers. One of the main aims of this doctoral thesis is just to propose a B-rep geometric modeller capable of coping with higher dimensional objects in some Euclidean space. Such a B-rep modeller should provide a general representation for bouquets of spheres or even complicated shapes. This requires the ability to represent and manipulate arbitrary shapes incident at a vertex (or base point) of a bouquet. Moreover, the study of the global shape of subsets of $\mathbb{R}^n$ as understood in homotopy theory suggests that the representation and manipulation of any subspace by a geometric modeller requires the ability to represent its boundary (and frontier) without ambiguity.

8.5. Convex shape classes. Let us now introduce a mathematical model for geometric feature modelling, as well as its axiomatics.

8.5.1. *Hadwiger ring.* A well-known class of sets in convexity theory is the Hadwiger convexity ring [**51**]. The *Hadwiger convexity ring H* is the class of sets in $\mathbb{R}^n$ which can be represented as a finite union of convex compact sets. The convexity ring is closed with respect to finite intersections, unions and projections on some spaces [**25**, p.177].

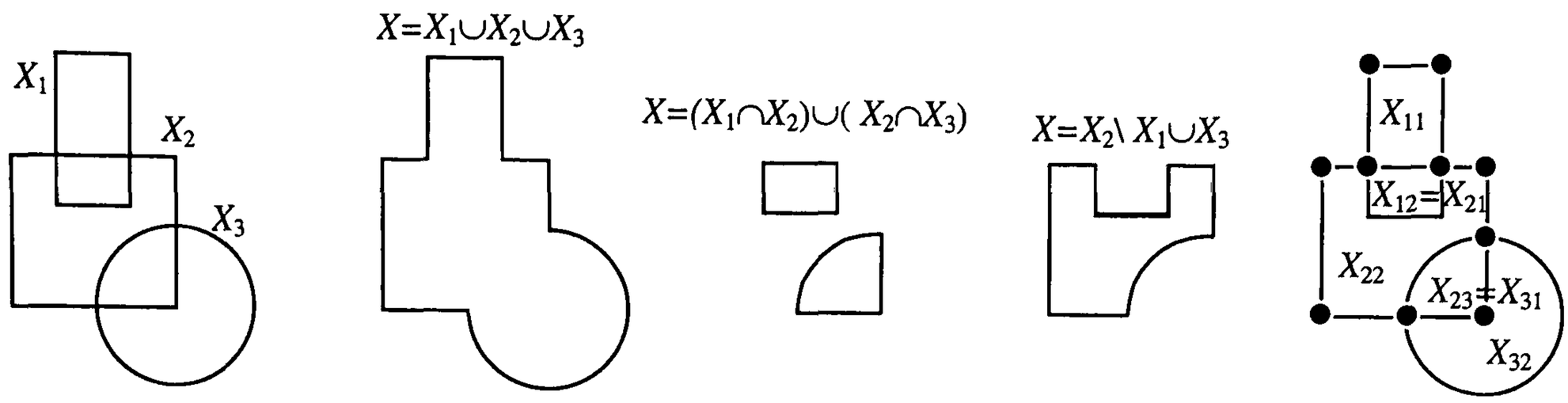

FIGURE 29. Illustrating the properties of the Hadwiger ring.

EXAMPLE 1.61. Let us consider three convex point sets X_1, X_2, X_3, Figure 29(a). They are in Hadwiger ring, as well as $X = X_1 \cup X_2 \cup X_3$ in (b) and $X = (X_1 \cap X_2) \cup (X_2 \cap X_3)$ in (c), because they are all decomposable into a finite union of convex compact sets. But, the point set $X = X_2 - (X_1 \cup X_3)$ in (d) is not in Hadwiger ring viewing that it does not admit a finite decomposition into convex subsets.

Example 1.61 shows that the Hadwiger ring is not closed with respect to differences. It is only closed in relation to unions and intersections of convex sets. Thus, Hadwiger sets are not necessarily convex. However, they are always decomposable into a finite union of convex sets. The intersection property is a direct consequence of a basic lemma in the convexity theory: *the intersection of an arbitrary collection of convex sets is convex* [**36**, p.3].

The Hadwiger ring provides a preliminary mathematical model for geometric feature modelling because:

- As any mathematical model, the Hadwiger ring is independent of any engineering, functional or technical specifications. Only the point set of each geometric feature (a protrusion or a depression) counts.
- The fact that the Hadwiger ring does not satisfy the difference axiom is not an handicap in geometric feature modelling, because the point set of any depression is represented in the model. It is eventually a problem for form feature recognition systems, but not for form feature modelling systems. It fact, from the point of view of the set theory, it does not make sense to distinguish between a protrusion and a depression.
- Both protrusions and depressions can be defined as Hadwiger sets. That is, a protrusion (respectively, a depression) is not required to be defined as a convex subset of a point set. Instead, a protrusion (respectively, a depression) is defined as a finite union of convex protrusions (respectively, depressions).

- It is independent of any feature shape interpretations. In other words, there are many possible form feature decompositions for a single engineering artefact because they depend on the designer intent or interpretation. However, they all have analogous Hadwiger decompositions, or, equivalently, decompositions with the same convex pattern.

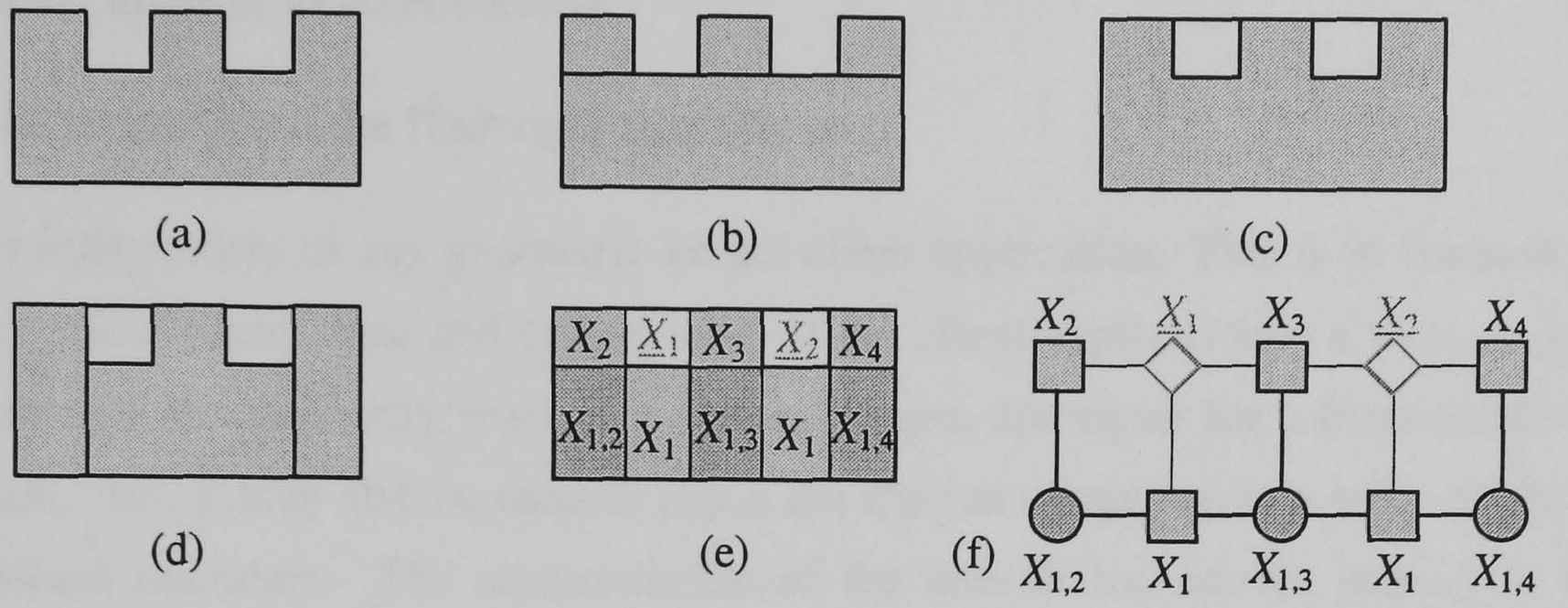

FIGURE 30. Convex pattern invariance in relation to engineering design operations.

EXAMPLE 1.62. Let us take a block with two rectangular depressions, Figure 30. This artefact can be designed either by unioning four blocks or by subtracting two blocks (two slotted depressions) from a bigger block (a block protrusion), or, alternatively, by unioning three blocks and subtracting two smaller blocks, as depicted in (b), (c), and (d), respectively. Nevertheless, they have the same Hadwiger decomposition, Figure 30(e), and thus the same convex pattern.

Therefore, the convex pattern of the resulting artefact is invariant to design-by features sequences to construct engineering artefacts. This makes possible to antecipate a convex pattern-based data structure underneath any geometric feature modeller that is independent of engineering design. That is, such a convex pattern-based data structure should support different engineering design views of an artefact simultaneously. This makes us to think of the convex pattern of an object as the 'neutral' convex decomposition or interplay between different geometric feature decompositions. This is important for several reasons, two of which come up immediately:

- It enables the multi-designer shape modification of the same engineering artefact under a cooperative design platform based on design-by-features, regardless of whether the designers have the same shape view of the corresponding geometric feature model or not. For example, one designer has introduced a rib on a block, but a second designer sees the resulting artefact as a block with two slots; hence the second designer should be able to, for example, to remove one of the slots.

- A designer's shape description of an engineering artefact into geometric features is not necessarily the same as the shape decomposition required by manufacturing processes. So, the Hadwiger convex decomposition seems to be more appropriate at the production stage than the designer's shape description, since it enables the re-interpretation of an engineering artefact in terms of form features

Other nice properties of the Hadwiger structure are:

- It is independent of any geometric-kernel client application. This is so because it does not 'recognise' protrusions and depressions. If the client application is a feature modeller, the Hadwiger structure may work as a convex pattern descriptor for a form feature decomposition. But, it may also be used to retain the Boolean structure of a solid object built upon Boolean operators. The representation of the intersection convex subsets in the convex pattern makes unnecessary to record the temporal course of modelling as usual for CSG modellers.
- The Hadwiger sets are easily editable. This is because their convex subsets are easily editable. This is possible because the Hadwiger structure retains the intersection convex subsets of both protrusions and depressions, as well any solid primitives used in solid modelling. This largely facilitates editing operations used in feature modelling and solid modelling.
- Because the design solid primitives (including protrusions and depressions) are basically convex, we can speed up time-consuming Boolean operations by using well-known algorithms of computational geometry [**95**], since we assume that any non-convex solid primitive is defined as part of a convex solid primitive.
- The fact that the difference axiom is not satisfied by the Hadwiger ring does not prevent the representation of solid blending primitives as usual in CSG, e.g. a blend between a cylinder and a rectangular block. The corresponding blending surface is a *saddle surface* (two valleys) which is neither convex nor concave, i.e. an anticlastic surface. The saddle surface has negative Gaussian curvature. In this case, the original cylinder has to be split into two, being one of them then defined as part of a convex object which also contains the solid blend primitive. However, the Hadwiger ring hardly applies to general anticlastic shapes, e.g. the so-called *monkey saddle*, which is similar to the saddle surface except that it has three valleys running down from the pass: two for the monkey's legs and one for its tail.
- Its convex pattern allows us to test whether or not two distinct point sets are in the same parametric shape family.

8.5.2. *Shape axiomatics for geometric feature modelling.* It is clear that protrusions and depressions are related to components, holes and voids. Altogether, components, through holes and voids provide us with the homotopic shape description of an object in $\mathbb{R}^3$, i.e. it provides us a *global* shape view of an object. Protrusions and depressions provide us the convex shape description of the same object, i.e. a *zonal* shape view of it. Thus, a shape axiomatics for geometric feature modelling could be possibly based on the following axioms:

- A protrusion is a Hadwiger set.
- A depression is a Hadwiger set.
- A component contains at least a protrusion.
- A through hole contains at least one depression.
- A void contains at least one depression.

EXAMPLE 1.63. In Figure 31(a), the through hole $H = D_1 \cup D_2 \cup D_3$ consists of three convex depressions D_1, D_2, and D_3. Note that other depression arrangements for H are possible. For example, $H = D$ may be considered as just a single depression D, which in turn consists of those three depressions, $D = D_1 \cup D_2 \cup D_3$. In contrast, the depression $D = D_1 \cup D_2$ in Figure 31(b) is not a through hole. It has two convex depressions D_1, D_2.

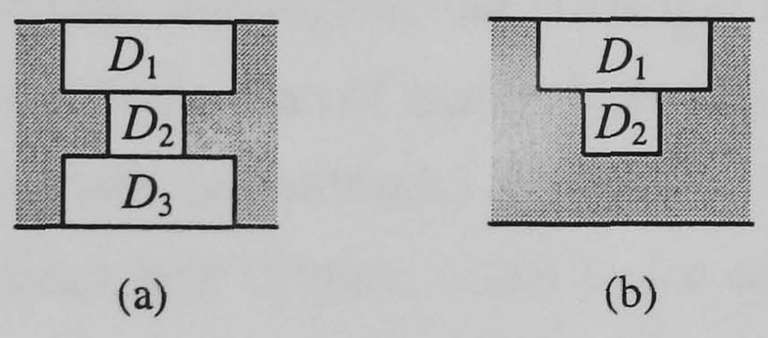

FIGURE 31

Thus, geometric feature modelling involves two mathematical theories: homotopy theory and convexity theory. They provide us with a general shape taxonomy for geometric feature modelling: homotopic shapes (components, through holes and voids) and Hadwiger shapes (protrusions and depressions). The axiomatics above complete a theory for geometric feature modelling. In particular, the last three axioms relate homotopic and Hadwiger shapes to each other by containment relationships. These axioms relating zonal and global shapes of an object imply a space decomposition which is not available in extant geometric modellers. This has in some extent justified the development of form feature modellers, and spread the idea that geometric feature modellers and geometric solid modellers are distinct shape modelling machines. It is our view that they are only representatives of

distinct shape views of an object. The geometric modellers provide us topological, differential and geometric shapes, while form feature modellers provide us homotopic and Hadwiger shapes. Our idea is to put them together into an integrated shape kernel responsible for all shape operations. This allows us to separate the functional aspects of engineering artefacts from the shape aspects of their underlying geometric objects.

9. Shape Kernel Architecture

9.1. Shape insufficiences of set-theoretic modellers. Set-theoretic modellers, usually known as CSG (Constructive Solid Geometry) modellers, typically include five parametric families of primitive solids (or homogeneously 3-dimensional geometric objects): blocks, wedges, spheres, cylinders, and tori. Each primitive solid is an element of a geometric equivalence class of congruent solids. Each primitive solid is parametrically defined by a finite number of parameter values. For example, a block is created or instantiated by assigning values to its length l, width w, and height h; symbolically, this is described by the function $CREATEBLOCK : \mathbb{R} \times \mathbb{R} \times \mathbb{R} \rightarrow \mathcal{B}$, where $\mathcal{B}$ is the family of blocks.

CSG modellers do not provide a shape interface suitable for feature-based modelling. In fact, they do not provide access to through holes, protrusions, etc. For example, a subtraction of one CSG solid from another may create a through hole, but it is very hard to recognize the existence of such a hole in a CSG tree. Besides, topological and Hadwiger shapes (e.g. a through hole consisting of three depressions) requires some kind of shape clustering machinery which is absent from CSG trees. Consequently, the automatic (algorithmic) detection of shape changes becomes difficult (e.g. the transmutation of the through hole (Figure 31(a)) into a stepped depression (Figure 31(b)) consisting of two convex depressions, after removing the bottom convex depression).

9.2. Shape insufficiences of B-Rep modellers. B-Rep modellers have some advantages over CSG modellers because they possess a lower level of shape incompleteness. In fact, they are able in principle to represent and manipulate manifolds or 'cells' of dimension up to 3 (i.e. points, lines, surfaces and solids), whether they possess holes and voids or not. The existence of these manifolds in B-Rep data strucutures is useful for many purposes. For example, it facilitates the direct, graphical interaction with the designer. Besides, B-Reps have explicit representatives, called shells, for components and voids. Shells are particular 'cellular' clustering entities. Unfortunately, through holes, depressions and protrusions do not have similar clustering representatives. There is no representation for the relationships between global topological shapes (components, through holes and voids) and their Hadwiger subsets (protrusions and depressions) either. Equivalently, there are no

hierarchical shape clustering entities, what makes difficult the representation of 'cellular' interactions between homotopic and Hadwiger shapes. To overcome these shape incompatibilities between 'cellular' boundary representations and feature representations, some authors have proposed external 'cellular' data structures associated with 'cellular' boundary representation data structures capable of emulating 'cellular' clusters for form features, their shape hierarchical or containment relationships, and their 'cellular' interactions as well. See [**11**] for a recent implementation of such external 'cellular' data structure associated with the ACIS boundary data structure. However, such external 'cellular' data structures on the top of a boundary data structure only strikes the shape deficiencies of the B-Rep modellers. In fact, they cannot be considered as extensions of B-Reps because the corresponding mathematical model has not been reformulated and extended. It is just an *ad-hoc* solution for a particular engineering application, as it is the case of feature-based modelling.

9.3. Shape requirements for applications. B-rep and CSG-rep are *complete* representations of solids in the sense of Requicha [**96**], i.e. they are unambiguous representations of solids. Requicha completeness refers to point sets of solids, i.e. their geometry or geometric shape. It does not cover other sorts of shape as those described in this chapter. In this sense, we can say that CSG-rep and B-Rep modellers are *shape-incomplete*, i.e. they are not capable of representing and processing all the shape types as necessary for most applications. Recall the difficulties that many researchers faced in the last two decades to integrate form feature modellers and geometric modellers. It is also known that B-reps and CSG-reps are not suited to efficient algorithms for extracting some shape properties nor for modification algorithms based on those properties. Even worse it is the inexistence of a shape framework that relates different shape types.

The problems mentioned above are largely due to insufficiences in the mathematical models of CSG-reps and B-Reps. The CSG-rep and B-Rep models were derived from the theory of semialgebraic sets [**96**] and theory of closed surfaces [**18**], respectively, but they were overconstrained by the notion of solidity. Consequently, they could not satisfy important shape requirements of a significant number of applications, even those related to design and manufacturing. To enable the effective integration of computer aided design and manufacturing systems we have to achieve an integrated shape kernel architecture. Otherwise, CADCAM integration in engineering environments will be always a mirage. The most important requirements to achieve an effective shape integration are:

- *General geometric coverage*. In the last twenty years, some efforts to integrate the geometries of solid modellers and free-form modellers have been attempted by integrating their

implicit and parametric representations. However, as explained in next chapters, an integrated geometry has to do more with a general geometric coverage than its representations. Such a general geometric coverage has been recently proposed by Middleditch, Reade and Gomes [**86**] to be the class of subanalytic sets. Subanalytic geometry is a generalisation of algebraic geometry, rational geometry and transcendental geometry; hence, it includes algebraic and semialgebraic sets (e.g. CSG objects) described by polynomials, rational sets (e.g. non-uniform rational B-splines, shortly NURBS) described ratios of polynomials, and transcendental sets (e.g. springs) described by transcendental functions, respectively. This is important for several reasons, namely: (i) to eliminate possible geometric incompatibilities in design and manufacturing, (ii) subanalytic sets form a Boolean class, i.e. they can be combined through Boolean operators to construct more complicated subanalytic sets, (iii) subanalytic sets are stratifiable, i.e. they admit partitions into manifolds or strata.

- *General shape coverage.* Geometry is only part of the business in shape modelling. By shape integration we mean not only geometry integration, but also the integration of geometry with other kinds of shape, namely homotopic, topological, differential and Hadwiger shapes. Geometry integration is far from complete but subanalytic sets look to be able to fill the gap between solid modelling and freeform modelling. Furthermore, the integration of homotopic and Hadwiger shapes in an application-independent or general shape modeller releases feature modellers from controlling shape representation and manipulation. This is advantageous in many respects, mainly because shape modelling is then application-independent. A feature modeller will be just a (functional) modelling system taking advantage of the facilities provided by a general-purpose shape modeller.
- *Multidimensional manifold structure.* The geometric structure of an object should be piecewise manifold and multidimensional. Amongst several reasons, we mention the following. First, it provides the unified representation for drafting, wireframe, surface, and solid models [**116**], as essential in interactive design. Second, it is necessary to model objects and spaces of arbitrary dimension, in applications such as robot path planning which uses n-dimensional configuration spaces [**83**]. Third, it is suited to the representation of finite element meshes, and solid models internal membranes.
- *General manifold clustering.* With the exception of the 'cellular' representation developed by Gomes and Teixeira [**46**], current 'cellular' geometric models do not provide general dimensionally nonhomogeneous clusters for cells. They usually use external, application-oriented 'cellular' clustering. These external 'cell' clusters were specifically designed to

represent the cell structures of form features, that is, they are application-oriented. This fact and the non-existence of a general shape theory have been the major barriers to the integration of geometric and feature modellers. Such clusters are called subcomplexes in the theory of complexes, and, more generally, in the theory of stratifications. Basically, the classical hierarchical 'cellular' structure of complex-shell(loop)-'cell' is replaced by the hierarchical stratified structure of complex-subcomplex-stratum. A subcomplex can represent the 'cellular' or stratified structure of a homotopic or Hadwiger shape, or even general shapes not necessarily homogeneous in dimension.

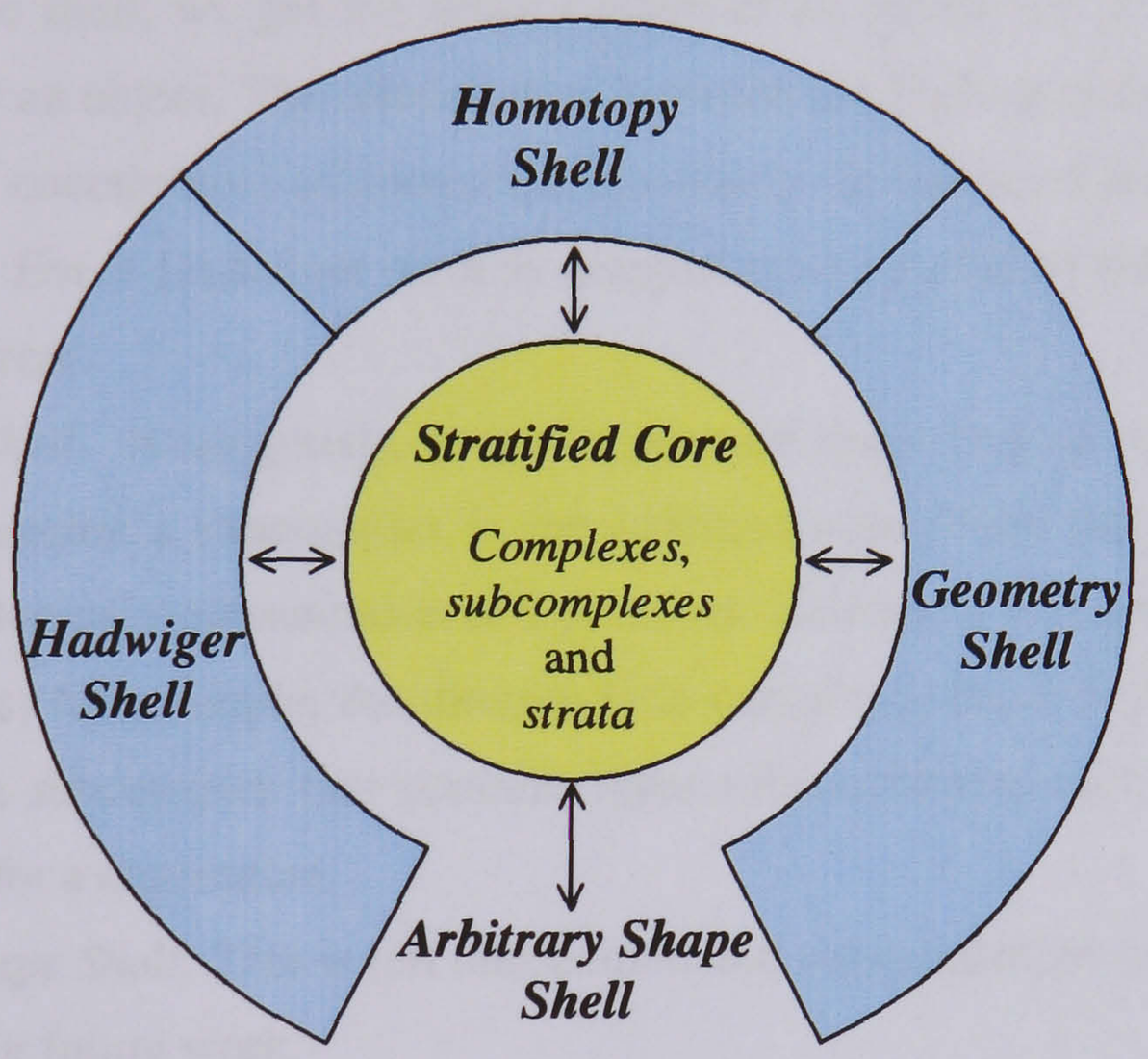

FIGURE 32. A shape kernel architecture.

9.4. A universal shape kernel architecture. A general shape modeller architecture should consist of the following modules, Figure 32.

- *Stratified Core.* The stratified core of the SKA (Shape Kernel Architecture) is a hierarchical stratified structure (complex-subcomplex-stratum). It is a generalisation of usual boundary cores, in the sense that any subcomplexes can represented and manipulated. Strata are the essential 'building blocks' and are, by definition, manifolds. In terms of the shape theory, they are then the fundamental topological shapes. Strata are usually called generalised 'cells' in geometric modelling. Therefore, the stratified core contains strata, i.e. vertices, edges, faces, solids, and even higher dimensional strata. In addition, the stratified core also

contains manifold subcomplexes, i.e. arbitrary finite clusters of manifolds, and complexes as a finite cluster of subcomplexes. These subcomplexes are not necessarily disjoint in a complex, but a subcomplex cannot belong to distinct complexes.

- *Geometric Shell.* The association of the stratified core with the geometric shell corresponds to the conventional design of B-rep modellers: topology alongside geometry. The geometry shell here implements the subanalytic geometry, i.e. it describes the geometry for points, lines, surfaces, and so on, via equalities and inequalities of analytic functions.
- *Hadwiger Shell.* The Hadwiger shell holds the convex pattern of an object. Together with the homotopic shell, we get the shape pattern of an object, i.e. a zonal and global shape description of an object. The relationships between the Hadwiger shell and homotopic shell represent the containment relationships previously axiomatised for Hadwiger and homotopic shapes. Every Hadwiger set X is mapped onto a stratified subset (or subcomplex) in the stratified core.
- *Homotopic Shell.* Analogously, every homotopic shape (e.g. components, through holes and voids) matches a subcomplex in the stratified core. Note that the stratified core contains a homological representation of a point set. Besides, a subcomplex may contain other subcomplexes; for example, the through hole containing three depressions in Figure 31 is stratified as a subcomplex that contains three subcomplexes, each of which is a stratified point subset for a depression.
- *Arbitrary Shape Shell.* This is left unspecified and concerns other sorts of shape which may be relevant for future work.

Putting this differently, a shape kernel consists of a stratified core (strata, clusters of strata, clusters of subcomplexes, homological reasoning algorithms, etc.) surrounded by a shape shell consisting of three modules: (differential) geometry, Hadwiger, and homotopy shells). Many applications need not to use all the modules. For example, in computer-aided geometric design of parametric curves and surfaces, the stratified core is likely unnecessary, but if a stratification is required for such geometric objects, they will be mapped onto strata and (sub)complexes. The algorithm of stratifying a geometric object is know in solid modelling as *boundary evaluation.* In solid modelling, the stratified core and the geometry shell are always on, while a form feature modeller demands the activation of the whole shape kernel. Note that a form feature modeller is not part of the shape kernel, because it holds a particular shape view, the designer's shape view.

Another important point is that every shape is one-to-one mapped onto either a cell or a subcomplex, but not all subcomplexes in the stratified nucleous correspond to a shape in the shape shell. For example, when two subcomplexes overlap, an overlapping-driven algorithm is triggered in order to achieve their intersection subcomplex. Then, this intersection subcomplex is defined as subcomplex of both overlapping subcomplexes, but it does not match any shape in the shape shell. Intersection subcomplexes constitute one of most important decisions in the design of our shape kernel. They are useful for many purposes, such as, for example, shape editing (undo, redo, resizing, deleting, etc) and shape matching for parametric families of objects.

This shape kernel is general-purpose, i.e. application-independent, regardless of whether or not it is included in a CAD system. It is necessary to bear in mind that some engineering terms used in feature modelling coincide with mathematical terms in shape theory; for example, a through hole is a form feature but also a homotopic (or global topological) shape. The distinction becomes apparent when we consider that there are so many kinds of through holes (straight holes, stepped holes, etc.) in engineering design, but they all have the same topological shape, just a through hole. A form feature combines technical function with shape, but its shape processing should be relegated to an application-independent shape kernel. That is, the 'cellular' clustering of a form feature is up to the shape kernel, not the form feature modeller itself. Thus, subcomplexes must be part of the stratified core in order to prevent external application-dependent cellular clustering.

10. Summary

A shape-theoretic framework for engineering artefacts has been proposed. Each type of shape is usually associated with a group of shape mappings of an Euclidean space into another, leaving intact certain properties of their subsets. Only homotopies do not form a group. So, we have a group of homeomorphisms, a group of diffeomorphisms, a group of isometries, etc. A general hierarchy of shapes has been derived from the hierarchy of shape mappings: homotopic shapes (i.e. n-holes) which are invariant under homotopies, Hadwiger shapes (i.e. Hadwiger sets) which are invariant under convexity-preserving mappings, differential geometric shapes (e.g. smooth manifolds or even piecewise smooth varieties) which are invariant under diffeomorphisms, and geometric shapes (e.g. semialgebraic manifolds and varieties) which are invariant under rational mappings (e.g. isometries).

The shape taxonomy here introduced and the understanding of the relationships between the various shapes type have led us to a preliminary design of a general shape kernel. In particular, the convexity theory and homotopy theory have been shown to be the mathematical theories supporting

form feature modelling. Besides, it has been understood that it is not good idea to have a separated and isolated view of the various branches of geometric modelling.

CHAPTER 2

Smoothness and singularities

'I fear that I bore you with these details,
but I have to let you see my little difficulties,
if you are to understand the situation.'

C. Doyle, A Scandal in Bohemia

This chapter deals with smoothness and singularities of manifolds and varieties. The context is the differential topology and geometry, but we are interested in their usefulness and applicability in geometric modelling. Although almost all the important examples and applications of differential geometry (e.g. engineering and geometric design in particular) deal with analytic manifolds, the discussion in this chapter is extended to smooth manifolds, restricting to the analytic category only when necessary. The objective is to exploit the smooth structure of manifolds (e.g. Euclidean spaces) to study the *intrinsic* properties of their subsets or subspaces, that is, independently of any choice of local coordinates (e.g. spherical coordinates, Cartesian coordinates, etc.). As suggested in subsection 6.2 (Chapter 1), manifolds provide us with the proper category in which most efficiently one can develop a coordinate-free approach to the study of the intrinsic geometry of point sets. It is obvious that the explicit formulæ for a subset may change when one goes from one set of coordinates to another. Thus, somehow, any geometric equivalence problem can be viewed as the problem of determining whether two different local coordinate expressions define the same intrinsic subset of a manifold. Such coordinate expressions (or change of coordinates) are defined by mappings between manifolds. Thus, by defining mappings between manifolds such as Euclidean spaces, we are able to uncover the local properties of their subspaces. In geometric modelling, we are particularly interested in properties such as, for example, local smoothness, i.e. to know whether the neighbourhood of a point in a submanifold is (visually) smooth, or the point is a singularity.

1. Differential of a smooth mapping

Let U, V be open sets in $\mathbb{R}^m, \mathbb{R}^n$, respectively. Let $f : U \to V$ be a mapping with component functions $f_1, \ldots, f_n$. Note that f is defined on every point $\mathbf{p}$ of U in the coordinate system $x_1, \ldots x_m$.

We call f smooth provided that all derivatives of the f_i of all orders exist and are continuous in U. Thus for f smooth, $\partial^2 f_i/\partial x_1 \partial x_2$, $\partial^3 f_i/\partial x_1^3$, etc., and $\partial^2 f_i/\partial x_1 \partial x_2 = \partial^2 f_i/\partial x_2 \partial x_1$, etc., all exist and are continuous. Therefore, a mapping $f : U \to V$ is *smooth* (or *differentiable*) if f has continuous partial derivatives of all orders. And we call f a *diffeomorphism* of U onto V when it is a bijection, and both f, f^{-1} are smooth.

Let $f : U \to V$ be a smooth (or differentiable or C^∞) and let $\mathbf{p} \in U$. The matrix

$$\mathrm{J}f(\mathbf{p}) = \begin{bmatrix} \partial f_1(\mathbf{p})/\partial x_1 & \partial f_1(\mathbf{p})/\partial x_2 & \cdots & \partial f_1(\mathbf{p})/\partial x_m \\ \vdots & \vdots & & \vdots \\ \partial f_n(\mathbf{p})/\partial x_1 & \partial f_n(\mathbf{p})/\partial x_2 & \cdots & \partial f_n(\mathbf{p})/\partial x_m \end{bmatrix}$$

where the partial derivatives are evaluated at $\mathbf{p}$, is called **Jacobian matrix** of f at $\mathbf{p}$ [**24**, p.51]. The linear mapping $\mathrm{D}f(\mathbf{p}) : \mathbb{R}^m \to \mathbb{R}^n$ whose matrix is the Jacobian is called the **derivative** or **differential** of f at $\mathbf{p}$; the Jacobian $\mathrm{J}f(\mathbf{p})$ is also denoted by $[\mathrm{D}f(\mathbf{p})]$. It is known in mathematics and geometric design that every polynomial mapping f (i.e. mappings whose component functions f_i are all polynomial functions) is smooth. If the components are rational functions, then the mapping is smooth provided none of the denominators vanish anywhere.

Besides, the composite of two smooth mappings, possibly restricted to a smaller domain, is smooth [**24**, p.51]. It is worth noting that the chain rule holds not only to smooth mappings, but also to differentials. This fact provides us with a simple proof of the following theorem.

THEOREM 2.1. *Let U, V be open sets in $\mathbb{R}^m, \mathbb{R}^n$, respectively. If $f : U \to V$ is a diffeomorphism, at each point $\mathbf{p} \in U$ the differential $\mathrm{D}f(\mathbf{p})$ is invertible, so that necessarily $m = n$.*

PROOF. See Gibson [**42**, p.9]. □

The justification for $m = n$ is that it is not possible to have a diffeomorphism between open subspaces of Euclidean spaces of different dimensions [**15**, p.41]. In fact, a famous theorem of algebraic topology (Brouwer's Invariance of Dimension) asserts that even a homeomorphism between open subsets of $\mathbb{R}^m$ and $\mathbb{R}^n$, $m \neq n$, is impossible (see Chapter 1).

Theorem 2.1 is very important not only to distinguish between two manifolds in the sense of differential geometry, but also to relate the invertibility of a diffeomorphism to the invertibility of the associated differential. More subtle is the hidden relationship between singularities and non-invertibility of the Jacobian. We should emphasize here that the direct inverse of Theorem 2.1 does not hold. However, there is a partial or local inverse, called Inverse Mapping Theorem, possibly

one of the most important theorems of the calculus. It is introduced in the next section, where it is discussed the relationship between invertibility of mappings and smoothness of manifolds.

2. Invertibility and smoothness

In Chapter 1 (Subsection 8.3), it is argued that the smoothness of a submanifold which is image of a mapping depends not only on smoothness but also invertibility of its associated mapping. This section generalises such a relationship between smoothness and *invertibility* to mappings of several variables. This generalisation is known in mathematics as the *Inverse Mapping Theorem*. This leads to a general mathematical theory behind geometric continuity in geometric modelling —not only confined to parametric free-form geometric design— as explained throughout this chapter. This generalisation is *representation-independent*, i.e. no matter whether a submanifold is parametrically or implicitly represented.

Before proceeding, let us briefly review the invertibility of mappings, linear case.

DEFINITION 2.1. Let X, Y be Euclidean spaces, and $f : X \to Y$ a continuous linear mapping. One says that f is **invertible** if there exists a continuous linear mapping $g : Y \to X$ such that $g \circ f = \mathrm{id}_X$ and $f \circ g = \mathrm{id}_Y$ where id_X and id_Y denote the identity mappings of X and Y respectively. Thus, by definition, we have:

$$g(f(x)) = x \quad \text{and} \quad f(g(y)) = y$$

for every $x \in X$ and $y \in Y$. We write f^{-1} for the inverse of f.

However, unless we have an algorithm to evaluate whether or not a mapping is invertible, smoothness analysis of a point set is useless from the computer-aided geometric modelling point of view. Fortunately, linear algebra is here to rescue us. Consider the particular case $f : \mathbb{R}^n \to \mathbb{R}^n$. The linear mapping f is represented by a matrix $A = [a_{ij}]$. It is known that f is invertible iff A is invertible (as a matrix), and the inverse of A, if it exists, is given by the formula

$$A^{-1} = \frac{1}{\det A} \mathrm{adj} A$$

where $\mathrm{adj} A$ is a matrix whose components are polynomial functions of the components of A. In fact, the components of $\mathrm{adj} A$ are subdeterminants of A. Thus, A is invertible iff its determinant $\det A$ is not zero.

Now, we are in position to define invertibility for differential mappings.

DEFINITION 2.2. Let U be an open subset of X and $f : U \to Y$ be a C^1 mapping, where X, Y are Euclidean spaces. We say that f is C^1-**invertible on** U if the image of f is an open set V in Y, and if there is a C^1 mapping $g : V \to U$ such that f and g are inverse to each other, i.e.

$$g(f(x)) = x \quad \text{and} \quad f(g(y)) = y$$

for all $x \in U$ and $y \in V$.

It is clear that f is C^0-invertible if the inverse mapping exists and is continuous. One says that f is C^r-invertible if f is itself C^r and its inverse mapping g is also C^r. In the linear case, we are interested in linear invertibility, which basically is the strongest requirement that we can make. By the Theorem 1.5, it turns out that if f is a C^1-invertible, and if f happens to be C^r, then its inverse mapping is also C^r. This is the reason why we emphasize C^1 at this point. However, a C^1 mapping with a continuous inverse is not necessarily C^1-invertible, as illustrated in the following example:

EXAMPLE 2.1. Let $f : \mathbb{R} \to \mathbb{R}$ be the mapping $f(x) = x^3$. It is clear that f is infinitely differentiable. Besides, f is strictly increasing, and hence has an inverse mapping $g : \mathbb{R} \to \mathbb{R}$ given by $g(y) = y^{1/3}$. The inverse mapping g is continuous at 0, but not differentiable at 0.

Let us now see the behaviour of invertibility under composition. Let $f : U \to V$ and $g : V \to W$ be invertible C^r mappings, where V is the image of f and W is the image of g. It follows that $g \circ f$ and $(g \circ f)^{-1} = f^{-1} \circ g^{-1}$ are C^r-invertible, because we know that a composite of C^r mappings is also C^r.

DEFINITION 2.3. Let $f : X \to Y$ be a C^r mapping, and let $\mathbf{p} \in X$. One says that f is **locally** C^r-**invertible** at $\mathbf{p}$ if there exists an open subset U of X containing $\mathbf{p}$ such that f is C^r-invertible on U.

This means that there is an open set V of Y and a C^r mapping $g : V \to U$ such that $f \circ g$ and $g \circ f$ are the corresponding identity mappings of V and U, respectively. Clearly, a composite of locally invertible mappings is locally invertible. Putting this differently, if $f : X \to Y$ and $g : Y \to Z$ are C^r mappings, with $f(\mathbf{p}) = \mathbf{q}$ for $\mathbf{p} \in U$, and f, g are locally C^r-invertible at $\mathbf{p}$, $\mathbf{q}$, respectively, then $g \circ f$ is locally C^r-invertible at $\mathbf{p}$.

In Example 2.1, we used the derivative as a test for invertibility of a real-valued function of one variable. That is, if the derivative does not vanish at a given point, then the inverse function exists, and we have a formula for its derivative. The Inverse Mapping Theorem generalises this result to mappings, not just functions.

THEOREM 2.2. **(Inverse Mapping Theorem)** *Let U be an open subset of $\mathbb{R}^m$, let $\mathbf{p} \in U$, and let $f : U \to \mathbb{R}^n$ be a C^1 mapping. If the derivative $\mathrm{D}f$ is invertible, f is* locally C^1-invertible *at $\mathbf{p}$. If f^{-1} is its local inverse, and $\mathbf{y} = f(\mathbf{x})$, then $\mathrm{J}f^{-1}(\mathbf{y}) = [\mathrm{J}f(\mathbf{x})]^{-1}$.*

PROOF. See Boothby [**15**, p.43]. □

It is equivalent to say that there exists open neighbourhoods U, V of $\mathbf{p}, f(\mathbf{p})$ respectively such that f maps U diffeomorphically onto V. Note that, by the Theorem 2.1, $\mathbb{R}^m$ has the same dimension as the Euclidean space $\mathbb{R}^n$, that is, $m = n$.

EXAMPLE 2.2. Let U be an open subset of $\mathbb{R}^2$ consisting of all pairs (r, θ), with $r > 0$ and arbitrary θ. Let $f : U \to V \subset \mathbb{R}^2$ be defined by $f(r, \theta) = (r\cos\theta, r\sin\theta)$, i.e. V represents a circle of radius r in $\mathbb{R}^2$. Then

$$\mathrm{J}f(r,\theta) = \begin{bmatrix} \cos\theta & -r\sin\theta \\ \sin\theta & r\cos\theta \end{bmatrix}$$

and

$$\det \mathrm{J}f(r,\theta) = r\cos^2\theta + r\sin^2\theta = r.$$

Thus, $\mathrm{J}f$ is invertible at every point, so that f is locally invertible at every point. The local coordinates f_1, f_2 are usually denoted by x, y so that we usually write

$$x = r\cos\theta \quad \text{and} \quad y = r\sin\theta.$$

The local inverse can be defined for certain zones of Y. In fact, let V be the set of all pairs (x, y) such that $x > 0$ and $y > 0$. Then the inverse on V is given by

$$r = \sqrt{x^2 + y^2} \quad \text{and} \quad \theta = \arcsin\frac{y}{\sqrt{x^2 + y^2}}.$$

An immediate consequence of the Inverse Mapping Theorem is the following corollary.

COROLLARY 2.1. *Let U be an open subset of $\mathbb{R}^n$ and $f : U \to \mathbb{R}^n$. A necessary and sufficient condition for the C^r mapping f to be a C^r diffeomorphism from U to $f(U)$ is that it be one-to-one and $\mathrm{J}f$ be nonsingular at every point of U.*

PROOF. Boothby [**15**, p.46]. □

Thus, diffeomorphisms have nonsingular Jacobians. This parallel between differential geometry and linear algebra provides us with a potential computable approach to evaluate whether or not a C^r mapping is a C^r diffeomorphism. Consequently, using computational techniques of differentiability and matrix calculus, we are able to establish smoothness conditions on a submanifold of $\mathbb{R}^n$.

Note that the domain and codomain of the mappings used in Theorem 2.1, Theorem 2.2 and its Corollary 2.1 have the same dimension. This may suggest that only smooth mappings between spaces of the same dimension are C^r invertible. This is not the case. Otherwise, this would be useless, at least for geometric modelling. For example, a parametrised k-manifold in $\mathbb{R}^n$ is defined by the *image* of a parametrisation $f : \mathbb{R}^k \to \mathbb{R}^n$, with $k < n$. On the other hand, an implicit k-manifold is defined by the *level set* of a function $f : \mathbb{R}^k \to \mathbb{R}$, i.e. by an equation $f(\mathbf{x}) = c$, where c is a real constant.

3. Level set, image, and graph of a mapping

Let us then review the essential point sets associated with a mapping. This will help us to understand how a manifold or even a variety[1] is defined, either implicitly, explicitly, or parametrically. Basically, we have three types of sets associated with any mapping $f : U \subset \mathbb{R}^m \to \mathbb{R}^n$ which play an important role in the study of manifolds and varieties — *level sets*, *images*, and *graphs*.

3.1. A mapping as a parametrisation of its image.

DEFINITION 2.4. (Baxandall and Liebeck [**9**, p.26]) Let U be open in $\mathbb{R}^m$. The **image** of a mapping $f : U \subset \mathbb{R}^m \to \mathbb{R}^n$ is the subset of $\mathbb{R}^n$ given by

$$\text{Image}\, f = \{\mathbf{y} \in \mathbb{R}^n \,|\, \mathbf{y} = f(\mathbf{x}),\ \forall \mathbf{x} \in U.\}$$

And, f is said to be a **parametrisation** of its image with parameters $(x_1, \ldots, x_m)$.

This definition suggests that *practically any mapping is a "parametrisation" of something* [**61**, p.263].

EXAMPLE 2.3. The mapping $f : \mathbb{R} \to \mathbb{R}^2$ defined by $f(t) = (\cos t, \sin t)$, $t \in \mathbb{R}$, has an image which is the unit circle $x^2 + y^2 = 1$ in $\mathbb{R}^2$ (Figure 1(a)). A distinct function with the same image as f is the mapping $g(t) = (\cos 2t, \sin 2t)$.

Example 2.3 suggests that two or more distinct mappings can have the same image. In fact, it can be proven that there is an infinity of different parametrisations of any non-empty subset of $\mathbb{R}^n$ [**9**, p.29]. Free-form curves and surfaces used in geometric design are just images in $\mathbb{R}^3$ of some parametrisation $\mathbb{R}^1 \to \mathbb{R}^3$ or $\mathbb{R}^2 \to \mathbb{R}^3$, respectively. The fact that an image can be parametrised by several mappings poses some problems to meet smoothness conditions when we patch together distinct parametrised curves or surfaces, simply because it is not easy to find a global reparametrisation for a compound

[1] A real, algebraic or analytic variety is a point set defined by a system of equations $f_1 = \ldots = f_k = 0$, where the functions f_i $(0 \leq i \leq k)$ are real, algebraic or analytic, respectively.

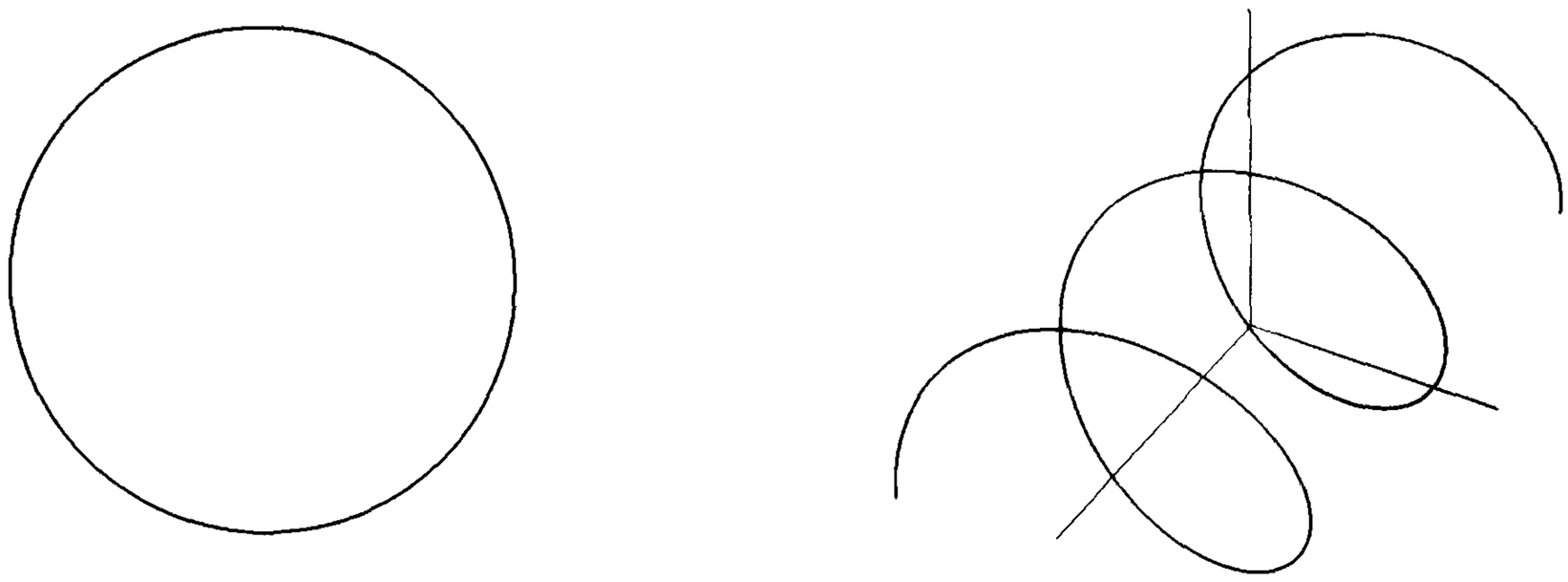

(a) (b)

FIGURE 1. (a) Image and (b) graph of $f(t) = (\cos t, \sin t)$.

curve or surface. Besides, the *smoothness of the component functions that describe the image of a mapping does not guarantee smoothness for its image.*

EXAMPLE 2.4. A typical example is the cuspidal cubic curve that is the image of a smooth mapping $f : \mathbb{R}^1 \to \mathbb{R}^2$ defined by $t \mapsto (t^3, t^2)$ which presents a cusp at $t = 0$, Figure 2(a). Thus, the cuspidal cubic is not a smooth curve.

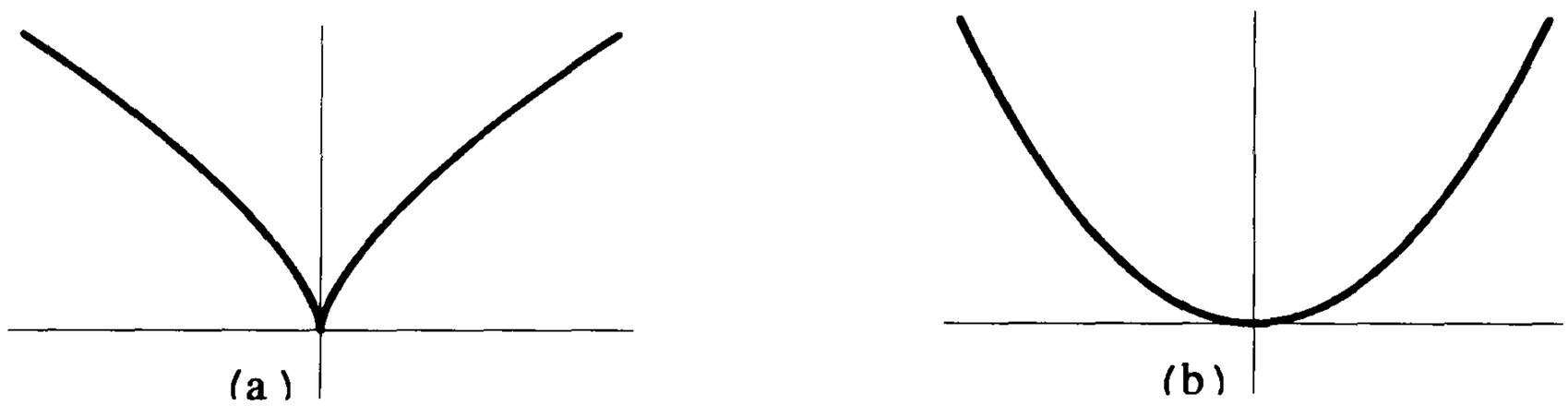

FIGURE 2. (a) Cuspidal cubic $x^3 = y^2$ and (b) parabola $y = x^2$ as *images* of different parametrisations.

Conversely, the *smoothness of the image of a mapping does not imply that such a mapping is smooth.* The following example illustrates this situation.

EXAMPLE 2.5. Let f, g and h be continuous mappings from $\mathbb{R}$ into $\mathbb{R}^2$ defined by the following rules:

$$f(t) = (t, t^2), \qquad g(t) = (t^3, t^6), \qquad \text{and} \qquad h(t) = \begin{cases} f(t), & t \geq 0, \\ g(t), & t < 0. \end{cases}$$

All three mappings have the same image, the parabola $y = x^2$ in $\mathbb{R}^2$, Figure 2(b). Their Jacobians are however distinct, $\mathrm{J}f(t) = [1 \quad 2t]$, $\mathrm{J}g(t) = [3t^2 \quad 6t^5]$, and $\mathrm{J}h(t) = \begin{cases} \mathrm{J}f(t), & t \geq 0, \\ \mathrm{J}g(t), & t < 0 \end{cases}$. As polynomials, f, g are differentiable or smooth everywhere. Furthermore, because of $\mathrm{J}f(t) \neq [0 \quad 0]$ for any $t \in \mathbb{R}$, f is C^1-invertible everywhere. Consequently, its image is surely smooth. The function g is also smooth, but its Jacobian is null at $t = 0$, i.e. $\mathrm{J}g(0) = [0 \quad 0]$. This means that g is not C^1-invertible, or, equivalently, g has a singularity at $t = 0$, even though its image is smooth. Thus, a singularity of a mapping does not necessarily determine a singularity on its image. Even more striking is the fact that h is not differentiable at $t = 0$ (the left and right derivatives have different values at $t = 0$). This is so despite the smoothness of the image of h. This kind of situation where a compound smooth curve is formed by piecing together smooth curve patches is common in geometric design of free-form curves and surfaces used in industry.

The discussion above shows that every parametric smooth curve, or, in general, a manifold can be described by several mappings, but at least one of them is surely smooth and invertible, i.e. a diffeomorphism. This is confirmed by the Corollary 2.1.

3.2. A level set of a mapping. Level sets of a mapping are varieties in some Euclidean space. That is, they are defined by equalities. Obviously, they are not necessarily smooth.

DEFINITION 2.5. (Dineen [**27**, p.6]) Let U be open in $\mathbb{R}^m$. Let $f : U \subset \mathbb{R}^m \to \mathbb{R}^n$ and $\mathbf{c} = (c_1, \ldots, c_n)$ a point in $\mathbb{R}^n$. A **level set** of f, denoted by $f^{-1}(\mathbf{c})$, is defined by the formula

$$f^{-1}(\mathbf{c}) = \{\mathbf{x} \in U \,|\, f(\mathbf{x}) = \mathbf{c}\}$$

In terms of coordinate functions $f_1, \ldots, f_n$ of f, we write

$$f(\mathbf{x}) = \mathbf{c} \Longleftrightarrow f_i(\mathbf{x}) = c_i \quad \text{for } i = 1, \ldots, n$$

and thus

$$f^{-1}(\mathbf{c}) = \bigcap_{i=1}^{n} \{\mathbf{x} \in U \,|\, f_i(\mathbf{x}) = c_i\} = \bigcap_{i=1}^{n} f_i^{-1}(c_i).$$

The smoothness criterion for a variety defined as a level set of a vector-valued function is given by the following theorem.

THEOREM 2.3. **(Implicit Function Theorem** , Baxandall [**9**, p.145]) *A set $X \subseteq \mathbb{R}^m$ is a smooth variety if it is a level set of a C^1 function $f : \mathbb{R}^m \to \mathbb{R}$ such that $\mathrm{J}f(\mathbf{x}) \neq 0$ for all $\mathbf{x} \in X$.*

This theorem is a particular case of the Implicit Mapping Theorem for mappings which are functions. The Implicit Mapping Theorem will be discussed later.

EXAMPLE 2.6. The circle $x^2+y^2=4$ is a variety in $\mathbb{R}^2$ that is a level set corresponding to the value 4 (i.e. point 4 in $\mathbb{R}$) of a function $f:\mathbb{R}^2\to\mathbb{R}$ given by $f(x,y)=x^2+y^2$. Its Jacobian is given by $\mathrm{J}f(x,y)=[2x \quad 2y]$ which is null at (0,0). However, the point $(0,0)$ is not on the circle $x^2+y^2=4$; hence the circle is a smooth curve.

EXAMPLE 2.7. The sphere $x^2+y^2+z^2=9$ is a smooth surface in $\mathbb{R}^3$. It is the level set for the value 9 of a C^1 function $f:\mathbb{R}^3\to\mathbb{R}$ defined by $f(x,y,z)=x^2+y^2+z^2$, and $\mathrm{J}f(x,y,z)\neq[0 \quad 0 \quad 0]$ at points on the sphere.

EXAMPLE 2.8. Let $f:\mathbb{R}^3\to\mathbb{R}$ be a function given by $f(x,y,z)=x^2+y^2-z^2$. Its level set corresponding to 0 is the right circular cone $z=\pm\sqrt{x^2+y^2}$, whose apex is the point $(0,0,0)$ as illustrated in Figure 3(a). The Jacobian $\mathrm{J}f(x,y,z)=[2x \quad 2y \quad -2z]$ is null at the apex. Hence, the cone is not smooth at the apex, and the apex is said to be a singularity. Nevertheless, the level sets of the same function for which $x^2+y^2-z^2=c\neq 0$ are smooth surfaces everywhere because the point $(0,0,0)$ is not on them. We have a hyperboloid of one sheet for $c>0$ and a hyperboloid of two sheets for $c<0$, as illustrated in Figure 3(b) and (c), respectively.

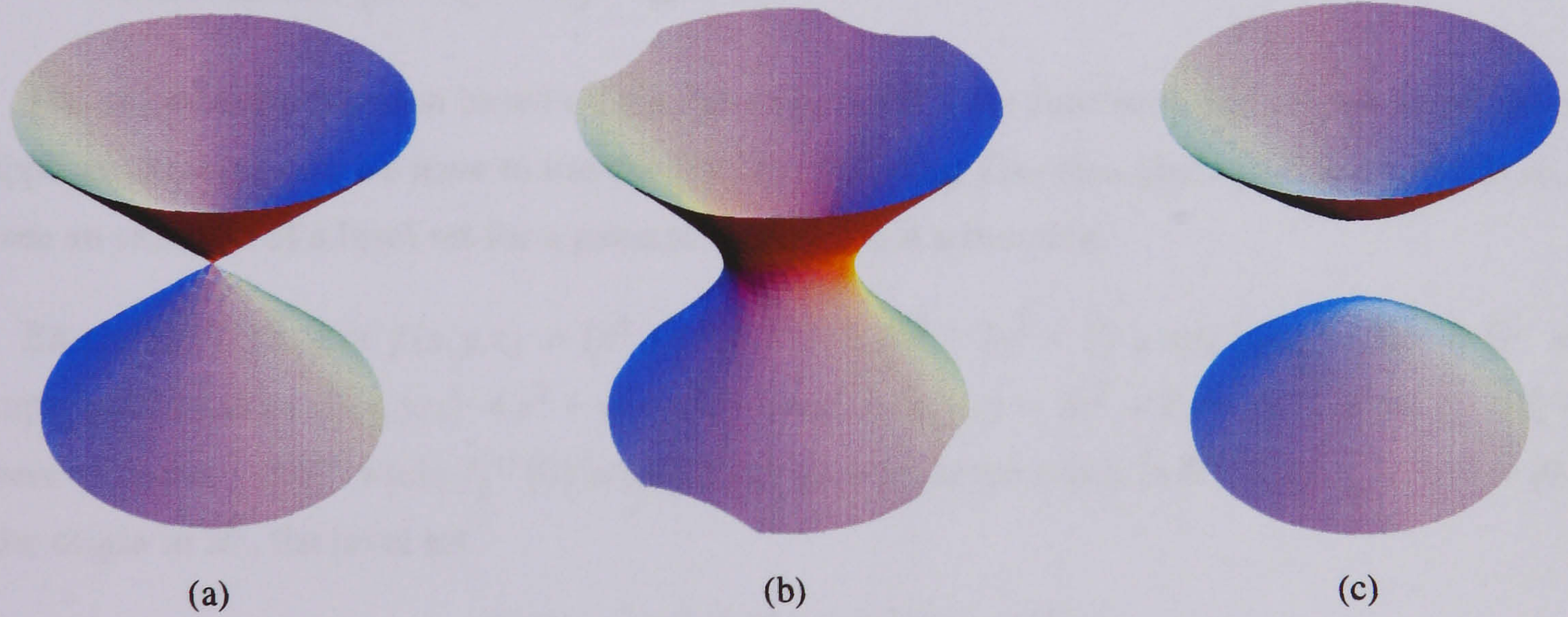

FIGURE 3. (a) Cone $x^2+y^2-z^2=0$; (b) hyperboloid of one sheet $x^2+y^2-z^2=a^2$; (c) hyperboloid of two sheets $x^2+y^2-z^2=-a^2$.

EXAMPLE 2.9. The Cartan umbrella with-handle $x^2-zy^2=0$ in $\mathbb{R}^3$ (Figure 4) is not smooth. It is defined as the zero set of the function $f(x,y,z)=x^2-zy^2$ whose Jacobian is $\mathrm{J}f(x,y,z)=$

$[2x \quad -2yz \quad -y^2]$. It is easy to see that the Cartan umbrella is not smooth along the z-axis, i.e. the singular point set $\{(0,0,z)\}$ where the Jacobian is zero. This singular point set is determined by the intersection $\{2x=0\}\cap\{-2yz=0\}\cap\{-y^2=0\}$, which basically yields the intersection of plane $\{x=0\}$ and plane $\{y=0\}$, i.e. the z-axis.

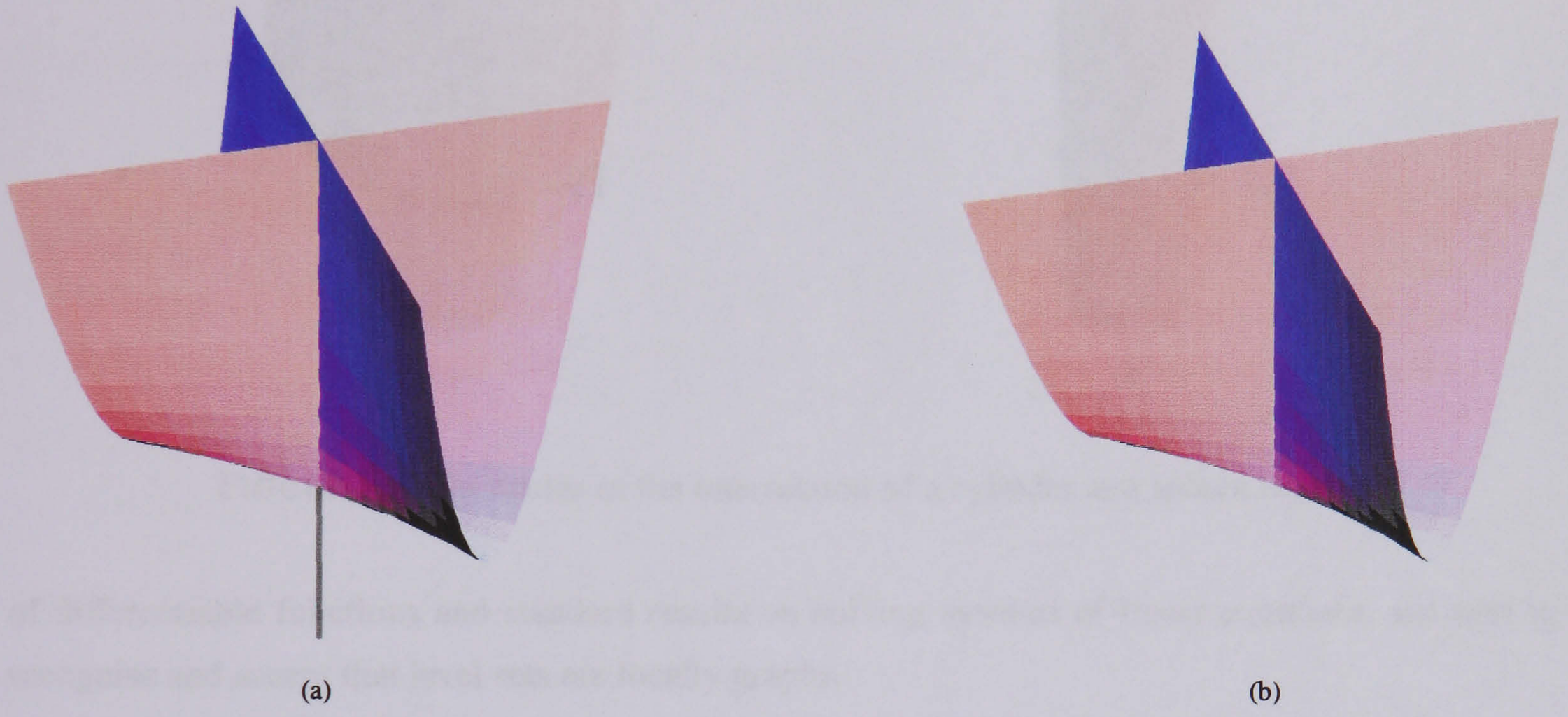

(a) (b)

FIGURE 4. (a) Cartan umbrella with-handle $x^2 - zy^2 = 0$; (b) Cartan umbrella without-handle $\{x^2 - zy^2 = 0\} - \{z < 0\}$.

The smoothness criterion based on the Jacobian is valid for functions and can be generalised to mappings. In this case, we have to use the Implicit Mapping Theorem given further on. Even so, let us see an example of a level set for a general mapping, not a function.

EXAMPLE 2.10. Let $f(x,y,z) = (x^2+y^2+z^2-1, 2x^2+2y^2-1)$ a mapping $f:\mathbb{R}^3 \to \mathbb{R}^2$ with component functions $f_1(x,y,z) = x^2+y^2+z^2-1$ and $f_2(x,y,z) = 2x^2+2y^2-1$. The set $f_1^{-1}(0)$ is a sphere of radius 1 in $\mathbb{R}^3$ while $f_2^{-1}(0)$ is a cylinder parallel to the z-axis in $\mathbb{R}^3$ (Figure 5). If $\mathbf{0} = (0,0)$ is the origin in $\mathbb{R}^2$, the level set

$$f^{-1}(\mathbf{0}) = f^{-1}(0,0) = f_1^{-1}(0)\cap f_2^{-1}(0)$$

is the intersection of a sphere and a cylinder in $\mathbb{R}^3$. Such an intersection consists of two circles on the sphere that can be obtained by solving the equations $f_1(x,y,z) = f_2(x,y,z) = 0$.

Let us see now the role of the differentiability in the local structure of level sets defined by general mappings as in Example 2.10. As noted in [**27**, p.11], by taking into account the linear approximation

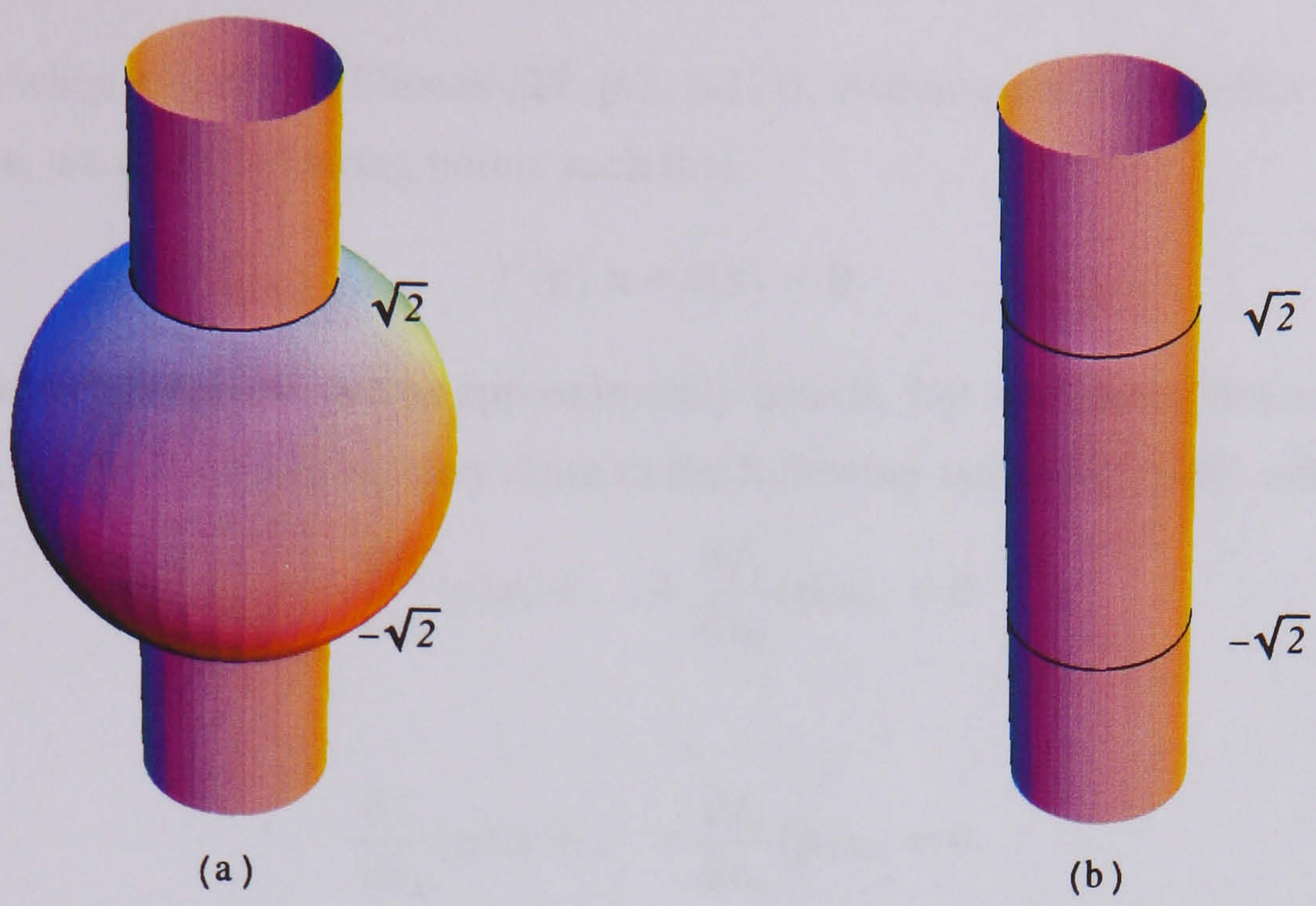

FIGURE 5. Two circles as the intersection of a cylinder and sphere in $\mathbb{R}^3$.

of differentiable functions and standard results on solving systems of linear equations, we start to recognise and accept that level sets are locally graphs.

Let $f : U \subset \mathbb{R}^m \to \mathbb{R}^n$, U an open subset of $\mathbb{R}^m$, $f = (f_1, \ldots, f_n)$, $\mathbf{c} = (c_1, \ldots, c_n)$. We assume that f is differentiable. Let us consider the level set $f^{-1}(\mathbf{c}) = \bigcap_{i=1}^{n} f_i^{-1}(c_i)$, i.e. the set whose points $(x_1, \ldots, x_m) \in U$ satisfy the equations

$$\begin{aligned} f_1(x_1, \ldots, x_m) &= c_1 \\ &\vdots \\ f_n(x_1, \ldots, x_m) &= c_n. \end{aligned} \tag{2}$$

We have m unknowns $(x_1, \ldots, x_m)$ and n equations. If each component function f_i is linear, we have a system of linear equations and the rank of the matrix gives us the number of linearly independent solutions, and information enough to identify a complete set of independent variables. The Implicit Mapping Theorem states that all this information can be *locally* obtained for differentiable mappings. This is due to the fact that differentiable mappings, by definition, enjoy a good local linear approximation.

If $\mathbf{p} \in f^{-1}(\mathbf{c})$, then $f(\mathbf{p}) = \mathbf{c}$. If $\mathbf{x} \in \mathbb{R}^n$ is close to zero, then, since f is differentiable, we have

$$f(\mathbf{p}+\mathbf{x}) = f(\mathbf{p}) + f'(\mathbf{p}).\mathbf{x} + \varepsilon(\mathbf{x})$$

where $\varepsilon(\mathbf{x}) \to 0$ when $\mathbf{x} \to 0$ (see Dineen [**27**, p.3, p.12]). Because we wish to find $\mathbf{x}$ close to $\mathbf{0}$ such that $f(\mathbf{p}+\mathbf{x}) = \mathbf{c}$, we are considering points such that

$$f'(\mathbf{p}).\mathbf{x} + \varepsilon(\mathbf{x}) = \mathbf{0}$$

and thus $f'(\mathbf{p}).\mathbf{x} \approx \mathbf{0}$ (where $\approx$ means approximately equal). Let us assume that $m \geq n$. Therefore, not surprisingly, we have something very close to the following system of linear equations

$$\begin{aligned} \frac{\partial f_1}{\partial x_1}(\mathbf{p})x_1 + \ldots + \frac{\partial f_1}{\partial x_m}(\mathbf{p})x_m &= 0 \\ &\vdots \\ \frac{\partial f_n}{\partial x_1}(\mathbf{p})x_1 + \ldots + \frac{\partial f_n}{\partial x_m}(\mathbf{p})x_m &= 0, \end{aligned} \tag{3}$$

whose matrix is the Jacobian $\mathrm{J}f$.

From linear algebra we know that

$$\begin{aligned} \operatorname{rank}\mathrm{J}f = n &\iff n \text{ rows of } \mathrm{J}f \text{ are linearly independent} \\ &\iff n \text{ columns of } \mathrm{J}f \text{ are linearly independent} \\ &\iff \mathrm{J}f \text{ contains } n \text{ columns, and the associated } n \times n \text{ matrix has non-zero determinant} \\ &\iff \text{the space of solutions of the system 3 is } (m-n)\text{-dimensional.} \end{aligned} \tag{4}$$

Besides, if any of the conditions (3) are satisfied, and we select n columns which are linearly independent then the variables concerning the remaining columns can be taken as a complete set of independent variables. If the conditions (3) are satisfied, we say that f has full or maximum rank at $\mathbf{p}$.

EXAMPLE 2.11. Let us consider the following system of equations

$$\begin{aligned} 2x - y + z &= 0 \\ y - w &= 0, \end{aligned}$$

whose matrix of coefficients is

$$\mathrm{A} = \begin{bmatrix} 2 & -1 & 1 & 0 \\ 0 & 1 & 0 & -1 \end{bmatrix}.$$

The submatrix $\begin{bmatrix} 2 & -1 \\ 0 & 1 \end{bmatrix}$ is obtained by taking the first two columns from A, and has determinant $2 \neq 0$. Thus, A has rank 2, or, equivalently, the two rows are linearly independent. So, the two

variables z, w in the remaining two columns can be taken as the independent variables. In other words, $y = w$, $2x = y - z = w - z$, and hence $\{(\frac{w-z}{2}, w, z, w) : z \in \mathbb{R}, w \in \mathbb{R}\}$ is the solution set. Alternatively, the solution set can be written in the following form

$$\{(g(z,w), z, w) : (z,w) \in \mathbb{R}^2\}$$

where $g(z,w) = (\frac{w-z}{2}, w)$ is a mapping $g : \mathbb{R}^2 \to \mathbb{R}^2$. In this format, the solution space is the graph of g (defined in the next subsection).

Assuming that the rows of $\mathrm{J}f(\mathbf{p})$ are linearly independent is equivalent to supposing that the gradient vectors $\{\nabla f_1(\mathbf{p}), \ldots, \nabla f_n(\mathbf{p})\}$ are linearly independent in $\mathbb{R}^m$. The Implicit Mapping Theorem states that with this condition we can solve the non-linear system of equations (2) near $\mathbf{p}$ and apply the same approach to identify a set of independent variables. The hypothesis of a good linear approximation in the definition of differentiable functions implies that the equation systems (2) and (3) are very close to one another [**27**, p.13]. Roughly speaking, this linear approximation is the tangent space to the solution set defined by the at $\mathbf{p}$.

THEOREM 2.4. *Let $f : U \subset \mathbb{R}^m \to \mathbb{R}^n$ $(m \geq n)$ be a differentiable mapping, let $\mathbf{p} \in U$ and assume that $f(\mathbf{p}) = \mathbf{c}$ and $\operatorname{rank} \mathrm{J}f(\mathbf{p}) = n$. For convenience, we also assume that the last n columns of the Jacobian are linearly independent. If $\mathbf{p} = (p_1, \ldots, p_m)$, let $\mathbf{p}_1 = (p_1, \ldots, p_{m-n})$ and $\mathbf{p}_2 = (p_{m-n+1}, \cdots, p_m)$ so that $\mathbf{p} = (\mathbf{p}_1, \mathbf{p}_2)$. Then, there exists an open set $V \subset \mathbb{R}^{m-n}$ containing $\mathbf{p}_1$, a differentiable mapping $g : V \to \mathbb{R}^n$, an open subset $U' \subset U$ containing $\mathbf{p}$ such that $g(\mathbf{p}_1) = \mathbf{p}_2$ and*

$$f^{-1}(\mathbf{c}) \cap U' = \{(\mathbf{x}, g(\mathbf{x})) : \mathbf{x} \in V\} = \operatorname{graph} g.$$

Therefore, locally every level set is a graph.

3.3. The graph of a mapping.

DEFINITION 2.6. (Dineen [**27**, p.6]) Let U be open in $\mathbb{R}^m$. The **graph** of a mapping $f : U \subset \mathbb{R}^m \to \mathbb{R}^n$ is the subset of the product space $\mathbb{R}^{m+n} = \mathbb{R}^m \times \mathbb{R}^n$ defined by

$$\operatorname{graph} f = \{(\mathbf{x}, \mathbf{y}) \,|\, \mathbf{x} \in U \text{ and } \mathbf{y} = f(\mathbf{x})\}$$

or

$$\operatorname{graph} f = \{(\mathbf{x}, f(\mathbf{x})) \,|\, \mathbf{x} \in U\}.$$

EXAMPLE 2.12. Let us consider both mappings $f(t) = (\cos t, \sin t)$ and $g(t) = (\cos 2t, \sin 2t)$ of Example 2.3. They have the same image in $\mathbb{R}^2$, say a unit circle. However, their graphs are distinct

point sets in $\mathbb{R}^3$. The graph of f is a circular helix $(t, \cos t, \sin t)$ in $\mathbb{R}^3$, Figure 1(b). But, although the graph of g is a circular helix with windings being around the same circular cylinder, those windings have half the pitch.

This suggests that there is a 1-1 correspondence between a mapping and its graph, that different mappings have distinct graphs. This leads us to think of a possible relationship between the smoothness of a mapping and the smoothness of its graph. In other words, the smoothness of a mapping determines the smoothness of its graph. This is corroborated by the following theorem.

THEOREM 2.5. (Baxandall [**9**, p.147]) *The* graph *of a* C^1 *mapping* $f : U \subseteq \mathbb{R}^m \to \mathbb{R}^n$ *is a smooth variety in* $\mathbb{R}^m \times \mathbb{R}^n$.

PROOF. Consider the mapping $F : U \times \mathbb{R}^n \subseteq \mathbb{R}^m \times \mathbb{R}^n \to \mathbb{R}^n$ defined by

$$F(\mathbf{x}, \mathbf{y}) = f(\mathbf{x}) - \mathbf{y}, \quad \mathbf{x} \in U, \mathbf{y} \in \mathbb{R}^n.$$

The graph of f is the level set of F corresponding to the value $\mathbf{0}$, that is

$$\operatorname{graph} f = \{(\mathbf{x}, \mathbf{y}) \in \mathbb{R}^m \times \mathbb{R}^n \mid f(\mathbf{x}) - \mathbf{y} = \mathbf{0}\}.$$

To prove that graph f is a smooth variety in $\mathbb{R}^m \times \mathbb{R}^n$ we show that:

(i) F is a C^1 mapping.

(ii) $J_F(\mathbf{x}, \mathbf{y}) \neq (\mathbf{0}, \mathbf{0})$ for all $\mathbf{x} \in U$, $\mathbf{y} \in \mathbb{R}^n$.

It follows from the definition of F above that for each $i = 1, \ldots, m$, $j = m+1, \ldots, m+n$ and each $\mathbf{x} \in U$, $\mathbf{y} \in \mathbb{R}^n$

$$\frac{\partial F}{\partial x_i}(\mathbf{x}, \mathbf{y}) = \frac{\partial f}{\partial x_i}(\mathbf{x}) \quad \text{and} \quad \frac{\partial F}{\partial y_j}(\mathbf{x}, \mathbf{y}) = -1.$$

Therefore the partial derivatives of F are continuous and so F is a C^1 mapping.

Also, for any $\mathbf{x} \in U$, $\mathbf{y} \in \mathbb{R}^n$

$$\mathrm{J}F(\mathbf{x}, \mathbf{y}) = (\mathrm{J}f(\mathbf{x}), -\mathbf{1}) \neq (\mathbf{0}, \mathbf{0}).$$

This completes the proof. □

EXAMPLE 2.13. Let us consider the curves sketched in Figure 6. In Figure 6(a) we have a curve $y = |x|$ in $\mathbb{R}^2$ that is not smooth. It is the graph of the function $f : \mathbb{R} \to \mathbb{R}$ that expresses y as a function of x, but f is not differentiable at $x = 0$. Nor is it the graph of a (inverse) function g expressing x as a function of y, because in the neighbourhood of $(0,0)$ the same value of y corresponds to two values of x.

In Figure 6(b) we see another non-smooth curve $xy = 0$ in $\mathbb{R}^2$ that is the union of the two coordinate axes, x and y. In fact, in any neighbourhood of $(0,0)$, there are infinitely many y's corresponding to $x = 0$, and infinitely many x's corresponding to $y = 0$, so it is not a graph of a function either way. Finally, the graph of the function $f(x) = x^{1/3}$, depicted in Figure 6(c), is a smooth curve. Note that the curve is smooth despite the function being not differentiable at $x = 0$. This happens because the curve is the graph of the function $x = f(y) = y^3$ is differentiable.

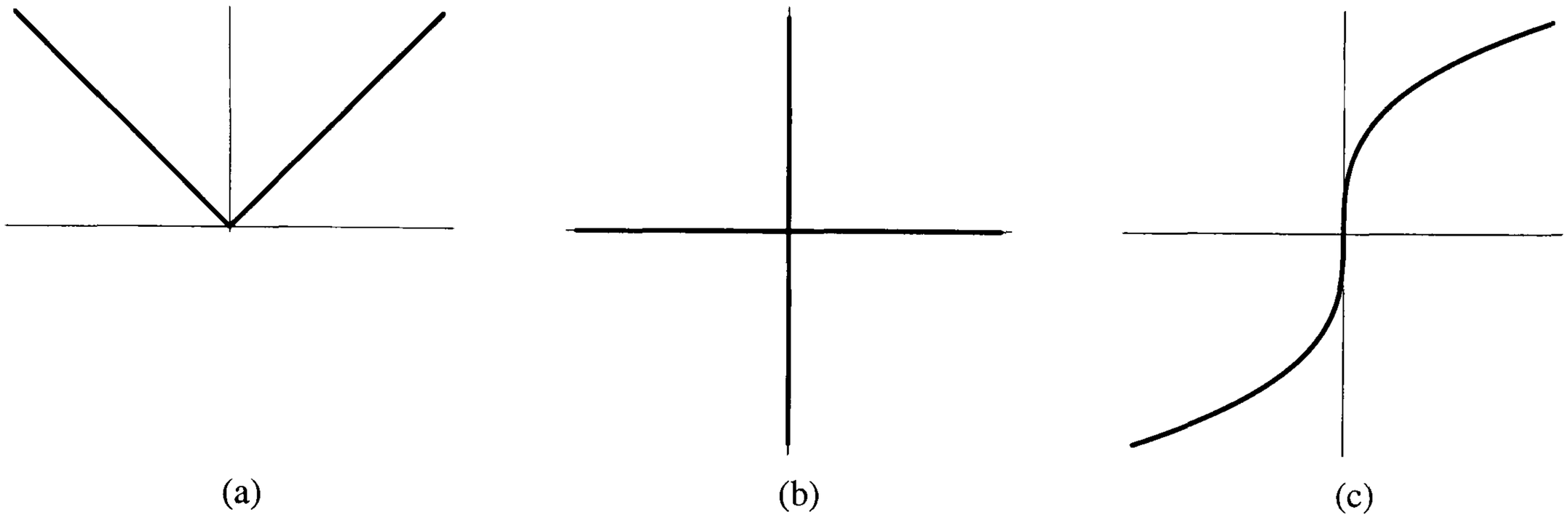

FIGURE 6. Not all point sets in $\mathbb{R}^2$ are graphs of a mapping.

From these examples, we come to the following conclusions:

- Rewording Theorem 2.5, every point set that is the graph of a differentiable mapping is smooth.
- The fact that a mapping is not differentiable does not imply that its graph is not smooth; but if the graph is smooth, then it is necessarily the graph of a related function by changing the roles of the variables, possibly the inverse function. This is the case for the curve $x = y^3$ in Figure 6(c).
- The graph of a mapping that is not differentiable is possibly non-smooth. This happens because of the differentiable singularities such as the cusp point in $y = |x|$, Figure 6.
- There are point sets in $\mathbb{R}^n$ which cannot be described as graphs of mappings, unless we break them up into pieces. For example, with appropriate constraints we could split $xy = 0$ (the union of axes in $\mathbb{R}^2$) into the origin and four half-axes, each piece described by a function. The origin is a cut point of $xy = 0$, that is, a topological singularity. The idea of partitioning a point set into smaller point sets by its topological singularities leads to a particular sort of stratification as detailed in the next chapter. Another alternative to describe a point set that is not describable by a graph of a function is to describe it as a level set of a function.

The relationship between graphs and level sets plays an important role in the study of varieties. It is easy to see that *every graph is a level set.* Let us consider a mapping $f : U \subseteq \mathbb{R}^m \to \mathbb{R}^n$. We define $F : U \times \mathbb{R}^m \to \mathbb{R}^n$ by $F(\mathbf{x}, \mathbf{y}) = f(\mathbf{x}) - \mathbf{y}$. If $\mathbf{0}$ is the origin in $\mathbb{R}^n$, we have

$$\begin{aligned}(\mathbf{x}, \mathbf{y}) \in F^{-1}(\mathbf{0}) &\iff F(\mathbf{x}, \mathbf{y}) = \mathbf{0} \\ &\iff f(\mathbf{x}) - \mathbf{y} = \mathbf{0} \\ &\iff (\mathbf{x}, \mathbf{y}) \in \operatorname{graph} f.\end{aligned}$$

Thus, $F^{-1}(\mathbf{0}) = \operatorname{graph} f$ and every graph is a level set. This fact has been used to prove the Theorem 2.5. As a summary, we can say that:

- Not all varieties in some Euclidean space are graphs of a mapping.
- Every variety as a graph of a mapping is a level set.
- Every variety is a level set of a mapping.

This shows us why the study of algebraic and analytic varieties in geometry is carried out using level sets of mappings, i.e. point sets defined implicitly. The reason is a bigger geometric coverage of point sets in some Euclidean space. In addition to this, many (not necessarily smooth) varieties admit a global parametrisation, whilst others can only be partially (locally) and piecewise parametrised.

EXAMPLE 2.14. Let $z = x^2 - y^2$ be a level set of a function $F : \mathbb{R}^3 \to \mathbb{R}$ defined by $F(x, y, z) = x^2 - y^2 - z$ corresponding to the value 0. It is observed that $JF(x, y, z) = [2x \quad -2y \quad -1]$ is not zero everywhere. So $z = x^2 - y^2$ in $\mathbb{R}^3$ is smooth everywhere. It is a variety known as a *saddle surface.* Note that z is explicitly defined in terms of x and y. So, the saddle surface can be viewed as the graph of the function $f : \mathbb{R}^2 \to \mathbb{R}$ given by $f(x, y) = x^2 - y^2$. Consequently, the saddle surface can be given a global parametrisation $g : \mathbb{R}^2 \to \mathbb{R}^3$ defined by $g(x, y) = (x, y, x^2 - y^2)$.

Not all varieties can be *globally* parametrised, even when they are smooth. But, as proved later, every smooth level set can be always *locally* parametrised, i.e. every smooth level set is locally a graph. This fact is proved by the Implicit Mapping Theorem.

Level sets correspond to implicit representations, say functions, on some Euclidean space, while graphs correspond to explicit representations. In fact, we have from calculus that

DEFINITION 2.7. (Baxandall and Liebeck [**9**, p.226]) Let $f : X \subseteq \mathbb{R}^m \to \mathbb{R}$ be a function, where $m \geq 2$. If there exists a function $g : Y \subseteq \mathbb{R}^{m-1} \to \mathbb{R}$ such that for all $(x_1, \ldots, x_{m-1}) \in Y$,

$$f(x_1, \ldots, x_{m-1}, g(x_1, \ldots, x_{m-1})) = 0,$$

then the function g is said to be defined **implicitly** on Y by the *equation*

$$f(x_1,\ldots,x_m)=0.$$

Likewise, the graph of $g: Y\subseteq\mathbb{R}^{m-1}\to\mathbb{R}$ is the subset of $\mathbb{R}^m$ given by

$$\{(x_1,\ldots,x_{m-1},x_m)\in\mathbb{R}^m \mid x_m=g(x_1,\ldots,x_{m-1})\}.$$

The expression $x_m=g(\mathbf{x})$ is called the *equation* of the graph [**9**, p.100]. Hence, g is said to be **explicitly** defined on Y by the *equation* $x_m=g(x_1,\ldots,x_{m-1})$.

EXAMPLE 2.15. The graph of the function $f(x,y)=-x^2-y^2$ has equation $-z=x^2+y^2$. This graph is a 2-manifold in $\mathbb{R}^3$ called a paraboloid (Figure 7). The equation $-z=x^2+y^2$ *explicitly* defines the paraboloid in $\mathbb{R}^3$. For $c<0$ the plane $z=c$ intersects the graph in a circle lying below the level set $x^2+y^2=-c$ in the (x,y)-plane. The equation $x^2+y^2=-c$ of a circle (i.e. a 1-manifold) in $\mathbb{R}^2$ is said to define y *implicitly* in terms of x. This circle is said to be an implicit 1-manifold.

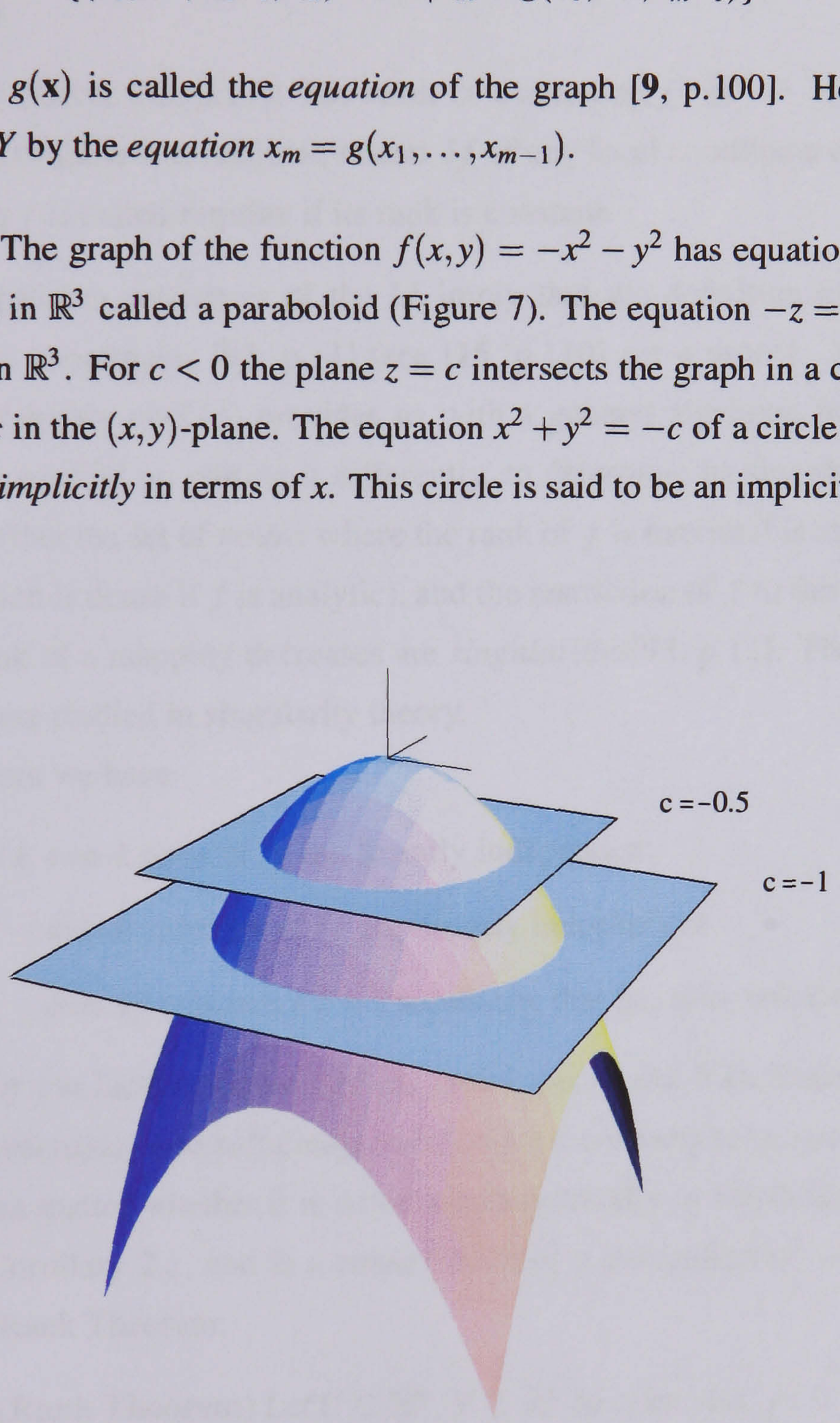

FIGURE 7. The paraboloid $-z=x^2+y^2$ in $\mathbb{R}^3$.

4. Rank-based smoothness

Now, we are in position to show that the rank of a mapping gives us a general approach to check the C^r invertibility or C^r smoothness of a mapping, and whether or not a variety is smooth. This smoothness test is carried out independently of how a variety is defined, implicitly, explicitly or parametrically, i.e. no matter whether a variety is considered a level set, a graph, or an image of a mapping, respectively.

DEFINITION 2.8. (Olver [**93**, p.11]) The **rank** of a mapping $f : \mathbb{R}^m \to \mathbb{R}^n$ at a point $\mathbf{p} \in \mathbb{R}^m$ is defined to be the rank of the $n \times m$ Jacobian matrix $\mathrm{J}f$ of any local coordinate expression for f at the point $\mathbf{p}$. The mapping f is called **regular** if its rank is constant.

Standard transformation properties of the $\mathrm{J}f$ imply that the definition of rank is independent of the choice of local coordinates [**93**, p.11] (see [**15**, p.110] for a proof). Moreover, the rank of the Jacobian matrix (shortly $\mathrm{rank}\mathrm{J}f$) provides us with a general algebraic procedure to check the smoothness of a submanifold or, putting it differently, to determine its singularities. It is proved in differential geometry that the set of points where the rank of f is maximal is an open submanifold of the manifold $\mathbb{R}^m$ (which is dense if f is analytic), and the restriction of f to this subset is regular. The subsets where the rank of a mapping decreases are *singularities*[**93**, p.11]. The types and properties of such singularities are studied in singularity theory.

From linear algebra we have

$$\begin{aligned}\mathrm{rank}\mathrm{J}f = k &\iff k \text{ rows of } \mathrm{J}f \text{ are linearly independent}\\ &\iff k \text{ columns of } \mathrm{J}f \text{ are linearly independent}\\ &\iff \mathrm{J}f \text{ contains a } k \times k \text{ submatrix that has non-zero determinant.}\end{aligned}$$

The fact that the $n \times m$ Jacobian matrix $\mathrm{J}f$ has rank k means that it includes a $k \times k$ submatrix that is invertible. Thus, a necessary and sufficient condition for a k-variety to be smooth is that $\mathrm{rank}\mathrm{J}f = k$ at every point of it, no matter whether it is defined parametrically or implicitly by f. This is clearly a generalisation of Corollary 2.1, and is a consequence of a generalisation of the Inverse Mapping Theorem, called the Rank Theorem:

THEOREM 2.6. (**Rank Theorem**) *Let $U \subset \mathbb{R}^m$, $V \subset \mathbb{R}^n$ be open sets, $f : U \to V$ be a C^r mapping, and suppose that* $\mathrm{rank}\mathrm{J}f = k$. *If $\mathbf{p} \in U$ and $\mathbf{q} = f(\mathbf{p})$, there exists open sets $U_0 \subset U$ and $V_0 \subset V$ with $\mathbf{p} \in U_0$ and $\mathbf{q} \in V_0$, and there exists C^r diffeomorphisms*

$$\phi : U_0 \to X \subset \mathbb{R}^m,$$

$$\psi : V_0 \to Y \subset \mathbb{R}^n$$

with X, Y *open in* $\mathbb{R}^m, \mathbb{R}^n$ *respectively,such that*

$$\psi \circ f \circ \phi^{-1}(X) \subset Y$$

and such that this mapping has the simple form

$$\psi \circ f \circ \phi^{-1}(p_1, \ldots, p_m) = (p_1, \ldots, p_k, 0, \ldots, 0).$$

PROOF. See Boothby [**15**, p.47]. □

This is a very important theorem because it states that a mapping of constant rank k behaves *locally* as a projection of $\mathbb{R}^m = \mathbb{R}^k \times \mathbb{R}^{m-k}$ to $\mathbb{R}^k$ followed by injection of $\mathbb{R}^k$ onto $\mathbb{R}^k \times \{0\} \subset \mathbb{R}^k \times \mathbb{R}^{n-k} = \mathbb{R}^n$.

4.1. Rank-based smoothness for parametrisations. The Rank Theorem for parametrisations is as follows:

THEOREM 2.7. (**Rank Theorem for parametrisations**) *Let* U *be an open set in* $\mathbb{R}^m$ *and* $f : U \to \mathbb{R}^n$. *A necessary and sufficient condition for the* C^∞ *mapping* f *to be a diffeomorphism from* U *to* $f(U)$ *is that it be one-to-one and the Jacobian* $\mathrm{J}f$ *have rank* m *at every point of* U.

PROOF. See Boothby [**15**, p.46]. □

This is a generalisation of Corollary 2.1, with $m \leq n$. It means that the kernel[2] of the linear mapping represented by $\mathrm{J}f$ is 0 precisely when the Jacobian matrix has rank m.

Let us review some simple examples of parametrised curves.

EXAMPLE 2.16. We know that the bent curve in $\mathbb{R}^2$ depicted in Figure 6 and defined by the parametrisation $f(t) = (t, |t|)$ is not differentiable at $t = 0$, even though its rank is 1 everywhere.

Example 2.16 shows that differentiability test should always precede the rank test in order to detect differentiable singularities.

EXAMPLE 2.17. A parametrised curve that passes the differentiability test, but not the rank test, is the cuspidal cubic in $\mathbb{R}^2$ given by $f(t) = (t^3, t^2)$ (Figure 2(a)). The component functions are polynomials and therefore differentiable. However, the $\operatorname{rank} \mathrm{J}f(t) = [3t^2 \quad 2t]$ is not 1 (i.e. its maximal

[2]Let $F : X \to Y$ be a linear mapping of vector spaces. By the *kernel* of F, denoted by kernel F, is meant the set of all those vectors $\mathbf{x} \in X$ such that $F(V) = \mathbf{0} \in Y$, i.e. kernel $F = \{\mathbf{x} \in X : F(\mathbf{x}) = \mathbf{0}\}$ (see Edwards [**33**, p.29]). In other words, the kernel of a linear mapping corresponds to the level set of a mapping.

value) at $t = 0$; in fact it is zero. This means that the parametrised cuspidal cubic is not smooth at $t = 0$, that is, it possesses a singularity at $t = 0$.

EXAMPLE 2.18. Let us take the parametrised parabola in $\mathbb{R}^2$ given by $f(t) = (t, t^2)$ (Figure 2(b)). f is obviously differentiable, and its rank is 1 everywhere, so it is globally smooth.

Nevertheless, algorithmic detection of singularities of a parametrised variety fails for self-intersections, i.e. topological singularities. Let us see some examples.

EXAMPLE 2.19. The curve parametrised by the differentiable mapping $f(t) = (t^3 - 3t - 2, t^2 - t - 2)$ is not smooth at $(0,0)$, despite the differentiability of f and its maximal rank. In fact, we get the same point $(0,0)$ on the curve for two distinct points $t = -1$ and $t = 2$ of the domain, that is, $f(-1) = f(2) = (0,0)$, and thus f is not one-to-one. These singularities are known as *self-intersections* in geometry or *topological singularities* in topology. In fact, the point $(0,0)$ of this curve is a cut point. Its local topological type is different from any other point.

The problem with a parametrised self-intersecting variety is that its self-intersections are topological singularities for the corresponding underlying topological space, but not for the parametrisation. However, it is an easy task to check whether a non-self-intersecting point in a parametrised variety is singular or not. A non-self-intersecting point is singular if the rank of Jacobian at this point is not maximal.

EXAMPLE 2.20. Let us consider a parametrisation $f(u,v) = (uv, u, v^2)$ of the Cartan umbrella without-handle (the negative z-axis) (Figure 4(b)). The effect of this parametrisation on $\mathbb{R}^2$ can be described as the 'fold' of the v-axis at the origin $(0,0)$ in order to superimpose negative v-axis and positive v-axis. The 'fold' is identified by the exponent 2 of the third component coordinate function. Thus, all points $(0,0,v^2)$ along v-axis are double points and determine that all points on the positive z-axis are singularities or self-intersecting points in $\mathbb{R}^3$. However, this is not so apparent if we restrict the discussion to the Jacobian and try to determine where the rank drops below 2. In fact,

$$\mathrm{J}f(u,v) = \begin{bmatrix} v & u \\ 1 & 0 \\ 0 & 2v \end{bmatrix}$$

and we observe that the rank drops below 2 only at $(0,0)$. This happens because only $(0,0)$ is a differential singularity, that is, the tangent plane is not defined at $(0,0)$. Any other point on the positive z-axis has a parametrised neighbourhood that can be approximated by a tangent plane in relation to the parametrisation.

EXAMPLE 2.21. Let $f : \mathbb{R}^2 \to \mathbb{R}^3$ be the mapping given by

$$f(x,y) = (\sin x, e^x \cos y, \sin y).$$

Then

$$\mathrm{J}f(x,y) = \begin{bmatrix} \cos x & 0 \\ e^x \cos y & -e^x \sin y \\ 0 & \cos y \end{bmatrix}$$

and hence

$$\mathrm{J}f(0,0) = \begin{bmatrix} 1 & 0 \\ 1 & 0 \\ 0 & 1 \end{bmatrix}$$

has rank 2, so that in a neighbourhood of $(0,0)$, the mapping f parametrises a subset of $\mathbb{R}^3$.

4.2. Rank-based smoothness for implicitations. The Implicit Function Theorem is particularly useful for geometric modelling because it provides us with a computational tool to test whether an implicit manifold, and more generally a variety, is smooth in the neighbourhood of a point. Specifically, it gives us a local parametrisation for which it is possible to check the local C^r-invertibility by means of its Jacobian.

Before proceeding, let us see how C^r-invertibility and smoothness is defined for implicit manifolds and varieties.

THEOREM 2.8. (**Rank Theorem for implicitations**) *Let U be open in $\mathbb{R}^m$ and let $f : U \to \mathbb{R}$ be a C^r function on U. Let $(\mathbf{p}, q) = (p_1, \ldots, p_{m-1}, q) \in U$ and assume that $f(\mathbf{p}, q) = 0$ but $\frac{\partial f}{\partial x_m}(\mathbf{p}, q) \neq 0$. Then the mapping*

$$F : U \to \mathbb{R}^{m-1} \times \mathbb{R} = \mathbb{R}^m$$

given by

$$(\mathbf{x}, y) \mapsto (\mathbf{x}, f(\mathbf{x}, y))$$

is locally C^r-invertible at $(\mathbf{p}, q)$.

PROOF. (See Lang [**68**, p.523]). All we need to do is to compute the derivative of F at $(\mathbf{p}, q)$. We write F in terms of its coordinates, $F = (F_1, \ldots, F_{m-1}, F_m) = (x_1, \ldots, x_{m-1}, f)$. Its Jacobian matrix is

therefore

$$\mathrm{J}F(\mathbf{x}) = \begin{bmatrix} 1 & 0 & \dots & & 0 \\ 0 & 1 & \dots & & 0 \\ \vdots & & \ddots & & \vdots \\ 0 & & \dots & 1 & 0 \\ \frac{\partial f}{\partial x_1} & \frac{\partial f}{\partial x_2} & \dots & & \frac{\partial f}{\partial x_m} \end{bmatrix}$$

and is invertible since its determinant is equal to $\frac{\partial f}{\partial x_m} \neq 0$ at $(\mathbf{p}, q)$. The Inverse Function Theorem guarantees that F is locally C^r-invertible at $(\mathbf{p}, q)$. □

As a corollary of this Theorem, we have the Implicit Function Theorem for functions of several variables.

THEOREM 2.9. (**Implicit Function Theorem**) *Let U be open in $\mathbb{R}^m$ and let $f : U \to \mathbb{R}$ be a C^r function on U. Let $(\mathbf{p}, q) = (p_1, \dots, p_{m-1}, q) \in U$ and assume that $f(\mathbf{p}, q) = 0$ but $\frac{\partial f}{\partial x_m}(\mathbf{p}, q) \neq 0$. Then there exists an open ball V in $\mathbb{R}^{m-1}$ centered at $\mathbf{p}$ and a C^r function*

$$g : V \to \mathbb{R}$$

such that $g(\mathbf{p}) = q$ and

$$f(\mathbf{x}, g(\mathbf{x})) = 0$$

for all $\mathbf{x} \in V$.

PROOF. (See Lang [**68**, p.524]). By Theorem 2.8 we know that the mapping

$$F : U \to \mathbb{R}^{m-1} \times \mathbb{R} = \mathbb{R}^m$$

given by

$$(\mathbf{x}, y) \mapsto (\mathbf{x}, f(\mathbf{x}, y))$$

is locally C^r-invertible at $(\mathbf{p}, q)$. Let $F^{-1} = (F_1^{-1}, \dots, F_m^{-1})$ be the local inverse of F such that

$$F^{-1}(\mathbf{x}, z) = (\mathbf{x}, F_m^{-1}(\mathbf{x}, z)) \quad \text{for} \quad \mathbf{x} \in \mathbb{R}^{m-1}, z \in \mathbb{R}.$$

We let $g(\mathbf{x}) = F_m^{-1}(\mathbf{x}, 0)$. Since $F(\mathbf{p}, q) = (\mathbf{p}, 0)$ it follows that $F_m^{-1}(\mathbf{p}, 0) = q$ so that $g(\mathbf{p}) = q$. Furthermore, since F, F^{-1} are inverse mappings, we obtain

$$(\mathbf{x}, 0) = F(F^{-1}(\mathbf{x}, 0)) = F(\mathbf{x}, g(\mathbf{x})) = (\mathbf{x}, f(\mathbf{x}, g(\mathbf{x}))).$$

This proves that $f(\mathbf{x}, g(\mathbf{x})) = 0$, as shown by previous equality. □

Note that we have expressed y as a function of $\mathbf{x}$ explicitly by means of g, starting with what is regarded as an implicit relation $f(\mathbf{x},y)=0$. Besides, from the Implicit Function Theorem, we see that the mapping G given by

$$\mathbf{x}\mapsto(\mathbf{x},g(\mathbf{x}))=G(\mathbf{x})$$

or writing down the coordinates

$$(x_1,\ldots,x_{m-1})\mapsto(x_1,\ldots,x_{m-1},g(x_1,\ldots,x_{m-1}))$$

provides a *parametrisation* of the variety defined by the *equation* $f(x_1,\ldots,x_{m-1},y)=0$ in the neighbourhood of a given point $(\mathbf{p},q)$. This is illustrated in Figure 8 for convenience. On the right, we have the surface $f(\mathbf{x})=0$, and we have also pictured the gradient $\operatorname{grad} f(\mathbf{p},q)$ at the point $(\mathbf{p},q)$ as in Theorem 2.9. Note that the condition $\frac{\partial f}{\partial x_m}(\mathbf{p},q)\neq 0$ in Theorem 2.9 implies that the $\operatorname{grad} f(\mathbf{p},q)=[\frac{\partial f}{\partial x_1}\quad\frac{\partial f}{\partial x_2}\quad\ldots\quad\frac{\partial f}{\partial x_m}]\neq 0$.

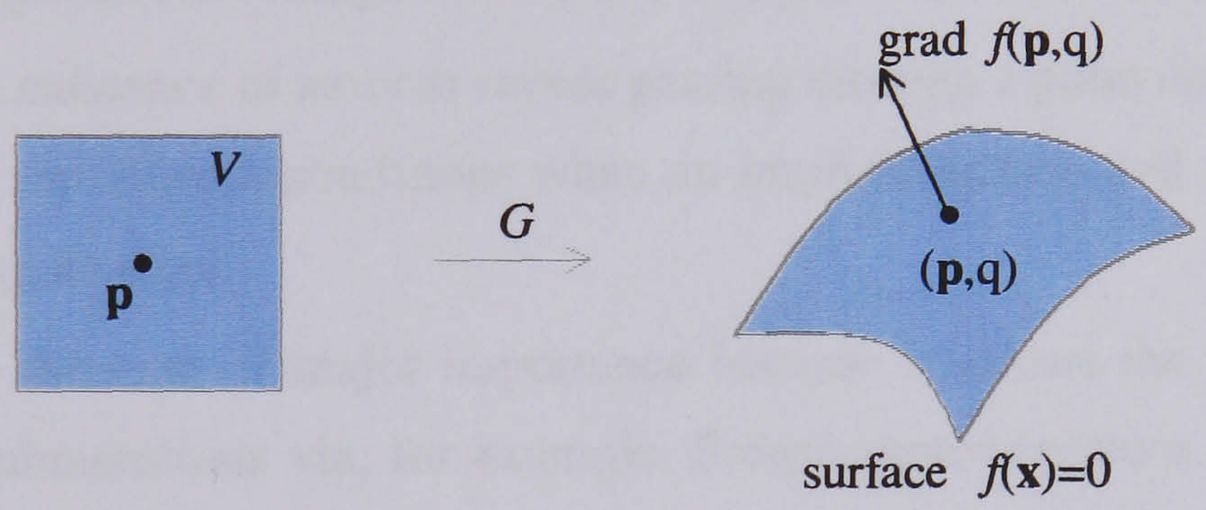

FIGURE 8. Local parametrisation of an implicitly-defined variety.

An example follows to illustrate the Implicit Function Theorem at work.

EXAMPLE 2.22. The Cartan umbrella $x^2-zy^2=0$ in $\mathbb{R}^3$ is the level set for the value 0 of the function $f:\mathbb{R}^3\to\mathbb{R}$ given by $f(x,y,z)=x^2-zy^2$. According to the Theorem 2.9, we have only to make sure that $\frac{\partial f}{\partial z}\neq 0$ in order to guarantee a regular neighbourhood for a point. But

$$\frac{\partial f}{\partial z}=-y^2=0\quad\Rightarrow\quad y=0$$

i.e. all points of $x^2-zy^2=0$ with $y=0$ are singular points. These singular points are then given by

$$\begin{cases} y=0\\ x^2-zy^2=0\end{cases}\quad\Leftrightarrow\quad\begin{cases} y=0\\ x=0\end{cases}\quad\Leftrightarrow\quad\{x=0\}\cap\{y=0\}$$

or, equivalently, the point set $\{(x,y,z)\in\mathbb{R}^3 : x=0,y=0\}$. That is, the singular set of the Cartan umbrella is the z-axis $0\times 0\times z$.

This result agrees with the fact that the Jacobian $\mathrm{J}f = [2x \quad 2yz \quad y^2]$ has maximal rank 1 for $(x,y,z) \neq (0,0,z)$. However, because the rank cannot fall below zero, we have no way to algorithmically detect via rank criterion any possible singularities in the z-axis. In fact, the z-axis is a smooth cut-line, but we know that the origin is a special singularity of the Cartan umbrella provided that, unlike the points of the positive z-axis, it is a cut-point.

The question now is whether or not there is any method to compute such singularities. An algorithm to determine the singularities of a variety is useful for many geometry-based packages. For example, the graphical visualisation of the Cartan umbrella with-handle $x^2 - zy^2 = 0$ in $\mathbb{R}^3$ is impossible because of the discontinuity at $y = 0$. Therefore, unless we use a parametric Cartan umbrella without-handle, such a point set cannot be visualised on a display screen. This is an example amongst others that shows how much a stratification algorithm of varieties can be useful.

Amongst other applications of Implicit Function Theorem, we can mention two:

- To prove the existence of smooth curves passing through a point on a surface [**68**, p.525].
- To state the smoothness conditions when an implicit surface and a parametric surface are stitched along an edge.

The first refers a theorem of major importance because it allows the study of smoothness of higher-dimensional submanifolds via, for example, Frénet approximations. We will come back to this point later in this chapter. The second is particularly important in geometric design because it makes it possible to avoid the conversion of an implicit surface patch to its parametric representation, or vice-versa. So, in principle, it is possible to design a smooth surface composed of parametric and implicit patches.

5. Submanifolds

By definition, a submanifold is a subset of a manifold that is a manifold in its own right. In geometric modelling, manifolds are usually Euclidean spaces, and submanifolds are points, curves, surfaces, etc. in some Euclidean space of equal or higher dimension. Manifolds and varieties in an Euclidean space are usually defined by either the image, level set or graph associated with a mapping.

5.1. Parametric submanifolds. As shown in previous sections, the smoothness characterisation of a submanifold clearly depends on its defining smooth mapping and its rank. We have seen that the notion of smooth mapping of constant rank leads to the definition of *smooth* submanifolds. In this respect, the Rank Theorem, and ultimately, the Inverse Function Theorem can be considered as the major milestones in the theory of smooth submanifolds. Notably, the smoothness of a mapping does

not ensure the smoothness of a submanifold. In fact, not all smooth submanifolds, say parametric smooth submanifolds, can be considered as topological submanifolds, i.e. submanifolds equipped with the submanifold topology.

Extreme cases of mappings $f : M \to N$ of constant rank are those corresponding to maximal rank, that is, the rank is the same as the dimension of M or N.

DEFINITION 2.9. Let $f : M \to N$ be a smooth mapping with constant rank. Then, for all $\mathbf{p} \in M$, f is called:

$$\text{an } \textbf{immersion} \quad \text{if} \quad \operatorname{rank} f = \dim M,$$

$$\text{a } \textbf{submersion} \quad \text{if} \quad \operatorname{rank} f = \dim N.$$

Let us now concentrate on immersions, that is, mappings whose images are parametric submanifolds. To say that $f : M \to N$ is an immersion means that the differential $\mathrm{D}f(\mathbf{p})$ is injective at every point $\mathbf{p} \in M$. This is the same as saying that the Jacobian matrix of f has rank equal to $\dim M$ (which is only possible if $\dim M \leq \dim N$). Then by the Rank Theorem, we have

COROLLARY 2.2. *Let M, N be two manifolds of dimensions m, n, respectively, and $f : M \to N$ a smooth mapping. The mapping f is an* immersion *if and only if for each point $\mathbf{p} \in M$ there are coordinate systems (U, φ), (V, ψ) about $\mathbf{p}$ and $f(\mathbf{p})$, respectively, such that the composite $\psi f \varphi^{-1}$ is a restriction of the coordinate inclusion $\iota : \mathbb{R}^m \to \mathbb{R}^m \times \mathbb{R}^{n-m}$.*

PROOF. See Sharpe [**103**, p.15]. □

This corollary provides the canonical form for immersed submanifolds:

$$(x_1, \ldots, x_m) \mapsto (x_1, \ldots, x_m, 0, \ldots, 0).$$

DEFINITION 2.10. A smooth (analytic) m-dimensional **immersed submanifold** of a manifold N is a subset $M' \subset N$ *parametrised* by a smooth (analytic), one-to-one mapping $f : M \to M' \subset N$, whose domain M, the *parameter space*, is a smooth (analytic) m-dimensional manifold, and such that f is everywhere regular, of maximal rank m.

Thus, a m-dimensional immersed submanifold M' is the *image* of an immersion $f : M \to M' = f(M)$. To verify that f is an immersion it is necessary to check that the Jacobian has rank m at every point. Observe that an immersed submanifold is defined by a *parametrisation*. Thus, an immersed submanifold is nothing more than a *parametrically-defined submanifold*, or simply a **parametric submanifold**. Despite its smoothness, an immersed or parametric submanifold may include

self-intersections. A submanifold with self-intersections is the image $M' = f(M)$ of an arbitrary regular mapping $f : M \to M' \subset N$ of maximal rank m, which is the dimension of the parameter space M. Examples of parametric submanifolds with self-intersections such as Bézier curves and surfaces are often found in geometric design activities. Immersed submanifolds constitute the largest family of parametric submanifolds. It includes the subfamily of parametric submanifolds without self-intersections, also known as *parametric embedded submanifolds.*

DEFINITION 2.11. An **embedding** is a one-to-one immersion $f : M \to N$ such that the mapping $f : M \to f(M)$ is a homeomorphism (where the topology on $f(M)$ is the subspace topology inherited from N). The *image* of an embedding is called an **embedded submanifold**.

In other words, the topological type is invariant for any point of an embedded submanifold. This is why embedded submanifolds are often called simply submanifolds. Obviously, $f : M \to N$ considered as a smooth mapping is called an embedding if $f(M) \subset N$ is a smooth manifold and $f : M \to f(M)$ is a diffeomorphism [**22**, p.10].

Parametric immersed submanifolds are attractive for geometric design of parametric curves and surfaces, but not for solid modelling that practically processes embedded submanifolds as the 'building blocks' of an engineering artifact. In order to integrate these two research areas of geometric modelling we have to somehow to reconcile immersed and embedded submanifolds. This has been taken into account in the design of the data structure of the Σ-geometric kernel.

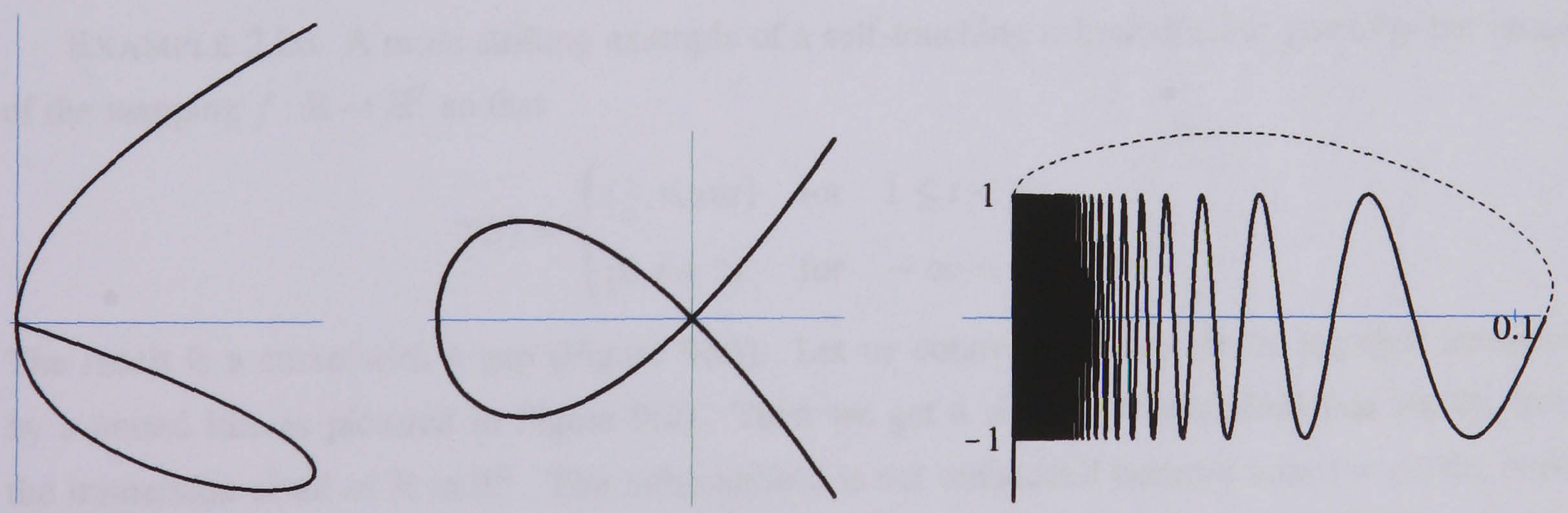

(a) (b) (c)

FIGURE 9

Let us see first some examples of 1-dimensional immersed that are not embedded manifolds.

EXAMPLE 2.23. Let $f:\mathbb{R}\to\mathbb{R}^2$ an immersion given by $f(t)=(\cos 2\pi t,\sin 2\pi t)$. Its image $f(\mathbb{R})$ is the unit circle $\mathbb{S}^1=\{(x,y)\,|\,x^2+y^2=1\}$ in $\mathbb{R}^2$. This shows that an immersion need not be one-to-one into (injective) in the large, even though it is one-to-one locally. In fact, for example, all the points $t=0,\pm1,\pm2,\ldots$ have the same image point $(0,1)$ in $\mathbb{R}^2$. Moreover, the circle intersects itself for consecutive unit intervals in $\mathbb{R}$, even though its self-intersections are not 'visually' apparent. Thus, this circle is an immersed submanifold, but not an embedded submanifold in $\mathbb{R}^2$. The same holds if we consider the immersion $f:[0,1]\to\mathbb{R}^2$ because $f(0)=f(1)$. But, if we take the immersion $f:]0,1[\to\mathbb{R}^2$, its image is an embedded manifold, that is, a unit circle less one of its points.

EXAMPLE 2.24. Let $f:]-\infty,2[\to\mathbb{R}^2$ be an immersion given by $f(t)=(-t^3+3t+2,t^2-t-2)$. Its image $f(]-\infty,2[)$ is a 1-dimensional immersed 6-shaped submanifold (Figure 9(a)). Although f is injective (say, injective globally, and consequently injective locally), that is, without self-intersections, its image is not an embedded manifold. This is so because $]-\infty,2[$ and its image $f(]-\infty,2[)$ are not homeomorphic. In fact the point $(0,0)$ in $f(]-\infty,2[)$ is a cut point of $f(]-\infty,2[)$, and hence the local topological type of such a 6-shaped submanifold is not constant. Note that the curve intersects itself at $t=-1$ and $t=2$, but because $t=2$ is not part of the domain, one says that the curve touches itself at the origin $(0,0)$.

EXAMPLE 2.25. $f:\mathbb{R}\to\mathbb{R}^2$ defined by $f(t)=(t^2-1,t^3-t)$ is an immersion (Figure 9(b)). It is not injective. However, it is injective when restricted to, say, the range $-1<t<\infty$.

EXAMPLE 2.26. A more striking example of a self-touching submanifold is given by the image of the mapping $f:\mathbb{R}\to\mathbb{R}^2$ so that

$$f(t)=\begin{cases}(\frac{1}{t},\sin\pi t) & \text{for}\quad 1\le t<\infty,\\ (0,t+2) & \text{for}\quad -\infty<t\le -1.\end{cases}$$

The result is a curve with a gap (Figure 9(c)). Let us connect the two pieces together smoothly by a dotted line as pictured in Figure 9(c). Then we get a smooth submanifold that results from the immersion of all of $\mathbb{R}$ in $\mathbb{R}^2$. This submanifold is not embedded because near $t=\infty$ the curve converges to the segment line $0\times[-1,1]$ in y-axis. In fact, while t converges to a point near ∞, its image converges to a line segment. Thus, the submanifold is not embedded because f is not a homeomorphism.

Embedded submanifolds are a subclass of immersed submanifolds that exclude self-intersecting submanifolds and self-touching submanifolds, that is, submanifolds that corrupt the local topological

invariance or type. Any other submanifold that keeps the same topological type everywhere in it is an embedded submanifold. Equivalently, a subset $f(M) \in N$ of a manifold N is called a smooth m-dimensional embedded submanifold if there is a covering $\{U_i\}$ of $f(M)$ by open sets (i.e. arbitrarily small neighbourhoods) of the ambient smooth manifold N such that the components of $U_i \cap f(M)$ are all connected open subsets of $f(M)$ of dimension m. Thus, there is no limitation on the number of components of an embedded submanifold in a chart of the ambient manifold; it may even be infinite [**103**, p.19]. This means that, even with differential and topological singularities removed, a smooth embedded submanifold may be non-regular. Regular submanifolds intersect more neatly with coordinate charts of the ambient manifold; in particular, the family of components of this intersection do not pile up.

DEFINITION 2.12. An m-dimensional smooth submanifold $M \subset N$ is **regular** if, in addition to the regularity of the parametrising mapping, there is a covering $\{U_i\}$ of M by open sets of N such that, for each i, $U_i \cap M$ is a *single* open connected subset of M.

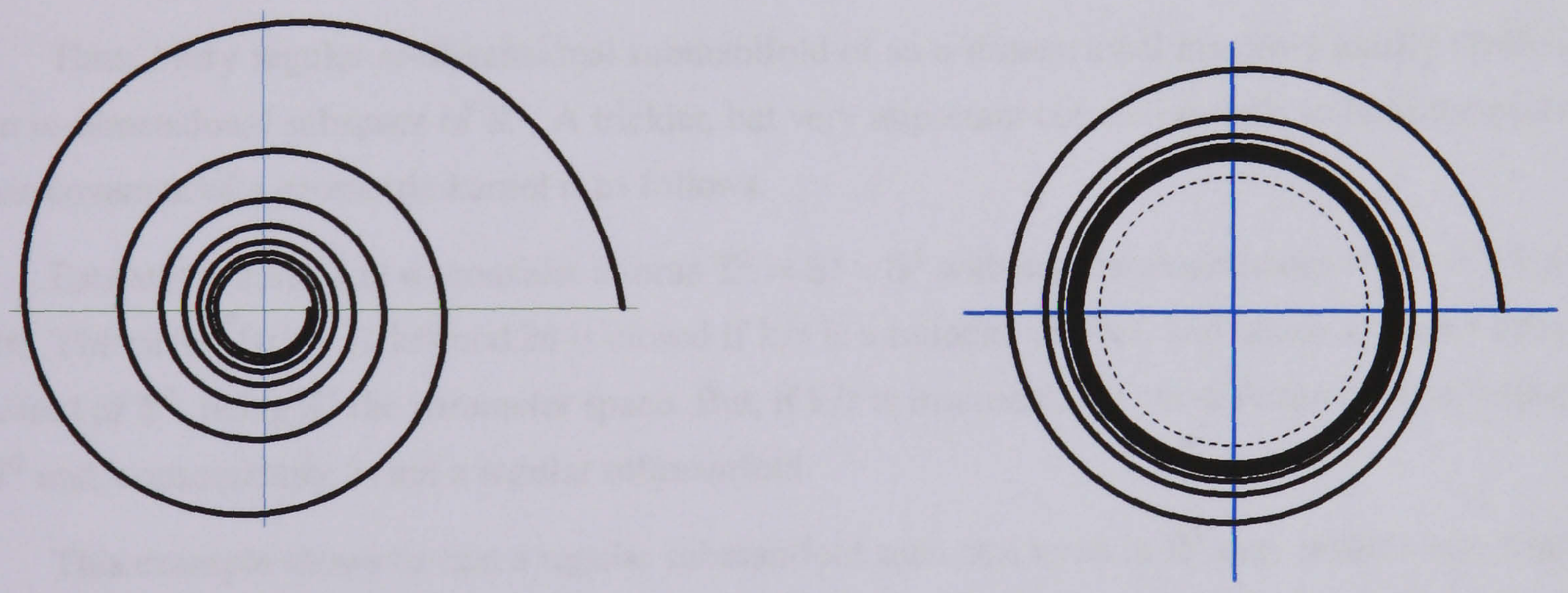

(a) (b)

FIGURE 10

By this definition, smooth regular submanifolds constitute a subclass of smooth embedded submanifolds. Three counterexamples are given below.

EXAMPLE 2.27. Let $f :]1, \infty[\to \mathbb{R}^2$ be a mapping given by

$$f(t) = (\frac{1}{t}\cos 2\pi t, \frac{1}{t}\sin 2\pi t).$$

Its image (Figure 10(a)) in $\mathbb{R}^2$ is an embedded curve because the image of every point $t \in]1,\infty[$ is a point in $\mathbb{R}^2$; hence, f is a homeomorphism. Note that even near $t = \infty$, f is still a homeomorphism because its image is a point, the origin $(0,0)$. That is, a point and its image have the same dimension. (This is not true in Example 2.26.) However, the image of $]1,\infty[$ is not a regular curve because it spirals to $(0,0)$ as $t \to \infty$ and tends to $(1,0)$ as $t \to 1$, Figure 10(a). This happens because near (in a neighbourhood of) $t = \infty$ the relative neighbourhood in the image curve has several (possibly an infinite number of) components.

EXAMPLE 2.28. Let us slightly change the previous mapping $f :]1,\infty[\to \mathbb{R}^2$ to be a mapping given by

$$f(t) = (\frac{t+1}{2t}\cos 2\pi t, \frac{t+1}{2t}\sin 2\pi t).$$

Its image (Figure 10(b)) in $\mathbb{R}^2$ is a non-regular embedded curve, now spiraling to the circle with center at $(0,0)$ and radius $1/2$ as $t \to \infty$, Figure 10(b). It is quite straightforward to check that the Jacobian is always 1. In fact, it could be 0 if both derivatives of the component functions could vanish simultaneously on $]1,\infty[$; this would happen if and only if $\cos 2\pi t = -\tan 2\pi t$, an impossible equality.

Thus, every regular m-dimensional submanifold of an n-dimensional manifold locally looks like an m-dimensional subspace of $\mathbb{R}^n$. A trickier, but very important counterexample to limit the geometric coverage of a geometric kernel is as follows.

EXAMPLE 2.29. Let us consider a torus $\mathbb{T}^2 = \mathbb{S}^1 \times \mathbb{S}^1$ with angular coordinates (θ,γ), $0 \leq \theta,\gamma < 2\pi$. The curve $f(t) = (t, \mathrm{k}t) \bmod 2\pi$ is closed if k/t is a rational number, and hence a regular submanifold of $\mathbb{T}^2$, being $\mathbb{S}^1$ the parameter space. But, if k/t is irrational, the curve forms a dense subset of $\mathbb{T}^2$ and, consequently, is not a regular submanifold.

This example shows us that a regular submanifold such as a torus in $\mathbb{R}^3$ may include non-regular submanifolds. One should be careful to avoid irrational numbers in the representation and construction of submanifolds in a geometric kernel.

5.2. Implicit submanifolds and varieties. An alternative to the parametric approach for submanifolds is to define them *implicitly* as a common or intersecting level set of a collection of functions [**93**, p.16]. We have seen this in Subsection 3.2, where the Implicit Mapping Theorem was introduced. This theorem provides an immediate canonical form for regular manifolds as follows:

THEOREM 2.10. (Olver [**93**, p.14]) *A n-dimensional submanifold $N \subset \mathbb{R}^m$ is regular if and only if for each point $\mathbf{p} \in N$ there exist local coordinates $\mathbf{x} = (x_1,\ldots,x_m)$ defined on a neighbourhood U of $\mathbf{p}$ such that $U \cap N = \{\mathbf{x} : x_1 = \cdots = x_{m-n} = 0\}$.*

Therefore, every regular n-dimensional submanifold of an m-dimensional manifold locally looks like a n-dimensional subspace of $\mathbb{R}^m$. This means that all regular n-dimensional submanifolds are locally equivalent. They are the basic constituents of the stratifications introduced in Chapter 3.

Let us study now varieties. They are generalisations of implicit submanifolds, and thus they are defined by submersions. In general, the variety $V_{\mathcal{F}}$ determined by a family of real-valued functions $\mathcal{F}$ is defined by the subset where they simultaneously vanish, that is,

$$V_{\mathcal{F}} = \{\mathbf{x} \,|\, f_i(\mathbf{x}) = 0 \text{ for all } f_i \in \mathcal{F}\}.$$

In particular case when these functions $\{f_i\}$ are components of a mapping $f : \mathbb{R}^m \to \mathbb{R}^n$, the variety $V_f = \{f(\mathbf{x}) = 0\}$ is just the set of solutions to the simultaneous system of equations $f_1(\mathbf{x}) = \cdots = f_n(\mathbf{x}) = 0$.

It is clear that the notion of rank has a natural generalisation to (infinite) families of smooth functions.

DEFINITION 2.13. Let $\mathcal{F}$ be a family of smooth real-valued functions $f_i : M \to \mathbb{R}$, with $M, \mathbb{R}$ smooth manifolds. The **rank** of $\mathcal{F}$ at a point $\mathbf{p} \in M$ is the dimension of the space spanned by their differentials. The family is **regular** if its rank is constant on M.

DEFINITION 2.14. A set $\{f_1, \ldots, f_k\}$ of smooth real-valued functions on a manifold M with a common domain of definition is called **functionally dependent** if, for each $\mathbf{p} \in M$, there is a neighbourhood U and a smooth function $H(y_1, \ldots, y_k)$, not identically zero on any subset of $\mathbb{R}^k$, such that $H(f_1(\mathbf{x}), \ldots, f_k(\mathbf{x})) = 0$ for all $\mathbf{x} \in U$. The functions are called **functionally independent** if they are not functionally dependent when restricted to any open subset of M.

EXAMPLE 2.30. The functions $f_1(x,y) = x/y$ and $f_2(x,y) = xy/(x^2+y^2)$ are functionally dependent on the upper halfplane $\{y > 0\}$ because the second can be written as a function of the first, $f_2 = f_1/(1+f_1^2)$.

Thus, for a regular family of functions, the rank gives us the number of functionally independent functions it contains. So, we obtain an Implicit Function Family Theorem generalising the Implicit Mapping Theorem as follows.

THEOREM 2.11. **(Implicit Function Family Theorem)** *If a family of functions $\mathcal{F}$ is regular of rank n, there exists n functionally independent functions $f_1, \ldots, f_n \in \mathcal{F}$ in the neighbourhood of any point, with the property that any other function $g \in \mathcal{F}$ can be expressed as a function thereof, $g = H(f_1, \ldots, f_n)$.*

PROOF. See Olver [**93**, p.13]. □

Thus, if $f_1, \ldots, f_r$ is a set of functions whose $m \times r$ Jacobian matrix has maximal rank r at $\mathbf{p} \in M$, they also have, by continuity, the same rank r in a neighbourhood of $U \subset M$ of $\mathbf{p}$, and hence are functionally independent near $\mathbf{p}$. As expected, Theorem 2.11 also implies that, locally, there are at most m functionally independent functions on any m-dimensional manifold M.

DEFINITION 2.15. A variety (or system of equations) $V_{\mathcal{F}}$ is **regular** if it is not empty and the rank of $\mathcal{F}$ is constant.

Clearly, the rank of $\mathcal{F}$ is constant if $\mathcal{F}$ itself is a regular family. In particular, regularity holds if the variety is defined by the vanishing of a mapping $f : N \to \mathbb{R}^r$ which has maximal rank r at each point $\mathbf{x} \in V_{\mathcal{F}}$, or equivalently, at each solution $\mathbf{x}$ to the system of equations $f(\mathbf{x}) = 0$ [**93**, p.16]. The Implicit Function Family Theorem 2.11, together with Theorem 2.10, shows that a regular variety is a regular submanifold, as stated by the following theorem.

THEOREM 2.12. *Let $\mathcal{F}$ be a family of functions defined on an m-dimensional manifold M. If the associated variety $V_{\mathcal{F}} \subset M$ is regular, it defines a regular submanifold of dimension $m - r$.*

PROOF. See Olver [**93**, p.17]. □

As for parametric submanifolds, to say that an implicit submanifold is regular means that it is smooth. However, a smooth parametric submanifold is not necessarily regular. But, for implicit submanifolds, regularity and smoothness coincide. This is so because, unlike a parametric submanifold, regularity of an implicit submanifold is completely determined by the regularity of its defining family of functions.

Thus, Theorem 2.12 gives us a simple criterion for the smoothness of a submanifold described implicitly.

EXAMPLE 2.31. Let $f : \mathbb{R}^3 \to \mathbb{R}$ be a function given by $f(x,y,z) = x^2 + y^2 + z^2 - 1$. Its Jacobian matrix $[2x \quad 2y \quad 2z]$ has rank 1 everywhere except at the origin, and hence its variety (the unit sphere) is a regular 2-dimensional submanifold of $\mathbb{R}^3$.

EXAMPLE 2.32. The function $f : \mathbb{R}^3 \to \mathbb{R}$ given by $f(x,y,z) = xyz$ is not regular, and its variety (the union of the three coordinate planes) is not a submanifold.

The fact that regularity and smoothness coincide for implicit submanifolds suggests that we may have an algorithm to determine singularities on a variety via the Jacobian matrix. Let us define

regular points and singular points before providing some examples that illustrate the computation of such singularities.

DEFINITION 2.16. Let $f : U \subset \mathbb{R}^m \to \mathbb{R}^r$ be a smooth mapping. A point $\mathbf{p} \in \mathbb{R}^m$ is a **regular point** of f, and f is called a submersion at $\mathbf{p}$, if the differential $\mathrm{D}f(\mathbf{p})$ is surjective. This is the same as saying that the Jacobian matrix of f at $\mathbf{p}$ has rank r (which is only possible if $r \leq m$). A point $\mathbf{q} \in \mathbb{R}^r$ is a **regular value** of f if every point of $f^{-1}(\mathbf{q})$ is regular.

Instead of 'non-regular' we can also say *singular* or *critical*. In general, we have:

DEFINITION 2.17. Let $f : U \subset \mathbb{R}^m \to \mathbb{R}^r$ be a smooth mapping. A point $\mathbf{p} \in \mathbb{R}^m$ is a **singular point** of f if the rank of its Jacobian matrix falls below its largest possible value $\min(m, r)$. Likewise, a **singular value** is any $f(\mathbf{p}) \in \mathbb{R}^r$ where $\mathbf{p}$ is a singular point.

Recall that a singular point of an immersion determines a singular point in a parametric submanifold, but its self-intersections are not determined by the singular points of its associated function. This happens because the regularity of an immersion at a given point is necessary but not sufficient to guarantee the regularity of its image. But, for implicit submanifolds and varieties, the regularity of functions is necessary and sufficient to ensure their regularity.

EXAMPLE 2.33. Let $f : \mathbb{R} \to \mathbb{R}$ given by $f(x) = x^2$. Then any $c \neq 0$ is a regular value of f. Its Jacobian $[2x]$ has rank 1 iff $x \neq 0$; hence $x = 0$ is the only singular point of f. This corresponds to the minimum point of the graph of f (i.e. the vertex of a parabola), but here we are concerned with implicit submanifolds that are defined by level sets, not graphs.

EXAMPLE 2.34. Let $f : \mathbb{R}^2 \to \mathbb{R}$ given by $f(x,y) = 2x^2 + 3y^2$. Its Jacobian $[4x \quad 6y]$ has rank 1 unless $x = y = 0$. So any $c \neq 0$ is a regular value of f. For $c > 0$, $f^{-1}(c)$ is an ellipse in the plane.

EXAMPLE 2.35. Let $f : \mathbb{R}^2 \to \mathbb{R}$ given by $f(x,y) = x^3 + y^3 - xy$. The maximal possible rank for its Jacobian $[3x^2 - y \quad 3y^2 - x]$ is 1, and we can find all points where this fails, i.e. all singular points, by solving the system $\partial f/\partial x = \partial f/\partial y = 0$, that is,

$$\begin{cases} 3x^2 - y &= 0 \\ 3y^2 - x &= 0\,. \end{cases}$$

This yields the points $(0,0)$ and $(\frac{1}{3}, \frac{1}{3})$ as the only singular points of f. Since $f(0,0) = 0$ and $f(\frac{1}{3}, \frac{1}{3}) = -\frac{1}{27}$ it follows that any c other than 0 or $-\frac{1}{27}$ is a regular value of f. Also, 0 is a regular value of restrictions $f|(\mathbb{R}^2 - \{(0,0)\})$ and $-\frac{1}{27}$ is a regular value of $f|(\mathbb{R}^2 - \{(\frac{1}{3}, \frac{1}{3})\})$. This is because the

singular points $(0,0)$, $(\frac{1}{3},\frac{1}{3})$ do not belong to the domain of the restrictions of f, say $f|(\mathbb{R}^2-\{(0,0)\})$, $f|(\mathbb{R}^2-\{(\frac{1}{3},\frac{1}{3})\})$, respectively. Figure 11 illustrates $f^{-1}(c)$ for some values of c. For $c=0$ we have the well-known folium of Descartes (Figure 11(a)). The folium of Descartes is the variety $x^3+y^3-xy=0$ which self-intersects at the singular point $(0,0)$, i.e. the level set defined by $f(x,y)=0$. The level set defined by $f(x,y)=-\frac{1}{27}$ is the variety $x^3+y^3-xy=-\frac{1}{27}$ (Figure 11(c)) whose singular point is the isolated point $(\frac{1}{3},\frac{1}{3})$. For $c=-\frac{1}{54}$, we have the regular variety $x^3+y^3-xy=-\frac{1}{54}$ (Figure 11(b)).

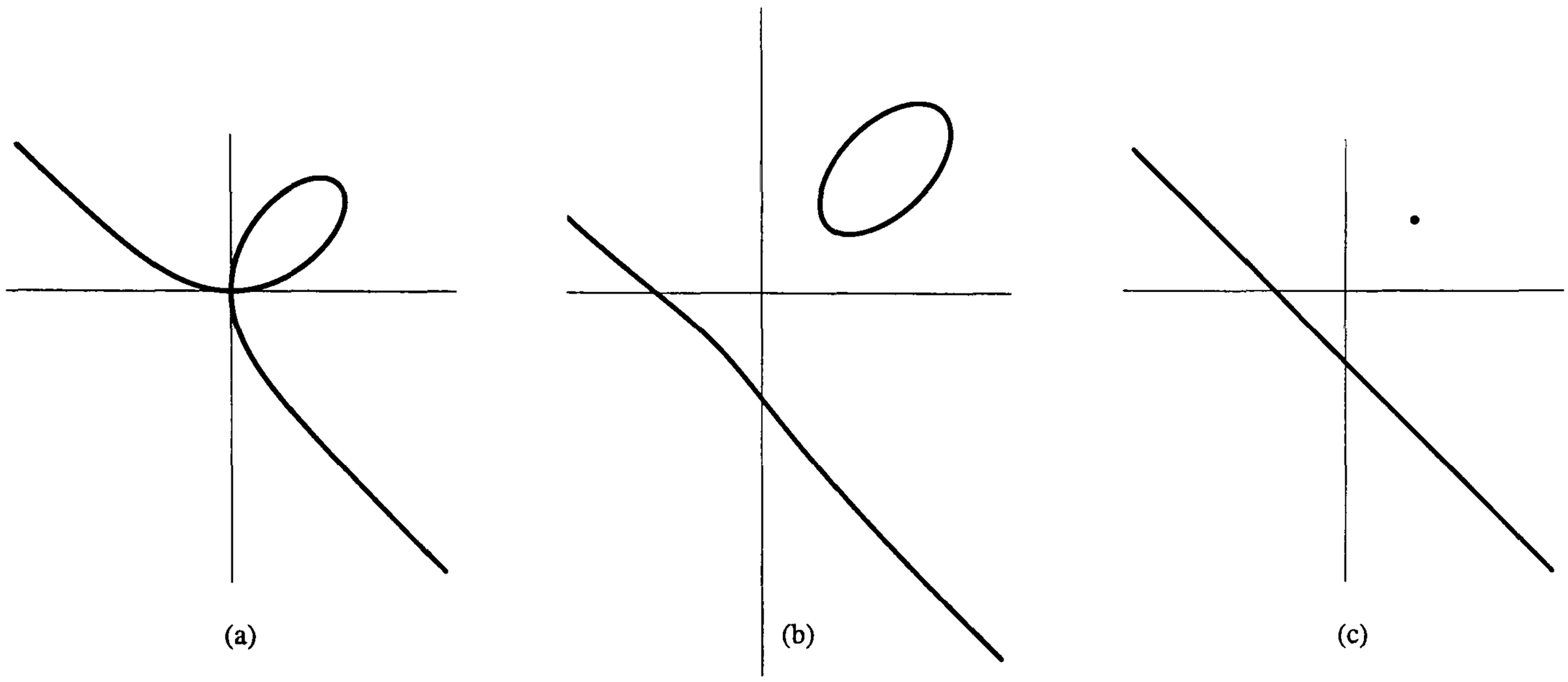

FIGURE 11. Varieties as level sets $x^3+y^3-xy=c$.

EXAMPLE 2.36. Let $f:\mathbb{R}^3\to\mathbb{R}$ be given by $f(x,y,z)=x^2-zy^2$. The associated variety has dimension $m-r=3-1=2$, but the maximal possible rank of its Jacobian $[2x\ -2zy\ -y^2]$ is 1. Its singular points are the solutions of the following system of equations:

$$\begin{cases} 2x=0 \\ -2zy=0 \\ -y^2=0 \end{cases} \iff \begin{cases} x=0 \\ zy=0 \\ y=0 \end{cases}.$$

The expressions $x=0$ and $y=0$ denote the two coordinate planes in $\mathbb{R}^3$, whose intersection is the z-axis. That is, the Jacobian vanishes along the z-axis, or, equivalently, Each point in the z-axis is a singular point. Since $f(0,0,z)=0$ it follows that any c other than 0 is a regular value of f. Also, 0 is a regular value of $f|(\mathbb{R}^3-\{(0,0,z)\})$. Figure 12(a) illustrates $f^{-1}(0)$, a variety known as the Cartan umbrella with-handle.

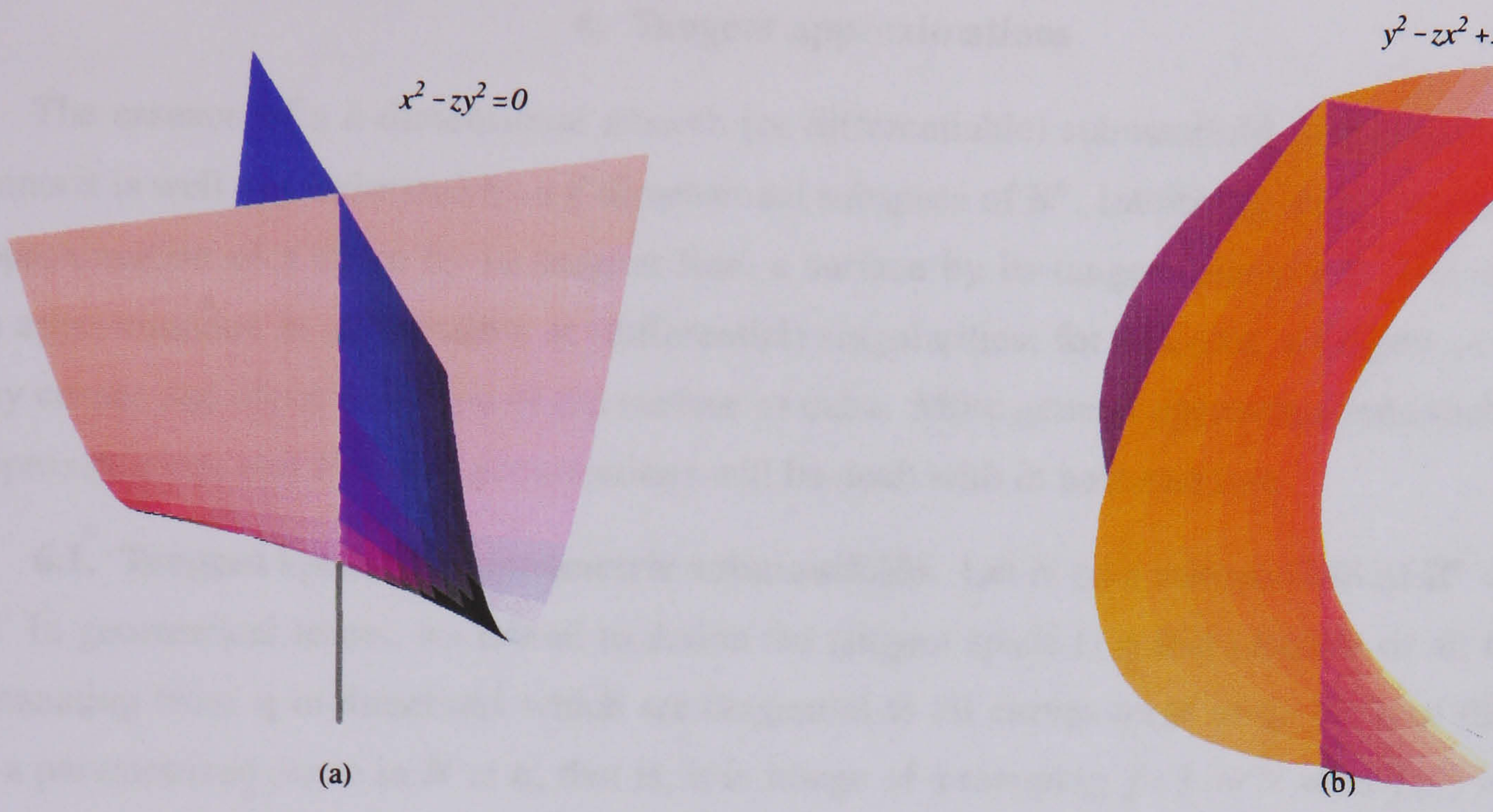

FIGURE 12. (a) Cartan umbrella with-handle as a level set $x^2 - zy^2 = 0$; (b) Butterfly as a level set $y^2 - z^2x^2 + x^3 = 0$.

EXAMPLE 2.37. Let $f : \mathbb{R}^3 \to \mathbb{R}$ be given by $f(x,y,z) = y^2 - z^2x^2 + x^3$. As for the previous example, the Jacobian $(-2z^2x + 3x^2 \quad 2y \quad -2zx^2)$ vanishes precisely on the z-axis. The z-axis is the line of "double points" where the surface intersects itself at $c = 0$. This is depicted in Figure 12(b) as the level set $f^{-1}(0)$, a variety known as the butterfly.

EXAMPLE 2.38. Let $f : \mathbb{R}^3 \to \mathbb{R}^2$ be the mapping given by $f(x,y,z) = (xy, xz)$. The Jacobian of f is $\begin{pmatrix} y & x & 0 \\ z & 0 & x \end{pmatrix}$ which has rank 2 unless all 2×2 minors are zero, i.e. unless $xz = xy = x^2 = 0$, which is equivalent to $x = 0$. Since $f(0,y,z) = (0,0)$, any point of $\mathbb{R}^2$ other than $(0,0)$ is a regular value. This variety (the union of the x-axis and the plane $x = 0$) has dimension 2 and is the intersection of two 2-dimensional varieties defined by the levels sets of the components functions of f. The first level set is the union of the planes $x = 0$ and $y = 0$, while the second level set is the union of the the planes $x = 0$ and $z = 0$ in $\mathbb{R}^3$.

Consequently, we have a systematic approach to get rank-based stratifications of varieties. In next chapter, we will come back to this point of discussion.

6. Tangent approximations

The essence of a k-dimensional smooth (or differentiable) submanifold is that near each of its points it is well approximated by a k-dimensional subspace of $\mathbb{R}^n$. Intuitively, this is just the standard approximation of a curve by its tangent line, a surface by its tangent plane, etc. Obviously, such an approximation is not possible at (differential) singularities; for example, a tangent plane flips at any corner and along any edge of the surface of cube. More general approximations such as Taylor approximations and Frénet approximations will be dealt with in next sections.

6.1. Tangent spaces for parametric submanifolds. Let N be a submanifold of $\mathbb{R}^n$ and let $\mathbf{q} \in N$. In geometrical terms, we intend to define the tangent space at $\mathbf{q}$ that consists of all the vectors emanating from $\mathbf{q}$ in directions which are tangential to all curves on N at $\mathbf{q}$. Each of these curves is a parametrised curve in N at $\mathbf{q}$, that is, it is image of a mapping $f : I \to N$ with $f(0) = \mathbf{q}$, where I is an open interval containing 0. A tangent vector to N at $\mathbf{q}$ has the form $\mathbf{q} + f'(0)$, where f is a parametrisation of a curve in N based at $\mathbf{q}$. Thus, apart from the point $\mathbf{q}$, a tangent vector is the image of the derivative $f'(0)$ at 0. This is illustrated in Figure 13.

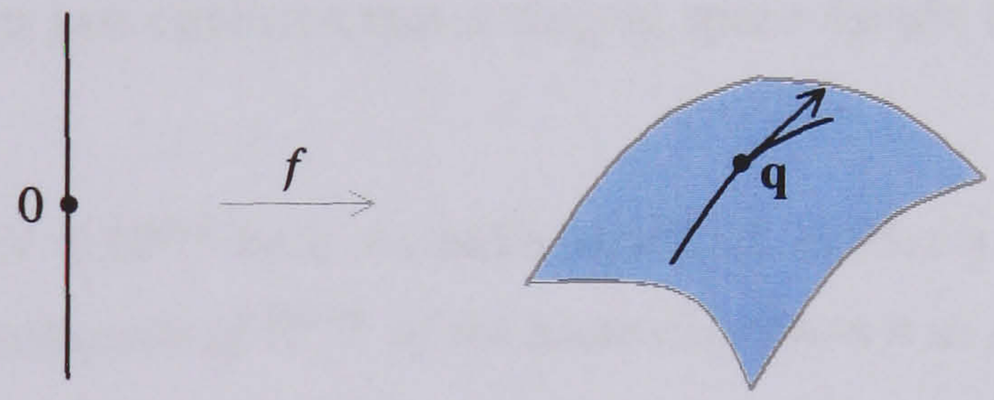

FIGURE 13. A tangent vector.

So, we can define a tangent space spanned by all vectors tangent to their corresponding curves on N at $\mathbf{q}$. This is a *geometric* definition of a tangent space to N at $\mathbf{q}$, and is called the *geometric* tangent space. An *analytic* generalisation of the geometric tangent space follows.

DEFINITION 2.18. Let $N \subseteq \mathbb{R}^{n+k}$ be a smooth n-submanifold, let $\mathbf{q} \in N$ and let $\mathbf{f} : U \subseteq \mathbb{R}^n \to \mathbb{R}^{n+k}$ be a parametrisation of a relatively open neighbourhood of $\mathbf{q}$ in N with $f(\mathbf{p}) = \mathbf{q}$. The **tangent space** $T_{\mathbf{q}}N$ at $\mathbf{q}$ to N is the *image*[3] of the differential $\mathbf{Df}(\mathbf{p}) : \mathbb{R}^n \to \mathbb{R}^{n+k}$.

The generality of this definition comes from the fact that we are no longer considering 1-dimensional tangent spaces to curves on N, but directly an n-dimensional tangent space to N at $\mathbf{q}$.

[3]By definition ([**61**, p.177]), the image of a linear mapping F is the set of vectors $\mathbf{a}$ for which there exists a solution of $F(\mathbf{x}) = \mathbf{a}$.

Furthermore, this tangent space is now spanned by partial derivatives of the Jacobian, that provide us with an analytical view of tangent spaces. This endows an analytic tangent space with a vector space structure. However, unlike a geometric tangent space, an analytic tangent space to a submanifold has the advantage that it is also a vector subspace of the ambient space (see Sharpe [**103**, p.41] for more details). As explained next, this is very important to define smoothness on a submanifold through Taylor approximations and its relatives such as, for example, Frénet approximations. Thus, from now on we drop the term *analytic*.

The tangent space $T_{\mathbf{q}}N$ at $\mathbf{q}$ to N is the vector subspace of $\mathbb{R}^{n+k}$ parallel to the affine subspace of $\mathbb{R}^{n+k}$ through $\mathbf{q}$ which best approximates N close to $\mathbf{q}$. By definition (see [**65**, p.7]), this affine subspace of $\mathbb{R}^{n+k}$ is given by

$$\mathbf{f}(\mathbf{p}) + (\mathbf{x} - \mathbf{p})\,\mathrm{D}\mathbf{f}(\mathbf{p}),$$

where $\mathrm{D}\mathbf{f}(\mathbf{p})$ spans a n-dimensional vector subspace of $\mathbb{R}^{n+k}$. This 'affine approximation' to $\mathbf{f}(\mathbf{x})$ near $\mathbf{p}$ is here called *tangent approximation*, and is a special case of the multidimensional Taylor's approximation.

The following theorem just confirms that a tangent space should be 'flat', rather than 'curved' like a manifold.

THEOREM 2.13. *Let $N \subseteq \mathbb{R}^{n+k}$ be a smooth n-manifold, and let $\mathbf{q} \in N$. Then the tangent space $T_{\mathbf{q}}N$ at $\mathbf{q}$ to N is a vector subspace of $\mathbb{R}^{n+k}$ of the same dimension n as N.*

PROOF. See Gibson [**42**, p.18]. □

It is clear that the smoothness of a submanifold N means that the neighbourhood of each point $\mathbf{q} = f(\mathbf{p})$ of N can be approximated by its tangent space. This has to do with the the number of linearly independent partial derivatives in the Jacobian, that is, with the rank of the Jacobian. If the rank falls below the dimension of N, we have a singularity.

6.2. Tangent spaces for implicit submanifolds. Before defining the tangent space $\mathrm{T}_{\mathbf{p}}M$ to an implicit manifold M at a point $\mathbf{p}$, it is convenient to generalise the idea of *local linear approximation* to a mapping between manifolds, that is, to define the differential at a point of a smooth mapping defined on a smooth manifold, rather than just on an open set.

Let $M \subseteq \mathbb{R}^{m+j}$, $N \subseteq \mathbb{R}^{n+k}$ be two smooth m-, n-manifolds respectively, let $f : M \to N$ be a smooth mapping, and let $\mathbf{p} \in M$ and $\mathbf{q} = f(\mathbf{p})$. The fact that f is smooth requires that there is an open neighbourhood U of $\mathbf{p}$ in $\mathbb{R}^{m+j}$, and a smooth mapping $F : U \to \mathbb{R}^{n+k}$ with $f = F$ on $U \cap M$. It is clear that the differential of F at $\mathbf{p}$ is a linear mapping $\mathrm{D}F(\mathbf{p}) : \mathbb{R}^{m+j} \to \mathbb{R}^{n+k}$. Then, $\mathrm{D}F(\mathbf{p})$

necessarily mappings the tangent space $\mathrm{T}_{\mathbf{p}}M$ into the tangent space $\mathrm{T}_{\mathbf{q}}N$ (see [**42**, p.19] for a proof). The restriction of the linear mapping $\mathrm{D}F(\mathbf{p})$ to $\mathrm{T}_{\mathbf{p}}M$ is the mapping $\mathrm{D}f(\mathbf{p}) : \mathrm{T}_{\mathbf{p}}M \to \mathrm{T}_{\mathbf{q}}N$, and is called the **differential** of f at $\mathbf{p}$.

We know that an m-dimensional implicit submanifold M of $\mathbb{R}^{m+j}$ has the form

$$M = \{\mathbf{x} : f(\mathbf{x}) = \mathbf{0}\}$$

where $f : \mathbb{R}^{m+j} \to \mathbb{R}^m$ is a differentiable mapping for which $\mathrm{D}f(\mathbf{p})$ has full rank m for each $\mathbf{p} \in M$. The tangent space to M at $\mathbf{p}$ is found by linearising f near $\mathbf{p}$.

THEOREM 2.14. *Let $M \subset \mathbb{R}^{m+j}$ be an m-dimensional submanifold described by the set of solutions to the equation $f(\mathbf{x}) = \mathbf{0}$. The tangent space $T_{\mathbf{p}}M$ to M at $\mathbf{p}$ is the* kernel *of $[\mathrm{D}f(\mathbf{p})]$, denoted by* kernel $[\mathrm{D}f(\mathbf{p})]$, *i.e. the set of solutions to the system of linear equations $[\mathrm{D}f(\mathbf{p})](\mathbf{x}) = \mathbf{0}$, where $[\mathrm{D}f(\mathbf{p})]$ is the Jacobian matrix.*

PROOF. See Hubbard and Hubbard [**61**, p.273]. □

The kernel is sometimes called the zero set of a linear mapping. In fact, by definition [**61**, p.177], the kernel of a linear mapping F is the set of vectors $\mathbf{x}$ such that $F(\mathbf{x}) = \mathbf{0}$. If F is represented by a matrix $[F]$, the kernel is the set of solutions to the system of linear equations $[F] = \mathbf{0}$. Kernels are related to uniqueness of solutions of linear solutions, whereas images are related to their existence [**61**, p.177]. If the kernel of F is not $\mathbf{0}$, there is more than a solution to $F(\mathbf{x}) = \mathbf{0}$.

7. Taylor approximations

In the previous section we used first-degree approximations (derivatives or tangent spaces) to curves, surfaces and higher-dimensional submanifolds. Now we are about to generalise such approximations to higher-order approximations, the so-called Taylor approximations. A kth order Taylor approximation has the intuitive meaning of deviating from successive tangent subspaces up to order k.

Approximation of functions of one and several variables by polynomials is a crucial issue in the calculus. It is also important for the purposes of computer-aided geometric since the techniques used to meet visual smoothness are essentially approximative in the sense of Taylor. The rest of this chapter is just devoted to showing this.

7.1. Taylor polynomials of functions and mappings. Let $U \subset \mathbb{R}^m$ be an open set, $f : U \to \mathbb{R}$ a real-valued function and $x \in U$. Let us denote by $(\partial f/\partial x_i)(\mathbf{x})$ the partial derivative of f with respect

to the ith variable x_i at $\mathbf{x}$. To denote a higher-order mixed partial derivative, we use multi-indices given by a m-tuple $\alpha = (\alpha_1, \ldots, \alpha_m)$ of non-negative integers. Then

$$\frac{\partial^{|\alpha|}}{\partial \mathbf{x}^\alpha} f = \frac{\partial^{|\alpha|}}{\partial {x_1}^{\alpha_1} \partial {x_2}^{\alpha_2} \ldots \partial {x_m}^{\alpha_m}} f \quad \textit{where} \quad |\alpha| = \alpha_1 + \cdots + \alpha_m \quad .$$

Recall that $f : U \to \mathbb{R}$ is *k-times differentiable* (or of class C^k, or C^k) if $(\partial^{|\alpha|} f / \partial \mathbf{x}^\alpha)(\mathbf{x})$ exists and is continuous for every m-tuple of non-negative integers α with $|\alpha| \leq k$. (Note that for $\alpha = (0, \ldots, 0)$, $(\partial^{|\alpha|} f / \partial \mathbf{x}^\alpha)(\mathbf{x})$ is just f.) f is *real analytic* on U if the Taylor series of f about each point in U converges to f in a neighbourhood of that point. In computer-aided geometric design, as for any computational geometry-based research area, we are interested in real analytic functions since only analytic functions possess *unique* Taylor approximations. This uniqueness is not guaranteed in the larger class of differentiable functions since that different differentiable functions may have the same Taylor series expansion (see Example 1.32 in Chapter 1, or Example 3 in [**98**, p.181] for a similar, but more detailed example).

DEFINITION 2.19. Let $U \subset \mathbb{R}^m$ be an open subset and $f : U \to \mathbb{R}$ be a C^k function. Then the polynomial of order k,

$$\mathrm{P}^k f(\mathbf{p}+\mathbf{h}) = \sum_{i=0}^{k} \sum_{\substack{|\alpha|=i \\ \alpha \in (\alpha_1, \ldots, \alpha_k)}} \frac{1}{\alpha!} \frac{\partial^{|\alpha|}}{\partial \mathbf{x}^\alpha} f(\mathbf{p})\, \mathbf{h}^\alpha$$

is called the kth order **Taylor polynomial approximation** (or, simply, Taylor polynomial) of f at $\mathbf{p}$.

EXAMPLE 2.39. (*Multi-index notation for a Taylor polynomial of a function in two variables*) Assume that f is a function in two variables $(x_1, x_2) = \mathbf{x}$. Its 2nd order Taylor polynomial at $\mathbf{p}$ is

$$\mathrm{P}^2 f(\mathbf{p}+\mathbf{h}) = \sum_{i=0}^{2} \sum_{\substack{|\alpha|=i \\ \alpha \in (\alpha_1, \alpha_2)}} \frac{1}{\alpha!} \frac{\partial^{|\alpha|}}{\partial \mathbf{x}^\alpha} f(\mathbf{p})\, \mathbf{h}^\alpha$$

$$= \underbrace{\frac{1}{0!0!} \frac{\partial^0}{\partial x_1^0 \partial x_2^0} f(\mathbf{p})\, h_1^0 h_2^0}_{f(\mathbf{p})}$$

$$+ \underbrace{\frac{1}{1!0!} \frac{\partial^1}{\partial x_1^1 \partial x_2^0} f(\mathbf{p})\, h_1^1 h_2^0 + \frac{1}{0!1!} \frac{\partial^1}{\partial x_1^0 \partial x_2^1} f(\mathbf{p})\, h_1^0 h_2^1}_{\text{terms of order 1: first derivatives}}$$

$$+ \underbrace{\frac{1}{2!0!} \frac{\partial^2}{\partial x_1^2 \partial x_2^0} f(\mathbf{p})\, h_1^2 h_2^0 + \frac{1}{1!1!} \frac{\partial^2}{\partial x_1^1 \partial x_2^1} f(\mathbf{p})\, h_1^1 h_2^1 + \frac{1}{0!2!} \frac{\partial^2}{\partial x_1^0 \partial x_2^2} f(\mathbf{p})\, h_1^0 h_2^2}_{\text{terms of order 2: second derivatives}}$$

or more simply

$$\begin{aligned} \mathrm{P}^2 f(\mathbf{p}+\mathbf{h}) = f(\mathbf{p}) \\ + \frac{\partial}{\partial x_1} f(\mathbf{p})\, h_1 + \frac{\partial}{\partial x_2} f(\mathbf{p})\, h_2 \\ + \frac{1}{2}\frac{\partial^2}{\partial x_1^2} f(\mathbf{p})\, h_1^2 + \frac{\partial^2}{\partial x_1 \partial x_2} f(\mathbf{p})\, h_1 h_2 + \frac{1}{2}\frac{\partial^2}{\partial x_2^2} f(\mathbf{p})\, h_2^2 \end{aligned}$$

EXAMPLE 2.40. Let us determine the 2nd order Taylor polynomial of the function $f(x,y) = \sin(x+y^2)$ at $(0,0)$. The first term of order 0 is $f(0,0) = \sin 0 = 0$ since the derivatives of order 1 are

$$\begin{aligned} \tfrac{\partial}{\partial x} f(x,y) &= \cos(x+y^2) \\ \tfrac{\partial}{\partial y} f(x,y) &= 2y\cos(x+y^2), \end{aligned}$$

hence $\frac{\partial}{\partial x} f(0,0) = 1$ and $\frac{\partial}{\partial y} f(0,0) = 0$. For the derivatives of order 2, we have

$$\begin{aligned} \tfrac{\partial^2}{\partial x^2} f(x,y) &= -\sin(x+y^2) \\ \tfrac{\partial^2}{\partial x \partial y} f(x,y) &= -2y\sin(x+y^2) \\ \tfrac{\partial^2}{\partial y^2} f(x,y) &= 2\cos(x+y^2) - 4y^2\sin(x+y^2), \end{aligned}$$

and $\frac{\partial^2}{\partial x^2} f(0,0) = 0$, $\frac{\partial^2}{\partial x \partial y} f(0,0) = 0$, and $\frac{\partial^2}{\partial y^2} f(0,0) = 2$. Analogously, for the derivatives of order 3, we can take advantage of the existence of crossed partials to determine

$$\begin{aligned} \tfrac{\partial^3}{\partial x^3} f(x,y) &= \tfrac{\partial}{\partial x}(\tfrac{\partial^2}{\partial x^2}) f(x,y) &&= -\cos(x+y^2) \\ \tfrac{\partial^3}{\partial x^2 \partial y} f(x,y) &= \tfrac{\partial}{\partial x}(\tfrac{\partial^2}{\partial x \partial y}) f(x,y) &&= -2y\cos(x+y^2) \\ \tfrac{\partial^3}{\partial x \partial y^2} f(x,y) &= \tfrac{\partial}{\partial y}(\tfrac{\partial}{\partial x \partial y^2}) f(x,y) &&= -2\sin(x+y^2) - 4y^2\cos(x+y^2) \\ \tfrac{\partial^3}{\partial y^3} f(x,y) &= \tfrac{\partial}{\partial y}(\tfrac{\partial^2}{\partial y^2}) f(x,y) &&= 4y\sin(x+y^2) - 8y\sin(x+y^2) - 8y^3\cos(x+y^2). \end{aligned}$$

At $(0,0)$ we have $\frac{\partial^3}{\partial x^3} f(0,0) = \frac{\partial^3}{\partial x^2 \partial y} f(0,0) = \frac{\partial^3}{\partial x \partial y^2} f(0,0) = 0$ and $\frac{\partial^3}{\partial y^3} f(0,0) = -1$. So the term of order 3 is $(-\frac{1}{3}!)h_1^3 = -\frac{1}{6}h_1^3$. Thus, the 3-order Taylor polynomial is

$$\mathrm{P}^3 f((0,0)+(h_1,h_2)) = 0 + h_1 + 0 + 0 + 0 + \frac{2}{2}h_2^2 + 0 + 0 + 0 - \frac{1}{6}h_1^3.$$

THEOREM 2.15. **(Taylor's Theorem)**

(1) *The polynomial* $\mathrm{P}^k f(\mathbf{p},\mathbf{h})$ *is the unique polynomial of total order* k *which has the same partial derivatives as* f *at* $\mathbf{p}$ *up to order* k.

(2) *The polynomial* $\mathrm{P}^k f(\mathbf{p},\mathbf{h})$ *is the unique polynomial of order* $\leq k$ *that best approximates* f *when* $\mathbf{h} \to 0$, *that is*

$$\lim \frac{f(\mathbf{p},\mathbf{h}) - \mathrm{P}^k f(\mathbf{p},\mathbf{h})}{|\mathbf{h}|^k} = 0.$$

PROOF. See Hubbard and Hubbard [**61**, p.284]. □

It can be also proved that the Taylor polynomial of the sum $f+g$ is the sum of the Taylor polynomials, the Taylor polynomial of the product $f\,g$ is the product of the Taylor polynomials [**61**, p.288], and the chain rule is satisfied for Taylor polynomials. Furthermore, all these results can be generalised to mappings $f:\mathbb{R}^m \to \mathbb{R}^n$. For that we have only to determine the Taylor polynomials corresponding to the n component functions of a mapping. The result is a mapping of Taylor polynomials.

7.2. Taylor polynomials of implicit functions. A computational geometric kernel should be able to represent and process Taylor polynomials of both parametric functions and implicit functions. This is important to set up smoothness conditions between two parametric submanifolds, two implicit manifolds, and between a parametric submanifold and an implicit submanifold. These general smoothness conditions are given in next section. Now, we are particularly interested in Taylor polynomials of functions given by the inverse and implicit function theorems.

In the setting of the Implicit Function Theorem, an implicit function g is given by $f(\mathbf{x},g(\mathbf{x})) = \mathbf{0}$ for all $\mathbf{x}$ in some neighbourhood of $\mathbf{p}$. Its corresponding Taylor polynomial is provided by the following theorem.

THEOREM 2.16. (**Taylor polynomial of an implicit function**) *If f is of class C^k for some $k \geq 1$, then g is also of class C^k, and its Taylor polynomial of order k is the unique polynomial mapping $\pi:\mathbb{R}^m \to \mathbb{R}^n$ of degree at most k such that*

$$\mathrm{P}^k f(\mathbf{p}+\mathbf{h}, \mathrm{P}^k g(\mathbf{p}+\mathbf{h})) \in o(|\mathbf{h}|^k).$$

PROOF. See Hubbard and Hubbard [**61**, p.289]. □

This theorem provides a technique to determine the coefficients of Taylor expansion of an implicit function. In fact, if we write the Taylor polynomial of the implicit function with undetermined coefficients, insert it into the equation $f(\mathbf{x},g(\mathbf{x})) = 0$ that specifies the implicit equation, and then identify like terms, we can determine such coefficients. Let us see an example that illustrates this technique.

EXAMPLE 2.41. The equation $f(x,y,z) = x^2+y^3+xyz^3-3=0$ determines z as an implicit function of x and y in a neighbourhood of $(1,1,1)$, since $\frac{\partial^3}{\partial z^3} f(1,1,1) = 3 \neq 0$. So, we can compute the Taylor polynomial of this implicit g to degree 2. Let

$$z = g(x,y) = g(1+u,1+v) = 1+a_1\,u+a_2\,v+\frac{1}{2}a_{1,1}\,u^2+\frac{1}{2}a_{2,2}\,v^2+o(u^2+v^2).$$

Substituting z in $x^2+y^3+xyz^3-3=0$, we obtain

$$(1+u)^2+(1+v)^3+(1+u)(1+v)(1+a_1\,u+a_2\,v+\frac{1}{2}a_{1,1}\,u^2+\frac{1}{2}a_{2,2}\,v^2+o(u^2+v^2)=0.$$

Now, multiplying out and identifying like terms, we get

- *Constant terms*:

$$3-3=0$$

- *Linear terms*:

$$2u+3v+u+v+3a_1u+3a_2v=0$$

yields $a_1=-1$, $a_2=-4/3$.

- *Quadratic terms*:

$$u^2(1+3a_1+3a_1^2+\frac{3}{2}a_{1,1})+uv(1+3a_1+3a_2+6a_1a_2+3a_{1,2})+v^2(3+3a_2+3a_2^2+\frac{3}{2}a_{2,2})=0$$

Identifying the coefficients with 0, and using the values of a_1 and a_2 calculated above, we get

$$a_{1,1}=-2/3,\quad a_{1,2}=10/9,\quad a_{2,2}=-26/9.$$

Finally, we can write down the 2nd order Taylor polynomial of g:

$$g(x,y)=1-(x-1)-\frac{4}{3}(y-1)-\frac{1}{3}(x-1)^2-\frac{13}{9}(y-1)^2+\frac{10}{9}(x-1)(y-1)+o((x-1)^2+(y-1)^2).$$

8. Contact and jet bundles

Most of this chapter has been dedicated to characterising visual smoothness —and the lack of it— for submanifolds in some Euclidean space. Visual smoothness is an essential issue in computer-aided geometric design of parametric curves and surfaces since there are boundary smoothness conditions to be satisfied whenever, for example, we patch together parametric surface patches (e.g. Bézier patches) to form a compound surface of an engineering artifact. Such a visual smoothness is called geometric continuity or G^r continuity for parametric submanifolds in computer-aided geometric design and C^r smoothness for submanifolds in differential geometry.

This section deals with the computation of such smoothness conditions under contact of C^r submanifolds. One way to do this locally is to approximate their associated functions, or mappings, by a *part* of their Taylor series at a given point. Such a part of a Taylor series is called a *jet* of a function or mapping at a given point.

DEFINITION 2.20. The $k-$**jet** of $f:\mathbb{R}^m \to \mathbb{R}^n$ at a given point $\mathbf{p}$ is just the k-degree Taylor polynomial

$$j^k f(\mathbf{p}) = \mathrm{P}^k f(\mathbf{p}+\mathbf{h}).$$

In particular, the k-jet of a function $f:\mathbb{R}\to\mathbb{R}$ at $\mathbf{p}$ is the polynomial

$$j^k f(\mathbf{p}) = f(\mathbf{p}) + t f'(\mathbf{p}) + \frac{t^2}{2!} f''(\mathbf{p}) + \cdots + \frac{1}{k!} t^k f^{(k)}(\mathbf{p})$$

obtained by truncating the Taylor series to degree k. Two k-jets are said to be equal when they are identically the same as polynomials. Some authors use a slightly different notion of k-jet by deleting the constant term.

DEFINITION 2.21. (Golubitsky and Guillemin [**44**, p.37]) Let M and N be smooth manifolds, and $\mathbf{p}\in M$. Assume that $f,g:M\to N$ are smooth mappings with $f(\mathbf{p})=g(\mathbf{p})=\mathbf{q}$.

(1) f has **1st order of contact** with g at $\mathbf{p}$ if $\mathrm{D}f(\mathbf{p}) = \mathrm{D}g(\mathbf{p})$ as mappings of $T_{\mathbf{p}}M \to T_{\mathbf{q}}N$.

(2) f has **k-th order of contact** with g at $\mathbf{p}$ if $\mathrm{D}f: TM \to TN$ has $(k-1)$st order of contact with $\mathrm{D}g$ at every point in $T_{\mathbf{p}}M$. This is written as $f \overset{k}{\sim} g$ at $\mathbf{p}$. TM and TN denote the tangent bundles to M and N, respectively. By definition, the *tangent bundle* to a manifold X is the union of tangent spaces at all points of X, $T(X) = \bigcup_{\mathbf{p}\in X} T_{\mathbf{p}}X$.

(3) A **k-jet from** M **to** N is an equivalence class $[j^k f(\mathbf{p})]$ under the equivalence relation $\overset{k}{\sim}$ at $\mathbf{p}$. We use the notation $j^k f(\mathbf{p})$ to denote the *k-jet of* f *at* $\mathbf{p}$.

(4) Let $J^k(M,N)_{\mathbf{p},\mathbf{q}}$ denote the set of equivalence classes under $\overset{k}{\sim}$ at $\mathbf{p}$ of mappings $f:M\to N$ where $f(\mathbf{p})=\mathbf{q}$. The disjoint union

$$J^k(M,N) = \bigcup_{(\mathbf{p},\mathbf{q})\in M\times N} J^k(M,N)_{\mathbf{p},\mathbf{q}}$$

is called the **k-jet bundle** from M to N.

As will be shown further below, these definitions are behind the mathematical smoothness theory in computer-aided geometric design for submanifold patch complexes. The mapping $j^k f: M \to J^k(M,N)$, that is the k-jet of a smooth mapping $f:M\to N$ defined by the equivalence class $[j^k f]$ of f in $J^k(M,N)_{\mathbf{p},f(\mathbf{p})}$ for all $\mathbf{p}\in M$, is a smooth invariant particularly useful to set up the smoothness conditions whenever we want to stitch together two submanifolds. This opens up a scenario of a mathematical theory for geometric continuity in computer-aided geometric design. In fact, as shown further on, $j^k f(\mathbf{p})$ is just an invariant way of describing the Taylor expansion of f at $\mathbf{p}$ up to order

k. It will also be shown that $j^k f(\mathbf{p})$ is a smooth mapping. This fact is very important for jet-based stratifications such as, for example, the Thom-Boardman stratifications, detailed in the next chapter.

Note that $J^0(M,N) = M \times N$, so f has $\overset{0}{\sim}$-contact with g at $\mathbf{p}$ iff $f(\mathbf{p}) = g(\mathbf{p})$, and $j^0 f(\mathbf{p}) = (\mathbf{p}, f(\mathbf{p}))$ is just the graph of f.

LEMMA 2.17. *Let U be an open subset of $\mathbb{R}^m$ and $\mathbf{p} \in U$. Let $f, g : U \to \mathbb{R}^n$ be smooth mappings. Then $f \overset{k}{\sim} g$ at $\mathbf{p}$ iff*

$$\frac{\partial^{|\alpha|} f_i}{\partial x^\alpha}(\mathbf{p}) = \frac{\partial^{|\alpha|} g_i}{\partial x^\alpha}(\mathbf{p}) \tag{5}$$

for every multi-index α with $|\alpha| \leq k$ and $1 \leq i \leq n$ where f_i and g_i are the coordinate functions determined by f and g, respectively, and $x_1, \ldots, x_m$ are coordinates on U.

PROOF. See Golubitsky and Guillemin [**44**, p.37]. □

The conditions (5) can be used as smoothness conditions for touching parametric curve or surface patches as is usual in computer-aided design. In fact, they generalise the G^k (kth order geometric continuity) conditions for two regular parametric submanifolds (see, for example, Gregory [**47**, p.335]) to any regular submanifolds with the same dimension, no matter whether they are parametrically or implicitly defined.

COROLLARY 2.3. *f and $g : U \to \mathbb{R}^n$ have kth order contact at $\mathbf{p}$ iff the Taylor expansions of f and g up to (and including) order k are identical at $\mathbf{p}$.*

PROOF. See Golubitsky and Guillemin [**44**, p.37]. □

The k-jet of f at $\mathbf{p} \in U$ has a canonical representative, namely the Taylor polynomial of f of order k at $\mathbf{p}$. Moreover, for the special case $M = \mathbb{R}^m$, $N = \mathbb{R}^n$, this polynomial mapping from $\mathbb{R}^m$ to $\mathbb{R}^n$ is *uniquely* determined by the list of derivatives of order k of f at $\mathbf{p}$.

9. Frénet approximations

In computer aided geometric design (CAGD), a classical way of ensuring the C^r smoothness or continuity of a parametric piecewise curve is to require the equality of the first r derivatives at its joints. This is generalised by Lemma 2.17 to higher dimensional manifolds regardless of whether they are implicitly or parametrically defined. Its Corollary 2.3 expresses the same result in terms of the Taylor expansions.

Another way of ensuring the C^r smoothness of a parametric piecewise curve is to require the equality of the geometric invariants of the curve at its joints, namely the Frénet frame and the curvatures. This suggests that it should be possible to express the Taylor expansion in terms of such geometric invariants. Also, this 'geometric' expansion can be in principle extended to higher dimensional (parametric and implicit) manifolds. Let us call it *Frénet expansion* or *approximation.*

The Frénet approximation of a mapping f —which is a parametric or implicit representation of a manifold— is a refinement of the Taylor approximation. Basically, each derivative $\mathbf{f}^{(i)}$ —which can be viewed as a geometric derivative invariant— of the Taylor series expansion is decomposed into subsidiary geometric invariants such tangents, curvatures, torsions, etc.

Frénet approximations can be used to establish the F^r continuity (or Frénet continuity of order r) of k-manifolds ($k \leq n$)—not only curves as usual in CAGD— in $\mathbb{R}^n$ (using the Gram-Schmidt orthogonalisation process for defining the Frénet frame). Thus, orthogonality seems to be the essence of Frénet approximations. This is true independently of whether the first k derivatives $\mathbf{f}^{(i)}$, with $i = 1, \ldots, k$, are linearly independent or not — as Mazure noted in [**81**] and [**80**]. In either case, Frénet approximations require we must supply $\mathbb{R}^n$ with an inner product in order to obtain the full geometric structure of $\mathbb{R}^n$ (including the concepts of distance, angles, and orthogonality). This is not explicitly stated in [**81**], but it is obviously assumed (see, for example, p.181 of [**81**]).

9.1. Orthogonality. Two vectors are called *orthogonal* (with respect to an inner product) if their inner product is zero. Thus, the angle between them is a right angle. A set of vectors is orthogonal if each pair of vectors is orthogonal. If all the vectors in a set are of unit length, such a set is further said to be *orthonormal.* Besides, if a set of nonzero vectors is orthogonal, then the vectors are linearly independent, and thus, they form an orthogonal basis for a vector space. An orthonormal basis is obtained by normalising the vectors of an orthogonal basis. A n-dimensional Frénet frame along a curve in $\mathbb{R}^n$ is an example of an orthonormal basis in $\mathbb{R}^n$. Remarkably, an orthonormal basis (e.g. Frénet frame for curves) can be inductively constructed using a fundamental tool of linear algebra, called Gram-Schmidt Orthogonalisation.

THEOREM 2.18. (**Gram-Schmidt Orthogonalisation**) *Let X be a vector space with an inner product $\langle , \rangle$ and $\mathbf{x}_1, \ldots, \mathbf{x}_n$ be n linearly independent vectors of X. Then the algorithm below constructs an orthonormal set of vectors $\mathbf{v}_1, \ldots, \mathbf{v}_n$ spanning the same subspace.*

PROOF. See Hubbard and West [**62**, p.407]. □

ALGORITHM. Define new vectors $\mathbf{u}_i$ and $\mathbf{v}_i$ inductively as follows:

$$\mathbf{u}_1 = \mathbf{x}_1, \qquad \mathbf{v}_1 = \frac{\mathbf{u}_1}{\|\mathbf{u}_1\|},$$

$$\mathbf{u}_2 = \mathbf{x}_2 - \langle \mathbf{x}_2, \mathbf{v}_1 \rangle \mathbf{v}_1, \qquad \mathbf{v}_2 = \frac{\mathbf{u}_2}{\|\mathbf{u}_2\|},$$

$$\mathbf{u}_3 = \mathbf{x}_3 - \langle \mathbf{x}_3, \mathbf{v}_1 \rangle \mathbf{v}_1 - \langle \mathbf{x}_3, \mathbf{v}_2 \rangle \mathbf{v}_2, \qquad \mathbf{v}_3 = \frac{\mathbf{u}_3}{\|\mathbf{u}_3\|},$$

$$\vdots$$

$$\mathbf{u}_n = \mathbf{x}_n - \sum_{i=1}^{n-1} \langle \mathbf{x}_n, \mathbf{v}_i \rangle \mathbf{v}_i, \qquad \mathbf{v}_n = \frac{\mathbf{u}_n}{\|\mathbf{u}_n\|}.$$

□

In linear algebra, the Gram-Schmidt Orthogonalisation Algorithm can be used to prove that any finite-dimensional vector space with an inner product has an orthonormal basis. In CAGD, it is used to construct the n-dimensional Frénet frame along a regular parametric curve M, starting with $\mathbf{x}_1$ a tangent vector at a given point $\mathbf{p} \in M$ (see [**47**, p.357] for more details). The construction of Frénet frames can be generalised to higher-dimensional submanifolds, say k-dimensional submanifolds ($1 < k < n$), with the first k vectors given by a basis of its k-dimensional tangent space at a given point and the remaining $n - k$ vectors given by Gram-Schmidt. The key for this generalisation, for example, to surfaces is the theorem that states the existence of smooth curves passing through a point on a surface [**68**, p.525]. Recall that a tangent space at a point $\mathbf{p} \in M$ has the same dimension as M. Subsequent subsections will deal with Frénet approximations to curves and surfaces in $\mathbb{R}^3$, leaving higher-dimensional Frénet approximations open to debate.

Before proceeding, we must review a few more notions related to orthogonality. Let X be an inner product space and T be a subspace of X. The *orthogonal projection* $\pi_T(\mathbf{x})$ of $\mathbf{x}$ onto T is the unique vector in T closest to X. If T is finite-dimensional, there is a formula for $\pi_T(\mathbf{x})$ in terms of an orthonormal basis for T given by the following theorem.

THEOREM 2.19. *If X is an inner product space and T is a finite-dimensional subspace with an orthonormal basis $\mathbf{v}_1, \ldots, \mathbf{v}_k$, then*

$$\pi_T(\mathbf{x}) = \sum_i \langle \mathbf{x}, \mathbf{v}_i \rangle \mathbf{v}_i.$$

PROOF. See Hubbard and West [**62**, p.408]. □

The geometric meaning of $\pi_T(\mathbf{x})$ is illustrated in Figure 14(a). Consider in $X = \mathbb{R}^3$, a vector $\mathbf{x}$ and a plane T through the origin. Then $\pi_T(\mathbf{x})$ is the vector lying in T that is obtained by dropping perpendiculars from the ends of the vector $\mathbf{x}$ to the plane T.

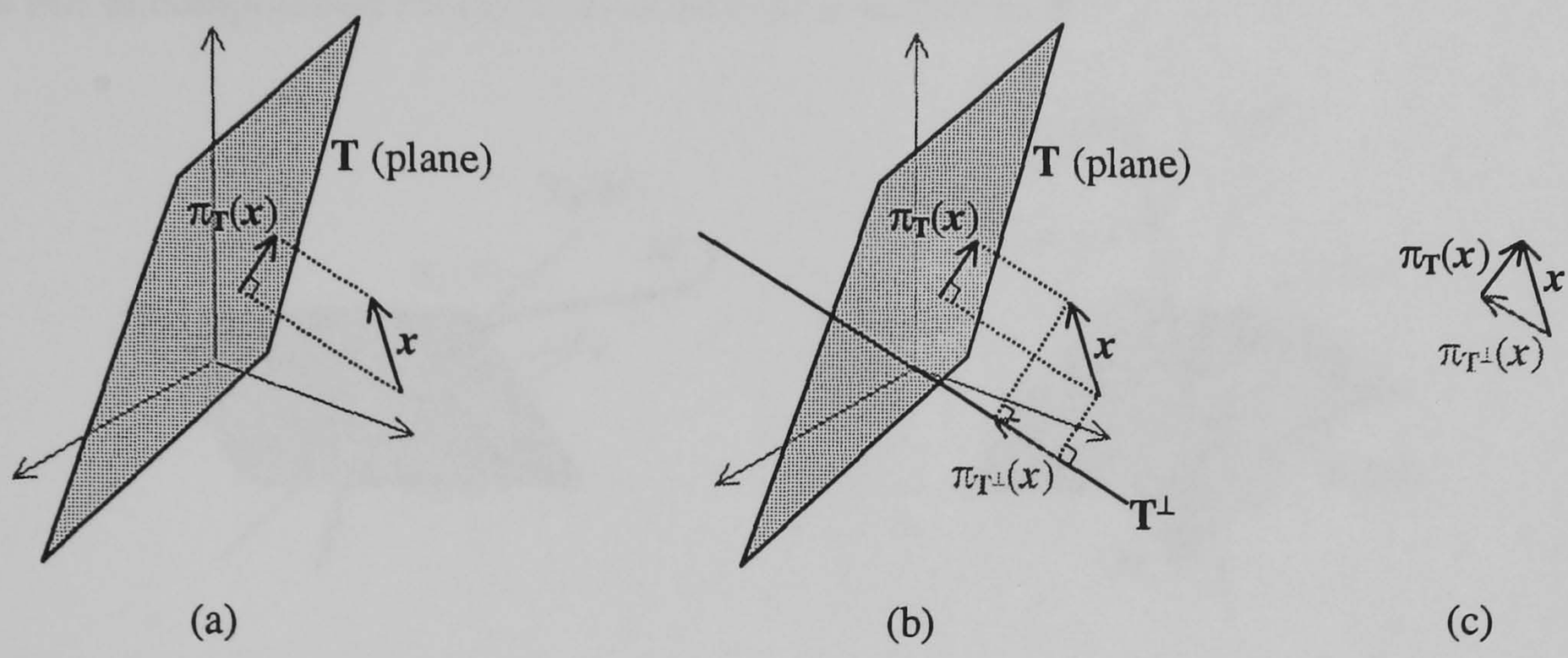

FIGURE 14. (a) Orthogonal projection of a vector $\mathbf{x}$, (b) orthogonal complement $T^\perp$ and projection $\pi_{T^\perp}(\mathbf{x})$, and (c) decomposition $\mathbf{x} = \pi_T(\mathbf{x}) + \pi_{T^\perp}(\mathbf{x})$.

Another important notion related to orthogonality is the *orthogonal complement* of a subspace T in X, which is defined by the following set of vectors

$$T^\perp = \{\mathbf{x} \in X \,|\, \langle \mathbf{x}, \mathbf{v} \rangle = 0 \text{ for all } \mathbf{v} \in T\}$$

In Figure 14(b), the orthogonal complement $T^\perp$ of the plane T is the line through the origin that is perpendicular to T. The projection $\pi_{T^\perp}(\mathbf{x})$ is the vector determined by dropping perpendiculars from the ends of $\mathbf{x}$ to the line $T^\perp$. Therefore, the vector $\mathbf{x}$ can be decomposed into two components, namely its orthogonal projection and its projection on the orthogonal complement, $\mathbf{x} = \pi_T(\mathbf{x}) + \pi_{T^\perp}(\mathbf{x})$, as illustrated in Figure 14(c). This leads to an important theorem:

THEOREM 2.20. (Hubbard and West [**62**, p.410]) *Any vector* $\mathbf{x} \in X$ *can be written uniquely as*

$$\mathbf{x} = \pi_T(\mathbf{x}) + \pi_{T^\perp}(\mathbf{x}).$$

In particular, any vector $\mathbf{x}$ defined at each point $\mathbf{p}$ of a submanifold (e.g. a curve or a surface) M but not necessarily tangent to M can be decomposed into two vectors; the first vector $\pi_T(\mathbf{x})$ lying in the tangent space $T_{\mathbf{p}}(M)$ of M at $\mathbf{p}$, and the second in the orthogonal complement of $T_{\mathbf{p}}(M)$, denoted by $T_{\mathbf{p}}^\perp(M)$. This reflects the direct sum[4] decomposition of $T_{\mathbf{p}}(\mathbb{R}^n) = T_{\mathbf{p}}(M) \oplus T_{\mathbf{p}}^\perp(M)$ into mutually

[4]Let M and N be linear spaces of X. If $M + N = X$ and $M \cap N = \{\mathbf{0}\}$ (where $\mathbf{0}$ stands for the zero vector of all vector spaces in sight), X is said to be the direct sum of M and N, written $X = M \oplus N$ [**10**, 24]. Equivalently, for each $\mathbf{x} \in X$, there exist *unique* elements $\mathbf{m} \in M$ and $\mathbf{n} \in N$ such that $\mathbf{x} = \mathbf{m} + \mathbf{n}$.

orthogonal subspaces: the *tangent* space $T_{\mathbf{p}}(M)$ and the *normal* or cotangent space $T_{\mathbf{p}}^{\perp}(M)$. Moreover, we have $\dim T_{\mathbf{p}}(\mathbb{R}^n) = \dim T_{\mathbf{p}}(M) + \dim T_{\mathbf{p}}^{\perp}(M)$. (Note that $T_{\mathbf{p}}(\mathbb{R}^n)$ and its subspace $T_{\mathbf{p}}(M)$ carry the standard inner product of $\mathbb{R}^n$ so M has the induced Riemannian metric [**15**, p.304].) Figure 15 illustrates this decomposition for (a) a curve and (b) a surface in $\mathbb{R}^3$.

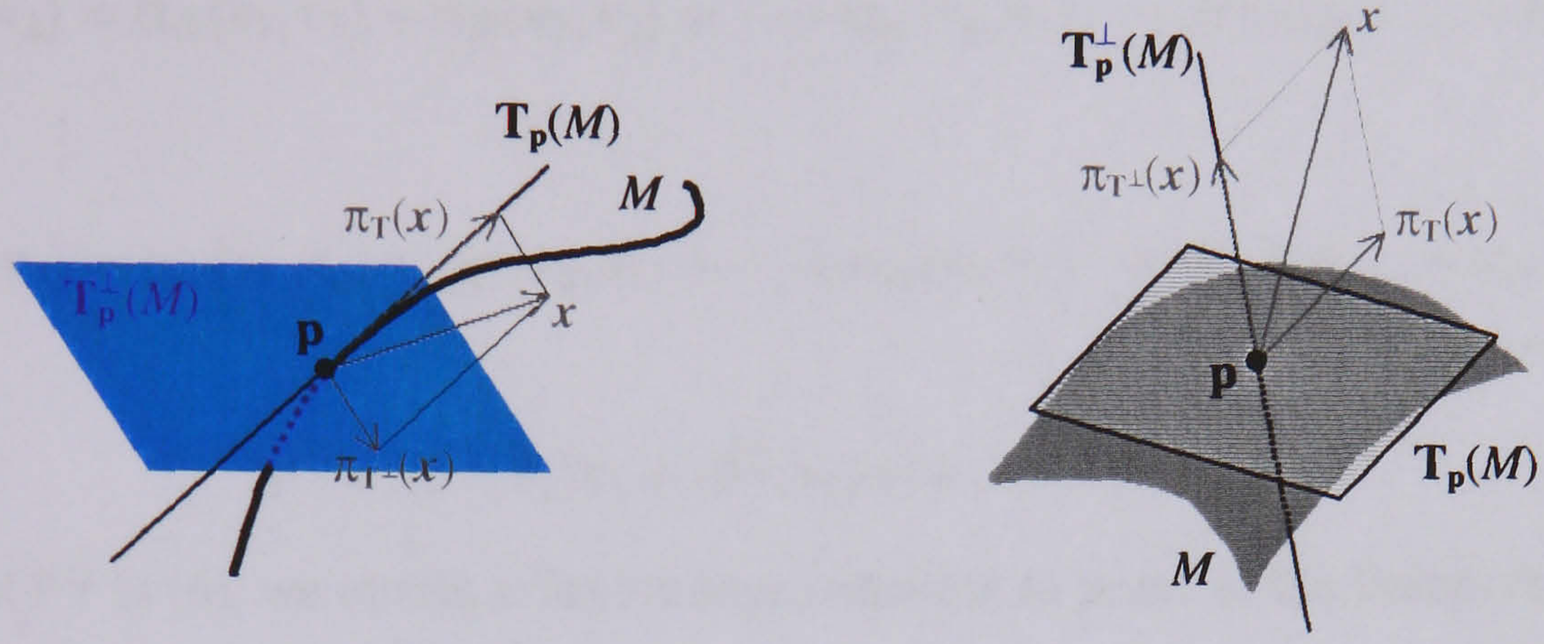

FIGURE 15

9.2. Frénet approximations for curves. A Frénet approximation of order n is a Taylor approximation that uses an orthogonal basis or frame $\mathbf{v}_1, \ldots, \mathbf{v}_n$ along a curve in $\mathbb{R}^n$.

Let $\mathbf{f} : [a,b] \subset \mathbb{R} \to \mathbb{R}^n$ be a regular parametric representation of class C^n and suppose that the n derivatives $\{\mathbf{f}^{(i)}(t)\}$ $(i = 1, \ldots, n)$ are linearly independent on $[a,b]$. The *Frénet frame* of the curve is the set of orthonormal vectors $\{\mathbf{v}_i(t)\}$ defined by the Gram-Schmidt orthogonalisation algorithm, that is

$$\mathbf{v}_i = \frac{\mathbf{u}_i}{\|\mathbf{u}_i\|}, \qquad \text{where} \qquad \mathbf{u}_i = \mathbf{f}^{(i)} - \sum_{k=1}^{i-1} \langle \mathbf{f}^{(i)}, \mathbf{v}_k \rangle \mathbf{v}_k.$$

Since $\mathbf{f}$ is C^n on $[a,b]$, its Taylor expansion up to order n at a point $p \in [a,b]$ gives:

$$\mathbf{f}(t) - \mathbf{f}(p) = t\mathbf{f}^{(1)}(p) + \frac{t^2}{2}\mathbf{f}^{(2)}(p) + \ldots + \frac{t^n}{n!}\mathbf{f}^{(n)}(p) + \mathbf{o}(t^n) \tag{6}$$

where $\mathbf{o}(t^r)$ denotes a real-valued mapping of t which is negligible with respect to t^n, i.e. that satisfies:

$$\lim_{t \to 0} \frac{1}{t^n} |\mathbf{o}(t^n)| = 0.$$

We are now in a position to make effective use of the orthonormal Frénet frame $\{\mathbf{v}_1, \mathbf{v}_2, \ldots, \mathbf{v}_n\}$. Since it is a basis any vector $\mathbf{f}^{(i)}$ can be written in the form

$$\mathbf{f}^{(i)} = \alpha_{i1}\mathbf{v}_1 + \alpha_{i2}\mathbf{v}_2 + \ldots + \alpha_{in}\mathbf{v}_n$$

with $\alpha_{i1}, \alpha_{i2}, \ldots, \alpha_{in}$ being real numbers. If we take the inner product of both sides successively with respect to $\mathbf{v}_1, \mathbf{v}_2, \ldots, \mathbf{v}_n$, we get

$$\begin{aligned}
\langle \mathbf{f}^{(i)}, \mathbf{v}_1 \rangle &= \alpha_{i1}\langle \mathbf{v}_1, \mathbf{v}_1 \rangle + \alpha_{i2}\langle \mathbf{v}_2, \mathbf{v}_1 \rangle + \cdots + \alpha_{in}\langle \mathbf{v}_n, \mathbf{v}_1 \rangle \quad &= \alpha_{i1} + 0 + \ldots + 0 = \alpha_{i1} \\
\langle \mathbf{f}^{(i)}, \mathbf{v}_2 \rangle &= \alpha_{i1}\langle \mathbf{v}_1, \mathbf{v}_2 \rangle + \alpha_{i2}\langle \mathbf{v}_2, \mathbf{v}_2 \rangle + \cdots + \alpha_{in}\langle \mathbf{v}_n, \mathbf{v}_2 \rangle \quad &= 0 + \alpha_{i2} + \ldots + 0 = \alpha_{i2} \\
&\vdots \\
\langle \mathbf{f}^{(i)}, \mathbf{v}_n \rangle &= \alpha_{i1}\langle \mathbf{v}_1, \mathbf{v}_n \rangle + \alpha_{i2}\langle \mathbf{v}_2, \mathbf{v}_n \rangle + \cdots + \alpha_{in}\langle \mathbf{v}_n, \mathbf{v}_n \rangle \quad &= 0 + 0 + \ldots + \alpha_{in} = \alpha_{in}.
\end{aligned}$$

Therefore,

$$\mathbf{f}^{(i)} = \langle \mathbf{f}^{(i)}, \mathbf{v}_1 \rangle \mathbf{v}_1 + \langle \mathbf{f}^{(i)}, \mathbf{v}_2 \rangle \mathbf{v}_2 + \ldots + \langle \mathbf{f}^{(i)}, \mathbf{v}_n \rangle \mathbf{v}_n$$

Substituting all $\mathbf{f}^{(i)}$ in (6), we obtain a Taylor approximation in terms of the Frénet frame, here called **Frénet approximation**, with

$$[\mathbf{f}^{(1)}, \ldots, \mathbf{f}^{(n)}]^T = \mathrm{L}[\mathbf{v}_1, \ldots, \mathbf{v}_n]^T$$

where L is a $n \times n$ matrix given by

$$\mathrm{L} = \begin{bmatrix}
\langle \mathbf{f}^{(1)}, \mathbf{v}_1 \rangle & \langle \mathbf{f}^{(1)}, \mathbf{v}_2 \rangle & \ldots & \langle \mathbf{f}^{(1)}, \mathbf{v}_n \rangle \\
\langle \mathbf{f}^{(2)}, \mathbf{v}_1 \rangle & \langle \mathbf{f}^{(2)}, \mathbf{v}_2 \rangle & \ldots & \langle \mathbf{f}^{(2)}, \mathbf{v}_n \rangle \\
\vdots & & & \\
\langle \mathbf{f}^{(n)}, \mathbf{v}_1 \rangle & \langle \mathbf{f}^{(n)}, \mathbf{v}_2 \rangle & \ldots & \langle \mathbf{f}^{(n)}, \mathbf{v}_n \rangle
\end{bmatrix}$$

The matrix L becomes a lower triangular because the Frénet frame is constructed by first making $\mathbf{v}_1$ the unit tangent vector to the curve at a given point, that is

$$\mathbf{f}^{(1)} = \alpha \mathbf{v}_1, \quad \text{with } \alpha = \|\mathbf{f}^{(1)}\|. \tag{7}$$

So, all $\mathbf{f}^{(i)}$ can be determined by successive differentiation from $\mathbf{f}^{(1)}$. But this requires we know the Frénet equations that give us $\{\mathbf{v}_i^{(1)}\}$ in terms of $\{\mathbf{v}_i\}$. This system of differential equations was developed in [**47**]. Since $\mathbf{v}_i^{(1)} \in \mathrm{span}\{\mathbf{v}_j\}_{i+1}^{j=1}$, it follows that

$$[\mathbf{v}_1^{(1)}, \ldots, \mathbf{v}_n^{(1)}]^T = \mathrm{K}[\mathbf{v}_1, \ldots, \mathbf{v}_n]^T \tag{8}$$

where $\mathrm{K} = [k_{ij}]$ is a lower Hessenberg matrix. From the orthonormality of the Frénet frame, we have

$$k_{ij} = \langle \mathbf{v}_i^{(1)}, \mathbf{v}_j \rangle.$$

Also, taking the orthonormality conditions $\langle \mathbf{v}_i, \mathbf{v}_j \rangle = \delta_{ij}$, and differentiating them, we get

$$k_{ij} + k_{ji} = 0.$$

The resulting matrix K for the Frénet differential equations (8) is therefore a lower Hessenberg, skew-symmetric matrix, and can now be written as

$$\mathrm{K} = \begin{bmatrix} 0 & \kappa_1 & & & \\ -\kappa_1 & 0 & \kappa_2 & & \\ & \ddots & \ddots & \ddots & \\ & & -\kappa_{n-2} & 0 & \kappa_{n-1} \\ & & & -\kappa_{n-1} & 0 \end{bmatrix}$$

where the quantities are called the curvatures of the curve. In particular, in $\mathbb{R}^2$, κ_1 is the curvature, while in $\mathbb{R}^3$, κ_1 is the curvature and κ_2 is the torsion (or second curvature). So, the Frénet equations (8) can be written as

$$\begin{aligned} \mathbf{v}_1^{(1)} &= \kappa_1 \mathbf{v}_2 \\ \mathbf{v}_2^{(1)} &= -\kappa_1 \mathbf{v}_1 + \kappa_2 \mathbf{v}_3 \\ &\vdots \\ \mathbf{v}_{n-1}^{(1)} &= -\kappa_{n-2} \mathbf{v}_{n-2} + \kappa_{n-1} \mathbf{v}_n \\ \mathbf{v}_n^{(1)} &= -\kappa_{n-1} \mathbf{v}_{n-1} \end{aligned}$$

Finally, we can determine the Frénet approximation in terms of Frénet frame and curvatures, i.e. against the Frénet-Serret apparatus $\{\mathbf{v}_1, \ldots, \mathbf{v}_n, \kappa_1, \ldots, \kappa_{n-1}\}$ in $\mathbb{R}^n$. Accordingly, we take the starting equation (7) and determine its successive derivatives by combining them with the differential Frénet equations. That is,

$$\begin{aligned} \mathbf{f}^{(1)} &= \alpha \mathbf{v}_1 \\ \mathbf{f}^{(2)} &= \alpha \mathbf{v}_1^{(1)} && = \alpha \kappa_1 \mathbf{v}_2 \\ \mathbf{f}^{(3)} &= \alpha \kappa_1 \mathbf{v}_2^{(1)} && = -\alpha \kappa_1^2 \mathbf{v}_1 + \alpha \kappa_1 \kappa_2 \mathbf{v}_3 \\ \mathbf{f}^{(4)} &= -\alpha \kappa_1^2 \mathbf{v}_1^{(1)} + \alpha \kappa_1 \kappa_2 \mathbf{v}_3^{(1)} && = -(\alpha \kappa_1^3 + \alpha \kappa_1 \kappa_2^2) \mathbf{v}_2 + \alpha \kappa_1 \kappa_2 \kappa_3 \mathbf{v}_4 \\ \mathbf{f}^{(5)} &= \ldots && = (\alpha \kappa_1^4 + \alpha \kappa_1^2 \kappa_2^2) \mathbf{v}_1 + (-\alpha \kappa_1^3 \kappa_2 - \alpha \kappa_1 \kappa_2^3 - \alpha \kappa_1 \kappa_2 \kappa_3^2) \mathbf{v}_3 + \alpha \kappa_1 \kappa_2 \kappa_3 \kappa_4 \mathbf{v}_5 \\ &\vdots \end{aligned}$$

Thus, the lower triangular matrix L is given by

$$\mathrm{L} = \begin{bmatrix} \alpha & & & & \\ 0 & \alpha\kappa_1 & & & \\ -\alpha\kappa_1^2 & 0 & \alpha\kappa_1\kappa_2 & & \\ 0 & -\alpha\kappa_1^3 - \alpha\kappa_1\kappa_2^2 & 0 & \alpha\kappa_1\kappa_2\kappa_3 & \\ \ddots & 0 & \ddots & 0 & \ddots \\ & \cdots & & & \alpha\kappa_1\kappa_2\ldots\kappa_{n-1} \end{bmatrix}$$

In short, the Frénet approximation is a refinement of the Taylor approximation with $\{\mathbf{f}^{(1)},\ldots,\mathbf{f}^{(n)}\}$ replaced by the Frénet-Serret apparatus.

9.3. Frénet approximations for surfaces and higher-dimensional submanifolds. In computer aided geometric design (CAGD) is not usual to determine a Frénet frame and higher-dimensional curvatures for surfaces and higher-dimensional submanifolds. The CAGD literature almost exclusively refers to Frénet frame and curvatures for parametric curves. The Gram-Schmidt orthogonalisation provides a process to determine a i-dimensional tangent space at a point of a i-dimensional submanifold.

In fact, looking at the expressions of Gram-Schmidt for curves in the previous subsection, we observe that $\sum_{k=1}^{i-1}\langle\mathbf{f}^{(i)},\mathbf{v}_k\rangle\mathbf{v}_k$ is nothing more than $\pi_{T^{i-1}}(\mathbf{f}^{(i)})$, the orthogonal projection of $\mathbf{f}^{(i)}$ onto the subspace $T^{i-1}\subset\mathbb{R}^n$ Gram-Schmidt generated by the subbasis $\mathbf{v}_1,\mathbf{v}_2,\ldots,\mathbf{v}_{i-1}$. This subspace T^{i-1} is called an $(i-1)$-dimensional *flag* of $\mathbb{R}^n$. The iterative nature of Gram-Schmidt orthogonalisation enables the construction of an ascending sequence of subspaces $T^1\subset T^2\subset\ldots\subset T^n=\mathbb{R}^n$ [**62**, p.462], with each subspace T^i of dimension i generated by the subbasis $\mathbf{v}_1,\mathbf{v}_2,\ldots,\mathbf{v}_{i-1},\mathbf{v}_i$, i.e. generated from the subbasis $\mathbf{v}_1,\mathbf{v}_2,\ldots,\mathbf{v}_{i-1}$ of T^{n-1} and $\mathbf{v}_i$ calculated by the Gram-Schmidt orthogonalisation process.

In case of an i-dimensional submanifold in $\mathbb{R}^n$ represented by a mapping $\mathbf{f}$, an i-dimensional flag in $\mathbb{R}^n$ can be viewed as an i-dimensional tangent space at a point of an i-dimensional submanifold. Such an i-dimensional tangent space can be generated by the k derivatives ($k=1,\ldots,i$) of $\mathbf{f}$. Thus, the Gram-Schmidt orthogonalisation technique can be applied to any i-dimensional submanifold ($i<n$) of $\mathbb{R}^n$ to determine its Frénet approximation. Besides, the Gram-Schmidt orthogonalisation can proceed up to dimension n to determine the Frénet frame.

10. Smoothness in geometric design and modelling

Some CAGD authors have argued that there are various kinds of visual smoothness or geometric continuity (e.g. Frénet frame continuity). But, what exists in the CAGD literature is different methods to achieve such a 'visual smoothness' for curves and surfaces. Well-known methods to achieve geometric continuity are those based on *geometric invariants* such tangents, curvatures and torsions. But, a geometric invariant may be not sufficient to guarantee 'visual smoothness' of a piecewise curve or surface. As any invariant, a geometric invariant is a mathematical tool to compare certain properties of geometric objects. For example, to obtain a bigger G^r curve from two touching G^r curves, it is required that they are joined with the same sided tangents, curvature, torsions, and higher order curvatures up to r. However, the fact that some geometric invariants are preserved does not guarantee that the resulting curve is G^r, for any positive integer r.

The essential thing about invariants is the kind of mappings we use to transform a set into another. In Chapter 1, we saw that homeomorphisms (i.e. continuous mappings with continuous inverses) are continuous deformation mappings which preserve certain properties, called topological properties, associated with topological invariants e.g. dimension, Betti numbers, etc.). Analogously, in the present chapter, the mappings associated with smoothness or geometric continuity as understood in CAGD are called *diffeomorphisms* in differential geometry. That is, from a CAGD point of view, a continuously geometric or G^r mapping is a C^r diffeomorphism, i.e. a C^r mapping whose inverse mapping is also C^r mapping. (Usually, this is ensured by imposing the condition that the first derivative is not zero [**47**, p.355].) This means that at a junction point of two C^r curves, the partial derivatives of a mapping C^r, as well as the partial derivatives of its inverse are identical. Notably, it is known that a C^r mapping that is a C^1 diffeomorphism is a C^r diffeomorphism (see Theorem 1.5 (Chapter 1)). Therefore, to guarantee that a C^r mapping is a C^r diffeomorphism, it is sufficient that it is a C^1 diffeomorphism, i.e. the first derivative of its inverse is C^1.

Thus, the concept of diffeomorphism is essential to define geometric continuity in CAGD. It is the starting point to establish the C^r contact conditions between two curves or higher dimensional manifolds (see Lemma 2.17). This implies the equality of their Taylor expansions, and their Frénet expansions as well. Therefore, diffeomorphisms preserve geometric invariants such as tangents, curvatures, torsions, and higher dimensional curvatures. Clearly, the essential kind of smoothness for manifolds is the C^r smoothness. Other sorts of smoothness found in CAGD literature are just particular techniques to achieve C^r smoothness.

Another important point related to smoothness or geometric continuity is the problem of *representation-independence*. Some geometric modelling applications may require that manifolds (e.g. curves and surfaces) are composed of touching submanifolds represented *implicitly* or *parametrically*. The question is how can we ensure geometric continuity between touching submanifolds defined by distinct kinds of point set representations (e.g. level set and image of two different mappings), i.e. implicit and parametric representations of point sets? In fact, as shown in the CAGD literature (see, for example, [39]), there are different methods to achieve visual smoothness, depending whether a curve or a surface is explicitly, *implicitly* or *parametrically* represented. However, no method has been devised for piecewise manifolds made up of patches with distinct representations (e.g. a parametric patch adjacent to an implicit patch of a surface). Obviously, this may be irrelevant in the 'massively parametric world' of free-form geometric modelling. However, in the general context of shape integration, the problem of representation-independent smoothness or 'geometric continuity' is critical, regardless of whether the representational conversion of a curve or surface is possible or not.

On the other hand, in geometric solid modelling, manifolds are usually constituents of a stratified set. Such constituents are called *strata* in stratification theory. In B-rep modelling, such stratified sets are known as B-rep objects and strata are called cells. Obviously, in B-rep modelling there is not too much concern about keeping smoothness conditions on, for example, the boundary of a solid object. But this does not mean that smoothness conditions are not relevant for geometric solid modelling. In fact, they are! For example, the creation of the non-smooth surface of a B-rep cube leads to the partition of its point set into a collection of smooth manifolds, namely: six smooth 2-manifolds (faces), twelve smooth 1-manifolds (edges), and eight smooth 0-manifolds (vertices). The surface of a cube is then a 2-dimensional non-smooth manifold that admits a partition into d-dimensional smooth submanifolds, with $0 \leq d \leq 2$. It is said to be a piecewise smooth manifold. The collection of 1-submanifolds and 0-submanifolds are *singularities* of the cube surface because a tangent plane suddenly flips there. That is, a cube surface is not a smooth manifold, since there is no tangent plane at the corners or along the edges. Therefore, the intuitive understanding of a solid object as composed of vertices, edges, faces and a solid meets the notion of a stratified set: a non-smooth point set is stratified into a piecewise smooth point set.

Therefore, manifolds can be either smooth or non-smooth. Non-smooth manifolds are in principle piecewise smooth manifolds. This leads us to the idea of partitioning a n-dimensional manifold into smooth k-dimensional submanifolds ($k \leq n$). The family of smooth submanifolds of dimension less than n are singularities of such a n-dimensional manifold. This simple idea is based on the pioneering work of two mathematicians, Whitney and Thom, nowadays known as Thom-Whitney stratification

theory. They showed that there is a close relationship between the concepts of differentiability and stratifiability of manifolds. Notably, both concepts are related even when they are applied to more general geometric point sets such as algebraic, analytic or even semianalytic varieties.

This discussion suggests that *smoothness* is a unifying concept in the theory of geometric modelling. Smoothness theory (from differential geometry), stratification theory, and singularity theory altogether constitute important mathematical cornerstones for geometric modelling theory.

11. Summary

We have shown that C^r smoothness from differential geometry generalises the concepts of visual smoothness found in the CAGD literature, and that it is representation-independent. The essential key to having smoothness on a manifold is the concept of diffeomorphism, that is, a differentiable mapping with a differentiable inverse. The differentiability of a mapping is not enough to guarantee the smoothness of a manifold (see Example 1.56); its inverse must be also differentiable. As noted in [37, p.106], smoothness and differentiability do not agree. Smoothness means that the defining mapping of a submanifold is a diffeomorphism.

Only a smooth mapping with smooth inverse, i.e. a diffeomorphism, ensures the smoothness of a parametric curve or surface. Thus, the smoothness of a submanifold depends more on the properties of the mapping used to define it than on its associated geometric invariants (e.g. curvature and torsion). The use of a geometric invariant may be not conclusive to ensure smoothness on a submanifold, as a topological invariant (e.g. Betti numbers) is not sufficient to characterise the continuity of a subspace. In geometric design, the relationships between diffeomorphisms and geometric invariants have not been very well understood yet. Usually, in geometric design, the smoothness criteria are based on geometric invariants, and this has led to the proliferation of many kinds of visual smoothness. Nevertheless, mathematicians have studied smoothness for decades. They proved that smoothness of a submanifold is only preserved by diffeomorphisms, regardless of whether the representation is implicit or parametric.

The relationship between the invertibility and smoothness of a mapping has led us to its algebraic counterpart, that is, the relationship between the invertibility of the Jacobian and smoothness of a submanifold. We have shown that this relationship is independent of whether we treat submanifolds as level sets, images, or graphs of mappings. So, we have shown that C^1 smoothness can be determined by the rank-based criterion. This suggests that we can determine the singularities of a submanifold by observing where the rank is not constant.

This smoothness analysis has also been extended to higher-order C^r smoothness by using the Taylor expansion, which can be refined by the Frénet approximation to get the usual geometric invariants in $\mathbb{R}^n$, namely the Frénet frame (i.e. i-dimensional tangent spaces) and curvatures.

The analysis of the rank of the Jacobian and the Taylor series have also suggested that we can envisage some rank-based and jet-based techniques to stratify varieties. This is developed in the next chapter.

The main contributions of this chapter (in the context of geometric modelling) are then the following:

- To show that the theory of functions allows us to have a unified view of point sets. The level set of a mapping corresponds to an implicit representation of a point set as usual in CSG, while its image corresponds to a parametric representation of another point set. Thus, this chapter shows that a unified mathematical theory for the representation of geometric objects exists indeed.
- To show that it is possible to establish C^r smoothness conditions on a submanifold that are coordinate-free and, consequently, representation-independent.
- To outline a computable approach to determine C^r smoothness on submanifolds. This approach generalises those found in computer aided geometric design of parametric curves and surfaces.
- To show that C^r smoothness (of manifolds) as defined in differential geometry is a generalisation of geometric continuity G^r often used in geometric design.
- To make clear that there is only one essential kind of smoothness, the C^r smoothness.
- To show that smoothness —or lack of smoothness— is central to geometric modelling.
- To show the intimate relationships between smoothness theory and both singularity theory and stratification theory.

CHAPTER 3

Stratifications and geometries

La possibilité d'utiliser le modèle differential est, à mes yeux,
la justification ultime de l'emploi des modèles quantitifs dans les sciences.

R. Thom, Stabilité Structurelle et Morphogénèse, 1972

Stratification is a fundamental concept in differential and algebraic geometry. The study of stratifications originated with the work of Whitney and Thom on singularities of analytic varieties (see [**119**] and [**110**]). The basic idea behind this study was to subdivide or partition a k-dimensional piecewise smooth variety into smooth submanifolds of dimension less than or equal to k. The singularities were just the union of all submanifolds of dimension less than k. This process was called 'removal of singularities'. A simple example of this process is the subdivision of a cube surface into faces, edges and vertices, where the edges and vertices are singularities. This simple idea developed into what is nowadays known as *Thom-Whitney stratification theory*. Basically, they demonstrated that there is a close relationship between the concept of differentiability and stratifiability of manifolds and varieties. Notably, both concepts are related even when they are applied to more general geometric point sets such as, for example, algebraic and analytic semivarieties. These semivarieties were studied by Gabrielov [**38**], Hironaka [**59, 58**], and Hardt [**55, 54**], as a natural extension of the theory of semianalytic sets developed by Lojasiewicz [**70, 71**].

Our purpose is to show that the Thom-Whitney stratification theory can work as a unifying mathematical theory in geometric modelling. It deals with stratifiable geometries, namely: algebraic, analytic, semialgebraic, semianalytic and, more generally, the subanalytic geometry. The objects in these geometries are commonly used in geometric design. The Thom-Whitney theory shows us the close relationship between geometry and stratifiability (or stratified structure) as a generalisation of the duality between geometry and structure of the well-known B-rep (boundary representations) data structures found in geometric modelling literature. This generalisation has led to the n-dimensional boundary representation described in next chapter.

1. Topological stratifications

The mathematical theory of stratifications was initially developed for the 'removal' of singularities or, equivalently, regularisation of analytic sets [**120**]. (This kind of regularisation has nothing to do with the regularisation of set-combinations commonly used in the geometric modelling research.) Perhaps the first attempt at an abstract theory of stratifications appears in Whitney's concept of a "complifold", or complex of manifolds [**118**, 1947]. However, only in the paper [**109**, 1962], Thom introduces the term "stratification" and the notion of "regularity" on how the strata of a stratification should fit together.

The basic idea of a *stratification* was to decompose an algebraic and, more generally, an analytic variety V into a finite, disjoint union of manifolds (just as with simplicial or CW complexes),

$$V = M_1 \cup M_2 \cup \ldots \cup M_k,$$

where each M_i is called a *stratum* of the stratification.

Stratifications are distinguished from each other by using a particular *local regularity* criterion of separation or partition. This section deals with only topological criteria, whilst next sections use differential criteria, the Whitney conditions in particular. The topological criteria appeal to the essence of topology as described in Chapter 1, and are not explicitly described and explained in the mathematical literature. However, they are useful because they help us to better understand the mathematical tools from the point-set topology and differential topology in the study of stratifications of varieties and semivarieties. Besides, some engineering applications based on geometric kernels (e.g. finite-element modelling and analysis) require stratifications whose submanifolds are not necessarily smooth, they may be just topological embedded submanifolds. So, it is convenient to be aware of these topological stratifications.

It is necessary to bear in mind that each stratum of any stratification must be a submanifold. Consequently, all cut-submanifolds (i.e. cut-points, cut-lines, cut-surfaces, and higher-dimensional cut-submanifolds) should be 'removed' in the sense they are singularities in a variety. (A cut-manifold is a generalisation of the the concept of cut-point introduced in Chapter 1.) These cut-submanifolds are topological singularities. Recall that there is a *topological singularity* at a point p of a variety V if the intersection of a small neighbourhood of p with V is not homeomorphic to a ball, that is, it does not have the topological type of a ball.

1.1. Ordinary topological stratifications. These stratifications, shortly *OrdT stratifications* or simply *stratifications*, do not satisfy any local regularity criterion, unless *manifoldness*. That is, as

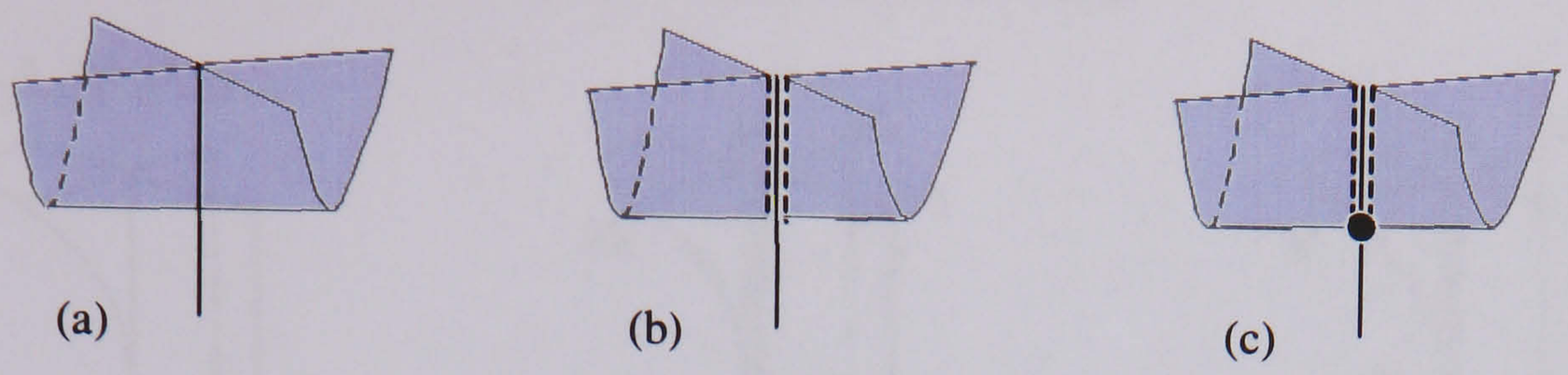

FIGURE 1

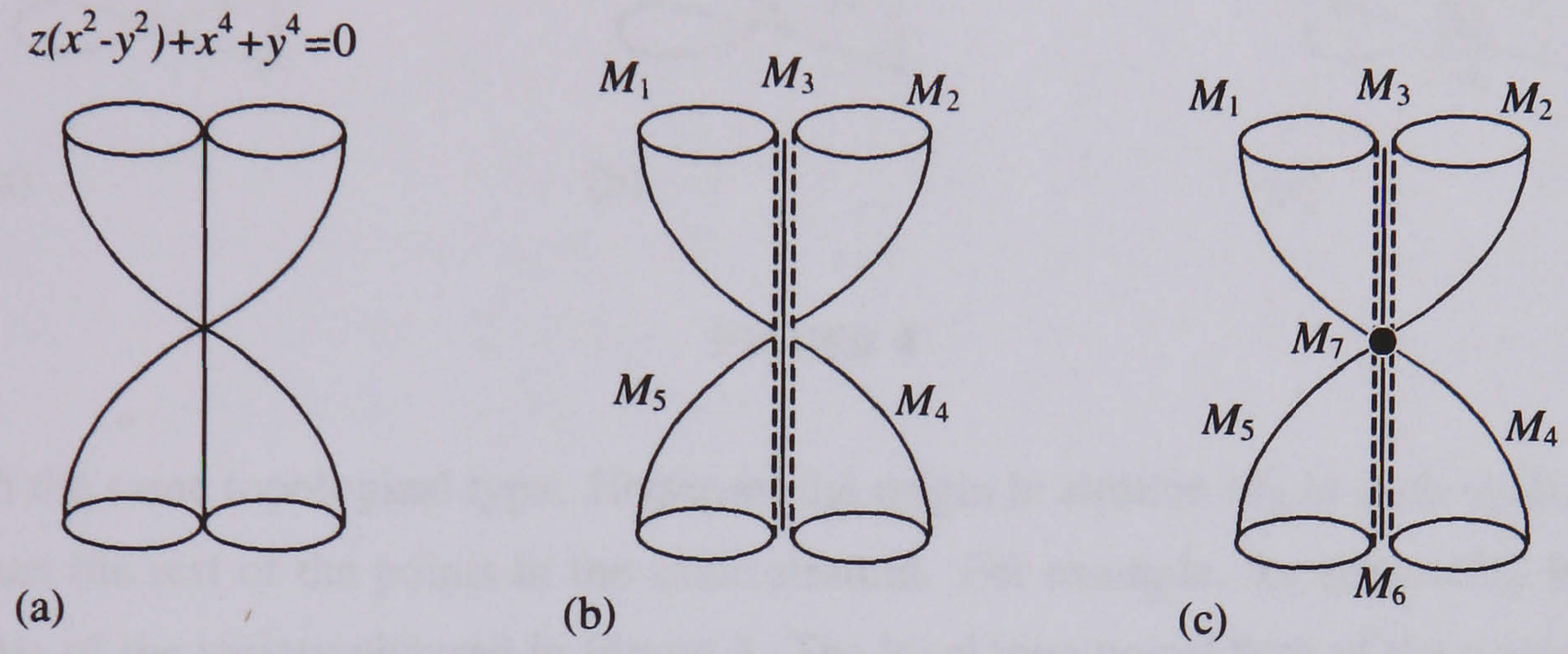

FIGURE 2

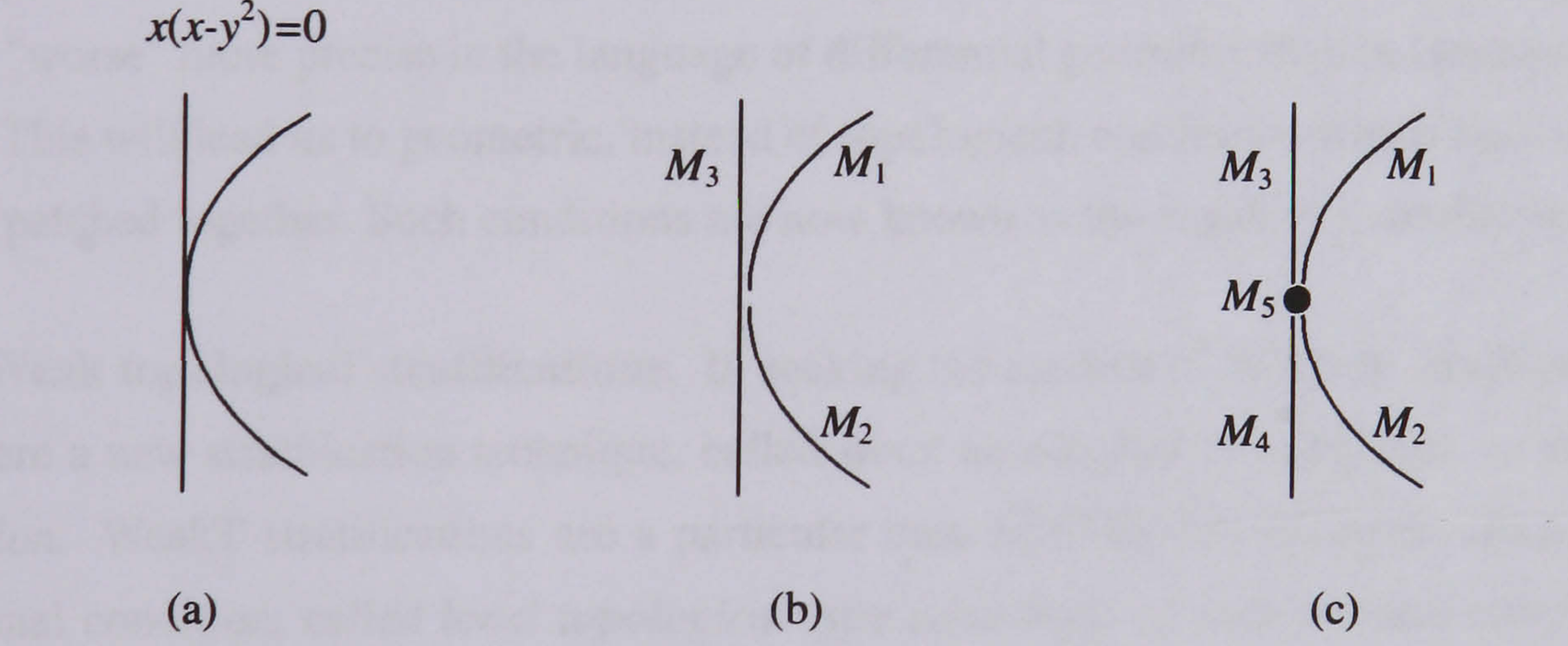

FIGURE 3

for any type of stratification, the strata must be manifolds. Thus, this is the most general type of stratification.

For example, all stratifications (b) and (c) depicted in Figures 1, 2, 3, 4 are OrdT stratifications. However, there is a significant difference between the stratifications (b) and the stratifications (c). Intuitively, unlike stratifications (c), stratifications (b) are not what we want in the sense that each stratum should consist of "equally bad" points. More formally, by "equally bad" points we mean

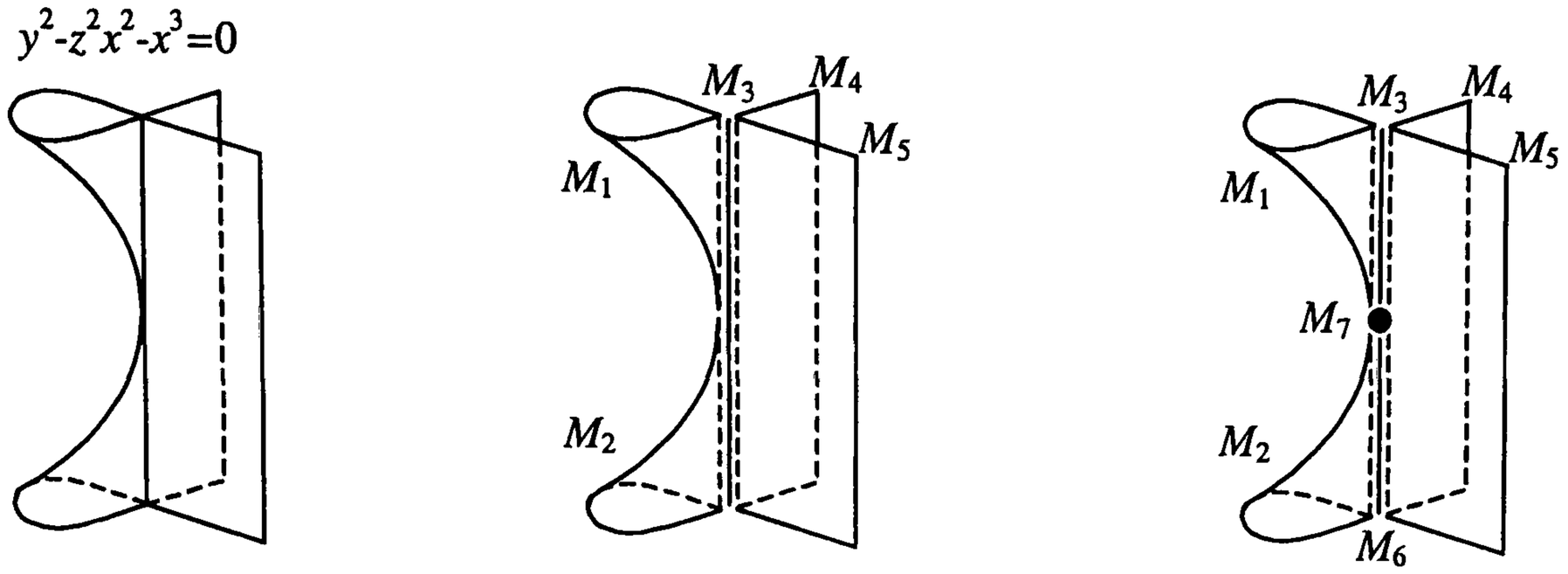

(a) (b) (c)

FIGURE 4

points with the same topological type. However, the origin in stratum M_3 in each stratification (b) is "worse" than the rest of the points in the same stratum. For example, for simplicity, let us take the manifold M_3 of the variety pictured in Figure 3. The local topological type of the origin in M_3 is the same as of a 1-dimensional cross-shaped (e.g. the xy-axes) object, while the local topological type of any other point in M_3 is that of a single open line segment. In next section we will make the words "bad" and "worse" more precise in the language of differential geometry than in language of point-set topology. This will lead us to geometric, instead of topological, conditions which state how the strata should be patched together. Such conditions are now known as the *regularity conditions of Whitney*.

1.2. Weak topological stratifications. In seeking the essence of Whitney stratifications, we introduce here a new stratification technique, called *weak topological stratification*, or shortly *WeakT stratification*. WeakT stratifications are a particular case of OrdT stratifications since they impose an additional condition, called *local topological type condition*, on each stratum *component*. It establishes that any two points of a stratum component have the same topological type (i.e. they are homeomorphs) in its ambient variety V. Using previous words, this is equivalent to say that the points of any stratum component are all "equally bad". Two points are "equally bad", say they have the same topological type, if their neighbourhoods in a variety (or, more generally, a point set) are homeomorphic or topologically equivalent. This topological condition leads to a regular adjacency of the stratum components in a stratified variety as we use to see in B-rep (boundary representation) data structures. Unfortunately, because of its topological nature, differential singularities such as cusps and corners are not detectable by geometric kernels based on topological type stratification techniques. Later on, we will see criteria to recognize such differential singularities.

The stratifications (c), but not the stratifications (b), in Figures 1, 2, 3, 4 are all WeakT stratifications. Both OrdT and WeakT stratifications 'remove' all topological singularities (i.e. cut submanifolds, and self-intersections in particular) of a variety. They remove topological singularities such that the resulting 'building blocks' are all connected submanifolds. However, only WeakT stratifications guarantee that all the points in each stratum possess the same topological type in a variety or semivariety.

EXAMPLE 3.1. Let us stratify the variety $V = \{(x,y,z) \in \mathbb{R}^3 : z(x^2 - y^2) + x^4 + y^4\}$ in Figure 2. Any point of V along the z-axis is topologically a singular point because an open neighbourhood of it in V is not homeomorphic to an open ball in V. Thus, the z-axis originates the stratum M_3 for the corresponding OrdT stratification in Figure 2(b). No further stratification is required for V because its partition against M_3 (z-axis) originates more four 2-dimensional sheets, M_1, M_2, M_4, M_5, all them manifolds. Taking now in consideration the local topological type condition, we see that all points of M_3 in Figure 2(b), except the origin $(0,0,0)$, have the same topological type. That is, the origin is "worse" than the other "bad" points in the z-axis. Therefore, the z-axis has to be further stratified into a 0-stratum M_7 (the origin) and two 1-strata, namely M_6 (the negative z-axis) and a redefined M_3 (the positive z-axis). The result is the WeakT stratification depicted in Figure 2(c).

Therefore, a WeakT stratification has in general more stratum components than an OrdT stratification due to the topological type condition. A WeakT stratification is then a refinement for a OrdT stratification. The term 'weak' is because the local topological type criterion is applicable to stratum components, not to strata. This means that the 'building blocks' of any WeakT stratification are stratum components, and that we are free to define the strata we want since all the components of each stratum are equidimensional. This is particularly useful for many geometry-based applications such as, for example, computer aided design and computer graphics, where often the user or designer enjoys how the geometric kernel machine is flexible to meet his/her human creative process. Thus, a WeakT stratification admits multi-component strata. That is, a WeakT stratification has two stratification levels, the first level for components and the second level for strata. At the first level, stratum components satisfy the local topological type regularity condition. At the second level, the stratum components are gathered into strata, each stratum with possibly more than one component.

EXAMPLE 3.2. The WeakT stratification of the Cartan umbrella in Figure 1(c) has four possible distributions Γ_i ($i = 1 \ldots 4$) for its strata, as shown in Figure 5. [The brackets denote that each stratum is a set of components.] All the strata of Γ_1 are connected; hence each stratum contains exactly one component. But, the only 2-stratum of Γ_2 has two components, the two sheets M_1, M_2; the remaining

strata of Γ_2 are connected. Similar distribution has Γ_3, but now it is its 1-stratum that possesses two components M_3, M_4. At last, Γ_4 has two strata which are not connected, namely its 1-,2-strata. The components of its 1-stratum are M_3 and M_4, while the components of its 2-stratum are M_1 and M_2.

	0-strata	1-strata	2-strata
Γ_1	$\{M_5\}$	$\{M_3\},\{M_4\}$	$\{M_1\},\{M_2\}$
Γ_2	$\{M_5\}$	$\{M_3\},\{M_4\}$	$\{M_1,M_2\}$
Γ_3	$\{M_5\}$	$\{M_3,M_4\}$	$\{M_1\},\{M_2\}$
Γ_4	$\{M_5\}$	$\{M_3,M_4\}$	$\{M_1,M_2\}$

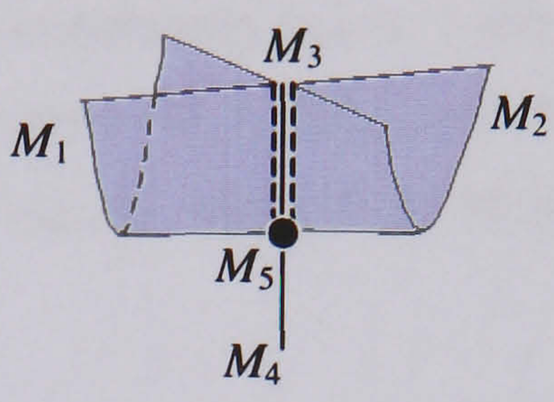

FIGURE 5. The four possible WeakT stratifications of the Cartan umbrella $x^2 - zy^2 = 0$.

Note that a WeakT stratification satisfies the local topological type condition. That is, all the points of a stratum component have the same topological type. However, its strata need not satisfy this criterion. For example, the strata of Γ_3 and Γ_4 do not satisfy the local topological type condition because the components M_3 and M_4 of their 1-stratum do not possess the same local topological type.

1.3. Strong topological stratifications. If we impose the local topological type condition on the strata, instead of their components, we get a more constrained topological stratification, called *strong topological stratification*, or *StrongT stratification.* It is clear that a StrongT stratification is a particular case of a WeakT stratification because if their strata satisfy the topological type condition, then their components also do. The word 'strong' just highlights that the topological type condition is satisfied not only for components but also for strata.

Obviously, if all the strata are connected, then a StrongT stratification and its underlying WeakT stratification coincide, as it is the case of the stratification Γ_1 of the Cartan umbrella above. The WeakT stratification Γ_2 is also a StrongT stratification, but not Γ_3 nor Γ_4. Thus, a StrongT stratification is nothing than a WeakT stratification whose strata also satisfy the local topological type criterion.

Unfortunately, StrongT stratifications are not very well adequate for interactive geometric design. Their topological type condition on strata is too restrictive and impose changes on the stratification that do not necessarily follow the intended design changes. Let us illustrate this situation with an example.

EXAMPLE 3.3. Let us consider again the WeakT-stratified variety in Figure 2(c). Assume that it has been organised into three strata, one for each dimension. Therefore, we have one 2-stratum

$\{M_1, M_2, M_4, M_5\}$ with four components, one 1-stratum $\{M_3, M_6\}$ with two components, and a connected 0-stratum $\{M_7\}$. Now, suppose that a designer intends to remove the sheet M_1. Deleting M_1 implies a re-arrangement of the remaining stratum components into strata. Otherwise, the topological type condition on strata is no longer satisfied, i.e. the topological consistency is lost. Such an arrangement requires the splitting of the 1-stratum $\{M_3, M_6\}$ into two 1-strata $\{M_3\}$, $\{M_6\}$, and the 2-stratum $\{M_1, M_2, M_4, M_5\}$ into two 2-strata $\{M_2\}$, $\{M_4, M_5\}$. But, the designer intent might be just to delete M_1 without changing anything else.

1.4. Topological splittings. The power of the topological type stratifications is that *all* topological invariants (e.g. dimension, cut-points and dimensional homogeneity) work simultaneously in the neighbourhood of each point of a component or a stratum. Obviously, *topological splittings* more general than topological stratifications are possible to envisage by relaxing the local topological type condition. These topological splittings are in a sense incomplete topological 'stratifications' viewing that they only satisfy particular collections of topological invariants. Nevertheless, no one expects that such topological splittings satisfy the topological type criterion, simply because a collection of topological invariants do not necessarily ensure the same local topological type over a connected component or stratum. Even so, these topological splittings are useful to better appreciate the topological type stratifications described above. Let us see then three kinds of these topological splittings.

1.4.1. *Topological splittings based on local dimension.* As shown in Chapter 1, dimension is a topological invariant. Let $X \subseteq \mathbb{R}^n$ a set and $\mathbf{x} \in \mathbb{R}^n$. There is a number $d \in \{-\infty, 0, \ldots, \dim X\}$ such that $\dim(U \cap X) = d$ for any sufficiently small neighbourhood U of $\mathbf{x}$ in $\mathbb{R}^n$. The number d defined by this property is called the *local dimension of* X *at* $\mathbf{x}$, notation $\dim_{\mathbf{x}}(X)$ [**29**, p.69]. Note that $\dim_{\mathbf{x}}(X) = -\infty$ iff $\mathbf{x} \notin \mathrm{Cl}(X)$. Consequently, if X is a d-dimensional manifold, then $\dim_{\mathbf{x}}(X) = d$ for all $\mathbf{x} \in \mathrm{Cl}(X)$. A topological splitting based on the local dimension (LD) criterion is here called LD splitting.

EXAMPLE 3.4. Let us partition the Cartan umbrella $X = \{(x, y, z) \in \mathbb{R}^3 : x^2 = zy^2\}$. All the points of the Cartan umbrella have dimension $d = 2$, except the points all over the negative z-axis which have dimension $d = 1$. So, we have only two pieces: a 1-dimensional submanifold $M = \{(x, y, z) \in \mathbb{R}^3 : x = 0, y = 0, z \leq 0\}$ and a non-manifold subset $Y = X - M$.

This example shows that the resulting pieces are not necessarily strata or submanifolds. The topological singularities are not necessarily removed. Thus, this kind of splitting is not a stratification, it is just a partition.

1.4.2. *Topological splittings based on local cut-manifoldness.* A topological splitting based on local cut-manifoldness is shortly designated by LCM splitting. As described in Chapter 2, a local cut n-manifold only exists for a set neighbourhood of dimension greater than n. Thus, a d-dimensional set may only contain $0-, 1-, 2-, \ldots, (d-1)-$dimensional cut manifolds.

EXAMPLE 3.5. All the points in $M = \{(x,y,z) \in \mathbb{R}^3 : x = 0, y = 0, z \leq 0\}$ of the Cartan umbrella are 0-dimensional cut submanifolds of order $k = 2$; hence, M is a non-manifold subset of the LCM splitting of the Cartan umbrella. Similarly, all the points in $N = \{(x,y,z) \in \mathbb{R}^3 : x = 0, y = 0, z > 0\}$ are contained in a 1-dimensional cut submanifold of order $k = 4$. The remaining points are part of 1-dimensional cut submanifolds of order $k = 2$. Therefore, the LCM splitting of the Cartan umbrella includes three pieces: the non-manifold subset M, the submanifold N, and the 2-dimensional submanifold $O = X - (M \cup N)$ with two components.

In general, the topological type of a point is determined using a finite collection of topological invariants such as, for example, dimension, cut-points and dimensional homogeneity. For locally 'well-behaved' spaces such as analytic varieties, dimension and dimensional homogeneity suffice to determine the local topological type of a space at a point. For example, each point in the negative z-axis of the Cartan umbrella has homogeneous dimension 1 because the intersection of its neighbourhood with X is a 1-ball. In contrast, each point in the positive z-axis, including the origin, has dimension 2; hence, points on that half-axis have different topological type. (Recall that dimension is a topological invariant.) Moreover, unlike the points in the positive z-axis, the point at the origin has a neighbourhood that includes points of dimension 1; that is, they have distinct topological types.

2. Mathematical design issues I: topological stratifications

From the discussion above, we come to the conclusion that, amongst the topological stratifications and splittings, *weak topological stratifications* are the suited mathematical model for stratified objects in $\mathbb{R}^n$. Let us summarise the advantages of the weak topological stratifications:

- *Local topological type invariance.* They resolve the topological singularities in such a way that all the 'building blocks' or connected strata of a geometric object are at least *embedded* submanifolds; otherwise, the invariance of the local topological type does not hold. This excludes *a priori* some pathological point sets, e.g. the topologist's curve. The local topological type condition imposes then that all strata are embedded (see previous chapter for details about embedded submanifolds). In fact, for any embedded submanifold M_i as a 'building block' of a LTT stratification we have $M_i \cap \mathrm{Fr}(M_i) = \emptyset$.

- *Frontier condition.* The local topological type invariance induces the frontier condition on the a WeakT-stratified point set. This is crucial for the design of any B-rep data structure, because it guarantees that the frontier of any connected stratum is the union of other connected strata of lower dimension. This is precisely the basic relationship between strata we have in extant B-rep data structures; for example, the face (a 2-dimensional stratum) is bounded by a collection of edges (1-dimensional strata) and vertices (0-dimensional strata). We will come back to the frontier condition in next sections.
- *Adaptability* By striking on the local topological type invariance of connected components, instead of strata, we allow application-oriented stratifications, i.e. WeakT stratifications whose strata are not necessarily connected, nor satisfy the frontier condition. For example, the stratification Γ_3 in Table 1 is a WeakT stratification which takes the negative z-axis and positive z-axis as components of the same stratum. This stratification is not LTT-invariant, and therefore it does not satisfy the frontier condition. In fact, the frontier of any of its 2-strata is not composed by any other strata of dimension 1 or 0. But, it is easy to observe that its refinement Γ_1 into connected strata is LTT-invariant and does satisfy the frontier condition. Thus, imposing the LTT criterion on stratum components, instead of strata, there is no need to rearrange the components of each stratum under any shape change operation carried out by a designer.

However, weak topological stratifications have some shortcomings because they do not satisfy important requirements in geometric modelling:

- *Lack of local finiteness* Since the submanifolds of a LTT stratification are not necessarily regular (see Chapter 2 for definitions) —they have only to be embedded submanifolds—, their components can pile up in the neighbourhood of a point. In this case it is said that the stratification is not locally finite. Stratifications that satisfy both frontier condition (or ultimately the LTT condition) and local finite condition are said to be *stable topological stratifications.* The terms of 'topological stability', 'stratification', 'regularity' were introduced by René Thom in his seminal paper [**109**] about stratifications.
- *Lack of computability.* They do not provide any algebraic machinery to resolve or detect in practice (i.e. a computational algorithm) singularities.
- *Undetectability of differential singularities.* Even if we could devise an algorithm based on LTT-invariance, only topological singularities would be identifiable. Differential singularities such as cusps, ridges, etc are not detectable by LTT-invariance. This makes unfeasible

the intuitive stratification of a cube surface into faces, edges and vertices; the cube surface would have only one face, the surface itself. Thus WeakT stratifications become useless for purposes of geometric modelling.

- *Lack of geometric persistence.* This a major issue in geometric modelling. Extant geometric kernels do not provide in general means to maintain the geometric identity of strata in a variety or subvariety. This can be illustrated as follows. The Cartan umbrella is an algebraic variety described by the equality $x^2 - zy^2 = 0$, but usually geometric kernels are not designed to retain the geometric identity of strata; for example, the 0-dimensional stratum at the origin of the Cartan umbrella is algebraically described by a triple of real numbers, not by the algebraic set $x^2 - zy^2 = 0$. This suggests that geometric persistence requires some kind of clustering for strata.
- *Lack of a general clustering scheme.* A weak topological stratification has been defined as a cluster of strata. But, many applications (e.g. form feature modelling) require that an object is viewed as a cluster of subobjects (respectively, form features), each one of which is in turn a cluster of strata. The inexistence of such a general scheme for clustering subobjects and strata in extant geometric modellers has undermined the effective integration of CAD (computer-aided design) technology in large-scale industries such as automobile, aircraft and shipbuilding industries. Quite often a design has to be changed, but even minor changes imply to redesign everything from the scratch because the geometric kernels that equip CAD systems do not allow local or zonal changes easily. Recall the difficulties that feature-based modelling researchers have faced for the last two decades to implement an effective feature-based modeller on the top of a geometric kernel. Without such in-built subobjects or clusters of strata (called *subcomplexes* in [**46**]), the representation and manipulation of subsets of an object is very difficult.

3. Whitney stratifications

It has also long been understood that there are many techniques of partitioning a real point set into submanifolds, each concerning a type of splitting or stratification. However, not all splittings or stratifications are valuable in mathematics, and even less in geometric modelling and design. From a mathematical point of view, Whitney stratifications are important because, by the existence of Whitney stratifications for subanalytic sets [**105**, p.44], one can reduce problems on subanalytic sets and maps to problems on Whitney stratifications. Although this is also relevant to the geometric design

theory as far as the unification of the extant geometric models, the importance of the Whitney stratifications —in terms of the design of a data structure for geometric objects— is due to their *nice local properties*. In fact, each stratum (connected or not) of a Whitney stratification consists of "equally bad" points. (This concept of "equal badness" is used intuitively by some mathematicians and means 'the same local topological type'.) The embedding of such nice local properties into a data structure has as a result a general boundary representation capable of representing and manipulating geometric objects in $\mathbb{R}^n$. (This general boundary representation is described in the next chapter.)

3.1. Whitney regularity conditions. The *regularity conditions* of Whitney are based on the concept of tangent space at a point of a manifold, which is obviously a geometric concept. Hence one says that the Whitney regularity conditions defined later, called (a)- and (b)-conditions, are essentially geometric.

Let $V = M_1 \cup M_2 \cup \ldots \cup M_k$ be a variety in $\mathbb{R}^n$ where M_1, M_2, ..., M_k are manifolds without boundary. Let $\mathbf{p} \in M_i$, and let $\mathrm{T}_{\mathbf{p}}M_i$ be a tangent space of M_i at $\mathbf{p}$. Let $\mathbf{q} \in M_j$, and let $\mathrm{N}_{\mathbf{q}}M_j$ be the normal space of M_j at $\mathbf{q}$. And denote by π some appropriate projection; for example, $\pi_{\mathrm{N}_{\mathbf{q}}M_j}(\tau)$ is the projection of τ into the normal space of M_j at $\mathbf{q}$

DEFINITION 3.1. M_j is **(a)-regular** over M_i at $\mathbf{p}$ if, for any tangent vector $\tau \in \mathrm{T}_{\mathbf{p}}M_i$,

$$\lim_{\mathbf{q}\to\mathbf{p}} \pi_{\mathrm{N}_{\mathbf{q}}M_j}(\tau) = 0$$

This means that for any tangent vector $\tau \in \mathrm{T}_{\mathbf{p}}M_i$, the projection of τ into the normal space of M_j at $\mathbf{q}$ approaches zero as $\mathbf{q}$ approaches $\mathbf{p}$. In other words, τ is nearly perpendicular to $\mathrm{N}_{\mathbf{q}}M_j$ when $\mathbf{q}$ is close to $\mathbf{p}$; equivalently, τ is nearly contained in $\mathrm{T}_{\mathbf{q}}M_j$ when $\mathbf{q}$ is close to $\mathbf{p}$. Thus we may restate the condition that M_j is (a)-regular over M_i at $\mathbf{p}$ as follows: $\mathrm{T}_{\mathbf{p}}M_i$ *is nearly contained in* $\mathrm{T}_{\mathbf{q}}M_j$ *as* $\mathbf{q}$ *approaches* $\mathbf{p}$. Therefore, $\|\pi_{\mathrm{N}_{\mathbf{q}}M_j}(\tau)\|$ can be viewed as the distance from τ to $\mathrm{T}_{\mathbf{q}}M_j$.

EXAMPLE 3.6. Let us look at the OrdT stratification of the variety V shown in Figure 2(b) first. Let $\mathbf{p}$ and $\mathbf{q}$ two points of V in the manifolds M_3 and M_2, respectively, as illustrated in Figure 6(a). As $\mathbf{q}$ approaches $\mathbf{p}$, we see that $\mathrm{T}_{\mathbf{q}}M_2$ is far from containing the tangent vector τ at $\mathbf{p}$. It is clear that $\|\pi_{\mathrm{N}(M_2,\mathbf{q})}(\tau)\|$ does not approach zero as $\mathbf{q}$ approaches $\mathbf{p}$. This shows that the OrdT stratification of V does not satisfy the (a)-regularity condition, or, equivalently, it is not stratified according to the (a)-regularity condition. In particular, M_2 is not (a)-regular over M_3 at $\mathbf{p}$.

EXAMPLE 3.7. Now, let us check whether the WeakT stratification of the variety V depicted in Figure 2(c) is (a)-regular. Consider, for example, the incident strata M_3, M_2 and M_7; M_7 is the point

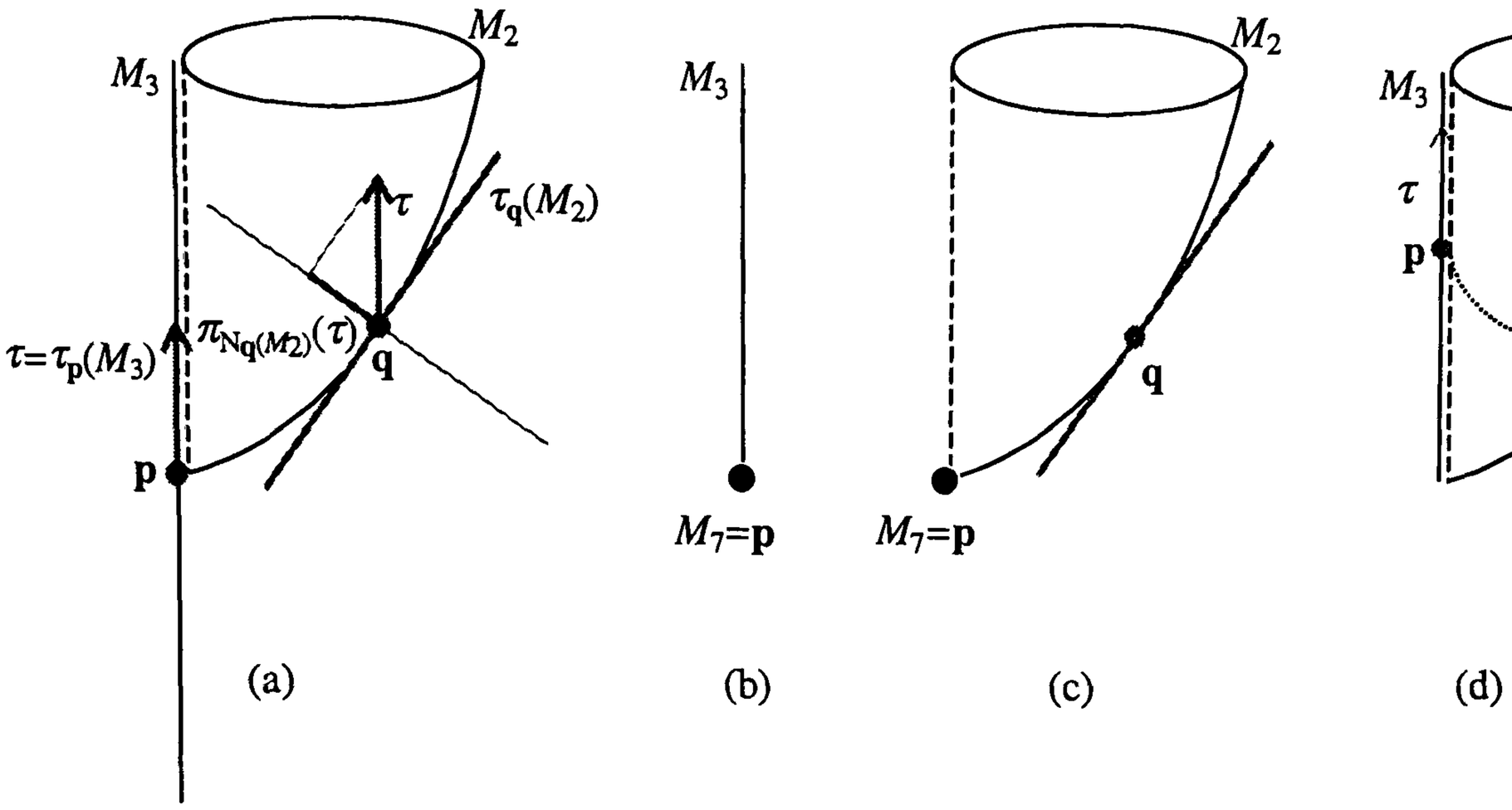

FIGURE 6. Testing the Whitney (a)-regularity condition.

p, M_3 is the positive z-axis, and M_2 is the top-right sheet of V.

(i) *Is M_3 (a)-regular over M_7 at* **p***?* (Figure 6(b)) This is a trivial case since M_7 is the point **p**, and in particular $T_{\mathbf{p}}M_7$ (i.e. the point **p** in this case) is clearly contained in $T_{\mathbf{q}}M_3$ for every $\mathbf{q} \in M_3$.

(ii) *Is M_2 (a)-regular over M_7 at* **p***?* (Figure 6(c)) This is also clear since $T_{\mathbf{p}}M_7$ (i.e. the point **p** in this case) is nearly contained in $T_{\mathbf{q}}M_2$ as **q** approaches **p**.

(iii) *Is M_2 (a)-regular over M_3 at any point* **p** *in M_3?* (Figure 6(d)) Let us take any sequence of points on M_2 such that **q** approaches **p** as denoted by the dotted line in Figure 6(d). The tangent space $T_{\mathbf{q}}M_2$ is a 2-dimensional linear space; thus it is obvious that the vector τ tangent to M_3 at **p** is nearly contained in $T_{\mathbf{q}}M_2$ as **q** approaches **p**. Hence M_2 is (a)-regular over M_3 at any **p** in M_3, that is M_2 is (a)-regular over M_3.

In short, because (i), (ii) and (iii) exhaust all possibilities in our checking process, the WeakT stratification of V depicted in Figure 2(c) satisfies the (a)-regularity condition.

EXAMPLE 3.8. Consider the WeakT stratification of the variety V depicted in Figure 3(c). For the same reason as we noted in the discussion of (i) in the previous example, it is clear that M_1 and M_3 are (a)-regular over M_5. Thus the WeakT stratification of V is also an (a)-regular stratification.

EXAMPLE 3.9. Consider now the OrdT stratification shown in Figure 3(b). For brevity, take the points **p** and **q** in the strata M_3 and M_1, respectively, as drawn in Figure 7(a). Unfortunately, in this case, M_1 is (a)-regular over M_3 at the origin **p**, since τ is clearly contained in $T_{\mathbf{q}}M_1$ as **q** approaches **p**. We say "unfortunately", because **p** in M_3 is obviously "worse" than the other points in M_3.

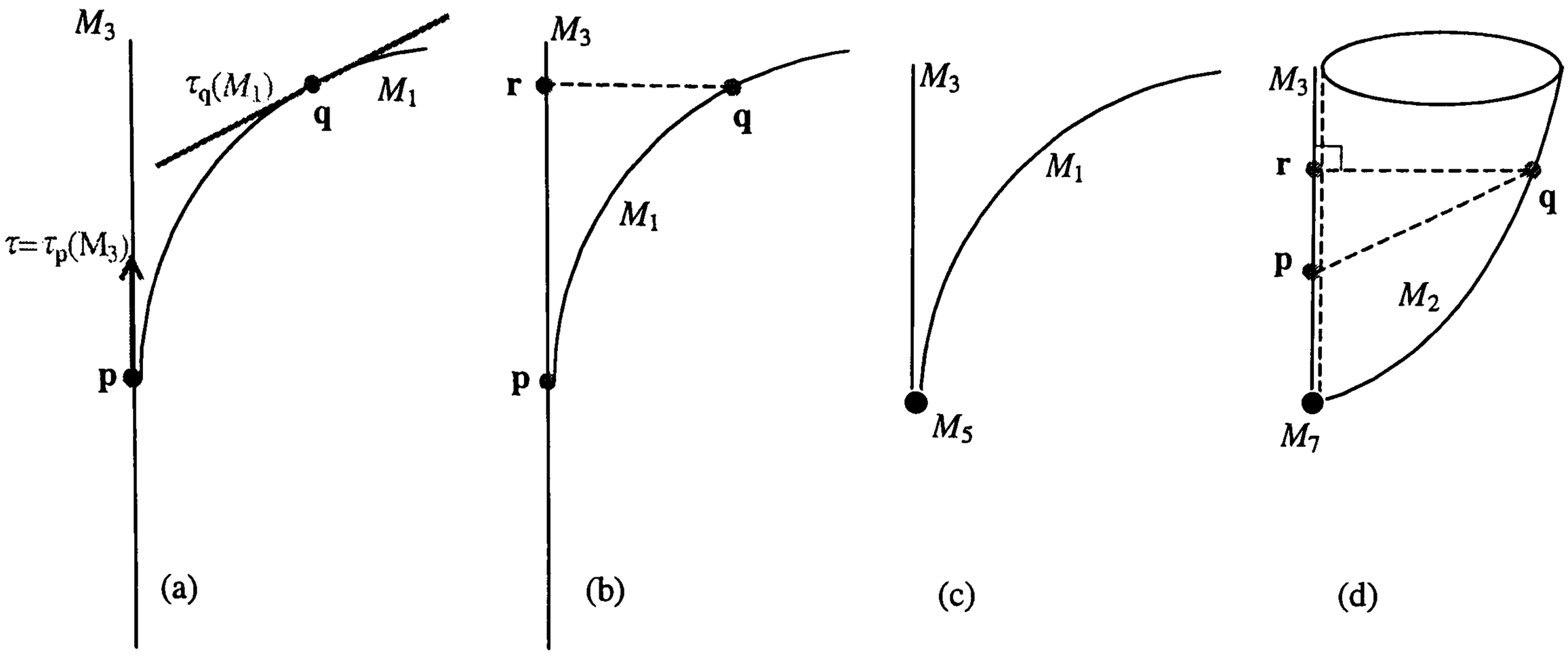

FIGURE 7. (a)-regularity insufficiency.

The previous example shows us the insufficiency of (a)-regularity to impose a WeakT stratification on a variety. Therefore, we need additional regularity conditions.

DEFINITION 3.2. Let $\mathbf{p} \in M_i$ and $\mathbf{q} \in M_j$. We say that M_j is **(b')-regular** over M_i at $\mathbf{p}$ if

$$\lim_{\mathbf{q}\to\mathbf{p}} \pi_{\mathrm{N_q}M_j} \frac{\vec{v}}{\|\vec{v}\|} = 0$$

where $\vec{v} = \vec{\mathbf{qp}} - \pi_{\mathrm{T_p}M_i}(\vec{\mathbf{qp}})$ and $\|\vec{v}\|$ is the Euclidean norm of $\vec{v}$.

In intuitive terms, this is equivalent to say that $\mathrm{T_q}M_j$ nearly contains the *direction* of the vector $\vec{v}$; that is, $\mathrm{N_q}M_j$ is nearly perpendicular to the direction of $\vec{v}$.

DEFINITION 3.3. Let $\{\mathbf{p_k}\}$ be a sequence of points in M_i, $\{\mathbf{q_k}\}$ a sequence of points in M_j. M_j is **(b)-regular** over M_i at $\mathbf{p}$ if

$$\lim_{k\to\infty} \pi_{\mathrm{N_{q_k}}M_j} \frac{\vec{v_k}}{\|\vec{v_k}\|} = 0$$

where $\vec{v_k} = \vec{\mathbf{q_k p_k}} - \pi_{\mathrm{T_{p_k}}M_i}(\vec{\mathbf{q_k p_k}})$.

REMARK 4. In [77], Mather proved that the regularity conditions (a) and (b) are equivalent to (a) and (b'). Moreover, he proved that (b) implies (a). Thus, it is enough to check the condition (b) for a regular stratification in the sense of Whitney. However, (b) is clearly harder to handle than (b'), and (a) is not difficult to check at all. Therefore, in mathematics, the conditions (a) and (b') are used preferably.

DEFINITION 3.4. (Whitney regularity conditions) A stratum M_j of the variety V is **Whitney-regular** over a stratum M_i of V if M_j is (a)-,(b)-regular (or (a)-,(b')-regular) over M_i at every point $\mathbf{p} \in M_i$.

DEFINITION 3.5. A stratification of a variety V is called a **Whitney stratification** if for any two strata M_j, M_i of V with $M_i \subset \mathrm{Cl}(M_j)$, M_j is Whitney-regular over M_i.

Thus, the conditions (b) and (b') overcome our problem in distinguishing the origin in the stratum M_3 of V in Figure 3(b).

EXAMPLE 3.10. Let us look again at this case as illustrated in Figure 7(b). Let $\mathbf{q} \in M_1$ and project $\vec{\mathbf{qp}}$ onto M_3 as $M_3 = \mathrm{T}_{\mathbf{p}}M_3$ in this case. We obtain $\vec{\mathbf{qr}} = \vec{\mathbf{qp}} - \pi_{\mathrm{T}_{\mathbf{p}}M_3}(\vec{\mathbf{qp}})$. This clearly shows that the direction (or unit vector) of $\vec{\mathbf{qr}}$ is not nearly contained in $\mathrm{T}_{\mathbf{q}}M_1$ as $\mathbf{q}$ approaches $\mathbf{p}$, which violates (b'). This implies that the stratification of V in Figure 3(b) is not Whitney-regular, i.e. a Whitney stratification.

EXAMPLE 3.11. On the other hand the stratification depicted in Figure 3(c) is a Whitney stratification. In fact, looking at its sub-stratification drawn in Figure 7(c), it is obvious that M_3 is Whitney-regular over M_5 and M_1 is Whitney-regular over M_5 since M_5 is just a point, and further $M_3 \not\subset \mathrm{Cl}(M_1)$ nor $M_1 \subset \mathrm{Cl}(M_3)$.

EXAMPLE 3.12. Using the same argument as in Example 3.10, it is clear that the OrdT-stratified variety V in Figure 2(b) is not (b')-regularly stratified. However, the stratification in Figure 2(c) is a Whitney stratification as illustrated in Figure 7(d). In fact, it is trivial to see that both M_2 and M_3 are Whitney-regular over M_7 since M_7 is a point. Therefore, we have only to check that M_2 is (b')-regular over M_3. So, let $\mathbf{p} \in M_3$ and $\mathbf{q} \in M_2$. Take any sequence of points in M_2 such that $\mathbf{q}$ approaches $\mathbf{p}$, i.e. $\mathbf{q} \to \mathbf{p}$. It is easy to see that as $\mathbf{q}$ approaches $\mathbf{p} \in M_3$ the vector $\vec{\mathbf{qr}} = \mathbf{q} - \pi_{\mathrm{T}_{\mathbf{p}}M_3}(\vec{\mathbf{qp}})$ is nearly contained in the (2-dimensional) tangent space $\mathrm{T}_{\mathbf{q}}M_2$ because the direction $\vec{\mathbf{qr}}$ is revolving about M_3. This shows that M_2 is (b')-regular over M_3 and hence V is Whitney-regular via Figure 2(c).

The examples above suggest that Whitney stratifications of algebraic and analytic varieties satisfy the LTT criterion, and therefore they are a subclass of weak topological stratifications. In fact the Thom-Mather Theorem confirms this for algebraic and analytic varieties as follows.

THEOREM 3.1. (**Thom-Mather Theorem [110, 78]**) *Let V be an analytic variety stratified under the (a) and (b) conditions. Along each stratum M_i the local topological type remain invariant in the following sense. If $\mathbf{p}, \mathbf{q}$ are two points in a connected component of the stratum M_i, then there is a*

neighbourhood U of $\mathbf{p}$ in V homeomorphic to a sufficient small neighbourhood U' of $\mathbf{q}$ in V and the homeomorphism $h : M_j \cap U \to M_j \cap U'$ preserves the stratification for each j.

PROOF. See [**73**]. □

The examples above suggest that if a variety V is stratified into $M_1 \cup M_2 \cup \ldots \cup M_n$ and if M_j is (a)-, (b)-regular over M_i such that $M_i \cap \mathrm{Cl}(M_j) \neq \emptyset$, then

$$\dim(M_i) < \dim(M_j), \tag{9}$$

as proved by Whitney in [**121**, p.541-547]. We call the inequality (9) the **dimensional inequality condition**. This inequality is not surprising given the Thom-Mather Theorem. However, despite the inequality (9) is valid for algebraic and analytic varieties, it is not satisfied in general, as the following counterexample shows.

COUNTEREXAMPLE 3.1. Let $M_1 = \{0\} \times [-1,1]$ a straight line segment in the y-axis of $\mathbb{R}^2$ and $M_2 = \{(x,y) | y = \sin(\frac{1}{x}), x \neq 0\}$ the *topologist*'s curve oscillating near $x = 0$. We have $M_1 \cap \mathrm{Cl}(M_2) \neq 0$ but $\dim(M_1) = \dim(M_2)$ (Figure 8). Thus, the variety $M_1 \cup M_2$ cannot be analytic. See [**120**, p.208-211] for more details about analytic varieties.

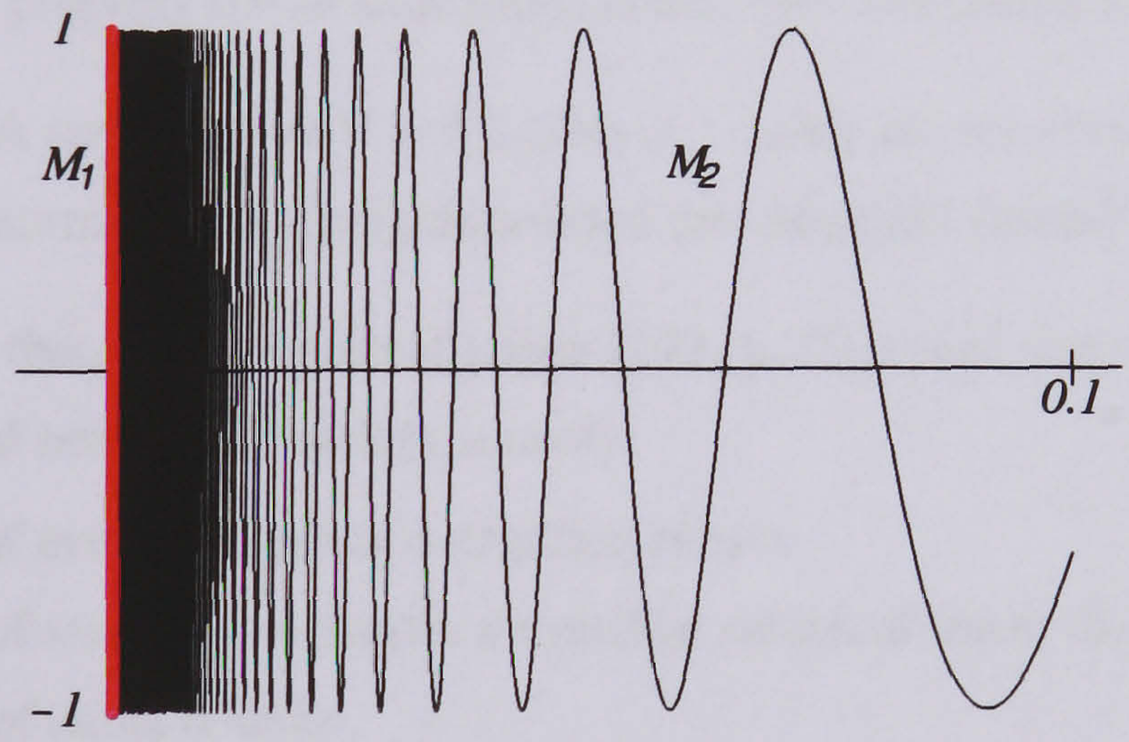

FIGURE 8. Topologist's curve.

The previous counterexample shows that:

- There seems to be an intimate relationship between Whitney stratifications and sorts of geometries, i.e. not all geometries admit Whitney stratifications.
- Stratifications can be used to study the geometric nature of point sets in $\mathbb{R}^n$; for example, to know whether that a point set is analytic or not.

- The incidence (a)-, (b)-conditions of Whitney on analytic varieties imply that Whitney stratifications of analytic varieties satisfy the LTT criterion, what allows us to rid of serious pathologies. This explains why analytic Whitney stratifications are sometimes said to have *nice local properties* [**120**].

Note that the inequality (9) does not imply that Whitney stratifications satisfy the frontier condition. For example, the ordinary topological stratifications (b) in Figures 1, 2, 3, 4 all satisfy the dimensional inequality of incident strata, but not the frontier condition. Obviously, one can conjecture that an analytic Whitney stratification satisfies the frontier condition. In fact, such conjecture is due to Thom and was proven by Mather [**77**].

THEOREM 3.2. *If a variety* $V = M_1 \cup M_2 \cup \ldots \cup M_n$ *is a (a)-,(b)-regular stratification and* $M_i \cap \mathrm{Cl}(M_j) \neq \emptyset$ *then* $M_i \subset \mathrm{Cl}(M_j)$.

This leads us to the following definition:

DEFINITION 3.6. A stratification $V = M_1 \cup M_2 \cup \ldots \cup M_n$ satisfies the **frontier condition** if whenever $M_i \cap \mathrm{Cl}(M_j) \neq \emptyset$ then $M_i \subset \mathrm{Cl}(M_j)$.

Another important property for stratifications is that one concerning *local finiteness* [**113**].

DEFINITION 3.7. A stratification $V = M_1 \cup M_2 \cup \ldots \cup M_n$ satisfies the **local finiteness condition** if each point of any stratum M_i has a neighbourhood meeting only finitely many strata.

It is worth noting that, in his seminal paper [**109**, p.25] about stratifications, Thom stated the properties that stratified sets should satisfy, namely:

(1) The closure of every stratum is a stratified subset.

(2) The frontier of stratum constitutes a stratified subset of lower dimension.

(3) The number of strata is finite.

(4) Any finite union and intersection of stratified subsets are stratified subsets.

The rationale behind the frontier condition —that includes the dimensional inequality condition— and the local finiteness condition is to guarantee *nice local properties*. They both ensure that strata are regular submanifolds. The frontier condition ensures that the strata are at least embedded submanifolds. The local finiteness condition imposes an additional restriction avoiding the "piling up" effect of some embedded submanifolds. Therefore, the local finiteness condition on strata means that all strata should be regular submanifolds (see previous chapter for more details about the various classes of submanifolds.)

What is more interesting is that these stratification properties proposed by Thom are essentially topological in the sense they do not depend on the nature of the geometry we may consider. They have been proposed to observe *topological stability*, i.e. to rid of possible pathologies. Therefore, the (a)-, (b)-conditions of Whitney are basically a geometric attempt to satisfy the local finiteness and frontier topological requirements. All this works quite well for algebraic and analytic varieties, as described above in this section. The properties of algebraic and analytic varieties guarantee *a priori* the local finiteness condition of a Whitney stratification. The frontier condition is a consequence of the local finiteness condition and (a)-, (b)-regular Whitney conditions [**113**, p.336] as proved by Mather [77]. Everything still works well for a more general class of closed semialgebraic and semianalytic sets. Moreover, the frontier condition still holds for Whitney stratifications of semialgebraic and semianalytic sets which are not closed, but the LTT condition may be violated. This is illustrated in next counterexample.

COUNTEREXAMPLE 3.2. Let us consider the stratified point set $X = M_1 \cup M_2 \cup M_3$, here called the *stratified double-flag*, as shown in Figure 9(a). The flagpole is the 1-stratum $M_1 = 0 \times 0 \times z$, the z-axis. The two flags M_2, M_3 are here taken as components of a 2-stratum. $M_2 = (x = 0) \cap (y < 0) \cap (z > 0)$ is the second quadrant of the plane $x = 0$ and $M_3 = (x = 0) \cap (y > 0) \cap (z < 0)$ is the fourth quadrant of the plane $x = 0$. It is trivial to check that Whitney conditions are satisfied because the tangent space at any point of the 2-stratum contains the tangent space at any point in the z-axis. Nevertheless, the frontier condition is still satisfied, but not the LTT condition. But, if we assume that all strata M_1, M_2, M_3 are connected, then the stratified double-flag in Figure 9(a) is no longer a Whitney-stratified set, and hence the frontier condition is not satisfied; consequently, the LTT condition cannot be satisfied either.

This counterexample shows us the following:

- Local finiteness and Whitney conditions imply the satisfaction of the frontier condition, a result due to Mather.
- Whitney stratifications do not necessarily satisfy the LTT condition, so the Thom-Mather Theorem is not always valid.
- The Thom-Mather Theorem is valid for Whitney stratifications with simply connected strata.
- Frontier condition does not imply LTT condition for multi-connected strata.
- Frontier condition implies LTT condition for connected strata.

In addition to connectedness, closedness property for strata seems to reinforce the LTT condition. This is illustrated in Figure 9(b), where a single connected 1-stratum M_4 has been attached along the

positive y-axis. This stratification is not a Whitney stratification because the M_1 and M_4 violate the (a)-condition at the origin. In fact, the tangent space at the origin, the M_1 itself, is not contained in the tangent space at any point of M_4 for a sequence of points in M_4 approaching the origin. To satisfy the Whitney conditions, we have to subdivide M_1 into two 1-strata, M_5 (the positive z-axis) and M_6 (the negative z-axis), by a 0-stratum M_7 (the origin), Figure 9(c).

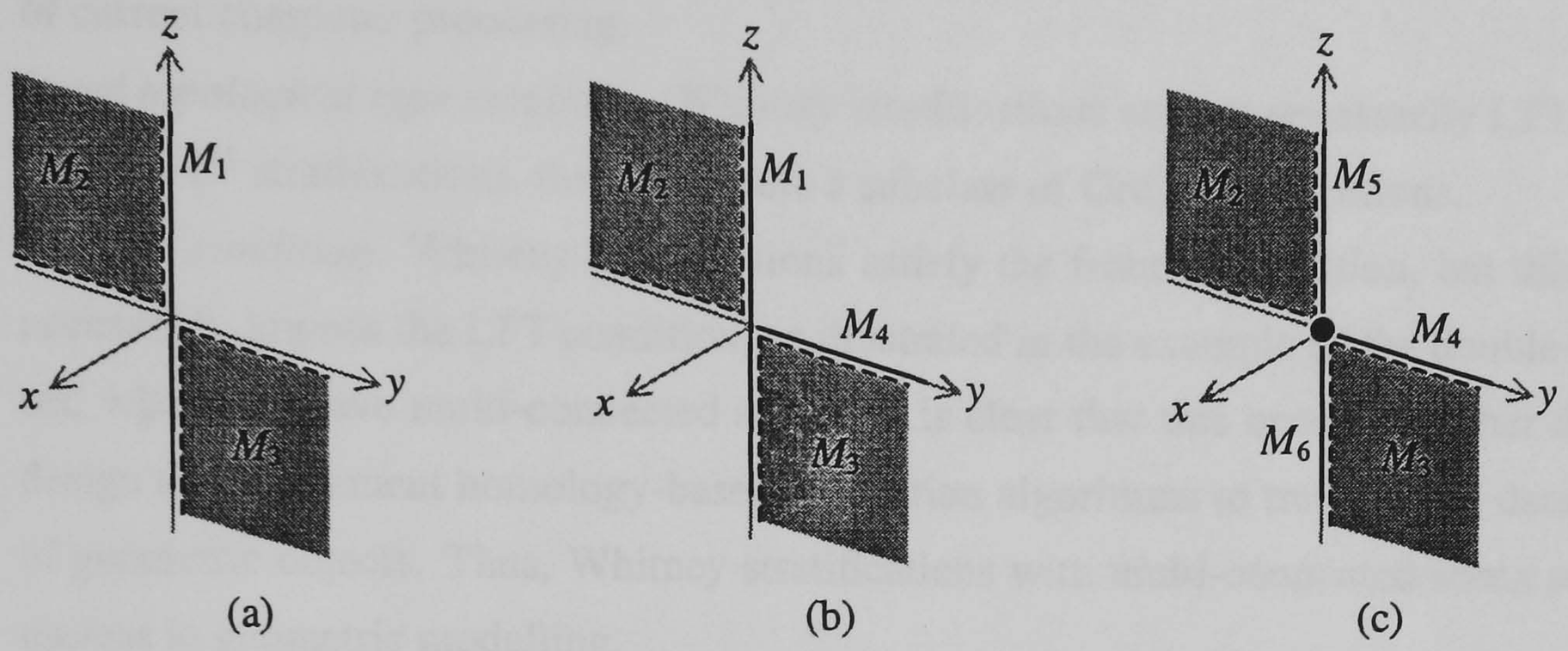

FIGURE 9. Stratifications of a double-flag point set.

4. Mathematical design issues II: Whitney stratifications

At this point of discussion, some facts about Whitney stratifications and their adequacy as a framework for processing geometric objects on computers can be pointed out. Let us enumerate them:

- *Local finiteness.* To be useful in geometric modelling, a stratification must be at least locally finite. A stratification satisfies the *local finiteness* condition if each point of a stratum has a neighbourhood meeting only finitely many strata [**113**]. This is essential to guarantee a computable representation for geometric objects. For example, an unbounded cone in $\mathbb{R}^3$ can be stratified into its apex and conical surface, since every point has a neighbourhood with just one 2-dimensional component. In contrast, if the conical surface is partitioned into an infinite number of lines, every point has a neighbourhood with an infinite number of 1-dimensional components; this stratification is not locally finite. As seen above, local finiteness is also essential to guarantee regular strata for a stratification, and therefore to rid of troublesome pathologies. This means that local finiteness heavily depends on the geometry of the point sets under study. That is, it is the local finiteness of a type of geometry that determines the local finiteness of a stratification, and not vice-versa. Local finiteness

condition together with the incidence Whitney conditions determine a Whitney stratification for a point set, but everything depends on the geometry nature of such point set. Remarkably, the local finiteness condition is inherent to algebraic, analytic, semialgebraic, semianalytic and, more generally, subanalytic sets because they are locally described by a finite number of subsets. Thus, the local finiteness matches the memory limitations and the discrete character of current computer processing.

- *Local topological type condition.* Whitney stratifications are not necessarily LTT-invariant. Thus, as C^1 stratifications, they constitute a subclass of OrdT stratifications.
- *Frontier condition.* Whitney stratifications satisfy the frontier condition, but this does not necessarily impose the LTT condition, as illustrated in the example of the double-flag point set, where we have multi-connected strata. It is clear that this becomes rather difficult to design and implement homology-based navigation algorithms to traverse the data structure of geometric objects. Thus, Whitney stratifications with multi-connected strata seem to be useless in geometric modelling.
- *Incidence scheme.* Even so, the dimensional inequality condition underlying the frontier condition guarantee that the incidence Whitney conditions lead to an *incidence scheme* for Whitney-stratified sets. The concept of an *incidence scheme* was introduced by Thom [**110**, p.245] and establishes that every stratum M of dimension d is associated with a finite number of strata of dimension less than d, $M_1 \ldots M_m$, the strata of the frontier of M; equivalently, we say that M_i is *incident* at M, or $M_i < M$. The incidence relation $<$ is transitive: $M_i < M_j$ and $M_j < M_k$ implies $M_i < M_k$.
- *Weak frontier condition.* Imposing the LTT condition on the stratum components of Whitney stratifications, they become a subclass of WeakT stratifications, regardless of whether the stratified set is closed or not. Whitney stratifications whose stratum components satisfy the frontier condition are said to satisfy the *weak frontier condition.* They are called here *Weak Whitney stratifications*, or just *WeakW stratifications.* The weak frontier condition is crucial to define an incidence scheme based on the order of the dimensions of the adjacent stratum components. Such a scheme is here called *weak incidence scheme.* Thus, the weak frontier condition is an important condition to ensure the satisfaction of the requirements of the design and implementation B-rep data structures. Besides, the design principles of a B-rep data structure can be extended to higher dimensions, as well as their navigation or traversal algorithms. This means that we have a mathematical validation for the incidence scheme of the extant B-rep data structures.

- *Computability.* It is possible —theoretically, at least— to computationally check the Whitney conditions for any two strata by using simultaneous approximation techniques of two sequences of points tending to a particular point in one of two strata, and calculation of tangent spaces in their respective Grassmannians. The tangent spaces can be determined by the Gram-Schmidt Orthogonalisation algorithm for any dimensions as explained in the previous chapter. Eventual problems with floating point arithmetic can be overcome by using, for example, the CORE Library for precision-driven exact computation with constructible real numbers [**126**].
- *Detectability of differential singularities.* The resolution of singularities makes usage of the criterion of C^r continuity, i.e. smoothness of order $r \geq 1$ [**44**]. (Recall that a point of a set X in $\mathbb{R}^n$ is C^r *regular* if it has a neighbourhood U in $\mathbb{R}^n$ such that $X \cap U$ is a C^r ball; otherwise it is said to be a C^r *singular* point [**44**].) Whitney stratifications are just C^1 stratifications, while topological stratifications are C^0 stratifications. Therefore, C^1 singularities such as cusps, ridges, etc. are in principle detectable and resolvable by Whitney stratifications. C^1 singularities are just the points where the rank of the Jacobian is not maximal and constant. As seen in the previous chapter, the points where the rank is constant and maximal are called regular points. Therefore, we can envisage a computational rank-based approach to detect C^1 singularities. Unfortunately, this approach is not sufficient to isolate all the singularities. For example, applying this approach to the Cartan umbrella with-handle has as a result the OrdT stratification in Figure 1(b), where the origin is in a C^∞ stratum M_3. This means that we cannot isolate the origin as a new stratum because the rank over M_3 is constant, even increasing continuity order, that is, using C^r Whitney stratifications with $r > 1$.
- *Adaptability.* WeakW stratifications are WeakT stratifications. Thus, during a shape operation on an object, there is no need to re-arrange the *internal* structure of existing multi-connected strata to conform with the frontier condition.
- *Lack of a general clustering scheme.* Similar to WeakT stratifications, the absence of general clusters of subobjects, each one of which is a cluster of strata, disables geometric persistence and adaptability to shape changes (e.g. deleting, undoing, redoing, resizing, etc. of form features).

5. Stratifiable geometries

The usefulness of a particular stratification depends on being able to find a sufficiently large class of sets for which they exist. Here we are interested in Whitney-stratifiable geometries. It is clear

that we need a geometry more general that algebraic or analytic geometries, and it is also Whitney-stratifiable. There are two major reasons behind this. The first is that algebraic and analytic geometries are restricted to point sets defined by algebraic and analytic equalities. Therefore their geometric coverage is limited to algebraic and analytic varieties, e.g. those found in parametric geometric design of curves and surfaces found in CAD systems, or algebraic geometry engines such as that one included in the *Mathematica* package. But, in solid modelling, we need more general geometries which enable the construction of geometric objects by using not only equalities but also inequalities of algebraic and analytic functions. (Nevertheless, Shapiro has shown that we can construct similar objects by using only equalities of R-functions [**102**].) For example, to define a square in $\mathbb{R}^2$ we need four inequalities. Otherwise, it does not make sense to think of geometry integration in engineering environments, CAD/CAM systems in particular, if we use different geometries for different tasks. The second is that a geometric framework as that one provided by Whitney stratifications satisfies many applications requirements. In addition to its adequacy to design and implementation of B-rep data structures, more applications are possible to envisage for Whitney stratifications. For example, they can be used to model Bézier polygons and polyhedra, to represent the stratification of semialgebraic and semianalytic point sets as a result of a boundary evaluation algorithm, and possibly to assist designers in the graphical visualisation of varieties which are unplottable because of their discontinuities. (Recall that, the Cartan umbrella with-handle $x^2 - y^2 z = 0$ cannot be plotted through Mathematica system.)

5.1. Semialgebraic geometry. Recall that a set $X \subseteq \mathbb{R}^m$ is *algebraic* when it is obtained by finitely many intersections of sets of the form $\{x \in \mathbb{R}^m \mid f(x) = 0\}$ with f a polynomial function on $\mathbb{R}^m$. That is, X is the intersecting set level of the zero-sets of a family of functions. Thus, algebraic sets are just algebraic varieties. A wider class of sets, closed under as many set-theoretic and topological operations as possible, is the class of semialgebraic sets.

DEFINITION 3.8. The class of **semialgebraic** subsets of $\mathbb{R}^m$ is the smaller Boolean algebra of subsets of $\mathbb{R}^m$ which contains all sets of the form

$$\{\mathbf{x} \in \mathbb{R}^m \mid f(\mathbf{x}) \geq 0\} \tag{10}$$

where $f : \mathbb{R}^m \to \mathbb{R}$ is a polynomial function.

Therefore, semialgebraic subsets of $\mathbb{R}^m$ are closed under finite unions, finite intersections and complements (and difference of any two) [**59**, p.166]. It also follows that the product of semialgebraic sets is semialgebraic [**41**, p.17], which mathematically validates sweeping operations usual in geometric modelling.

REMARK 5. (Hironaka [**59**, p.167]) In (10), we may replace $\geq$ by $>$, because

$$\{\mathbf{x} \in \mathbb{R}^m \mid f(\mathbf{x}) > 0\} = \mathbb{R}^m - \{\mathbf{x} \in \mathbb{R}^m \mid -f(\mathbf{x}) \geq 0\}.$$

This implies that the semialgebraic Boolean class includes the algebraic sets viewing that

$$\{\mathbf{x} \in \mathbb{R}^m \mid f(\mathbf{x}) = 0\} = \{\mathbf{x} \in \mathbb{R}^m \mid f(\mathbf{x}) \geq 0\} \cap \{\mathbf{x} \in \mathbb{R}^m \mid -f(\mathbf{x}) \geq 0\}.$$

REMARK 6. (Hironaka [**59**, p.167]) A subset $X \in \mathbb{R}^m$ is semialgebraic if and only if there exist a finite family of polynomials f_i, g_j on $\mathbb{R}^m$ such that

$$X = \{\cup_i \{\mathbf{x} \in \mathbb{R}^m \mid f_i(\mathbf{x}) > 0\}\} \cup \{\cup_j \{\mathbf{x} \in \mathbb{R}^m \mid g_j(\mathbf{x}) = 0\}\}$$

Taking into account that the topological operations, say closure, interior and frontier, are defined in terms of set-theoretic operations (see Chapter 1), we have:

THEOREM 3.3. *If X is semialgebraic in $\mathbb{R}^m$, then its closure (hence also its interior and frontier) is also semialgebraic in $\mathbb{R}^m$.*

PROOF. See Gibson [**41**, p.18] for an elegant proof using the Tarski-Seidenberg Theorem. □

By the definition of semialgebraicity above, the inverse image of a semialgebraic subset of $\mathbb{R}^n$ under a polynomial map $f : \mathbb{R}^m \to \mathbb{R}^n$ is semialgebraic [**41**, p.17]. The converse of this is Tarski-Seidenberg Theorem.

THEOREM 3.4. (**Tarski-Seidenberg Theorem**) *The* image *of a semialgebraic subset of $\mathbb{R}^m$ under a polynomial map $f : \mathbb{R}^m \to \mathbb{R}^n$ is semialgebraic.*

PROOF. See Seidenberg [**101**]. □

This theorem is important for two reasons:

- It formalises our intuition that parametric curves and surfaces (e.g. Bézier curves and surfaces) as images of polynomial functions are semialgebraic indeed.

- In the theory of semialgebraic geometry it is only needed in the particular case of a linear projection $f : \mathbb{R}^{n+k} \to \mathbb{R}^n$ to ensure that semialgebraic subsets are closed under linear projections. This is because a linear projection of an algebraic set is not in general algebraic but semialgebraic such as, for example, the projection of a circle in $\mathbb{R}^2$ into $\mathbb{R}$.

Another important property of semialgebraic subsets of $\mathbb{R}^m$ is as follows:

THEOREM 3.5. *A semialgebraic set has only finitely many connected components, each of which is semialgebraic.*

The smoothness theory and singularity theory provide the interplay between the semialgebraic geometry and stratification theory. Let $X \subset \mathbb{R}^m$ be semialgebraic, and let $\mathbf{p} \in X$. We say $\mathbf{p}$ is a **regular point** of X if there exists a neighbourhood U of $\mathbf{p}$ in $\mathbb{R}^m$ and a family of real analytic functions $f_1, \ldots, f_k$, defined in U, such that $\mathrm{D}f_1, \ldots, \mathrm{D}f_k$ are linearly independent elements of $\mathrm{T}_{\mathbf{p}}X$, and

$$X \cap U = \{\mathbf{x} \in U \mid f_1(\mathbf{x}) = \ldots = f_k(\mathbf{x}) = 0\}.$$

It follows from the Implicit Function Theorem that $\mathbf{p}$ is a regular point of X if and only if there is an open neighbourhood U of $\mathbf{p}$ in $\mathbb{R}^m$ such that $U \cap X$ is an analytic submanifold of U. Moreover, this analytic submanifold (and thus smooth) is of dimension k. The set of regular points ΔX of a semialgebraic set X is also semialgebraic, and open and dense in X [**79**, p.131]. The set of regular points ΔX is an analytic manifold which may contain components of distinct dimensions. The dimension of ΔX is defined to be the dimension of the largest component, which is also the dimension of X; that is $\dim X = \dim \Delta X$.

A point of X is a **singular point** of X if it is not a regular point of X. The set ΣX of singular points of X is also semialgebraic, since $\Sigma X = X - \Delta X$. Note that ΣX is closed in X. Besides, we have $\dim \Sigma X < \dim X$ and $\dim (\mathrm{Cl}(X) - X) < \dim X$ [**41**, p.19].

The regular and singular points of a semialgebraic set X can be dimensionally related to each other by a *filtration* $X^k \supseteq X^{k-1} \supseteq \ldots X^0$ of X by taking $X^k = X$, where $k = \dim X$, and defining X^{i-1} to be ΣX^i if $\dim X^i = i$, and to be X^i if $\dim X^i < i$. Obviously, there are finitely many differences $X^i - X^{i-1}$, each a smooth manifold of dimension i which altogether yield a finite stratification of X.

Now we come closer to the matter in hand that semialgebraic sets are Whitney-stratifiable. Let M, N be smooth submanifolds of $\mathbb{R}^m$. The **bad set** $\Xi(M,N)$ is defined as the set of points $\mathbf{x} \in M$ where N fails to be Whitney regular over M at $\mathbf{x}$.

THEOREM 3.6. **(Whitney Theorem)** *Let M, N be semialgebraic smooth submanifolds of $\mathbb{R}^m$. Then the bad set $\Xi(M,N)$ is semialgebraic and its dimension $\dim \Xi(M,N) < \dim M$.*

Besides, for any semialgebraic sets $X, Y \in \mathbb{R}^m$, it follows from the preceding results that the set

$$\amalg(X,Y) = \Sigma X \cup \Xi(X - \Sigma X, Y - \Sigma Y)$$

is also semialgebraic, and $\dim \amalg(X,Y) < \dim X$. At last, we are in position to prove the Whitney-stratifiability of the semialgebraic sets.

THEOREM 3.7. *Any semialgebraic set $X \subseteq \mathbb{R}^m$ admits a Whitney stratification $\mathcal{X}$ having finitely many semialgebraic strata.*

PROOF. We follow here the proof given in [**41**, p.20]. Let $k = \dim X$ and $X^k \supseteq X^{k-1} \supseteq \ldots X^0$ a filtration of X by semialgebraic sets X^i closed in X with $\dim X^i \leq i$ and each difference $X^i - X^{i-1}$ a smooth manifold of dimension i (or empty). Suppose inductively that $X^k, X^{k-1}, \ldots, X^i$ have been constructed according to the following prescription. If $\dim X^i < i$ we simply put $X^{i-1} = X^i$. If $\dim X^i = i$ we put

$$X^{i-1} = \mathrm{Cl}_X\{ \bigcup_{j=i+1}^{k} \Xi(X^i, X^j - X^{j-1})\}.$$

($\mathrm{Cl}_X Y$ means closure a subset $Y \subseteq X$ in X.) It follows from the preceding notes that X^{i-1} is semialgebraic of dimension $\leq (i-1)$. And $X^i - X^{i-1}$ is a smooth manifold viewing that it is obtained from the smooth manifold $X^i - \Sigma X^i$ by removing a closed set. We take $\mathcal{X}$ to be a stratification of X whose strata are the $X^i - X^{i-1}$. It follows from the construction that $\mathcal{X}$ is a Whitney stratification which has of course finitely many semialgebraic strata. □

5.2. Semianalytic geometry. Analytic functions are particularly useful in geometric design because they can be *uniquely* approximated by Taylor series expansion. They include the algebraic or polynomial functions, rational functions, transcendental functions, etc. Analytic functions are used to define semianalytic subsets of $\mathbb{R}^m$, as polynomial functions are used to define semialgebraic subsets of $\mathbb{R}^m$.

Similar to semialgebraic sets, semianalytic sets are defined not only by analytic equalities —what characterises the analytic geometry—, but also by analytic inequalities. This means that semialgebraic sets form a subclass of the semianalytic sets since polynomial functions are in the class of analytic functions. For example, the straight line segment from the point $(0,0)$ and $(1,0)$ in $\mathbb{R}^2$ is given by the semianalytic point set $\{y = 0\} \cap \{x > 0\} \cap \{x < 1\}$. This point set is the intersection of the analytic set $\{y = 0\}$ with two semianalytic sets, $\{x > 0\}$ and $\{x < 0\}$, respectively. Obviously, this straight line segment is not analytic. Thus, analytic varieties are just a subclass of semianalytic sets. That is,

every analytic variety is semianalytic, but not vice-versa. For another example, observe that the line $y = x$ and the half-plane $y \geq x$ in $\mathbb{R}^2$ are both semianalytic, but only the former is analytic.

All this makes us to wonder whether or not all the nice local properties of semialgebraic sets can be extended to semianalytic sets. In particular, we are interested in to know whether semianalytic sets are or not Whitney-stratifiable. This study was carried out by Lojasiewicz and is summarised as follows:

- *Local finiteness.* Every semianalytic set is locally finite [**71**, p.76] [**53**, p.112].
- *Boolean algebra.* Taking into account that the product, the sum of squares, or the Cartesian product of two analytic functions is analytic, we readily verify that the *union* of a locally finite family of semialgebraic sets is semianalytic, the *intersection* of a finite family of semialgebraic sets is semianalytic, the complement (or difference of any two) of a semianalytic set is also semianalytic, as well as the *Cartesian product* of two semianalytic sets [**71**, p.67] [**53**, p.109].
- *Topological operations.* It follows that the *closure*, *interior*, and *frontier* of a semianalytic set is also semianalytic, as well as any of its *connected components* [**71**, p.76] [**53**, p.112].
- *Images.* The *inverse image* under an analytic map of a semianalytic set is semianalytic. Unfortunately, the Tarski-Seidenberg Theorem may fail, i.e. the *direct image* under an analytic map of even a compact analytic set may fail to be semianalytic. [**71**, p.] [**53**, p.110].
- *Whitney-stratifiability.* Semianalytic sets admit Whitney stratifications [**71**, p.97].
- *Triangulability.* Every semianalytic set is triangulable [**70**, p.463]. This generalises the triangulability of semialgebraic sets first proven by Hironaka [**59**, p.170].

Thus, with the exception of the Theorem Tarski-Seidenberg, semianalytic sets enjoy all the good properties of semialgebraic sets. In fact, the semianalyticity of sets is not preserved by *projection* operations (see, for example, [**72**, p.1587]), even when such sets are compact. As noted in [**58**, p.453], this failure causes various difficulties in dealing with semianalytic, or even closed real-analytic, subsets in geometric problems. In geometric modelling, the lack of projective invariance makes to think of semianalytic geometry as inadequate for operations of graphical visualisation and projection. But, as shown later, there is no problem if we project objects of dimension at most 3, as usual in geometric modelling. Problems turn out for higher dimensions. Nevertheless, the image of any semianalytic set by an analytic isomorphism (i.e. diffeomorphism) is semianalytic [**70**, p.450]. The following two examples show us that the semianalyticity is not preserved by projections.

EXAMPLE 3.13. (Hironaka, [**58**, p.453]) Let $f : \mathbb{R}^3 \to \mathbb{R}^2$ be a projection $(x,y,z) \mapsto (x,y)$. Let $X = \{(x,y,z) \in \mathbb{R}^3 \,|\, xz = 1 \text{ and } y = \sin(1/x), x > 0\}$, which is closed real analytic and hence semianalytic in $\mathbb{R}^3$. But $f(X)$, the graph of $y = \sin(1/x)$, $x > 0$, called the *topologist's curve*, is not semianalytic at the origin of $\mathbb{R}^2$.

This example shows us that if f is not *proper*, the image of a semianalytic subset by f can be pretty wild, that is, non-semianalytic. (Recall that a map f from Y to X is proper if whenever A is compact in X, $f^{-1}(A)$ is compact in Y.) But, semianalyticity fails to preserve even for compact subsets. Semianalyticity may fail even if the map is real analytic and *proper*, as illustrated by next example.

EXAMPLE 3.14. (Lojasiewicz, [**72**, p.1587]) The point set $X = \{x = 1, z = e^y, 0 \leq y \leq x\} \subset \mathbb{R}^3$ is not semialgebraic. (This is clear because the point set $z = e^y$ is not semialgebraic.) Consequently, by the theorem of the semianalytic cones that asserts that 'every semianalytic cone of $\mathbb{R}^n$ is semialgebraic', the cone $[0,\infty)X$ cannot be semianalytic, what implies that the point set $Y = [0,\infty)X \cap \{0 \leq x \leq 1\}$, i.e. $Y = 0 \cup \{z = xe^{y/x}, 0 < x \leq 1, 0 \leq y \leq x\}$, is not semianalytic either. But Y is the image of the compact semianalytic set $Z = \{y = xu, z = xe^u, 0 \leq x \leq 1, 0 \leq u \leq 1\} \subset \mathbb{R}^4$ by the projection $(x,y,z,u) \mapsto (x,y,z)$.

5.3. Subanalytic geometry. Tarski and Seidenberg shown that semialgebraicity is preserved by rational maps (not only algebraic or polynomial maps) [**108, 101**] (see also [**42**, p.223] for a simple proof). Namely, if $X \subseteq \mathbb{R}^m$ is semialgebraic, and $f : X \to \mathbb{R}^n$ is rational, then $f(X)$ is also semialgebraic in $\mathbb{R}^n$. Examples 3.13 and 3.14 have shown that the Tarski-Seidenberg Theorem may fail to preserve semianalyticity under projections.

The question is now whether or not there is a bigger class of sets that not only enjoy the properties of semianalytic sets, but also does satisfy the Tarski-Seidenberg Theorem. As noted by Lojasiewicz in [**72**, p.1588], a natural candidate is the class of sets which are *locally* images by projections of relatively compact semianalytic sets. (Recall that a set X is relatively compact whenever its closure $\overline{X}$ is compact [**30**, p.237].) Thus, we are interested in a class of *locally compact* sets. In fact, by definition, a Hausdorff space is locally compact if each point has a relatively compact neighbourhood [**30**, p.237], that is, a neighbourhood with compact closure. Obviously, a locally compact space not need to be compact, but every compact space is locally compact. For example, $\mathbb{R}^n$ is locally compact, but not compact. Also, an open interval in $\mathbb{R}$ is locally compact, but not compact. Local compactness rids of serious problems such as, for example, to have the set of rationals as image of a projection. In fact, it is known that the set of rationals in $\mathbb{R}$ is not a locally compact space.

DEFINITION 3.9. (Lojasiewicz,[72, p.1589]) Let $V \subseteq \mathbb{R}^n$ a real analytic variety. A subset X of V is said to be **subanalytic** if its trace in the neighbourhood of any point of V is the image, by the projection $V \times \mathbb{R}^k \to V$, of a relatively compact semianalytic subset of $V \times \mathbb{R}^k$ (where k depends on **x**).

It is clear that a relatively compact subanalytic set is the image of a projection of a relatively compact semianalytic set, and vice-versa [72, p.1589].

REMARK 7. (Hironaka [58, p.465]) It is easy to prove that $X \subset \mathbb{R}^n$ is subanalytic if and only if for every $\mathbf{x} \in \overline{X}$, we can find an open neighbourhood U of $\mathbf{x}$ in $\mathbb{R}^n$ and a finite number of *proper* real analytic maps of real analytic spaces $f_{ij} : Y_{ij} \to U$, $j = 1,2$, such that

$$X \cap U = \bigcup_i (\text{Image } f_{i1} - \text{Image } f_{i2}).$$

REMARK 8. (Hironaka [58, p.465]) Using resolution of singularities, we may assume that all the Y_{ij} of Remark 7 are real analytic manifolds (smooth and connected).

According to Remark 7, a subanalytic set is a set which locally is the proper analytic image of some semianalytic set. This disables the existence of spirals in the neighbourhood of any point of a subanalytic set. The same applies to the neighbourhood of any point of a subanalytic stratum. For example, the spiral in $\mathbb{R}^2$ that is image of the map $f : [0,\infty) \to \mathbb{R}^2$ analytically given $f(r) = (\frac{\cos r}{r}, \frac{\sin r}{r})$ is compact, but f is not proper in spite of f is a 1-1 immersion. Thus the strata of a subanalytic stratification are regular. In fact, a proper one-to-one immersion is an embedding [103, p.16], and its image is a closed regular submanifold [15, p.81]. Thus, unlike semianalytic sets, subanalytic sets are closed under proper projections. As noted in [58, p.454], "the class of subanalytic subsets is the smallest one which contains all the semianalytic subsets and is closed under the operation of taking the images by proper real analytic maps".

THEOREM 3.8. *If X is semianalytic in $\mathbb{R}^n$, then it is also subanalytic in $\mathbb{R}^n$.*

PROOF. See Hironaka [58, p.467]. □

Semianalytic and subanalytic sets coincide up to dimension 2, and start to differ from each other from the dimension 3. (An example of a subanalytic set in $\mathbb{R}^3$ that is *not* semianalytic is the set Y in Example 3.14.)

In addition to projective invariance, subanalytic sets enjoy the properties of semianalytic sets which are relevant for geometric modelling. In short, we have:

- *Local finiteness.* Every subanalytic set in $\mathbb{R}^n$ is locally finite [**58**, p.472].
- *Boolean algebra.* The property of being subanalytic is closed under finite union, finite intersection, and difference of any two [**58**, p.466]. This follows from the definition given in Remark 7.
- *Topological operations.* The closure, the interior, and frontier of a subanalytic set $X \in \mathbb{R}^n$ is also subanalytic [**58**, p.480-481] [**59**, p.179].
- *Images.* Subanalyticity is preserved by proper real-analytic maps [**58**, p.480]. Let $f : \mathbb{R}^m \to \mathbb{R}^n$ be a proper real-analytic map. If Y is a subanalytic subset of $\mathbb{R}^n$, then so is $f^{-1}(Y)$ in $\mathbb{R}^m$. If X is a subanalytic subset of $\mathbb{R}^m$, then so is $f(X)$ in $\mathbb{R}^n$.
- *Whitney-stratifiability.* Subanalytic sets admit Whitney stratifications [**58**, p.488].
- *Triangulability.* Every subanalytic set is triangulable [**59**, p.180].

Bounded and unbounded subanalytic sets (for example, a line segment with a finite length and a line with infinite length, respectively) are often useful in geometric modelling. Bounded subanalytic sets have a finite number of connected components. But, as Middleditch and Reade noted in [**84**, p.83], a subanalytic set may possess an infinite number of components. For example, the set-intersection of an unbounded sine curve with an unbounded straight line can yield an infinite set of isolated points. To overcome this problem, Middleditch and Reade have proposed to reduce the geometric coverage of Djinn* API to finitely subanalytic sets. Another way to round this problem is to make sure that at least one of the Boolean operands is bounded.

6. Mathematical design issues: stratifiable geometries

Let us review such important issues related to the geometric nature of point sets in $\mathbb{R}^n$ and stratifiability, and their applicability to the mathematical design of a geometric kernel:

- *Geometric coverage.* Subanalytic geometry provides a wide geometric coverage in $\mathbb{R}^n$ that includes the geometries commonly used in solid modelling, free-form modelling of curves and surfaces, and algebraic geometry engines such as, for example, the *Mathematica.*
- *Topological coverage.* In geometric modelling, we use *topologically stable* spaces, i.e. spaces that enjoy nice local properties. Therefore, we are interested in topological spaces which are rid of pathologies. Otherwise, it will be rather difficult to control and process their geometry on computers. We have seen that subanalytic geometry ensures the required nice local properties, since the strata of a stratified subanalytic set are all regular manifolds.

Note that a subanalytic set need not to be neither closed nor open as, for example, the union of a relatively open square and a relatively open edge in $\mathbb{R}^2$ is a subanalytic subset in $\mathbb{R}^2$.

- *Stratifiability.* For mathematicians, stratifiability is useful to study the local properties of point sets. For example, if the dimensional inequality condition is not satisfied for a point set, we can conclude immediately that such a point set is not subanalytic. For us, geometric modelling researchers, this is also important because it helps us to understand the intimate relationship between stratifiability and geometric nature of point sets. But, above all, stratifiability is relevant for the mathematical design of geometric kernel data structures. In fact, a weak Whitney stratification endows a space with a homological structure similar to those of conventional B-reps, which is essential to devise traversal, interrogation and geometric reasoning algorithms. Remarkably, any Whitney stratification of a locally closed set in $\mathbb{R}^n$ satisfies the weak frontier condition [**105**, p.24], what shows that weak Whitney-stratifiability depends more essentially on the topological stability than geometric stability of a point set. Moreover, stratifiability is a first step to guarantee the triangulability of a geometric object, what is necessary for finite-element modelling applications.
- *Geometric operators.* Together with the shape coverage (types of shape) and stratifiability (structure), the set of operators definable for a class of subsets of $\mathbb{R}^n$ is the third most important part of the triangular mathematical design architecture of the Σ-geometric kernel proposed in Chapter 1. Taking into account that subanalytic sets form a Boolean class, the set-theoretic operators are here considered the basic operators to construct geometric objects. But, because the inner kernel of the Σ-geometric kernel processes stratified subanalytic sets, we have to define some sort of stratified set-theoretic operators, i.e. set-theoretic operators which are stratifiability-preserving, similar to those proposed in [**87**]. Alternatively, the geometric kernel can be provided by a set of Euler operators as proposed in Chapter 5.
- *Shape coverage and clustering.* In order to be able to process sorts of shapes (global topological shapes, homotopic shapes, convex and concave shapes, etc.) other than geometric ones, and preserve the geometric identity of manifolds and varieties under stratification and subdivision operations, we need an effective technique of clustering strata. This point will be tackled in next chapter.

7. Thom-Boardman stratifications

Singularities can be discussed in terms of the Inverse Map Theorem: they occur where the theorem fails [**43**, p.585]. A map $f : M \to N$ of one n-manifold M into another n-manifold N is nonsingular at $\mathbf{p} \in M$ if it is locally invertible. The test for local invertibility is given explicitly by the Inverse Map Theorem. If $x_1, \ldots, x_n$ is a system of coordinates around $\mathbf{p} \in M$, and $f_1, \ldots, f_n$ a system around $f(\mathbf{p}) \in N$, then f is locally invertible if and only if the Jacobian of the transformation is nonsingular, i.e. $\det \mathrm{D}f(\mathbf{p}) \neq 0$. But, as seen in Chapter 2, this is a rudimentary way to determine singularities. For example, we know from the previous chapter that the singular set of the Cartan umbrella with-handle $x^2 - zy^2 = 0$ is the z-axis, what leads to an OrdT stratification. However, we have no way to distinguish the origin from the remaining singular points in the z-axis, though we know that it has a rather different topological type.

A more accurate approach to calculate singularities has been outlined in Chapter 2 and is based on the rank of the first differential. In fact, by the Implicit Mapping Theorem, all *regular* points of a map $f : M \to N$, where $\dim M = m$ and $\dim N = n$, that is, points at which the rank of the first differential is equal to $\min(m,n)$, are equivalent. On the hand, points at which the rank is less than $\min(m,n)$ are called *singular* points of the map and the number yielding the deficiency of the rank is the simplest invariant that distinguishes nonequivalent singular points. Such a number is called the *corank* of the singularity. However, the corank criterion may fail to isolate singularities from the singular set either.

EXAMPLE 3.15. Let us consider the Cartan umbrella $x^2 - zy^2 = 0$. It is a level set of the function $f : \mathbb{R}^3 \to \mathbb{R}$ given by $f(x,y,z) = x^2 - zy^2$. We know that the maximal rank of the Jacobian $\mathrm{J}f = [2x \quad -2zy \quad -y^2]$ associated with the Cartan umbrella is 1, so the corank is 0 for the regular point set (the two umbrella sheets) or 1 for the singular point set (z-axis); hence the corank cannot increase further, and the origin is not distinguishable from the other singular points in the singular point set.

In order to overcome these difficulties, we have to use a finer approach to resolve singularities. Basically, it consists of determining the singularities of the sucessive C^r derivatives of a map. That is, we determine the C^r singularities by taking the Jacobian of the C^{r-1} derivative. This leads to an increasingly refinement of the conjunctive form of C^1 singular set towards a union of smooth submanifolds.

EXAMPLE 3.16. Let us consider again the Cartan umbrella. Intuitively, self-intersections as those which occur in the Cartan umbrella have a conjunctive form. The singular set of the Cartan umbrella

is given by the conjunction of the zero sets of the derivatives of the Jacobian, i.e.

$$\{x=0\}\wedge\{yz=0\}\wedge\{y=0\}=\{0\times 0\times z\}. \tag{11}$$

The singular set is then the z-axis. The first and third terms of (11) are smooth submanifolds in $\mathbb{R}^3$, the planes $\{x=0\}$ and $\{y=0\}$. So, we need not decompose them further. But, $\{yz=0\}$ is not smooth because it is the union of two planes, $\{y=0\}$ and $\{z=0\}$. The Jacobian concerning this variety $yz=0$ is $[z \quad y]$, so its singular set is given by

$$\begin{cases} z=0 \\ y=0 \end{cases}$$

or, in the conjunctive form,

$$\{z=0\}\wedge\{y=0\} \tag{12}$$

Replacing (12) in (11), we get

$$\{x=0\}\wedge\{y=0\}\wedge\{z=0\}=\{0\times 0\times 0\}. \tag{13}$$

i.e. the origin. Note that $\{z=0\}\wedge\{y=0\}=\{x\times 0\times 0\}$ is the x-axis. Thus, the singularity at the origin can be viewed as the intersection of the z-axis (the singularity set of first order) and the x-axis (the singularity set of second order), i.e. $\{0\times 0\times z\}\wedge\{x\times 0\times 0\}=\{0\times 0\times 0\}$.

This intuitive technique was formally studied and developed by Thom and Boardman. It is now know as Thom-Boardman stratification.

7.1. Transversality. *Transversality* is the key idea behind Thom-Boardman stratifications.

DEFINITION 3.10. Two linear subspaces of a finite-dimensional linear space are said to be **transverse** if their sum[1] is the whole space.

This makes us think of transversality for more general spaces in $\mathbb{R}^n$ depends on their associated tangent bundles, i.e. the tangent spaces at every point of them. In previous chapter we have used a particular case of transversality, namely the notion of orthogonality of tangent and cotangent spaces in $\mathbb{R}^n$.

---

[1]Let U and V be subspaces of the vector space X. Their *sum* $U+V$ is the set of all vectors $\mathbf{x}=\mathbf{u}+\mathbf{v}$, where $\mathbf{u}\in U$ and $\mathbf{v}\in V$. Besides, $U+V$ is a subspace of X [**34**, p.171].

EXAMPLE 3.17. In $\mathbb{R}^3$, two 1-dimensional subspaces are never transversal, while two non-parallel 2-dimensional subspaces are always transversal. Similarly, a 1-dimensional and a 2-dimensional subspace are transversal only if the former subspace does not lie in a 2-dimensional subspace parallel to the latter subspace.

The notion of objects intersecting transversally (or in general position) is fundamental in singularity theory. It can be easily extended to smooth submanifolds of a smooth manifold.

DEFINITION 3.11. Let M_1, M_2 be two submanifolds of a manifold M. They **intersect transversally at** $x \in M_1 \cap M_2$ when the tangent spaces T_xM_1, T_xM_2 intersect transversally in T_xM; and they **intersect transversally in** M when they do so at every point of $M_1 \cap M_2$.

This is illustrated in Figure 10, where some examples of non-transverse and transverse submanifolds in (a) $\mathbb{R}^2$ and (b) $\mathbb{R}^3$ are depicted. Note that two tangential lines in $\mathbb{R}^2$ are not transverse, whereas two crossing lines in $\mathbb{R}^3$ are transverse. The idea behind this is that we can slightly perturb two crossing lines in $\mathbb{R}^2$ without destroying the intersection, but not two tangential lines. Similarly, two crossing lines in $\mathbb{R}^3$ are not transverse since a slight perturbation of them destroy their intersection. This is very important from the floating point arithmetic because it is *a priori* ensured that floating point inaccuracies in the representation of strata do not alter their transversality. As seen later, this leads us to the notion of *genericity* or *infinitesimal stability*.

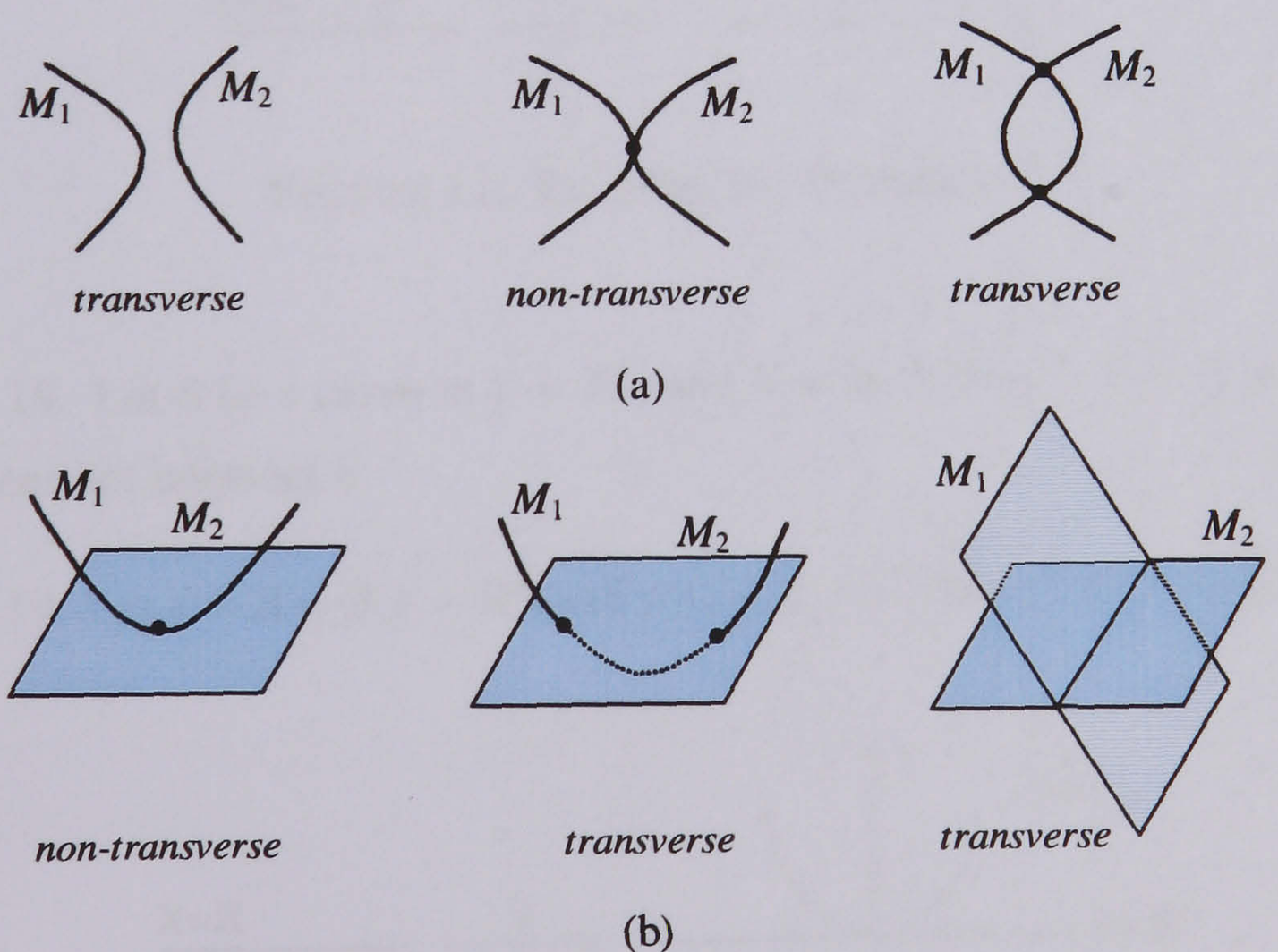

FIGURE 10

In order to exploit the idea of transversality in geometric modelling, we have to define it in terms of mappings. Doing so, we are able to study transversality for images, level sets, and graphs of mappings, i.e. the (parametric, implicit, and explicit) representations of geometric objects as usual in geometric modelling.

DEFINITION 3.12. Let X and Y be smooth manifolds and $f : X \to Y$ be a smooth map. Let B be a smooth submanifold of Y and $\mathbf{p} \in X$. The map is said to be **transverse** to B at $\mathbf{p}$ (denoted by $f \pitchfork B$ at $\mathbf{p}$), or , in other words, f intersects B **transversely** at $\mathbf{p}$ if either

(a) $f(\mathbf{p}) \notin B$, or

(b) $f(\mathbf{p}) \in B$ and the image of the tangent space to X at $\mathbf{p}$ under the derivative $\mathrm{D}f$ is transverse to the tangent space to B, that is,

$$\mathrm{T}_{f(\mathbf{p})}Y = \mathrm{T}_{f(\mathbf{p})}B + \mathrm{D}f(\mathrm{T}_{\mathbf{p}}X). \tag{14}$$

Of course, the map f is said to be **transverse to** B if it is transverse to B at every point of X, and we write $f \pitchfork B$. The equation (14) is known as T-condition, or transversality condition, and is illustrated in Figure 11.

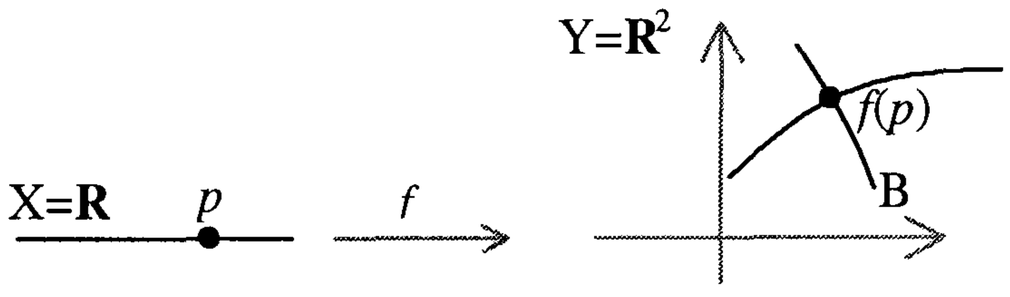

FIGURE 11. Picturing the T-condition.

EXAMPLE 3.18. Let B be a curve in $Y = \mathbb{R}^3$, and $X = \mathbb{R}$. Then $f : X \to Y$ is transverse to B iff the image of X does not intersect B.

EXAMPLE 3.19. Let $X = \mathbb{R} = B, Y = \mathbb{R}^2$, and $f(t) = (t, t^2)$. Then $f \pitchfork B$ at all nonzero x, Figure 12.

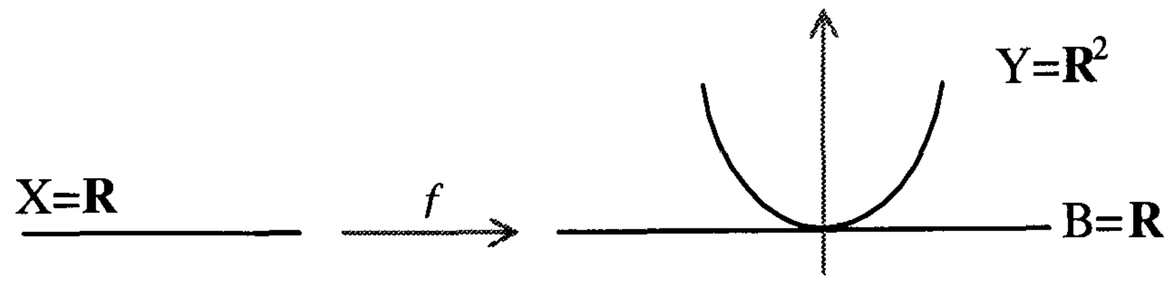

FIGURE 12

Inclusion maps $f : X \subset \mathbb{R}^m \to \mathbb{R}^m$ are possibly the best way to further develop our intuition about transversality. The condition for f to be transverse to a manifold $Y \subset \mathbb{R}^m$ then reduces to

$$\mathrm{T}_{\mathbf{y}}X + \mathrm{T}_{\mathbf{y}}Y = \mathrm{T}_{\mathbf{y}}\mathbb{R}^m, \quad \text{for all } \mathbf{y} \in X \cap Y, \tag{15}$$

and we write $X \pitchfork Y$, and say that X *transverse to* Y, [**24**, p.161].

EXAMPLE 3.20. Let X, Y be the x-axis and y-axis in $\mathbb{R}^2$, respectively. Clearly, $X \pitchfork Y$.

EXAMPLE 3.21. Let X, Y be the x-axis and y-axis in $\mathbb{R}^3$, respectively. In spite of they intersect at the origin $\mathbf{0} = (0,0,0)$, X is not transverse to Y. In fact, $\dim X + \dim Y = 2 < 3 = \dim \mathbb{R}^3$, hence $\mathrm{T}_{\mathbf{0}}X + \mathrm{T}_{\mathbf{0}}Y$ cannot yield $\mathbb{R}^3$.

EXAMPLE 3.22. Let X be a unit sphere $\mathbb{S}^1 = \{(x,y) \in \mathbb{R}^2 \,|\, x^2 + y^2 = 1\}$ and Y be the line $Y_1 = \{(0,y) \,|\, y \in \mathbb{R}\}$ (respectively, the lines $Y_2 = \{(2,y) \,|\, y \in \mathbb{R}\}$, $Y_3 = \{(1,y) \,|\, y \in \mathbb{R}\}$). In each case other than the latter we do have transverse intersection.

It is apparent that the relative dimensions of X, Y and B play an important role in determining the transversality for a particular instance.

THEOREM 3.9. *Let X and Y be smooth manifolds, $B \subset Y$ a smooth submanifold. Assume that* $\dim X + \dim B < \dim Y$, *or, equivalently,* $\dim X < \operatorname{codim} Y$. *Let $f : X \to Y$ be smooth and suppose that $f \pitchfork B$. Then $f(X) \cap B = \varnothing$.*

PROOF. See Golubitsky [**44**, p.51]. □

THEOREM 3.10. *If $f : X \to Y$ is transverse to B then $f^{-1}(B)$ is a smooth submanifold in X with the same codimension in X as B has in Y, that is,* $\operatorname{codim} f^{-1}(B) = \operatorname{codim} B$. *In particular, if* $\dim X = \operatorname{codim} B$, *then $f^{-1}B$ consists only of isolated points.*

PROOF. See Golubitsky [**44**, p.52]. □

It is clear that, for any trio X, Y, and B, the set of of transverse maps is quite large. The formalisation of this fact is known as the Thom Transversality Theorem.

THEOREM 3.11. (**Thom Transversality Theorem**) *Let X and Y be smooth manifolds and B a smooth submanifold of $J^k(X,Y)$. Let*

$$T_B = \{f \in C^\infty(X,Y) \,|\, j^k f \pitchfork B\}. \tag{16}$$

Then T_B is a residual subset of $C^\infty(X,Y)$ in the C^∞ topology. Moreover, if B is closed, then T_B is open.

PROOF. See Golubitsky and Guillemin [**44**, p.54]. □

REMARK 9. $C^\infty(X,Y)$ is the family of all smooth mappings of $X \to Y$, i.e. $C^\infty(X,Y) = \{f : X \to Y : f \text{ of class } C^\infty\}$. C^∞ is the Whitney C^∞-topology associated to $C^\infty(X,Y)$ as explained in [**1**, pp.180-181].

REMARK 10. A subset of a topological space is residual if it is a countable intersection of open dense subsets of such a topological space.

REMARK 11. Note that if B is closed, the maps transverse to B form an open everywhere dense set. If B is not closed, the maps transverse to B form a countable intersection of open dense sets. Examples: (1) Y a torus, B an "irrational line" winding round it and X a circle; (2) Y a plane, X a circle on it and B one of its tangents (without the point of contact). In either example, the embedding of X in Y is transverse to B but there exist maps non-transverse to B arbitrarily close to this embedding.

We are also interested in dealing with cases where B is not a smooth manifold, but a manifold or a variety with singularities. In particular, we are interested in mappings which are transverse to a stratified set. A mapping is said to be transverse to a stratified set B if it is transverse to each stratum [**4**, p.41]

EXAMPLE 3.23. Let B the union of two planes intersecting along a line in $\mathbb{R}^3$, and the stratification $\mathcal{B}$ its partition into the line of intersection and four halfplanes. Transversality to $\mathcal{B}$ means transversality to each of the planes as well as transversality to the intersection line. For example, a curve that is transverse to $\mathcal{B}$ does not intersect its line of singularities.

Of course, the Thom Transversality Theorem also extends to the case of a stratified set B. However, in this case the theorem only guarantees that transverse maps form an everywhere dense intersection of a countable number of open sets, not just an open everywhere dense set. Nevertheless, for the transverse maps to form an open everywhere dense set it is sufficient for the stratification to satisfy the following further condition [**4**, p.41]: *every embedding transverse to a stratum of smaller dimension is transverse to all adjacent strata of larger dimension in some neighbourhood of this stratum of smaller dimension.* This is called here the **transversal adjacency condition**.

EXAMPLE 3.24. Let B be the cone $x^2 = y^2 + z^2$ in $\mathbb{R}^3$ as depicted in Figure 13(a), and $\mathcal{B}$ its stratification into the point $M_1 = \mathbf{0} = (0,0,0)$ and the two sheets M_2 and M_3, Figure 13(b). Clearly, this stratification satisfies the transversal adjacency condition.

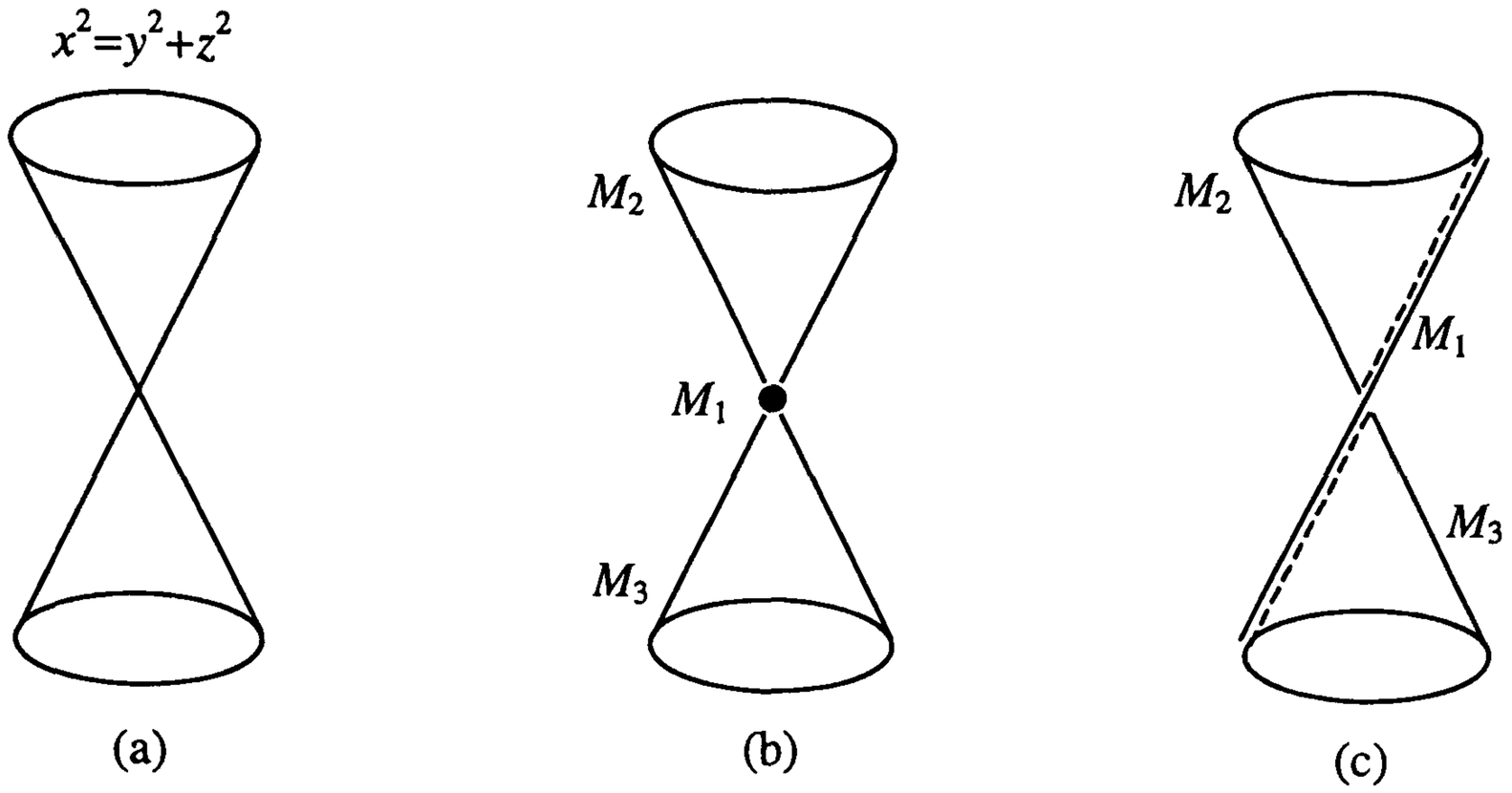

FIGURE 13. Stratifications of a cone.

EXAMPLE 3.25. Let us take again the cone in Figure 13(a), but now stratified into a straight line M_1 passing through the apex and the two sheets (now homeomorphic to $\mathbb{R}^2$) M_2, M_3. From transversality to the 1-dimensional stratum M_1 there does not follow transversality to M_2 and M_3. In fact, any plane tangent to M_2 or M_3 intersects M_1 transversely at the apex. But, such tangent planes are not obviously transverse to M_2 or M_3. Consequently, transversal adjacency condition is not satisfied, that is, transversality to M_1 does not imply transversality to higher dimensional strata M_2 and M_3. The transversal adjacency condition would be satisfied if M_1 were partitioned into two halflines (two 1-dimensional strata) by the apex (a 0-dimensional stratum).

EXAMPLE 3.26. Let B be the Cartan umbrella with-handle given by $x^2 = zy^2$. A rank-based stratification of B consists of two 2-dimensional sheets and a singular line $x = y = 0$, the z-axis in $\mathbb{R}^3$. As for the previous example, transversality to the singular line does not imply transversality to the submanifold of regular points of the surface close to this line. In fact, the plane $z = 0$ is transverse to the singular line but is not transverse to the surface. Therefore, similar to local topological type condition, the transversal adjacency condition leads to the partition of the z-axis into the negative z-axis, the origin, and the positive z-axis.

If the transversal adjacency condition is satisfied for the stratification B, that is, if

transversality to lower-dimensional strata

$$\Downarrow$$

transversality to higher-dimensional strata,

then transversality to the whole stratification is achieved as follows:

ALGORITHM 3.1. (**Thom Stratification Algorithm**)[**4**, p.42])

(1) Strata of the lowest dimension are smooth, and thus the Thom Transversality Theorem applies.
(2) In a neighbourhood of strata of least dimension transversality is achievable to all strata.
(3) Discard from the containing manifold the closure of a neighbourhood of the strata of least dimension and proceed to process the strata of the next smallest dimension.

The examples above and the Thom Stratification Algorithm suggest that T-regular Thom stratifications satisfy the topological type criterion. This was proven by Thom in [**109**] indeed. Moreover, it can be proved that it is possible to decompose any algebraic stratification further in such a way that the transversal adjacency condition becomes fulfilled [**4**, p.43].

7.2. First-order Thom-Boardman singularity sets. Our purpose now is to use Thom Transversality Theorem to show that for a dense set of smooth maps $f : \mathbb{R}^m \to \mathbb{R}^n$ the singular set Σf can be partitioned into finitely many smooth manifolds on each of which f has constant rank.

Recall that a singular point of a smooth map $f : X \to Y$ is a point $\mathbf{x} \in X$ for which the rank of the differential $\mathrm{D}f(\mathbf{x})$ falls bellow its possible maximal value of $\min(\dim X, \dim Y)$. A rudimentary classification of singularities of f is provided then by distinguishing one singular point from another by the value taken by the corank of the differential at it. We say that f has a singularity of type Σ^i at $\mathbf{x} \in X$ if $\mathrm{D}f(\mathbf{x})$ drops rank by i, or, equivalently, if $\mathrm{rank}\,\mathrm{D}f(\mathbf{x}) = \min(\dim X, \dim Y) - i$. Denote by $\Sigma^i f$ the singularities of f of type Σ^i.

DEFINITION 3.13. The **first-order Thom-Boardman singularity sets** are defined by

$$\Sigma^i f = \{\mathbf{x} \in X \,|\, \mathrm{D}f(\mathbf{x}) \text{ has kernel corank } i, \}$$

or

$$\Sigma^i f = \{\mathbf{x} \in X \,|\, \mathrm{D}f(\mathbf{x}) \text{ has kernel dimension } i, \}$$

REMARK 12. Let $r = \mathrm{rank}\,\mathrm{D}f(\mathbf{x})$ and let $m = \dim X$ and $n = \dim Y$. The differences $m - r$ and $n - r$ are called the *coranks* of $\mathrm{D}f(\mathbf{x})$ at X and Y, respectively.

REMARK 13. The coranks are related to the dimension i of the kernel by the formulas $m - r = i$, $n - r = n - m + i$.

The first-order Thom-Boardman singularity sets are determined by observing where the rank of the Jacobian falls below $\min(\dim X, \dim Y)$. In this way we get a stratification by rank of X into

finitely many sets on each on each of which f has constant rank. One might reasonably expect that these singularity sets were submanifolds of X, but as shown below that is not necessarily the case.

EXAMPLE 3.27. Let $f : \mathbb{R}^2 \to \mathbb{R}^2$ be defined by $f(x,y) = (x^2, y^2)$. This is called the "folded handkerchief" map because it is the composite of the two maps

$$(x,y) \mapsto (x,y^2)$$

$$(x,y) \mapsto (x^2,y)$$

which "fold" the plane along the x-axis and y-axis, respectively, as illustrated in Figure 14. The respective Jacobian is given by

$$\mathrm{J}f(x,y) = \begin{bmatrix} 2x & 0 \\ 0 & 2y \end{bmatrix},$$

so the overall singular set is given by $xy = 0$, the union of the axes $x = 0$ and $y = 0$. It can be decomposed into three first-order Thom-Boardman singularity sets, namely: the origin is the only Σ^2 point, other points on the axes being Σ^1 points, and the remaining points being Σ^0 points (the regular points). This fits in with the fact that the origin is folded twice, other points on the axes just once, and the rest not at all.

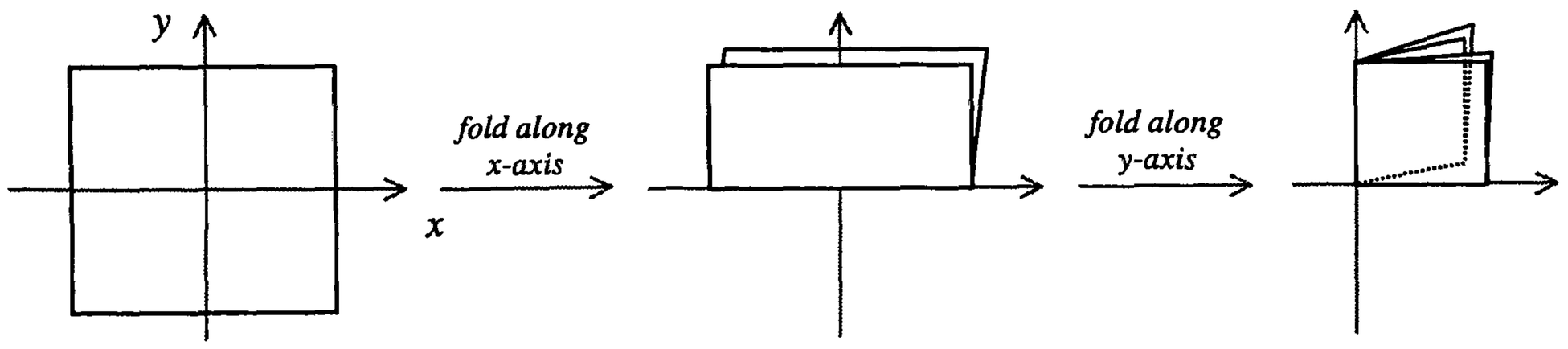

FIGURE 14. Folding an handkerchief using a composite of two maps.

In Example 3.27, the first Thom-Boardman singularity sets $\Sigma^0 f$, $\Sigma^1 f$ and $\Sigma^2 f$ are all submanifolds. However, not always this is the case, as shown in the following example.

EXAMPLE 3.28. Let us take the smooth map $f : \mathbb{R}^2 \to \mathbb{R}^2$ given by $f(x,y) = (x^2 + y, y^2)$. Its Jacobian matrix is $\begin{bmatrix} 2x & 1 \\ 0 & 2y \end{bmatrix}$, and therefore the Σ^1 points are given by the union of the two axes $xy = 0$, which is not then a submanifold. Note that there are no Σ^2 points, since the rank cannot drop below 1. This happens because $\frac{\partial f_1}{\partial y} = 1 \neq 0$.

THEOREM 3.12. *Σ^i is a smooth submanifold of $J^1(m,n)$ of codimension $i(m-n+i)$.*

PROOF. See Gibson [**42**, p.56-57]. □

7.3. Higher-order Thom-Boardman singularity sets. The Thom-Boardman theory has to do with the behaviour of maps restricted to their singular sets [**44**, p.145].

DEFINITION 3.14. A map $f : X \to Y$ is said to be **1-generic** if $j^1 f \pitchfork \Sigma^i$ for all i.

Thus, if $f : X \to Y$ is 1-generic, $\Sigma^i f$ is a submanifold, so the restriction $f|\Sigma^i$ is again a map between manifolds, and we can again ask whether it has singularities generically. Such singularities are denoted by $\Sigma^{i,j} f$, the set of points where the map $f : \Sigma^i \to Y$ drops rank j. By the theorem 3.12, we have $\operatorname{codim} \Sigma^i f > \dim X - \dim Y$, so $\dim \Sigma^i f < \dim Y$. Therefore, $\mathbf{x} \in \Sigma^{i,j} f$ if and only if $\mathbf{x} \in \Sigma^i f$ and the kernel of $\mathrm{D} f(\mathbf{x})$ intersects the tangent space to $\Sigma^i f$ in a j-dimensional subspace [**44**, p.152].

THEOREM 3.13. *Let $f : X \to Y$ be 1-generic. Then*

$$\mathbf{x} \in \Sigma^{i,j} f \iff j^2 f(\mathbf{x}) \in \Sigma^{i,j}.$$

PROOF. See Golubitsky [**44**, p.154]. □

COROLLARY 3.1. *Let $f : X \to Y$ be 1-generic. If $j^2 f \pitchfork \Sigma^{i,j} f$, then $\Sigma^{i,j} f$ is a submanifold of $\Sigma^i f$ whose codimension is given by the formula*

$$(m-n+i)i + \frac{j}{2}[(m-n+i)(2i-j+1) - 2i + 2j],$$

where $m = \dim X$ and $n = \dim Y$.

Thus, $\Sigma^{i,j} f$ is a submanifold of X, being its dimension given by $\dim \Sigma^{i,j} f = \dim X - \operatorname{codim} \Sigma^i f - \operatorname{codim} \Sigma^{i,j} f$, where obviously $\operatorname{codim} \Sigma^i f$ is the codimension of $\Sigma^i f$ in X and $\operatorname{codim} \Sigma^{i,j} f$ is the codimension of $\Sigma^{i,j} f$ in $\Sigma^i f$. Moreover, by the Transversality Theorem, we know that the condition $j^2 f \pitchfork \Sigma^{i,j}$ is satisfied by a residual set of maps. These maps for which this condition is satisfied for all i, j are called **2-generic**.

It seems reasonable to think of this process in higher order versions of $\Sigma^{i,j}$. So, if $f : X \to Y$ is 2-generic, $\Sigma^{i,j,k} f$ is defined to be the set of points in $\Sigma^{i,j} f$ where the map

$$f : \Sigma^{i,j} \to Y$$

drops rank by k. This definition makes sense provided that $\Sigma^{i,j} f$ is a submanifold of X. Analogously, if, by chance, $\Sigma^{i,j,k} f$ comes out to be a manifold, we can then define $\Sigma^{i,j,k,l} f$. Boardman proved this process can be continued indefinitely by the following theorem.

THEOREM 3.14. **(Boardman Theorem)** *For every sequence of integers $i_1,\ldots,i_k$ such that $i_1 + \max(0,\dim X - \dim Y) \geq i_2 \geq \ldots \geq i_k \geq 0$, one can define a fiber subbundle $\Sigma^{i_1,\ldots,i_k}$ of $J^k(X,Y)$ (relative to the fibration $J^k(X,Y) \to X \times Y$) such that if $j^1 f$ is transversal to all manifolds $\Sigma^{i_1,\ldots,i_j}$ where $j < k$, then $\Sigma^{i_1,\ldots,i_k} f$ is well-defined and*

$$\mathbf{x} \in \Sigma^{i_1,\ldots,i_k} f \Longleftrightarrow j^k f(\mathbf{x}) \in \Sigma^{i_1,\ldots,i_k}.$$

PROOF. See Boardman [**14**]. □

DEFINITION 3.15. ([**44**, p.157]) A **Boardman map** is a map $f : X \to Y$ whose k-jet extension $j^k f$ is transversal to $\Sigma^{i_1,\ldots,i_k}$, for all k.

Thus, if $f : X \to Y$ is a Boardman map, then, by the Boardman Theorem 3.14, we can partition X into a disjoint union of subsets consisting of the regular points $X - \bigcup \Sigma^i f$ and the Boardman submanifolds $\Sigma^{i_1,\ldots,i_k} f$ with $i_k = 0$. The map

$$f : X - \bigcup_{i \neq 0} \Sigma^i f \to Y$$

is either an immersion or a submersion, what depends on whether $\dim X \leq \dim Y$ or $\dim X \geq \dim Y$; and if $i_k = 0$ the map

$$f : \Sigma^{i_1,\ldots,i_k} f \to Y$$

is an immersion. This partition of X which we have just described is called the **Thom-Boardman stratification** [**44**, p.159].

COROLLARY 3.2. *Let $f : X \to Y$ be* (k-1)*-generic. If $j^k f \pitchfork \Sigma^{i_1,\ldots,i_k} f$ and $\Sigma^{i_1,\ldots,i_k} f$ is non-empty, then $\Sigma^{i_1,\ldots,i_k} f$ is a submanifold of $\Sigma^{i_1,\ldots,i_{k-1}} f$ whose codimension is given by the formula*

$$(m-n+i)\,\mu(i_1,\ldots,i_k) - (i_1 - i_2)\,\mu(i_2,\ldots,i_k) - \cdots - (i_{k-1} - i_k)\,\mu(i_k)$$

where $\mu(i_1,\ldots,i_k)$ stands for the number of sequences $(l_1,\ldots,l_k)$ of integers which satisfy the following conditions:

(i) $l_1 \geq l_2 \geq \cdots \geq l_k \geq 0$

(ii) $i_j \geq l_j$ *for all* $1 \leq j \leq k$ *and* $l_1 > 0$.

The singularity sets $\Sigma^{i_1,\ldots,i_k}$ are called the **Boardman submanifolds** of $J^k(m,n)$. Also, from the Thom Transversality Theorem we have:

THEOREM 3.15. *The set of all smooth maps $f : X \to Y$ for which $j^k f$ is transverse to all the Boardman submanifolds $\Sigma^{i_1,\ldots,i_k}$ is dense in $C^\infty(X,Y)$.*

We say that a smooth map $f : X \to Y$ is **k-generic** when $j^k f \pitchfork \Sigma^{i_1,\ldots,i_k}$, i.e. $j^k f$ is transverse to all the Boardman submanifolds $\Sigma^{i_1,\ldots,i_k}$, for every integer $k \geq 1$. For such a map the set

$$\Sigma^{i_1,\ldots,i_k} f = (j^k f)^{-1}(\Sigma^{i_1,\ldots,i_k})$$

is also a smooth submanifold of X having the same codimension as $\Sigma^{i_1,\ldots,i_k}$. Moreover, as Boardman showed in [**14**], we have

THEOREM 3.16. *Let $f : X \to Y$ be a generic map. Then*

$$\Sigma^{i_1,\ldots,i_k,i_{k+1}} f = \Sigma^{k+1}(f|\Sigma^{i_1,\ldots,i_k} f).$$

From the two last theorems we have the following. Any smooth map $f : X \to Y$ can be forced to be generic by an arbitrarily small perturbation. Besides, the sets $\Sigma^{i_1,\ldots,i_k} f$ are smooth manifolds and coincide precisely with the Thom singularity sets [**42**, p.187]. Besides, a trivial consequence of the theorem 3.16 is that

$$\Sigma^{i_1} f \supseteq \Sigma^{i_1,i_2} f \supseteq \Sigma^{i_1,i_2,i_3} f \supseteq \ldots$$

EXAMPLE 3.29. Which are Thom singularity sets associated with a k-generic map $f : \mathbb{R}^3 \to \mathbb{R}^3$? Let us take first $k = 1$, so by the formula above we have $\mu(i) = i$, and therefore the codimension of Σ^i in $J^1(3,3)$ is $(m-n+i)i = (3-3+i)i = i^2$. Hence, $\Sigma^i f$ has codimension i^2 in $\mathbb{R}^3$. It is then clear that $\Sigma^1 f$ with codimension 1 is the only first-order Thom singularity set which can occur. $\Sigma^1 f$ splits into $\Sigma^{1,0} f$ and $\Sigma^{1,1} f$ with codimensions 1,2 respectively, and in turn $\Sigma^{1,1} f$ splits into $\Sigma^{1,1,0} f$ and $\Sigma^{1,1,1} f$ with codimensions 2 and 3, respectively. No further further splittings are possible in $\mathbb{R}^3$ since the kth order Thom singularity set $\Sigma^{1,\ldots,1} f$ has codimension k, so it does not appear for $k \geq 4$.

EXAMPLE 3.30. Let us take the dovetail map $f : \mathbb{R}^3 \to \mathbb{R}^3$ given by $f(x,y,z) = (x,y,z^4 - xz - yz^2)$, whose Jacobian matrix is then

$$\begin{bmatrix} 1 & 0 & 0 \\ 0 & 1 & 0 \\ -z & -z^2 & 4z^3 - x - 2yz \end{bmatrix}.$$

Taking into account that the rank only drops when $\frac{\partial f_3}{\partial z} = 0$, it is easy to see that the possible Thom singularities sets $\Sigma^{1,\dots,1} f$ are given by the following equations:

$$\Sigma^1 f : \frac{\partial f_3}{\partial z} = 0$$

$$\Sigma^{1,1} f : \frac{\partial f_3}{\partial z} = 0 \quad \text{and} \quad \frac{\partial^2 f_3}{\partial z^2} = 0$$

$$\Sigma^{1,1,1} f : \frac{\partial f_3}{\partial z} = 0 \quad \text{and} \quad \frac{\partial^2 f_3}{\partial z^2} = 0 \quad \text{and} \quad \frac{\partial^3 f_3}{\partial z^3} = 0.$$

These Thom singularities are pictured in Figure 15: $\Sigma^1 f$ is the folded surface, $\Sigma^{1,1} f$ is the fold curve, and $\Sigma^{1,1,1} f$ is the origin.

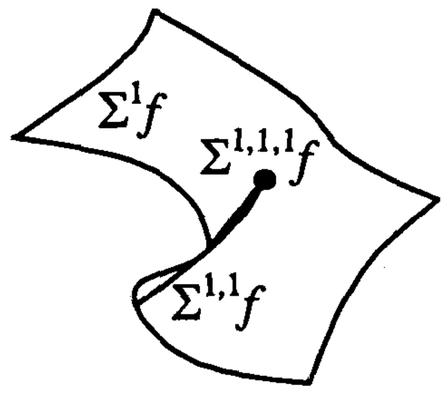

FIGURE 15. Thom-Boardman singularities of the dovetail map.

A Thom-Boardman stratification enjoys the property that the restriction of f to each stratum is a stable map, namely either a submersion or an immersion with normal crossings. Obviously, for geometric modelling purposes, we can ask how do the strata fit together, or, equivalently, how do the closures of the higher-dimensional strata intersect the lower-dimensional ones. Taking into account the transversality theorem, they are expected to be transverse, what it is the same as saying that they satisfy the local topological type condition.

8. Mathematical design issues: Thom-Boardman stratifications

Whitney theory and Thom-Boardman theory together with subanalytic geometry have been just discussed and assessed in the context of geometric modelling and design. Whitney stratifications are based on the idea of connectedness and containment of tangent 1-planes at two points of adjacent strata, while Thom-Boardman stratifications are based on the idea of transversality.

Both of them lead to topological type stratifications, and that is essential to develop a homological structure (cycles, boundaries and chains) on subanalytic sets in $\mathbb{R}^n$. This is fundamental for the design and implementation of a combinatorial boundary representation in $\mathbb{R}^n$.

However, Thom-Boardman stratifications take advantage because:

- They have been formulated for any kind of map, and consequently we can have stratifications for level sets and images. That is, Thom-Boardman stratifications are applicable to both implicit and parametric representations of point sets. Certainly, this is very encouraging for the geometry integration in geometric modelling.
- They are essentially computable stratifications, i.e. there is an matrix calculus algorithm to steadily stratify subanalytic sets.
- They provide a natural way to establish the geometric continuity conditions under contact equivalence, by just looking at the Boardman symbols. In fact, Boardman symbols are contact invariant.
- They generalise Whitney stratifications because we are able to detect higher-order singularities.

9. Summary

Topological stratifications have been introduced to understand the local properties of point sets. This study has led to the notions of topological singularities and partition of a point set into manifolds (i.e. point subsets without topological singularities). These topological stratifications have two major problems. First, they do not provide any algebraic machinery (i.e. a computational algorithm) to resolve singularities. Second, they cannot detect differential singularities such as cusps, inflection points, maxima, minima, etc.

These problems were resolved by mathematicians by using differential stratifications. One of the first attempts to solve the first problem was carried out by Whitney, who introduced the Whitney stratifications, say C^1 Whitney stratifications. Unfortunately, the rank-based algebraic machinery used to resolve singularities usually originates OrdT stratifications, not Whitney stratifications. Despite the existence of an algorithm to check whether a stratification is a Whitney stratification [**67**], no algorithm has ever been proposed —at the best knowledge of the author— to construct a Whitney stratification for a general algebraic variety in $\mathbb{R}^n$, using exclusively the Whitney machinery.

Besides, the ultimate objective of geometry integration is only possible if we are able to *uniformly* handle implicit representations (i.e. level sets such as algebraic varieties) and parametric representations (i.e. images such as Bézier curves and surfaces). Unfortunately, Whitney stratifications only works for level sets (or kernels) of maps. In fact, as seen before, self-intersections are not usually detectable for parametric varieties.

The importance of the Thom-Boardman stratifications stems from the fact they look adequate to solve these problems. In fact, they work quite well for level sets and images of maps, that is, for

implicit and parametric representations of point sets. This makes us to think of Thom-Boardman stratifications as a promising cornerstone for geometry-integrated systems, say integration of solid modelling, free-form modelling of curves and surfaces, and algebraic geometry systems. For example, we could imagine the construction of a smooth surface compound of implicit and parametric patches without loosing the control of C^r smoothness along their borders.

The geometry integration is reinforced by the existence of an algorithm to determine regular stratifications of implicit and parametric point sets: the Thom Stratification Algorithm. The existence of such an algorithm to automatically decompose an algebraic variety into a regular stratification makes possible in principle the graphical visualisation of dimensionally non-homogeneous varieties (e.g. the Cartan umbrella with-handle) through geometry machines (e.g. *Mathematica*). Note that current geometry machines are only able to plot dimensionally homogeneous subsets of varieties (e.g. Cartan umbrella without-handle) through their parametric counterparts. This may be not relevant for most 3D geometric modellers that basically use shape composition techniques, instead of shape decomposition techniques, to build up application-oriented geometric objects. But, it is certainly a significant step towards the integration of geometric modellers (e.g. ACIS modeller [**64**]) and algebraic geometry machines (e.g. Mathematica [**123**]).

CHAPTER 4

Σ-representation

With all these data you should be able to draw some just inference.

C. Doyle, The Sign of Four

To represent n-dimensional geometric objects has been an interesting research topic for years in geometric modelling, computational geometry, and computer graphics. Some representations for 3-dimensional objects were introduced mainly in 70's and 80's and then used in most commercial CAD systems. Only a few representations have been extended to higher dimensional objects in 90's. With some exceptions (e.g. the CSG representations of the Goffannon modeller (Brunel University) and Svlis modeller (Bath University)), these dimension-independent representations were limited to simplicial and cell complexes.

Our purpose now is to introduce a dimension-independent representation for regular stratified objects in $\mathbb{R}^n$, eventually with relatively non-compact strata. It is here called Σ-*representation.* (Σ is a Greek character for *s* and denotes here the first character of both words 'stratified shape by subcomplexes'.) The main idea is then to generalise previous representations.

1. Representation requirements

An object representation should fulfill a set of general requirements in order to be useful in practice. Let us enumerate them:

- *Separation of shape structures.* The representation core should be a stratified structure. It should be separated from other shape structures such as geometry structure, homotopy structure, Hadwiger structure, or else. This enables us to extend the Σ-kernel to other kinds of shape structures eventually required for some geometric application. This separation of the description of shape from stratified structure is similar to that one of conventional B-reps, with the difference that now we have more shape structures coupled to the stratified core. The stratified structure also enables the graphical interaction with geometric objects displayed on a computer screen. The designer is so able to pick up or select one or more

strata to carry out a particular design operation on an object. Besides, the lack of a stratified structure in surface models causes a number of difficulties in interfacing them to rapid prototyping processes [**104**]. Without this stratified structure, verifying the completeness and correctness of a geometric object which has been transferred from a CAD system to another is difficult because cracks and improper intersections most likely occur as a consequence of the inaccuracy of floating-point computations. Nevertheless, in healing-software industry practice, such a stratified structure has been revealed as a necessary condition (not a sufficient one) to prevent such inaccuracies.

- *Dimension independence.* It enables the convergence of multivariate viewpoints from solid and geometric modelling, computational geometry, computer aided design, computer graphics, and other geometry-based activities. This makes possible to tackle in a unified manner several geometric problems, such as solid modelling of articulated objects, simplicial approximation of curved manifolds, motion encoding and interference detection, free configuration space computation, and graphical representation of multidimensional data [**94**, p.56]. Besides, it facilitates the design of dimension-independent operators such as, for example, set-theoretic operators for both point sets and stratified sets and Euler operators, as detailed in the next chapter.

- *Order and incidence representation.* A series of computational geometry algorithms make usage of order information; for example, the optimal three-dimensional convex hull algorithm [**95**] and the divide-and-conquer approach for building the two-dimensional Voronoi diagram [**49**]. In solid modelling, order information is essential to traverse or navigate through an object. Examples of orderings are: (i) an ordering of vertices and edges incident to a face, (ii) an ordering of faces incident to an edge, (iii) an ordering of edges and faces incident at a vertex, etc.
- *Compactness representation* The boundaries and frontiers of an object and its strata must have a consistent representation. This is needed because objects encountered in many geometric-application domains have frontiers. But, there may be others with boundaries partially missing. For example, a crack of an object can be represented by a missing boundary. Therefore, the relative compactness of strata must be carefully represented.
- *Subobject representation.* Current geometry-based machines cannot cope with the representation and manipulation of subsets of geometric objects. This is essential for applications that require other shape structures other than geometry. Representation of subobjects allows to directly couple a new kind of shape structure (e.g. Hadwiger structure or form feature

structure) to the stratified structure. That is, it is important and necessary for applications which require stratum clustering. In fact, current geometric modellers cannot cope with the representation and manipulation of such stratum clusters. Such clusters are usually implemented and coupled to a geometric modeller as auxiliary data structures, and are dependent of a particular geometric application.

2. Representation state-of-art

In computational geometry, the most widely used representation of a stratified structure is the *incidence graph* [**32**], [**48**], [**100**]. It consists of *nodes* for cells and *arcs* connecting nodes if the corresponding cells are incident and differ by one in dimension. Although the incidence graph has came up in the context of polytopes, cell complexes and simplicial complexes, it can be easily extended to represent regular stratifications. Unfortunately, it does not provide any direct access to ordering information. Accessing ordering information requires graph searching algorithms or, alternatively, auxiliary data structures, e.g. linked lists [**21**, p.389].

In the case of 2-dimensional objects, ordering representation may be associated to edges. This kind of representation was called *edge-based representation.* The first edge-based representation is called *winged-edge representation*, and was proposed by Baumgart [**8**] in the context of computer vision research. Similar edge-based representations appeared in computational geometry [**26**], [**90**], and solid modelling [**6**], [**18**], [**31**], and [**74**]. For a detailed comparative analysis of edge-based representations, see the work of Weiler [**116**], [**117**], [**115**]. These edge-based representation schemes work quite well since an edge is incident at most two vertices and two faces.

Weiler extended a variant of an edge-based representation due to Mäntylä and Sulonnen [**74**], called *half-edge representation*, to inhomogeneous relatively compact objects in $\mathbb{R}^3$. It was coined as *radial-edge representation.* The key feature of the radial-edge representation is the cyclic ordering of oriented edges —they were called edge-uses— around an edge, each one representing the use of such an edge by a loop bordering one out of two oriented faces —they were called face-uses— of a face. However, radial-edge representation has no provision for correctly forming shells when a cut-vertex has to be traversed. This fact was noted by Gursoz and Prinz [**50**] and is due to the fact that the radial-edge representation lacks an ordering around a vertex. Gursoz and Prinz proposed an alternative vertex-based representation to remedy this deficiency of radial-edge representation. They called it *cusp-based representation.* These edge-based representations have been used in the design and implementation of commercial geometric kernels for objects of dimension up to 3.

In the late 80's, computational geometry researchers have tried to generalise representations to higher dimensions. A complete characterization of the adjacencies in a CW complex of an n-dimensional polyhedron was given by Lienhardt [**69**]. Lienhardt shows how to compute the number of boundaries, the Euler characteristic, orientability, and genus of 2-G-maps representing surfaces. Similar work, but using a different approach, was done independently by Brisson [**20**]. Brisson introduced a representation for a CW complex of a d-dimensional manifold (not necessarily without boundary), called *cell-tuple representation.* The Brisson's representation contains in a easily accessible form the cellular structure, ordering information, the topological dual of the cellular structure, and boundaries [**21**]. It consists of a set of cell-tuples which yields a dimension-ascending description or skeletal description of the cellular structure of a manifold. Each cell-tuple consists of a sequence of incident cells of increasing dimension, where any two consecutive cells differ in dimension by one. This means that a d-cell comes before a $(d+1)$-cell in a cell-tuple, what denotes that such a d-cell is in the boundary of a $(d+1)$-cell. Cell-tuples were implemented as arrays of pairs of indices such that the first index points to the constituent cells, and the second one is used by a switch operator to determine a particular adjacent cell-tuple. Brisson shows that cell-tuple representation is equivalent to the representations used by Guibas and Stolfi [**49**] in dimension 2 and Dobkin and Lazlo [**28**] in dimension 3, whose implementations were called the quad-edge data structure and the facet-edge data structure, respectively.

Similar efforts to extend representations of geometric objects to higher dimensions were attempted in solid and geometric modelling. Rossignac and O'Connor proposed *selective geometric complexes*, or SG complexes, as a new mathematical model in the attempt to extend the geometric coverage of solid and geometric modelling over curved point sets with internal structures and incomplete boundaries. However, SG complexes lack mathematical rigour for two major reasons. First, labelling is used to define the relative compactness of cells, attaching to each of them an attribute with one out two values, either *active* or *inactive.* It is clear that labelling is much more a representation issue than a mathematical issue. Second, removing now the adjective 'selective', we end up with geometric complexes which were vaguely defined as stratifications of real algebraic varieties. They wrote on the footer of p.156 [**99**], "The theory of stratifications provides a geometric decomposition of a variety, which is more than sufficient for our purposes". It remains to know which sort of stratification they had in mind. For example, what about the dimensional inequality condition to prevent the representation of non-analytic varieties such as the topologist curve. In fact, geometric complexes are equivalent to a kind of stratification which satisfies the local finiteness condition but not the frontier condition, because it misses the local topological stability or regularity required by

the dimension inequality condition. Consequently, there is not a one-to-one correspondence between a real algebraic variety and a geometric complex. Geometric complexes cover a bigger class of varieties, including non-analytic varieties. Obviously, this *a priori* undermines the representation of geometric complexes because the incidence scheme of Thom is not ensured. They also recognised that a general ordering representation is absent from the representation of SG complexes [**99**, p.161]. The ordering representation is confined to the ordering of cells bounding a cell.

The present work introduces the *subcomplex-tuple representation* for regular stratifications in $\mathbb{R}^n$ of subanalytic objects. It extends the cell-tuple representation of Brisson to a bigger class of geometric objects, say subanalytic sets, and to more general complexes than CW complexes, say Whitney stratifications and Thom-Boardman stratifications. It synthesises the topological structure, ordering information, topological dual, boundaries, and subcomplexes. The basic elements are tuples of subcomplexes. There is also a set of basic operators which act on the components of these tuples in order to easily access the information required.

3. Regular stratifications

In Chapter 3, we explained the mathematics behind subanalytic sets and their possible stratifications. We came to the conclusion that regular stratifications such as Whitney stratifications and Thom-Boardman stratifications match the topological stability of subanalytic sets. We also explained why Whitney conditions do not guarantee the frontier condition for multi-component strata. Therefore, a regular stratification can be defined as follows:

DEFINITION 4.1. A *regular stratification* $\mathbf{X} = (|X|, X)$ is a pair consisting of a set $X = \{M_i\}$ of connected strata and its underlying point set $|X|$, which satisfies the following conditions:

(i) (*Local finiteness*). Each point has a neighbourhood meeting only finitely many strata.

(ii) (*Boundary condition*). The boundary of each stratum is a union of lower-dimensional strata.

(iii) (*Whitney regularity*). For each pair M_i, M_j of strata and each $\mathbf{p} \in M_i \cap \mathrm{Fr}M_j$, M_j is regular over M_i at $\mathbf{p}$.

Here we are interested in *subanalytic stratifications*, i.e. stratifications of subanalytic sets into subanalytic manifolds or strata. In fact, one of the most important properties of subanalytic sets is that they are stratifiable, i.e. they can be partitioned into *manifolds* or *strata*.

3.1. Strata. Let us see some examples of connected strata in lower dimensional Euclidean spaces. In $\mathbb{R}^0$ we have only one 0-manifold, the $\mathbb{R}^0$ itself. In $\mathbb{R}^1$, there are only 0-manifolds (points) and

1-manifolds (open intervals), where $\mathbb{R}^1$ itself is the biggest 1-manifold. In $\mathbb{R}^2$ we have the previous manifolds, 1-manifolds with holes (e.g. the circle $x^2+y^2=1$ of radius 1), 2-manifolds without holes (e.g. the relative interior of a square), and 2-manifolds with holes (e.g. the relative interior of square with a closed disc removed from it). In $\mathbb{R}^3$ we have the manifolds described previously, and 3-manifolds. These 3-manifolds may possess holes and voids. For example, the interior $x^2+y^2+z^2<1$ of a solid sphere is a 3-manifold without any holes and voids, while the interior $(x^2+y^2+z^2+a^2-b^2)^2<4a^2(x^2+y^2)$ of a solid torus is a 3-manifold with a hole. Removing a closed solid 3-sphere from the interior of a 3-manifold results in a 3-manifold with a void. Note that in $\mathbb{R}^3$, 2-manifolds may also contain holes and voids; for example, the frontier $(x^2+y^2+z^2+a^2-b^2)^2=4a^2(x^2+y^2)$ of a closed solid torus in $\mathbb{R}^3$ is a 2-manifold with a hole and a void.

Nevertheless, *manifolds are not necessarily connected* i.e. they may contain several components. In fact, by definition, a d-manifold is a topological space *locally* homeomorphic to $\mathbb{R}^d$. (*Locally* means 'in the neighbourhood of any point'.) For example, two points in $\mathbb{R}^n$ may be considered as just one 0-manifold with two components (each component with a point); analogously, five non-intersecting open 3-spheres may form just one 3-manifold with five components (an open 3-sphere each), or two 3-manifolds (the first with $1 \leq k \leq 4$ open 3-spheres and the second with $5-k$ 3-spheres), or just five 3-manifolds with a 3-sphere each.

Manifolds or strata of the Σ-kernel are all *connected*, i.e. they all have only one component. There are two major reasons for that, namely:

- *Boundary condition breakdown.* The failure of regularity conditions of Whitney for multi-connected strata cause the breakdown the boundary condition. But, Middleditch *et al.* [**86**] showed that it is possible to define a stratification which satisfies the boundary condition with multi-component strata. This stratification, called *strong relative topological stratification*, is the stratification of the Djinn API [**2**].
- *Theoretical intractability.* They are hardly tractable theoretically. The problem is that multi-component strata place difficulties in satisfying the boundary (assembly) condition whenever the designer intends to attach or detach a new stratum to an object. This problem was noted by Middleditch *et al.* [**84**] in the design of Djinn API. They showed that to hold the boundary condition, a complex re-arrangement of stratum components is almost always necessary.

- *Computational intractability.* It is hard to computationally manage such re-arrangements of strata in order to hold the boundary condition.
- *Design intent overriding.* Such re-arrangements of strata are often undesirable because they may override the designer intent. The organization of strata is compelled to change, overriding the design intent.
- *Traversal algorithm unreliability.* Unless we guarantee the satisfaction of the boundary condition —using, for example, a strong relative topological stratification—, it is difficult to design reliable algorithms to traverse the data structure.

The solution proposed by the Σ is to consider the existence of two kinds of 'building blocks': superstrata (or multi-component strata) and strata (or connected strata). This guarantees that the *weak boundary condition* is always satisfied, but not necessarily the boundary condition.

3.2. (Weak) boundary condition. A stratification $\{M_i\}$ satisfies the *frontier condition* if for any two (multi-component) strata M_1 and M_2 such that $M_1 \cap \mathrm{Fr}(M_2) \neq \emptyset$ implies $M_1 \subset \mathrm{Fr}(M_2)$. Taking the components of strata instead the strata themselves, we say that a stratification satisfies the *weak frontier condition* if the family of the connected components of all M_i satisfies the frontier condition [**105**, p.4]. Analogously, we say that a stratification $\{M_i\}$ satisfies the *boundary condition* or the *weak boundary condition* by replacing Fr by Bd and frontier by boundary in the previous two definitions. The frontier condition (respectively, boundary condition) basically states that the frontier (respectively, boundary) of each stratum is a union of lower dimensional strata [**113**]. The weak frontier condition (respectively, weak boundary condition) basically says that the frontier (respectively, boundary) of each connected component of a stratum is a union of lower dimensional components of other strata.

It is clear that the frontier condition and the weak frontier condition are equivalent to the boundary condition and the weak boundary condition, respectively, because all strata M_i are part of the same stratified set. Besides, the frontier condition (respectively, boundary condition) implies the weak frontier condition (respectively, weak boundary condition), but not vice-versa. For convenience, from now on we only refer to the boundary condition and the weak boundary condition. The boundary condition is important primarily because it refers to 'part of the frontier' of a stratum *already* in the data structure of a geometric kernel. It has the advantage that the 'missing part of the frontier' do not need to be considered and represented in the data structure. This is particularly useful for the representation of 'non-manifold' stratified sets whose strata may have 'incomplete' frontiers.

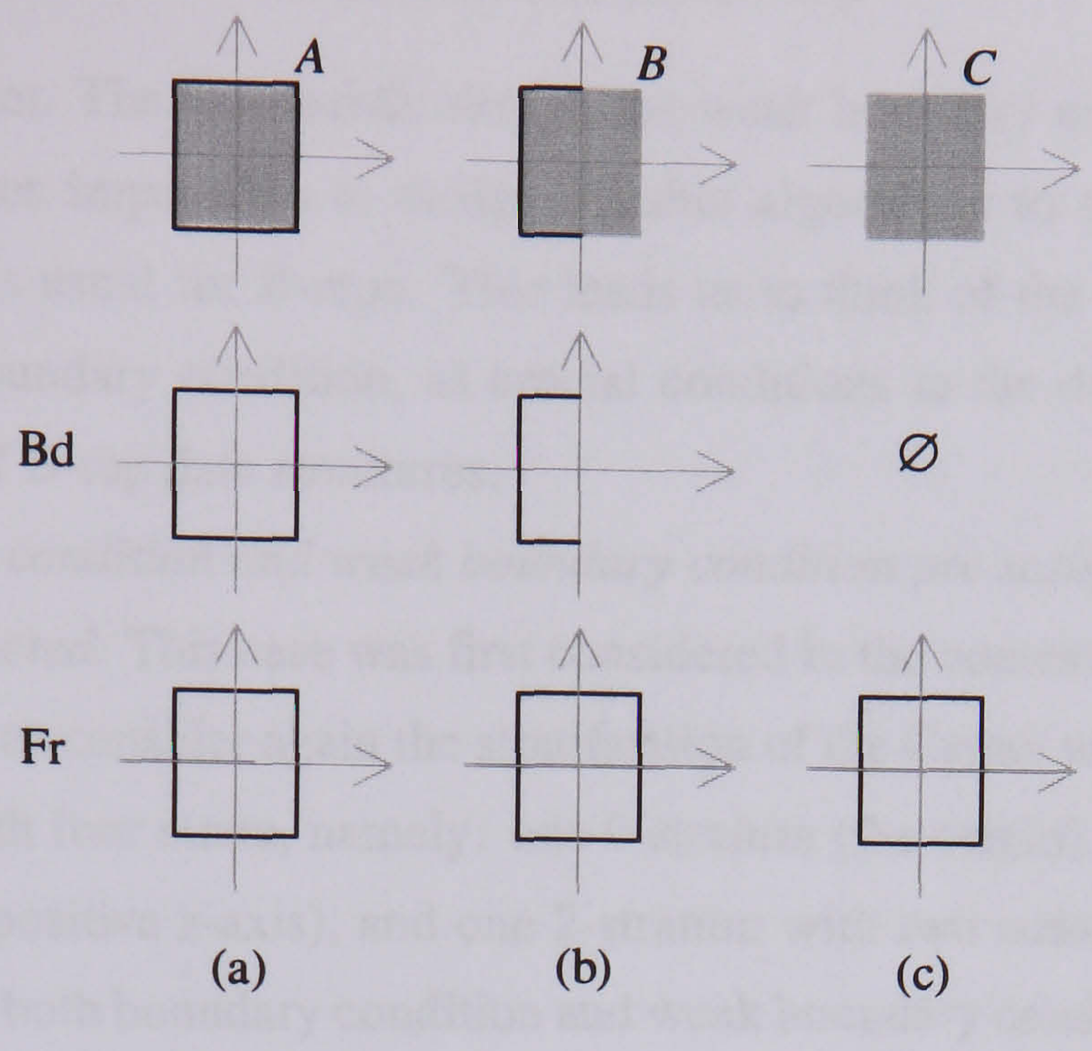

FIGURE 1

For example, the boundary and the frontier of the 2-stratum of the stratified sets B, C depicted in Figure 1 do not coincide, what means that only 'part of the frontier', here called boundary, of such a 2-stratum is represented by the stratified set. Thus, in a general setting, it is more adequate to use the (weak) boundary condition than the (weak) frontier condition.

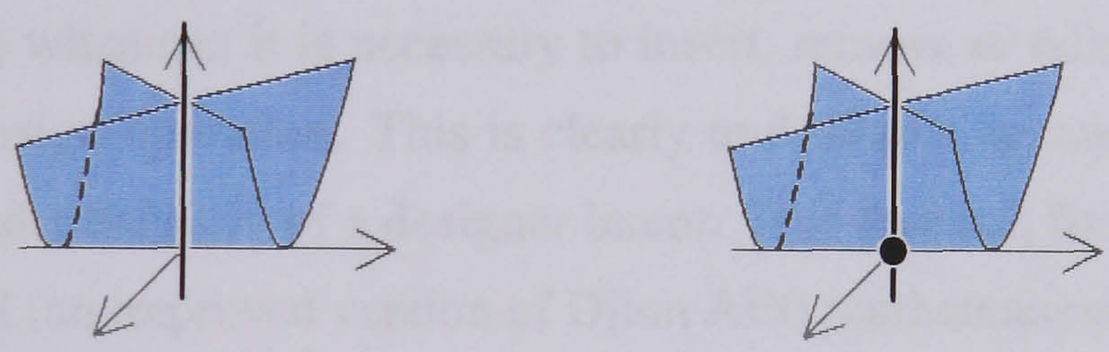

FIGURE 2

Let us consider different stratifications of the Cartan umbrella for which the boundary condition and weak boundary condition may or not be satisfied:

- *Neither boundary condition nor weak boundary condition are satisfied.* An example of this case is the Cartan umbrella stratified into two sheets and the z-axis as shown in Figure 2(a). In fact, this stratified set does not satisfy the weak boundary condition because the boundary of any of its 2-dimensional components (sheets) is the union of the origin and the positive z-axis, which are not strata in it. The origin and the positive z-axis are just subsets of the only 1-stratum (the z-axis) in this stratified set. Consequently, the boundary condition cannot

be satisfied either. The non-satisfaction of the weak boundary condition (and the boundary condition) makes impossible to design reliable algorithms to traverse or navigate in the data structure as usual for B-reps. This leads us to think of the weak boundary condition, and also the boundary condition, as crucial conditions in the design, implementation and manipulation of B-rep data structures.

- *Both boundary condition and weak boundary condition are satisfied, but strata are not necessarily connected.* This case was first considered in the context of the development of the Djinn API. Let us consider again the stratification of the Cartan umbrella illustrated in Figure 2(b) now with four strata, namely: one 0-stratum (the origin), two 1-strata (the negative z-axis and the positive z-axis), and one 2-stratum with two components (two sheets). It is easy to see that both boundary condition and weak boundary condition are satisfied. But, the fact that strata are not necessarily connected makes difficult to hold the boundary condition. For example, the user is not allowed to define the positive z-axis and negative z-axis as components of one 1-stratum because this violates the boundary condition; the negative z-axis is not in the boundary of the 2-stratum with two sheets. Imposing the boundary condition on a stratification with multi-connected strata has as a result an intricate re-arrangement of the strata and their components (with possible creation of new strata from components of the existing strata) whenever it is necessary to insert, remove or edit strata from the model via a geometric design operation. This is clearly undesirable because it changes the structure of an object independently of a designer intent. This fact led, for example, the designers of the Djinn* API (an improved version of Djinn API) mathematical kernel to option for strata with a single component [**84**].
- *Both boundary condition and weak boundary condition are satisfied, being all strata connected.* This is the case of most B-rep geometric kernels, including Gnomes (see [**107**] for this implementation of SGCs) and the Djinn* API. Here, the boundary condition and the weak boundary condition are equivalent because all strata are connected, i.e. each stratum possesses a single connected component. For example, let us consider again the stratified Cartan umbrella in Figure 2(b.5), now with five connected strata, namely: one 0-stratum (the origin), two 1-strata (the negative z-axis and the positive z-axis), and two 2-strata (two sheets). The boundary of any stratum of this stratified set is a union of strata in it; for example, the boundary of either 2-stratum (a sheet) is the union of a 0-stratum (the origin) and a 1-stratum (the positive z-axis).

- *Only the weak boundary condition is satisfied, with strata not necessarily connected.* This is the case of the Σ-geometric kernel. It does not impose any restrictions on the number of components of any stratum, except that it must be finite. Therefore, the user/designer is free to define and edit (i.e. insert, remove and update components of) any stratum, no matter the boundary relationships between strata. The important thing here is the boundary relationships between components. This kind of stratification that satisfies the weak boundary condition is called *weak topological stratification* or, shortly, WeakT stratification. A WeakT stratification does not depend on the number of components defined for each stratum. For example, any WeakT-stratification of the Cartan umbrella in Figure 2(b) contains two 2-dimensional components (the sheets), two 1-dimensional components (the positive and negative z-axes) and one 0-dimensional component (the origin). But, there are four possible WeakT stratifications of the Cartan umbrella. All them include a 0-stratum with the 0-component (the origin); the two open z-half-axes give rise to two 1-strata, one z-half-axis for each 1-stratum, or, alternatively, just one 1-stratum with both z-half-axes; the two sheet components may form one 2-stratum, or, alternatively, two 2-strata, one sheet component for each 2-stratum. Thus, the number of strata of a WeakT stratification is determined by the application or design intent. WeakT stratifications constitute an important step towards a universal and unified boundary representation for geometric modelling and design.

Despite, the (weak) boundary condition is something of an embarrassment in mathematical practice, since it is not preserved under natural operations on stratifications (e.g. taking intersections of stratifications in general position) [**41**, p.16-17], and therefore in the stratified Boolean operators, it must be hold in the design and implementation of any n-dimensional boundary representation, for the following reasons:

- It enables the identification of the frontier of each stratum in a geometric modelling system.
- To use the same algorithms of topological nagivation and interrogation, independently of the dimension of the strata in an geometric object.
- To use general homological algorithms to geometric shape reasoning, independently of the dimension of the strata in an geometric object.
- To facilitate computations of the physical properties of a geometric object, what requires that the frontier of each stratum is well-defined in the data structure.
- To keep the algebraic consistency via Euler-Poincaré formula if a combinatorial data structure is being used.

3.3. Local finiteness. To be useful in geometric modelling, a stratification must be at least locally finite. A stratification is said to be *locally finite* if each point of a stratum has a neighbourhood meeting only finitely many strata [**113**]. Fortunately, *local finiteness* is a property satisfied by subanalytic sets, i.e. they are locally described by a finite number of subsets. For example, an unbounded cone in $\mathbb{R}^3$ can be stratified into its apex and conical surface, since every point has a neighbourhood with just one 2-dimensional component. In contrast, if the conical surface is partitioned into an infinite number of lines through the apex, every point has a neighbourhood with an infinite number of 1-dimensional components; this stratification is not locally finite.

4. Covering stratified objects with subcomplexes

Let $\mathbf{X} = (|X|, X)$ be a stratified object or complex, $Y \subset X$ a subset of strata in X, and $|Y| = \bigcup\{M : M \in Y\}$ its union. Then, $\mathbf{Y} = (|Y|, Y)$ is called *subcomplex* of $\mathbf{X} = (|X|, X)$ if $\mathbf{Y} = (|Y|, Y)$ is also a stratified object or complex. Note that a complex, and thus also a subcomplex, may be an empty complex, a singleton complex, or any collection of disjoint strata which satisfy the regularity axioms. A complex or a subcomplex is not required to be relatively compact.

A series of consequences follow from the definition of subcomplex, namely:

- An arbitrary intersection of subcomplexes is also a subcomplex.
- An arbitrary union of subcomplexes is also a subcomplex.
- Every union of k-strata in X with $X^{k-1} = \{M : M \in X, \dim(M) \leq k-1\}$ forms a subcomplex.
- Every stratum lies in a locally finite subcomplex.
- Every locally finite subset of a complex is contained in a locally finite subcomplex.

Thus, alternatively, a complex $\mathbf{X} = (|X|, \mathcal{X})$ may be defined as a point set $|X|$ with a subcomplex decomposition $\mathcal{X}$. That is, a *subcomplex decomposition* of a complex is a *covering* of $\mathbf{X}$ into subcomplexes. Recall that there are basically two main ways to decompose a complex: partitions and coverings. So, a complex may be defined as a partition of strata, or, alternatively, as a covering of subcomplexes. In the latter case, the subcomplexes are not required to be disjoint. Nevertheless, either strata or subcomplexes must cover the whole complex, i.e. the union of the underlying point sets of either strata or subcomplexes is the whole point set $|X|$. Also, if $\mathcal{Y}$ is a subset of $\mathcal{X}$ such that $\bigcup\{Y_i : Y_i \in \mathcal{Y}\} = X$, then $\mathcal{Y}$ is called a *subcovering* of $\mathcal{X}$.

In addition to stratum decomposition and subcomplex decomposition, a complex can be also defined through a *filtration* or *skeletal decomposition* $X^0 \ldots \subseteq X^{k-1} \subseteq X^k$ by taking $X^k = X$, where $k = \dim X$, and defining $X^k = \bigcup\{M : M \in X, \dim(M) \leq k\}$ as the union of strata of dimension $\leq k$. X^k

is called the *k-skeleton* of X. That is, X^i is homeomorphic to a space obtained by attaching a number of i-strata to X^{i-1}. Doing so for any positive i, we obtain the containment sequence $X^0 \subseteq X^1 \subseteq \ldots \subseteq X^{k-1} \subseteq X^k = X$. Note that $X^i - X^{i-1}$ is homeomorphic to a locally finite disjoint union of relatively open i-strata, which are the i-strata of X.

5. The subcomplex-tuple representation

Let us then define the basic elements of the subcomplex-tuple structure. If $\mathbf{X} = (|X|, X)$ is a dimensional regular complex, a tuple $(\Sigma_0, \Sigma_1, \ldots, \Sigma_d)$ of subcomplexes from $\mathbf{X}$ such that $\Sigma_i \subseteq \mathbf{X}$ and $\Sigma_0 \subseteq \Sigma_1 \subseteq \ldots \subseteq \Sigma_d$ is called a *subcomplex-tuple*. This containment relation between subcomplexes defines a partial order. In fact, a subcomplex of dimension k cannot contain a subcomplex of dimension greater than k. Thus, each subcomplex is a subcomplex of another subcomplex, or the complex which represents the entire object. In the subcomplex-tuple representation, this is expressed by putting a subcomplex before another into a subcomplex-tuple. In case two subcomplexes intersect, an intersection subcomplex must be defined for them in order to keep the containment relation. In the subcomplex-tuple representation, this is expressed by putting the intersection subcomplex before its intersecting subcomplexes into their corresponding subcomplex tuples.

The simplest subcomplex consists of a single stratum. Every stratum forms a subcomplex. This is important for two major reasons, namely:

- *Integration of distinct coverings on the same object.* The stratum covering is the simplest covering. It corresponds to the idea of a complex as a collection of strata. All the stratified models include this sort of structure. However, not all are able to support simultaneous coverings of subcomplexes as required for many applications in design engineering (e.g. engineering drafting, set-theoretic operators, and form feature modelling). The first integrated model of coverings for engineering artefacts in $\mathbb{R}^3$ was proposed by Gomes and Teixeira [**46**] in the context of form feature modelling.
- *Integration of the boundary covering with any other covering.* The boundary covering provides an unique representation for a stratified subanalytic object in $\mathbb{R}^n$. This representation consists of stratum boundary-tuples, each component representing the boundary of a stratum. Thus, instead of cells or even strata, we have boundaries of strata in the representation. It generalises the cell-tuple representation of Brisson to the representation of inhomogeneous and non-compact objects in $\mathbb{R}^n$.

The key for integrating distinct coverings (including the boundary covering) is the definition of intersection subcomplexes. Whenever two or more subcomplexes intersect, they are overstratified in order to accommodate and share a new subcomplex. This new subcomplex is called *intersection subcomplex*. This avoids the verbosity of external clustering of strata for particular applications such as form-feature based modelling (e.g. [**11**]) and boolean operations (e.g. [**76**]).

EXAMPLE 4.1. Figure 3 shows a single subcomplex covering of an object which may be used for distinct purposes or applications. The complex X is covered by three subcomplexes A, B, and C. There are two intersection subcomplexes, namely $I = A \cap B$ and $J = B \cap C$. The subcomplexes A and B share the subcomplex I, while B and C share the subcomplex J. The subcomplex-tuples are then: (I,A,X), (I,B,X), (J,B,X), and (J,C,X). In geometric modelling, A, B, and C may represent geometric primitives combined through either appropriate set-theoretic operators or eventually other operators. In the context of form feature design, the subcomplexes A, B, C may be considered as stratified subobjects corresponding to convex protrusions, while X is a non-convex protrusion which a embodies a mechanical component or part. The designer may even amalgamate geometric primitives with form features that intersection subcomplexes prevent eventual compatibility problems between applications running on the top of Σ-kernel.

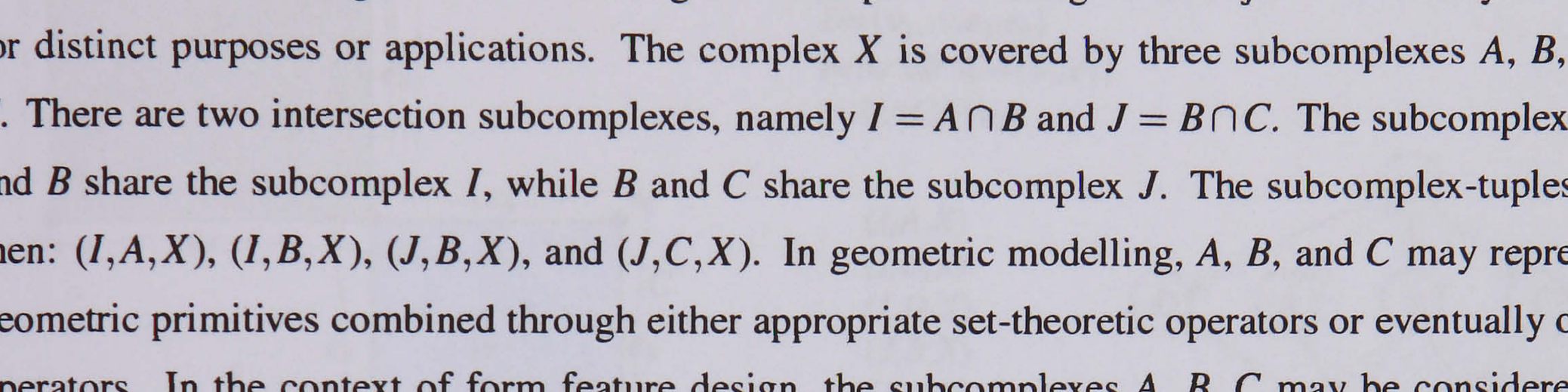

(a) Subcomplex covering (b) Subcomplex-tuples (c) Subcomplex-tuple graph

FIGURE 3. A subcomplex covering of a stratified object.

EXAMPLE 4.2. Let us look now at Figure 4 for a more detailed subcomplex covering of a stratified object X. Subcomplexes are pictured as dashed lines. The entire complex consists of seven vertices, nine edges and two faces, $X = \{v_1, v_2, v_3, v_4, v_5, v_6, v_7 e_1, e_2, e_3, e_4, e_5, e_6, e_7, e_8, e_9 f_1, f_2\}$. Four subcomplexes have been defined for X, namely: $A = \{v_1, e_2, e_3\}$, $B = \{v_1, v_2, v_3, e_1, e_3, e_4, f_1\}$, $C = \{v_2, v_4, v_5, v_6, e_5, e_6, e_7, e_8, f_2\}$, and $D = \{v_1, v_7, e_3, e_9\}$. Consequently, two intersection subcomplexes

have been generated, namely: $I = A \cap B \cap D = \{v_1, e_3\}$ and $J = B \cap C = \{v_2\}$. So, we have the following subcomplex-tuples: (I,A,X), (I,B,X), (I,D,X), (J,B,X), and (J,C,X).

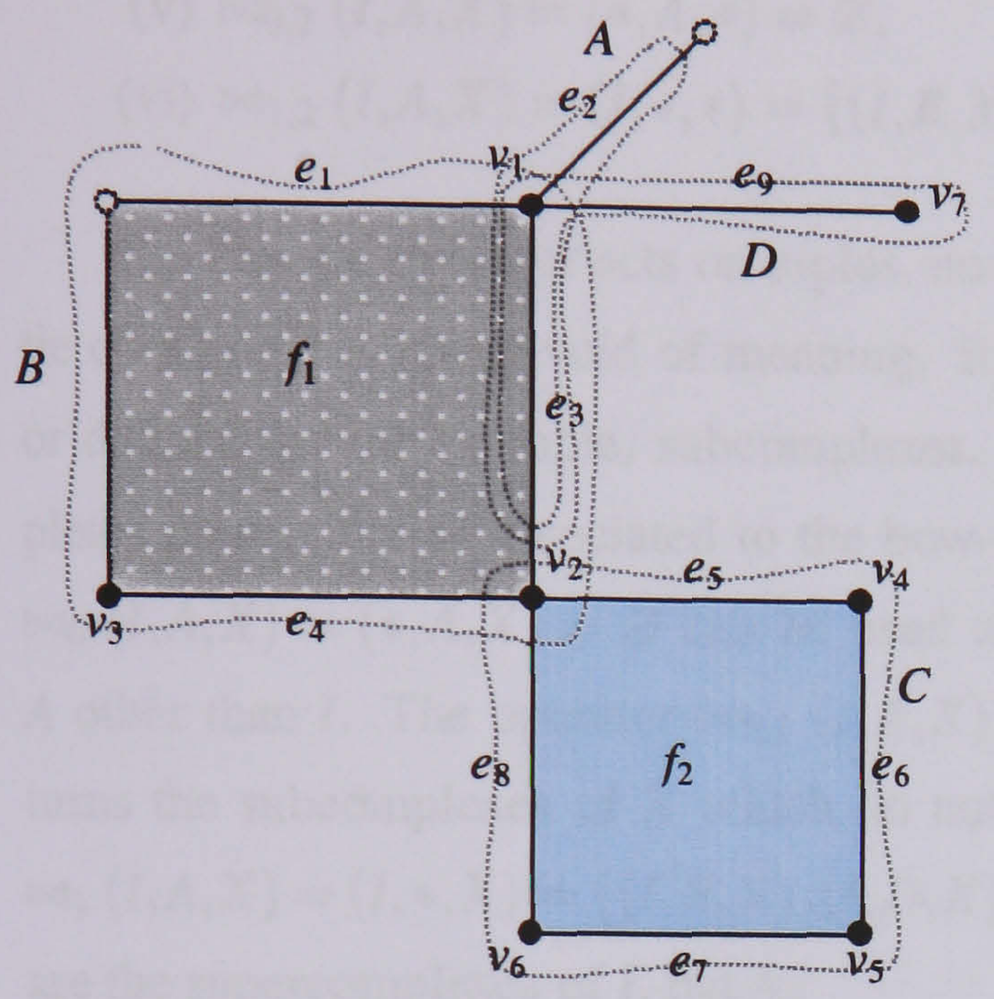

(a) Subcomplex covering

$X=\{v_1,v_2,v_3,v_4,v_5,v_6,v_7,e_1,e_2,e_3,e_4,e_5,e_6,e_7,e_8,e_9,f_1,f_2\}$
$A=\{v_1,e_2,e_3\}$
$B=\{v_1,v_2,v_3,e_1,e_3,e_4,f_1\}$
$C=\{v_2,v_4,v_5,v_6,e_5,e_6,e_7,e_8,f_2\}$
$D=\{v_1,v_7,e_3,e_9\}$
$I=A\cap B\cap D=\{v_1,e_3\}$
$J=B\cap C=\{v_2\}$

(I,A,X)
(I,B,X)
(I,D,X)
(J,B,X)
(J,C,X)

(b) Subcomplex-tuples

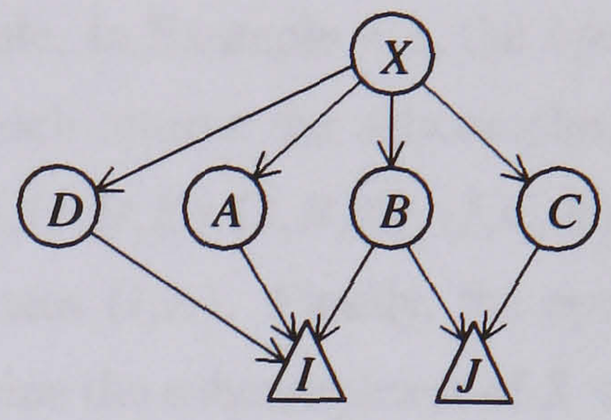

(c) Subcomplex-tuple graph

FIGURE 4. A subcomplex covering of another stratified object.

The set $T(\mathbf{X}) = \{(\Sigma_1, \ldots, \Sigma_k) : \Sigma_i \in \mathbf{X}, \Sigma_1 \subseteq \ldots \subseteq \Sigma_k\}$ is the set of all the subcomplex-tuples for $\mathbf{X}$, and $t_i = \Sigma_i$ is called the i-component of the subcomplex-tuple $t = (\Sigma_1, \ldots, \Sigma_k)$. The *resolution* of a subcomplex-tuple t is the number of its components, written $\mathrm{Res}\, t$. The largest resolution found in $T(\mathbf{X})$ is called resolution of $T(\mathbf{X})$, or resolution of the representation, and is denoted by $\mathrm{Res}\, T(\mathbf{X})$.

A set of basic operators handle the components of subcomplex-tuples. Its cardinality depends on the resolution $r = \mathrm{Res}\, T(\mathbf{X})$. For $0 \leq i \leq r-1$, define the operator $\bowtie_i : T(\mathbf{X}) \to T(\mathbf{X})$ by $\bowtie_i (t) = U(\mathbf{X})$, where $U(\mathbf{X})$ is a subset of tuples of $T(\mathbf{X})$ such that $t_i \neq u_i$ and $t_j = u_j$ for $i \neq j$, $\forall u \in U(\mathbf{X})$. That is, the operator $\bowtie_i (t)$ returns a subset of subcomplex-tuples which match t on all except the i-th component. It is called *bow-tie* operator. The bow-tie operator can be even generalised to multiple indices. In this case, the bow-tie operator $\bowtie_{i_1,\ldots,i_l} (t)$ returns a set of tuples matching t on all but the $i_1, \ldots, i_l$-th components, with $0 \leq i_1 < \ldots < i_l \leq r-1$.

EXAMPLE 4.3. Let us take the tuple (I,A,X) in Figure 4. Its resolution is 3. Thus, there are 6 possible bow-tie operators for (I,A,X):

(i) $\bowtie_0 (I,A,X) = (*,A,X) = \varnothing$,

(ii) $\bowtie_1 (I,A,X) = (I,*,X) = \{(I,B,X),(I,D,X)\}$,

(iii) $\bowtie_2 (I,A,X) = (I,A,*) = \varnothing$,

(iv) $\bowtie_{0,1} (I,A,X) = (*,*,X) = \{(I,B,X),(I,D,X),(J,B,X),(J,C,X)\}$,

(v) $\bowtie_{0,2} (I,A,X) = (*,A,*) = \varnothing$,

(vi) $\bowtie_{1,2} (I,A,X) = (I,*,*) = \{(I,B,X),(I,D,X)\}$,

The bow-tie operator acts on tuples, no matter the nature of their components. That is, the bow-tie operator is *a priori* void of meaning. It means something when its components are instantiated or defined as, for example, subcomplexes. The containment relation between subcomplexes completes the semantics associated to the bow-tie operator. For example, in Example 4.3, the operator $\bowtie_0 (I,A,X) = (*,A,X) = \varnothing$ can be used to define an operator which returns the subcomplexes of A other than I. The operator $\bowtie_{0,1} (I,A,X) = (*,*,X) = \{(I,B,X),(I,D,X),(J,B,X),(J,C,X)\}$ returns the subcomplexes of X which do not include the subcomplexes (I,A). Finally, the operator $\bowtie_1 (I,A,X) = (I,*,X) = \{(I,B,X),(I,D,X)\}$ can be used to determine the subcomplexes of X which are the supercomplexes of I, but A.

Note that the bow-tie operator only returns subcomplex-tuples of $T(\mathbf{X})$. It does not return subcomplex-subtuples. To obtain such subtuples of subcomplexes we need more two operators, called *left bow-tie* and *right bow-tie*.

DEFINITION 4.2. Let $\mathbf{Y} = (|Y|,Y,\mathcal{Y})$ be a subcomplex of the complex $\mathbf{X} = (|X|,X,\mathcal{X})$. Let $T(\mathbf{Y})$, $S(\mathbf{Y})$ be the set of all subcomplex-tuples of $\mathbf{Y}$ and the set of subcomplex-subtuples of $\mathbf{Y}$, respectively. The *left bow-tie* of $\mathbf{Y}$ in relation to s is the filter $\ltimes : \mathcal{X} \times S(\mathbf{X}) \to S(\mathbf{X})$ defined by

$$\ltimes(Y,s) = L(\mathbf{Y})$$

which returns the set $L(\mathbf{Y}) \subseteq S(\mathbf{Y})$ of subcomplex-subtuples of $\mathbf{Y}$ having

(i) s as a subtuple of every $l \in L(\mathbf{Y})$.

(ii) $l = (y_0,y_1,\ldots,y_{k-2})$ for some $y \in T(\mathbf{Y})$, with $\mathrm{Res}\, y = k$. (Hence, l does not include the higher-order component of y.)

Analogously, *right bow-tie* of $\mathbf{Y}$ in relation to s is the filter $\rtimes : \mathcal{X} \times S(\mathbf{X}) \to S(\mathbf{X})$ defined by

$$\rtimes(Y,s) = R(\mathbf{Y})$$

which returns a set $R(\mathbf{Y}) \subseteq S(\mathbf{X})$ of subcomplex-subtuples of $\mathbf{X}$ having

(i) s as a subtuple of every $r \in R(\mathbf{Y})$.

(ii) $r = (x_k, x_{k+1}, \ldots, x_{i-1})$ for some $x = (y_0, y_1, \ldots, y_{k-1}, x_k, x_{k+1}, \ldots, x_{i-1}) \in T(\mathbf{X})$, with $\mathrm{Res}\, x = i$, and $y = (y_0, y_1, \ldots, y_{k-1}) \in T(\mathbf{Y})$, with $\mathrm{Res}\, y = k$. (Hence, r does not include the subcomplex $\mathbf{Y}$ and its subcomplexes.)

Roughly speaking, the left bow-tie operator gives us the subcomplexes of a given subcomplex $\mathbf{Y}$, with the restriction that they must include a (possibly empty) collection of other subcomplexes, i.e. the subcomplexes of the tuple $\mathbf{s}$. The right bow-tie operator uses the same restriction, but it returns supercomplexes of $\mathbf{Y}$ instead.

EXAMPLE 4.4. In Figure 4, the operator $\rtimes(I, \varnothing) = \{(A,X), (B,X), (D,X)\}$ returns all the subtuples of supercomplexes of I, while the operator $\ltimes(X, (B)) = \{(I,B), (J,B)\}$ returns all the subtuples of subcomplexes of X containing the singular subtuple (B).

The key of the subcomplex-tuple representation is the existence of intersection subcomplexes. They prevent duplications of stratum clusters as two or more subcomplexes intersect. These duplications are usual in extensions or external data structures associated to current geometric modellers. Intersection subcomplexes make unnecessary the existence of such supplementary data structures. Intersection subcomplexes are also important to reinforce the containment relation between subcomplexes. In a way, this containment relation portrays a global incidence scheme for subcomplexes. For example, in Figure 4, we can say that the subcomplexes A, B, D are 'incident to' the intersection subcomplex I somehow. This global incidence relationship is a consequence of two facts:

- The existence of intersection subcomplexes in the representation.
- The transitivity property of the containment relation. $\mathbf{A} \subseteq \mathbf{B}$ and $\mathbf{B} \subseteq \mathbf{C}$ implies $\mathbf{A} \subseteq \mathbf{C}$.

The containment relation $\subseteq$ is transitive for subcomplexes. The question now is to know whether this containment relation guarantees an incidence scheme in the sense of Thom [**110**, p.245]. The answer is affirmative, since the subcomplexes in the incidence relation are well-defined. Recall that the *Thom incidence scheme*, associated to a regular stratum complex, states that every d-dimensional stratum M is associated with a finite number of strata of dimension less than d, say $M_1, \ldots, M_m$, the strata of the frontier of M. Equivalently, M_i is said to be *incident* to M, or $M_i < M$ $(0 \leq i \leq m)$. For regular stratified sets, this incidence scheme is ensured by the dimensional inequality condition underlying the frontier condition. The incidence relation $<$ is obviously transitive for strata: $M_i < M_j$ and $M_j < M_k$ implies $M_i < M_k$. Note that $<$ is a strict partial order of X. A sequence $M_0, \ldots, M_k$ of strata satisfying $M_0 < \ldots < M_k$ is called a *ascending chain* of strata. Brisson used this incidence scheme for cells of a 'subdivided' manifold [**21**]. Its representation, called *cell-tuple structure*, was

defined as a set of cell-tuples representing ascending chains of cells and an operator $switch_k$ to get all the information related to cellular structure, ordering, dual, and boundaries.

Our idea is to integrate the cell-tuple structure into the subcomplex-tuple structure, in order to get similar information through such a single operator. To successfully integrate these two representations we have to show that the subcomplex-tuple structure generalises the cell-tuple structure. In fact, this generalisation occurs at various levels:

- A stratum is a generalisation of a cell. Unlike a cell, a stratum may possess holes.
- A regular stratified set is a generalisation of a 'subdivided' manifold because it need not be homogeneous in dimension, neither relatively compact. That is, a regular stratified object may have dangling strata and its strata are not necessarily relatively compact. They may present incomplete boundaries.
- Redefinition of stratum-tuples as subcomplex-tuples. Stratum-tuples are generalisations of Brisson cell-tuples. They cannot work as subcomplex-tuples provided that a stratum in a regular stratification is never a subset of another stratum. The strata are disjoint. The disjointedness of strata prevent the satisfaction of the containment relation as usual in the subcomplex-tuple structure. To avoid the existence of two sorts of tuples for strata and subcomplexes, respectively, we have to redefine stratum-tuples as subcomplex-tuples. A redefined stratum-tuple is a subcomplex-tuple, in which each component refers to the boundary (or boundary subcomplex) of a stratum, instead the stratum itself. Note that the boundary condition of regular stratified objects implies a transitive relation on boundary or incident strata: $\frac{1}{2}(M_i) \subset \frac{1}{2}(M_j)$ and $\frac{1}{2}(M_j) \subset \frac{1}{2}(M_k)$ implies that $\frac{1}{2}(M_i) \subset \frac{1}{2}(M_k)$, where $\frac{1}{2}$ denotes the stratified boundary of some stratum. This partial order implies the incident relation $<$ on strata: $M_i < M_j$ and $M_j < M_k$ implies $M_i < M_k$, respectively. A sequence $M_0, \ldots, M_k$ of strata that satisfies $M_0 < \ldots < M_k$ is here called a *skeletal chain* of strata, and is the stratum counterpart for an ascending chain of cells. Thus, the incidence scheme is subsumed under the containment schema of boundaries of strata. This is possible because: (i) there is a one-to-one correspondence between a stratum and its boundary (and, consequently, its frontier); (ii) the dimensional inequality condition underlying the boundary (frontier) condition ensures an incidence scheme for regular stratified objects.
- Finally, the bow-tie operator $\bowtie$ generalises the operator *switch* of Brisson. It corresponds to the single-index bow-tie operator.

In short, the *subcomplex-tuple structure* for regular stratified objects $\mathbf{X}$ is the pair $(T(\mathbf{X}), \Omega)$, where $T(\mathbf{X})$ is the set of all subcomplex-tuples (including the boundary subcomplex-tuples for strata) for $\mathbf{X}$, and $\Omega = \{\bowtie_{i_1,\ldots,i_l}, \ltimes, \rtimes\}$ is the set of operators consisting of the the multi-index bow-tie $\bowtie_{i_1,\ldots,i_l}$, the left bow-tie $\ltimes$, and right bow-tie $\rtimes$. It generalises the cell-tuple structure as explained above.

6. Representation of incidence and order

Incidence and order are important requirements of any representation of geometric objects. They facilitate the computation of the physical properties of objects via integration, as required in many engineering applications (e.g. finite element analysis and modelling). For example, the circular order of strata in the boundary of face enables the integration of such a face in order to compute its area. In other words, ordering is the combinatorial counterpart for orientation. Note that only orientable objects are integrable. In addition, incidence and order are also essential to develop and write homology-based algorithms, which are used in the stepwise construction of objects and ongoing shape analysis and recognition.

In geometric modelling, the ordering information is explicitly represented by (topologically) oriented strata. These oriented strata have several names in the literature, namely: half-cells (Mäntylä and Sulonnen representation), cell-uses (Weiler representation), co-cells (ACIS modeller), etc. This explicit representation of order through oriented strata has as a result a highly verbose representation. For example, in the radial-edge representation of Weiler, one thousand faces incident to an edge requires two thousands of oriented faces, two thousand of loops for such oriented faces, and two thousand of oriented edges for just one edge.

Oriented representations are manageable in up to $\mathbb{R}^3$, but hardly they can be generalised to higher dimensions. Even so, this generalisation was done by Lienhardt [**69**]. In contrast, we have chosen to an orientable, but not oriented, representation of regular stratified objects. These orientable representations are sometimes called 'implicit' representations, while the oriented are called 'explicit' representations of 'subdivided' or stratified objects. Orientable representations have the advantage that they also support the representation of non-oriented stratified objects such as, for example, the stratified Möbius band.

The cell-tuple structure, proposed by Brisson [**21**], is a general representation of incidence and order, but only for stratified manifolds in $\mathbb{R}^n$. The cell-tuple structure is not valid for stratified 'non-manifold' objects. As Yamaguchi and Kimura noted in [**125**], despite the mathematical background that makes the cell-tuple structure of Brisson —as well as the n-G-maps of Lienhardt— rigorous,

its power to represent shapes is very limited. For example, they cannot handle strata with holes or dangling strata.

To be more accurate, we should say that if strata, instead cells, are used, we still get a valid representation for arbitrary regular stratified objects. Let us call it stratum-tuple structure. Unfortunately, only incidence is completely represented. The representation of order becomes uncertain or fuzzy. A fuzzy representation of order contradicts the Lemma 2 in [**21**, p.399]. It states that given a tuple $t \in T(\mathbf{X})$, there is a unique $u \in T(\mathbf{X})$ such that $u_i \neq t_i$ and $u_j = t_j$ for all $i \neq j$. Thus, the result of applying the single-index switch operator is always *only one* cell-tuple. Equivalently, an object has a deterministic order representation if and only if the single-index bow-tie operator always retrieves a single tuple. The uniqueness of the single-index bow-tie operator is ensured since the following conditions are satisfied:

- *Local manifoldness of an object.* The stratified object is locally a manifold, i.e. the neighbourhood of any of its points has the topological type of a manifold-with-boundary or a manifold-without boundary.
- *Local manifoldness of each stratum boundary.* The boundary of any stratum is also locally a manifold. Thus, a stratum is not allowed to have a boundary with dangling strata.
- *Non-intersecting boundaries of an object.* The boundary of a stratified object must not intersect with itself. This is a consequence of the local manifoldness condition.

6.1. Order representation in stratified manifolds-without-boundary. Let us see some examples of stratified manifolds-without-boundary.

EXAMPLE 4.5. (*Stratified tetrahedron*). Let us take the stratified tetrahedron depicted in Figure 5. It is a 'subdivided' manifold in the sense of Brisson. It satisfies his Lemma 2. So, we have a one-to-one correspondence between the cell-tuples of Brisson and our boundary subcomplex-tuples. They are equivalent for any stratified manifold. For example, $switch_0(v_1, e_1, f_1) = (v_2, e_1, f_1)$ and, analogously, $\bowtie_0 (\boxplus(v_1), \boxplus(e_1), \boxplus(f_1)) = (\boxplus(v_2), \boxplus(e_1), \boxplus(f_1))$. It is easy to see that Brisson Lemma is valid for every cell-tuple, and corresponding boundary subcomplex-tuple, of a tetrahedron.

EXAMPLE 4.6. (*Stratified cylinder*). The stratified cylinder pictured in Figure 6(a) is also a 'subdivided' manifold. Thus, the Brisson Lemma holds. The understratified cylinder (b) is not a 'subdivided' manifold because the cylindrical face is not a cell. Likewise, the understratified cylinder (c) is not a 'subdivided' manifold because both edges are not cells. This suggests that the Brisson Lemma may not be satisfied. In fact, f_3 in (b) possesses a hole through it as a result of its amalgamation with

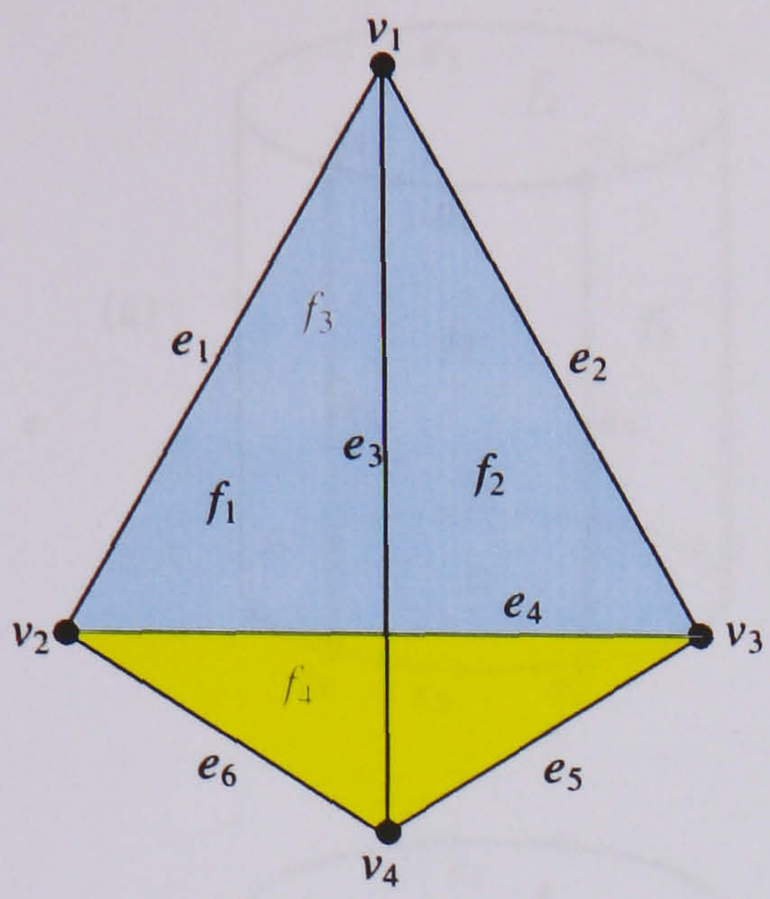

(a) Tetrahedron

$\sqsubset(v_1),\sqsubset(e_1),\sqsubset(f_3)$
$\sqsubset(v_1),\sqsubset(e_1),\sqsubset(f_1)$
$\sqsubset(v_1),\sqsubset(e_2),\sqsubset(f_2)$
$\sqsubset(v_1),\sqsubset(e_2),\sqsubset(f_3)$
$\sqsubset(v_1),\sqsubset(e_3),\sqsubset(f_1)$
$\sqsubset(v_1),\sqsubset(e_3),\sqsubset(f_2)$

$\sqsubset(v_2),\sqsubset(e_1),\sqsubset(f_3)$
$\sqsubset(v_2),\sqsubset(e_1),\sqsubset(f_1)$
$\sqsubset(v_2),\sqsubset(e_4),\sqsubset(f_3)$
$\sqsubset(v_2),\sqsubset(e_4),\sqsubset(f_4)$
$\sqsubset(v_2),\sqsubset(e_6),\sqsubset(f_1)$
$\sqsubset(v_2),\sqsubset(e_6),\sqsubset(f_4)$

$\sqsubset(v_3),\sqsubset(e_2),\sqsubset(f_2)$
$\sqsubset(v_3),\sqsubset(e_2),\sqsubset(f_3)$
$\sqsubset(v_3),\sqsubset(e_4),\sqsubset(f_3)$
$\sqsubset(v_3),\sqsubset(e_4),\sqsubset(f_4)$
$\sqsubset(v_3),\sqsubset(e_5),\sqsubset(f_2)$
$\sqsubset(v_3),\sqsubset(e_5),\sqsubset(f_4)$

$\sqsubset(v_4),\sqsubset(e_5),\sqsubset(f_2)$
$\sqsubset(v_4),\sqsubset(e_5),\sqsubset(f_4)$
$\sqsubset(v_4),\sqsubset(e_6),\sqsubset(f_1)$
$\sqsubset(v_4),\sqsubset(e_6),\sqsubset(f_4)$
$\sqsubset(v_4),\sqsubset(e_3),\sqsubset(f_1)$
$\sqsubset(v_4),\sqsubset(e_3),\sqsubset(f_2)$

(b) Subcomplex-tuples

FIGURE 5

e_1, e_4, and f_4. This causes the annihilation of eight tuples containing e_1 and e_4, namely: (v_1,e_1,f_3), (v_1,e_1,f_4), (v_2,e_1,f_3), (v_2,e_1,f_4), and (v_3,e_4,f_3), (v_3,e_4,f_4), (v_4,e_4,f_3), (v_4,e_4,f_4). Besides, the merge of f_3 with f_4 causes the replacement of f_4 by f_3 in the remaining tuples containing f_4. The circled f_3 in Figure 6(b) denote such replacements or mergings. This makes the family of stratum-tuples of (b) a subfamily of stratum-tuples of (a). It is easy to see that the Brisson Lemma holds seeing that the outcome of the single-index bow-tie operator for any tuple is a single tuple. Let us pay attention now to the cylinder (c) which result from cylinder (b) after merging its four vertices with vertices they bound. The amalgamation of e_2, v_3, and e_5 implies the deletion of all tuples including v_3 and the replacement of e_5 by e_2 in its container tuples. Analogously, the amalgamation of e_3, v_4, and e_6 causes the deletion of all tuples containing v_4 and the replacement of e_5 by e_2 in its container tuples. The resulting family of tuples consists of four tuples: (v_1,e_2,f_2), (v_1,e_2,f_3), (v_2,e_3,f_3), (v_2,e_3,f_1). Then, the amalgamation of v_1 with e_2 and v_2 with e_3 determines the elimination of v_1 and v_2 from the previous four tuples, as illustrated in Figure 6(c). Again, the resulting family of tuples of cylinder (c) is a subfamily of that one of cylinder (b), with the vertex components being now null. Consequently, the incidence of their higher strata must hold. It is easy to see that Brisson Lemma does not hold, but the cardinality of the single-index bowtie operator is *at most* a tuple singleton, or, equivalently, either a tuple singleton or an empty set.

This suggests that Brisson Lemma can be generalised to regular stratified manifold objects as follows.

(a)

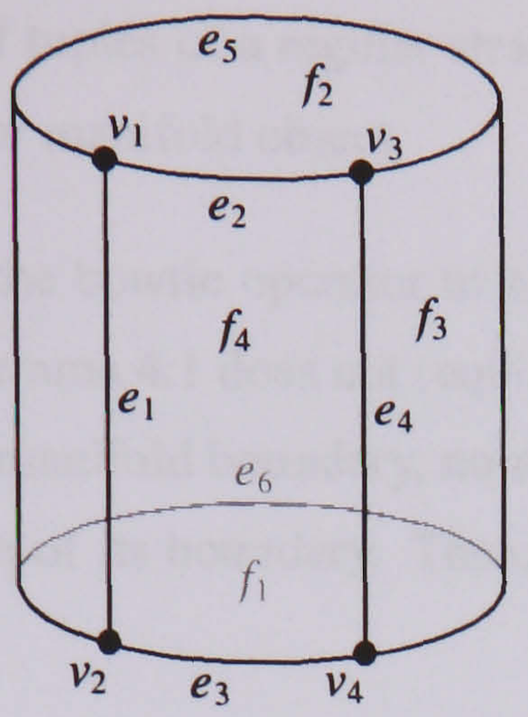

$\sqsubset(v_1),\sqsubset(e_2),\sqsubset(f_2)$ $\sqsubset(v_3),\sqsubset(e_2),\sqsubset(f_2)$
$\sqsubset(v_1),\sqsubset(e_2),\sqsubset(f_4)$ $\sqsubset(v_3),\sqsubset(e_2),\sqsubset(f_4)$
$\sqsubset(v_1),\sqsubset(e_1),\sqsubset(f_4)$ $\sqsubset(v_3),\sqsubset(e_4),\sqsubset(f_4)$
$\sqsubset(v_1),\sqsubset(e_1),\sqsubset(f_3)$ $\sqsubset(v_3),\sqsubset(e_4),\sqsubset(f_3)$
$\sqsubset(v_1),\sqsubset(e_5),\sqsubset(f_2)$ $\sqsubset(v_3),\sqsubset(e_5),\sqsubset(f_2)$
$\sqsubset(v_1),\sqsubset(e_5),\sqsubset(f_3)$ $\sqsubset(v_3),\sqsubset(e_5),\sqsubset(f_3)$
$\sqsubset(v_2),\sqsubset(e_1),\sqsubset(f_3)$ $\sqsubset(v_4),\sqsubset(e_4),\sqsubset(f_3)$
$\sqsubset(v_2),\sqsubset(e_1),\sqsubset(f_4)$ $\sqsubset(v_4),\sqsubset(e_4),\sqsubset(f_4)$
$\sqsubset(v_2),\sqsubset(e_3),\sqsubset(f_4)$ $\sqsubset(v_4),\sqsubset(e_3),\sqsubset(f_4)$
$\sqsubset(v_2),\sqsubset(e_3),\sqsubset(f_1)$ $\sqsubset(v_4),\sqsubset(e_3),\sqsubset(f_1)$
$\sqsubset(v_2),\sqsubset(e_6),\sqsubset(f_1)$ $\sqsubset(v_4),\sqsubset(e_6),\sqsubset(f_1)$
$\sqsubset(v_2),\sqsubset(e_6),\sqsubset(f_3)$ $\sqsubset(v_4),\sqsubset(e_6),\sqsubset(f_3)$

(b)

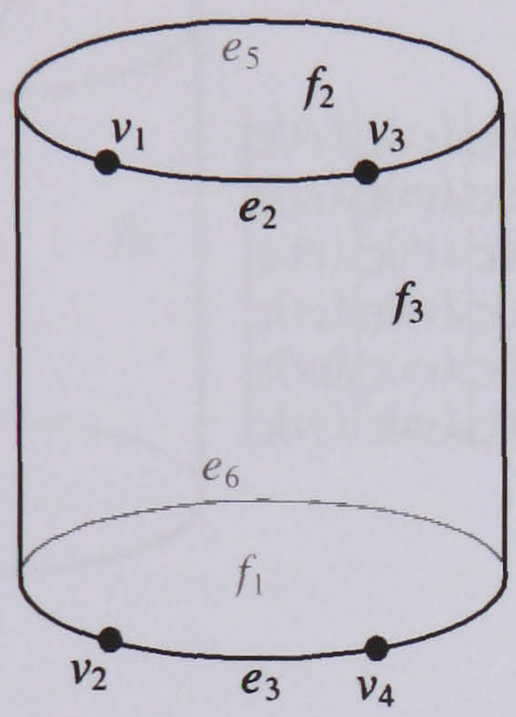

$\sqsubset(v_1),\sqsubset(e_2),\sqsubset(f_2)$ $\sqsubset(v_3),\sqsubset(e_2),\sqsubset(f_2)$
$\sqsubset(v_1),\sqsubset(e_2),\sqsubset(f_3)$ $\sqsubset(v_3),\sqsubset(e_2),\sqsubset(f_3)$
$\sqsubset(v_1),\sqsubset(e_5),\sqsubset(f_2)$ $\sqsubset(v_3),\sqsubset(e_5),\sqsubset(f_2)$
$\sqsubset(v_1),\sqsubset(e_5),\sqsubset(f_3)$ $\sqsubset(v_3),\sqsubset(e_5),\sqsubset(f_3)$
$\sqsubset(v_2),\sqsubset(e_3),\sqsubset(f_3)$ $\sqsubset(v_4),\sqsubset(e_3),\sqsubset(f_3)$
$\sqsubset(v_2),\sqsubset(e_3),\sqsubset(f_1)$ $\sqsubset(v_4),\sqsubset(e_3),\sqsubset(f_1)$
$\sqsubset(v_2),\sqsubset(e_6),\sqsubset(f_1)$ $\sqsubset(v_4),\sqsubset(e_6),\sqsubset(f_1)$
$\sqsubset(v_2),\sqsubset(e_6),\sqsubset(f_3)$ $\sqsubset(v_4),\sqsubset(e_6),\sqsubset(f_3)$

(c)

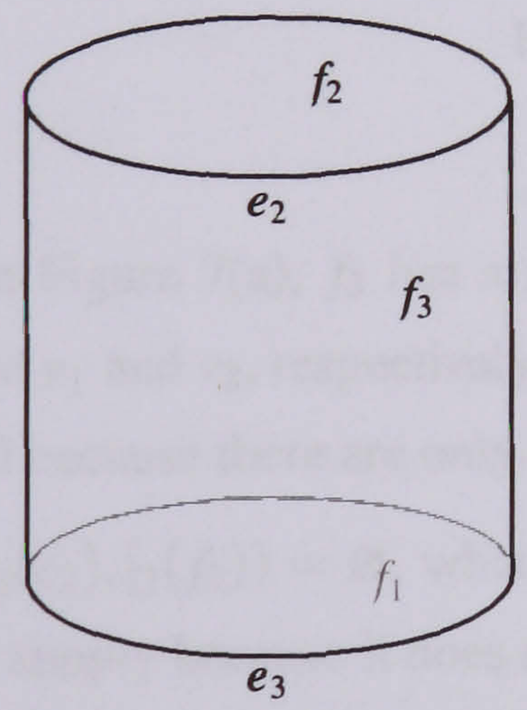

$\sqsubset(-),\ \sqsubset(e_2),\sqsubset(f_2)$
$\sqsubset(-),\ \sqsubset(e_2),\sqsubset(f_3)$
$\sqsubset(-),\ \sqsubset(e_3),\sqsubset(f_3)$
$\sqsubset(-),\ \sqsubset(e_3),\sqsubset(f_1)$

FIGURE 6

LEMMA 4.1. *Let* $\mathbf{X}$ *be a regular stratified manifold object. Let us assume that the boundary of each k-stratum has at most two* $(k-1)$*-strata incident at each one of its* $(k-2)$*strata. Given a tuple* $t \in T(\mathbf{X})$*, there is at maximum another tuple* $u \in T(\mathbf{X})$ *such that* $u_i \neq t_i$ *and* $u_j = t_j$ *for any* $i \neq j$.

PROOF. The set of tuples of a regular stratified manifold object is always a subset of its corresponding regular cellular manifold object. □

That is, applying the bowtie operator to any tuple, the result is always the empty set or a tuple singleton. Note that Lemma 4.1 does not require that the boundary of a k-stratum is manifold. But, if a k-stratum has a non-manifold boundary, no more than two $(k-1)$-strata are allowed to be incident at each $(k-2)$-stratum of its boundary. Thus, Lemma 4.1 admits some strata with self-intersecting boundaries.

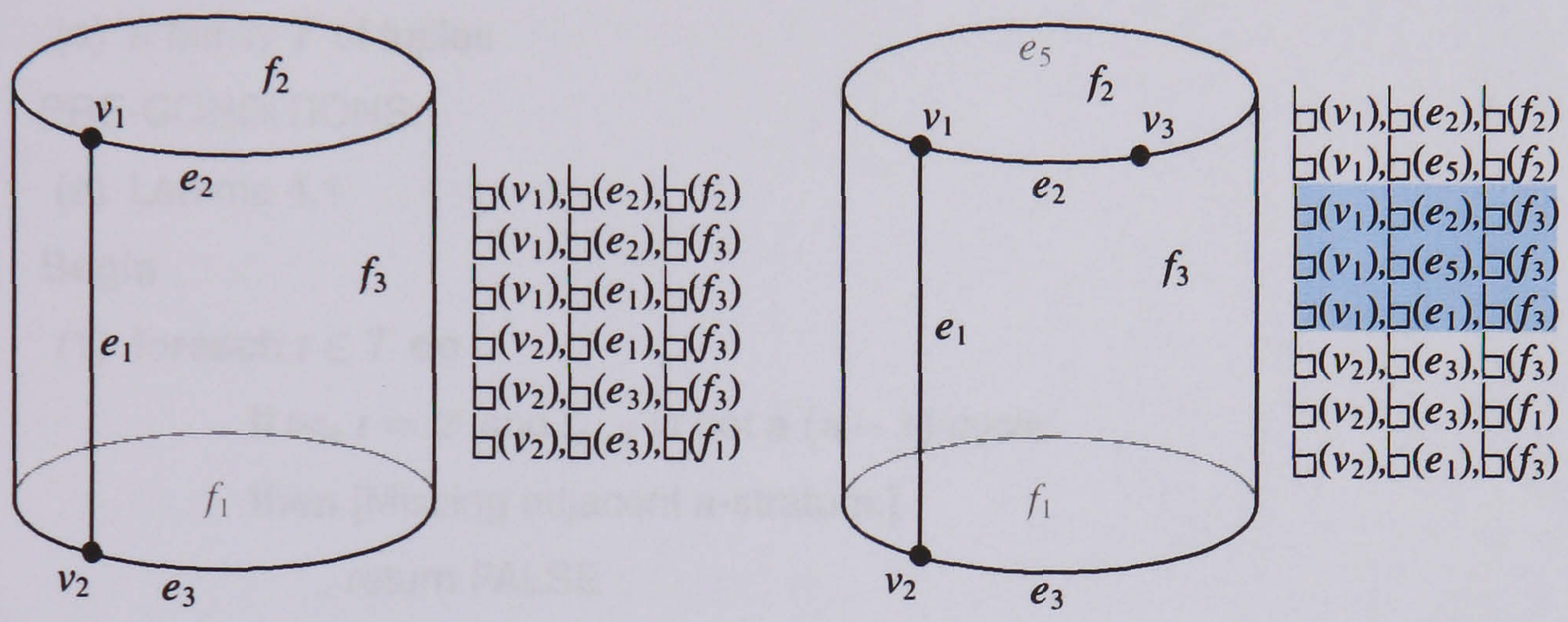

FIGURE 7

EXAMPLE 4.7. In Figure 7(a), f_3 has a non-manifold boundary consisting of two circles connected by an edge e_1 at v_1 and v_2, respectively. The cylinder (a) does not satisfy Brisson Lemma, but Lemma 4.1 is satisfied because there are only two edges incident at v_1 and v_2. In fact, we have:

(i) $\bowtie_0 (\sqcup(v_1),\sqcup(e_2),\sqcup(f_2)) = \varnothing$, what means that the it is not possible to go to next vertex bounding e_2 simply because it does not exist.

(ii) $\bowtie_1 (\sqcup(v_1),\sqcup(e_2),\sqcup(f_2)) = \varnothing$, i.e. there is no more edges bounding f_2 at v_1.

(iii) $\bowtie_2 (\sqcup(v_1),\sqcup(e_2),\sqcup(f_2)) = \{(\sqcup(v_1),\sqcup(e_2),\sqcup(f_3))\}$, i.e. there is a face f_3 adjacent to f_2, both of them incident to e_2.

Thus, the Brisson Lemma does not hold, but the cardinality of the tuple family that is returned by the single-index bow-tie operator is at most 1. A counterexample is the cylinder in Figure 7(b). In fact, the vertex v_1 has three incident edges bounding f_3. Despite the manifoldness of the cylinder, the set of tuples does not provide enough order information to determine the ordering of edges about v_1. This

order is said to be fuzzy. In fact, the result of the operator $\bowtie(\natural(v_1),\natural(e_1),\natural(f_3))$ is a set of three tuples, namely: $(\natural(v_1),\natural(e_4),\natural(f_3))$, $(\natural(v_1),\natural(e_5),\natural(f_3))$, and $(\natural(v_1),\natural(e_6),\natural(f_3))$.

The order fuzziness will be resolved in Section 6.3. The algorithm to check whether or not a family of tuples define a n-manifold-without-boundary is as follows:

ALGORITHM 4.1. (Manifold-without-boundary)

INPUT:

(a) a family T of tuples

PRE-CONDITIONS:

(a) Lemma 4.1

Begin

(1) **foreach** $t \in T$ **do**

if $\bowtie_n t = \varnothing$ and t_{n-1} is not a $(n-1)$-cycle

then [Missing adjacent n-stratum.]

return FALSE

else if card$(\bowtie_n t > 1)$

then [Non-manifoldness condition.]

return FALSE

(2) return TRUE.

End

Alternatively, we could emulate the homology-based algorithm given in [**3**, pp.173-175], though with a few changes to conform with Lemma 4.1, to determine whether or not a given family of tuples form a 2-cycle.

6.2. Order representation in stratified manifolds-with-boundary. The Brisson Lemma still holds for 'subdivided' manifolds-with-boundary. As noted in [**21**, p.416], in generalising the cell-tuple structure to the manifolds-with-boundary, the problem is that $switch_k(t)$ is not defined if t_{k-1} belongs to the stratified boundary of a manifold-with-boundary. The result of $switch_k(t)$ will be to go 'nowhere'. The immediate consequence is that the topological dual cannot be determined. Brisson proposed two equivalent approaches to overcome this problem. Intuitively, the solution consists of imagining the space 'outside' of the k-dimensional manifold-with-boundary as simply another k-cell that encloses it up on itself.

EXAMPLE 4.8. (*Stratified tetrahedral manifold-with-boundary*) Let us take again the tetrahedron in Figure 5, but now with the face f_2 removed. The resulting object is a tetrahedral stratified manifold-with-boundary. The cell-tuple representation requires that family of cell-tuples remain the same, but f_2 is labelled as 'absent', 'closing up', 'off', or anything else. In our representation, the number of tuples decreases because all tuples containing f_2 are removed. Thus, the outcome of the $\bowtie$ operator will be either a tuple singleton for any stratum in the interior of a stratified manifold or the empty set for any stratum in the boundary of a stratified manifold.

ALGORITHM 4.2. (Manifold-with-boundary)

INPUT:

(a) a family T of tuples

PRE-CONDITIONS:

(a) Lemma 4.1

Begin

(1) **foreach** $t \in T$ **do**

if res$(t) \neq n+1$ or card$(\bowtie_n t) > 1$

then [Non-manifoldness condition.]

return FALSE

else if $\bowtie_n t = \varnothing$ and t_{n-1} is not a $(n-1)$-cycle

then [Missing adjacent n-stratum.]

return FALSE

(2) return TRUE.

End

The identification of the boundary of an n-dimensional manifold-with-boundary is essential when an n-stratum is attached to it, transforming it into a manifold-without-boundary.

6.3. Order representation in stratified non-manifold objects. As seen above, the order becomes fuzzy if the boundary of any stratum is not locally a manifold or, more generally, if Lemma 4.1 is not satisfied. The order also becomes fuzzy for dimensionally inhomogeneous stratified objects, usually called 'non-manifold' objects in geometric modelling.

COUNTEREXAMPLE 4.1. (*Stratified non-manifold tetrahedral object*) Let us remove the face f_2 from the tetrahedron-with-boundary pictured in Figure 5. The result is a tetrahedron-with-boundary consisting of three faces f_1, f_3, and f_4, as depicted in Figure 8(a). Deleting now f_1 from it, we

(a)

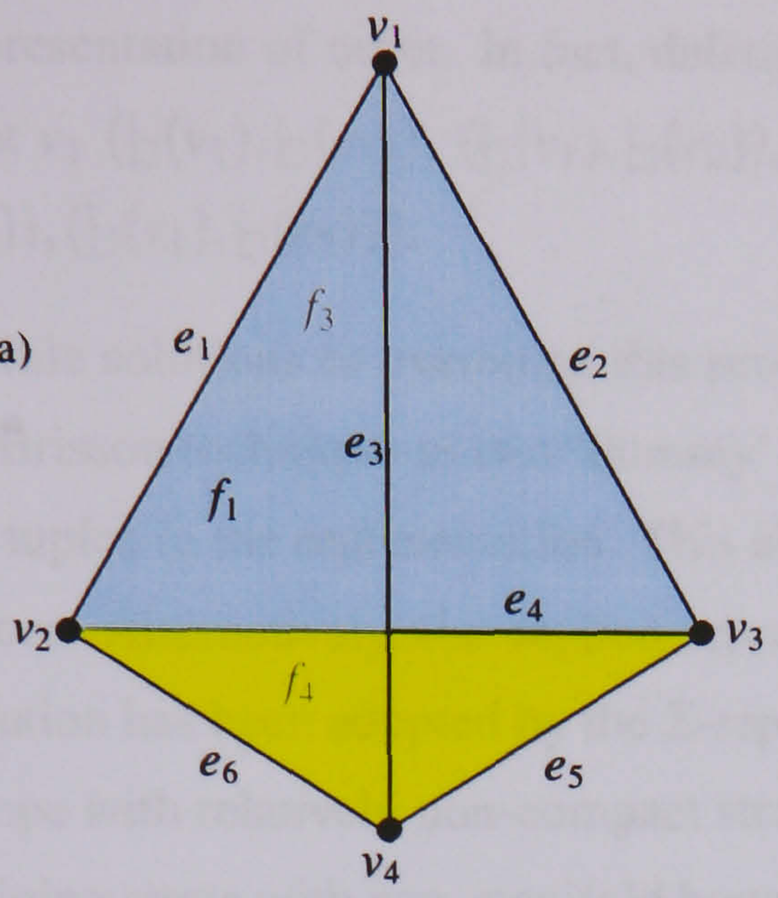

$\sqsubset(v_1),\sqsubset(e_1),\sqsubset(f_3)$
$\sqsubset(v_1),\sqsubset(e_1),\sqsubset(f_1)$

$\sqsubset(v_1),\sqsubset(e_2),\sqsubset(f_3)$
$\sqsubset(v_1),\sqsubset(e_3),\sqsubset(f_1)$

$\sqsubset(v_3),\sqsubset(e_2),\sqsubset(f_3)$
$\sqsubset(v_3),\sqsubset(e_4),\sqsubset(f_3)$
$\sqsubset(v_3),\sqsubset(e_4),\sqsubset(f_4)$

$\sqsubset(v_3),\sqsubset(e_5),\sqsubset(f_4)$

$\sqsubset(v_2),\sqsubset(e_1),\sqsubset(f_3)$
$\sqsubset(v_2),\sqsubset(e_1),\sqsubset(f_1)$
$\sqsubset(v_2),\sqsubset(e_4),\sqsubset(f_3)$
$\sqsubset(v_2),\sqsubset(e_4),\sqsubset(f_4)$
$\sqsubset(v_2),\sqsubset(e_6),\sqsubset(f_1)$
$\sqsubset(v_2),\sqsubset(e_6),\sqsubset(f_4)$

$\sqsubset(v_4),\sqsubset(e_5),\sqsubset(f_4)$
$\sqsubset(v_4),\sqsubset(e_6),\sqsubset(f_1)$
$\sqsubset(v_4),\sqsubset(e_6),\sqsubset(f_4)$
$\sqsubset(v_4),\sqsubset(e_3),\sqsubset(f_1)$

(b)

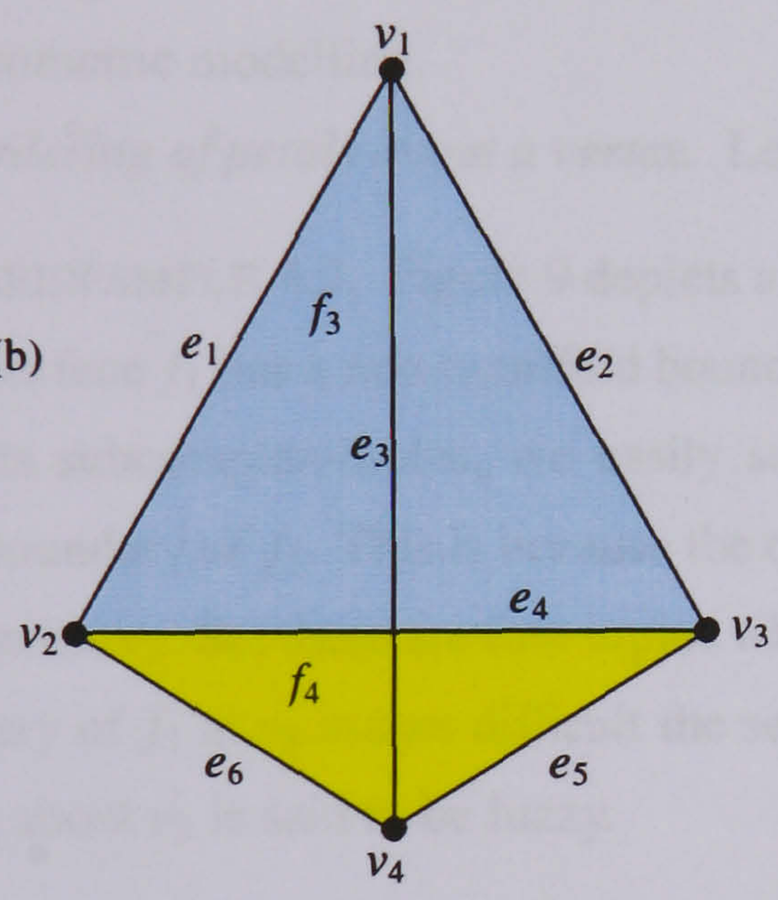

$\sqsubset(v_1),\sqsubset(e_1),\sqsubset(f_3)$
$\sqsubset(v_1),\sqsubset(e_1),\sqsubset(f_1)$

$\sqsubset(v_1),\sqsubset(e_2),\sqsubset(f_3)$
$\sqsubset(v_1),\sqsubset(e_3),$

$\sqsubset(v_3),\sqsubset(e_2),\sqsubset(f_3)$
$\sqsubset(v_3),\sqsubset(e_4),\sqsubset(f_3)$
$\sqsubset(v_3),\sqsubset(e_4),\sqsubset(f_4)$

$\sqsubset(v_3),\sqsubset(e_5),\sqsubset(f_4)$

$\sqsubset(v_2),\sqsubset(e_1),\sqsubset(f_3)$

$\sqsubset(v_2),\sqsubset(e_4),\sqsubset(f_3)$
$\sqsubset(v_2),\sqsubset(e_4),\sqsubset(f_4)$

$\sqsubset(v_2),\sqsubset(e_6),\sqsubset(f_4)$

$\sqsubset(v_4),\sqsubset(e_5),\sqsubset(f_4)$

$\sqsubset(v_4),\sqsubset(e_6),\sqsubset(f_4)$
$\sqsubset(v_4),\sqsubset(e_3),$

FIGURE 8

obtain a non-manifold tetrahedral object as drawn in Figure 8(b). The non-manifoldness is obvious because the resolution is not the same for all tuples. An immediate consequence is that the order round v_1 and v_4 is no longer completely represented. For example, three tuples are definable for v_1: $(\sqsubset(v_1),\sqsubset(e_1),\sqsubset(f_3))$, $(\sqsubset(v_1),\sqsubset(e_2),\sqsubset(f_3))$, and $(\sqsubset(v_1),\sqsubset(e_3))$. Thus, it is allowed to go from e_1 to e_2 through $\bowtie_0 (\sqsubset(v_1),\sqsubset(e_1),\sqsubset(f_3)) = (\sqsubset(v_1),\sqsubset(e_2),\sqsubset(f_3))$. However, the bow-tie operator does not enable to path the way from e_3 to e_2 or somewhere else since $\bowtie_0 (\sqsubset(v_1),\sqsubset(e_3)) = \varnothing$. However, from the homology point of view, there is an order for all those edges incident at v_1. Each one belongs two different 1-cycles. This is an unsolved problem in geometric modelling, since only 1-cycles bounding faces are usually represented. The situation gets worse as long as f_3 is removed from the non-manifold tetrahedral object. An incomplete representation of order at v_1 gives place

to a fuzzy representation of order. In fact, deleting f_3 gives rise to the appearance of three tuples of resolution 2 at v_1 $(\llcorner(v_1),\llcorner(e_1))$, $(\llcorner(v_1),\llcorner(e_2))$, $(\llcorner(v_1),\llcorner(e_3))$, and therefore $\bowtie_1$ $(\llcorner(v_1),\llcorner(e_1)) = \{(\llcorner(v_1),\llcorner(e_2)),(\llcorner(v_1),\llcorner(e_3))\}$.

Two possible solutions to overcome this problem come to mind immediately. The first consists of extending Brisson technique to two 'dummy' or missing faces by labelling them as 'off', though keeping their tuples in the representation. This allows one to traverse the 1-cycles which bounded f_1 and f_2 as before. Alternatively, the explicit representation of cycles in the tuples solve the problem. The latter solution has been adopted by the Σ-representation, and as explained further below it is also essential to cope with relatively non-compact strata and objects. Note that Brisson technique fails for objects containing strata with non-manifold boundaries, i.e. boundaries with spikes or dangling strata as usual in geometric modelling.

6.3.1. *Ordering of petals about a vertex.* Let us start with a face with non-manifold boundary.

COUNTEREXAMPLE 4.2. Figure 9 depicts a stratified manifold object and its boundary subcomplex-tuples. Its face f_1 has a non-manifold boundary, and therefore it does not satisfy the Lemma 4.1. Looking at its subcomplex-tuples, we easily see that they do not provide a deterministic way to traverse the boundary of f_1. This is because the object has four edges bounding f_1 which are incident at the same vertex v_3. So, there are four tuples whose first component is the vertex v_3. The bifurcation of the boundary of f_1 at v_3 makes difficult the selection of the next edge to go in the boundary of f_1. The ordering about v_3 is said to be fuzzy.

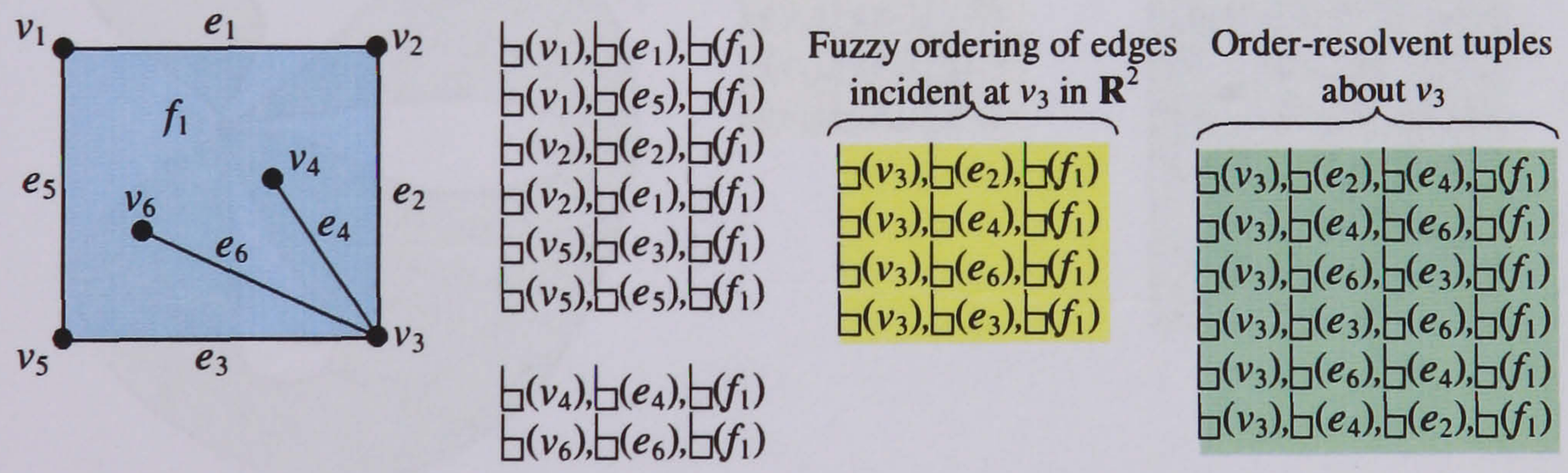

FIGURE 9

The existence of subcomplexes in the representation allows to solve this problem easily. For example, in Figure 9, $\llcorner(e_4)$ can be considered as an intersection subcomplex of two subcomplexes, $\llcorner(e_2)\cup\llcorner(e_4)$ and $\llcorner(e_4)\cup\llcorner(e_6)$, so that to go from e_2 to e_6, the edge e_4 must be visited first. So, for each pair of consecutive fuzzy tuples, two additional tuples are defined. For example, $(\llcorner(v_3),\llcorner(e_2),$

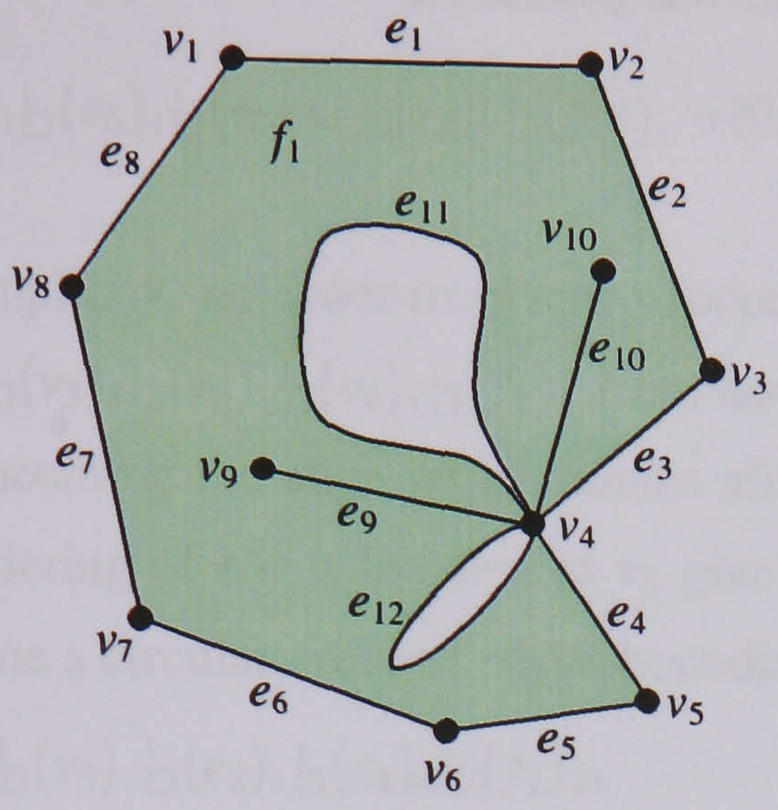

$\sqsubset(v_1),\sqsubset(e_1),\sqsubset(f_1)$
$\sqsubset(v_1),\sqsubset(e_8),\sqsubset(f_1)$
$\sqsubset(v_2),\sqsubset(e_1),\sqsubset(f_1)$
$\sqsubset(v_2),\sqsubset(e_2),\sqsubset(f_1)$
$\sqsubset(v_3),\sqsubset(e_2),\sqsubset(f_1)$
$\sqsubset(v_3),\sqsubset(e_3),\sqsubset(f_1)$
$\sqsubset(v_5),\sqsubset(e_4),\sqsubset(f_1)$
$\sqsubset(v_5),\sqsubset(e_5),\sqsubset(f_1)$
$\sqsubset(v_6),\sqsubset(e_5),\sqsubset(f_1)$
$\sqsubset(v_6),\sqsubset(e_6),\sqsubset(f_1)$
$\sqsubset(v_7),\sqsubset(e_6),\sqsubset(f_1)$
$\sqsubset(v_7),\sqsubset(e_7),\sqsubset(f_1)$
$\sqsubset(v_8),\sqsubset(e_7),\sqsubset(f_1)$
$\sqsubset(v_8),\sqsubset(e_8),\sqsubset(f_1)$

$\sqsubset(v_9),\sqsubset(e_9),\sqsubset(f_1)$
$\sqsubset(v_{10}),\sqsubset(e_{10}),\sqsubset(f_1)$

Fuzzy ordering of edges incident at v_4 in $\mathbf{R}^2$

$\sqsubset(v_4),\sqsubset(e_3),\sqsubset(f_1)$
$\sqsubset(v_4),\sqsubset(e_4),\sqsubset(f_1)$
$\sqsubset(v_4),\sqsubset(e_9),\sqsubset(f_1)$
$\sqsubset(v_4),\sqsubset(e_{10}),\sqsubset(f_1)$
$\sqsubset(v_4),\sqsubset(e_{11}),\sqsubset(f_1)$
$\sqsubset(v_4),\sqsubset(e_{12}),\sqsubset(f_1)$

Order-resolvent tuples about v_4

$\sqsubset(v_4),\sqsubset(e_3),\sqsubset(e_{10}),\sqsubset(f_1)$
$\sqsubset(v_4),\sqsubset(e_{10}),\sqsubset(e_{11}),\sqsubset(f_1)$
$\sqsubset(v_4),\sqsubset(e_{11}),\sqsubset(e_9),\sqsubset(f_1)$
$\sqsubset(v_4),\sqsubset(e_9),\sqsubset(e_{12}),\sqsubset(f_1)$
$\sqsubset(v_4),\sqsubset(e_{12}),\sqsubset(e_4),\sqsubset(f_1)$
$\sqsubset(v_4),\sqsubset(e_4),\sqsubset(e_{12}),\sqsubset(f_1)$
$\sqsubset(v_4),\sqsubset(e_{12}),\sqsubset(e_9),\sqsubset(f_1)$
$\sqsubset(v_4),\sqsubset(e_9),\sqsubset(e_{11}),\sqsubset(f_1)$
$\sqsubset(v_4),\sqsubset(e_{11}),\sqsubset(e_{10}),\sqsubset(f_1)$
$\sqsubset(v_4),\sqsubset(e_{10}),\sqsubset(e_3),\sqsubset(f_1)$

FIGURE 10

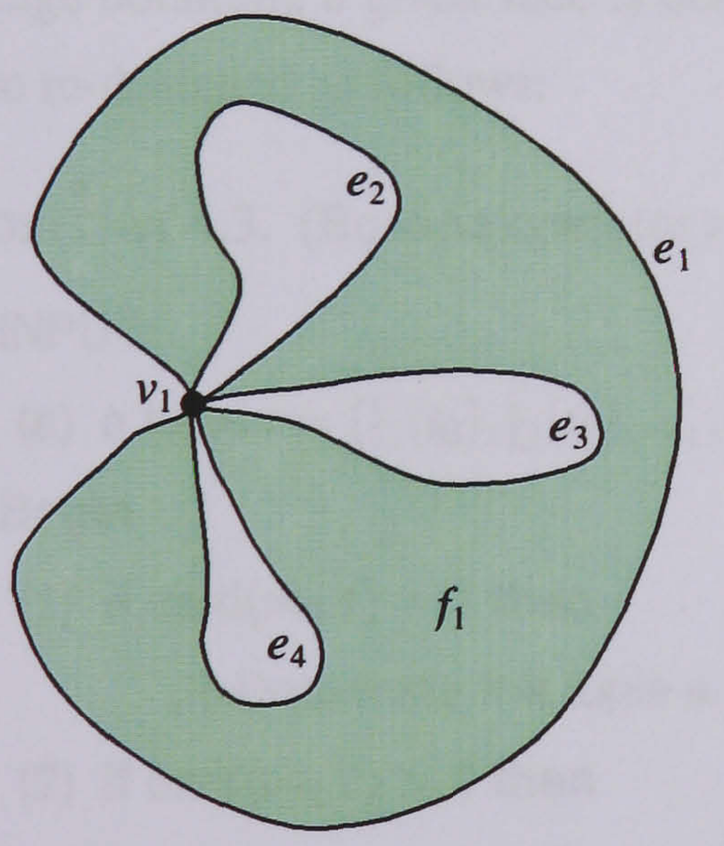

Fuzzy ordering of edges incident at v_1 in $\mathbf{R}^2$

$\sqsubset(v_1),\sqsubset(e_1),\sqsubset(f_1)$
$\sqsubset(v_1),\sqsubset(e_2),\sqsubset(f_1)$
$\sqsubset(v_1),\sqsubset(e_3),\sqsubset(f_1)$
$\sqsubset(v_1),\sqsubset(e_4),\sqsubset(f_1)$

Order-resolvent tuples about v_1

$\sqsubset(v_1),\sqsubset(e_1),\sqsubset(e_4),\sqsubset(f_1)$
$\sqsubset(v_1),\sqsubset(e_4),\sqsubset(e_3),\sqsubset(f_1)$
$\sqsubset(v_1),\sqsubset(e_3),\sqsubset(e_2),\sqsubset(f_1)$
$\sqsubset(v_1),\sqsubset(e_2),\sqsubset(e_1),\sqsubset(f_1)$
$\sqsubset(v_1),\sqsubset(e_1),\sqsubset(e_2),\sqsubset(f_1)$
$\sqsubset(v_1),\sqsubset(e_2),\sqsubset(e_3),\sqsubset(f_1)$
$\sqsubset(v_1),\sqsubset(e_3),\sqsubset(e_4),\sqsubset(f_1)$
$\sqsubset(v_1),\sqsubset(e_4),\sqsubset(e_1),\sqsubset(f_1)$

FIGURE 11

$\sqsubset(f_1)$) containing e_2 bounding f_1 at v_3 is given two supplementary tuples, $\langle\sqsubset(v_3),\sqsubset(e_2),\sqsubset(e_2)\cup\sqsubset(e_4),\sqsubset(f_1)\rangle$ and $\langle\sqsubset(v_3),\sqsubset(e_4),\sqsubset(e_4)\cup\sqsubset(e_2),\sqsubset(f_1)\rangle$, one for each orientation about v_3. Likewise, $(\sqsubset(v_3),\sqsubset(e_4),\sqsubset(f_1))$ is associated with two additional tuples, $\langle\sqsubset(v_3),\sqsubset(e_4),\sqsubset(e_4)\cup\sqsubset(e_6),\sqsubset(f_1)\rangle$

and $\langle \boxplus(v_3), \boxplus(e_6), \boxplus(e_6) \cup \boxplus(e_4), \boxplus(f_1) \rangle$, with the first tuple defining the opposite orientation to the second.

For simplicity, an order-resolvent subcomplex-tuple $\langle \boxplus(v_3), \boxplus(e_6), \boxplus(e_6) \cup \boxplus(e_4), \boxplus(f_1) \rangle$ is denoted as $\langle \boxplus(v_3), \boxplus(e_6), \boxplus(e_4), \boxplus(f_1) \rangle$ from now on. Such order-resolvent tuples have one more component concerning the edge which comes after another. Thus, in Figure 9, the four tuples defining a fuzzy ordering of edges incident at v_3 give rise to $2(n-1) = 2(4-1) = 6$ order-resolvent tuples which define a circular order of edges bounding f_1 at v_3, namely:

(i) $\langle \boxplus(v_3), \boxplus(e_2), \boxplus(e_4), \boxplus(f_1) \rangle$,
(ii) $\langle \boxplus(v_3), \boxplus(e_4), \boxplus(e_6), \boxplus(f_1) \rangle$,
(iii) $\langle \boxplus(v_3), \boxplus(e_6), \boxplus(e_3), \boxplus(f_1) \rangle$,
(iv) $\langle \boxplus(v_3), \boxplus(e_3), \boxplus(e_6), \boxplus(f_1) \rangle$,
(v) $\langle \boxplus(v_3), \boxplus(e_6), \boxplus(e_4), \boxplus(f_1) \rangle$,
(vi) $\langle \boxplus(v_3), \boxplus(e_4), \boxplus(e_2), \boxplus(f_1) \rangle$.

Now, the boundary of f_1 of the object depicted in Figure 9 can be traversed without fuzziness. For example, $\bowtie_1 (\boxplus(v_3), \boxplus(e_2), \boxplus(f_1)) = (\boxplus(v_3), \boxplus(e_4), \boxplus(f_1))$, with the intermediate tuple $\langle \boxplus(v_3), \boxplus(e_2), \boxplus(e_4), \boxplus(f_1) \rangle$ to be determined before returning $(\boxplus(v_3), \boxplus(e_4), \boxplus(f_1))$. Thus, accessing next edge bounding a given face is done as before, using the bow-tie operator $\bowtie_1$, but internally it has to be re-designed as follows:

ALGORITHM 4.3. (Bow-tie operator $\bowtie_1$)

INPUT:

(a) a tuple $t = (\boxplus(t_0), \boxplus(t_1), \ldots, \boxplus(t_i))$

Begin

(1) **if** card$(\bowtie_1 t) = 1$ **then**

(i) Determine the tuple $u = (\boxplus(t_0), \boxplus(t_*), \boxplus(t_2), \ldots, \boxplus(t_i))$ such that $\boxplus(t_*) \neq \boxplus(t_1)$.

(2) **if** card$(\bowtie_1 t) > 1$ **then**

Begin

(i) Determine the tuple $u = (\boxplus(t_0), \boxplus(t_1), \boxplus(t_*), \boxplus(t_2), \ldots, \boxplus(t_i))$ such that dim(t_1)=dim(t_*).

(ii) Remove t_1 from u.

End

(3) Return u.

End

Note that $\sqcup\!\!\!\!\sqcup(e_4)$ (respectively, $\sqcup\!\!\!\!\sqcup(e_6)$) of the object pictured in Figure 9 is the second component of two order-resolvent tuples, each one of which concerns an orientation of f_1. This is so because e_4 (respectively, e_6) is a spike edge bounding f_1. Thus, applying $\bowtie_1$ $(\sqcup\!\!\!\!\sqcup(v_3), \sqcup\!\!\!\!\sqcup(e_4), \sqcup\!\!\!\!\sqcup(f_1))$ yields two tuples: its predecessor (e.g. $(\sqcup\!\!\!\!\sqcup(v_3), \sqcup\!\!\!\!\sqcup(e_2), \sqcup\!\!\!\!\sqcup(f_1))$) and sucessor (e.g. $(\sqcup\!\!\!\!\sqcup(v_3), \sqcup\!\!\!\!\sqcup(e_4), \sqcup\!\!\!\!\sqcup(f_1))$). For obvious reasons, the predecessor is eliminated in the traversal of the frontier of f_1. Thus, the uniqueness of the bowtie operator holds. In case that the traversal of the frontier of f_1 starts with a spike edge, we have only to pick up either the predecessor or the sucessor. This determines an orientation in the traversal of the frontier of f_1. This is not described in the Algorithm 4.3 for simplicity.

Other examples are provided in Figure 10 and Figure 11. In these cases, we have some 1-cycles bounding f_1, instead a single 1-cycle for cells. Note that it does not matter whether a bounding edge is part of 1-cycle or a spike in the circular order about a vertex. However, the object depicted in Figure 11 has four fuzzy tuples for edges incident at v_1, but $2n = 2 \times 4 = 8$ order-resolvent tuples, i.e. more two tuples than expected. This is because e_1 is first and the last edge in the ordering about v_1.

Let us now generalise the circular ordering of edges bounding a face at a vertex to just the circular ordering of edges about a vertex. This generalisation only makes sense in $\mathbb{R}^2$. In fact, it is not possible to order dangling edges incident at a vertex in $\mathbb{R}^3$ or higher dimensional spaces, unless they belong to a 1-cycle or they bound a face. Then, it is possible to have a partial ordering of edges about a vertex for such a 1-cycle or face, respectively. But, this is what the bow-tie operator above does.

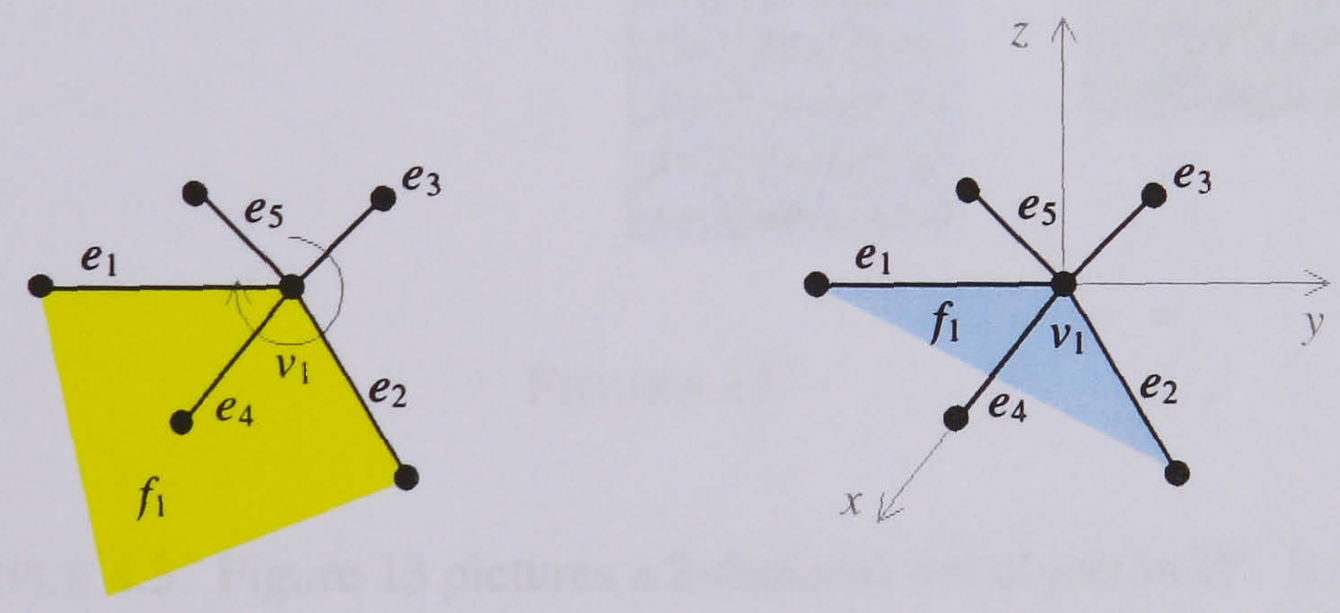

(a) Circular order about v in $\mathbf{R}^2$ (b) Fuzzy circular order about v in $\mathbf{R}^3$

FIGURE 12

Before proceeding, let us illustrate this by considering five edges incident at a vertex in $\mathbb{R}^3$, Figure 12(b). Assume that f_1 has not been attached to the object yet. There is no circular order round such a vertex, because intuitively it is not possible to say which edge comes first. This implies that attaching a face f_1 to edges e_1 and e_2 incident at v_1 is an easy task in $\mathbb{R}^3$ because there is not order. However, after attaching f_1 to e_1, v_1, e_2, the edges e_1 and e_2 are said to have a partial ordering at v_1

for f_1, Figure 12(b). That is, f_1 imposes an ordering to e_1 and e_2. But, in $\mathbb{R}^2$, we cannot do the same without including the intermediate edge e_4 in the boundary of the attached face, Figure 12(a).

Therefore, to generalise the ordering of edges round a vertex, we have to consider the case of a bouquet of 1-dimensional petals (edges) and 2-dimensional petals (with faces) incident at a vertex in $\mathbb{R}^2$. The ordering technique is similar to that one used for faces, in which the target face is $\mathbb{R}^2$ itself. Basically, it consists of ordering edges independently of possible faces in $\mathbb{R}^2$.

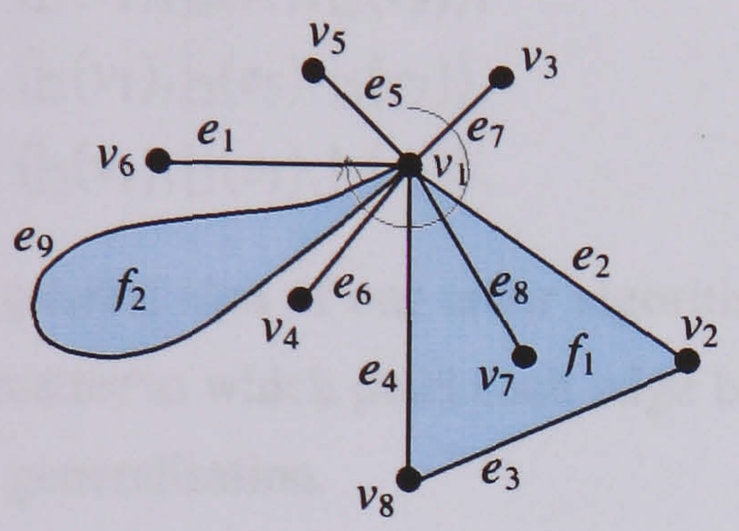

$\square(v_3),\square(e_7)$
$\square(v_5),\square(e_5)$
$\square(v_6),\square(e_1)$
$\square(v_4),\square(e_6)$
$\square(v_7),\square(e_8),\square(f_1)$
$\square(v_8),\square(e_4),\square(f_1)$
$\square(v_8),\square(e_3),\square(f_1)$
$\square(v_2),\square(e_3),\square(f_1)$
$\square(v_2),\square(e_2),\square(f_1)$

Fuzzy ordering of edges incident at v_1 in $\mathbf{R}^2$

$\square(v_1),\square(e_1)$
$\square(v_1),\square(e_5)$
$\square(v_1),\square(e_7)$
$\square(v_1),\square(e_6)$
$\square(v_1),\square(e_2),\square(f_1)$
$\square(v_1),\square(e_8),\square(f_1)$
$\square(v_1),\square(e_4),\square(f_1)$
$\square(v_1),\square(e_9),\square(f_2)$

Order-resolvent tuples of edges about v_1 in $\mathbf{R}^2$

$\square(v_1),\square(e_1),\square(e_5)$
$\square(v_1),\square(e_5),\square(e_7)$
$\square(v_1),\square(e_7),\square(e_2)$
$\square(v_1),\square(e_4),\square(e_6)$
$\square(v_1),\square(e_6),\square(e_9)$
$\square(v_1),\square(e_9),\square(e_1)$

Order-resolvent tuples of edges about v_1 for f_1

$\square(v_1),\square(e_2),\square(e_8),\square(f_1)$
$\square(v_1),\square(e_8),\square(e_4),\square(f_1)$
$\square(v_1),\square(e_4),\square(e_8),\square(f_1)$
$\square(v_1),\square(e_8),\square(e_2),\square(f_1)$

FIGURE 13

COUNTEREXAMPLE 4.3. Figure 13 pictures a 2-dimensional object in $\mathbb{R}^2$. It is clear that there is a circular order of edges about v_1. The partial orderings of edges bounding f_1 and f_2 are easily given by the previous bow-tie operator. But, the dangling edges at v_1 are fuzzy-ordered. The existence of dangling edges incident at v_1 makes difficult to determine a total ordering of edges round it. There are two reasons for that. First, the bow-tie operator does not allow to snap between tuples with distinct resolutions. Therefore, it is not allowed to go from an edge of an 1-dimensional petal to another edge of an 2-dimensional petal through a vertex. For example, it is not possible to go from e_6 to e_4 by using the bow-tie operator $\bowtie_1 (\boxplus(v_1),\boxplus(e_6))$ because their corresponding tuples have different resolutions. Second, the result of the single-index bow-tie operator is not unique. For example,

$\bowtie_1 (\natural(v_1), \natural(e_6)) = \{(\natural(v_1), \natural(e_1)), (\natural(v_1), \natural(e_5)), (\natural(v_1), \natural(e_7))\}$. The ordering round v_1 is then fuzzy. It is not possible to order edges round a vertex in $\mathbb{R}^2$ without additional fuzzy-resolvent tuples for dangling edges, namely:

(i) $\langle \natural(v_1), \natural(e_4), \natural(e_6) \rangle$,
(ii) $\langle \natural(v_1), \natural(e_6), \natural(e_9) \rangle$,
(iii) $\langle \natural(v_1), \natural(e_9), \natural(e_1) \rangle$,
(iv) $\langle \natural(v_1), \natural(e_1), \natural(e_5) \rangle$,
(v) $\langle \natural(v_1), \natural(e_5), \natural(e_7) \rangle$,
(vi) $\langle \natural(v_1), \natural(e_7), \natural(e_2) \rangle$.

The general idea of our order algorithm about a vertex is then to snap from an edge to the next one, no matter to which petal each edge belongs. Algorithm 4.3 has then to be modified to conform with our generalisation.

ALGORITHM 4.4. (Generalised bow-tie operator $\bowtie_1$)

INPUT:

(a) the set of tuples $T(\mathbf{X})$ of an object $\mathbf{X}$
(b) a tuple $t = (\natural(t_0), \natural(t_1), \ldots, \natural(t_i))$
(c) the ambient space $\mathbb{A}$

PRE-CONDITIONS:

(a) $t \in T(\mathbf{X})$ **or** $t \in S(\mathbf{X})$

Begin

(1) **if** Res$(t) = 1$ **then** [A vertex tuple] Return $\varnothing$.
(2) **if** Res$(t) = 2$ **then**
  if dim$\mathbb{A} = 2$ **then**
    (i) Determine $R(t)$ [The set of fuzzy-resolvent tuples for edges in $\mathbb{A}$.]
    (ii) Determine $S(t)$ [The set of fuzzy-resolvent subtuples for edges bounding faces in $\mathbb{A}$.]
    (iii) $S(t) = S(t) \cup R(t)$.
    (iv) Determine $s = (t_0, t_1, s_2) \in S(t)$ such that $t = (t_0, t_1)$.
    (v) Return s.
  else [dim$\mathbb{A} \geq 3$] Return $\varnothing$
(3) **if** Res$(t) \geq 3$ **then** [an edge bounding a face] Former operator applies.

End

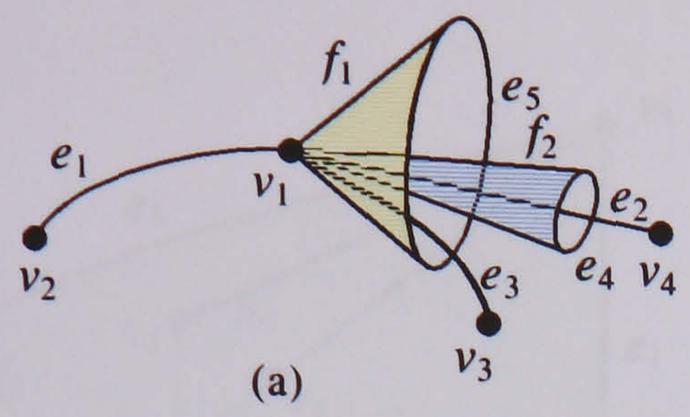

(a)

			Spherical ordering of petals about v_1 in $\mathbf{R}^3$
$\sqcup(v_2),\sqcup(e_1)$	$\sqcup(v_1),\sqcup(e_1)$	$\sqcup(v_1),\sqcup(e_1),\sqcup(P_1)$	$(P_1,-)$
$\sqcup(v_3),\sqcup(e_3)$	$\sqcup(v_1),\sqcup(e_2)$	$\sqcup(v_1),\sqcup(e_2),\sqcup(P_2)$	(P_2,P_5)
$\sqcup(v_4),\sqcup(e_2)$	$\sqcup(v_1),\sqcup(e_3)$	$\sqcup(v_1),\sqcup(e_3),\sqcup(P_3)$	(P_3,P_4)
$\sqcup(-),\ \sqcup(e_4),\sqcup(f_2)$	$\sqcup(v_1),\sqcup(f_1)$	$\sqcup(v_1),\sqcup(f_1),\sqcup(P_4)$	$(P_4,-)$
$\sqcup(-),\ \sqcup(e_5),\sqcup(f_1)$	$\sqcup(v_1),\sqcup(f_2)$	$\sqcup(v_1),\sqcup(f_2),\sqcup(P_5)$	(P_5,P_4)

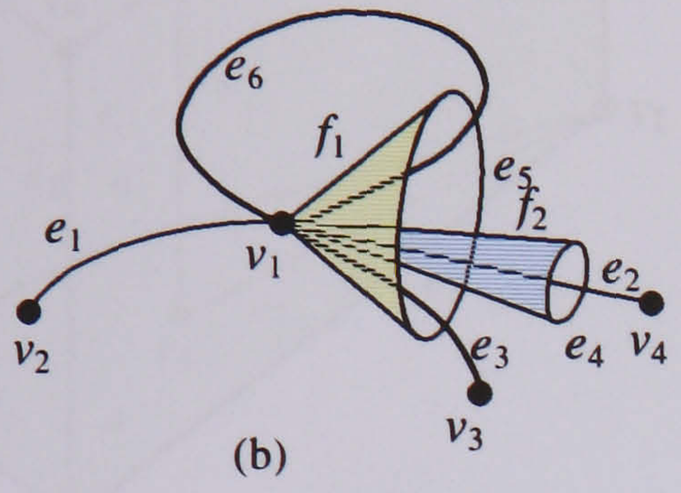

(b)

			Spherical ordering of petals about v_1 in $\mathbf{R}^3$
$\sqcup(v_2),\sqcup(e_1)$	$\sqcup(v_1),\sqcup(e_1)$	$\sqcup(v_1),\sqcup(e_1),\sqcup(P_1)$	$(P_1,-)$
$\sqcup(v_3),\sqcup(e_3)$	$\sqcup(v_1),\sqcup(e_2)$	$\sqcup(v_1),\sqcup(e_2),\sqcup(P_2)$	(P_2,P_5)
$\sqcup(v_4),\sqcup(e_2)$	$\sqcup(v_1),\sqcup(e_3)$	$\sqcup(v_1),\sqcup(e_3),\sqcup(P_3)$	(P_3,P_4)
$\sqcup(-),\ \sqcup(e_4),\sqcup(f_2)$	$\sqcup(v_1),\sqcup(f_1)$	$\sqcup(v_1),\sqcup(f_1),\sqcup(P_4)$	$(P_4,-)$
$\sqcup(-),\ \sqcup(e_5),\sqcup(f_1)$	$\sqcup(v_1),\sqcup(f_2)$	$\sqcup(v_1),\sqcup(f_2),\sqcup(P_5)$	(P_5,P_4)
	$\sqcup(v_1),\sqcup(e_6)$	$\sqcup(v_1),\sqcup(e_6),\sqcup(P_6)$	$(P_6,-)$
			(P_6,P_4)

FIGURE 14

Attaching strata in higher dimensional spaces seems to be easier because there are less ordering constraints to satisfy. However, the variety of shapes is larger in higher-dimensional spaces, what means that more new ordering configurations are possible. Figure 14 shows two objects with distinct ordering configurations at a vertex. Gursoz and Prinz [**50**] and Yamaguchi and Kimura [**125**] extended the Weiler technique to define a circular ordering about a vertex, using explicitly oriented cells in $\mathbb{R}^3$. However, their technique is only applicable to vertices whose ordering configurations are similar to that one depicted in Figure 14(a). Their methods only work if there is a clear hierarchy of petals round a vertex. A petal cannot be a subpetal at the same vertex, as it is the case of the petal P_6 containing e_6 at v_1, Figure 14(b). This petal at v_1 is also a subpetal of the petal P_4 containing the face f_1. Thus, there is not any circular order of edges incident at a vertex in $\mathbb{R}^3$. What exists is a partial circular ordering for each petal, and a spherical ordering about a vertex based on the containment relationship of petals. This containment relationship is derived from the partition of a small neighbourhood of a vertex into sectors or regions. For example, in Figure 14(a) the face f_1 subdivides a small neighbourhood of v_1 into two sectors.

6.3.2. *Ordering of sheets of a book about an edge.* Let us consider now the circular ordering round an edge. In $\mathbb{R}^2$, no non-manifold situation is possible because two faces at maximum are adjacent to an edge. In $\mathbb{R}^3$, several faces may be incident to an edge, what is a non-manifold situation. It is the counterpart of edges incident at a vertex in $\mathbb{R}^2$.

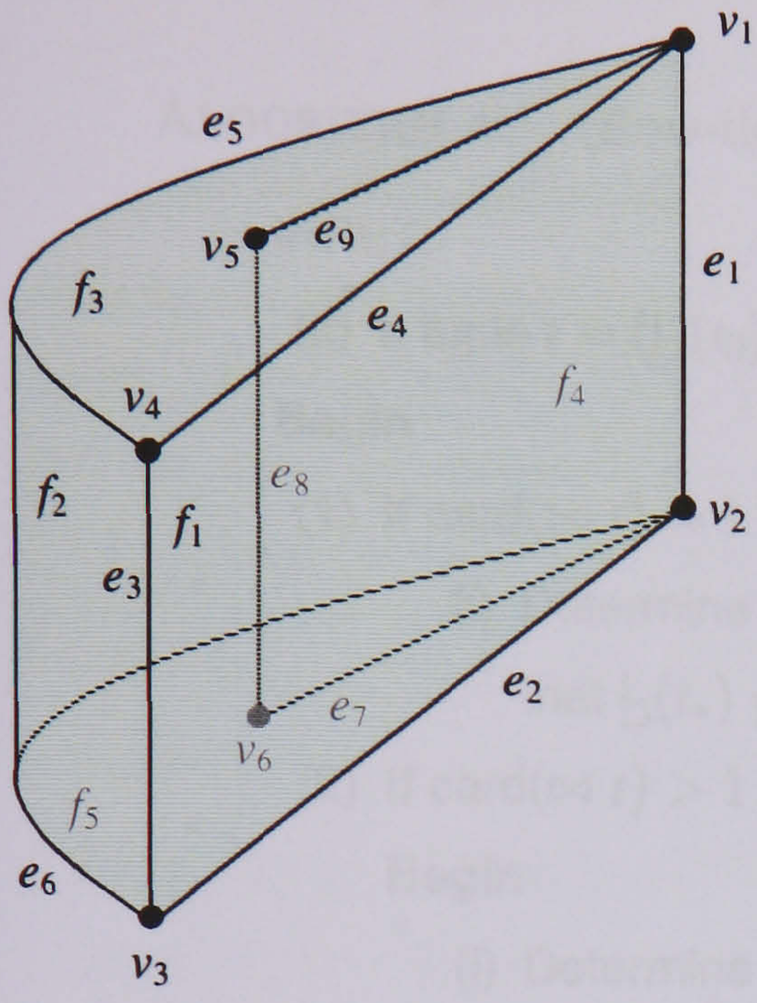

$\sqsubset(v_3),\sqsubset(e_3),\sqsubset(f_1),\sqsubset(s_1)$
$\sqsubset(v_3),\sqsubset(e_3),\sqsubset(f_2),\sqsubset(s_1)$
$\sqsubset(v_3),\sqsubset(e_2),\sqsubset(f_1),\sqsubset(s_1)$
$\sqsubset(v_3),\sqsubset(e_2),\sqsubset(f_5),\sqsubset(s_1)$
$\sqsubset(v_3),\sqsubset(e_6),\sqsubset(f_2),\sqsubset(s_1)$
$\sqsubset(v_3),\sqsubset(e_6),\sqsubset(f_5),\sqsubset(s_1)$
$\sqsubset(v_4),\sqsubset(e_3),\sqsubset(f_1),\sqsubset(s_1)$
$\sqsubset(v_4),\sqsubset(e_3),\sqsubset(f_2),\sqsubset(s_1)$
$\sqsubset(v_4),\sqsubset(e_4),\sqsubset(f_1),\sqsubset(s_1)$
$\sqsubset(v_4),\sqsubset(e_4),\sqsubset(f_3),\sqsubset(s_1)$
$\sqsubset(v_4),\sqsubset(e_5),\sqsubset(f_2),\sqsubset(s_1)$
$\sqsubset(v_4),\sqsubset(e_5),\sqsubset(f_3),\sqsubset(s_1)$
$\sqsubset(v_1),\sqsubset(e_4),\sqsubset(f_1),\sqsubset(s_1)$
$\sqsubset(v_1),\sqsubset(e_5),\sqsubset(f_2),\sqsubset(s_1)$
$\sqsubset(v_2),\sqsubset(e_2),\sqsubset(f_1),\sqsubset(s_1)$
$\sqsubset(v_2),\sqsubset(e_6),\sqsubset(f_2),\sqsubset(s_1)$
$\sqsubset(v_5),\sqsubset(e_9),\sqsubset(f_4),\sqsubset(s_1)$
$\sqsubset(v_5),\sqsubset(e_9),\sqsubset(f_3),\sqsubset(s_1)$
$\sqsubset(v_6),\sqsubset(e_7),\sqsubset(f_5),\sqsubset(s_1)$
$\sqsubset(v_6),\sqsubset(e_7),\sqsubset(f_4),\sqsubset(s_1)$

Fuzy circular order of edges bounding f_3 at v_1

$\sqsubset(v_1),\sqsubset(e_4),\sqsubset(f_3),\sqsubset(s_1)$
$\sqsubset(v_1),\sqsubset(e_5),\sqsubset(f_3),\sqsubset(s_1)$
$\sqsubset(v_1),\sqsubset(e_9),\sqsubset(f_3),\sqsubset(s_1)$

Fuzy circular order of edges bounding f_5 at v_2

$\sqsubset(v_2),\sqsubset(e_2),\sqsubset(f_5),\sqsubset(s_1)$
$\sqsubset(v_2),\sqsubset(e_7),\sqsubset(f_5),\sqsubset(s_1)$
$\sqsubset(v_2),\sqsubset(e_6),\sqsubset(f_5),\sqsubset(s_1)$

Fuzy circular order of faces about e_1

$\sqsubset(v_1),\sqsubset(e_1),\sqsubset(f_1),\sqsubset(s_1)$
$\sqsubset(v_1),\sqsubset(e_1),\sqsubset(f_2),\sqsubset(s_1)$
$\sqsubset(v_1),\sqsubset(e_1),\sqsubset(f_4),\sqsubset(s_1)$
$\sqsubset(v_2),\sqsubset(e_1),\sqsubset(f_1),\sqsubset(s_1)$
$\sqsubset(v_2),\sqsubset(e_1),\sqsubset(f_2),\sqsubset(s_1)$
$\sqsubset(v_2),\sqsubset(e_1),\sqsubset(f_4),\sqsubset(s_1)$

Circular order of faces about e_1

$\sqsubset(v_1),\sqsubset(e_1),\sqsubset(f_1),\sqsubset(f_4),\sqsubset(s_1)$
$\sqsubset(v_1),\sqsubset(e_1),\sqsubset(f_4),\sqsubset(f_2),\sqsubset(s_1)$
$\sqsubset(v_1),\sqsubset(e_1),\sqsubset(f_2),\sqsubset(f_4),\sqsubset(s_1)$
$\sqsubset(v_1),\sqsubset(e_1),\sqsubset(f_4),\sqsubset(f_1),\sqsubset(s_1)$
$\sqsubset(v_2),\sqsubset(e_1),\sqsubset(f_1),\sqsubset(f_4),\sqsubset(s_1)$
$\sqsubset(v_2),\sqsubset(e_1),\sqsubset(f_4),\sqsubset(f_2),\sqsubset(s_1)$
$\sqsubset(v_2),\sqsubset(e_1),\sqsubset(f_2),\sqsubset(f_4),\sqsubset(s_1)$
$\sqsubset(v_2),\sqsubset(e_1),\sqsubset(f_4),\sqsubset(f_1),\sqsubset(s_1)$

FIGURE 15

EXAMPLE 4.9. Let us look at the object depicted Figure 15. The boundary of the interior solid (or 3-stratum) s_1 is not manifold along the edge e_1. There are three faces f_1, f_4, f_2 incident to e_1. The circular order of these faces about e_1 is then fuzzy. To eliminate the uncertainty in selecting the next face through e_1, eight tuples of resolution 5 have to be generated. They are:

(i) $\langle\sqsubset(v_1),\sqsubset(e_1),\sqsubset(f_1),\sqsubset(f_4),\sqsubset(s_1)\rangle$,
(i) $\langle\sqsubset(v_1),\sqsubset(e_1),\sqsubset(f_4),\sqsubset(f_2),\sqsubset(s_1)\rangle$,
(i) $\langle\sqsubset(v_1),\sqsubset(e_1),\sqsubset(f_2),\sqsubset(f_4),\sqsubset(s_1)\rangle$,
(i) $\langle\sqsubset(v_1),\sqsubset(e_1),\sqsubset(f_4),\sqsubset(f_1),\sqsubset(s_1)\rangle$, and
(i) $\langle\sqsubset(v_2),\sqsubset(e_1),\sqsubset(f_1),\sqsubset(f_4),\sqsubset(s_1)\rangle$,
(i) $\langle\sqsubset(v_2),\sqsubset(e_1),\sqsubset(f_4),\sqsubset(f_2),\sqsubset(s_1)\rangle$,
(i) $\langle\sqsubset(v_2),\sqsubset(e_1),\sqsubset(f_2),\sqsubset(f_4),\sqsubset(s_1)\rangle$,
(i) $\langle\sqsubset(v_2),\sqsubset(e_1),\sqsubset(f_4),\sqsubset(f_1),\sqsubset(s_1)\rangle$.

These tuples order faces about e_1. For example,

$$\bowtie_2(\sqsubset(v_1),\sqsubset(e_1),\sqsubset(f_1),\sqsubset(s_1)) = \langle\sqsubset(v_1),\sqsubset(e_1),\sqsubset(f_1),\sqsubset(f_4),\sqsubset(s_1)\rangle$$
$$= (\sqsubset(v_1),\sqsubset(e_1),\sqsubset(f_4),\sqsubset(s_1)),$$

i.e. f_4 comes after f_1.

Thus, the Algorithm 4.3 can be generalised to higher dimensions as follows:

ALGORITHM 4.5. (Bow-tie operator $\bowtie_k$)

INPUT:

(a) a tuple $t = (\natural(t_0), \natural(t_1), \ldots, \natural(t_i))$

Begin

(1) **if** card$(\bowtie t) = 1$ **then**

(i) Determine the tuple $u = (\natural(t_0), \natural(t_1), \ldots, \natural(t_{k-1}), \natural(t_*), \natural(t_{k+1}), \ldots, \natural(t_i))$ such that $\natural(t_*) \neq \natural(t_k)$.

(2) **if** card$(\bowtie t) > 1$ **then**

Begin

(i) Determine the tuple $u = (\natural(t_0), \natural(t_1), \ldots, \natural(t_{k-1}), \natural(t_k), \natural(t_*), \natural(t_{k+1}), \ldots, \natural(t_i))$ such that dim(t_k)=dim(t_*).

(ii) Remove t_k from u.

End

(3) Return u.

End

A possible problem with these order resolvent tuples is that the local order is repeated for each vertex bounding the stratum for which the order is defined. For example, in Example 4.9, each bounding vertex of e_1 gives rise to four uncertainty resolvent tuples. That is, the resolution of uncertainty is repeated for each vertex bounding a fuzzy-order stratum. Similar to edges incident at a vertex in $\mathbb{R}^2$, there is an order for faces incident to an edge in $\mathbb{R}^3$. Therefore, if f_4 were outside of the solid s_1, we would still have an order of three faces incident to e_1. In this case, the fuzzy circular orderings of edges bounding f_3 and f_5 at v_1 and v_2, respectively, would disappear, but the fuzzy circular ordering of faces incident to e_1 would remain. However, the partial ordering of faces bounding s_1 along e_1 would be deterministic. In order to keep the total ordering of faces incident to e_1, we have only to replace the component s_1 by s_* in the tuples $(\natural(v_1), \natural(e_1), \natural(f_4), \natural(s_1))$ and $(\natural(v_2), \natural(e_1), \natural(f_4), \natural(s_1))$, with s_* denoting the exterior anti-solid.

7. Representation of relatively non-compact objects

In this chapter, we have only considered relatively compact stratified objects, i.e. objects whose strata have no missing frontier stratum. By a relatively non-compact stratified object we then mean an

object with at least one stratum with at leat one missing frontier stratum. The problem with relatively non-compact strata is that they introduce ambiguity in the representation.

COUNTEREXAMPLE 4.4. Figure 16 depicts two 1-dimensional objects, **X** and **Y**. Both objects contain a vertex v_1 and an edge e_1. They are then represented by the same tuple $(\sqcup(v_1), \sqcup(e_1))$. Thus, they are indistinguishable in the Σ-representation. This is a problem because they are quite different. **X** is a relatively non-compact object, while **Y** is relatively compact. Besides, **Y** has a hole through it, what means that they are homotopy inequivalent.

COUNTEREXAMPLE 4.5. Figure 17 shows two 2-dimensional objects, **X** and **Y**. **X** is a 2-manifold-with-frontier, while **Y** is a 2-manifold-without-frontier. Both objects contain a vertex v_1 and a face f_1. Their Σ-representation consists of a single tuple $(\sqcup(v_1), -, \sqcup(f_1))$. They are then representation-indistinguishable. But, their compactness and homotopy properties are distinct. **X** is a relatively non-compact object, while **Y** is relatively compact. Also, **X** has no holes at all, while **Y** possesses a 2-hole.

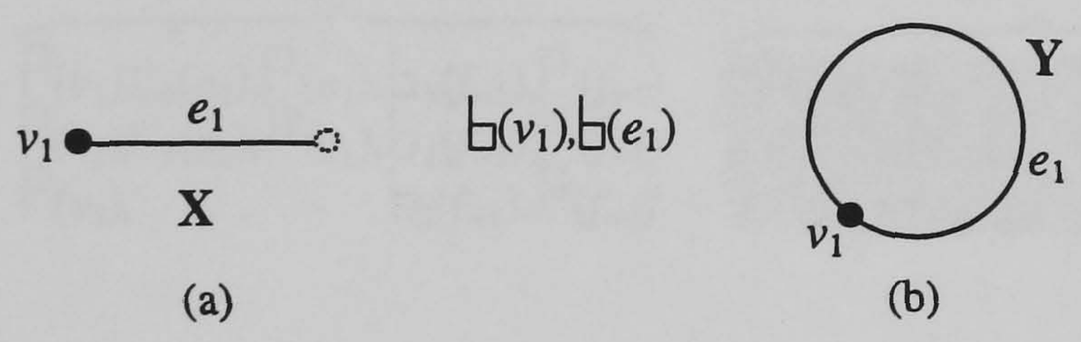

FIGURE 16

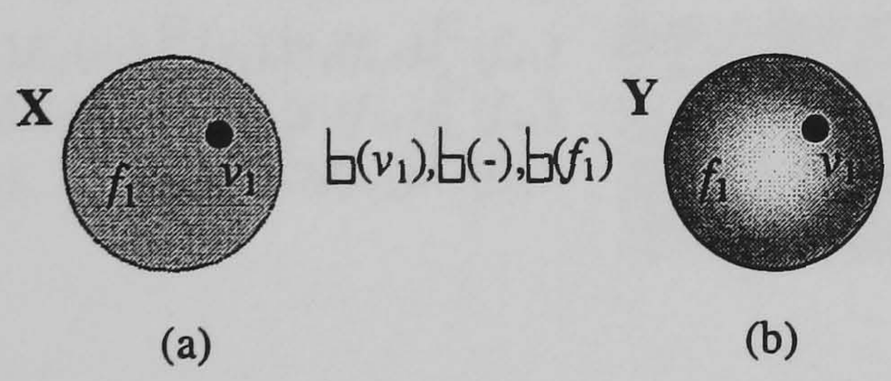

FIGURE 17

To overcome this representation ambiguity problem, we have embedded compactness, homology and homotopy information into the subcomplex-tuples of the Σ-representation. (All this information is also crucial for the Euler operators to be introduced and described in Chapter 5.) Recall that the components of the tuples describing relatively compact objects are related by the containment of the boundaries of strata in a skeletal chain. All this works quite well for relatively compact strata because their boundaries coincide with their frontiers. But, for relatively non-compact strata, boundaries do

not necessarily coincide with frontiers. This is the case of the object **X** depicted in Figure 16(a). The boundary of the edge e_1 consists of a single vertex v_1, but its frontier includes e_1 and a second 'missing' vertex.

In order to cope with relatively non-compact objects, the Σ-representation has been re-designed as follows:

- *Shape-descriptors tuples.* The shape of each stratum is described by a family of shape-descriptor tuples. This shape information is the core of shape reasoning algorithms. The Euler operators introduced in Chapter 5 make usage of this information extensively. It includes the cycles, boundary components, holes, and frontier components of each stratum.
- *Augmented boundary subcomplex-tuples.* The essential shape-descriptor component of each stratum is incorporated into each boundary subcomplex-tuple. This eliminates the ambiguity of Σ-representation of relatively non-compact objects and strata. That is, Σ-representation becomes a *complete* representation for objects, being possible to distinguish two objects by comparing their families of tuples.

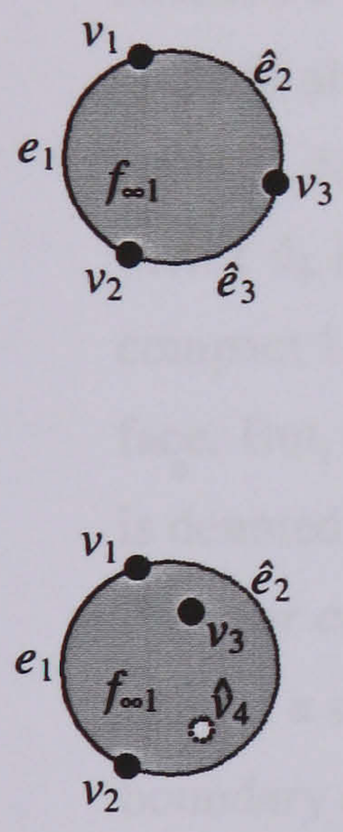

FIGURE 18

7.1. Shape-descriptors tuples of strata. By definition, a shape-descriptor of a stratum is a tuple of five shape components which satisfies the containment relationship that features the Σ-representation. These five shape components are:

- *Cycle*. Every cycle in a stratum gives rise to a distinct shape descriptor. It comes before any other shape component. It the most essential shape in a stratum. It denotes the existence of a hole of the same dimension. A k-cycle is the homological counterpart for a k-hole. A cycle is denoted by the symbol $\sqsubset$.
- *Boundary component.* Every boundary component of a stratum is the second component of a shape-descriptor tuple. It comes in second place because it may contain a cycle. The symbol $\sqsubset\!\!\sqcup$ is used to denote a boundary component of a stratum, and its boundary as well.
- *Hole*. The third component denotes the existence of a hole in a stratum. It is necessary because a k-hole in relatively non-compact stratum does not correspond to a k-cycle. A k-cycle is always manifold, but a k-hole can be degenerated, i.e. it can be non-manifold in a stratum. Moreover, a hole is not necessarily relatively-compact. For example, the 'missing' vertex $\hat{v}_4$ in the relatively non-compact face $f_{\infty 1}$ in Figure 18(b) defines a relatively non-compact 1-hole through $f_{\infty 1}$, while v_3 defines a relatively compact 1-hole through the same face. But, none of these two holes corresponds to a 1-cycle bounding $f_{\infty 1}$. A stratified hole is denoted by the symbol $\sqsubset\!\sqcap$.
- *Frontier component.* A frontier component contains a hole if it is an inner frontier component of a stratum. Otherwise, the hole shape-component is null. Note that its corresponding boundary component may be also null, seeing that it may not include any boundary stratum. A frontier component and its frontier are denoted by the symbol $\sqsubset\!\sqcap\!\sqcup$.
- *Frontier.* A stratified frontier of a stratum has at least one frontier component.

EXAMPLE 4.10. Figure 18(a) shows an object with a single relatively non-compact face $f_{\infty 1}$. Its stratified frontier $\sqsubset\!\sqcap\!\sqcup(f_{\infty 1})$ has only one component $\sqsubset\!\sqcap\!\sqcup_1(f_{\infty 1})$. It has no holes, but its frontier component $\sqsubset\!\sqcap\!\sqcup_1(f_{\infty 1})$ has two boundary components, $\sqsubset\!\sqcup_1(f_{\infty 1})$ and $\sqsubset\!\sqcup_2(f_{\infty 1})$. The first boundary component $\sqsubset\!\sqcup_1(f_{\infty 1})$ consists of v_1, v_2, and e_1, while the second boundary component $\sqsubset\!\sqcup_2(f_{\infty 1})$ includes only v_3.

So, we have:

$$\begin{aligned}
\mathsf{P}(f_{\infty 1}) &= \mathsf{P}_1(f_{\infty 1}),\\
\mathsf{P}_1(f_{\infty 1}) &= \mathsf{b}_1(f_{\infty 1}) \cup \mathsf{b}_2(f_{\infty 1}) \cup \{\hat{e}_2, \hat{e}_3\},\\
\mathsf{b}_1(f_{\infty 1}) &= \{v_1, v_2, e_1\},\\
\mathsf{b}_2(f_{\infty 1}) &= \{v_3\}.
\end{aligned}$$

Note that the 'missing' edges $\hat{e}_2$, $\hat{e}_3$ are not part of the Σ-representation. They are used here only to better differentiate the boundary from the frontier of $f_{\infty 1}$. The two shape-descriptors tuples for $f_{\infty 1}$ are shown alongside the object (a). There is also one shape descriptor for e_1. It includes a 0-cycle $\mathsf{c}_1\ (e_1)$ because its frontier consists of two vertices. Note there is no shape-descriptors tuples for vertices for obvious reasons.

EXAMPLE 4.11. In Figure 18(b), the stratified frontier $\mathsf{P}(f_{\infty 1})$ has three components, $\mathsf{P}_1(f_{\infty 1})$, $\mathsf{P}_2(f_{\infty 1})$, and $\mathsf{P}_3(f_{\infty 1})$. The first component $\mathsf{P}_1(f_{\infty 1})$ concerns the outer frontier component of $f_{\infty 1}$. It has no holes and cycles, but includes a boundary component $\mathsf{b}_1(f_{\infty 1}) = \{v_1, v_2, e_1\}$. The corresponding shape-descriptor tuple is then $(-, \mathsf{b}_1(f_{\infty 1}), -, \mathsf{P}_1(f_{\infty 1}), \mathsf{P}(f_{\infty 1}))$. The second frontier component $\mathsf{P}_2(f_{\infty 1})$ has no cycles, one boundary component $\mathsf{b}_{\infty 2}(f_{\infty 1}) = \{v_3\}$ which coincides with a relatively compact 1-hole $\mathsf{h}_1(f_{\infty 1})$; hence, the shape tuple $(-, \mathsf{b}_2(f_{\infty 1}), \mathsf{h}_1(f_{\infty 1}), \mathsf{P}_2(f_{\infty 1}), \mathsf{P}(f_{\infty 1}))$.

EXAMPLE 4.12. In Figure 18(c), the stratified frontier $\mathsf{P}(f_{\infty 1})$ consists of three frontier components, $\mathsf{P}_1(f_{\infty 1})$ and $\mathsf{P}_2(f_{\infty 1})$. The outer frontier component $\mathsf{P}_1(f_{\infty 1})$ forms a 1-cycle $\mathsf{c}_1\ (f_{\infty 1}) = \{v_1, e_1\}$, which coincides with its only one boundary component $\mathsf{b}_1(f_{\infty 1})$. This shape description is synthesised by the shape-descriptor tuple $(\mathsf{c}_1\ (f_{\infty 1}), \mathsf{b}_1(f_{\infty 1}), -, \mathsf{P}_1(f_{\infty 1}), \mathsf{P}(f_{\infty 1}))$. The inner frontier component $\mathsf{P}_2(f_{\infty 1})$ concerns a relatively non-compact 1-hole $\mathsf{h}_{\infty 1}(f_{\infty 1})$. It contains a relatively non-compact boundary component $\mathsf{b}_{\infty 2}(f_{\infty 1}) = \{v_2, e_2, e_{\infty 3}\}$, which in turn comprises a 1-cycle $\mathsf{c}_2\ (f_{\infty 1}) = \{v_2, e_2\}$. So, $(\mathsf{c}_2\ (f_{\infty 1}), \mathsf{b}_2(f_{\infty 1}), \mathsf{h}_{\infty 1}(f_{\infty 1}), \mathsf{P}_2(f_{\infty 1}), \mathsf{P}(f_{\infty 1}))$ is the corresponding shape-descriptor tuple. In addition to the shape-descriptors for $f_{\infty 1}$, we have a single shape-descriptor for each edge. The frontier of edge e_1 has only one frontier component $\mathsf{P}_1(e_1) = \mathsf{b}_1(e_1) = \{v_1\}$. The edge e_2 also has only one frontier component $\mathsf{P}_1(e_2) = \mathsf{b}_1(e_2) = \{v_2\}$. But, the relatively non-compact edge $e_{\infty 3}$ has two frontier components. The first is given by $\mathsf{P}_1(e_{\infty 3}) = \mathsf{b}_1(e_{\infty 3}) = \{v_2\}$, while the second is $\mathsf{P}_2(e_{\infty 3}) =$ concerns the 'missing' vertex $\hat{v}_3$. So, the shape-descriptor tuples for edges are: $(-, \mathsf{b}_1(e_1), -, \mathsf{P}_1(e_1), \mathsf{P}(e_1))$, $(-, \mathsf{b}_1(e_2), -, \mathsf{P}_1(e_2), \mathsf{P}(e_2))$, and $(-, -, -, \mathsf{P}_2(e_{\infty 3}), \mathsf{P}(e_1))$.

7.2. Frontier subcomplex-tuples. The generalisation of the Σ-representation to relatively non-compact objects and strata makes mandatory the replacement of boundary subcomplex-tuples by frontier subcomplex-tuples. This happens because the boundary of a stratum is no longer necessarily identical to its frontier. Thus, the symbol $\sqcup$ gives place to the symbol $\sqcap$ in the boundary subcomplex-tuples. It is clear that this generalisation does not imply any loss of incidence and order information. Only a few small changes have to be carried out in the bow-tie operator because the subcomplex tuples have been almost doubled in size in order to include shape information. With the exception of the first component, each one of the remaining components concerning edges, faces, solids, ..., n-strata is preceded by the first component of its corresponding shape-descriptor which contains it.

EXAMPLE 4.13. Let us look again at the object shown in Figure 18(c). Let us construct their frontier subcomplex tuples without any shape information. They are as follows:

(i) $(\sqcap(v_1), -, \sqcap(e_1), -, \sqcap(f_{\infty 1}))$,
(ii) $(\sqcap(v_2), -, \sqcap(e_2), -, \sqcap(f_{\infty 1}))$, and
(iii) $(\sqcap(v_2), -, \sqcap(e_{\infty 3}), -, \sqcap(f_{\infty 1}))$.

Looking at the shape descriptor of e_1, we see that the first shape component that includes v_1 is $\sqcup_1(e_1)$. Likewise, we obtain the first shape component $\sqsubset_1 (f_{\infty 1})$ that contains e_1 for $f_{\infty 1}$. After introducing this shape information into $\sqcap(v_1), -, \sqcap(e_1), -, \sqcap(f_{\infty 1}))$, we get the tuple $\sqcap(v_1), \sqcup_1(e_1), \sqcap(e_1), \sqsubset_1 (f_{\infty 1}), \sqcap(f_{\infty 1}))$. Analogously, the first shape components of e_2 and $f_{\infty 1}$ which include v_2 and e_2 are $\sqcup_1(e_2)$ and $\sqsubset_2 (f_{\infty 1})$, respectively. So, the second frontier subcomplex-tuple must be updated to $\sqcap(v_2), \sqcup_1(e_2), \sqcap(e_2), \sqsubset_2 (f_{\infty 1}), \sqcap(f_{\infty 1}))$. At last, the third frontier subcomplex-tuple gives to the augmented frontier subcomplex-tuple $\sqcap(v_2), \sqcup_1(e_{\infty 3}), \sqcap(e_{\infty 3}), \sqcup_{\infty 2}(f_{\infty 1}), \sqcap(f_{\infty 1}))$. Note that the first shape component of $f_{\infty 1}$ that contains $e_{\infty 3}$ is not the first component of its shape descriptor, but the second one. This is so because $e_{\infty 3}$ does not belong to the 1-cycle $\sqsubset_2 (f_{\infty 1})$. It belongs to the relatively non-compact boundary component $\sqcup_{\infty 2}(f_{\infty 1})$, which includes $\sqsubset_2 (f_{\infty 1})$.

8. Summary

One of the main problems in geometric modelling is the non-existence of general data structures capable of representing objects independently of dimension, manifoldness, and compactness. Another problem of current geometric data structures is their known inability to cope with separate manipulation of subobjects as required by CAD systems, and feature-based modellers in particular. The result is a poor abstraction and design of geometric modellers and proliferation of *ad hoc* solutions, say external data structures, for new problems, with consequent difficulties in software maintenance.

As shown in Chapter 1, the theory of homotopy allows us to get a better understanding of the shape structure of objects in higher dimensions and the relation between objects and their boundaries. As seen above, this is absolutely crucial for the design of a n-dimensional boundary representation as the Σ-representation. It represents regular stratified subanalytic objects in $\mathbb{R}^n$.

Σ-representation has been designed to cope with:

- The representation of regular stratified objects as a generalisation of regular cellular objects.
- The representation of subcomplexes as required for a variety of geometry-based applications.
- The representation of incidence and order even under non-manifold conditions.
- The representation of incidence and order even under non-compactness conditions.
- The representation of shape.
- The representation of incidence and order independently of the implementation i.e. the data structure.

There are several possible implementations or data structures for the Σ-representation. It can be implemented as a set of 2-dimensional arrays whose rows represent subcomplex-tuples, a graph data structure, or even as a database which is particularly adequate for Web-based applications and multiresolution geometric systems. List-based languages as Prolog and Lisp are particularly adequate to implement the Σ-representation, with the advantage that effective and natural shape reasoning techniques can be easily developed and implemented. A language as LogTalk [**89**] which combines the advantages of Prolog, object-oriented languages, and event-driven programming provides another excellent support to quickly implement the Σ-representation.

In short, Σ-representation can be characterised as follows:

- Geometric objects can be represented in higher dimensions.
- Geometric objects are regular stratified subanalytic sets. That is, both geometry and structure are general enough to cover practically all engineering artefacts. The geometry (subanalytic geometry) comes alongside structure (regular stratification).
- The building blocks are strata, not just topological cells.
- The structure of any geometric object extends the two-layered structure 'complex-cell' of conventional boundary representations to a three-layered structure 'complex-subcomplex-manifold'.

- Every complex is primarily viewed as a collection of subcomplexes. These subcomplexes may be used as stratified subobjects for geometric features (Hadwiger shapes), boolean primitives, or even user-defined subobjects.
- The geometric objects are not oriented, neither geometrically nor topologically. There is no need to having topologically oriented strata in the data structure. These oriented manifolds (e.g. 'halfedges', 'coedges', 'face-use', etc.) are usual in boundary representation data structures, but are extremely verbose. Besides, oriented strata are not easily extendable to higher dimensions. Σ-representation makes use of orientable strata, not oriented strata. All the incidence and order information is retrieved by a bow-tie operator.
- Any geometric object satisfies a general Euler-Poincaré formula valid for regular stratifications in $\mathbb{R}^n$ (see Chapter 5).

CHAPTER 5

Shape operators

Where there is no imagination there is no horror.

C. Doyle, A Study in Scarlet

This chapter deals with the third module of the Σ-geometric kernel architecture: *shape operators*. Euler operators will be subject to considerable discussion, but other shape operators will be described.

Euler operators here proposed enjoy the *dimension-independence* property. They are appropriate to stepwise construct regular stratifications of subanalytic varieties, semi-varieties, and, in general, stratified subanalytic sets in $\mathbb{R}^n$.

Compactness-independence is their second property. They do not impose restrictions on the relative compactness a regular stratified object and their strata. This means that the stratified frontier of a stratum is not required to be in its ambient object. Unbounded lines, semi-surfaces, and other relatively non-compact point sets are admissible strata.

The third fundamental property enjoyed by these Euler operators is that they are *design-order independent*, i.e. they do not constrain the construction order of an object. This means that any stratum can be attached to or detached from an object at any time. This facilitates and significantly shortens the re-designing tasks of engineering artefacts which do not meet manufacture requirements.

Altogether, these properties provide the user with a significant freedom in interactive geometric applications and programming, namely computer graphics, computer aided design and computational geometry.

1. Euler formulæ review

Let us remember that this work follows the guidelines of the geometric kernel architecture here proposed: shape (geometry), structure (stratification), and operators (e.g. Euler operators).

The focus now is on the operators, namely Euler operators. A set of Euler operators have been designed for regular stratified subanalytic objects, after finding out an appropriate Euler formula. An important aspect in boundary representation modellers is precisely whether an *algebraic invariant* (i.e. Euler formula) is used or not. If so, a boundary representation is said to be combinatorial, and

non-combinatorial otherwise. The combinatorial method relies on an elementary process of counting through invariants, the Euler characteristic in particular. This reliance on counting is what distinguishes a representation from another, as it distinguishes algebraic topology from other branches of topology and geometry [**57**, p.5]. In this sense, SGC-rep [**99**] and Djinn-rep [**2**] cannot be considered as combinatorial boundary representations. On the contrary, boundary representations used by Parasolid, ACIS, Σ-kernel are combinatorial. Combinatorial representations enable not only the construction of complicated objects from simple ones but also the inference of properties (e.g. incidence, order, shape, etc.) of the complicated from the simple.

The operators we use (e.g. bowtie operator, Euler operators, etc.) depend on the conceptual structure (say stratification) of an object. The converse is not true, that is, the (data) structure should be independent of the operators. For example, an object with strata other than relatively open strata does not satisfy any Euler formula used in geometric modelling. Therefore, Euler operators could not be used in this case. On the other hand, the structure of an object depends on the sort of geometry or geometric coverage of the objects. Recall that regular stratifications are admissible for subanalytic sets, but it is difficult to believe that non-analytic sets admit any sort of regular stratification.

In respect to the topological coverage of a *combinatorial* boundary representation, it depends on its associated Euler formula. (Obviously, this dependence does not exist for non-combinatorial boundary representations.) As shown below, the Euler formula may restrict the topological coverage of a boundary representation. In fact, the higher topological coverage, the lesser topological consistency problems for boundary representations.

1.1. Baumgart's Euler formula. The boundary representation of Baumgart [**7**], usually called *winged edge representation*, used Euler operators satisfying the Euler equation

$$v - e + f = 2B - 2H \tag{17}$$

where v, e, f, B and H stand for the number of vertices, edges, faces, bodies and handles in bodies (or 'visual' holes through bodies). In spite of the geometric coverage of the Baumgart's objects is restricted to planar faceted objects, the formula (17) covers a larger class of geometric objects, for example, spheres and tori. Baumgart used faceted approximations for these curved objects, but his formula enables an exact geometric representation for some curved objects.

EXAMPLE 5.1. A sphere $\mathbb{S}^2 = \{\mathbf{x} = (x,y,z) \in \mathbb{R}^3 : \|\mathbf{x}\| = 1\}$ has a stratification generated by the Euler operator `mBfe` (*make body, face and vertex*). The result is a new body $B_1 \approx \mathbb{S}^2$ consisting of a

new face f_1 and a new vertex v_1, Figure 1(a). The vertex v_1 is redundant, but without it the topological validity of the formula (17) is broken.

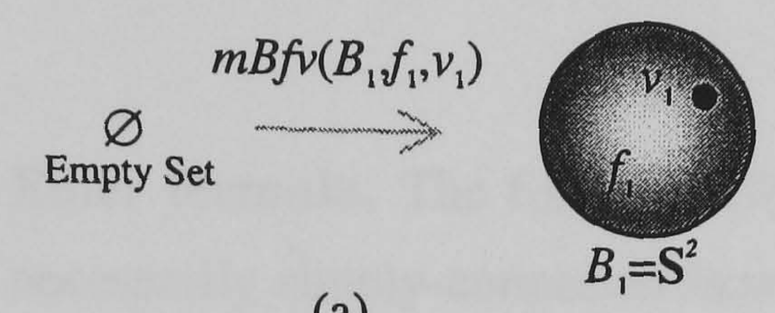

FIGURE 1. Construction of a 2-sphere $\mathbb{S}^2$, a cylinder C and a torus $\mathbb{T}^2$.

EXAMPLE 5.2. In Figure 1(c), the stratification of a torus $\mathbb{T}^2$ includes one vertex v_1, two edges e_1 and e_2, and one face f_1. The construction of any conventional B-rep object starts with the creation of a topological 2-sphere stratified into a face f_1 and a vertex v_1, as in Figure 1(a). It seems unlikely that we can topologically deform a 2-sphere into a torus. However, this is consistent with formula (17) since we apply a topological operation called *connected sum* (#) of two 2-spheres (they can be the same). First, we topologically deform such a sphere $\mathbb{S}^2$ into a cylinder C with an edge connecting two vertices, each bounding a circular edge of C, Figure 1(b). (Note that $\mathbb{S}^2$ and C are topologically equivalent or homeomorphic.) Finally, we apply the Euler operator corresponding to the *connected sum* of the cylinder with itself, which is described as follows: (i) first, we proceed to a tearing operation of cutting or eliminating the top and bottom circular faces f_2, f_3 of the cylinder; (ii) and then sew up their boundaries together by identifying or merging the vertices v_1, v_2 and the circular edges e_2, e_3. Thus, this Euler operator eliminates two faces (f_2 and f_3) (tearing operation), one edge (e_3) and one

vertex (v_2) (sewing up or merging operation), and generates one handle in the object. Altogether, these operations are carried by the Euler operator `k(2 f) evmH` (*kill two faces, edge, vertex, make handle*). The resulting torus consists of the face f_1, the edges e_1 and e_2, and the vertex v_1, but only the stratum f_1 is not redundant.

1.2. Braid-Hillyard-Stroud's Euler formula. The formula (17) can be extended in order to include 2-strata with holes, i.e. not necessarily simply-connected faces. (Note that the face f_1 of $\mathbb{T}^2$ in Figure 1(c) does not contain any through hole.) This extended formula is given by

$$v - e + (f - f_h) = 2B - 2H \tag{18}$$

where the new variable f_h denotes the number of holes through faces. In geometric modelling literature, these holes through faces are called "rings". In homotopy theory, they are called 1-holes, and 1-cycles in homology theory. This formula was introduced by CAD Group of Cambridge University in the construction of Build modeller, in the late 70s. This formula reduces slightly the redundancy of a boundary representation because faces need not to be homeomorphic to $\mathbb{R}^2$, they may contain holes.

EXAMPLE 5.3. The formula (18) enables the construction of a torus $\mathbb{T}^2$ from a cylinder without the intermediate edge e_1 pictured in Figure 1(c). In fact, according to formula (18), the face f_1 is now allowed to have a hole. The resulting cylinder has one edge less, but now f_1 possesses one through hole such that the formula (18) holds. The connected sum of this cylinder with itself —as described in previous example— implies the identification of two vertices (v_1 and v_2) and two edges (e_2 and e_3), i.e. the elimination of one vertex and one edge. The result is a torus with one face, one edge, and one vertex. In summary, one redundant edge e_1 has been thrown away, but two redundant strata, v_1 and e_2, still remain.

Note that the elimination of redundant strata only aims to generalise the Euler invariant. It can be seen as a de-subdivision algorithm that undoes the subdivision algorithm that supports the mathematical proof of the Euler formula. However, redundant strata may be useful to have a more complete shape description of a stratum or manifold. For example, a torus $\mathbb{T}^2$ has the homotopy type of $\mathbb{S}^1 \times \mathbb{S}^1$, and, consequently, it is easier for shape recognition algorithms to identify its shape if two edges —one for each $\mathbb{S}^1$— incident at a vertex bound a toroidal surface.

1.3. General Euler formula for closed surfaces. As suggested by the examples above, the topological redundancy of boundary representations (B-reps) can be eliminated by increasing the topological coverage of the manifolds or strata which constitute a closed surface. The immediate

consequence is the generalisation of the Euler formula, although it has not been accomplished by geometric modelling researchers. An important step towards such a general Euler formula for closed surfaces in $\mathbb{R}^3$ is the following formula:

$$v-(e-e_h)+(f-f_h+f_v)=2B-2H \tag{19}$$

where the new variables e_h, f_v stand for the number of holes through edges (or 1-holes, or closed edges without boundary, or spheres $\mathbb{S}^1$) and voids in faces (or 2-holes, or closed faces without boundary, or spheres $\mathbb{S}^2$), respectively. A circle is an example of an edge with a hole, and a sphere $\mathbb{S}^2$ is an example of a face with a void. Therefore, the topological coverage is higher for this formula than for Euler formulas used in conventional B-reps. This allows us to construct less-stratified closed surfaces, and thus with a lower number of Euler operators.

EXAMPLE 5.4. A sphere $\mathbb{S}^2$ without any 'dummy' vertex can be now generated by using the operator $\texttt{mBff}_v$ (*make body and face with a 2-hole*), Figure 2(a). The topological deformation of a sphere $\mathbb{S}^2$ into a cylinder is made by using twice the operator $\texttt{mee}_h\texttt{ff}_h$ (*make edge with a 1-hole and face with a 1-hole*), Figure 2(b). Once again, no 'dummy' vertices or edges are required. At last, the topological deformation of such a cylinder into a torus is made by the connected sum $C\#C=\texttt{k(2f)ee}_h\texttt{mH}$ (*kill two faces and edge with 1-hole, make handle*), which deletes f_1 and f_2, identifies e_1 with e_2, and creates an handle (the torus itself), Figure 2(c).

The Euler formula (19) disables the generation of a torus with a single 2-stratum or face. A redundant edge is still required to comply with (19). This suggests a new generalisation of the Euler formula. However, no other sorts of strata are admissible for closed surfaces than those of (19). This means that the left-side of (19) has reached the maximum generalisation for surfaces. But, the right-side of (19) can be re-interpreted by taking components (C) with possibly 1-holes (C_h) or 2-holes (C_c), instead of components (C) and handles (H).

THEOREM 5.1. *Every relatively compact surface $\mathcal{S}$ satisfies the Euler formula*

$$v-(e-e_h)+(f-f_h+f_v)=C-C_h+C_c \tag{20}$$

where C, C_h, C_c stand for the number of components of $\mathcal{S}$, 1-holes through components, and 2-holes or cavities (voids) in components, respectively.

PROOF. The *global* Euler characteristic $\chi(\mathcal{S})=C-C_h+C_c$ is well-known in mathematics; it is the alternate sum of the first three Betti numbers, namely $\beta_0=C$, $\beta_1=C_h$, and $\beta_2=C_c$. They describe

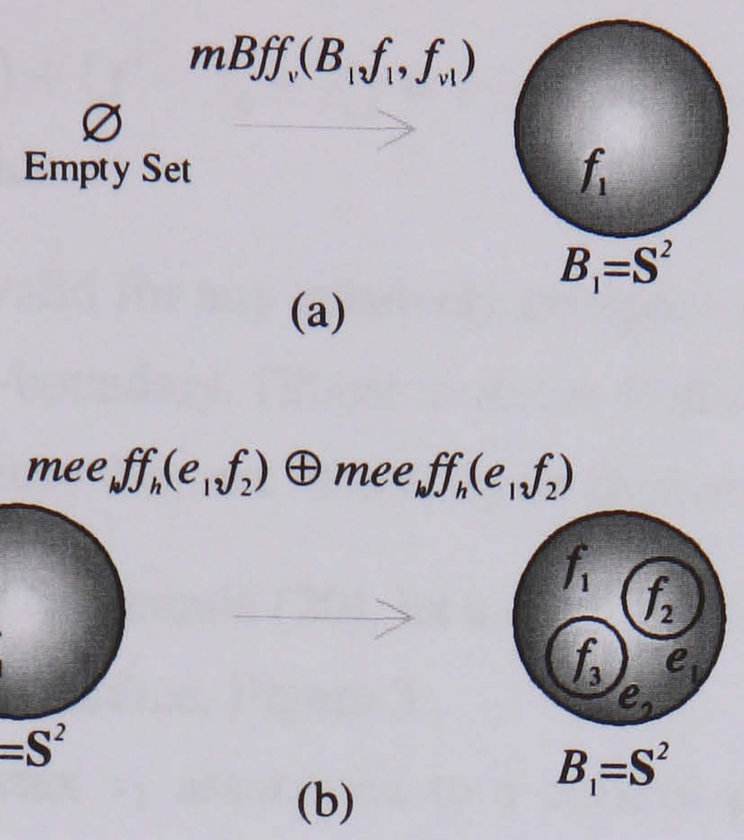

FIGURE 2. Construction of a 2-torus $\mathbb{T}^2$ using the Euler formula $v-(e-e_h)+(f-f_h+f_v)=2B-2H$ for closed surfaces.

the *global* topological properties (or homotopic properties) of a topological space, in particular a surface, no matter their constituents or strata. Surfaces cannot possess holes other than through holes (or 1-holes) and voids (2-holes), even in $\mathbb{R}^n$, $n>3$.

On the other hand, the *local* Euler characteristic $\chi(\mathcal{S})=v-(e-e_h)+(f-f_h+f_v)$ is basically the alternate sum of the number of strata of increasing dimension in $\mathcal{S}$. Because edges only admit holes (or 1-holes) through them, and faces admit holes through them and holes (or 2-holes) which are voids, we conclude that the formula (20) is the most general Euler formula for surfaces.

The alternate sums can be explained by subdivision techniques similar to those illustrated in [**66**, Section 5.4]. In fact, let X, Y be two stratified sets such that Y is obtained from X after applying the Euler operator $\texttt{mekf}_h$ (*make edge, kill hole through face*), which inserts a new edge between two frontier components (e.g. between the outer frontier component and a defining-hole inner frontier component). The result is the merge of such two frontier components into one, and the elimination of a face hole. Denote the vertices, edges, edge 1-holes, faces, face 1-holes, face 2-holes of X by v, e, e_h, f, f_h, f_v and those of Y by v', e', e'_h, f', f'_h, f'_v. Note that $v'=v$, $e'=e+1$, $e'_h=e_h$, $f'=f$, $f'_h=f_h-1$,

and $f_c' = f_c$ so $\chi(Y) = v' - (e' - e_h') + (f' - f_h' + f_c') = v - [(e+1) - e_h] + [f - (f_h - 1) + f_c] = \chi(X)$.
That is, the Euler characteristic holds. □

Note that the formula (20) is valid for any relatively compact surfaces, either they are surfaces-with-boundary or surfaces-without-boundary. (These surfaces-without-boundary are sometimes called closed surfaces because in some sense they are closed up on themselves.)

EXAMPLE 5.5. With reference to formula (20), let us see how to construct a regular stratification of, for example, a four-sided Bézier surface, Figure 3.

mvC. This operator creates a vertex v_1 associated to a control point, which constitutes a point-component from the homotopy point of view.

3⊗mve. The operator mve is used three times to introduce the other three vertices v_2, v_3, v_4 and the edges e_1, e_2, and e_3.

meC$_h$. It introduces the new edge e_4 which originates the appearance of a new 1-hole through the object.

mfkC$_h$. Such a hole disappears from the object after inserting the face f_1.

mee$_h$ff$_h$. This operator subdivides f_1 into two faces f_2 and f_3 by a new edge e_1 with a 1-hole.

kfmC$_h$. At last, f_3 is removed from the surface, what becomes the 1-hole through f_2 also a global 1-hole of the whole surface.

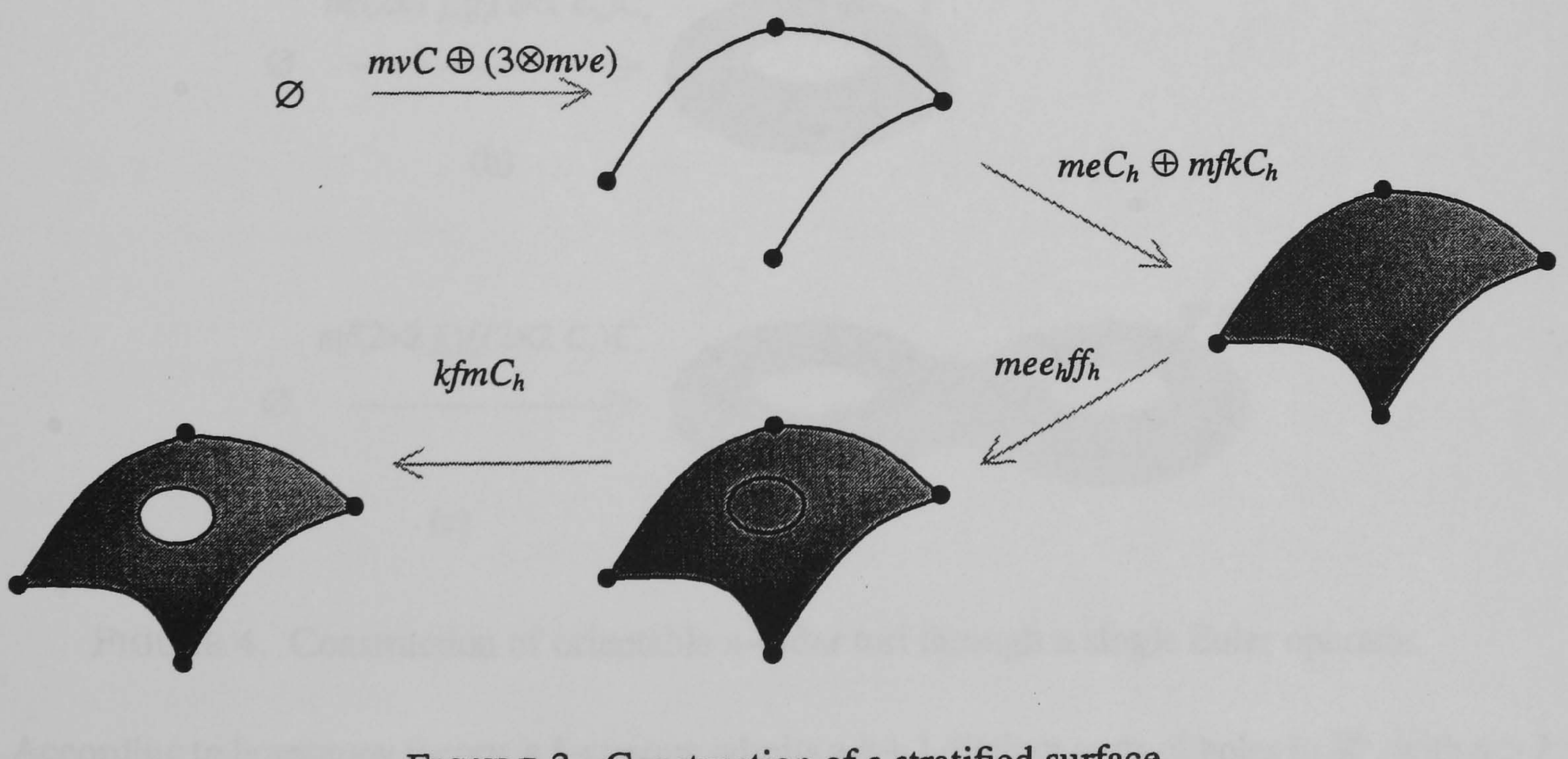

FIGURE 3. Construction of a stratified surface.

EXAMPLE 5.6. The formula (20) also admits the construction of any orientable surface-without-boundary in $\mathbb{R}^3$. According to Theorem of Surface Classification (see, for example, [3, p.18]) any

orientable closed surface is homeomorphic to the sphere or to the sphere with a finite number of handles, say a finite connected sum of tori. Figure 4 illustrates the generation of a regular stratification for each one of these surfaces. So, we have:

$\underline{\texttt{mf}(2\times 0\ \ \texttt{f}_h)\,\texttt{f}_c(2\times 0\ \ \texttt{C}_h)\,\texttt{C}_c}$. This operator creates a stratification for a sphere without handles, Figure 4(a), which consists of a single 2-stratum, the sphere itself.

$\underline{\texttt{mf}(2\times 1\ \ \texttt{f}_h)\,\texttt{f}_c(2\times 1\ \ \texttt{C}_h)\,\texttt{C}_c}$. In this case, the result is also a stratification with a single 2-stratum corresponding to a sphere with one handle, i.e. a torus, Figure 4(b).

$\underline{\texttt{mf}(2\times 2\ \ \texttt{f}_h)\,\texttt{f}_c(2\times 2\ \ \texttt{C}_h)\,\texttt{C}_c}$. This operator generates a stratification with a single stratum for a double torus, Figure 4(c).

⋮

$\underline{\texttt{mf}(2\times n\ \ \texttt{f}_h)\,\texttt{f}_c(2\times n\ \ \texttt{C}_h)\,\texttt{C}_c}$. This operator creates a stratification with a single stratum for the n-order torus (i.e. a sphere with n handles), and thus is a generalisation for the preceding operators.

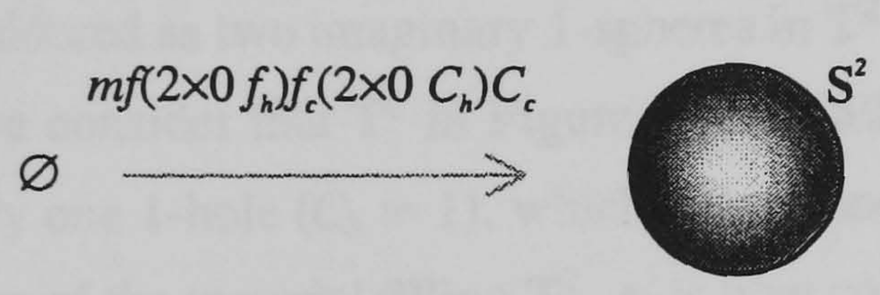

FIGURE 4. Construction of orientable n-order tori through a single Euler operator.

According to homotopy theory, a k-stratum admits a $k+1$ distinct sorts of holes in $\mathbb{R}^n$, with $n > k$. For example, a 0-stratum may only possess 0-holes, a 1-stratum may have 0-holes and 1-holes, a 2-stratum may contain 0-holes, 1-holes and 2-holes, a 3-stratum may have 0-holes, 1-holes, 2-holes, and 3-holes, etc.

A *0-hole of a stratum* is related to the number of components of a stratum. For example, a 0-stratum with three components (or points) is said to be a 0-stratum with two 0-holes. A 0-hole denotes the absence of a path between two points of a stratum; analogously, a 1-stratum with two components (or edges) possesses a 0-hole, etc. Therefore, the number of 0-holes of any stratum is equal to the number of its components less one. In terms of Euler formula, such stratum components are counted. Alternatively, if multi-connected strata are admissible for a geometric modeller, the variables v, e, f stand for the number of *components* for 0-strata, 1-strata, 2-strata, respectively, instead of *strata* themselves.

A *1-hole of a stratum* has the homotopy type of a 1-sphere $\mathbb{S}^1$ (or circle). This hole prevents the contraction of a loop in such a stratum into a point. For example, the circle $x^2+y^2=1$ is the simplest 1-stratum with a 1-hole. The toroidal surface $\mathbb{T}^2$ as a whole (right-hand side of formula 20) has two 1-holes ($C_h=2$) because it contains two non-contractible 1-spheres (e.g. the edges e_1 and e_2 in Figure 1(c) considered as two imaginary 1-spheres in $\mathbb{T}^2$ are not contractible to a point in $\mathbb{T}^2$; hence $e_h=2$). But, if we consider that $\mathbb{T}^2$ in Figure 1(c) is 'filled' with material, then the corresponding solid torus has only one 1-hole ($C_h=1$), which corresponds to the imaginary 1-sphere e_1 ($e_h=1$) in $\mathbb{T}^2$. In fact, because of the material filling $\mathbb{T}^2$, e_2 is now contractible to a point in such material. Also, a sphere $x^2+y^2+z^2=1$ has no 1-holes because every 1-sphere in it is contractible to a point.

A *2-hole of a stratum* is homotopy-equivalent to a 2-sphere $\mathbb{S}^2$ in such a stratum. This hole prevents the contraction to a point of any balloon contained in such a stratum. The sphere $x^2+y^2+z^2=1$ is the simpler 2-stratum with a 2-hole. It is its own balloon.

Analogously, a *3-hole of a stratum* is homotopy-equivalent to a 3-sphere $\mathbb{S}^3$ in such a stratum that is not contractible to a point in it. The sphere $x^2+y^2+z^2+w^2=1$ is the simplest 3-stratum with a 3-hole.

As demonstrated later, this process can be generalised to higher dimensions and used to find out the corresponding Euler formula for multi-dimensional objects in $\mathbb{R}^n$. For the time being, it is convenient to retain that a k-hole is only definable for strata of dimension greater or equal to k. For example, a 2-stratum only admits 0-, 1-, and 2-holes, that is, 2-dimensional components less 1, through holes and voids, respectively. They are denoted by the variables f, f_h and f_v. But the ambient space may restrict the strata and their holes definable in it. No stratum of dimension greater than n is definable in $\mathbb{R}^n$, while no k-hole ($k \geq n$) is definable in $\mathbb{R}^n$. This is because the general Euler formula for closed surfaces does not include holes of dimension greater or equal to 3. Therefore, the formula (20) is absolutely general for current B-reps. Furthermore, the redundancy of B-rep data structures can be eliminated by generalisation of the Euler formula that rules the creation and manipulation of

surfaces and their manifold constituents or strata. This allows programmers and users to make use of geometric kernels in a more flexible and intuitive manner.

1.4. Masuda's Euler formula. Before proceeding let us note that 'non-manifoldness' is a term to name modern B-reps. This is because the neighbourhood of a k-dimensional stratum point is not necessarily homeomorphic to a k-dimensional manifold in the ambient object. But, both 'manifold' and 'non-manifold' boundary representations are data structures for regular stratified objects. So, we prefer to call them stratified representations, or simply Σ-representations.

The first 'non-manifold' B-rep was introduced by Weiler in his doctoral work [**116**]. However, Weiler did not propose *explicitly* any Euler formula in order to cover general relatively compact objects. Such formulas were introduced later by Wu [**124**], Masuda [**76**], and Yamaguchi [**125**].

The Masuda's Euler formula [**76**] is certainly the most general formula for relatively compact 'non-manifold' objects found in the geometric modelling literature. It is given by

$$v - e + (f - f_h) - (s - s_h + s_c) = C - C_h + C_c \tag{21}$$

where the new variables s, s_h, s_c stand for the number of solids, 1-holes through solids, and 2-holes or cavities (voids) in solids, respectively.

Following the guidelines of our discussion, we see that Masuda's objects suffer from topological redundancy because holes through edges (e_h) and voids in faces (f_v) have not been considered. A major novelty of the Masuda's B-rep data structure is that for the first time solids or 3-strata are used to model engineering parts and assemblies. However, the Masuda's interpretation of the global Euler characteristic was a bit misleading because C, C_h, and C_c were supposed to stand for the number of complexes, holes through complexes, and voids in complexes, respectively, instead of the number of components (of a complex), holes through these components, and voids in these components. Consequently, the Masuda's model considers that each complex has only one component.

EXAMPLE 5.7. Figure 5 illustrates a 'non-manifold' technique to construct a torus. It differs from the 'manifold' technique in the sense that it does not require the attachment of an handle to a sphere, neither the topological deformation of a surface-without-boundary. The sequence of operators is as follows:

2⊗mvC. This operator is called twice to create a vertex v_1 (and then v_2) and a point-component C_1 (C_2, respectively).

2⊗meC_h. This operator is applied twice to the current object to create two 1-holes C_{h_1}, C_{h_2} by attaching the edges e_1, e_2, respectively.

mff$_h$kCC$_h$. Despite this operator has not been introduced by Masuda, it can be used to attach a face with a 1-hole to an object.

kvemC$_h$C$_v$. This operator has not been introduced by Masuda, but it can be used to attach a surface to itself by identifying two of its frontier components.

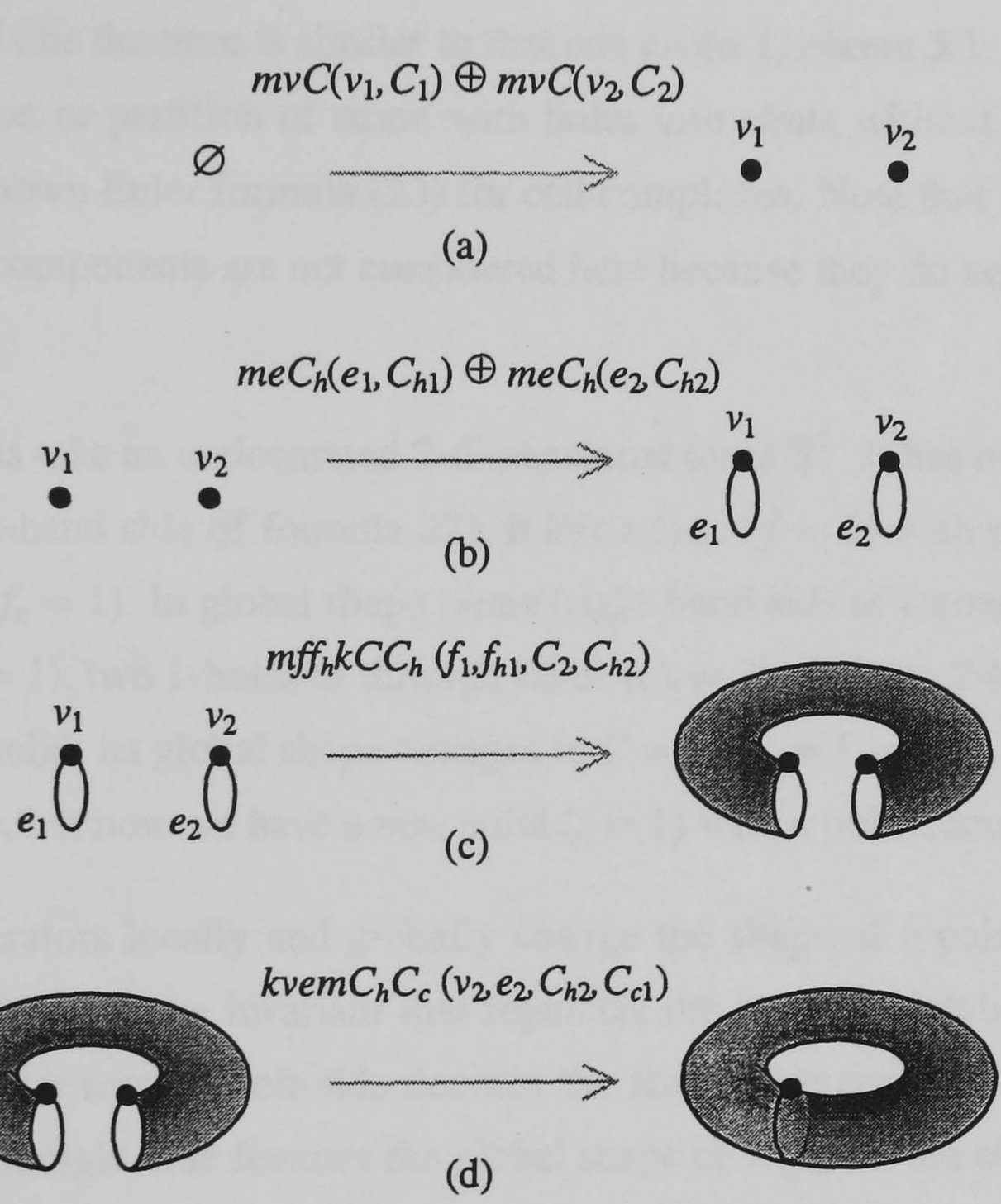

FIGURE 5. The 'non-manifold' construction of 2-torus $\mathbb{T}^2$ based on the Masuda's formula.

2. General Euler formulæ

The Masuda's Euler formula can be generalised by including edges with a 1-hole and faces with a 2-hole:

THEOREM 5.2. *Every relatively-compact regular stratified point set X in* $\mathbb{R}^3$ *satisfies the following Euler formula*

$$v-(e-e_h)+(f-f_h+f_v)-(s-s_h+s_v)=C-C_h+C_c \tag{22}$$

where v, e, f, s stand for the number of connected 0-, 1-, 2-, 3-strata (or vertices, edges, faces and solids), respectively, and C the number of components of the X. The other variables denote holes

in strata and components; the subscripts h and v denote through holes and holes which are voids, respectively. So, e_h, f_h, s_h denote holes through edges, faces and solids, respectively; and f_v, s_v denote voids in faces and solids; at last, C_h and C_c stand for the number of holes through components and voids in components, respectively.

PROOF. The proof of this theorem is similar to that one given Theorem 5.1. The proof technique is based on the subdivision or partition of strata with holes into strata without holes in such a way that we obtain the well-known Euler formula (23) for cell complexes. Note that 3-holes for solids (or 3-strata) and 3-holes for components are not considered here because they do not exist in $\mathbb{R}^3$, only in $\mathbb{R}^4$ and above. □

EXAMPLE 5.8. Let us take an undecorated 2-dimensional torus $\mathbb{T}^2$. It has no vertices and edges. In local shape terms (left-hand side of formula 22), it has a face ($f = 1$) with two essential 1-holes ($f_h = 2$) and one 2-hole ($f_c = 1$). In global shape terms (right-hand side of formula 22), it is a surface with one component ($C = 1$), two 1-holes or through holes ($C_h = 2$), and one 2-hole or hollow cavity (C_c). Filling in it with a solid, its global shape changes to $C = 1$, $C_h = 1$, and $C_c = 0$. No local shape changes occur in the face, but now we have a new solid ($s = 1$) with a hole through it ($s_h = 1$).

Therefore, Euler operators locally and globally change the shape of a point set or space. The Euler formula is an algebraic shape invariant that regulates the local and global shape changes on an object. In fact, the Euler formula left-side denotes the shape changes on strata of an object. In contrast, the Euler formula right-side features the global shape changes on the object as a whole.

Let us now generalise formula (22) as follows:

1. The generalisation is extended to objects in $\mathbb{R}^n$.
2. The objects are not necessarily compact, and each of its strata is not required to be relatively compact[1].

2.1. General Euler formula left-side. It is known from mathematics that a point set regularly-stratified into strata *without holes* has the Euler characteristic $\mathcal{X}(X)$ given by the alternate sum of the number of strata of each dimension, that is,

$$\mathcal{X}(X) = \sum_{i=0}^{n} (-1)^i s^i \tag{23}$$

[1]Only by abuse of language, we can say that a stratum is *relatively compact*. In fact, a stratum is, by definition, relatively open (e.g. an open line segment in $\mathbb{R}^1$). By a relatively compact stratum we mean here a relatively open stratum whose boundary and frontier in its ambient stratified object coincide.

where s^i denotes the number of relatively compact i-dimensional strata in the object.

If a regular stratified object X contains strata *with holes*, the Euler characteristic becomes

$$\chi(X) = \sum_{i=0}^{n} (-1)^i [s^i + \sum_{j=1}^{i} (-1)^j h_i^j] \tag{24}$$

where h_i^j stands for the number of j-dimensional holes of relatively compact i-dimensional strata. This formula takes into account that a i-dimensional stratum has at most holes of dimension $(i-1)$.

In fact, by induction on the dimension, and for:

- $i = 0$, we have $(-1)^0[s^0 + 0] = s^0 = v$
- $i = 1$, we have $(-1)^1[s^1 + (-1)^1 h_1^1] = -(s^1 - h_1^1) = -(e - e_h)$
- $i = 2$, we have $(-1)^2[s^2 + (-1)h_2^1 + h_2^2] = s^2 - h_2^1 + h_2^2 = f - f_h + f_c$
- $i = 3$, we get $(-1)^3[s^3 + (-1)h_3^1 + h_3^2 + (-1)h_3^3] = -(s^3 - h_3^1 + h_3^2 - h_3^3) = -(s - s_h + s_c - h_3^3)$
- $\vdots$

Dropping down the *compactness condition*, we have the following Euler characteristic:

$$\chi(X) = \sum_{i=0}^{n} (-1)^i [s^i + \sum_{j=1}^{i} (-1)^j h_i^j] + \sum_{i=1}^{n} (-1)^i [s_\infty^i + \sum_{j=1}^{i-1} (-1)^j h_{\infty i}^j] \tag{25}$$

where s_∞^i denotes the number of relatively non-compact i-dimensional strata in the object, and $h_{\infty i}^j$ the number of j-dimensional holes for relatively non-compact i-dimensional strata. Therefore, the formula (25) consists of two terms. The first term concerns the relatively compact subset of X, while the second term concerns the relatively non-compact subset of X. Note that the stratum dimension i of the second term starts at 1, because 0-strata or vertices are always relatively compact. Note that $h_3^3 = 0$ in $\mathbb{R}^3$; it only exists in $\mathbb{R}^4$ and above.

In $\mathbb{R}^3$, the formula (25) becomes

$$\begin{aligned} \chi(X) = [v - (e - e_h) + (f - f_h + f_c) - (s - s_h + s_c)] + \\ + [-(e_\infty) + (f_\infty - f_{\infty h}) - (s_\infty - s_{\infty h} + s_{\infty c})] \end{aligned} \tag{26}$$

where e_∞, f_∞ and s_∞ stand for the number of relatively non-compact edges, faces and solids, respectively; $f_{\infty h}$ and $s_{\infty h}$ denote the number of non-compact 1-holes through faces and solids, respectively, and $s_{\infty c}$ the number of non-compact 2-holes in solids.

EXAMPLE 5.9. Figure 6 shows three objects which have relatively non-compact strata and holes. The object (a) has one relatively non-compact edge $e_{\infty 1}$ because one of its frontier vertices is missing. Its circular face $f_{\infty 1}$ is also relatively non-compact because its boundary and frontier do not coincide.

These two strata are not compact because they are not closed in the relative topology. The object (b) is a regular stratification of the Cartan umbrella. The positive z-axis corresponds to the relatively non-compact edge $e_{\infty 1}$, while the negative z-axis concerns the relatively non-compact edge $e_{\infty 2}$. The Cartan sheets refer to relatively non-compact strata $f_{\infty 1}$ and $f_{\infty 2}$. In this case, the strata are not compact because they are not bounded, i.e. their size is infinite. At last, the object (c) consists of a non-compact solid $s_{\infty 1}$ because it is bounded by a relatively non-compact face $f_{\infty 1}$. This face is relatively non-compact because it has two points missing. The absence of these two points implies the existence of a non-compact 1-hole $f_{\infty h1}$ through such a face. Besides, there is a missing line inside $s_{\infty 1}$ between the those two missing points of $f_{\infty 1}$; hence, the non-compact 1-hole $s_{\infty h1}$ through $s_{\infty 1}$.

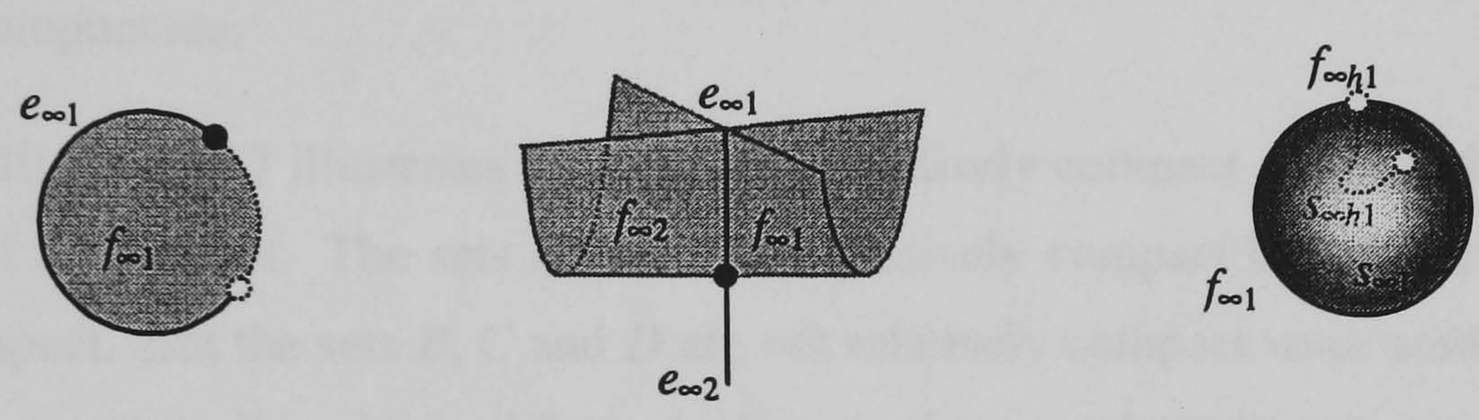

FIGURE 6. Some examples of relatively non-compact strata and holes.

2.2. General Euler formula right-side. In mathematics, the Euler characteristic $\chi(X)$ of a compact point set X in $\mathbb{R}^n$ may be also given by

$$\chi(X) = C + \sum_{i=1}^{n} (-1)^i H^i \tag{27}$$

where C stands for the number of components of X, and H^i the number of i-dimensional holes for these components. So, $H^1 = C_h$ denotes the number of 1-holes through components (simply called through holes in geometric modelling literature), $H^2 = C_c$ denotes the number of 2-holes in components (usually called voids in components), etc.

Relaxing the compactness condition, the relatively compact subset of X still satisfies (27), but not its complement in X. In this general situation, we have the following formula:

$$\chi(X) = [C + \sum_{i=1}^{n} (-1)^i H^i] + \sum_{i=1}^{n} (-1)^i [C_\infty^i + \sum_{j=1}^{i-1} (-1)^j H_{\infty i}^j] \tag{28}$$

The first term is concerns the relatively compact subset of X as in (27), while the second term has to do with the relatively non-compact subset of X. C_∞^i denotes the number of i-dimensional relatively non-compact components, or, in other words, the number of relatively non-compact i-strata in X. Note

that all components in X are always disjoint, no matter whether they are compact or not. Therefore, every relatively non-compact i-stratum in X constitutes a non-compact component of dimension i. On the other hand, every relatively compact i-stratum in X is part of a relatively compact component of dimension $\geq i$.

In $\mathbb{R}^3$, the formula (28) becomes

$$\chi(X) = (C - C_h + C_c) - (E_\infty) + (F_\infty - F_{\infty h}) - (S_\infty - S_{\infty h} + S_{\infty c}) \tag{29}$$

where E_∞, F_∞ and S_∞ stand for the number of relatively non-compact edge components, face components and solid components, respectively; $F_{\infty h}$ and $S_{\infty h}$ denote the number of non-compact 1-holes through face components and solid components, respectively, and $S_{\infty c}$ the number of non-compact 2-holes in solid components.

EXAMPLE 5.10. Figure 7 illustrates the notions of relatively compact subset and relatively non-compact subset of a point set. The sets A and E are relatively compact because all of their strata are relatively compact. But the sets B, C and D are not relatively compact since some of their strata are not relatively compact. B is obtained from A after attaching a relatively non-compact edge $e_{\infty 1}$, and, therefore, A is the relatively compact subset of B. So, A constitutes the only relatively compact component of B, while $e_{\infty 1}$ constitutes the only relatively non-compact edge component $E_{\infty 1}$ of B. Similarly, C results from B by attaching a new relatively non-compact edge $e_{\infty 2}$ to B. Thus, the relatively compact subset of C is still A, but now we have two relatively non-compact edge components, $E_{\infty 1} = \{e_{\infty 1}\}$ and $E_{\infty 2} = \{e_{\infty 2}\}$. Analogously, D stems from E by attaching a relatively non-compact face $f_{\infty 1}$ to E. This introduces a new relatively non-compact face component $F_{\infty 1} = \{f_{\infty 1}\}$ into D. At last, we get E from D by attaching a new vertex to D. Consequently, the three relatively non-compact components disappear since their underlying strata $e_{\infty 1}$, $e_{\infty 2}$, and $f_{\infty 1}$ are transformed into the relatively compact strata e_1, e_2, and f_1, respectively. That is, the relatively non-compact subset of E is now the empty set.

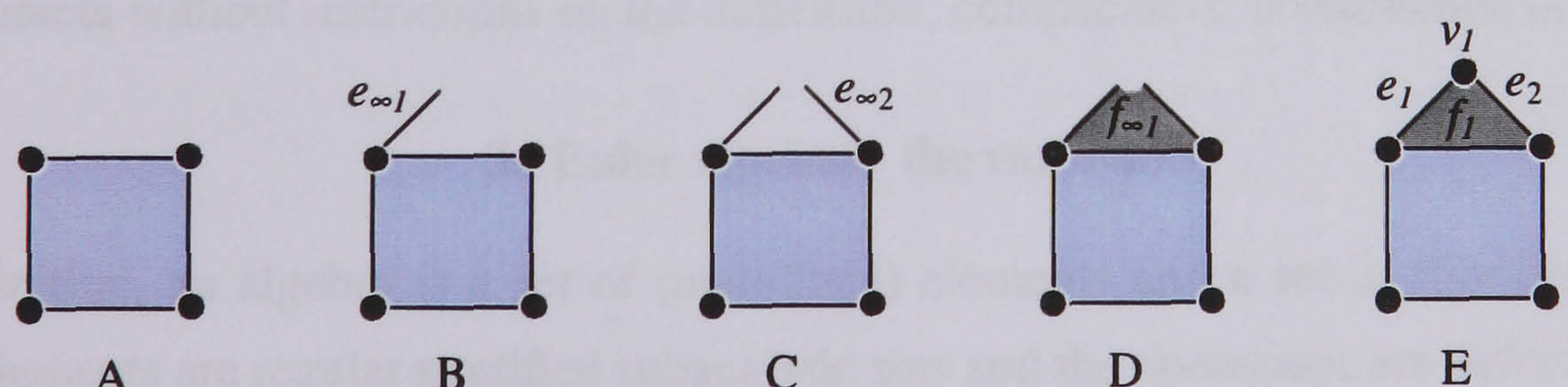

FIGURE 7. The relatively compact subset and relatively non-compact subset of a point set.

Let us see now the second term of (29) in more detail for each dimension:

- For $i=0$, we have no relatively non-compact components since any vertex is relatively compact.
- For $i=1$, we have $(-1)^1[C^1_\infty+0]=-E_\infty$, where $C^1_\infty=E_\infty$ denotes the number of relatively non-compact edge components in X. Note that edges with 1-holes are not considered here because they are compact indeed.
- For $i=2$, we have $(-1)^2[C^2_\infty+(-1)^1H^2_{\infty 1}]=F_\infty-F_{\infty h}$, where $C^2_\infty=F_\infty$ and $H^2_{\infty 1}=F_{\infty h}$ denote the number of relatively non-compact face components and the number of 1-holes through these face components, respectively. Again, faces with 2-holes are not considered here since they are compact faces.
- For $i=3$, we have $(-1)^3[C^3_\infty+(-1)^1H^3_{\infty 1}+(-1)^2H^3_{\infty 2}]=-(S_\infty-S_{\infty h}+S_{\infty c})$, where $C^3_\infty=S_\infty$, $H^3_{\infty 1}=S_{\infty h}$ and $H^3_{\infty 2}=S_{\infty c}$ denote the number of relatively non-compact solid components, the number of 1-holes through these solid components, and the number of 2-holes in such solid components, respectively. Again, solids with 3-holes are not considered here since they are compact solids.
- $\vdots$

In summary, the Euler formula for regularly-stratified subanalytic point sets is formed by equating the right-side of (25) to the right-side of (29):

$$\sum_{i=0}^{n}(-1)^i[s^i+\sum_{j=1}^{i}(-1)^j h^j_i]+\sum_{i=1}^{n}(-1)^i[s^i_\infty+\sum_{j=1}^{i-1}(-1)^j h^j_{\infty i}]= \tag{30}$$
$$[C+\sum_{i=1}^{n}(-1)^i H^i]+\sum_{i=1}^{n}(-1)^i[C^i_\infty+\sum_{j=1}^{i-1}(-1)^j H^j_{\infty i}]$$

This algebraic topological invariant is the cornerstone of the design and implementation of the Σ-geometric kernel Euler operators. Its generality allows us to construct geometric objects and engineering artefacts without restrictions on the dimension, compactness, construction order, etc.

3. Euler algebra: the rationale

By definition, an algebra is a set of (undefined) elements and a set of (undefined) operations. Here, our elements are regular stratified subanalytic sets and the operations are Euler operators which satisfy the formula (30). Hence, the *Euler algebra* of regular stratified subanalytic sets. Subanalyticity of a point set guarantees its regular stratification in the sense of Whitney or Thom-Boardman, that is, the topological regularity is *a priori* guaranteed.

To be useful for geometric modelling purposes, an Euler algebra of regular stratified subanalytic sets must be closed. This ensures that the outcome of any Euler operator applied to a regular stratified subanalytic set is also a regular stratified subanalytic set. The closure of this Euler algebra is then guaranteed by observing two points:

- *Stratification closure.* The action of applying an Euler operator to a regular stratified object is also a regular stratified object. That is, the resulting object satisfies the Whitney regularity conditions or Thom regularity condition.
- *Subanalyticity closure.* An object is subanalytic if and only if its constituent strata are subanalytic. This means that subanalyticity of a stratified set is preserved by Euler operators since its constituent strata are all subanalytic sets.

Euler operators are essentially shape operators. They change the shape of an object from many different ways at distinct levels of understanding and describing shape. In general terms, Euler operators carry out shape changes on objects according to the shape taxonomy introduced in Chapter 1, namely:

- *Geometric changes.* The shape changes at the geometric level can be local or global. *Global* geometric changes occur whenever the underlying point set of an object changes, e.g. by attaching or detaching a stratum or by re-defining the geometry of a particular stratum or even the whole object. *Local* geometric changes do not change the underlying point set of an object are due to topological subdivision of a stratum, e.g. the subdivision of a face into two by a new edge.
- *Topological changes.* Topological shape changes also occur locally and globally. They happen whenever the topological properties of any stratum or an object change. *Local* topological changes are related to shape changes on strata. If the number of strata changes, we say that a local topological change has occurred because the local Euler characteristic changes. If we remove an edge bounding a compact face, it becomes a non-compact face, what constitutes a local topological change. Obviously, this local compactness change implies a global compactness change on the whole object. In this case, we say that a *global* topological change has occurred.
- *Homotopic changes.* Homotopic changes are also called *global* topological changes. They are related to the number of holes associated to strata and their ambient object.
- *Differential changes.* They may occur in the resolution of singularities or at setting up the continuity conditions of two touching surfaces.

- *Convex changes.* They occur by changing the geometry of a stratum or an object, e.g. during a morphing operation as usual in animation systems or after detaching a form feature from an object modelled through a CAD system.

Let us see some examples:

EXAMPLE 5.11. Let us take the objects (a) and (b) in Figure 8 and apply the Euler operator $\mathtt{mee_hff_h}$ (*make edge with 1-hole and face with 1-hole*) to (a) to obtain (b). It subdivides a face into two by a new edge e with a 1-hole $\mathtt{e}_h$. The resulting two faces are a simply-connected face f and the original face now reshaped to a face with a 1-hole $\mathtt{f}_h$. So, we can count these shape changes as follows:

Geometric changes. The global geometric shape has not changed because the point set underlying the object has not changed either. But, locally, the geometry of the original face has been re-defined.

Topological changes. The *local* topological changes are: (i) a new edge e has been introduced, (ii) a new face f has been generated by the subdivision of the original face by e.

Homotopic changes. The object has not suffered any *global* topological changes. But, the original face has acquired a new hole after its subdivision by e.

Differential changes. None. All the strata remain smooth.

Convex changes. None. The geometry has not changed.

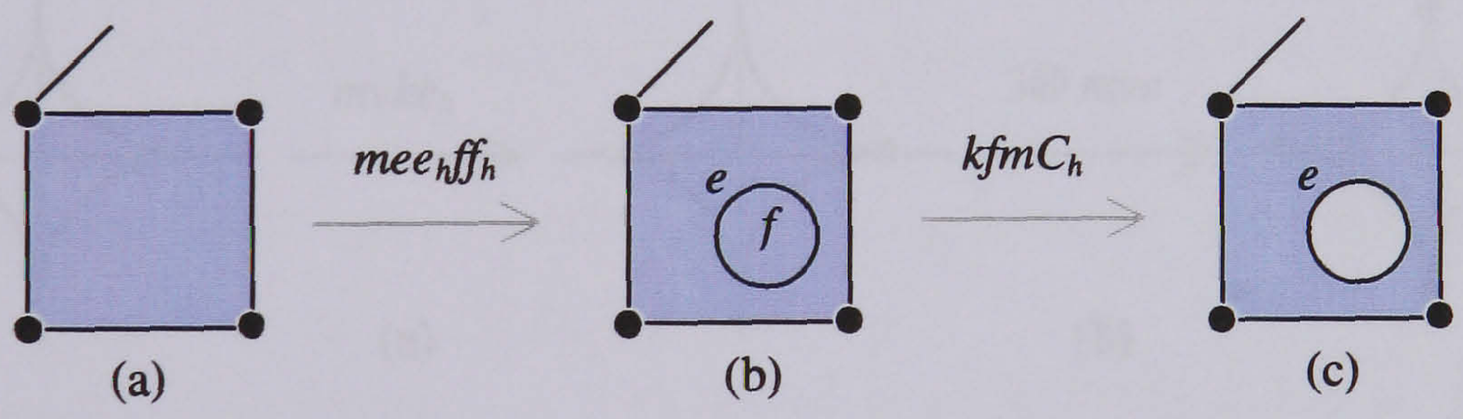

FIGURE 8. Illustrating shape changes through Euler operators.

EXAMPLE 5.12. Let us consider now the object (c) in Figure 8 which is obtained from (b) by applying the Euler operator $\mathtt{kfmC}_h$ (*kill face, make component 1-hole*) to 8(b). It removes the simply-connected face f, from (b). The consequent shape changes are then:

Geometric changes. The point subset corresponding to the simply-connected face f has been deleted. This is a local geometric change that implies a global geometric change on the object.

Topological changes. A face f has been deleted, so the number of strata has changed. This is a local topological change.

Homotopic changes. The removal of f also implies a global topological change on the object. In fact, the hole through the only face of the object (b) has also become a hole through the object (c).

Differential changes. None. All the remaining strata are smooth.

Convex changes. The edge e defines now a concavity in the object.

EXAMPLE 5.13. Let $V = \{(x,y) \in \mathbb{R}^2 : x^{2/3} + y^{2/3} = 1\}$ an 1-dimensional algebraic variety in $\mathbb{R}^2$, Figure 9. It is named astroid. It is also a C^0 manifold, so it can be taken as a topological stratification of itself with just one non-smooth edge e. This edge possesses a 1-hole e_h. However, it has differential singularities at the points $(1,0)$, $(0,1)$, $(-1,0)$, and $(0,-1)$. So, its differential singularities can be "removed" by applying two Euler operators:

mvke$_h$. The operator mvke$_h$ (*make vertex, kill edge 1-hole*) introduces a vertex at the singularity $(1,0)$, breaking up the 1-hole e_h of e, Figure 9(a).

3⊗mve. The Euler operator mve (*make vertex and edge*) is called three times to subdivide the current longest edge into two by a new vertex at each remaining singularity, Figure 9(b) and (c).

At any time we can undo these operators by means of their inverses, getting back —no matter the order— non-smooth strata.

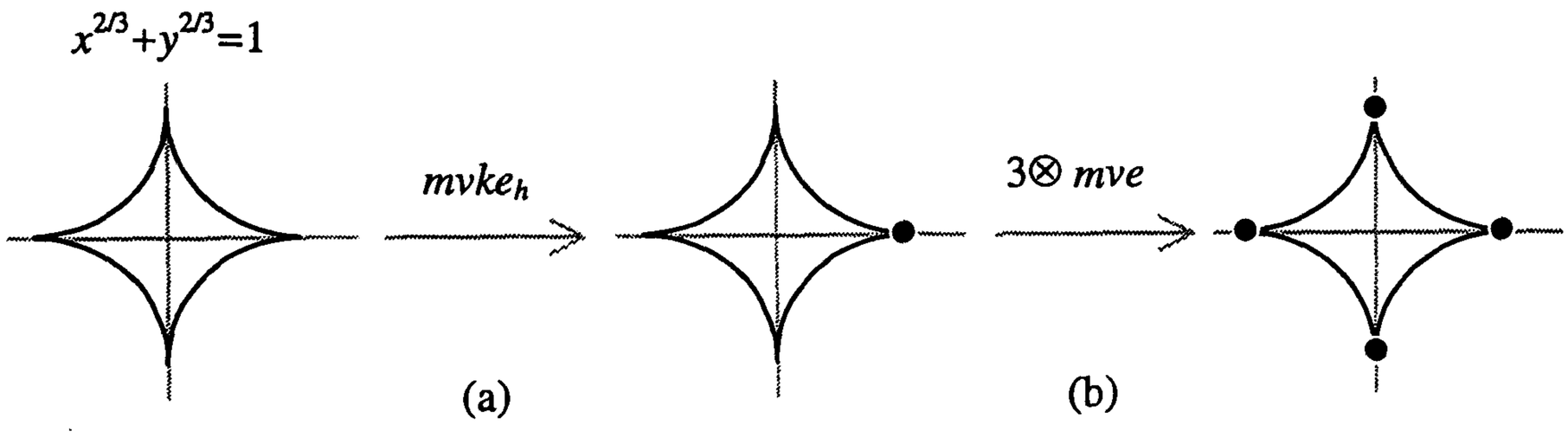

FIGURE 9. Differential shape changes through Euler operators.

As illustrated in Figure 9, Euler operators may carry out differential shape changes on strata, which correspond to subdivisions (also unsubdivisions) of strata into other strata. Note that the resolution of differential singularities on a variety does not change its geometric shape, neither its homotopic shape. What changes is its local topological shape.

In the Σ-geometric kernel there are particularly important Euler operators to handle the compactness of an object and its strata. They are topological operators seeing that they change the topological property of compactness. Some Euler operators act on the non-compact subset of an object, some operators operate on the compact subset of an object, and other operators bridge both subsets.

4. Euler algebra I: family of global hole constructors (SAT)

There two subfamilies of n-hole constructors which use the stratum attaching technique (SAT). The first is defined by attaching a stratum homeomorphic to $\mathbb{R}^n$. The second subfamily is generated by taking an attaching stratum with holes.

4.1. n-hole constructor by attaching a n-stratum homeomorphic to $\mathbb{R}^n$. In this case, we intend to construct a global hole as a result of attaching a stratum homeomorphic to $\mathbb{R}^n$. These Euler operators are then homotopic operators, that is, they operate on the global shape properties of an object. Besides, they are local hole-invariant because the attaching stratum has no holes. In particular, we impose the condition that the dimension of the attaching stratum is equal to the dimension of the resulting global hole. In short, this global hole constructor must satisfy two conditions:

- The attached n-stratum is homeomorphic to $\mathbb{R}^n$, i.e. a n-cell.
- The dimensions of the attached stratum and resulting global hole are identical.

The general n-hole constructor is achieved by using the induction method on the dimension:

(i) mvC, kvC. The operator mvC (*make vertex and Component*) adds a new isolated vertex to an object, and, consequently, a new component, Figure 10(a). Alternatively, Figure 10(b), we can think of this operator as a subdivider for a 0-hole: adding a vertex to 0-hole subdivides this 0-hole into two 0-hole. So, this operator introduces a new 0-stratum $\mathtt{s}^0$ and a new 0-hole $\mathtt{H}^0$, and we can write $\mathtt{mvC}=\mathtt{ms}^0\mathtt{H}^0$. The result is a new 0-sphere in the object. The inverse operator kvC (*kill vertex and Component*) undoes the action of mvC, i.e. it eliminates a 0-hole by the removal of a point-component.

(ii) $\mathtt{meC}_h$, $\mathtt{keC}_h$. The operator $\mathtt{meC}_h$ (*make edge and 1-dimensional Component hole*) creates a 1-hole $\mathtt{H}^1=\mathtt{C}_h$ by attaching a new edge $\mathtt{s}^1=\mathtt{e}$, Figure 11(a). Alternatively, a 1-hole can be generated by subdividing a 1-hole into two 1-holes by a new edge, as illustrated in Figure 11(b). The result is a new 1-sphere in the object. Its inverse Euler operator is $\mathtt{keC}_h$ which eliminates a 1-hole $\mathtt{C}_h$ by deleting a 1-stratum e.

(iii) $\mathtt{mfC}_c$, $\mathtt{kfC}_c$. The Euler operator $\mathtt{mfC}_c$ (*make face and 2-dimensional Component hole*) forms a 2-hole $\mathtt{H}^2=\mathtt{C}_c$ by attaching a new 2-stratum $\mathtt{s}^2=\mathtt{f}$ or face, Figure 12(a). The result is a new 2-sphere in the object. This operator also subdivides a 2-hole into two 2-holes by attaching a new face as depicted in Figure 12(b). The operator $\mathtt{kfC}_c$ undoes a 2-hole by deleting a constituent face, eventually merging two 2-holes.

⋮

(n) $\mathtt{ms}^n\mathtt{H}^n$, $\mathtt{ks}^n\mathtt{H}^n$. The operator $\mathtt{ms}^n\mathtt{H}^n$ encloses a n-hole by attaching a new n-stratum, or, alternatively, subdivides a n-hole into two n-holes by a new n-stratum. Its inverse is the operator $\mathtt{ks}^n\mathtt{H}^n$.

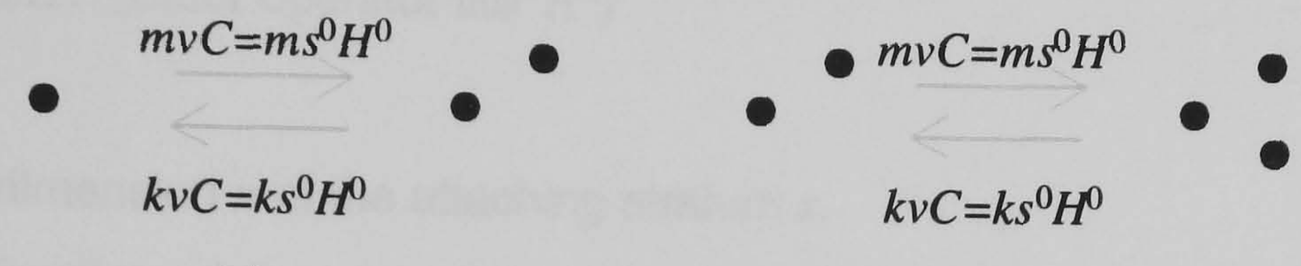

FIGURE 10. The operator mvC: construction of 0-holes.

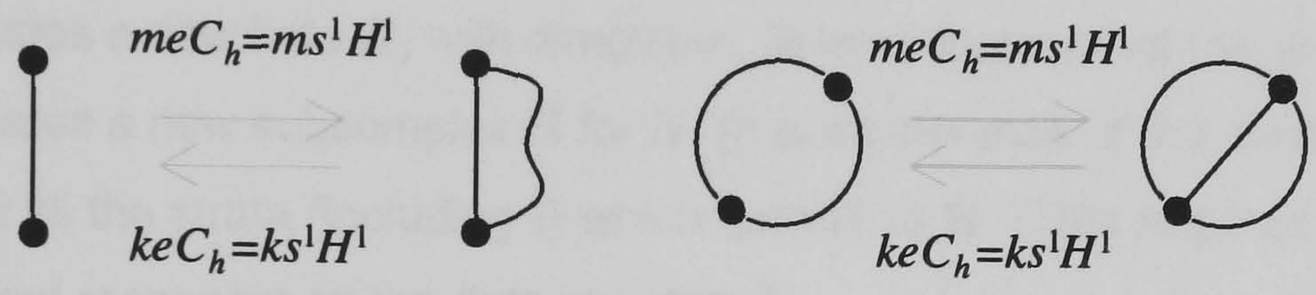

FIGURE 11. The operator $\mathtt{meC}_h$: construction of 1-holes.

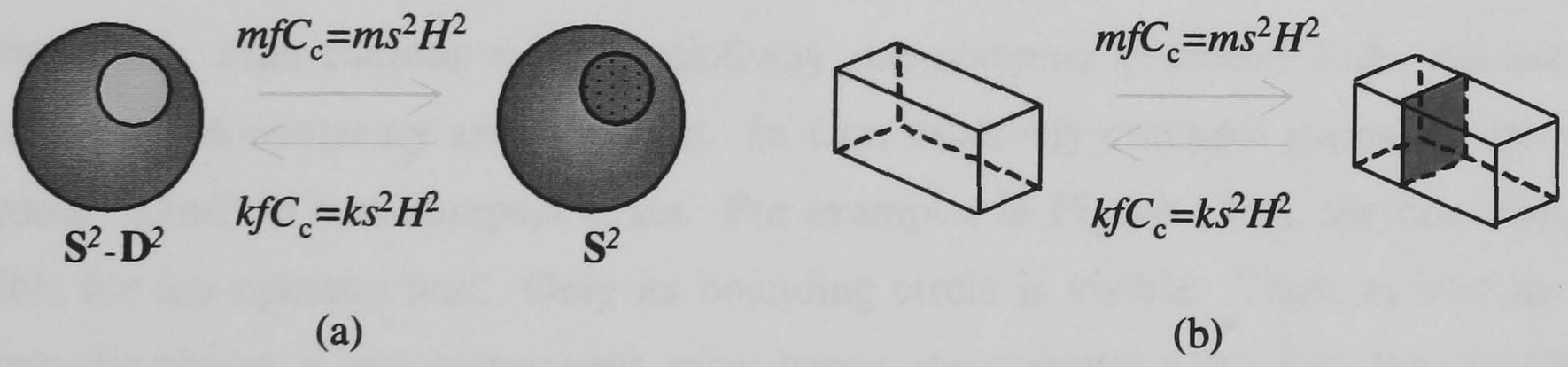

FIGURE 12. The operator $\mathtt{mfC}_c$: construction of 2-holes.

The Algorithm 5.1 for the Euler operator $\mathtt{ms}^n\mathtt{H}^n$ (and its inverse $\mathtt{ks}^n\mathtt{H}^n$) is dimension-independent. There is no need to have a Euler operator for each dimension as usual in 3-dimensional geometric kernels. However, the usual operators mvC, $\mathtt{meC}_h$, and $\mathtt{mfC}_c$, as well as their inverses, have been included in Σ-geometric kernel for convenience of developers of 3D applications. These 3D operators just call the dimension-independent Euler operator $\mathtt{ms}^n\mathtt{H}^n$ (resp. $\mathtt{ks}^n\mathtt{H}^n$) by instantiating the dimension n.

The fact that a global n-hole, say a n-sphere $\mathbb{S}^n$, is formed by attaching a n-stratum implies that the relatively compact subset of the modelling object is to be changed. Thus, we can say that these hole constructors are in the class of relatively *compact* geometry operators. However, as illustrated

in Figure 13, these operators work identically well even in conjunction with relatively non-compact strata.

ALGORITHM 5.1. (Euler operator $\mathtt{ms}^n\mathtt{H}^n$)

INPUT:

(a) the dimension n of the attaching stratum s.

(b) the frontier subcomplex of the attaching stratum s, i.e. a $(n-1)$-cycle.

Begin

(1) Creates a new stratum s, with dim(s)=n. [It is an instance of the class Stratum.]

(2) Set up the frontier relationships between s and the strata of its frontier subcomplex.

(3) Creates a new hole H, with dim(H)=n. [It is an instance of the class Hole.]

(4) Creates a new subcomplex $\mathbf{H}$ for H. [It is an instance of the class Subcomplex.]

(5) Add all the strata (including s) which form H to $\mathbf{H}$. [This requires homotopic and homological reasoning on the data structure.]

(6) Re-arrange possible containment and intersection relationships between the new subcomplex $\mathbf{H}$ and pre-existing subcomplexes.

End

Nevertheless, after running $\mathtt{ms}^n\mathtt{H}^n$, relatively *non-compact* geometry Euler operators must be called to make the necessary arrangements. In fact, relatively compact geometry operators are in some extent 'blind' to non-compact strata. For example, in Figure 13(a), the non-compact face is not visible for the operator mvC. Only its bounding circle is visible. Thus, as long as we insert a vertex into the object, a new component arise; hence, the operator mvC. But, the resulting object is no longer non-compact, so other Euler operators must called to compact the object and its relatively non-compact face. These operators which look for the non-compact subset of an object, as long as those responsible for controlling the compactness of its strata will be detailed ahead.

Analogously, in Figure 13(b), the operator $\mathtt{meC}_h$ ignores the presence of the both non-compact faces in the object. It only recognises the presence of two 1-dimensional components, and thus linking two vertices by a new edge results into a new global 1-hole; hence, the operator $\mathtt{meC}_h$. This easily generalises to higher-dimensional objects.

4.2. n-hole constructor by attaching a n-stratum with a n-hole. Attaching a n-stratum with a n-hole to an object gives rise to the appearance of a global n-hole in the object. Let us see how this works at each dimension.

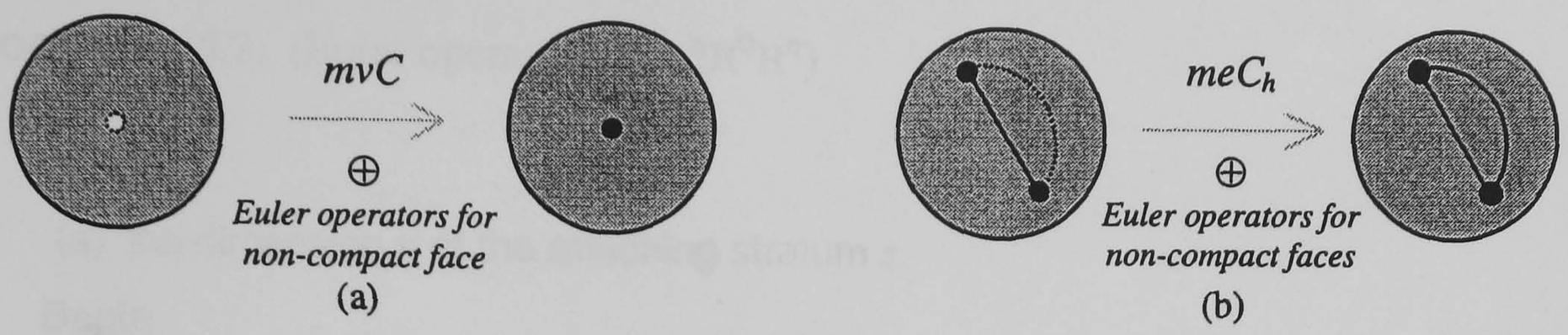

FIGURE 13

(i) $\mathtt{mee}_h\mathtt{CC}_h$, $\mathtt{kee}_h\mathtt{CC}_h$. The Euler operator $\mathtt{mee}_h\mathtt{CC}_h$ forms a 1-sphere $\mathbb{S}^1$ from the empty set. The global 1-hole $\mathtt{H}^1{=}\mathtt{C}_h$ is due to insertion of an edge that contains a 1-hole $\mathtt{h}^1{=}\mathtt{e}_h$. Conversely, the operator $\mathtt{kee}_h\mathtt{CC}_h$ eliminates a global 1-hole by deleting an edge that contains a 1-hole. This is illustrated in Figure 14.

(ii) $\mathtt{mff}_c\mathtt{CC}_c$, $\mathtt{kff}_h\mathtt{CC}_c$. The Euler operator $\mathtt{mff}_h\mathtt{CC}_c$ forms a 2-sphere $\mathbb{S}^2$ from the empty set. The global 2-hole $\mathtt{H}^2{=}\mathtt{C}_c$ comes up by inserting a face with a 2-hole $\mathtt{h}^2{=}\mathtt{f}_c$. Conversely, the operator $\mathtt{kff}_h\mathtt{CC}_c$ undoes a 2-hole by deleting a face with a local 2-hole. This is illustrated in Figure 15.

⋮

(n) $\mathtt{ms}^n\mathtt{h}_n^n\mathtt{H}^0\mathtt{H}^n$, $\mathtt{ks}^n\mathtt{h}_n^n\mathtt{H}^0\mathtt{H}^n$. These operators generalise previous operators to higher dimensions. The superscript n of $\mathtt{h}_n^n$ denotes the dimension of the local hole, while its subscript n denotes the dimension of the hosting stratum $\mathtt{s}^n$.

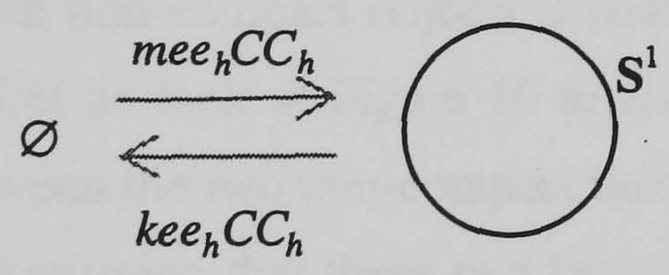

FIGURE 14. The operator $\mathtt{mee}_h\mathtt{CC}_h$.

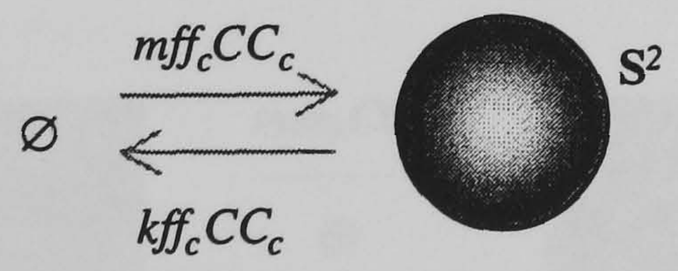

FIGURE 15. The operator $\mathtt{mff}_c\mathtt{CC}_c$.

Note that the stratum attached by this Euler operator has minimum dimension $n = 1$, because a vertex does not have holes. The coresponding algorithm is then as follows:

ALGORITHM 5.2. (Euler operator $\mathrm{ms}^n\mathrm{h}^n_n\mathrm{H}^0\mathrm{H}^n$)

INPUT:

(a) the dimension n of the attaching stratum s.

Begin

(1) Creates a new stratum s, with dim(s)=n. [It is an instance of the class Stratum.]

(2) Creates a new local hole h, with dim(h)=n. [It is an instance of the class Hole.]

(3) Creates a new subcomplex $\mathbf{h}$ for h. [It is an instance of the class Subcomplex.]

(4) Adds s to $\mathbf{h}$.

(5) Creates a new component C. [It is an instance of the class Component.]

(6) Creates a new global hole H, with dim(H)=n. [It is an instance of the class Hole.]

(7) Assigns H to C, and vice-versa.

(8) Creates a new subcomplex $\mathbf{H}$ for H. [It is an instance of the class Subcomplex.]

(9) Adds s to $\mathbf{H}$.

(10) Re-arrange possible containment and intersection relationships between the new subcomplex $\mathbf{H}$ and pre-existing subcomplexes.

End

The operator $\mathrm{ms}^n\mathrm{h}^n_n\mathrm{H}^0\mathrm{H}^n$ clearly belongs to the class of compact geometry operators. But, as for previous operator, its usage with non-compact objects is straightforward, because it ignores the presence of non-compact strata. Let us look at Figure 16 to show how this works. We intend to fill in the 1-dimensional space between the two non-compact faces by inserting a new circular edge, i.e. an edge e with a 1-hole e_h. Assuming that these two faces are absent from the object, such a circular edge comes into the object by applying the operator $\mathrm{mee}_h\mathrm{CC}_h$. The arrangements to be done to validate the resulting object are up to non-compact geometry Euler operators described later.

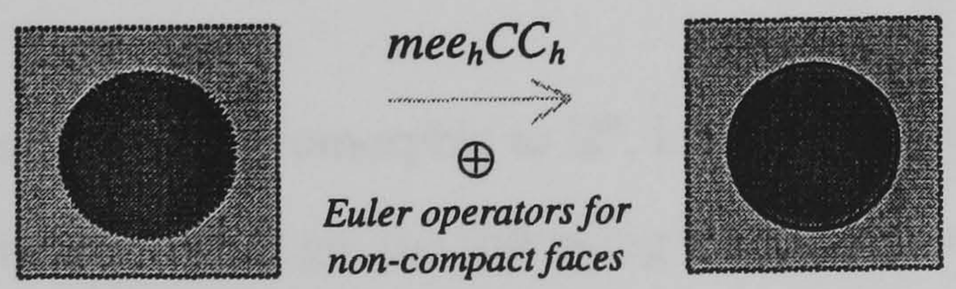

FIGURE 16

5. Euler algebra II: family of global hole constructors (SDT)

There two classes of Euler operators to construct a global $(n-1)$-hole by detaching a n-stratum from an object. Simply-connected strata feature the first class, while the second class generalises the construction of a $(n-1)$-hole by detaching a n-stratum with holes.

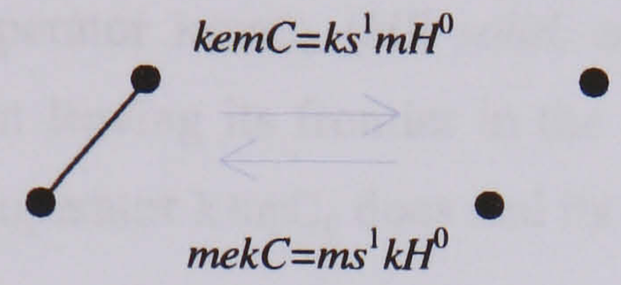

FIGURE 17. The operators kemC and mekC.

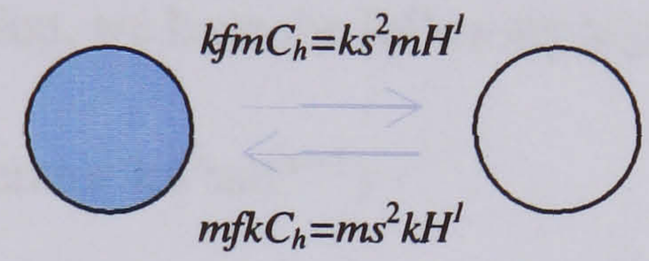

FIGURE 18. The operators $\mathtt{kfmC}_h$ and $\mathtt{mfkC}_h$.

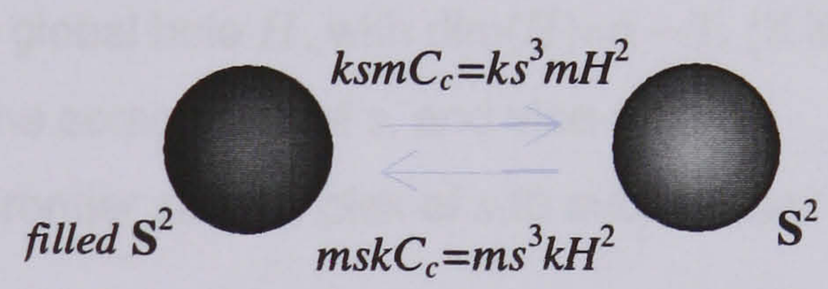

FIGURE 19. The operators $\mathtt{ksmC}_c$ and $\mathtt{mskC}_c$.

5.1. $(n-1)$-hole constructor by detaching a n-stratum without holes. A $(n-1)$-hole can be created by removing a n-stratum. This occurs whenever we remove a n-stratum from an object, but its frontier remains in the object. Its frontier becomes a $(n-1)$-a hole. Thus, the following condition must be satisfied:

- The detaching n-stratum is homeomorphic to $\mathbb{R}^n$, i.e. it is a n-cell.

Using induction on the dimension, we get the following hole constructors at each dimension:

(i) kemC, mekC. The Euler operator kemC (*kill edge, make Component*) generates a 0-hole $\mathtt{H}^0{=}\mathtt{C}$ or component by deleting an edge $\mathtt{s}^1{=}\mathtt{e}$ between two vertices, Figure 17. The operator mekC is its inverse.

(ii) $\mathtt{kfmC}_h$, $\mathtt{mfkC}_h$. The operator $\mathtt{kfmC}_h$ (*kill face, make 1-dimensional Component hole*) creates a 1-hole $\mathtt{H}^1{=}\mathtt{C}_h$ by deleting a face $\mathtt{s}^2{=}\mathtt{f}$ is carried out by the operator $\mathtt{kfmC}_h$, Figure 18. Thus, the frontier of $\mathtt{f}$ becomes a 1-hole in the resulting object. Its inverse is the operator $\mathtt{mfkC}_h$.

(iii) $\mathtt{ksmC}_c$, $\mathtt{mskC}_c$. The operator $\mathtt{ksmC}_c$ (*kill solid, make 2-dimensional Component hole*) deletes a solid $\mathtt{s}^3{=}\mathtt{s}$, but leaving its frontier in the object. Its frontier becomes a 2-hole $\mathtt{H}^2{=}\mathtt{C}_c$. This is what the operator $\mathtt{ksmC}_c$ does and its inverse $\mathtt{mskC}_c$ undoes.

⋮

(n) We abstract these operators and their inverses in higher dimensions as $\mathtt{ks}^n\mathtt{mH}^{n-1}$, $\mathtt{ms}^n\mathtt{kH}^{n-1}$, respectively.

According to this generalisation, we have the following algorithm:

ALGORITHM 5.3. (Euler operator $\mathtt{ks}^n\mathtt{mH}^{n-1}$)

INPUT:

(a) the detaching stratum s.

Begin

(1) Creates a new global hole H, with $\dim(H){=}n-1$. [It is an instance of the class Hole.]

(2) Assigns H to the component of s, and vice-versa.

(3) Promotes the frontier subcomplex of s to subcomplex $\mathbf{H}$ of H.

(4) Removes s.

(5) Re-arrange possible containment and intersection relationships between the re-defined subcomplex $\mathbf{H}$ and pre-existing subcomplexes.

End

5.2. $(n-1)$-hole constructor by detaching a n-stratum with $(n-1)$-holes. Let us consider now a detaching n-stratum with a $(n-1)$-hole. This relaxes the previous condition that the detached stratum must be simply connected. The result is another class of Euler operators that can be also generalised to higher dimensions.

(i) $\mathtt{kff}_h\mathtt{mCC}_h$, $\mathtt{mff}_h\mathtt{kCC}_h$. The $\mathtt{kff}_h\mathtt{mCC}_h$ means *kill face and 1-dimensional local face hole, kill Component and 1-dimensional global Component hole*. Let us look at Figure 20. The idea is to remove a face $\mathtt{f}{=}\mathtt{s}^2$ with a 1-hole $\mathtt{f}_h{=}\mathtt{h}^1_2$ from an object. The result is the appearance of a new component $\mathtt{C}{=}\mathtt{H}^0$ and a new 1-hole $\mathtt{C}_h{=}\mathtt{H}^1$; hence we get the Euler operator $\mathtt{kff}_h\mathtt{mCC}_h$ or $\mathtt{ks}^2\mathtt{h}^1_2\mathtt{mH}^0\mathtt{H}^1$. The operator $\mathtt{mff}_h\mathtt{kCC}_h$ or $\mathtt{ms}^2\mathtt{h}^1_2\mathtt{kH}^0\mathtt{H}^1$ is its inverse.

(ii) $\mathtt{kss}_c\mathtt{mCC}_c$, $\mathtt{mss}_c\mathtt{kCC}_c$. The semantics behind the operator $\mathtt{kss}_c\mathtt{mCC}_c$ (*kill solid and 2-dimensional local solid hole, kill Component and 2-dimensional global Component hole*) is the analogous as for the previous operator. The difference is that now we have solids instead of faces and 2-holes instead of 1-holes. Let us then consider a 2-sphere inside another 2-sphere with the inner 2-sphere filled with material, as well as the space between them, Figure 21. Here the idea is to remove the solid $\mathtt{s}{=}\mathtt{s}^3$ placed between the outer and inner 2-spheres, i.e. a solid with a 2-hole $\mathtt{s}_c{=}\mathtt{h}_3^2$. This 2-hole is nothing more than the inner 2-sphere. Doing so, the result is the appearance of a new component $\mathtt{C}{=}\mathtt{H}^0$ consisting of the outer 2-sphere, and a new 2-hole $\mathtt{C}_c{=}\mathtt{H}^2$ concerning the outer 2-sphere; hence the Euler operator $\mathtt{ks}\,\mathtt{s}_c\mathtt{mCC}_c$ or $\mathtt{ks}^3\mathtt{h}_3^2\mathtt{mH}^0\mathtt{H}^2$. The operator $\mathtt{ms}\,\mathtt{s}_c\mathtt{kCC}_c$ or $\mathtt{ms}^3\mathtt{h}_3^2\mathtt{kH}^0\mathtt{H}^2$ is its inverse.

⋮

(n) For higher dimensions, we get the Euler operators $\mathtt{ks}^n\mathtt{h}_n^{n-1}\mathtt{mH}^0\mathtt{H}^{n-1}$ and $\mathtt{ms}^n\mathtt{h}_n^{n-1}\mathtt{kH}^0\mathtt{H}^{n-1}$.

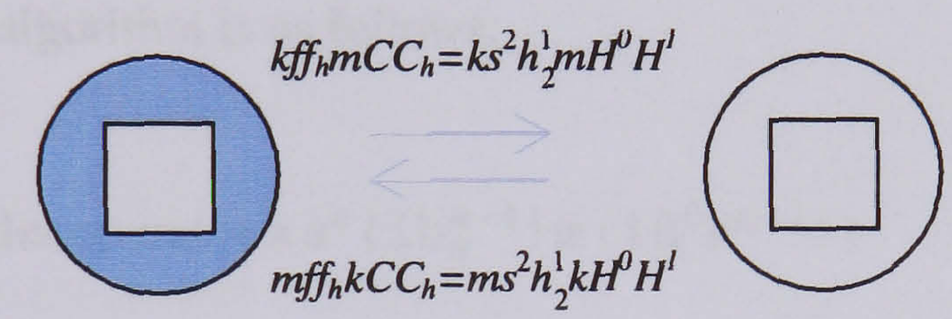

FIGURE 20. The operators $\mathtt{kff}_h\mathtt{mCC}_h$ and $\mathtt{mff}_h\mathtt{kCC}_h$.

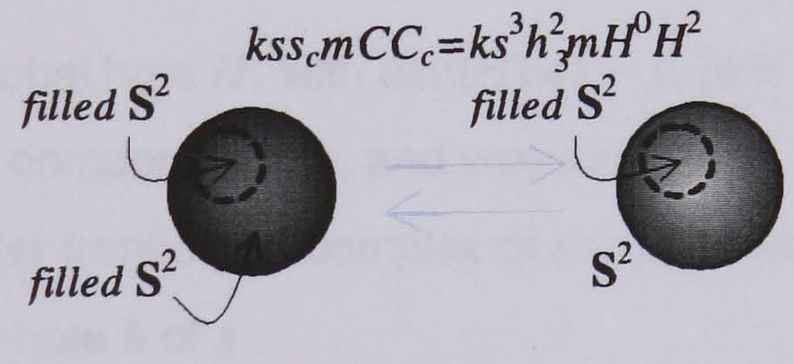

FIGURE 21. The operators $\mathtt{kss}_c\mathtt{mCC}_c$ and $\mathtt{mss}_c\mathtt{kCC}_c$.

We have implicitly assumed that the removing stratum had only one hole. But, if the removing stratum has more holes, the operator is no longer correct. In order to overcome this difficulty, a more general operator must be used. So, if a removing n-stratum has i number of $(n-1)$-holes, we have the Euler operator $\mathtt{ks}^n\,(\mathtt{ih}_n^{n-1})\,\mathtt{m}\,(\mathtt{iH}^0)\,\mathtt{H}^{n-1}$, being $\mathtt{ms}^n\,(\mathtt{ih}_n^{n-1})\,\mathtt{k}\,(\mathtt{iH}^0)\,\mathtt{H}^{n-1}$ its inverse. This is illustrated in Figure 22 for a face with $i=2$ number of 1-holes. Deleting this face we get two new components, each for a 1-hole.

Note that each $(n-1)$-dimensional local hole of the n-stratum originates a $(n-1)$-dimensional global hole in the resulting object. This means that, we have to be sure that each $(n-1)$-dimensional

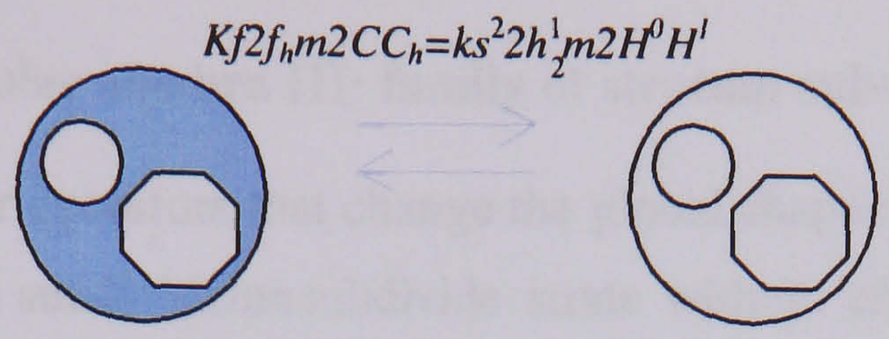

FIGURE 22. The operator $\mathtt{kf2f}_h\mathtt{m2CC}_h$.

local hole will be part of a single global component after removing the n-stratum. But, this is should be decided by the geometric kernel engine, not by an Euler operator. This means that the geometric kernel engine observe a set of rules that determine how a stratum is detached. In other words, which Euler operators are called when the user or programmer wants to remove a stratum.

So, the corresponding algorithm is as follows:

ALGORITHM 5.4. (Euler operator $\mathtt{ks}^n(\mathtt{ih}_n^{n-1})\mathtt{m}(\mathtt{iH}^0\mathtt{H}^{n-1})$)

INPUT:

(a) the detaching stratum s.

Begin

(1) Creates a new global hole H, with dim(H)=$n-1$. [It is an instance of the class Hole.]

(2) Assigns H to the component of s, and vice-versa.

(3) Promotes the outer frontier subcomplex of s to subcomplex $\mathbf{H}$ of H.

(4) **For** each $(n-1)$-hole h of s

Begin

(i) Determines the $(n-1)$-hole H of the object that coincides with h.

(ii) Creates a new component C. [It is an instance of the class Component.]

(iii) Assigns H to C, and vice-versa.

(iv) Removes h.

End

(5) Removes s.

(6) Re-arrange possible containment and intersection relationships between the re-defined subcomplex $\mathbf{H}$ and pre-existing subcomplexes.

End

6. Euler algebra III: family of stratum subdividers

We have described Euler operators that change the global shape of an object. Let us concentrate now on operations that just subdivide/unsubdivide strata without changing the global shape of an object. A *subdivider* is an Euler operator that subdivides a n-stratum into two n-strata and a $(n-1)$-stratum, called the subdividing stratum.

6.1. n-stratum subdivider by a $(n-1)$-stratum without holes. The Euler operators `mve` (*make vertex and edge*), `mef` (*make edge and face*), and `mfs` (*make face and solid*) are the usual subdividers in B-Rep geometric kernels; their inverses `kve`, `kef`, and `kfs` are the corresponding coalescers. In the Σ-geometric kernel, subdivision operators encapsulate the dimension-independent Euler operator $\mathtt{ms}^{n-1}\mathtt{s}^n$, while coalescing operators encapsulate the inverse dimension-independent Euler operator $\mathtt{ks}^{n-1}\mathtt{s}^n$. Note that the subdividing stratum $\mathtt{s}^{n-1}$ has a dimension $n-1$ and the subdivided stratum $\mathtt{s}^n$ has a dimension n. In addition to conventional subdividers for compact strata, this operator $\mathtt{ms}^{n-1}\mathtt{s}^n$ is also encapsulated by subdividers for non-compact strata in the data structure.

Thus, these operators can be characterised by:

- *Key feature.* A stratum is cut off into two equidimensional strata. More precisely, n-stratum is split into three pieces: two n-strata and one $(n-1)$-stratum, called the subdividing stratum.
- *Shape invariance.* Subdivision and coalescence Euler operators do not change the global or homotopic shape of an object. Besides, the resulting three strata are all point subsets of the original stratum, what means that the geometric shape of the object is not changed either.
- *Compactness invariance.* They do not depend on the compactness of the stratum to be subdivided. That is, the operator works identically well for relative compact and non-compact strata.

So, this local-invariant T-shaped Euler operator only must satisfy two conditions:

- The subdividing $(n-1)$-stratum is homeomorphic to $\mathbb{R}^{n-1}$, i.e. it is a $(n-1)$-cell.
- The dimension of the subdivided stratum is n.

Let us see this subdivision Euler operator at each dimension:

(i) `mve`, `kve` [edge subdivider (coalescer)]. The operator `mve` (*make vertex and edge*) subdivides an edge into two by a new vertex. In first case, Figure 23(a), the vertex subdivides a non-compact edge into two non-compact edges; hence we have $\mathtt{mve}_\infty$. In the second case,

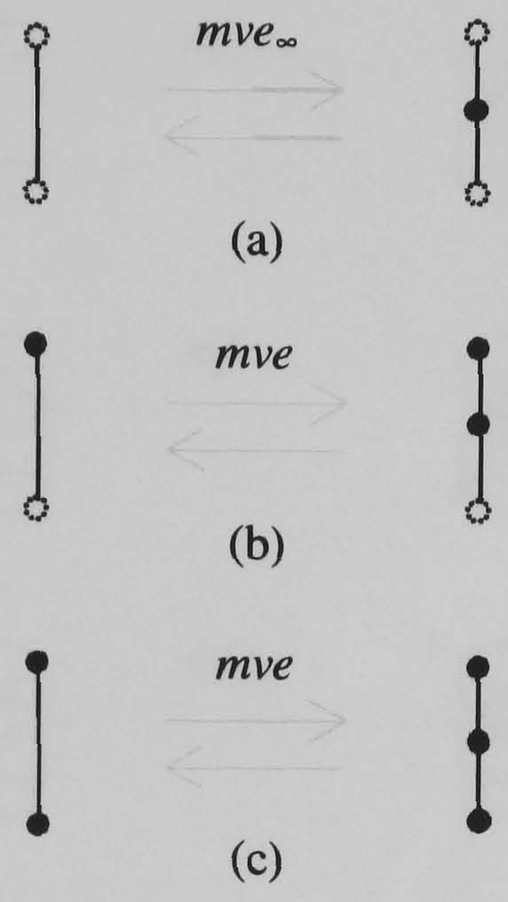

FIGURE 23. The operators mve and $\texttt{mve}_\infty$ to subdivide an edge by a new vertex.

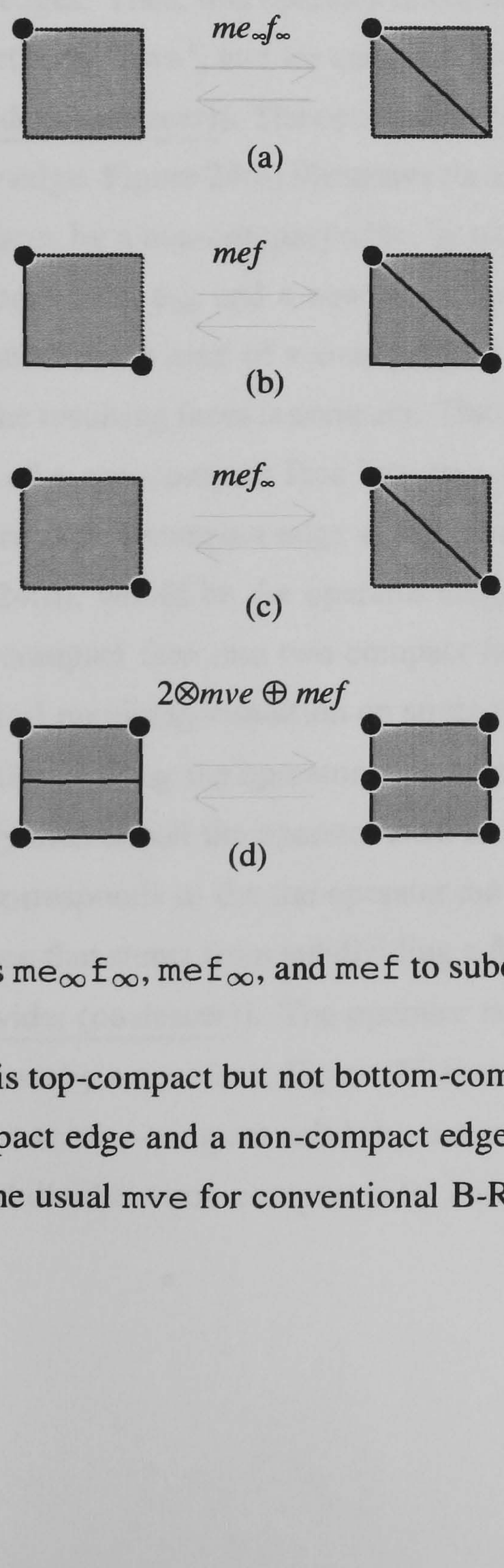

FIGURE 24. The operators $\texttt{me}_\infty\texttt{f}_\infty$, $\texttt{mef}_\infty$, and mef to subdivide a face by a new edge.

Figure 23(b), the edge is top-compact but not bottom-compact, so the subdivision by a vertex gives rise to a compact edge and a non-compact edge; hence, we have mve. The third case, Figure 23(c), is the usual mve for conventional B-Reps, which subdivides a compact

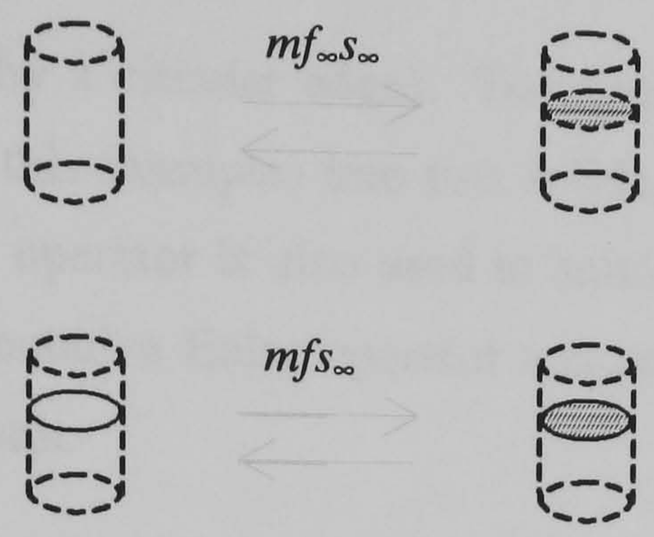

FIGURE 25. The operators $\mathtt{mf}_\infty\mathtt{s}_\infty$, $\mathtt{mfs}_\infty$, and $\mathtt{mfs}$ to subdivide a solid by a new face.

edge into two compact edges. Thus, this operator introduces a new vertex $\mathtt{v}=\mathtt{s}^0$ and a new (eventually non-compact) edge $\mathtt{e}=\mathtt{s}^1$, and we can write $\mathtt{mve}=\mathtt{ms}^0\mathtt{s}^1$.

(ii) `mef`, `kef` [face subdivider (coalescer)]. The operator `mef` (*make edge and face*) subdivides a face into two by a new edge. Figure 24(a) illustrates the subdivision of a non-compact face into two non-compact faces by a non-compact edge, by using the operator $\mathtt{me}_\infty\mathtt{f}_\infty$. So, we obtain a new non-compact edge $\mathtt{e}_\infty$ and a new non-compact face $\mathtt{f}_\infty$. The second case, in Figure 24(b), is the subdivision `mef` of a non-compact face into two faces by a compact edge. Note that one of the resulting faces is compact. The third case, in Figure 24(c), depicts the subdivision $\mathtt{mef}_\infty$ of a non-compact face into two non-compact faces by a compact edge. The new strata are now a compact edge `e` and a non-compact face $\mathtt{f}_\infty$. A possible fourth case, in Figure 24(d), would be the operator $\mathtt{me}_\infty\mathtt{f}$, but it is meaningless because we cannot subdivide a compact face into two compact faces by a new non-compact edge. Otherwise, the topological regularity condition on strata is broken. Thus, geometric engine must manage this situation, calling the operator `mve` twice to subdivide each vertical edge by a new vertex, an only then to call the operator `mef` as usual. In short, the subdivision of a face by a new edge corresponds to the the operator $\mathtt{ms}^1\mathtt{s}^2$, where $\mathtt{s}^1$ a new subdividing edge and $\mathtt{s}^2$ is a new face that stems from subdividing a face.

(iii) `mfs`, `kfs` [solid subdivider (coalescer)]. The operator $\mathtt{mfs}=\mathtt{ms}^2\mathtt{s}^3$ (*make face and solid*) subdivides a solid into two by a new face. Figure 25(a) shows the subdivision $\mathtt{mf}_\infty\mathtt{s}_\infty$ of a non-compact solid into two non-compact solids by a new non-compact face. The operator $\mathtt{mfs}_\infty$, Figure 25(b), subdivides a non-compact solid into two non-compact solids by a new

compact face (bounded by a circular edge). The operator mfs, Figure 25(c), subdivides a non-compact solid (in this example) into two solids, being the new solid compact, by a new compact face. This operator is also used to subdivide a compact solid by a compact face. In respect to the tentative Euler operator $\mathtt{mf}_{\infty}\mathtt{s}$, once again we have a topological regularity-breaking operator.

⋮

(n) Thus, by generalisation, we obtain the dimension-independent operators $\mathtt{ms}^{n-1}\mathtt{s}^n$ (respectively, $\mathtt{ks}^{n-1}\mathtt{s}^n$) to subdivide (respectively, coalesce) a n-stratum into two by a simply-connected $(n-1)$-stratum.

The corresponding algorithm is as follows:

ALGORITHM 5.5. (Euler operator $\mathtt{ms}^{n-1}\mathtt{s}^n$)

INPUT:

(a) the n-stratum t to be subdivided.

(b) the frontier subcomplex b of the subdividing $(n-1)$-stratum s.

Begin

(1) Subdivides the boundary subcomplex c of t into two subcomplexes, c^* and c_1, by the frontier subcomplex b of s. [c^* is c reshaped after subtracting the strata going into c_1. The boundary subcomplex c_1 is created just before this transference of strata by instantiating the class Subcomplex.]

(2) Adds b to c^* and c_1.

(3) Creates the new subdividing stratum s with dim(s)=$n-1$. [It is an instance of the class Stratum.]

(4) Adds s to c^* and c_1.

(5) Creates a new stratum t_1, with dim(t_1)=n, as a result of the subdivision of t into t^* and t_1. [It is an instance of the class Stratum.]

(6) Updates the bounding relationships between t^* and c^*.

(7) Sets up the bounding relationships between t_1 and c_1.

(8) Re-arrange possible containment and intersection relationships between the re-defined subcomplex **H** and pre-existing subcomplexes.

End

6.2. n-stratum subdivider by a $(n-1)$-stratum with a $(n-1)$-hole. Unlike the first class of stratum subdividers (respectively, coalescers), this second class *directly* change the homotopic shape

of the stratum to be subdivided. These shape changes result from inserting a $(n-1)$-dimensional hole in such a stratum. However, these subdividers do not introduce any global holes in the object, i.e. they do not imply global shape changes. Thus, a n-stratum subdivider by a $(n-1)$-stratum with a $(n-1)$-hole is a topological operator.

To understand how it works, let us remember that the simpler $(n-1)$-dimensional hole is $\mathbb{S}^{n-1}$. Moreover, a $(n-1)$-hole may be the frontier of a n-stratum. Thus, a $(n-1)$-hole only exists in a n-dimensional Euclidean space ($i > n$), possibly bounding a n-stratum. For example, $\mathbb{S}^0$ is embeddable in $\mathbb{R}^{>0}$, $\mathbb{S}^1$ is embeddable in $\mathbb{R}^{>1}$, $\mathbb{S}^2$ is embeddable in $\mathbb{R}^{>2}$, and so on.

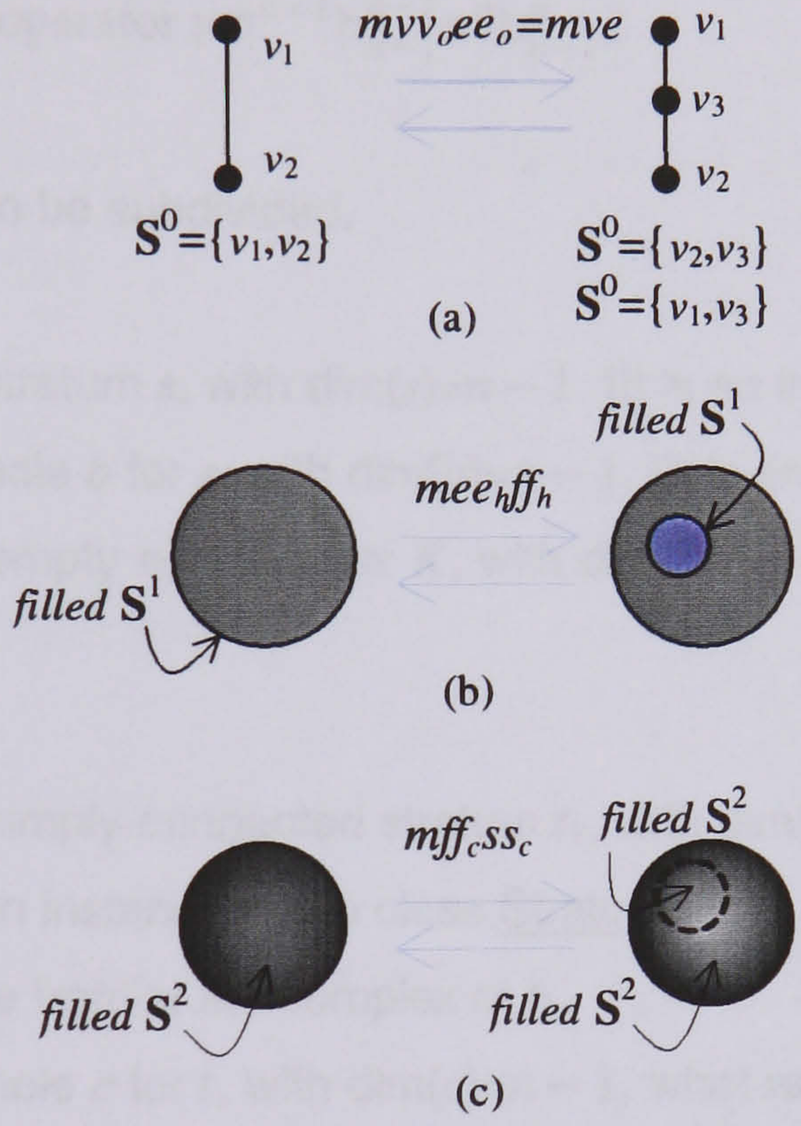

FIGURE 26. Subdivision operators by holes.

This suggests that, once again, we can use the induction method on dimension to define a dimension-independent subdivider denoted by $\mathtt{ms}^{n-1}\mathtt{h}_{n-1}^{n-1}\mathtt{s}^{n}\mathtt{h}_{n-1}^{n}$, where $\mathtt{h}_i^j$ denotes a j-hole in a i-stratum:

(i) $\mathtt{mee}_h\mathtt{ff}_h$, $\mathtt{kee}_h\mathtt{ff}_h$ [subdivider (coalescer) of a face by 1-hole $\mathbb{S}^1$]. The operator $\mathtt{mee}_h\mathtt{ff}_h$ (*make edge, 1-dimensional edge hole, face and 1-dimensional face hole*) subdivides a face into two faces by an edge with a 1-dimensional hole. This edge is homeomorphic to $\mathbb{S}^1$, which leaves a 1-hole in the original face. So, the corresponding Euler operator is $\mathtt{mee}_h\mathtt{ff}_h$ or $\mathtt{ms}^1\mathtt{h}_1^1\mathtt{s}^2\mathtt{h}_2^1$. This is illustrated in Figure 26(a).

(ii) $\mathtt{mff}_c\mathtt{ss}_c$, $\mathtt{kff}_c\mathtt{ss}_c$ [subdivider (coalescer) of a solid by 2-hole $\mathbb{S}^2$]. The operator $\mathtt{mff}_c\mathtt{ss}_c$ (*make face, 2-dimensional face hole, solid and 2-dimensional solid hole*) or $\mathtt{ms}^2\mathtt{h}_2^2\mathtt{s}^3\mathtt{h}_2^3$

subdivides a solid into two solids by a 2-hole, i.e. a hole homeomorphic $\mathbb{S}^2$ or 2-sphere. The 2-hole is filled in by the new solid. This is illustrated in Figure 26(b).

⋮

(n) Thus, by generalisation, we obtain the dimension-independent operators $\mathtt{ms}^{n-1}\mathtt{h}_{n-1}^{n-1}\mathtt{s}^{n}\mathtt{h}_{n}^{n-1}$ (respectively, $\mathtt{ks}^{n-1}\mathtt{h}_{n-1}^{n-1}\mathtt{s}^{n}\mathtt{h}_{n}^{n-1}$) to subdivide (respectively, coalesce) a n-stratum into two by a $(n-1)$-stratum with a $(n-1)$-hole.

The algorithm is as follows:

ALGORITHM 5.6. (Euler operator $\mathtt{ms}^{n-1}\mathtt{h}_{n-1}^{n-1}\mathtt{s}^{n}\mathtt{h}_{n-1}^{n}$)

INPUT:

(a) the n-stratum t to be subdivided.

Begin

(1) Creates a new stratum s, with dim(s)=$n-1$. [It is an instance of the class Stratum.]

(2) Creates a new hole b for s, with dim(b)=$n-1$. [It is an instance of the class Hole.]

(3) Creates a new empty subcomplex K, with dim(K)=$n-1$. [It is an instance of the class Subcomplex.]

(4) Adds s to K.

(5) Creates a new simply-connected stratum t_1, with dim(t_1)=n, as a result of splitting t into t^* and t_1. [It is an instance of the class Stratum.]

(6) Sets up K as the frontier subcomplex of t_1.

(7) Creates a new hole c for t, with dim(c)=$n-1$, what reshapes t into t^*. [It is an instance of the class Hole.]

(8) Sets up K as a new frontier subcomplex for t^*.

(9) Sets up K as the subcomplex for c.

(10) Re-arrange possible containment and intersection relationships between the re-defined subcomplex $\mathbf{H}$ and pre-existing subcomplexes.

End

6.3. Subdivider of a n-stratum with a n-hole by a $(n-1)$-stratum with a $(n-1)$-hole. Let us consider a n-stratum with a n-hole; for example, the 2-sphere $\mathbb{S}^2$ is a 2-stratum with a 2-hole. The idea here is to subdivide $\mathbb{S}^2$ by $\mathbb{S}^1$ (a 1-stratum with a 1-hole). The outcome consists of two faces without holes, but the global 2-hole remains. Thus, the global or homotopic shape of the original object is unchanged by local subdivision of a stratum. However, the local or homotopic shape of the subdivided stratum changes. The result is a local shape operator.

(i) $\mathtt{mee}_h\mathtt{fkf}_c$, $\mathtt{kee}_h\mathtt{fmf}_c$ [subdivider (coalescer) of a face with a 2-hole by 1-hole $\mathbb{S}^1$]. The operator $\mathtt{mee}_h\mathtt{fkf}_c$ (*make edge, 1-dimensional edge hole, and face, kill 2-dimensional face hole*) subdivides a face with a 2-hole into two faces without 2-holes by a edge with a 1-dimensional hole, as illustrated in Figure 27. Thus, $\mathtt{mee}_h\mathtt{fkf}_c=\mathtt{ms}^1\mathtt{h}_1^1\mathtt{s}^2\mathtt{kh}_2^2$ subdivides a 2-stratum with a 2-hole $\mathtt{f}_c=\mathtt{h}_2^2$ by a 1-stratum $\mathtt{e}=\mathtt{s}^1$ with a 1-hole $\mathtt{e}_h=\mathtt{h}_1^1$ implies the disappearance of the former 2-hole in the 2-stratum.

$\vdots$

(n) Generalising this operator to higher dimensions, we have the dimension-independent Euler operator $\mathtt{ms}^{n-1}\mathtt{h}_{n-1}^{n-1}\mathtt{s}^n\mathtt{kh}_n^n$, that is, the subdivider of a n-stratum with a n-hole by a $(n-1)$-stratum with a $(n-1)$-hole. The corresponding coalescer is then $\mathtt{ks}^{n-1}\mathtt{h}_{n-1}^{n-1}\mathtt{s}^n\mathtt{mh}_n^n$.

The algorithm is as follows:

ALGORITHM 5.7. (Euler operator $\mathtt{ms}^{n-1}\mathtt{h}_{n-1}^{n-1}\mathtt{s}^n\mathtt{kh}_n^n$)

INPUT:

(a) the n-stratum t to be subdivided.

PRE-CONDITION:

(a) t has the shape of a n-hole.

Begin

(1) Creates a new (subdividing) stratum s, with $\dim(s)=n-1$. [It is an instance of the class Stratum.]

(2) Creates a new hole b for s, with $\dim(b)=n-1$. [It is an instance of the class Hole.]

(3) Creates a new empty subcomplex K, with $\dim(K)=n-1$. [It is an instance of the class Subcomplex.]

(4) Adds s to K.

(5) Sets up b has hole of s.

(6) Creates a new simply-connected stratum t_1, with $\dim(t_1)=n$, as a result of splitting t into t^* and t_1. [It is an instance of the class Stratum.]

(7) Sets up K as the frontier subcomplex of t_1.

(8) Sets up K as the frontier subcomplex of t^*. [t^* is the reshaped t after subdivision.]

(9) Re-arrange possible containment and intersection relationships between the re-defined subcomplex $\mathbf{H}$ and pre-existing subcomplexes.

End

FIGURE 27. The Euler operator $\mathtt{mee}_h\mathtt{fkf}_c$.

7. Euler algebra IV: family of *local* hole constructors

Local hole constructors change the homotopic shape of strata, but not the homotopic shape of an object. Thus, these operators are local shape operators. As shown in the sequel, these operators can be considered as *partial* stratum coalescers. Thus, the point set or geometry of the underlying object is not changed.

There are two subclasses of local hole constructors:

(i) The first makes use of a Stratum Merging Technique (STA): two adjacent strata are merged into one. Because the merging involves two, instead of three strata, we say that this class is also a class of partial stratum coalescers.

(ii) The second follows a Stratum Emerging Technique (SET): a manifold point subset of dimension m of a n-stratum, with $(m < n)$ emerges as or is transformed into a m-stratum. That is, the original n-stratum is split into two, instead three, strata: a n-stratum a m-stratum.

Therefore, a pre-condition must be satisfied: both merging stratum (first case) and emerging stratum (second case) cannot possess any holes; otherwise, they fall in a different class of operators.

7.1. Local hole constructors by merging a stratum. These operators must observe that following pre-conditions:

- A merging stratum nust be void of holes; otherwise, the merging operation would involve three strata, instead of two.
- A merging stratum cannot be part of any cycle of the same dimension bounding the absorbing stratum; otherwise, the merging operation would involve three strata, instead of two.

It is worthy to note the following:

- A merging n-stratum need not to be relatively closed in the object, because the first pre-condition imposes that it is homeomorphic to $\mathbb{R}^n$.
- As a first consequence, the frontier of the 'disappearing' stratum is not required to exist in the object.

- As a second consequence, a merging stratum is not required to be a cut stratum for the boundary of the absorbing stratum. Equivalently, the merge does not necessarily cause the separation of the boundary of the absorbing stratum into two boundary components.

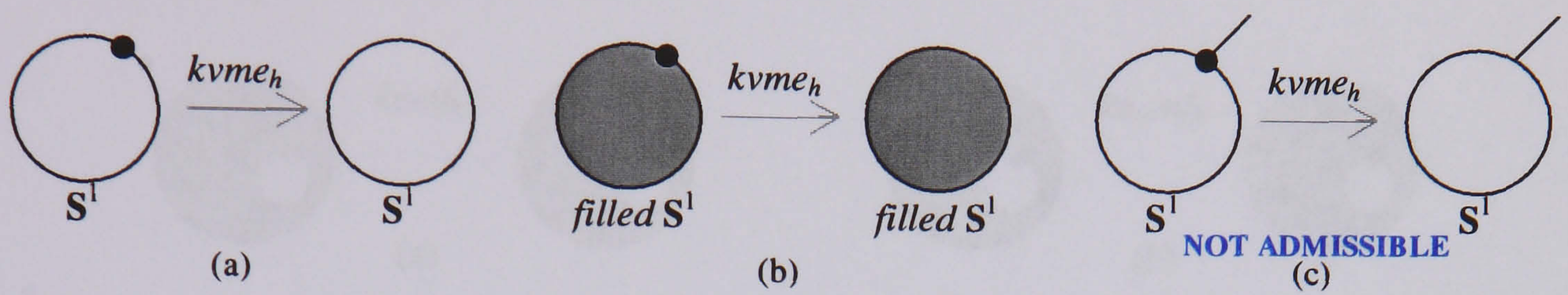

FIGURE 28. The Euler operator $\mathtt{kvme}_h$.

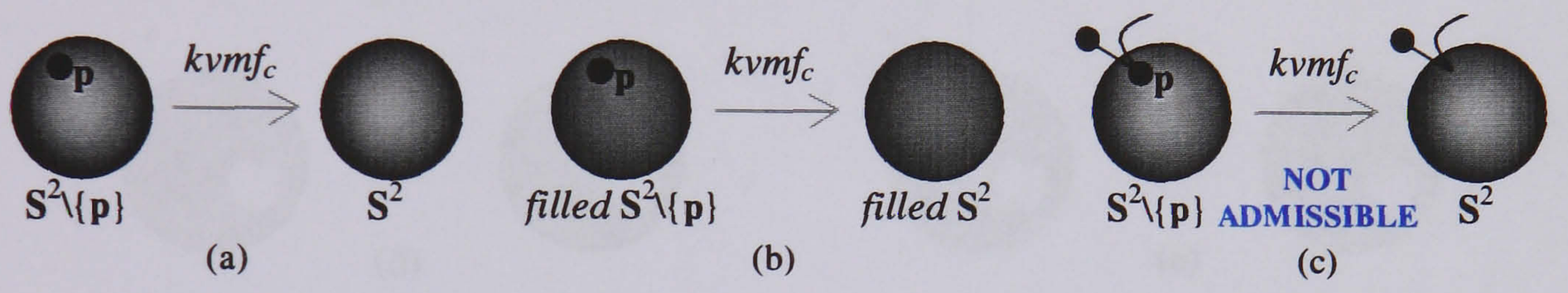

FIGURE 29. The Euler operator $\mathtt{kvmf}_c$.

Let us consider the local n-hole constructors by merging a **vertex** with a stratum of dimension > 0:

(i) $\mathtt{kvme}_h$, $\mathtt{mvke}_h$ [*Vertex* bounding edge]. The operator $\mathtt{kvme}_h$ (*kill vertex, make 1-dimensional edge hole*) also $\mathtt{ks}^0\mathtt{mh}_1^1$, merges a vertex $\mathtt{v}$ with its bounding edge, which homeomorphic to $\mathbb{R}$ The result is a 1-dimensional edge hole $\mathtt{e}_h$, Figure 28(a). Note that $\mathtt{v}$ cannot bound any other edges; otherwise, the topological regularity condition is broken, Figure 28(c).

(ii) $\mathtt{kvmf}_c$, $\mathtt{mvkf}_c$ [*Vertex* bounding face.] The operator $\mathtt{kvmf}_c$ (*kill vertex, make 2-dimensional face hole*), also $\mathtt{ks}^0\mathtt{mh}_2^2$, merges a vertex $\mathtt{v}$ with its bounding face, which homeomorphic to $\mathbb{R}^2$. The result is a 2-dimensional face hole $\mathtt{f}_c$, Figure 29(a). Analogously, $\mathtt{v}$ cannot bound any other faces, in order to keep topological regularity on the stratification, Figure 29(c).

⋮

(n) $\mathtt{kvmh}_n^n$, $\mathtt{mvkh}_n^n$ [*Vertex* bounding n-stratum.] The operator $\mathtt{kvmh}_n^n$ (*kill vertex, make n-dimensional stratum hole*), also $\mathtt{ks}^0\mathtt{mh}_n^n$, merges a vertex with an absorbing n-stratum, what originates a new n-hole $\mathtt{h}_n^n$ in the n-stratum. The operator $\mathtt{mvkh}_n^n$ is its inverse operator.

The $\mathtt{kvmh}^n_n$ is only operator of this class that is inherently a compact Euler operator because the result is always a n-stratum with a n-hole, i.e. a relatively compact edge. However, its performance is not affected whether the resulting n-stratum with a n-hole bounds a relatively compact stratum, a relatively non-compact stratum, or neither.

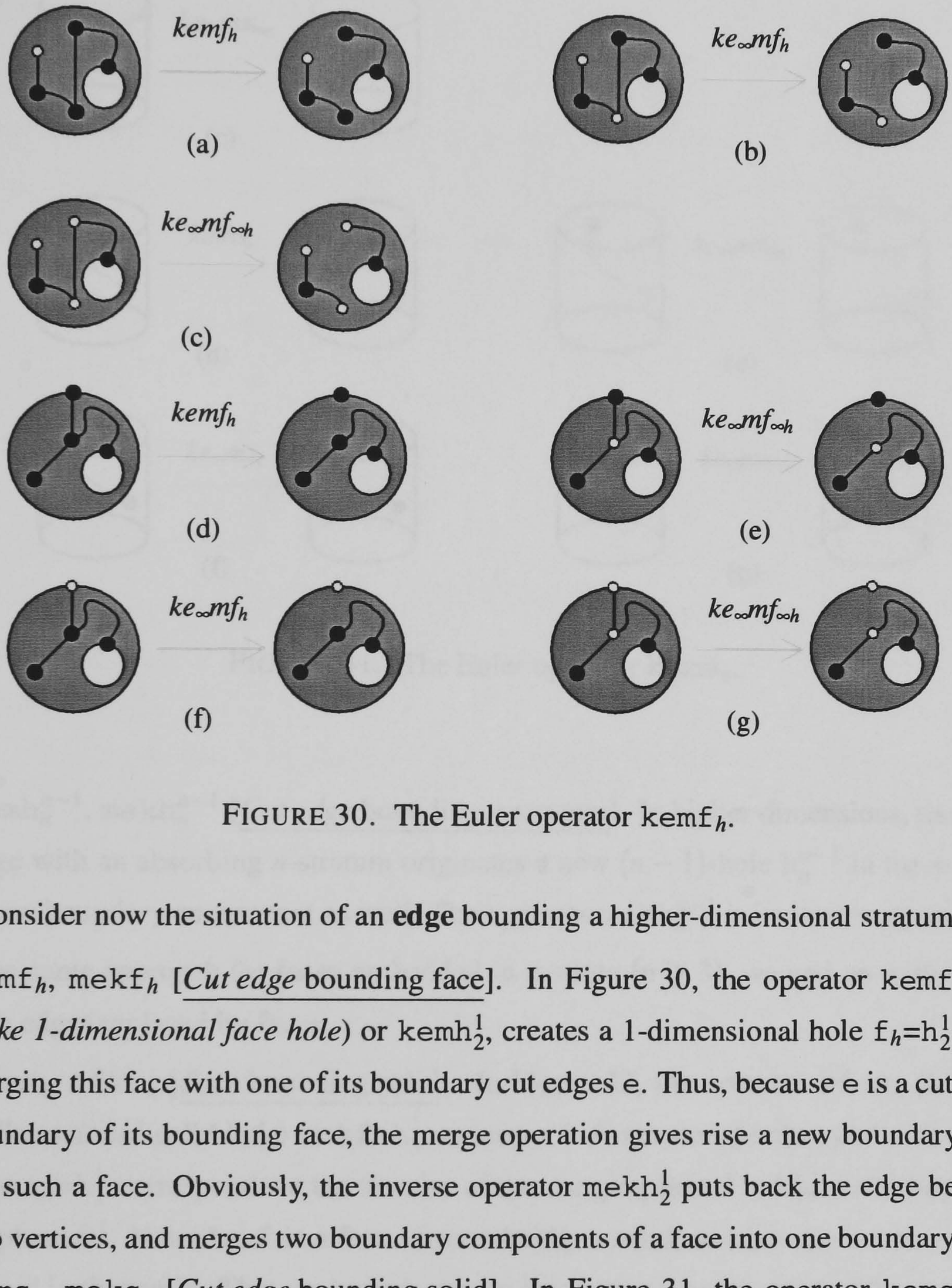

FIGURE 30. The Euler operator $\mathtt{kemf}_h$.

Let us consider now the situation of an **edge** bounding a higher-dimensional stratum:

(i) $\mathtt{kemf}_h$, $\mathtt{mekf}_h$ [*Cut edge* bounding face]. In Figure 30, the operator $\mathtt{kemf}_h$ (*kill edge, make 1-dimensional face hole*) or $\mathtt{kemh}^1_2$, creates a 1-dimensional hole $\mathtt{f}_h=\mathtt{h}^1_2$ in a face by merging this face with one of its boundary cut edges e. Thus, because e is a cut edge for the boundary of its bounding face, the merge operation gives rise a new boundary component for such a face. Obviously, the inverse operator $\mathtt{mekh}^1_2$ puts back the edge between those two vertices, and merges two boundary components of a face into one boundary component.

(ii) $\mathtt{kems}_c$, $\mathtt{meks}_c$ [*Cut edge* bounding solid]. In Figure 31, the operator $\mathtt{kems}_c$ (*kill edge, make 2-dimensional solid hole*) or $\mathtt{kemh}^2_3$, creates a 2-dimensional hole $\mathtt{s}_c=\mathtt{h}^2_3$ in a solid by merging it with one of its boundary cut edges e. Obviously, this originates a new boundary component for the absorbing solid.

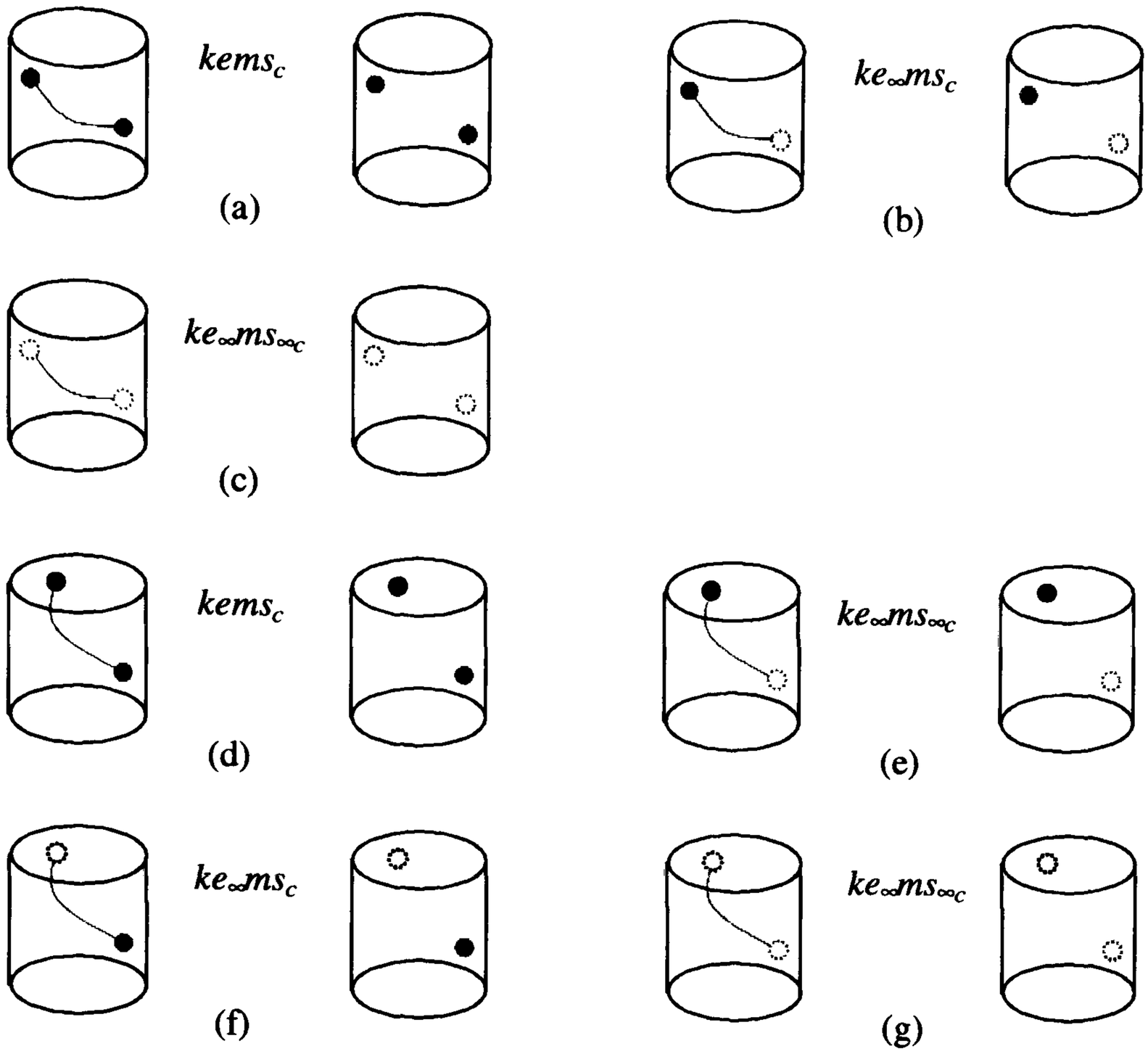

FIGURE 31. The Euler operator $\texttt{kems}_c$.

$\vdots$

(n) $\texttt{kemh}_n^{n-1}$, $\texttt{mekh}_n^{n-1}$ [*Cut edge* bounding *n*-stratum]. In higher dimensions, the merge of an edge with an absorbing *n*-stratum originates a new $(n-1)$-hole $\texttt{h}_n^{n-1}$ in the *n*-stratum, and a new boundary component as well. The operator $\texttt{mekh}_n^{n-1}$ is its inverse operator.

Using the same approach for **faces** embedded in *n*-strata ($n \geq 3$), we end up with an analogous operator with edges replaced by faces:

(i) $\texttt{kfms}_h$, $\texttt{mfks}_h$ [*Face* bounding solid]. In Figure 32, the operator $\texttt{kfms}_h$ (*kill face, make 1-dimensional solid hole*) or $\texttt{kfmh}_3^1$, creates a 1-dimensional hole $\texttt{s}_h$=$\texttt{h}_3^1$ for a solid. This hole $\texttt{s}_h$=$\texttt{h}_3^1$ corresponds to the frontier of the merging face $\texttt{f}$, which is homeomorphic to a 1-sphere $\mathbb{S}^1$. Note that $\texttt{f}$ is a face surrounded by a solid, and it is not necessarily relatively closed in that solid. That, its boundary may have several components. The inverse operator $\texttt{mfks}_h$ puts back the face, what eliminates the corresponding 1-dimensional hole $\texttt{s}_h$ in a solid.

$\vdots$

(n) $\mathtt{kfmh}_n^{n-1}$, $\mathtt{mfkh}_n^{n-1}$ [*Face* bounding *n*-stratum]. In higher dimensions, merging a face c with its surrounding *n*-stratum originates a new $(n-1)$-hole $\mathtt{h}_n^{n-1}$ in a *n*-stratum. Again, the new hole is determined by the frontier of f, and its boundary may have several components. Some of these boundary components of f will be transformed into boundary components for the *n*-stratum after merging f with it. The operator $\mathtt{mfkh}_n^{n-1}$ is the inverse operator.

All this process can be generalised for any *k*-stratum bounding a *n*-stratum of dimension $n > k$. Merging such a bounding *k*-stratum with a surrounding *n*-stratum gives rise to a $(n-k)$-hole for the *n*-stratum. So, the corresponding operator is $\mathtt{ks}^k\mathtt{mh}_n^{n-k}$, with $n > k$, being $\mathtt{ms}^k\mathtt{kh}_n^{n-k}$ its inverse operator. The corresponding algorithm is as follows:

ALGORITHM 5.8. (Euler operator $\mathtt{ks}^k\mathtt{mh}_n^{n-k}$)

INPUT:

(a) the merging *k*-stratum s.

(b) the absorbing *n*-stratum u.

PRE-CONDITIONS:

(a) $s \in \mathrm{Bd}(u)$, what means that $\dim(s) < \dim(u)$.

(b) s is not in any *k*-cycle.

Begin

(1) Subdivides frontier component $f(u)$ (which contains s) into two by s, i.e. $f(u) = f_1(u) \cup \{s\} \cup f_2(u)$. [This implies an analogos subdivision of the boundary component $b(u) \subseteq f(u)$, i.e. $b(u) = b_1(u) \cup \{s\} \cup b_2(u)$ such that $b_1(u) \subseteq f_1(u)$ and $b_2(u) \subseteq f_2(u)$.]

(2) Creates a new $(n-k)$-dimensional local hole h for u. [It is an instance of the class Hole.]

(3) **If** $f_2(u) \neq \emptyset$ **then** [particular case of $f(s) = \mathbb{S}^0$]

(i) Identifies h with the new frontier component $f_2(u)$.

(4) **If** $b_1(u) \subseteq f_1(u)$ has c components **then**

Begin

(i) Creates at most $(c-1)$ new boundary components for the surrounding stratum u.

(ii) Identifies h with the frontier of s.

End

(5) Unites the point set of s to the point set of t. [Geometric merging.]

(6) Deletes s.

End

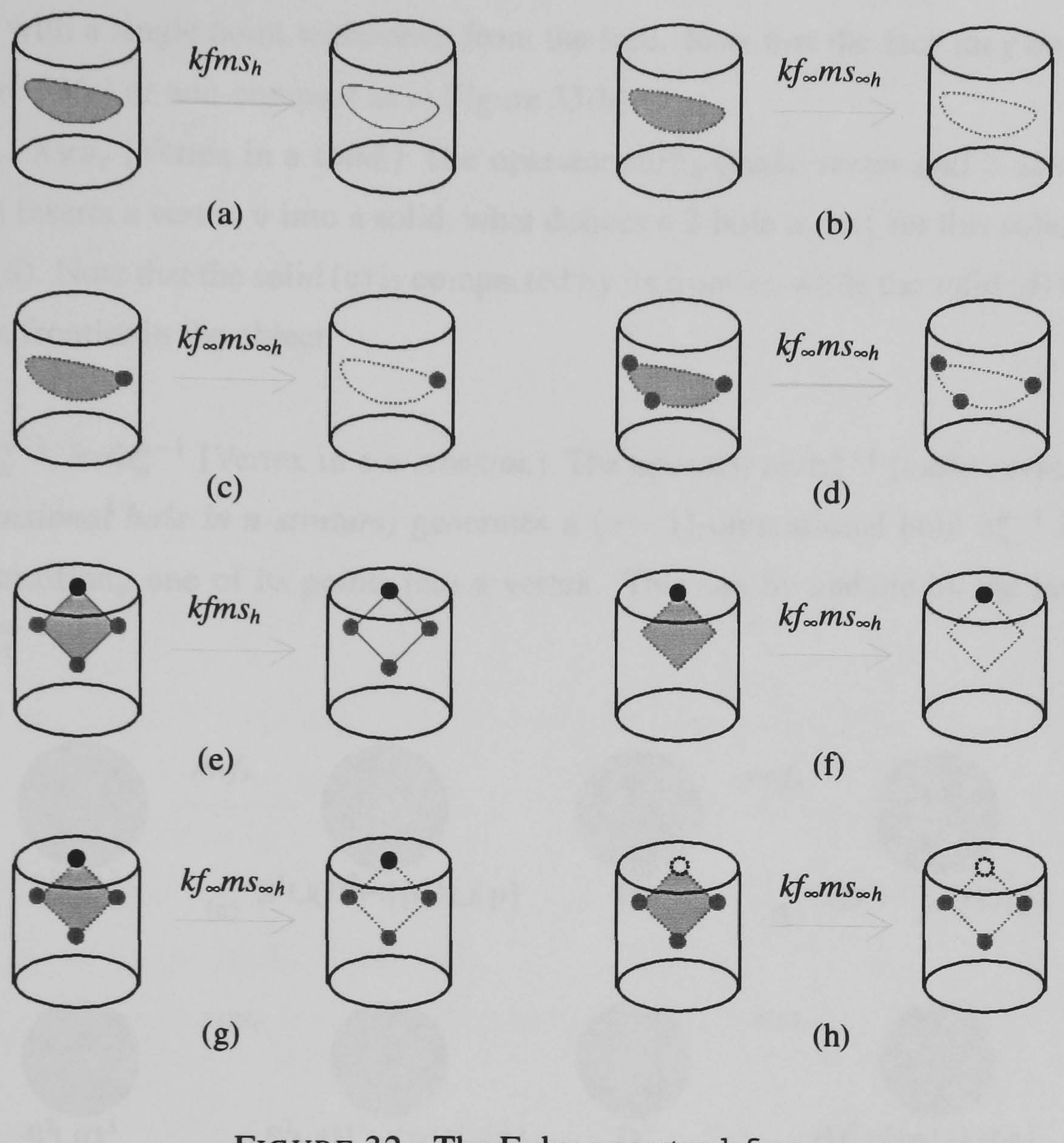

FIGURE 32. The Euler operator $\texttt{kfms}_h$.

7.2. Local hole constructors by emerging a stratum. Merging operators are caracterised by the union of the point sets of two adjacent strata. Unlike these Merging Euler operators, Emerging Euler operators are local hole constructors which are characterised by an emerging stratum, that is, a stratum whose point set is subtracted to the point set of another stratum of an object. Again, we impose the condition that the emerging k-stratum must be homeomorphic to $\mathbb{R}^k$. The ambient n-stratum has no restrictions in respect to shape and compactness. Such an emerging k-stratum will determine a $(n-1-k)$-dimensional hole in a n-stratum, with $n > k+1$.

Let us start with the case of a **vertex** emerging from faces and higher dimensional strata, Figure 33:

- $\texttt{mvf}_h$, $\texttt{kvf}_h$ [Vertex in a *face*.] The operator $\texttt{mvf}_h$ (*make vertex and 1-dimensional face hole*) introduces an isolated vertex v in a face, what originates a 1-dimensional hole $\texttt{f}_h$=$\texttt{h}_2^1$ through such a face, Figure 33(a) and (b). The point set of the new vertex is a singleton, i.e.

a set with a single point withdrawn from the face. Note that the face may be compact as in Figure 33(a) or non-compact as in Figure 33(b).

- $\mathtt{mvs}_c$, $\mathtt{kvs}_c$ [Vertex in a *solid.*] The operator $\mathtt{mvf}_h$ (*make vertex and 2-dimensional solid hole*) inserts a vertex v into a solid, what defines a 2-hole $\mathtt{s}_c$=$\mathtt{h}_3^2$ for this solid, Figure 33(c) and (d). Note that the solid (c) is compacted by its frontier, while the solid (d) is not bounded by its frontier in the object.

⋮

- $\mathtt{mvh}_n^{n-1}$, $\mathtt{kvh}_n^{n-1}$ [Vertex in a *n-stratum.*] The operator $\mathtt{mvh}_n^{n-1}$ (*make vertex and* $(n-1)$*-dimensional hole in n-stratum*) generates a $(n-1)$-dimensional hole $\mathtt{h}_n^{n-1}$ in a n-stratum by stratifying one of its points into a vertex. This can be undone by the inverse operator $\mathtt{kvh}_n^{n-1}$.

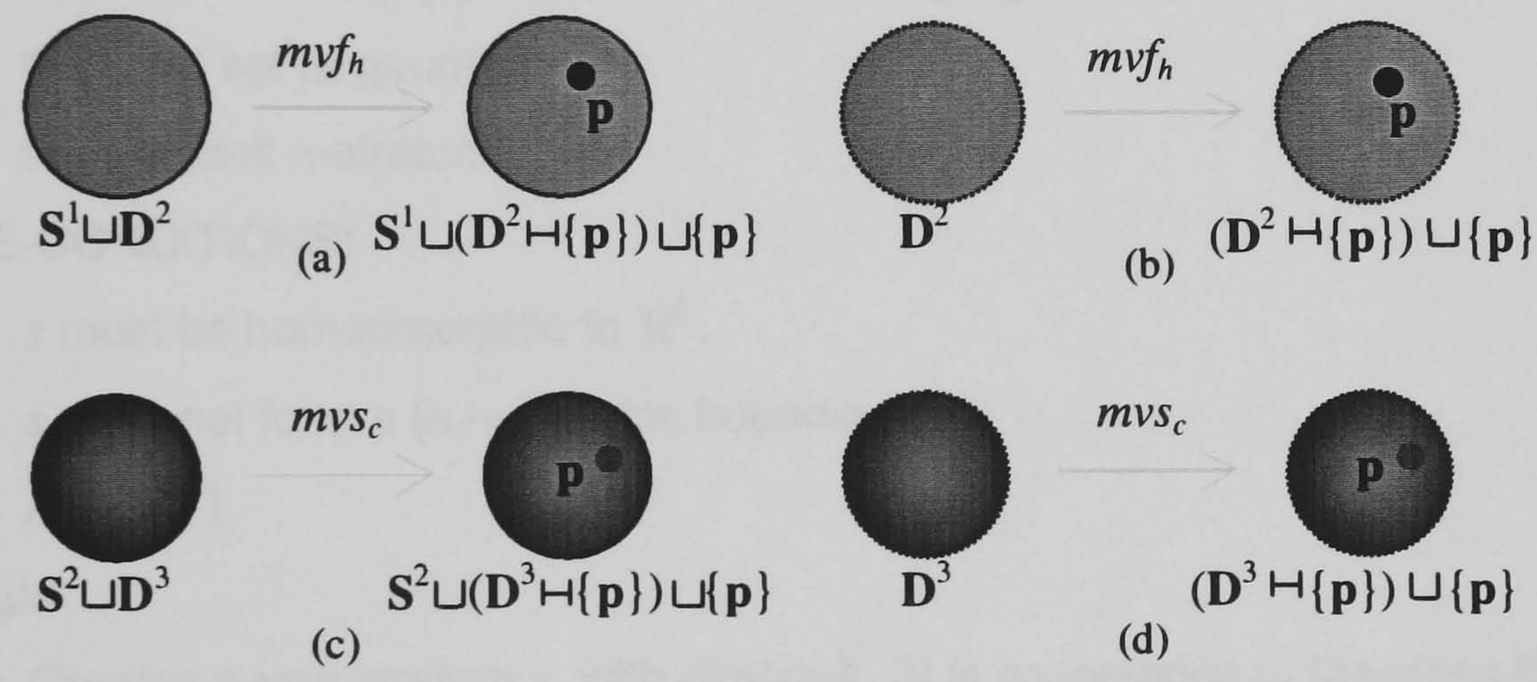

FIGURE 33. The Euler operator $\mathtt{mvh}_n^{n-1}$ that inserts a vertex with an stratum.

Let us take now **edges** as emerging strata:

- $\mathtt{mes}_h$, $\mathtt{kes}_h$ [Edge through or in a *solid.*] The operator $\mathtt{mes}_h$ (*make edge and 1-dimensional solid hole*) transforms a 1-dimensional manifold point subset of a solid into an edge e, with the restriction that the new edge must start and end at a frontier of such a solid. Several cases are shown in Figure 34. The new edge must be then homeomorphic to $\mathbb{R}^1$. Inserting e through or in a solid produces a new 1-dimensional hole $\mathtt{s}_h$ through or in such a solid. The inverse operator $\mathtt{kes}_h$ undoes this hole $\mathtt{s}_h$ by merging e with a solid.
- $\mathtt{meh}_4^2$, $\mathtt{keh}_4^2$ [Edge through or in a 4-*stratum.*] Following the same restrictions described just above, a 2-hole $\mathtt{h}_4^2$ is defined by an edge e embedded in a 4-stratum.

⋮

- $\mathtt{meh}_n^{n-2}$, $\mathtt{keh}_n^{n-2}$ [Edge through or in a *n-stratum*.] The operator $\mathtt{meh}_n^{n-2}$ creates a $(n-2)$-hole h_n^{n-2} defined by an edge $\mathtt{e}$ embedded in a n-stratum. The new edge is homeomorphic to $\mathbb{R}^2$, and its point set is subtracted from the ambient stratum point set. The operator $\mathtt{keh}_n^{n-2}$ undoes the action of $\mathtt{meh}_n^{n-2}$ by merging the point sets of $\mathtt{e}$ and its ambient stratum point set.

Thus, in general, we have the operator $\mathtt{ms}^k\mathrm{h}_n^{n-1-k}$ that inserts a k-stratum (homeomorphic to $\mathbb{R}^k$) with an embedding n-stratum, in which such a k-stratum defines a $(n-1-k)$-hole h_n^{n-1-k}.

The algorithm for this Euler operator follows:

ALGORITHM 5.9. (Euler operator $\mathtt{ms}^k\mathrm{h}_n^{n-1-k}$)

INPUT:

(a) the dimension $\dim(s) = k$ of the new emerging k-stratum s.

(b) the point set or geometry of s.

(c) the ambient n-stratum u.

PRE-CONDITIONS:

(a) s must be homeomorphic to $\mathbb{R}^k$.

(b) s must not form a $(n-1)$-cycle bounding u.

(c) $n > k+1$

Begin

(1) Creates a new stratum s, with $\dim(s)=k$. [It is an instance of the class Stratum.]

(2) Creates a new local hole h for u, with $\dim(h)=n-1-k$. [It is an instance of the class Hole.]

(3) Creates a new subcomplex **h** for h. [It is an instance of the class Subcomplex.]

(4) Adds s to **h**.

End

8. Euler algebra V: family of stratum attachers

This section deals with a new class of Euler operators which allow us to attach (respectively, detach) relatively non-compact strata to (respectively, from) an object. The attaching (respectively, detaching) n-stratum must be homeomorphic to $\mathbb{R}^n$.

These operators feature the following properties:

- *Shape variance.* The global shape of the object changes because a new point set is added to an object. In particular, a new non-compact stratum component is inserted into the object.

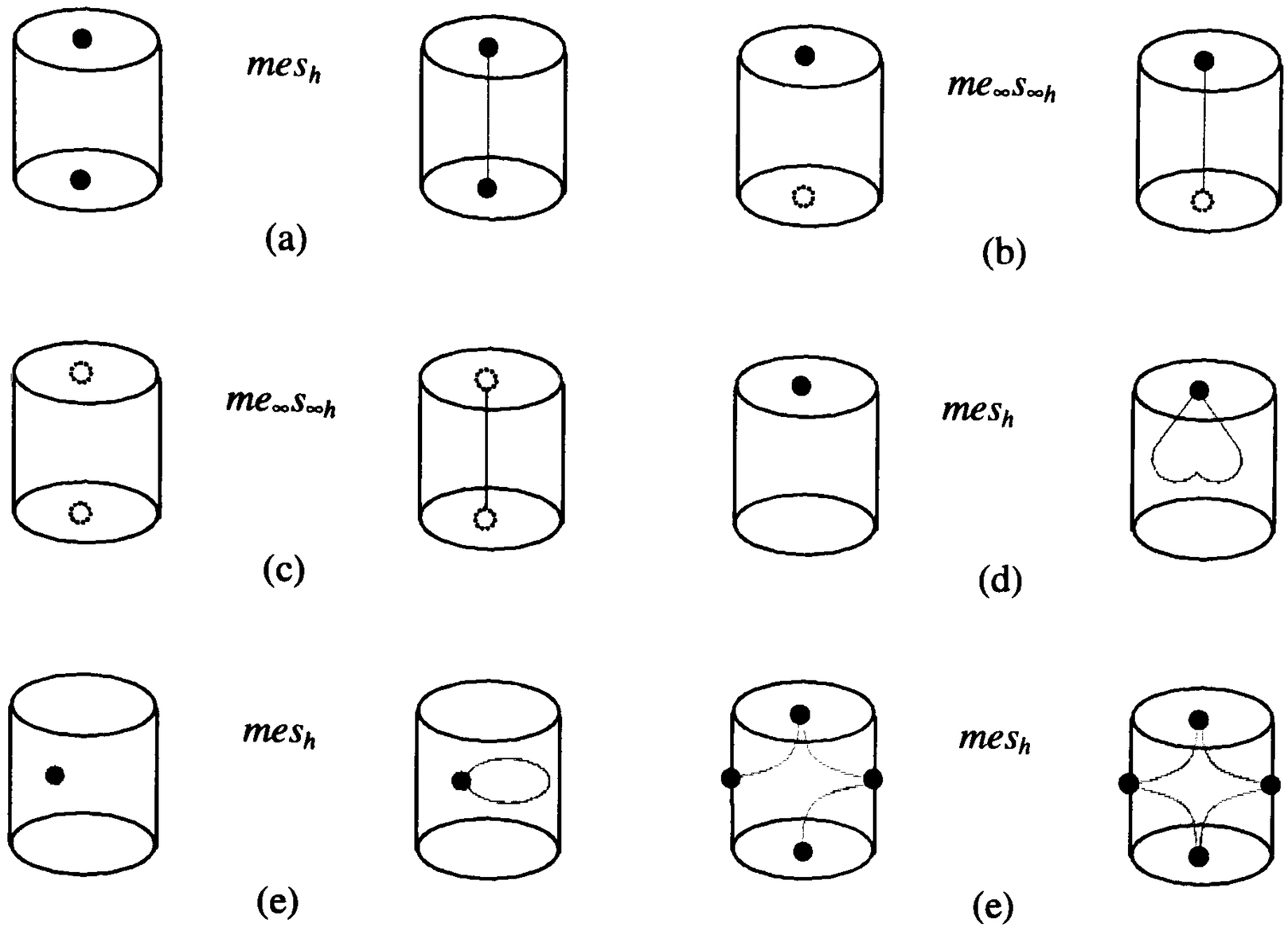

FIGURE 34. The Euler operator $\mathtt{mes}_h$.

However, the number of global holes does not change, and the number of local holes of strata neither.

- *Compactness variance.* The compact point subset of an object does not change either. However, because a relatively non-compact stratum is to be attached to (respectively, detached from) an object, the non-compact point subset of an object will certainly change.

Therefore, these operators deal with the non-compact strata and components of the object in the relative topology induced by the ambient space. Let us enumerate them:

(i) $\mathtt{me}_\infty\mathtt{E}_\infty$, $\mathtt{ke}_\infty\mathtt{E}_\infty$. The operator $\mathtt{me}_\infty\mathtt{E}_\infty$ (*make edge and edge component*) introduces a new relatively non-compact edge $\mathtt{e}_\infty$ and its corresponding non-compact edge component $\mathtt{E}_\infty$ into the object, Figure 35(a). The subscript ∞ says us that the new edge is not compact in the data structure, i.e. at least one of its frontier strata is missing in the data structure. The operator $\mathtt{ke}_\infty\mathtt{E}_\infty$ undoes the effect of $\mathtt{me}_\infty\mathtt{E}_\infty$, and is then its inverse.

(ii) $\mathtt{mf}_\infty\mathtt{F}_\infty$, $\mathtt{kf}_\infty\mathtt{F}_\infty$. The operator $\mathtt{mf}_\infty\mathtt{F}_\infty$ (*make face and face component*) introduces a new relatively non-compact face $\mathtt{f}_\infty$, as well as its respective non-compact face component $\mathtt{e}_\infty$, into the object Figure 35(b). As for the operator for edges, at least one of the frontier strata of the new face must be missing in the object. The operator $\mathtt{kf}_\infty\mathtt{F}_\infty$ is the inverse

operator of $\mathtt{mf}_\infty\mathtt{F}_\infty$, and deletes a non-compact face and its corresponding component from an object.

⋮

(n) $\mathtt{ms}^n_\infty\mathtt{S}^n_\infty$, $\mathtt{ks}^n_\infty\mathtt{S}^n_\infty$. The operator $\mathtt{ms}^n_\infty\mathtt{S}^n_\infty$ (*make stratum and stratum component*) and its inverse $\mathtt{ks}^n_\infty\mathtt{S}^n_\infty$ (*kill stratum and stratum component*) generalise previous operators for non-compact n-dimensional strata.

The dimension-independent Euler operator $\mathtt{ms}^n_\infty\mathtt{S}^n_\infty$ has then the following algorithm:

ALGORITHM 5.10. (Euler operator $\mathtt{ms}^n_\infty\mathtt{S}^n_\infty$)

INPUT:

(a) the dimension $\dim(s_\infty) = n$ of the new relatively non-compact n-stratum s_∞.

(b) the point set or geometry of s_∞.

(c) the boundary subcomplex **b** of s_∞.

PRE-CONDITIONS:

(a) s_∞ must be homeomorphic to $\mathbb{R}^n$.

(b) **b** must not belong to a $(n-1)$-hole.

Begin

(1) Creates a new stratum s_∞, with $\dim(s_\infty)$=n. [It is an instance of the class Stratum.]

(2) Creates a new frontier subcomplex **f** for s_∞. [It is an instance of the class Subcomplex.]

(3) Sets up **b** as boundary subcomplex **b** for f.

(4) Creates a new non-compact stratum component S_∞, with $\dim(S_\infty)$=n. [It is an instance of the class Component.]

(5) Adds S_∞ to the set of components of the object.

End

For convenience, the Σ-geometric kernel includes explicitly the attachers (detachers) $\mathtt{me}_\infty\mathtt{E}_\infty$ ($\mathtt{ke}_\infty\mathtt{E}_\infty$), $\mathtt{mf}_\infty\mathtt{F}_\infty$ ($\mathtt{kf}_\infty\mathtt{F}_\infty$), $\mathtt{ms}_\infty\mathtt{S}_\infty$ ($\mathtt{kv}_\infty\mathtt{S}_\infty$) for non-compact edges, faces and solids, because most applications in geometric modelling handle objects in $\mathbb{R}^3$. All these operators call the dimension-independent Euler operators $\mathtt{ms}^n_\infty\mathtt{S}^n_\infty$ (*make n-stratum and n-dimensional stratum component*) and $\mathtt{ks}^n_\infty\mathtt{S}^n_\infty$ (*kill n-stratum and k-dimensional stratum component*), respectively.

REMARK 14. The fact that $\mathtt{s}^n_\infty$ must be homeomorphic to $\mathbb{R}^n$ does not prevent the insertion (respectively, deletion) a non-compact stratum with holes into (respectively, from) and object. This can be carried out with the proto-Euler operator $\mathtt{ms}_{\infty\_}$ which calls first the Euler operators that

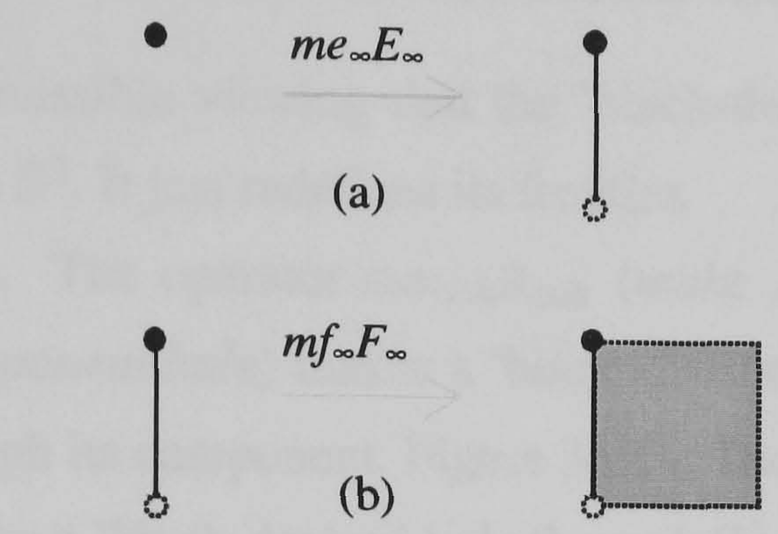

FIGURE 35. Attachers and detachers of relatively non-compact strata.

remove all the holes of such a stratum $\mathtt{s}^n_\infty$, and then calls the operator $\mathtt{ms}^n_\infty \mathtt{S}^n_\infty$ to proceed to its deletion.

9. Euler algebra VI: family of 'black & decker' hole constructors

These operators could be named *direct* hole constructors or 'black & decker' hole constructors. They constitute the first class of Euler operators which do not change the number of strata of an object. Only the number of holes is changed. Hence, we call them 'black & decker' hole constructors.

For obvious reasons, the new hole to be made in or through a n-stratum has dimension k at most, with $1 \leq k \leq n-1$, and such an n-stratum cannot have the shape of a n-hole. Note that $k \geq 1$ because only faces and higher dimensional strata may carry holes of lower dimension holes. According to the Euler formula, all strata are connected, i.e. they do not possess 0-holes.

Besides, it is assumed that such a n-stratum is already relatively non-compact. But, if we want to make a 'black & decker' hole in a compact stratum, we have to uncompact it first by means of adequate Euler uncompacters, and only then a 'black & decker' hole maker can be invoked. Such Euler uncompacters will be described further ahead.

The 'black-decker' makers for holes are:

- $\mathtt{mf}_{\infty h}\mathtt{F}_{\infty h}$, $\mathtt{kf}_{\infty h}\mathtt{F}_{\infty h}$. The operator $\mathtt{mf}_{\infty h}\mathtt{F}_{\infty h}$ (*make 1-dimensional face hole and 1-dimensional face component hole*) makes a hole $\mathtt{f}_{\infty h}$ through a face and, consequently, a hole $\mathtt{F}_{\infty h}$ through its face component, Figure 36(a). Note that the situation illustrated in

Figure 36(b) is not admissible viewing that the 'black-decker' perforation of $\mathbb{S}^2$ does not make any hole through $\mathbb{S}^2$. It just redefines its frontier.

- $\mathtt{ms}_{\infty h}\mathtt{S}_{\infty h}$, $\mathtt{ks}_{\infty h}\mathtt{S}_{\infty h}$. The operator $\mathtt{ms}_{\infty h}\mathtt{S}_{\infty h}$ (*make 1-dimensional solid hole and 1-dimensional solid component hole*) makes a 'black-decker' hole through a solid, what also originates a hole through its component, Figure 36(c). The inadmissible situation occurs in $\mathbb{R}^4$ when we try to make a 'black-decker' hole through $\mathbb{S}^3$.

- $\mathtt{ms}_{\infty c}\mathtt{S}_{\infty c}$, $\mathtt{ks}_{\infty c}\mathtt{S}_{\infty c}$. The operator $\mathtt{ms}_{\infty c}\mathtt{S}_{\infty c}$ (*make 2-dimensional solid hole and 2-dimensional solid component hole*) makes a 2-dimensional 'black-decker' hole in a solid, Figure 36(d). Note the missing point inside the solid prevents any 2-sphere containing it in the solid to contract into a point.

  ⋮

- $\mathtt{mh}^k_{\infty n}\mathtt{H}^k_{\infty n}$, $\mathtt{kh}^k_{\infty n}\mathtt{H}^k_{\infty n}$. The generalisation to higher dimensions gives these operators, with $1 \leq k \leq n-1$.

Therefore, the algorithm for the Euler operator $\mathtt{mh}^k_{\infty n}\mathtt{H}^k_{\infty n}$ is as follows:

ALGORITHM 5.11. (Euler operator $\mathtt{mh}^k_{\infty n}\mathtt{H}^k_{\infty n}$)

INPUT:

(a) the ambient non-compact stratum s, with $\dim(s) = n$

(b) the dimension of the new 'black & decker' hole h, with $\dim(h) = k$.

(c) the point set or geometry g of h in s.

PRE-CONDITIONS:

(a) s must be relatively non-compact .

(b) $1 \leq k \leq n-1$.

Begin

(1) Determines the non-compact component S of s.

(2) Creates a new 'black & decker' hole h for s, with $\dim(h)=k$. [It is an instance of the class Hole.]

(3) Sets up g as the geometry of h.

(4) Creates a new component hole H for S, with $\dim(H)=k$. [It is an instance of the class Hole.]

(5) Sets up h as the local counterpart for H.

End

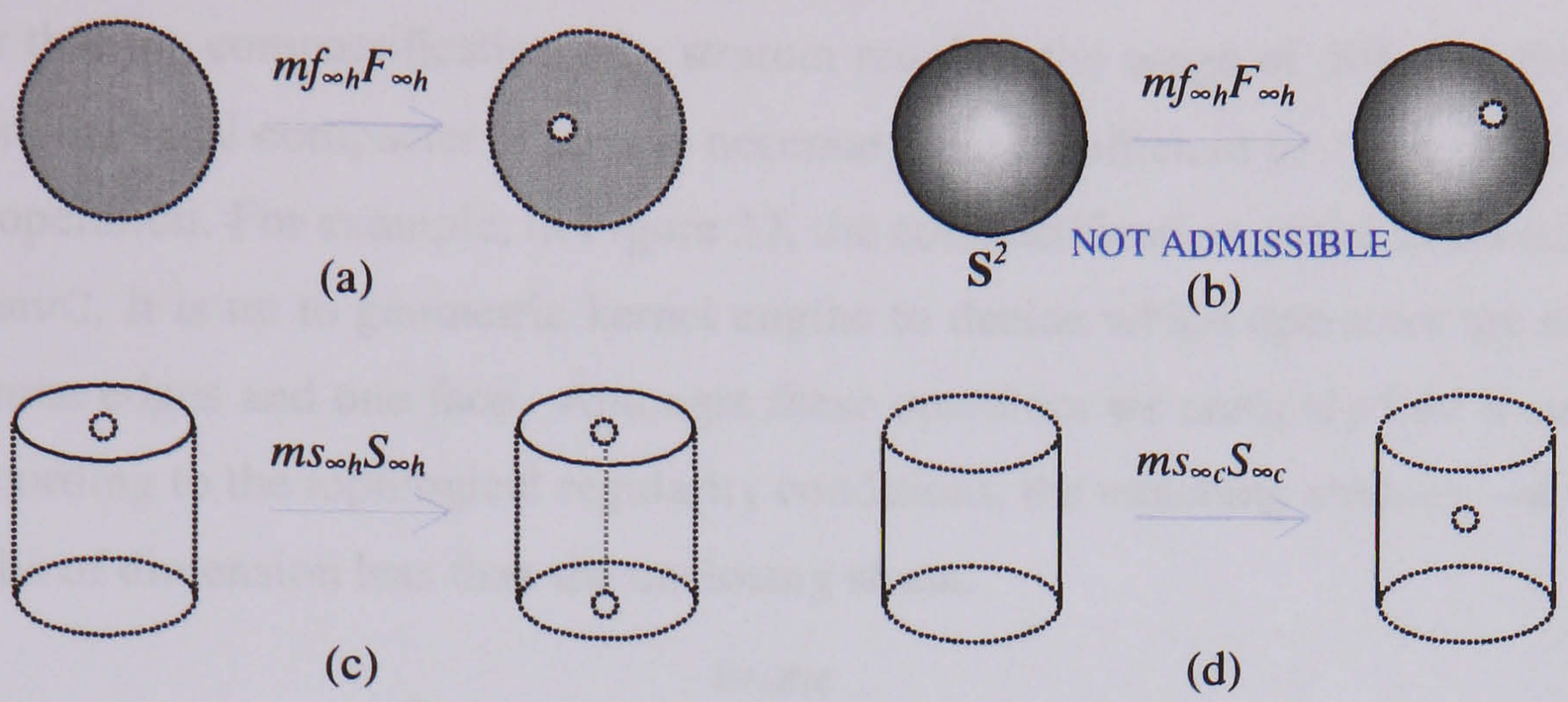

FIGURE 36. 'Black & Decker' hole constructors for relatively non-compact strata.

10. Euler algebra VII: family of local compacters

Because the Σ-geometric kernel handles both compact and non-compact strata, we need Euler operators capable of transforming a compact stratum into a non-compact stratum, and vice-versa. These Euler operators are here called *local compacters*. They are subsumed under general attachers and detachers of strata. In fact, they are invoked by the geometric kernel engine whenever the attachment or detachment of a stratum changes the local compactness of adjacent strata.

Let us see how they work:

- $\texttt{ke}_\infty\texttt{me}$, $\texttt{me}_\infty\texttt{ke}$. [*Edge compacter*] The operator $\texttt{ke}_\infty\texttt{me}$ (*kill non-compact edge, make compact edge*) transforms a non-compact edge into a compact edge by only changing its compactness state. Figure 37 gives us an example of application of this operator. It is invoked three times after the insertion of a new vertex at the origin in $\mathbb{R}^2$ to compact three edges. The bottom edge remains a non-compact edge because, despite the new vertex, another vertex is missing in its frontier.
- $\texttt{kf}_\infty\texttt{mf}$, $\texttt{mf}_\infty\texttt{kf}$. [*Face compacter*] The operator $\texttt{kf}_\infty\texttt{mf}$ (*kill non-compact face, make compact face*) is the compacter for faces. It transforms a non-compact face into a compact face by changing its compactness state. This is illustrated in Figure 37, where the only face in the object becomes a compact face as another consequence of the incoming vertex.

  ⋮
- $\texttt{ks}^n_\infty\texttt{ms}^n$, $\texttt{ms}^n_\infty\texttt{ks}^n$. [*Stratum compacter*] The generalised n-dimensional stratum compacter $\texttt{ks}^n_\infty\texttt{ms}^n$ is used to compact a n-stratum.

It is clear that the compactification of a stratum requires the usage of different Euler operators. The corresponding local compacter is always necessary, but insufficient to complete the entire compactification operation. For example, in Figure 37, the compactification of the strata starts by calling the operator mvC. It is up to geometric kernel engine to decide which operators are called in order to compact three edges and one face. Amongst these operators we certainly find local compacters. Note that, according to the topological regularity conditions, the attaching stratum —a vertex, in this case— must be of dimension less than the enclosing strata.

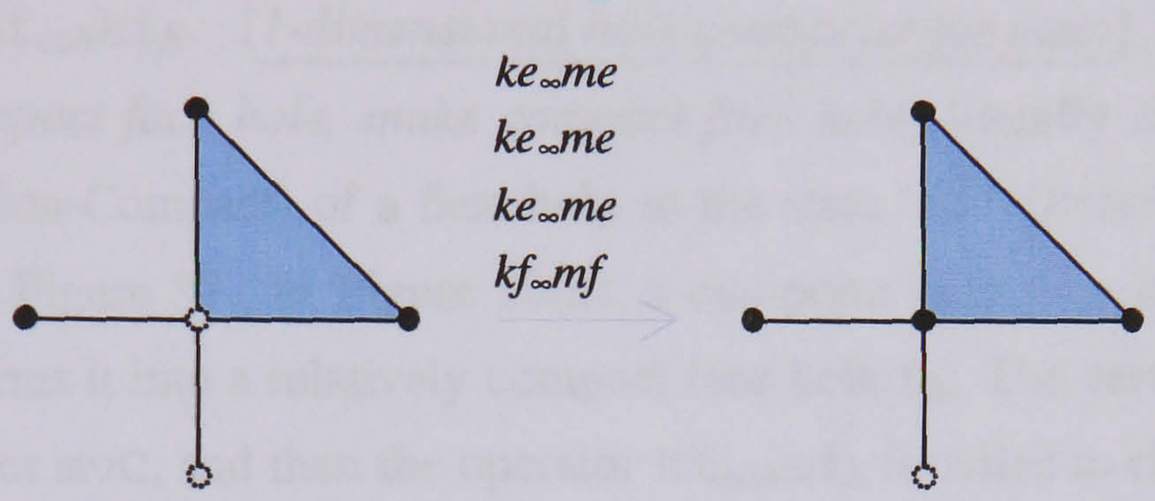

FIGURE 37. Use of stratum compacters after attaching a vertex.

The algorithm for the Euler operator $\mathtt{ks}^n_\infty\mathtt{ms}^n$ can be described as follows:

ALGORITHM 5.12. (Euler operator $\mathtt{ks}^n_\infty\mathtt{ms}^n$)

INPUT:

(a) the non-compact stratum s, with $\dim(s) = n$

(b) the compactifying stratum u.

PRE-CONDITIONS:

(a) $\dim(u) < \dim(s)$ [To conform with regularity conditions.]

Begin

(1) Adds u to boundary subcomplex $\mathbf{b}(s)$ of s, which is now a $(n-1)$-cycle. [The frontier subcomplex $\mathbf{f}(s)$ is droped from the point set of u, which is now associated with $\mathbf{b}(s)$ by means of u itself.]

(2) Changes the compactness state of s from 'RNC' ('Relatively Non-Compact') to 'RC' ('Relatively Compact').

End

For convenience, the Σ-geometric kernel includes the operators $\mathtt{ke}_\infty\mathtt{me}$, $\mathtt{kf}_\infty\mathtt{mf}$, $\mathtt{kv}_\infty\mathtt{mv}$, and respective inverses for geometric modelling applications up to $\mathbb{R}^3$. These operators are particular cases of the dimension-independent operator $\mathtt{ks}^n_\infty\mathtt{ms}^n$. Thus, internally, they call $\mathtt{ks}^n_\infty\mathtt{ms}^n$.

11. Euler algebra VIII: family of local hole compacters

In addition to strata, local holes can be also compacted. A non-compact local hole becomes compact by filling in it with a suited stratum, or just a point set. This family of local hole compacters assumes that the filling 'material' is a point set already associated to a stratum.

The local hole compacters are:

- $\mathtt{kf}_{\infty h}\mathtt{mf}_h$, $\mathtt{mf}_{\infty h}\mathtt{kf}_h$. [*1-dimensional hole compacter for faces*] The operator $\mathtt{kf}_{\infty h}\mathtt{mf}_h$ (*kill non-compact face hole, make compact face hole*) literally changes the state 'RNC' (Relatively Non-Compact) of a face hole to the state 'RC' (Relatively Compact). This is illustrated in Figure 38. In Figure 38(a), a one-point hole $\mathtt{f}_{\infty h}$ is filled in with a vertex, what transforms it into a relatively compact face hole $\mathtt{f}_h$. The vertex is attached by means of the operator mvC, and then the operator $\mathtt{kf}_{\infty h}\mathtt{mf}_h$ is called to change compactness state of the face hole. In Figure 38(b), the non-compact face hole $\mathtt{f}_{\infty h}$ consists of the union of three point sets: two one-point sets, each one associated with a vertex, and 1-dimensional point set between those two vertices. So, filling in $\mathtt{f}_{\infty h}$ with an edge between these two vertices results in a compact face hole $\mathtt{f}_h$ with the same underlying point set, but now completely stratified and relatively closed. Thus, the operator $\mathtt{kf}_{\infty h}\mathtt{mf}_h$ comes after attaching the edge to that face through the operator mekC. Still, in Figure 38(c), another $\mathtt{f}_{\infty h}$ is transformed into $\mathtt{f}_h$ after attaching a circular edge, i.e. an edge with the shape of a 1-hole. This attachment is, of course, carried out the operator $\mathtt{mee}_h\mathtt{CC}_h$.

  No more hole compacters are possible for faces because every face with the shape of a 2-hole is already compact.

- $\mathtt{ks}_{\infty h}\mathtt{ms}_h$, $\mathtt{ms}_{\infty h}\mathtt{ks}_h$. [*1-dimensional hole compacter for solids*] The operator $\mathtt{ks}_{\infty h}\mathtt{ms}_h$ (*kill 1-dimensional non-compact solid hole, make 1-dimensional compact solid hole*) is the 1-dimensional hole compacter for solids. It transforms a non-compact solid hole $\mathtt{s}_{\infty h}$ into a compact solid hole $\mathtt{s}_h$. Figure 38(d) illustrates the most simple case of a solid hole $\mathtt{s}_{\infty h}$ through a non-compact solid: just a missing point. Filling in $\mathtt{s}_{\infty h}$ with such a point transforms $\mathtt{s}_{\infty h}$ into a 1-dimensional compact solid hole $\mathtt{s}_h$. The usage of $\mathtt{ks}_{\infty h}\mathtt{ms}_h$ in Figure 38(c) is far more subtle. In this case, non-compact edge completely fills in a 1-dimensional non-compact solid hole $\mathtt{s}_{\infty h}$; hence the compactification of $\mathtt{s}_{\infty h}$ into $\mathtt{s}_h$. To be sure of this just imagine the homotopic contraction of this non-compact edge into a point. The result is a deformation of the non-compact cylinder in Figure 38(c) into the non-compact torus in Figure 38(d).

$\mathtt{ks}_{\infty c}\mathtt{ms}_c$, $\mathtt{ms}_{\infty c}\mathtt{ks}_c$. [*2-dimensional hole compacter for solids*] The operator $\mathtt{ks}_{\infty c}\mathtt{ms}_c$ (*kill 2-dimensional non-compact solid hole, make 2-dimensional compact solid hole*) is a 2-dimensional hole compacter for solids. Figure 38(e), a simple 2-dimensional non-compact hole $\mathtt{s}_{\infty c}$ in a solid is depicted. It becomes a 2-dimensional compact hole $\mathtt{s}_c$ by filling in it with a vertex. In Figure 38(f), the compactification of the only 2-hole in a solid is obtained by attaching an edge.

No more hole compacters are possible for solids because every solid with the shape of a 3-hole is already compact in $\mathbb{R}^4$.

⋮

- $\mathtt{kh}^k_{\infty n}\mathtt{mh}^k_n$, $\mathtt{mh}^k_{\infty n}\mathtt{kh}^k_n$. [*k-dimensional hole compacter for n-strata*] The generalised k-dimensional hole compacter $\mathtt{kh}^k_{\infty n}\mathtt{mh}^k_n$ is used to compact a k-dimensional hole of a n-stratum, with $1 \leq k \leq n-1$.

Its algorithm is as follows:

ALGORITHM 5.13. (Euler operator $\mathtt{kh}^k_{\infty n}\mathtt{mh}^k_n$)

INPUT:

(a) the non-compact local hole h, with $\dim(h) = k$

(b) the compactifying stratum u.

PRE-CONDITIONS:

(a) $1 \leq k \leq n-1$, where n is the dimension of the ambient stratum.

Begin

(1) Determines the ambient stratum s of h.

(2) Adds u to boundary subcomplex **b**(s) of s, which has the homotopic shape of a (k)-hole. [The frontier subcomplex **f**(s) is droped from the point set of u, which is now associated with **b**(s) by means of u itself.]

(3) Changes the compactness state of s from 'RNC' ('Relatively Non-Compact') to 'RC' ('Relatively Compact').

End

12. Euler algebra IX: family of global compacters

Global compactness-handling Euler operators constitute a new class of operators. The designer is free to add/remove any stratum to/from an object at any time and order, so the Σ-geometric kernel provides various families of Euler operators to handle the relative compactness of strata and objects.

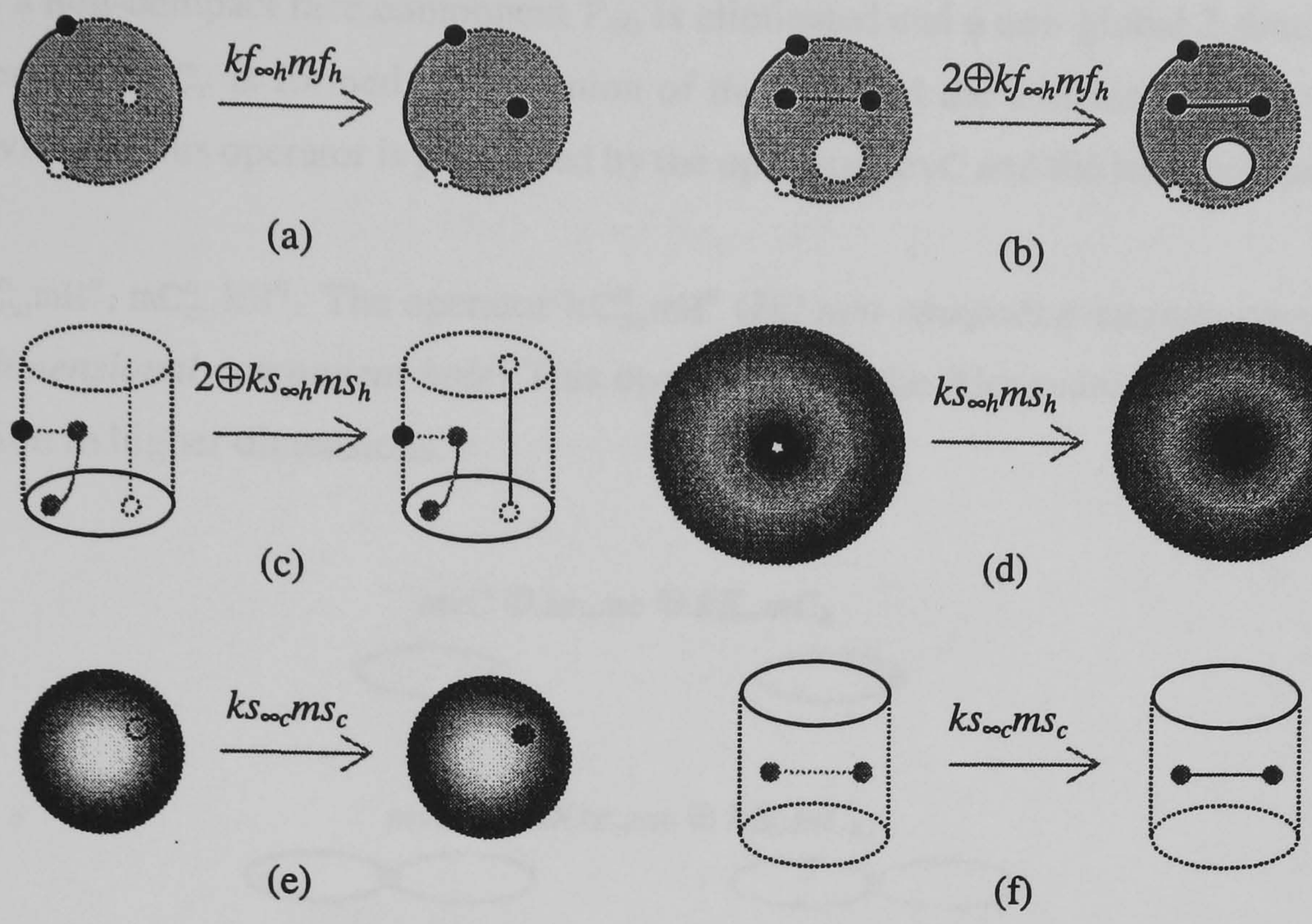

FIGURE 38. Local hole compacters.

The focus of this section is on families of global compacters, i.e. compacters that regulate the global or homotopic shape of an object.

12.1. Alexandroff one-point compacters. These global compacters perform Alexandroff one-point compactifications on manifolds or strata. They are aplicable whenever we want to compact a stratum whose frontier is a point. This surely implies global shape changes on an object.

Let us see how they work:

- $\mathtt{kE}_\infty\mathtt{mC}_h$, $\mathtt{mE}_\infty\mathtt{kC}_h$. The operator $\mathtt{kE}_\infty\mathtt{mC}_h$ (*kill non-compact edge component, make 1-dimensional component hole*) is a global compacter that finishes the Alexandroff one-compactification of an edge, as illustrated in Figure 39(a). The overall Alexandroff one-point compactification involves three Euler operators, namely: mvC, $\mathtt{ke}_\infty\mathtt{me}$, and the global compacter $\mathtt{kE}_\infty\mathtt{mC}_h$. The non-compact edge component $\mathtt{E}_\infty$ is eliminated by the incoming vertex, whose attachment to the non-compact edge also produces a new 1-dimensional global hole $\mathtt{C}_h$. That is, the attaching vertex changes the relative compactness of the target edge, as well as the global shape of an object.
- $\mathtt{kF}_\infty\mathtt{mC}_c$, $\mathtt{mF}_\infty\mathtt{kC}_c$. The operator $\mathtt{kF}_\infty\mathtt{mC}_c$ (*kill non-compact face component, make 2-dimensional component hole*) finishes the Alexandroff one-point compactification of a face.

So, a non-compact face component $\mathtt{F}_\infty$ is eliminated and a new global 2-dimensional component hole $\mathtt{C}_c$ is formed by the union of the face and the attaching vertex, Figure 40(a). Obviously, this operator is preceeded by the operators mvC and the local compacter $\mathtt{kf}_\infty\mathtt{mf}$.

⋮

- $\mathtt{kC}^n_\infty\mathtt{mH}^n$, $\mathtt{mC}^n_\infty\mathtt{kH}^n$. The operator $\mathtt{kC}^n_\infty\mathtt{mH}^n$ (*kill non-compact n-stratum component, make n-dimensional component hole*) This operator takes the Alexandroff one-point compactification to higher dimensions.

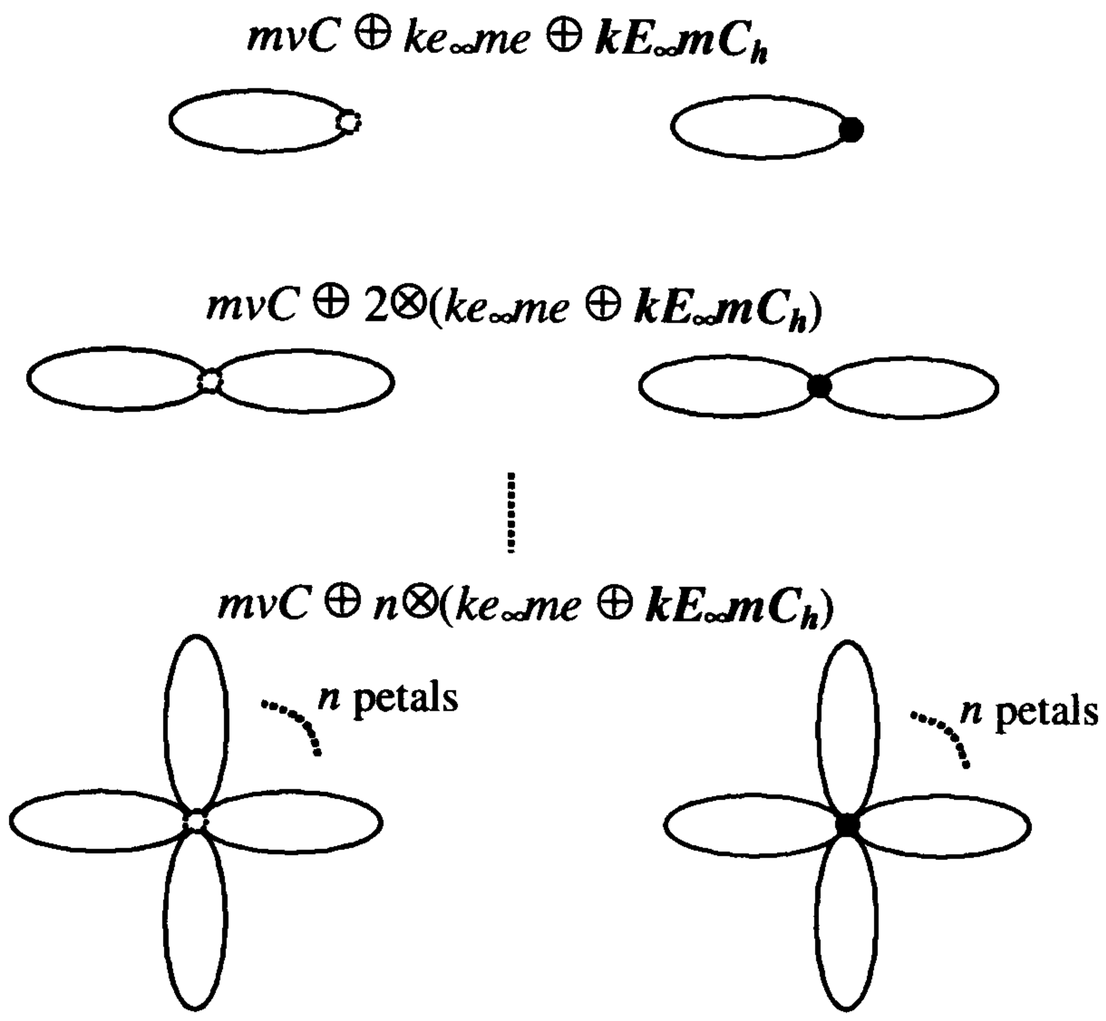

FIGURE 39. Alexandroff one-point compactification of edge bouquets through the local compacter $\mathtt{ke}_\infty\mathtt{me}$ and global compacter $\mathtt{kE}_\infty\mathtt{mC}_h$.

A nice property of the compacters (and, in general, the Euler operators) is their independence in relation to shape complexity. The following two examples corroborate our statement.

EXAMPLE 5.14. Let us look again at Figure 39. It illustrates the construction of bouquets of 1-holes by attaching a vertex. The compact geometry Euler operator mvC is called to attach a vertex and a vertex-component to each bouquet.

Bouquet with one edge petal, Figure 39(a). After attaching a vertex by means of mvC, the first bouquet consists of only one petal. This petal consists of an edge. This edge will become a compact edge after applying the local compacter $\mathtt{ke}_\infty\mathtt{me}$. Because a 1-hole is formed by attaching a vertex, the non-compact geometry Euler operator $\mathtt{kE}_\infty\mathtt{mC}_h$ is called.

Bouquet with two edge petals, Figure 39(b). Now, suppose we have two edge petals instead of only one. After calling the operator mvC to attach a vertex, we invoke both the operators $\mathtt{ke}_\infty\mathtt{me}$ and $\mathtt{kE}_\infty\mathtt{mC}_h$ for each petal.

Bouquet with n edge petals, Figure 39(c). In case we have a bouquet of n edge petals, we call the attaching-vertex operator mvC once, and both operators $\mathtt{ke}_\infty\mathtt{me}$ and $\mathtt{kE}_\infty\mathtt{mC}_h$ for each one of the n petals. The first operator will make each edge a compact edge, and the second will eliminates an edge-component $\mathtt{E}_\infty$ and at the same time creates a 1-hole $\mathtt{C}_h$.

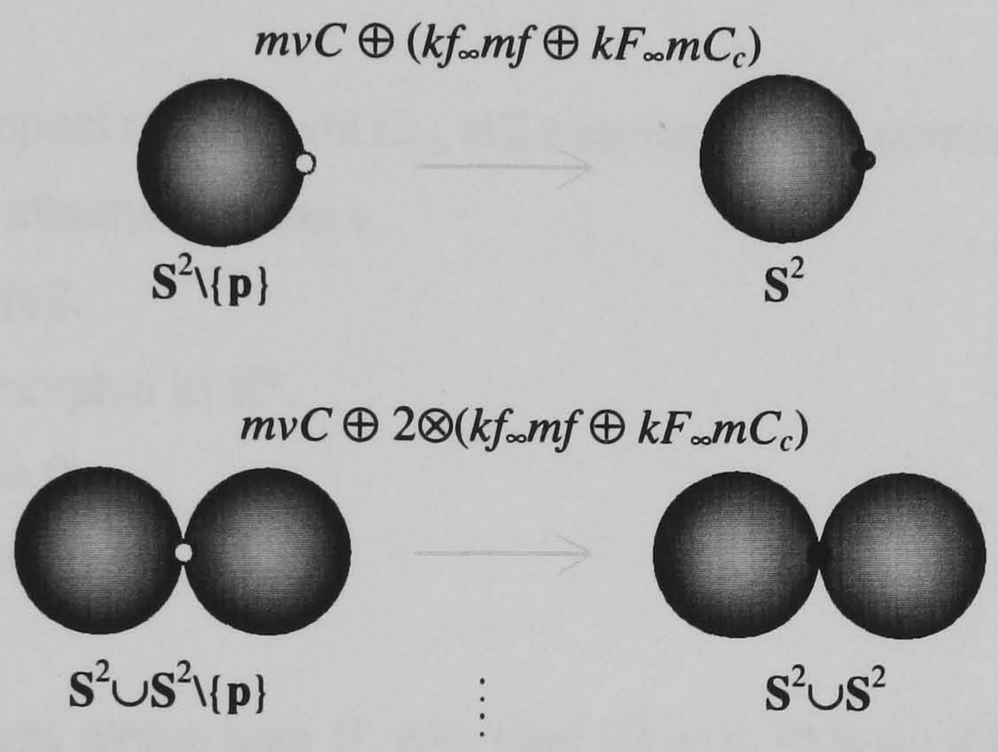

FIGURE 40. Alexandroff one-point compactification of face bouquets through the local compacter $\mathtt{kf}_\infty\mathtt{mf}$ and global compacter $\mathtt{kF}_\infty\mathtt{mC}_c$.

EXAMPLE 5.15. Let us look at the face bouquets in Figure 40. It illustrates the construction of n-bouquets of 2-dimensional holes by attaching a vertex to n faces simultaneously. The compact geometry Euler operator mvC is called once for each bouquet to attach a vertex and a vertex-component.

Bouquet with one face petal, Figure 40(a). After attaching a vertex, the first bouquet has only one face petal. The local compacter $\mathtt{kf}_\infty\mathtt{mf}$ transforms its non-compact face $\mathtt{kf}_\infty$ into a compact face f. At last, the global compacter $\mathtt{kF}_\infty\mathtt{mC}_c$ finishes the Alexandroff one-point compactification of the face petal, what originates the appearance of a new global 2-dimensional hole $\mathtt{C}_c$ and the elimination of the non-compact face component $\mathtt{kF}_\infty$.

Bouquet with two face petals, Figure 40(b). Now, suppose we have two face petals instead of only one. In this case, all we have to do is to call both operators $\mathtt{kf}_\infty\mathtt{mf}$ and $\mathtt{kF}_\infty\mathtt{mF}_c$ for each petal.

Bouquet with n face petals. For a bouquet of n face petals, both operators $\mathtt{kf}_\infty\mathtt{mf}$ and $\mathtt{kF}_\infty\mathtt{mC}_c$ are called n times, once for each petal. The operator $\mathtt{kf}_\infty\mathtt{mf}$ carries out the local compactification of each face $\mathtt{f}_\infty$, while the operator $\mathtt{kF}_\infty\mathtt{mC}_c$ does the global compactification of its corresponding component $\mathtt{F}_\infty$.

Remarkably, these operators work quite well independently of whether a petal stratum bounds higher dimensional strata or not. For example, let us consider a 1-bouquet of edges bounding one or more faces, as illustrated in Figure 41. The sequence of Euler operators to be used is the same as in Figure 39(a). The difference is that we need now additional operators to compact the bounded faces.

The algorithm for these Alexandroff one-point compacters is then as follows:

ALGORITHM 5.14. (Euler operator $\mathrm{kC}^n_\infty\mathrm{mH}^n$)

INPUT:

(a) the non-compact component C_∞ still associated to a compact stratum s, with $\dim(s) = n$

(b) the already attached vertex v.

PRE-CONDITIONS:

(a) s is homeomorphic to $\mathbb{R}^n$.

(b) $\dim(\mathrm{Fr}(s)) = 0$

(c) Fr(s) is connected.

Begin

(1) Creates a new global hole H, with $\dim(H) = n$. [It is an instance of the class Hole.]

(2) Creates a new subcomplex **H** for H. [It is an instance of the class Subcomplex.]

(3) Adds s and v to **H**.

(4) Labels **H** as a n-cycle. Determines the subcomplex **I** of the vertex component C concerning v.

(5) Adds s to **I**, updating $\dim(\mathbf{I}) = \dim(s)$.

(6) Adds v to the boundary subcomplex of s. [This automatically poses v in the frontier subcomplex of s.]

(7) Drops down the point set or geometry g of v from the frontier subcomplex of s. [At this stage v and its geometry g are already subsumed to boundary subcomplex of s, and, consequently, to frontier subcomplex.]

(8) Eliminates the non-compact component C_∞ associated to s.

End

12.2. Global compacters for non-compact stratum components without holes. This subfamily of global compacters is defined by removing the pre-conditions (b) and (c) of the Alexandroff one-point compacters. However, the condition (a) holds. Remember that the compacting stratum u must be in the frontier of the stratum s to be compacted, and therefore $\dim(u) < \dim(s)$ for spaces

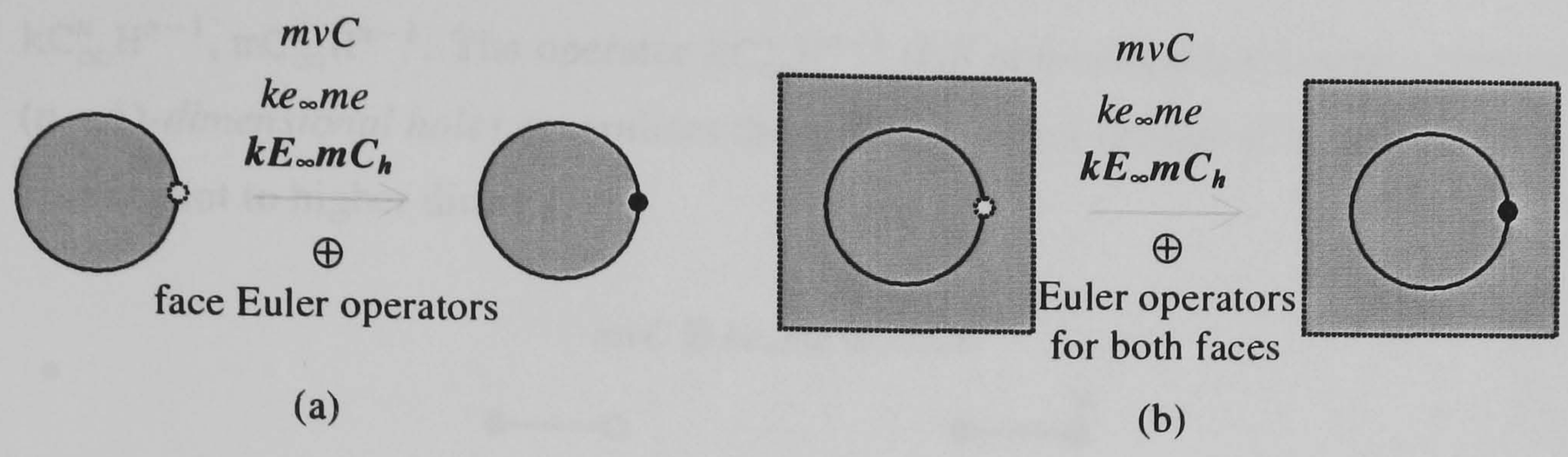

FIGURE 41. Compactness handler $\mathtt{kE}_\infty\mathtt{mC}_h$ for edge bounding faces.

with nice local properties like subanalytic sets. Thus, if $\dim(s) = 3$, then $\dim(u)$ can be 0, 1, or 2 at maximum. That is, a solid can be compacted by a vertex, an edge, or a face.

These global compacters are as follows:

- $\mathtt{kE}_\infty\mathtt{C}$, $\mathtt{mE}_\infty\mathtt{C}$. The operator $\mathtt{kE}_\infty\mathtt{C}$ (*kill non-compact edge component and component*) is the global compacter for a non-compact edge component $\mathtt{E}_\infty$ whose frontier is not connected. More precisely, its frontier consists of two point components, Figure 42(a) and (b). This operator carries out the global compactification of an edge, after it has been locally compacted, i.e. after using the local compacter $\mathtt{ke}_\infty\mathtt{me}$. This global compactification is made by eliminating the non-compact edge component $\mathtt{E}_\infty$. Simultaneously, this global compacter is also a global shaper because it bridges the two frontier components of an edge by the edge itself, being then necessary to eliminate one of those vertex components $\mathtt{C}$.
- $\mathtt{kF}_\infty\mathtt{C}_h$, $\mathtt{mF}_\infty\mathtt{C}_h$. The operator $\mathtt{kF}_\infty\mathtt{C}_h$ (*kill non-compact face component and 1-dimensional hole*) terminates the compactification of a non-compact face component $\mathtt{F}_\infty$. Its frontier is required to be already in the object and forms a global 1-dimensional hole $\mathtt{C}_h$. Taking into account that $\mathtt{F}_\infty$ fills in $\mathtt{C}_h$, this hole has to be eliminated from the object; hence, $\mathtt{kF}_\infty\mathtt{C}_h$. Figure 43 shows the three possible ways (a), (b), (c) to compact a non-compact face component by means of a vertex, an edge, and an edge with a 1-hole, respectively.
- $\mathtt{kS}_\infty\mathtt{C}_c$, $\mathtt{mS}_\infty\mathtt{C}_c$. The operator $\mathtt{kS}_\infty\mathtt{C}_c$ (*kill non-compact solid component and 2-dimensional hole*) runs the last stage of the compactification of a solid component $\mathtt{S}_\infty$. At this stage, the frontier of $\mathtt{kS}_\infty$ is already compacted, and thus it has already the shape of a 2-hole $\mathtt{C}_c$. Therefore, this 2-hole is already filled in by a solid. Consequently, both the non-compact solid component $\mathtt{S}_\infty$ and the 2-hole $\mathtt{C}_c$ must be eliminated from the object. Figure 44 shows some cases (a), (b), (c), (d) to compact a non-compact solid component as explained later.

⋮

- $\mathrm{kC}^n_\infty\mathrm{H}^{n-1}$, $\mathrm{mC}^n_\infty\mathrm{H}^{n-1}$. The operator $\mathrm{kC}^n_\infty\mathrm{H}^{n-1}$ (*kill non-compact n-stratum component and* $(n-1)$*-dimensional hole*) generalises the global compactification of a non-compact stratum component to higher dimensions.

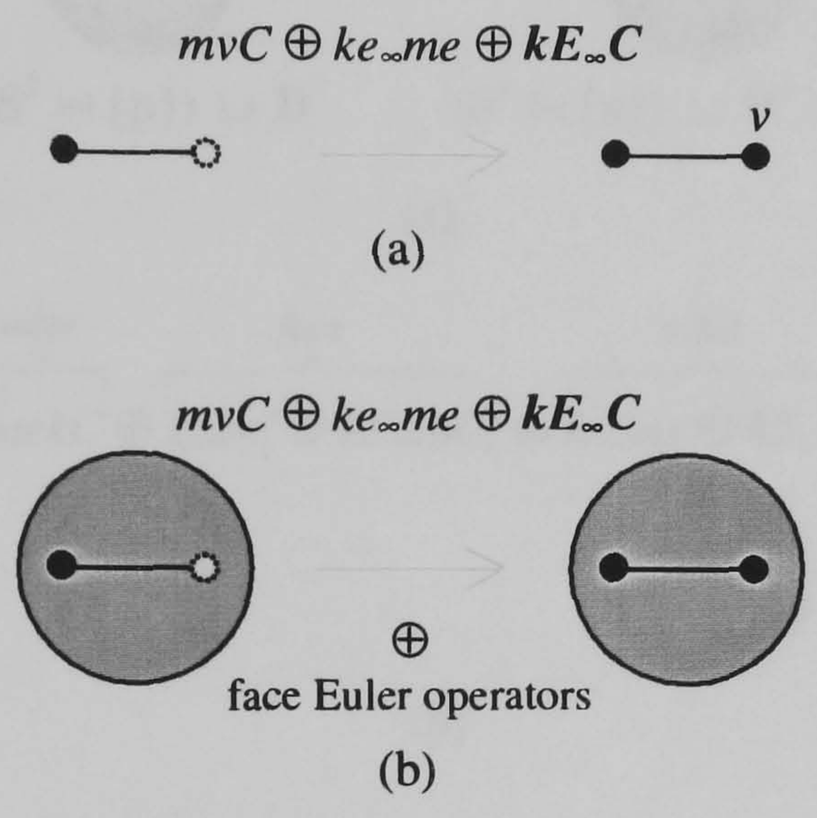

FIGURE 42. Global compacter $\mathrm{kE}_\infty\mathrm{C}$ for non-compact edge components.

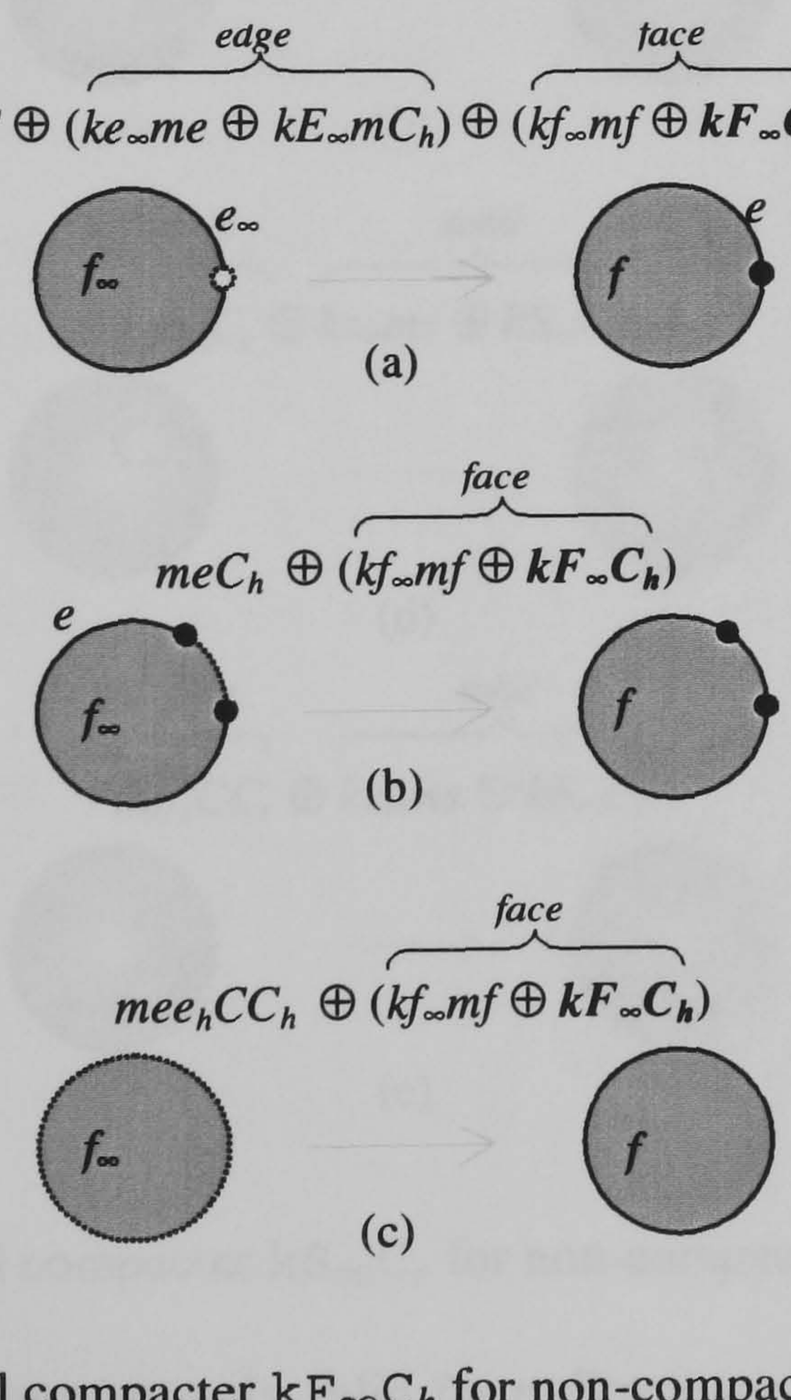

FIGURE 43. Global compacter $\mathrm{kF}_\infty\mathrm{C}_h$ for non-compact face components.

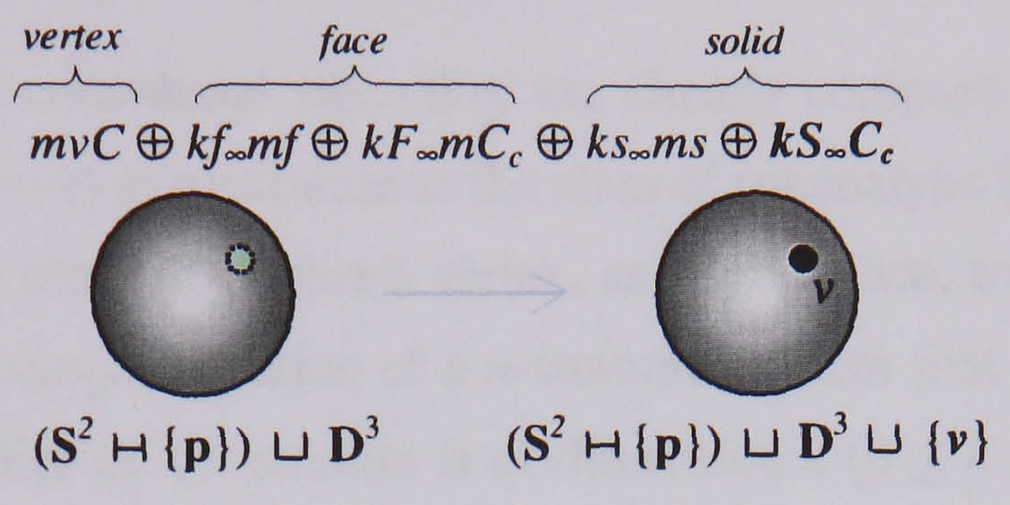

(a)

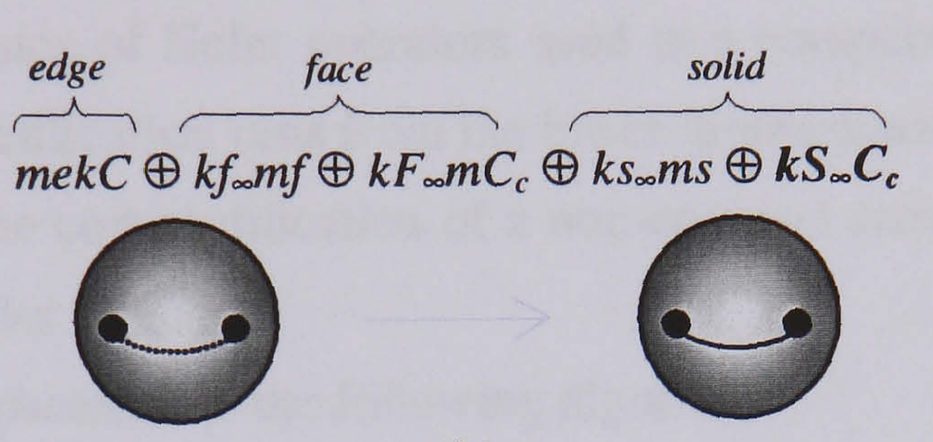

(b)

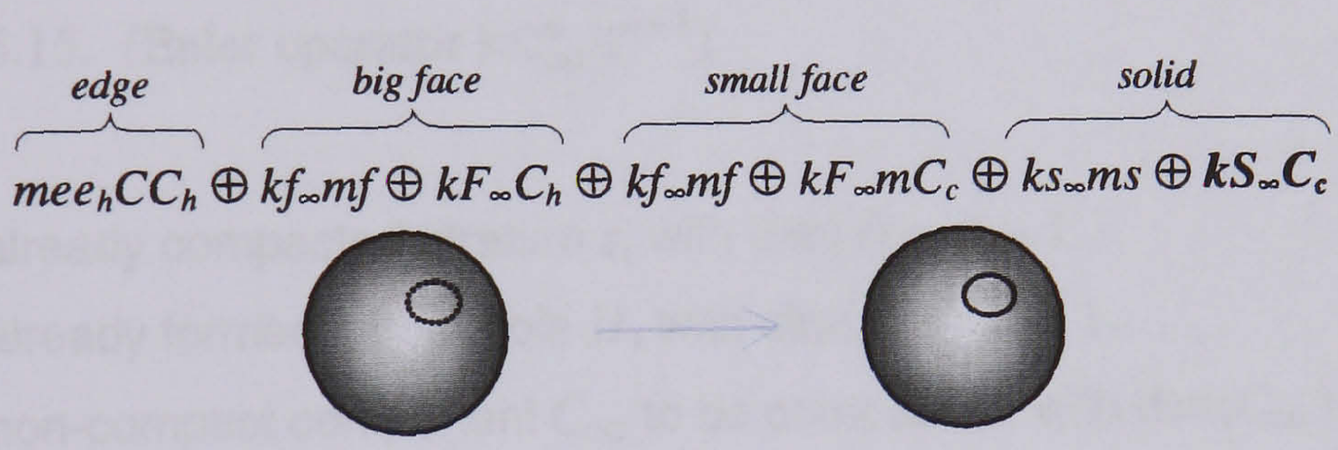

(c)

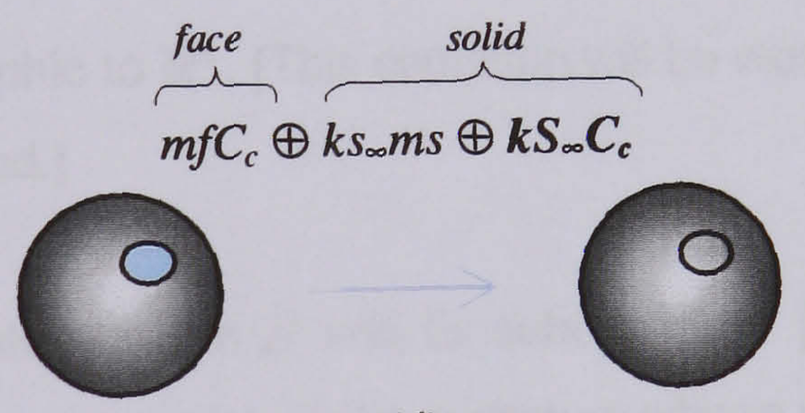

(d)

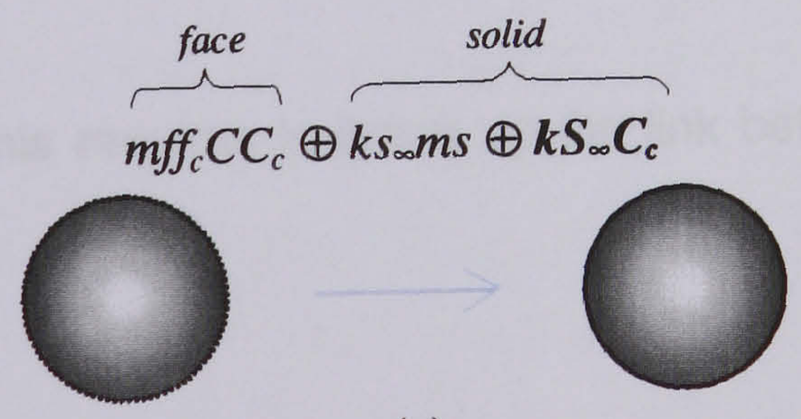

(e)

FIGURE 44. Global compacter $kS_\infty C_c$ for non-compact solid components.

This class of global compacters are only valid for n-dimensional non-compact stratum components which are homeomorphic to $\mathbb{R}^n$ and are not Alexandroff one-point compactifiable. n-strata

homeomorphic to $\mathbb{S}^n$ are not considered since they are already compact. Besides, the frontier of a n-stratum is of dimension $(n-1)$ at maximum in the class of subanalytic sets. That is, the frontier of a n-stratum is compacted by attaching either a vertex, an edge, a face, a solid, or a $(n-1)$-stratum. It is also expected that the compactification of a n-stratum requires first the compactification of its frontier. That is, if the frontier of a n-stratum is of dimension k $(0 \leq k \leq n-1)$, edge compacters are invoked first, followed by face compacters, solid compacters, ..., and $(n-1)$-stratum compacters at last. Therefore, the sequence of Euler operators used in a compactification operation follows a predefined order. The compactification runs from the lower-dimensional strata to higher-dimensional strata. And, it is clear that the compactification of a non-compact stratum component always starts with a compact-geometry Euler operator.

This class of global compacters has the following algorithm:

ALGORITHM 5.15. (Euler operator $\mathrm{kC}^n_\infty\mathrm{H}^{n-1}$)

INPUT:

(a) the already compacted stratum s, with $\dim(s) = n-1$.

(b) the already formed global hole H, with $\dim(H) = n-1$.

(c) the non-compact component C_∞ to be compacted, with $\dim(C_\infty) = n$.

PRE-CONDITIONS:

(a) C_∞ is homeomorphic to $\mathbb{R}^n$. [This condition will be weakened to C_∞ with all of its holes already compacted.]

Begin

(1) Breaks up the link between H and its subcomplex. [This subcomplex remains in the object as frontier subcomplex of the n-stratum whose non-compact component is C_∞.]

(2) Deletes H.

(3) Deletes C_∞. [This requires to break up the link between C_∞ and its corresponding stratum.]

End

Let us detail these global compacters with some examples.

EXAMPLE 5.16. *Compactification of an edge by attaching a vertex*, Figure 42(a). All we want to do is to attach a new vertex v to the object. The original object consists of one vertex $\mathtt{v=1}$, one non-compact edge $\mathtt{e}_\infty\mathtt{=1}$, one vertex component $\mathtt{C=1}$, and one non-compact edge component $\mathtt{E}_\infty\mathtt{=1}$. The resulting object after attaching the new vertex has two vertices $\mathtt{v=2}$, one relatively closed edge

e=1, and one relatively compact component C=1. That is, resulting object has no longer non-compact strata and non-compact stratum components. In other words, the attachment of v determines the global compactification of the non-compact edge component, what involves the sequence $\mathtt{mvC} \oplus \mathtt{ke}_\infty\mathtt{me} \oplus \mathtt{kE}_\infty\mathtt{C}$ of Euler operators:

mvC. This operator introduces an isolated vertex v and, consequently, a vertex component C into the object. Recall that it is a compact geometry operator. It works as the relatively non-compact edge was not there.

$\mathtt{ke}_\infty\mathtt{me}$. Despite the attachment of the second vertex, the edge remains a non-compact edge in the object. This means that the object is left temporarily, topologically inconsistent. To come back a consistent topological state, we first call the local edge compacter $\mathtt{ke}_\infty\mathtt{me}$. In addition to change the compactness state of current edge, this operator attaches the previous vertex to the frontier of such an edge.

$\mathtt{kE}_\infty\mathtt{C}$. After that, we apply the global compacter $\mathtt{kE}_\infty\mathtt{C}$ to finish the compactification of the edge. The compactification of this edge terminates with the elimination of the corresponding non-compact edge component $\mathtt{E}_\infty$. Such an edge bridges now its two frontier vertices. Consequently, the vertex component C must be eliminated. The result is an object with just one component.

EXAMPLE 5.17. *Compactification of an edge bounding a face by attaching a vertex*, Figure 42(b). Once again, remember that compactification operators work quite independently of the strata adjacent to the compactifying stratum. This is illustrated in Figure 42(b), where the compactifying stratum is a vertex. There two strata to be compacted: an edge and a face. In this case, the edge to be compacted bounds a face, but the Euler operators to compact it are exactly the same as those for the object in Figure 42(a). The difference is that now we have also a face to compact.

EXAMPLE 5.18. *Compactification of a face by attaching a vertex*, Figure 43(a). Let f_∞ be such a face to which lacks a vertex. Thus, to compact f_∞ we have first to attach a single vertex to its frontier, i.e. to compact its frontier $\mathrm{Fr}(f_\infty)$. The compactification of $\mathrm{Fr}(f_\infty)$ is made by compactifying first the frontier edge e_∞ through the operators $\mathtt{ke}_\infty\mathtt{me}$ and $\mathtt{kE}_\infty\mathtt{mC}_h$. The compactification of $\mathrm{Fr}(f_\infty)$. implies the compactification of the f_∞ itself, so the compactifiers $\mathtt{kf}_\infty\mathtt{mf}$ and $\mathtt{kF}_\infty\mathtt{C}_h$ must be called afterwards. That is, the compactification of f_∞ is made by calling the following Euler operators:

mvC. This is the first Euler operator to go into action, a compact-geometry Euler operator. It attaches the missing vertex to frontier of the face. It triggers on the following operators.

$\mathtt{ke}_\infty\mathtt{me}$. As a consequence of attaching the missing vertex, we have to compact first the edge bounding our face. This is carried out by calling the compactness transformer $\mathtt{ke}_\infty\mathtt{me}$ for edges.

$\underline{\mathtt{kE}_{\infty}\mathtt{mC}_h}$. Compacting an edge by attaching a missing vertex gives rise to a 1-hole C_h; hence the operator $\mathtt{kE}_{\infty}\mathtt{mC}_h$. This operator finishes the compactification of the edge by eliminating the non-compact edge component E_{∞}.

$\underline{\mathtt{kf}_{\infty}\mathtt{mf}}$. After that, we have to compact our face by calling the compactness transformer $\mathtt{kf}_{\infty}\mathtt{mf}$ for faces.

$\underline{\mathtt{kF}_{\infty}\mathtt{C}_h}$. The compactification of the face terminates after eliminating its non-compact face component F_{∞}, and the 1-hole C_h formed previously by the operator $\mathtt{kE}_{\infty}\mathtt{mC}_h$ used to compact $\mathrm{Fr}(f_{\infty})$. Consequently, the face fills in the 1-hole C_h originated by the compactification of the bounding edge; in other words, the 1-hole C_h is eliminated. Hence, the operator $\mathtt{kF}_{\infty}\mathtt{C}_h$ is called.

EXAMPLE 5.19. *Compactification of a face by attaching an edge*, Figure 43(b). Here, $\mathrm{Fr}(f_{\infty})$ lacks an edge in the object. Note that $\mathrm{Bd}(f_{\infty})$ is compact, but even so $\mathrm{Fr}(f_{\infty})$ has to be completed. The compactification of f_{∞} is carried out by calling the following Euler operators:

$\underline{\mathtt{meC}_h}$. This compact-geometry Euler operator forms a 1-hole $\mathtt{C}_h$ by attaching an edge e to the model. In this case, attaching e completes $\mathrm{Fr}(f_{\infty})$; in fact, $\mathrm{Fr}(f_{\infty})$ has the global shape of a 1-hole.

$\underline{\mathtt{kf}_{\infty}\mathtt{mf}}$. After completing $\mathrm{Fr}(f_{\infty})$, the compactness transformer $\mathtt{kf}_{\infty}\mathtt{mf}$ is called to transform the non-compact face f_{∞} into the compact face f.

$\underline{\mathtt{kF}_{\infty}\mathtt{C}_h}$. The completion of $\mathrm{Fr}(f_{\infty})$ has introduced a 1-hole C_h into the object that is eliminated by filling in it with a face f. This compact face f has been introduced in the object by the previous operator, which has transformed $\mathtt{f}_{\infty}$ into f. However, the corresponding non-compact face component $\mathtt{F}_{\infty}$ has remained. Hence, we call the operator $\mathtt{kF}_{\infty}\mathtt{C}_h$ to maintain the topological validity of the object. Thus, the operators $\mathtt{kf}_{\infty}\mathtt{mf}$ and $\mathtt{kF}_{\infty}\mathtt{C}_h$ have been called to transform f_{∞} into f and eliminate the 1-hole C_h generated by the completion of $\mathrm{Fr}(f_{\infty})$.

EXAMPLE 5.20. *Compactification of a face by attaching an edge with a 1-hole*, Figure 43(c). Here, $\mathrm{Fr}(f_{\infty})$ as a whole is missing in the model, that is, $\mathrm{Bd}(f_{\infty}) = \varnothing$. The frontier $\mathrm{Fr}(f_{\infty})$ can be introduced into the object as a whole by attaching an edge e with a 1-hole e_h. Thus, the compactification of f_{∞} is carried out by calling the following Euler operators:

$\underline{\mathtt{mee}_h\mathtt{CC}_h}$. This compact-geometry Euler operator adds an edge e with a 1-hole e_h to the object, which constitutes a component C with the global shape of a 1-hole C_h. This ring-shaped edge will be the frontier of the face to be compacted, say $\mathrm{Fr}(f_{\infty})$.

$\underline{\mathtt{kf}_{\infty}\mathtt{mf}}$. After attaching the previous ring-shaped edge, the compactness transformer $\mathtt{kf}_{\infty}\mathtt{mf}$ is called to transform the non-compact face $\mathtt{f}_{\infty}$ into the compact face f.

$\underline{\mathtt{kF}_{\infty}\mathtt{C}_h}$. The remaining non-compact face component F_∞ and global 1-hole C_h are eliminated by invoking the operator $\mathtt{kF}_{\infty}\mathtt{C}_h$.

EXAMPLE 5.21. *Different ways to compact of a solid*, Figure 44. It is clear that a solid can be compacted by attaching (a) a vertex, (b) an edge homeomorphic to $\mathbb{R}^1$, (c) an edge with the shape of a 1-hole, (d) a face homeomorphic to $\mathbb{R}^2$, or (e) by a face with the shape of a 2-hole. As usual, the compactification starts with a compact-geometry Euler operator and proceeds by compactifying the strata of increasing dimension. Therefore, the compactification of a solid requires the preliminary compactification of its bounding edges and faces. It finishes with the corresponding local and global compacters, say $\mathtt{ks}_{\infty}\mathtt{ms}$ and $\mathtt{kS}_{\infty}\mathtt{C}_c$.

12.3. Global compacters for non-compact stratum components with holes. Let us suppose now that non-compact components possess holes. That is, we relax the condition (a) of the previous two subfamilies of global compacters. So, we have:

(i) $\mathtt{kF}_{\infty h}\mathtt{C}, \mathtt{mF}_{\infty h}\mathtt{C}$. The operator $\mathtt{kF}_{\infty h}\mathtt{C}$ (*kill 1-dimensional non-compact hole of non-compact face component and component*) is called to finish the compactification of a face component hole $F_{\infty h}$. It compactifies a hole through a non-compact face, not the face itself. A face with holes is compacted as a face without holes, with the pre-condition that all of its holes are already compacted. The compactification of a face with holes (i.e. not homeomorphic to $\mathbb{R}^2$) is accomplished by attaching either a compacting vertex or compacting edge to its last non-compact frontier component, no matter whether it is a inner or outer component. For example, the face with holes depicted in Figure 45 becomes a compact face after filling in the last non-compact hole with a vertex or attaching a circular edge to its outer frontier. In any case, such a face becomes compact after calling the operator $\mathtt{kF}_{\infty h}\mathtt{C}$ for each hole, in order to compact each non-compact face component hole, and the operators $\mathtt{kf}_{\infty}\mathtt{mf}$ and $\mathtt{kF}_{\infty}\mathtt{C}_h$. These two latter operators behaviour as the face were a face without holes, seeing they compact the outer frontier component of it. In short, the compactification of a face with holes terminates by calling the compacter $\mathtt{kF}_{\infty h}\mathtt{C}$ as many times as the number of holes through such a face, followed by the usual local and global compacters for faces without holes, $\mathtt{kf}_{\infty}\mathtt{mf}$ and $\mathtt{F}_{\infty}\mathtt{C}_h$.

(ii) $\mathtt{kS}_{\infty c}\mathtt{C}, \mathtt{mS}_{\infty c}\mathtt{C}$. The operator $\mathtt{kS}_{\infty c}\mathtt{C}$ (*kill 2-dimensional non-compact hole of non-compact solid component and component*) is the compacter for 2-dimensional non-compact holes in solid components. It compacts holes, not components. Similar to face components, a non-compact solid component is compacted by the usual local and global compacters for solids

without holes. If a solid has holes, we have first to compact its holes, and only then the outer frontier component.

⋮

(n) $\mathrm{kH}^{n-1}_{\infty n}\mathrm{C}$, $\mathrm{mH}^{n-1}_{\infty n}\mathrm{C}$. The operator $\mathrm{kH}^{n-1}_{\infty n}\mathrm{C}$ (*kill* (n-1)*-dimensional non-compact hole of* n*-dimensional non-compact component and component*) generalises previous operators to higher dimensional non-compact holes. It compactifies a $(n-1)$-dimensional hole $\mathrm{H}^{n-1}_{\infty n}$ of a n-dimensional non-compact component. Such compactification of a hole determines a compact component (that coincides with a inner frontier component of a n-stratum) C in the object that is deleted from the object because of its merging to the outer frontier component of such a n-stratum.

This class of global compacters has the following algorithm:

ALGORITHM 5.16. (Euler operator $\mathrm{kH}^{n-1}_{\infty n}\mathrm{C}$)

INPUT:

(a) the non-compact hole H of non-compact face component F_∞.

(b) the corresponding compacted, but not yet inner frontier component C.

PRE-CONDITIONS:

(a) the corresponding face hole h is already compacted.

Begin

(1) Determines the face f of h.

(2) Detaches H from F_∞.

(3) Detaches H from h.

(4) Deletes H.

(5) Detaches the subcomplex of C from C and attaches it to boundary subcomplex of f.

(6) Deletes C.

End

EXAMPLE 5.22. Let us consider a non-compact face ($f_\infty = 1$) with three 1-dimensional non-compact holes ($f_{\infty h} = 3$), Figure 45. This determines a non-compact face component ($F_\infty = 1$) with three 1-dimensional non-compact holes ($F_{\infty h} = 3$). Figure 45 illustrates two ways to compact such a non-compact face component and its corresponding non-compact face.

First alternative on right: *First inner frontier components or holes, then outer frontier component.* Each inner frontier component of the non-compact face is compacted by first attaching a single vertex

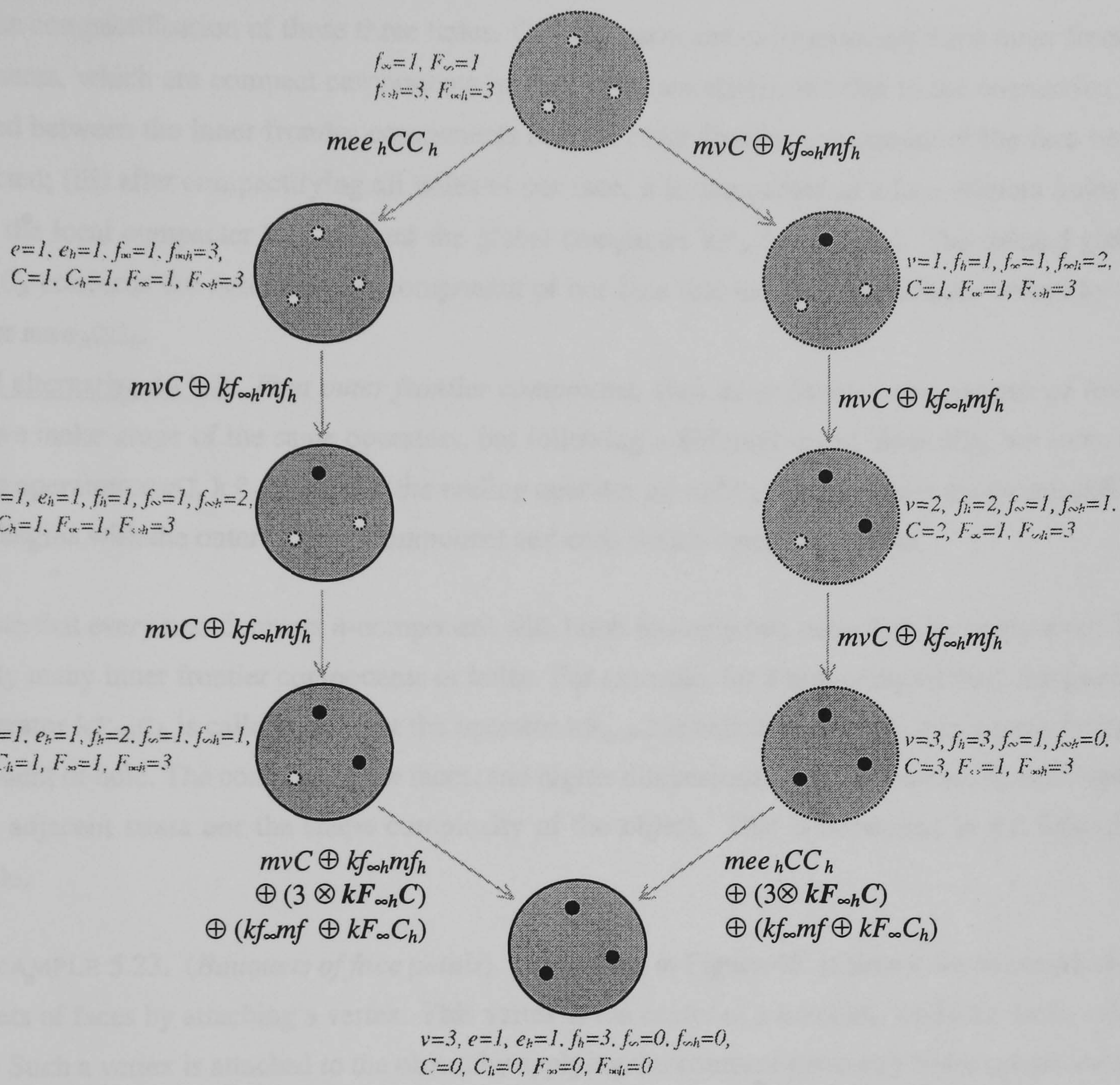

FIGURE 45. Compactification of outer and inner frontier components of a face using $\mathtt{kF}_{\infty}\mathtt{C}_{\infty}$ and $\mathtt{kF}_{\infty h}\mathtt{C}$, respectively.

through the compact-geometry Euler operator mvC. Each vertex constitutes an inner frontier of our face. Consequently, each 1-dimensional non-compact hole $f_{\infty h}$ through such a face is transformed into a compact 1-hole f_h by running the Euler operator $\mathtt{kf}_{\infty h}\mathtt{mf}_h$.

On the other hand, the outer frontier component of our face is compacted as follows: (i) the compact-geometry operator $\mathtt{mee}_h\mathtt{CC}_h$ is called to attach an edge e with a 1-hole e_h, which is, in global shape terms, a component C with a 1-hole C_h, and constitutes the outer frontier of our face; (ii) as long as the last frontier component —the outer frontier component, in this case— is formed in the object we apply the operator $\mathtt{kF}_{\infty h}\mathtt{C}$ three times, one for each non-compact 1-hole of our non-compact face to

finish the compactification of those three holes. Consequently, the corresponding three inner frontier components, which are compact components in their own, are eliminated due to the connection established between the inner frontier components and the outer frontier component of the face being compacted; (iii) after compactifying all holes of our face, it is compacted as a face without holes by calling the local compacter $\mathtt{kf}_{\infty}\mathtt{mf}$ and the global compacter $\mathtt{kF}_{\infty}\mathtt{C}_h$ as usual. The deleted global 1-hole C_h concerns the outer frontier component of our face that has been introduced before by the operator $\mathtt{mee}_h\mathtt{CC}_h$.

Second alternative on left: *First outer frontier component, then inner frontier components or holes.* Here, we make usage of the same operators, but following a different order. Basically, we swap the starting operators mvC, $\mathtt{kf}_{\infty h}\mathtt{mf}_h$ and the ending operator $\mathtt{mee}_h\mathtt{CC}_h$, because now the compactification is begins with the outer frontier component and ends with a inner component.

Note that every non-compact n-component with holes has only one outer frontier component, but possibly many inner frontier components or holes. For example, for a non-compact face component, the operator $\mathtt{kF}_{\infty}\mathtt{C}_h$ is called once, but the operator $\mathtt{kF}_{\infty h}\mathtt{C}$ is called to compact every inner frontier component or hole. The compacters for faces, and higher dimensional strata in general, do not depend on the adjacent strata nor the shape complexity of the object. This is illustrated in the following example.

EXAMPLE 5.23. (*Bouquets of face petals*). Let us look at Figure 46. It shows the construction of bouquets of faces by attaching a vertex. This vertex is the centre of a bouquet, while the faces are its petals. Such a vertex is attached to the object by applying the compact-geometry Euler operator mvC. The result is a bouquet with one or more face-petals. Nevertheless, we have to proceed the local and global shape changes (e.g. compactness, connectivity, etc) on the petals and the object.

1-bouquet, Figure 46(a). After attaching a vertex to the object, we obtain a bouquet consisting of only one face-petal. The necessary local and global shape arrangements to be made on face-petals are described by the following sequence of Euler operators:

(i) $\mathtt{kf}_{\infty h}\mathtt{mf}_h$ to compact a 1-dimensional non-compact hole of a petal face;

(ii) $\mathtt{kF}_{\infty h}\mathtt{C}$ to compact the corresponding 1-dimensional non-compact hole of its non-compact face component;

(iii) $\mathtt{kf}_{\infty}\mathtt{mf} \oplus \mathtt{kF}_{\infty}\mathtt{C}_h$ to compact the outer frontier component of a petal face;

2-bouquet, Figure 46(b). After attaching the vertex to the bouquet, we call the previous sequence of Euler operators twice, one for each petal face.

n-bouquet, Figure 46(c). Analogously, if a bouquet has n face-petals, such a sequence of Euler operators is called n times, once for each petal.

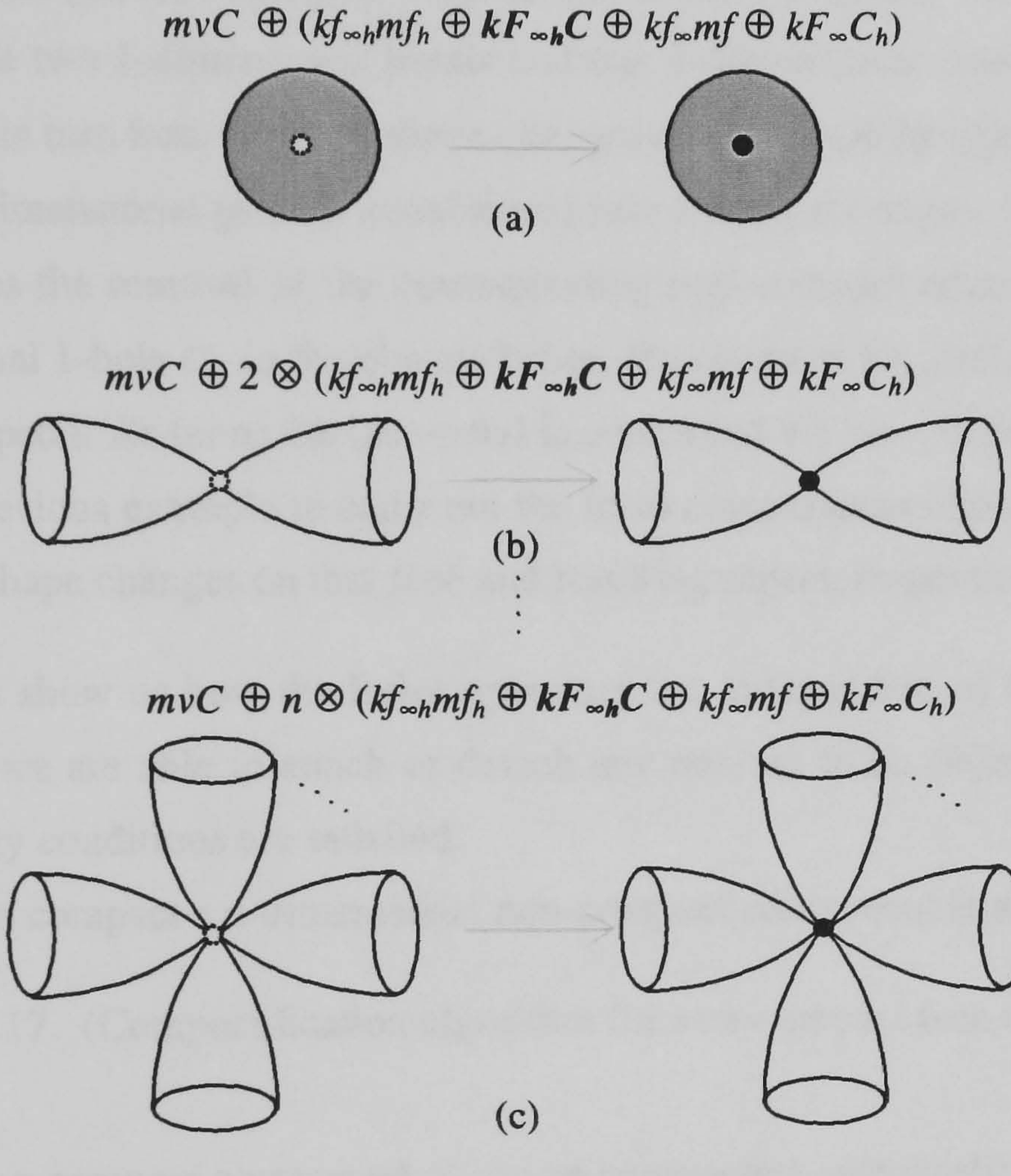

FIGURE 46. Global compacters $\mathrm{kF}_{\infty}\mathrm{C}h$ and $\mathrm{kF}_{\infty h}\mathrm{C}$ for bouquets of faces.

Note that, the petals of a bouquet may be of any dimension > 0. In Figure 47, the bouquet has two edge petals and a face petal.

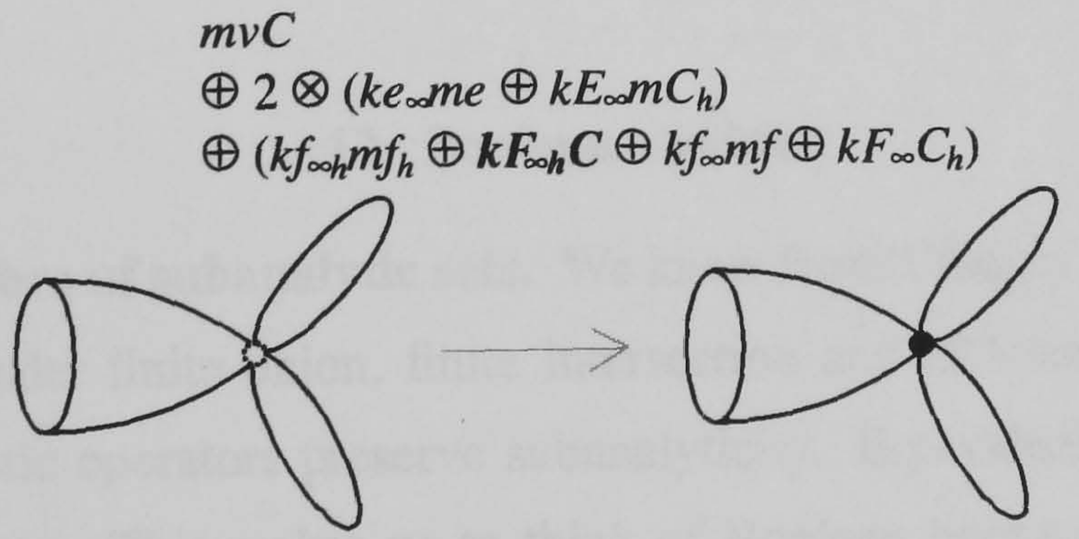

FIGURE 47. Compacters for a mixed-dimensional bouquet.

EXAMPLE 5.24. Figure 47 illustrates the attachment of a vertex to a mixed-dimensional bouquet. As before, we use the compact-geometry Euler operator mvC to attach the vertex to a bouquet. Consequently, it is up to the geometric engine to detect the number of petals and dimension of each one. Doing so, we see that two 1-dimensional petals and one 2-dimensional petal require local compactness changes, which in turn lead to global shape changes on the resulting object. So, the non-compact edge e_∞ of each 1-dimensional petal is transformed into a compact edge e by applying the operator $\mathtt{ke}_\infty\mathtt{me}$. This causes the removal of the corresponding non-compact edge-component $\mathtt{E}_\infty$ and the appearance of a global 1-hole $\mathtt{C}_h$ in the object; hence, the operator $\mathtt{kE}_\infty\mathtt{mC}_h$ is called twice, one for each 1-dimensional petal. As far as the face-petal is concerned we have to call the sequence of Euler operators used in previous example to carry out the local compactness changes on that face, as well as local and global shape changes on that face and resulting object, respectively.

These examples show us how the Euler operators are independent of the shape complexity of an object. That is, we are able to attach or detach any stratum to an object at any time, since the topological regularity conditions are satisfied.

The algorithm to compact a n-dimensional non-compact component is as follows:

ALGORITHM 5.17. (Compactification algorithm for non-compact face components)

INPUT:

(a) the non-compact component F_∞ to be compacted, with $\dim(F_\infty) = 2$.

Begin

(1) **If** F_∞ has i inner 1-holes **then**

(i) Calls $i \oplus \mathtt{kF}_{\infty h}\mathtt{C}$

(2) Calls $\mathtt{kf}_\infty\mathtt{mf} \oplus \mathtt{kF}_\infty\mathtt{C}_h$ [Compact F_∞ as if it were a face without holes.]

End

13. Boolean algebras

13.1. Boolean algebra of subanalytic sets. We know from Chapter 3 that the property of being subanalytic is closed under finite union, finite intersection and difference of any two subanalytic sets. That is, set-theoretic operators preserve subanalyticity. Equivalently, we say that subanalytic sets form a Boolean class. This makes us to think of Boolean operators as possible operators to construct (subanalytic) objects in general. This is not a new idea in geometric modelling as the early geometric modellers (e.g. PADL modeller, [**112, 97**]) emulated a Boolean algebra of semialgebraic sets to construct regularised solid objects.

Unfortunately, a Boolean algebra of point sets, either they are semialgebraic, semianalytic or subanalytic, is alone useless to shape objects because of the following shortcomings:

- *Small shape coverage.* They are strictly *geometric operators* since they operate only on point sets. No other sorts of shape can be handled. For a point set, we can check whether or not a point belongs to it (point membership test), to its interior, exterior or frontier. But, a point set is not a stratified set. Consequently, it is not possible to distinguish a point at a corner from any other point in the frontier of, for example, a cube. Thus, Boolean operators can not be used as general shape operators seeing that they are confined to geometric shapes. They are inadequate to operate on other sorts of shape as, for example, homotopic shapes.
- *Small interactivity.* The manipulation of point sets on computers is basically symbolic. Point sets lack a stratified structure, so the graphical or algorithmic interaction with geometric entities as vertices or edges of a solid is not possible, simply because they do not exist in a point set. In a point set, we have only points, no strata at all. This prevents an engineering designer to pick up or select vertices, edges, and so on, of a geometric object in order to carry out a particular design operation.

In short, Boolean operators are essentially *geometric operators* because they only handle point sets. They are of less importance as general shape operators to model objects of interest for most geometric applications. However, they may have an important role in definition of the geometry of strata of an object, or even subobjects as required by some applications as, for example, finite element modelling.

13.2. Boolean algebra of stratified subanalytic sets. Let us consider now stratified sets instead of point sets. Recall that a stratified set $\mathbf{X} = (X, |X|)$ is a pair that consists of a set $X = \{M_i\}$ of strata and its underlying point set $|X|$, and satisfies a set of conditions of how strata fit together, as seen in Chapter 3. By abuse of language, we sometimes call X a stratified set. A basic property of a stratified set X is that $X = \bigcup M_i$ is the disjoint union of its strata M_i. Therefore, each point of $|X| = \bigcup |M_i|$ lies in the interior of exactly one stratum of X.

Let us see under which conditions stratified sets form a closed Boolean algebra.

EXAMPLE 5.25. Let us look at Figure 48. It shows a stratified set X with two spanning stratified subsets K and L; hence, $X = K \cup L = \{v_1, v_2, v_3, v_4, v_5, e_1, e_2, e_3, e_4, e_5\}$. That is, the union of two stratified subsets is a stratified subset of a stratified set, Figure 48(a). Besides, the intersection $K \cap L = \{v_2, v_3\}$ is also a stratified subset of X, Figure 48(b). This agrees to a Thom property required for stratifications that any finite union and intersection of stratified subsets are stratified subsets (see

Chapter 3 for more details). This mimics a similar property for cell complexes and simplicial complexes. In respect to difference operator between two stratified subsets, the result is also a stratified subset, but not relatively compact one. Figure 48(c) shows the difference between K and L, that is, $K - L = \{v_1, v_4, v_5, e_1, e_4, e_5\}$.

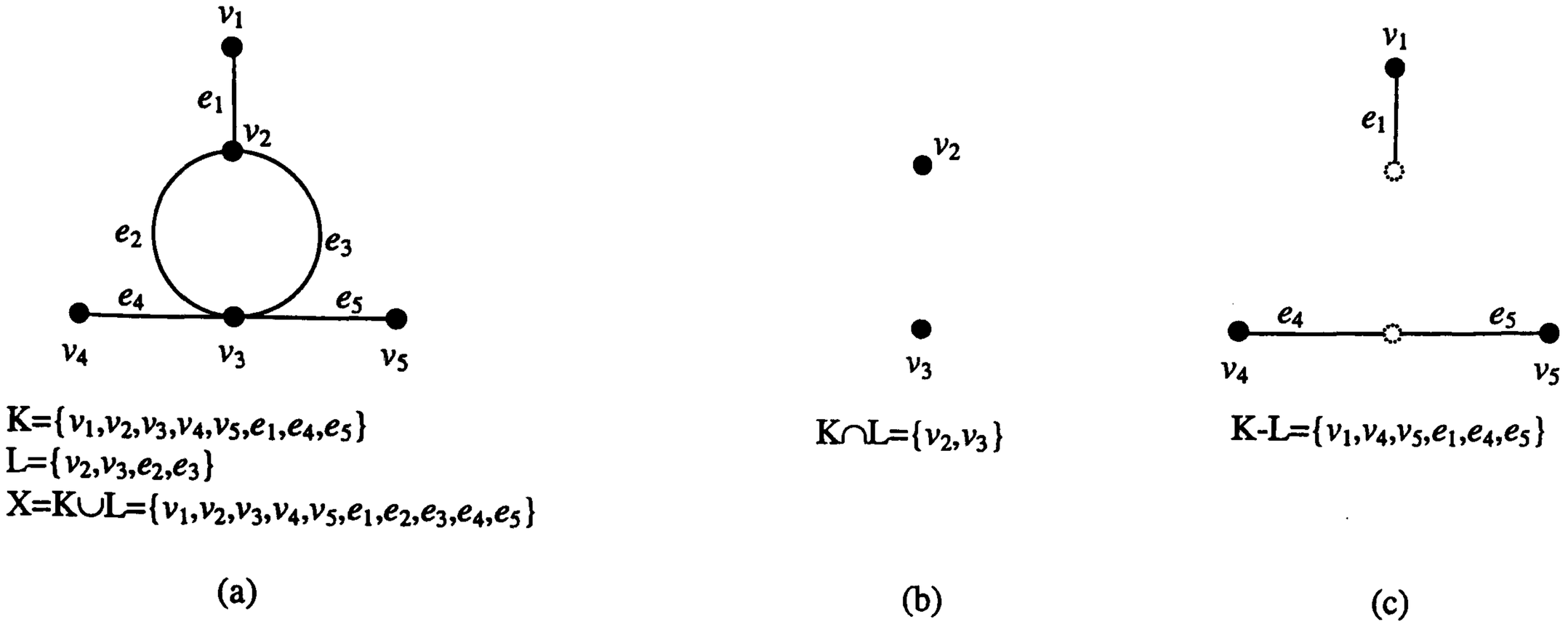

FIGURE 48. Boolean operators of subsets of a stratified set.

FIGURE 49. Boolean operators of stratified sets.

Despite the subsets of a stratified set X form a Boolean algebra in X, in general, stratified sets do not constitute a Boolean class. This is illustrated by the following example.

EXAMPLE 5.26. Let us take the stratified sets $X = \{v_1, v_2, e_1\}$ and $Y = \{v_3, v_4, v_5, v_6, e_2, e_3, e_4\}$ in $\mathbb{R}^2$, Figure 49. The union of X and Y is a set that consists of the strata of X and the strata of Y,

i.e. $X \cup Y = \{v_1, v_2, e_1, v_3, v_4, v_5, v_6, e_2, e_3, e_4\}$, which is not a stratified set because e_1 intersects e_2 and e_4, that is, there are two points shared by different strata. Therefore, $X \cup Y$ is *not* a stratified set, although $|X| \cup |Y|$ is a subanalytic set and $|X| \cup |Y| = |X \cup Y|$. The intersection of two stratified sets is always a stratified set, but $|X| \cap |Y| \neq |X \cap Y|$. In fact, in Figure 49, $X \cap Y = \varnothing$, so $|X \cap Y| = \varnothing$, but $|X| \cap |Y| = \{\mathbf{p}, \mathbf{q}\}$, where $\mathbf{p}$ is the intersection point of $|e_1| \cap |e_2|$, and $\mathbf{q}$ is the intersection point of $|e_1| \cap |e_4|$. The fact that there are no strata shared by both stratified sets X and Y implies that $X - Y = X$, which is also a stratified set. But, unfortunately, $|X| - |Y| = |X| - \{\mathbf{p}, \mathbf{q}\}$ which is not equal to $|X - Y| = |X|$.

This example shows that stratified sets do not constitute a Boolean class. However, a Boolean algebra can be generated by first overstratifying both operands in such a way that overlapping or intersecting points are 'eliminated'[2]. More formally, we have:

DEFINITION 5.1. The *stratified intersection* $\mathbf{X} \sqcap \mathbf{Y}$ of two stratified sets, $\mathbf{X} = (|X|, X)$ and $\mathbf{Y} = (|Y|, Y)$, is defined as follows:

(i) $X \sqcap Y = X^* \cap Y^*$, where X^* and Y^* are overstratifications of X and Y, respectively, due to their intersecting stratified subset;

(ii) $|X| = |X^*|$ and $|Y| = |Y^*|$;

(iii) $|X^*| \cap |Y^*| = |X^* \cap Y^*|$.

DEFINITION 5.2. The *stratified union* $\mathbf{X} \sqcup \mathbf{Y}$ of two stratified sets, $\mathbf{X} = (|X|, X)$ and $\mathbf{Y} = (|Y|, Y)$, is defined as follows:

(i) $X \sqcup Y = X^* \cup Y^*$, where X^* and Y^* are overstratifications of X and Y, respectively, due to their intersecting stratified subset;

(ii) $|X| = |X^*|$ and $|Y| = |Y^*|$;

(iii) $|X^*| \cup |Y^*| = |X^* \cup Y^*|$.

DEFINITION 5.3. The *stratified difference* $\mathbf{X} \sqcap\!\!- \mathbf{Y}$ of two stratified sets, $\mathbf{X} = (|X|, X)$ and $\mathbf{Y} = (|Y|, Y)$, is defined as follows:

(i) $X \sqcap\!\!- Y = X^* - Y^*$, where X^* and Y^* are overstratifications of X and Y, respectively, due to their intersecting stratified subset;

(ii) $|X| = |X^*|$ and $|Y| = |Y^*|$;

(iii) $|X^*| - |Y^*| = |X^* - Y^*|$.

---

[2]Conversely, Djinn partitions (i.e. overstratifications) are defined in terms of set operators (see, for example, [85] and [87]). Thus, the algorithms underlying our stratified set operators are distinct from those of Djinn.

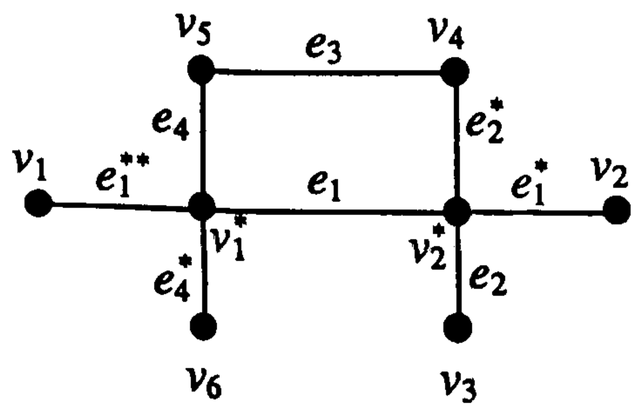

$X^*=\{v_1,v_1^*,v_2^*,v_2,e_1^{**},e_1,e_1^*$
$Y^*=\{v_3,v_2^*,v_4,v_5,v_1^*,v_6,e_2,e_2^*,e_3,e_4,e_4^*\}$

(a) $X \sqcup Y$

(b) $X \sqcap Y$

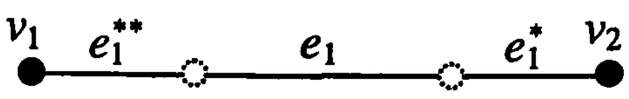

(c) $X \mapsto Y$

FIGURE 50. Stratified Boolean operators of stratified sets.

EXAMPLE 5.27. Let us take again the two stratified sets X, Y depicted in Figure 49(a). First, we have to compute their intersection subset, which consists of two strata, v_1^* and v_2^* corresponding to intersection points **p** and **q**, respectively. Each intersection stratum subdivides overlapping strata of X and Y. So, v_2^* subdivides $e_1 \in X$ and $e_2 \in Y$, whilst v_1^* subdivides $e_1 \in X$ and $e_4 \in Y$. That is, the intersecting subset imposes an overstratification X^* for X and an overstratification Y^* for Y. The resulting stratified union of X and Y is pictured in Figure 50(a). The stratified intersection $X \sqcap Y$ is nothing more than the intersection subset of X^* and Y^*, Figure 50(b). At last, the stratified difference $X \mapsto Y$ is drawn in Figure 50(c).

The *stratified Boolean algebra* $(\mathcal{S}, \{\sqcup, \sqcap, \mapsto\})$ is surely closed in the class $\mathcal{S}$ of stratified subanalytic sets, where $\{\sqcup, \sqcap, \mapsto\}$ is the set of stratified Boolean operators, as defined above. Stratified Boolean operators are useful to implement high-level geometric operations such as set-theoretic operations of extant geometric modellers, or even attachment and detachment of design form features of current CAD/CAM systems. Therefore, they are richer shape operators than conventional Boolean operators. Besides, they admit graphical interaction with the designer. However, they do not provide any means to control locally and globally the shape of an object. However, stratified Boolean operators must satisfy the requirement that all the strata of their operands are at least C^1. That is, strata are not allowed to have differential singularities. Otherwise, the result may not be a stratified set. This is illustrated by the following example. (An analogous counterexample can be found in [87, p.690].)

COUNTEREXAMPLE 5.1. Let $X = \{v_1, v_2, e_1\}$ and $Y = \{v_3, v_4, e_2\}$ be two stratified sets, three strata each, Figure 51(a). The corresponding point sets are $|X| = |v_1| \cup |e_1| \cup |v_2| = (0 \times 1) \cup$

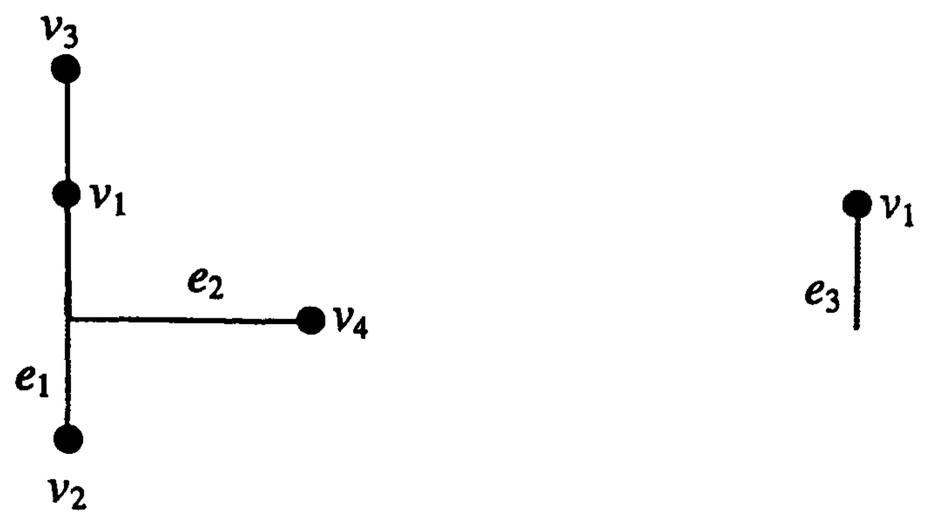

(a) (b)

FIGURE 51. Stratified Boolean operators may fail for non-smooth strata.

$(0\times]-1,1[) \cup (0 \times (-1))$ and $|Y| = |v_3| \cup |e_2| \cup |v_4| = (0 \times 2) \cup (0 \times [0,1[\cup]0,2[\times 0) \cup (2 \times 0)$, respectively. The stratified intersection $X \sqcap Y = \{v_1, e_3\}$ is depicted in Figure 51(b) is not a stratified set because e_3 is not a relatively open stratum. In fact, $|e_3| = |e_1| \cap |e_2| = (0\times] - 1, 1[) \cap (0 \times [0,1[\cup]0,2[\times 0) = 0 \times [0,1[$, which is not relatively open in the y-axis as the origin 0×0 is included.

Thus, stratified Boolean operators require smooth strata for stratified set operands. This forces the stratification of non-smooth strata. However, some geometric applications such as, for example, finite element applications may require such non-smooth strata. A possible solution for this problem is to keep such non-smooth strata as stratified subsets or subcomplexes in their object. This enables the geometric persistence of non-smooth strata of an object.

14. Mathematical design issues: shape operators

Boolean operators are important shape operators because they may be used as:

- *Set-theoretic operators of point sets.* They can be used for sets which are point sets, i.e. sets defined as subsets of some Euclidean space. They are geometric operators, i.e. they operate on point sets, regardless whether those point sets are point sets of strata, varieties, semivarieties, or even more complicated point sets. Thus, they are essential either for purely geometric kernels (e.g. CSG modellers) or for stratified geometric kernels (B-rep modellers) which define the geometry of each stratum as a Boolean combination of point sets. For example, in Figure 52, the de-partition of f_1 and f_2 into f_3 by e_2 implies the geometric union of $|f_1|$, $|f_2|$, and $|e_2|$, i.e. the point set $|f_3| = |f_1| \cup |e_2| \cup |f_2|$. This shows that Boolean operators may be subsumed under Euler operators to carry out geometric operations on point sets of strata. Equivalently, the geometric union of $|f_1|$, $|f_2|$, and $|e_3|$ may be demanded by merging of f_2, f_3, and e_1 through the Euler operator `kef` (*kill edge and face*). Even in

the case that the geometry of a stratum is not defined by booleans, but by its supporting or relative geometry instead, set-theoretic operators are still important to determine geometric intersection of strata, i.e. the point set that results from the intersection of two stratum point sets. Clearly, this geometric intersection can be easily generalised to all stratum point sets of two objects in order to determine the geometric intersection of them. Thus, set-theoretic operators of point sets are indispensable to any kind of geometric modeller.

- *Set-theoretic operators of strata.* They do not constitute a Boolean algebra in the class of regular stratified sets. Nevertheless, they can be used to construct and de-construct stratified objects if the following condition is satisfied: strata of both operands are disjoint, i.e. they do not overlap. Otherwise, the resulting set of strata is not surely a stratified set. Recall that stratified set-theoretic operators overstratify the overlapping strata of their operands before applying the corresponding set-theoretic operators. Therefore, apart of the overlapping strata, the stratified set-theoretic operators work as usual set-theoretic operators because it is ensured *a priori* that combining strata do not overlap. They can be used to define other stratified operators such as those introduced by Middleditch *et al.* [87], the partition and de-partition operators in particular.
- *Attachment operations* ($\boxplus$). By definition, an attacher is an operator that changes the geometry (or the point set underlying) of an object by the attachment of a stratum. They are said to be *constructors* or *makers* of stratified objects. They allow the stepwise construction of stratified objects by attaching strata, as illustrated in Figure 53. To attach a stratum to a stratified object X we use an Euler operator, or alternatively the set-theoretic union of X with a stratified singleton containing such a stratum. We start with the empty stratified set $X = \varnothing$. The subsequent steps attach $\{v_1\}$, $\{e_1\}$, $\{v_2\}$, $\{e_2\}$, $\{f_1\}$, and $\{f_2\}$, namely:

(1) $X = X \cup \{v_1\} = \{v_1\}$
(2) $X = X \cup \{e_1\} = \{v_1, e_1\}$
(3) $X = X \cup \{v_2\} = \{v_1, e_1, v_2\}$
(4) $X = X \cup \{e_2\} = \{v_1, e_1, v_2, e_2\}$
(5) $X = X \cup \{f_1\} = \{v_1, e_1, v_2, e_2, f_1\}$
(6) $X = X \cup \{f_2\} = \{v_1, e_1, v_2, e_2, f_1, f_2\}$

Note that the point sets of the operands do no overlap. So, this disjoint union is also called *disjoint attacher*. Obviously, the same result is obtained by using the stratified set-theoretic union. In case of overlapping of underlying point sets, we cannot use set-theoretic union as an attacher. Instead, we use the stratified set-theoretic union, to which we call

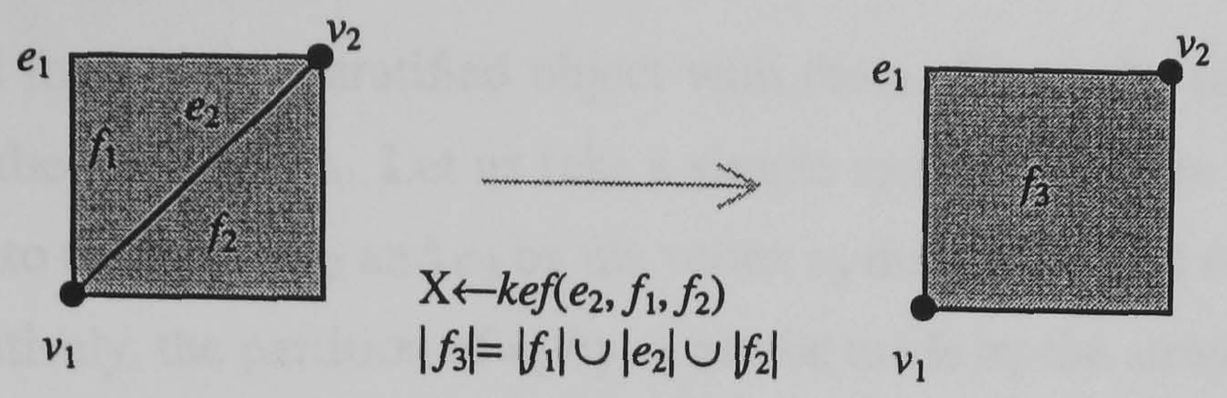

FIGURE 52. Topological and geometric departitions of two faces and an edge into a face.

jointed attacher. These attachers can be easily generalised for stratified objects that embody, for example, form features. Why do we need these operators if they are just stratified set operators? Because they are more closely related to the design level than set operators. Some design operations such as, for example, the interactive attachment of a through hole to a part or just a vertex to a line segment, can be carried out by a designer without explicitly referring to set operators. The attachment operation of two stratified sets X and Y is denoted by $X \boxplus Y$.

- *Detachment operations* ($\boxminus$). Analogously, the set-theoretic difference operator can be used to detach strata from a stratified object. For example, to delete the edge e_2 from X in Figure 54(a), we apply the set-theoretic difference such that $X = X - \{e_2\}$. The result is shown in Figure 54(b). The same set-theoretic operator is used to delete the relatively non-compact face $f_{\infty 1}$, Figure 54(c). This is a *disjoint detacher* seeing that the point sets of both operands of the set-theoretic difference do not overlap. It is equivalent to the disjoint detacher based on the stratified set-theoretic difference. Analogously, a *jointed detacher* can be defined in terms of the stratified set-theoretic difference. However, it cannot be given in terms of the usual set-theoretic difference because the point sets of operands may overlap. The detachment operation of two stratified sets X and Y is denoted by $X \boxminus Y$.
- *Partition operations* ($\boxplus$). Partition or subdivision operators are 'trivial' Euler operators. The question now is to know whether these partitioners can be implemented through set-theoretic operators. To answer to this question, we have first to remember that set-theoretic operations of stratified objects operate on sets of strata, not on point sets. Consequently, attaching or uniting an edge to a face in order to subdivide it into two faces is nonsense. The result is an edge overlapping a face; no subdivision occurs through this face. Thus, we obtain a set of strata which is not a stratified set. We can think of boolean intersection as possible solution to subdivide strata, but what it does is a mere selection of strata shared by both stratified

operands and form a new stratified object with them. Thus, the only solution here is the stratified set-theoretic union. Let us take a simple example, Figure 55. The subdivision of the edge e_1 into two edges e_2 and e_3 by the vertex v_3 may be carried out by the Euler operator mve. Alternatively, the partition of e_1 by v_3 can be made by the stratified set-theoretic union of X which includes e_1 and Y that is a singleton stratified set which includes v_3. The partition operation of two stratified sets X and Y is denoted by $X \boxplus Y$.

- *De-partition operations* ($\boxminus$). De-partition operator is the inverse of the partition operator, and is denoted by $X \boxminus Y$. Basically, it merges two equi-dimensional strata of dimension k incident at a common stratum of dimension $k-1$ into one stratum of dimension k. Besides, the point set of the resulting stratum is the set-theoretic union of the point sets of the three involved strata. Let us look at the Figure 56. In (a), we have two stratified objects $X = \{v_1, v_2, v_3, e_2, e_4\}$ and $Y = \{v_3\}$. So, Y is the intersection set of X and Y. What we want to do is to de-partition X against Y. In other words, we intend to merge v_3 with e_2 and e_3. The de-partition operation proceeds at two levels. At the first level, the geometric level, a new point set $|e_1| = |e_2| \cup |v_1| \cup |e_3|$ is created as the union of the point sets of the merging strata. At the second level, the stratification level, the de-partition operation consists of three steps: (i) first, the set $Z = \{v_3, e_2, e_3\}$ of merging strata is created; (ii) Z is detached from X, i.e. we determine $X \boxminus Z$; (iii) a new stratum e_1 and a stratified singleton $W = \{e_1\}$ are generated; (iv) e_1 is attached to the current object through the attachment operator such that the final result is $X \boxminus Z = X \boxminus Z \boxplus W$.

In short, the stratified set-theoretic operators seem to be an alternative to Euler operators as the fundamental shape operators of regular stratified subanalytic objects. In fact, the attachment, detachment, partition, and departition operators can be implemented on the top of stratified set-theoretic operators. A possible disadvantage of these operators is that they basically operate on strata and their corresponding point sets. They do not operate on absent point sets, say holes. So, unless we have adequate shape reasoning algorithms to infer and control the homotopic shape of strata and stratified objects, a stratified geometric kernel based on stratified set-theoretic operators may fail to satisfy significant requirements in some geometric applications such as, for example, form-feature based modelling. Stratified set-theoretic operators are good enough to attach and detach form features, but inadequate to recognise their shape transmutations as explained in [**46**]. Obviously, this problem can be solved by implementing such stratified set-theoretic operators on the top of the Euler operators described in this chapter, similar to what is usual in conventional B-rep modellers.

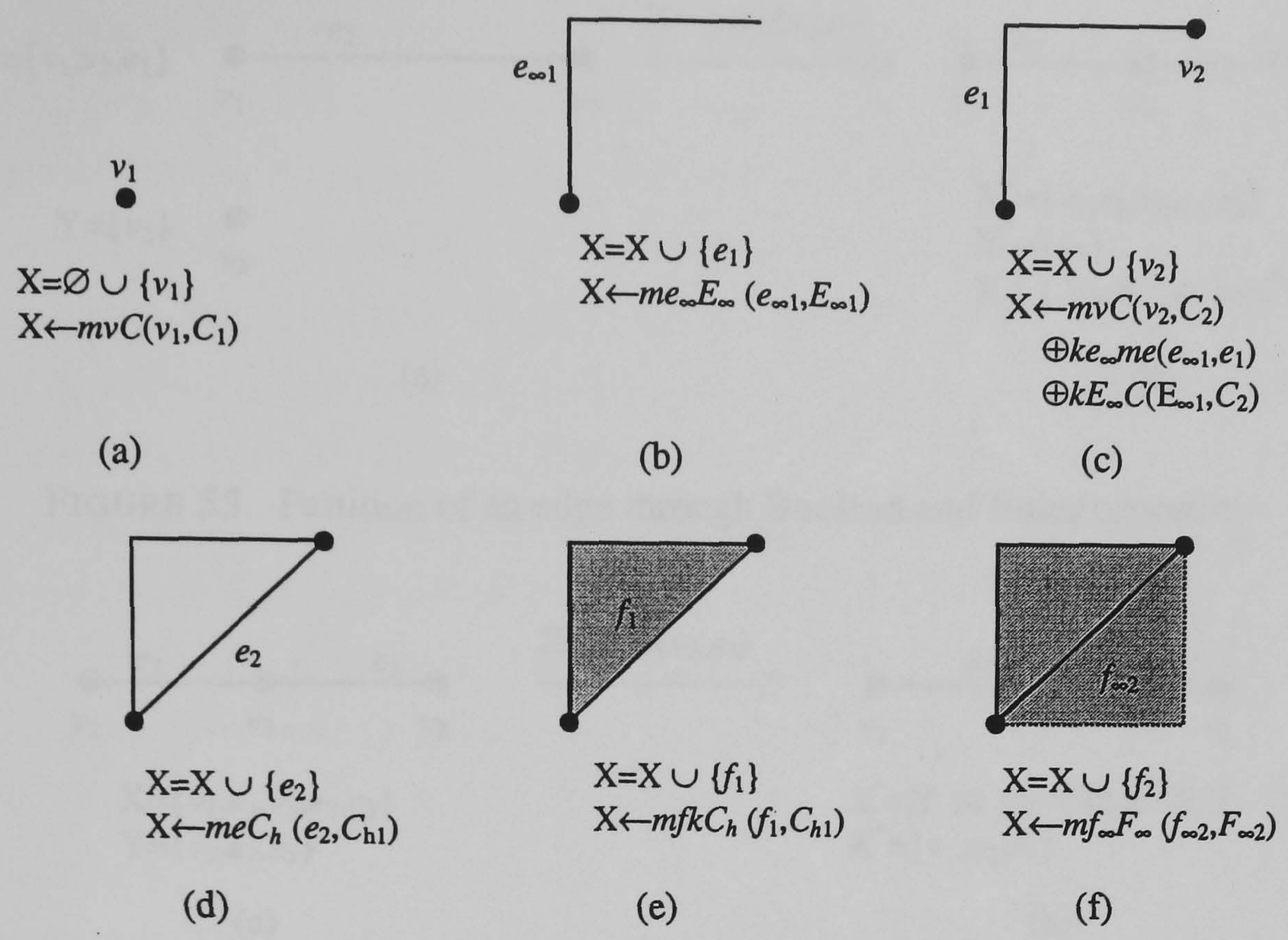

(a) X=∅ ∪ {v_1}
X←$mvC(v_1,C_1)$

(b) X=X ∪ {e_1}
X←$me_{\infty}E_{\infty}$ ($e_{\infty 1}$,$E_{\infty 1}$)

(c) X=X ∪ {v_2}
X←$mvC(v_2,C_2)$
$\oplus ke_{\infty}me(e_{\infty 1},e_1)$
$\oplus kE_{\infty}C(E_{\infty 1},C_2)$

(d) X=X ∪ {e_2}
X←meC_h (e_2,C_{h1})

(e) X=X ∪ {f_1}
X←$mfkC_h$ (f_1,C_{h1})

(f) X=X ∪ {f_2}
X←$mf_{\infty}F_{\infty}$ ($f_{\infty 2}$,$F_{\infty 2}$)

FIGURE 53. Stratum attachment through Boolean and Euler operators.

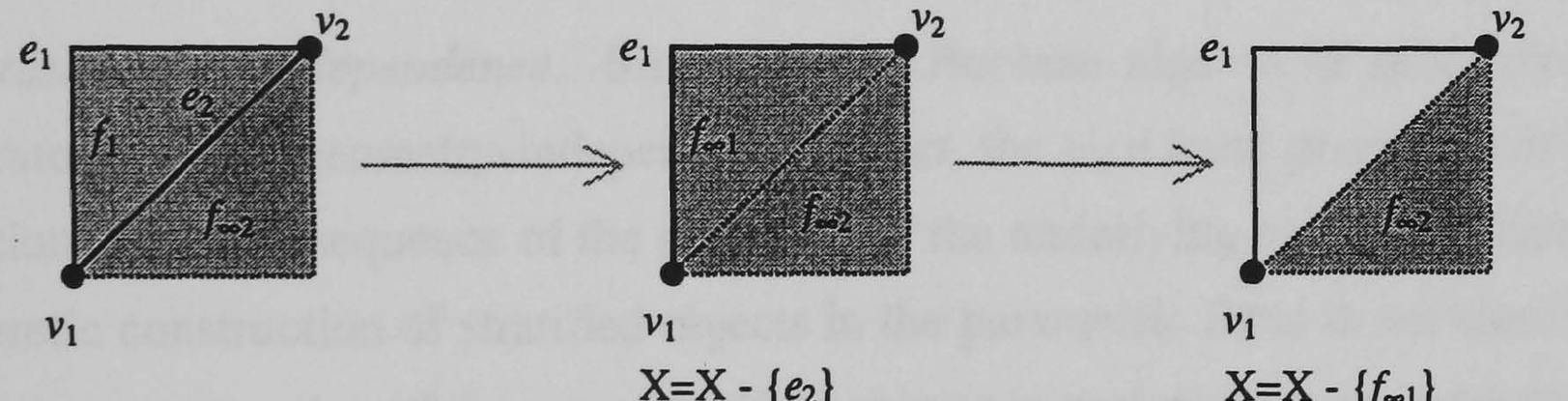

(a)

(b) X=X - {e_2}
X←$mF_{\infty}C_h(F_{\infty 1},C_{h1})$
$\oplus mf_{\infty}kf(f_{\infty 1},f_1)$
$\oplus keC_h(e_2,C_{h1})$

(c) X=X - {$f_{\infty 1}$}
X←$kf_{\infty}F_{\infty}(f_{\infty 1},F_{\infty 1})$

FIGURE 54. Stratum detachment through Boolean and Euler operators.

The fundamental shape operators of the Σ-kernel are Euler operators because:

- *Geometric coverage*. They are applicable to a large class of point sets, say subanalytic sets. Thus, they are general from the geometry point of view. At this point, we can say that they have the same advantages as the Boolean algebra of subanalytic sets.

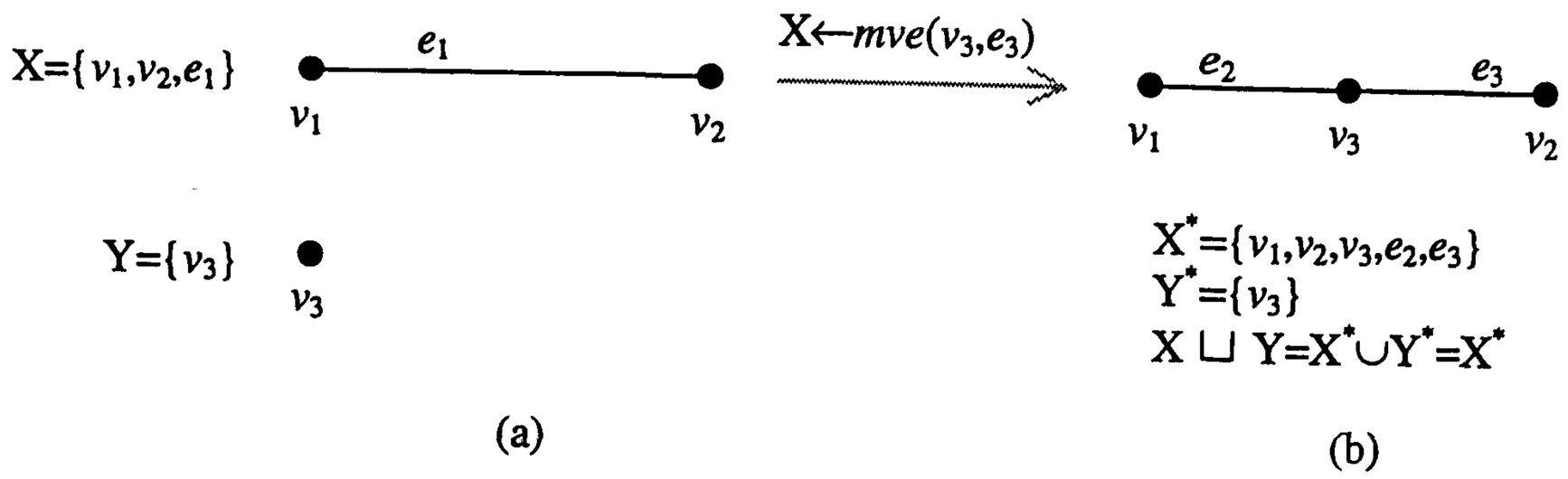

FIGURE 55. Partition of an edge through Boolean and Euler operators.

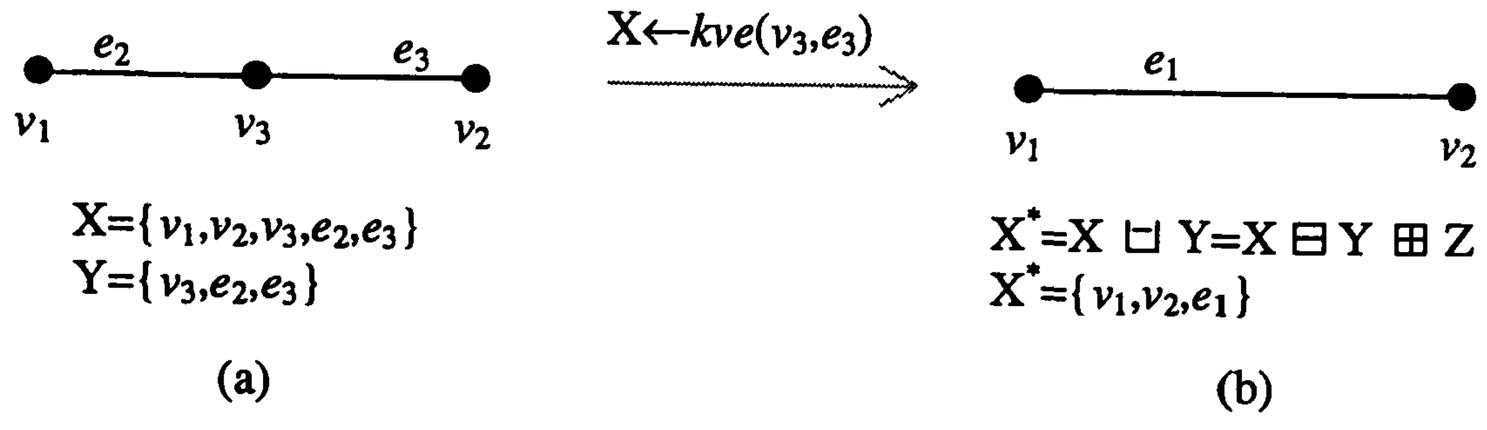

FIGURE 56. De-partition of an edge through Boolean and Euler operators.

- *Representation independence.* Similar to the Boolean algebra of subanalytic sets, Euler operators are not geometry-independent. In fact, the nice local properties of regular stratifications are a consequence of the geometry of the underlying point sets. However, the set-theoretic construction of stratified objects in the parametric form is not clear yet, while the Eulerian construction of the same stratified objects is straightforward, regardless of whether stratum point sets are implicit representations and parametric representations of geometry. Thus, the Σ-kernel admits the simultaneous representation of point sets which are either level sets (or 'kernels') or images of maps. It is even possible to stitch two surfaces with distinct geometric representations to observe a pre-defined order of continuity or smoothness, by making use of the Boardman symbols of contact. But, this is an open issue to future research.
- *Topological coverage.* Either Eulerians or stratified Booleans do not impose restrictions of the topological coverage of strata or stratified objects. Strata are not required to be relatively closed, neither relatively open, or both. They are not required to be relatively bounded either. That is, they not required to be relatively compact. For Euler operators, this is a consequence of the general Euler formula we have used.

- *Homotopic coverage.* Some Euler operators manipulate local holes, some Euler operators global holes, and other Euler operators handle both local and global holes. Thus, Euler operators enable the design of data structures that enable the representation of homotopic shapes, as well as homology-based homotopic reasoning algorithms. The Σ-kernel even enables the construction of 'black & decker' holes, i.e. pure point set holes in the sense that no stratum is used to denote such a hole. Unlike Euler operators, stratified set-theoretic operators do not recognize homotopic shapes. They operate only on sets of strata, independently of their homotopic shape. Obviously, this places difficult problems to overcome during shape processing and construction of objects, unless such stratified Booleans operate on a homological structure or Thom incidence scheme. Thus, Euler operators allow us to have a complete control on the homotopic shape of strata and objects.
- *Algebraic atomicity.* All stratified operators such as stratified set-theoretic operators, stratum attachers and detachers, partitioners and de-partitioners, and respective variants as those introduced in [87] can be expressed and implemented in terms of Euler operators.
- *Hadwiger shape coverage.* Stratified set-theoretic operators are better adequate to manipulate Hadwiger or convex shapes than Euler operators. In fact, Hadwiger shapes as stratified subobjects are *a priori* easily removed from or inserted into an object by applying the stratified difference or the stratified union, respectively. However, to the light of the shape theory axioms of Chapter 1, Hadwiger shapes are related to homotopic shapes. Therefore, any change in the Hadwiger ring of an object most probably changes the homotopy shape structure of it. Unfortunately, stratified Booleans are alien to homotopic shape changes. In order to keep the control on the shape of an object is then necessary to implement stratified set-theoretic operators on the top of Euler operators.
- *Stratification closure.* They inherently control the topological regularity or topological stability of the stratification of an object whenever its shape changes. This is not clear for shape changes caused by stratified set-theoretic operators.
- *Dimension-independence.* A significant disadvantage of conventional Euler operators is that they have been restricted to objects of dimension up to 3. One of the achievements of this thesis is just their generalisation to multi-dimensional objects in $\mathbb{R}^n$. Moreover, such objects, and their strata, need not be relatively compact. In terms of software engineering design, dimension-independence has two immediate consequences. First, it has a smaller kernel in terms of programming language code. The second consequence is ease of maintenance.

- *Order independence.* Usually, conventional Euler operators are associated with relatively compact objects. They follow the principle that a stratum cannot be created before its frontier. This means that there is an order in the construction of objects. Unlike these conventional Euler operators, those of Σ-kernel allow us to construct objects without a predefined order of attaching or detaching strata. Equivalently, a stratum or a subobject may be removed from or inserted into the target object at any time and order. This is possible because the strata and objects are not necessarily relatively compact. In other words, this is a consequence of having a bigger topological coverage or a more general Euler formula. Order-independent design of objects is another significant achievement of this thesis.

15. Σ-geometric kernel revisited

The Σ-geometric kernel has been designed to meet the requirements of a general-purpose shape modeller, either it is a geometric modeller, a feature modeller, a CAD system, a finite element system, or any other possible geometry machines such as, for example, morphing and animation systems. Its general design comes from three important points: representation independence, dimension independence, and design-order independence of objects. Let us focus on the latter two issues.

15.1. Dimension independence. In Chapter 4, a dimension-independent data structure has been introduced. It enables a unified view of disparate research areas such as computer graphics, solid and geometric modelling, and computational geometry. But, without an algebra of dimension-independent shape operators capable of handling a variety of objects with distinct properties as required for the more diverse geometric applications, such a data structure would be possibly useless. Moreover, shape operators must be atomic in such a way that any shape operation required for any geometric application can be constructed or programmed by a sequence of those atomic shape operators. The dimension-independent Euler operators fulfill these important requirements.

15.2. Design order independence. Current CAD systems imposes serious design restrictions. For example, CAD systems usually do not provide any means, say n-dimensional design operators, to construct an object by attaching or detaching strata stepwise by direct graphical interaction. An n-dimensional design operator simply either attaches a n-stratum to an object or detaches a n-stratum from it. So, a design attacher is denoted by `mv` (*make vertex*), `me` (*make edge*), `mf` (*make face*), and so on. The corresponding design detachers are the inverses of the attachers; so, we have `kv` (*kill vertex*), `ke` (*kill edge*), `kf` (*kill face*), etc. It is clear that they internally call an appropriate Euler operator

to make the corresponding attachment of a stratum. These n-dimensional design operators have two major advantages:

- *Operator encapsulation.* They encapsulate the details of seemingly complicated Euler operators.
- *Drafting-like design.* They enable the design of objects by following the principles of manual drafting and computer-assisted drafting.

However, the use of n-dimensional design operators is only possible if we have an approach to map each n-dimensional design operator into a sequence of Euler operators. Surely, such an approach requires important homology-based reasoning algorithms and some kind of event-driven programming. It is an open issue for future research. The stepwise construction of a tetrahedron through design operators is illustrated in Figure 57, and described by the following example.

EXAMPLE 5.28. (*Construction of a tetrahedron without order constraints on the strata to be attached to it.*) The construction steps illustrated in Figure 57 are as follows:

mv. This design operator intends to add a vertex to an empty object. It calls the Euler operator mvC to add a point-component to the empty object.

3×me. The designer uses the operator me three times to add three edges to the object. The operator me calls the Euler operator $\mathtt{me}_{\infty}\mathtt{E}_{\infty}$ to add a non-compact edge to the object.

2×mv. Adding two vertices to the object makes two of its edges compact. So, the Euler operators mvC and $\mathtt{ke}_{\infty}\mathtt{me}$ are called twice.

3×me. The first operator me calls the Euler operator $\mathtt{meC}_h$ which makes a 1-dimensional hole $\mathtt{C}_h$ by inserting an edge between two vertices. The second operator me calls $\mathtt{me}_{\infty}\mathtt{E}_{\infty}$ which adds a non-compact edge to the object.

mf. It calls $\mathtt{mfkC}_h$ to kill a previously created 1-dimensional hole by attaching a face (the back face).

mv. The attaching of the fourth vertex connecting the remaining two non-compact edges gives rise to the appearance of a 1-dimensional hole. This is made by calling the following Euler operators: mvC to create a vertex-component, 2× $\mathtt{Ke}_{\infty}\mathtt{me}$ to make two edges compact, $\mathtt{kE}_{\infty}\mathtt{C}$ to kill an edge-component and a vertex-component, and $\mathtt{kE}_{\infty}\mathtt{mC}_h$ to kill the remaining edge-component and create the left 1-dimensional hole.

me. It calls $\mathtt{meC}_h$ to attach an edge between two vertices. It implies the appearance of the right 1-dimensional hole.

3×mf. The first mf eliminates the left 1-dimensional hole by calling $\texttt{mfkC}_h$. The second mf eliminates the right 1-dimensional hole by calling $\texttt{mfkC}_h$. The third mf calls $\texttt{mfC}_c$ to attach the bottom face producing a 2-cycle (or shell), what, in homotopy terms, is called a 2-dimensional hole.

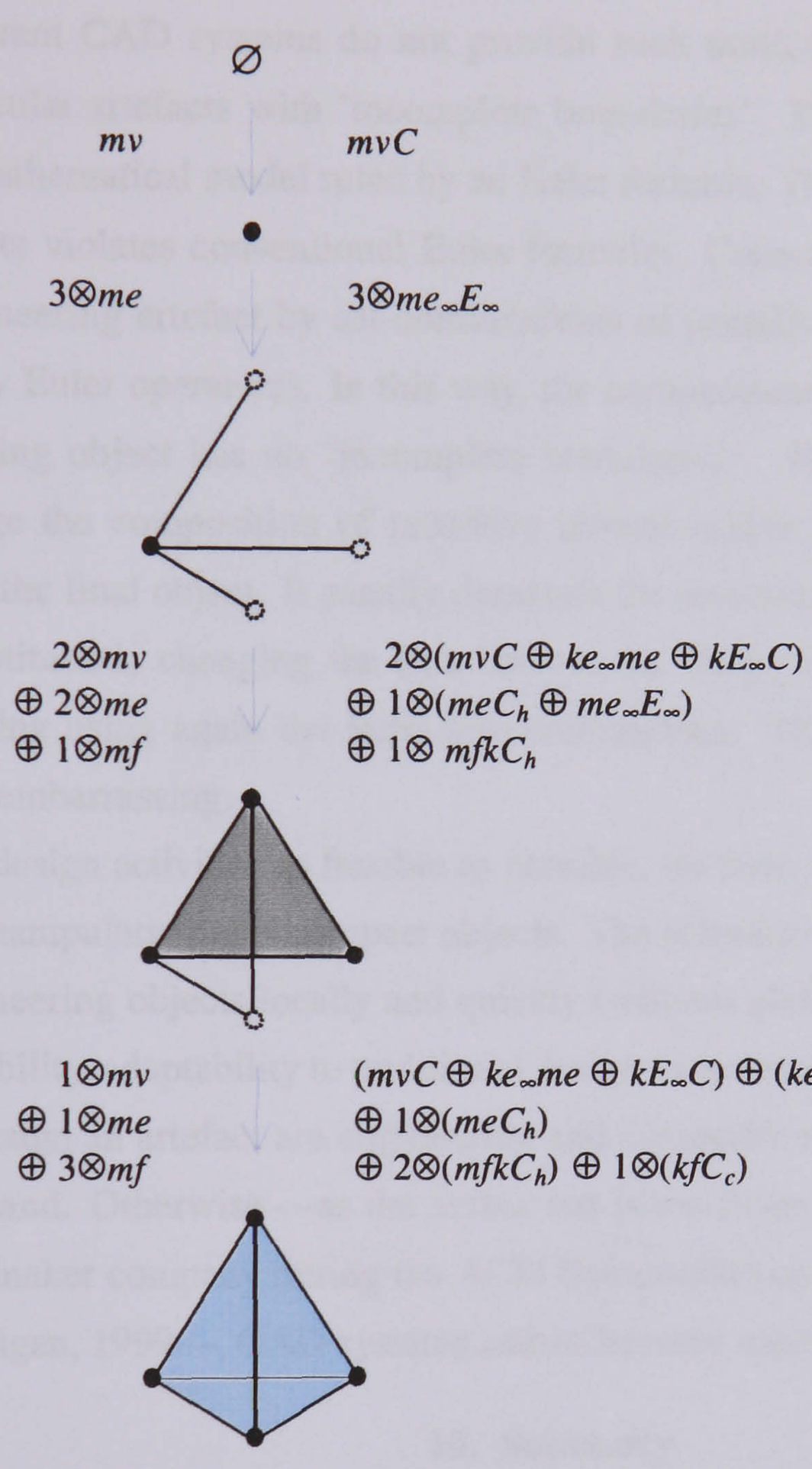

FIGURE 57. Construction of a tetrahedron.

The design operators are not Euler operators. The designer need not know too much about the mathematics underlying the geometric kernel. The designer usually intends to add or remove vertices, edges, faces, etc. to construct an engineering artefact. Usually, a designer does not have a rigorous idea of shape of an object, and thus he/she is not aware of shape changes that may occur by adding or removing a stratum. It should be up to geometric engine to process such shape changes, either they are local, zonal, or global to an object. Surely, homological reasoning algorithms are required

in order to determine which shape changes may occur in consequence of inserting or removing a stratum. This causes a series of Euler operators to be called in order to perform such shape changes. Therefore, design operators encapsulate Euler operators.

However, current CAD systems do not provide such multi-dimensional facilities in designing artefacts, in particular artefacts with 'incomplete boundaries'. This has been essentially due to the lack of a sound mathematical model ruled by an Euler formula. The non-compactness of 'incomplete boundary' artefacts violates conventional Euler formulæ. Consequently, the designer is induced to construct an engineering artefact by set-combinations of primitive solid objects (even for primitive objects defined by Euler operators). In this way, the compactness of the resulting object is ensured, that is, the resulting object has no "incomplete boundaries". The fact that it is not, in principle, possible to change the composition of primitive objects makes difficult to proceed to even small shape changes in the final object. It usually demands the de-construction of the resulting object into its primitive constituents, changing the size but not the shape of one or more primitives, and re-construct everything using again the same set-combinations. This lack of flexibility against shape changes is rather embarrassing.

To make the design activities as flexible as possible, we have to have operators, say Euler operators, capable of manipulating non-compact objects. The relaxation of compactness is also important to re-design engineering objects locally and quickly (without global reconstruction) just before their production. Flexibility, adaptability to traditional design techniques (or drafting), capability of locally and quickly re-design an artefact are engineering and competitive requirements that many industrial practitioners demand. Otherwise —as the author has learnt from an industrial manager working for a worldwide car-maker company during the ACM Symposium on Solid Modeling and Applications, Ann Arbor, Michigan, 1999—, CAD systems risk to become useless.

16. Summary

Euler formulæ are central to the design and implementation of combinatorial B-rep data structures. We have made a series of generalisations to these formulæ —what is also of significant mathematical interest— in order to encompass regular stratified objects. These stratified objects can be of any dimension and not necessarily compact. The compactness relaxation has enabled the construction of an object without a pre-defined order to attach or detach strata. Thus, the rather restrictive principle of conventional B-reps according to which a stratum must be attached only after its frontier strata is no longer necessary. This is quite useful for many geometry-based applications where significant a freedom degree is required in the conception and design of geometric objects.

Conclusions

Well, really, I came to seek a theory, not to propound one.

C. Doyle, The Noble Bachelor

The mathematical design of a general-purpose geometric kernel involves many aspects related to algebra, function theory, point set topology, differential topology and geometry, homotopy, convexity theory, algebraic geometry, which altogether should match important requirements such as computability, human-machine interactivity, design intent, editing facilities, etc.

The ultimate objective of this mathematical design is just to make possible the effective integration of shape through engineering environments based on computer aided design and manufacturing. Such an integration requires:

- The integration of geometries used in solid modelling and free-form modelling of curves and surfaces.
- The integration of geometries with their structures. Recall the subanalytic geometry admits regular stratifications.
- The integration of geometric structures used in B-reps and CSG-reps. This is only possible if a stratified geometric structure with subcomplexes is available.
- The integration of geometric structures with other shape structures such as convex structures and homotopy structures. Once again, this is only possible if a stratified geometric structure with subcomplexes is available.

So, the main contributions of current PhD work are:

- *Chapter 1.* It proposes a general shape theory that encompasses the solid modelling, free-form modelling of curves and surfaces, and form feature modelling. The role of the mathematics has been shown to be very important to be able to relate these research areas through a hierarchy of mappings. This hierarchy of shape mappings allows to establish the (containment) relationships between different shapes in an object. As a consequence, a shape taxonomy has been introduced in Chapter 1. In particular, we have proposed a possible

axiomatics for form feature modelling based on the relationships between homotopy shapes and convex shapes.

- *Chapter 2*. It shows that parametric representations and (explicit) implicit representations of objects are part of the same theory, which combines function theory with manifold theory. So, the C^r continuity conditions can be obtained for both parametric and implicit formulations of manifolds in a similar way. Moreover, it is shown that the different notions of geometric continuity found in the computer-aided geometric design literature are just particular cases of the mathematical notion of C^r smoothness or continuity.
- *Chapter 3*. It presents a mathematical theory that generalises and unifies the theories behind B-reps (boundary representations) and CSG-reps (constructive solid geometry representations) of solids. The corresponding mathematical model congregates subanalytic geometry and Whitney stratifications of varieties. This theory has been extended to parametric objects via Thom-Boardman stratifications of the same subanalytic sets.
- *Chapter 4*. It introduces a dimension-independent representation for regular stratified objects, called *subcomplex-tuple representation*, or simply *Σ-representation*. It generalises current boundary representations to higher dimensions. It generalises the *cell-tuple representation* of Brisson to regular stratified objects, not necessarily homogeneous in dimension nor relatively compact. The existence of subcomplexes in the data structure facilitates the integration of geometric modellers and form feature modellers, and provides the designer with significant flexibility in designing engineering artefacts.
- *Chapter 5*. It introduces Euler operators which are dimension-independent, compactness-independent, and construction order-independent. These three generalisations of the Euler operators, together with the subcomplexes embedded in the data structure, provide the designers and manufacturers with virtually full flexibility to *locally* re-design engineering artefacts without the need to reconstructing the whole object.

That's all!

Bibliography

[1] R. Abraham, J. Marsden, and T. Ratiu. *Manifolds, tensor analysis, and applications*. Addison-Wesley Publishing Company, Inc., Reading, U.S.A., 1983.

[2] C. Armstrong, A. Bowyer, S. Cameron, J. Corney, G. Jared, R. Martin, A. Middleditch, M. Sabin, and J. Salmon. *Djinn, a geometric interface for solid modelling: specification and report*. Information Geometers Ltd., Winchester, England, 2000.

[3] M. Armstrong. *Basic topology*. McGraw-Hill Book Company (UK) Limited, 1979.

[4] B. Arnold, S. Gusein-Zade, and A. Varchenko. *Singularities of differentiable maps: volume I*, volume 82 of *Monographs in Mathematics*. Birhäuser Boston, Inc., 1962.

[5] L. Auslander and R. MacKenzie. *Introduction to differentiable manifolds*. McGraw-Hill Series in Higher Mathematics. McGraw-Hill Book Company, Inc. (New York), 1985.

[6] A. Baer, C. Eastman, and M. Henrion. A survey of geometric modeling. Research Report 66, Institute of Physical Planning, Carnegie-Mellon University, March 1977.

[7] B. Baumgart. Winged edge polyhedron representation. Stanford Artificial Intelligence Project, MEMO AIM-179 STAN-CS-320, Computer Science Department, Stanford University, 1972.

[8] B. Baumgart. A polyhedron representation for computer vision. In *AFIPS Conf. Proc.*, volume 44, pages 589–596, 1975.

[9] P. Baxandall. *Vector Calculus*. Oxford Applied Mathematics and Computing Science Series. Clarendon Press, Oxford, England, Oxford, UK, 1986.

[10] S. Berberian. *Linear algebra*. Oxford University Press, Oxford, England, 1992.

[11] R. Bidarra, K. Kraker, and W. Bronsvoort. Representation and management of feature information in a cellular model. *Computer Aided Design*, 30(4):301–313, April 1998.

[12] H. Blum. A transformation for extracting new descriptors of shape. In W. Whaten-Dunn, editor, *Models for Speech and Visual Form*. MIT Press, Cambridge, Massachusetts, USA, 1967.

[13] L. Blumenthal and K. Menger. *Studies in geometry*. W.F. Freeman and Company, 1970.

[14] J. Boardman. Singularities of differentiable maps. *Publ. Math. I.H.E.S.*, 33:21–57, 1967.

[15] W. Boothby. *An introduction to differentiable manifolds and Riemannian geometry*. Number 63 in Pure and Applied Mathematics. Academic Press Inc. (New York), 1975.

[16] K. Borsuk. Some remarks concerning the theory of shape in arbitrary metrizable spaces. In J. Novak, editor, *General topology and its relations to modern analysis and algebra III*, pages 77–81. Academic Press Inc.

[17] K. Borsuk. Concerning homotopy properties of compacta. *Fundamenta Mathematicae*, 62:223–254, 1968.

[18] I. Braid, R. Hillyard, and I. Stroud. Stepwise construction of polyhedra in geometric modelling. In K. Brodlie, editor, *Mathematical Methods in Computer Graphics and Design*, pages 123–141. Academic Press Inc. (London) Ltd., England, 1980.

[19] G. Bredon. *Topology and geometry*. Number 139 in Graduate Texts in Mathematics. Springer-Verlag, New York, USA, 1993.

[20] E. Brisson. *Representation of d-dimensional geometric objects*. PhD thesis, Department of Computer Science and Engineering, University of Washington, Washington, USA, 1990.

[21] E. Brisson. Representing geometric structures in d dimensions: topology and order. *Discrete & Computational Geometry*, 9(4):387–426, 1993.

[22] T. Brocker and K. Janich. *Introduction to differential topology*. Cambridge University Press, Cambridge, England, 1982.

[23] R. Brown. *Topology: a geometric account of general topology, homotopy types and the fundamental groupoid.* Mathematics and Its Applications. Ellis Horwood Ltd, Chicester, England, 1988.

[24] J. Bruce and P. Giblin. *Curves and singularities*. Cambridge University Press, Cambridge, England, 1984.

[25] Y. Burago and V. Zalgaller. *Geometric inequalities*, volume 285 of *A Series of Comprehensive Studies in Mathematics*. Springer-Verlag (Berlin), 1988.

[26] G. Danaraj and V. Klee. A representation of 2-dimensional pseudomanifolds and its use in the design of a linear-time shelling algorithm. *Annals of Discrete Mathematics*, 2:53–63, 1978.

[27] S. Dineen. *Multivariate calculus and geometry*. Springer Undergraduate Mathematics Series. Springer-Verlag, London, Great Britain, 1998.

[28] D. Dobkin and M. Laszlo. Primitives for the manipulation of three-dimensional subdivisions. *Algorithmica*, 4(1):3–32, 1989.

[29] L. Dries. *Tame topology and O-minimal Structures*, volume 248 of *London Mathematical Society Lecture Notes Series*. Cambridge University Press, 1998.

[30] J. Dugundji. *Topology*. Allyn and Bacon Series in Advanced Mathematics. Allyn and Bacon, Inc., Boston, USA, 1966.

[31] C. Eastman and K. Weiler. Geometric modelling using the euler operators. In *Proc. First Ann. Conf. Computer Graphics and CADCAM Systems*, pages 248–254, 1979.

[32] B. Edelsbrunner. *Algorithms in combinatorial geometry*, volume 10 of *EATCS Monographs on Theoretical Computer Science*. Springer-Verlag, Berlin, Germany, 1987.

[33] C. Edwards. *Advanced calculus of several variables*. Academic Press, New York, USA, 1973.

[34] C. Edwards. *Elementary linear algebra*. Prentice-Hall, Inc., 1988.

[35] M. Eisenberg. *Topology*. Holt, Rinehart and Winston, Inc., New York, USA, 1974.

[36] G. Ewald. *Combinatorial convexity and algebraic geometry*, volume 168 of *Graduate Texts in Mathematics*. Springer-Verlag (New York), 1996.

[37] G. Farin. *Curves and surfaces for CAGD: a pratical guide*. Academic Press, Inc., Boston, U.S.A. (3rd edition), 1993.

[38] A. Gabrielov. Projections of semi-analytic sets. *Functional Anal. Appl.*, 2(4):282–291, 1968.

[39] T. Garrity and J. Warren. Geometric continuity. *Computer Aided Geometric Design*, 8(51-65), 1991.

[40] M. Gemignami. *Axiomatic geometry*. Addison-Wesley Series in Mathematics Education. Addison-Wesley Publishing Company, Inc., Reading, Massachusetts, USA, 1971.

[41] C. Gibson. Construction of canonical stratifications. In A. Dold and B. Eckman, editors, *Topological stability of smooth mappings*, volume 552 of *Lecture Notes in Mathematics*, pages 8–34. Springer-Verlag, Berlin, 1976.

[42] C. Gibson. *Singular points of smooth mappings*. Number 25 in Research Notes in Mathematics. Pitman Publishing Limited, London, England, 1979.

[43] R. Gilmore. *Catastrophe theory for scientists and engineers*. John Wiley & Sons, Inc. New York, 1981.

[44] M. Golubitsky and V. Guillemin. *Stable mappings and their singularities*. Number 14 in Graduate Texts in Mathematics. Springer-Verlag, 1986.

[45] A. Gomes and A. Middleditch. Synthesis of a unified approach to shape modelling. In W. Strasser, R. Klein, and R. Rau, editors, *Geometric Modeling: Theory and Practice*. Springer-Verlag, 1997.

[46] A. Gomes and J. Teixeira. Modelling shape through a cellular representation scheme. In J. Teixeira and J. Rix, editors, *Proceedings of the Workshop on Graphics and Modelling in Science & Technology*, ANMP, Coimbra, Portugal, 1996. Springer-Verlag.

[47] J. Gregory. Geometric continuity. In T. Lyche and L. Schumaker, editors, *Mathematical methods in computer aided design*, pages 353–371. Academic Press, Inc., 1989.

[48] B. Grunbaum. *Convex polytopes*, volume 16 of *Pure and Applied Mathematics*. Interscience Publishers (John Wiley & Sons), London, England, 1967.

[49] L. Guibas and J. Stolfi. Primitives for the manipulation of general subdivisions and the computation of voronoi diagrams. *ACM Transactions on Graphics*, 4(2):74–123, 1985.

[50] E. Gursoz and F. Prinz. A point set approach in geometric modelling. In F. Krause and H. Jansen, editors, *Advanced Geometric Modeling for Engineering Applications (International GI-IFIP Symposium 89)*, pages 73–87. Elsevier Science Publishers B.V. (North-Holland), 1990.

[51] H. Hadwiger. *Vorlesungen uber Inhalt, Oberflache und Isoperimetrie*. Springer-Verlag (Berlin), 1957.

[52] J. Hahn. Geometric continuous patch complexes. *Computer Aided Geometric Design*, 6:55–67, 1989.

[53] R. Hardt. Homology theory for real analytic and semianalytic sets. *Annali Della Scuola Normale de Pisa*, 3rd Series, 29:107–148, 1975.

[54] R. Hardt. Stratification of real analytic mappings and images. *Inventiones Math.*, 28:193–208, 1975.

[55] R. Hardt. Topological properties of subanalytic sets. *Transactions of the American Mathematical Society*, 211, October 1975.

[56] S. Helgason. *Differential geometry, Lie groups, and symmetric spaces*. Pure and Appllied Mathematics' Series. Academic Press, Inc. (New York), 1978.

[57] M. Henle. *A combinatorial introduction to topology*. W.F. Freeman and Company, 1979.

[58] H. Hironaka. Subanalytic sets. In Y. Kusunoki, S. Mizohata, M. Nagata, H. Toda, M. Yamaguti, and H. Yoshizawa, editors, *Number Theory, Algebraic Geometry and Commutative Algebra*, pages 453–493. Kinokuniya Book-Store Co., Ltd., Tokyo, Japan, 1973.

[59] H. Hironaka. Triangulations of algebraic sets. In R. Hartshorne, editor, *Proceedings of Symposia in Pure Mathematics: Algebraic Geometry, Vol. 29*, pages 165–185. American Mathematical Society (AMS), 1974.

[60] M. Hirsch. *Differential topology*. Number 33 in Graduate Texts in Mathematics. Springer-Verlag (New York), 1976.

[61] J. Hubbard and B. Hubbard. *Vector calculus, linear algebra, and differential forms: a unified approach.* Prentice-Hall Inc., New Jersey, USA, 1999.

[62] J. Hubbard and B. West. *Differential equations: a dynamical systems approach.* Texts in Applied Mathematics 18. Springer-Verlag, New York, USA, 1995.

[63] W. Hurewicz. Beitrage zur topologie der deformationen iii. klassen und homologietypen von abbildungen. In *Proceedings of the Koninklijke Nederlandse Akademie van Wetenschapen, Amsterdam*, pages 117–125, 1936.

[64] Spatial Technology Inc. *ACIS Geometric Modeler: Technical Overview*. Spatial Technology Inc., 1990.

[65] A. Jones, A. Gray, and R. Hutton. *Manifolds and mechanics*. Lecture Series 2. Australian Mathematical Society, Cambridge University Press, Cambridge, England, 1987.

[66] L. Kinsey. *Topology of Surfaces*. Undergraduate Texts in Mathematics. Springer-Verlag (New York), 1993.

[67] T. Kuo. The ratio test for analytic whitney stratifications. volume 192 of *Lecture Notes in Mathematics*, pages 141–149. Springer-Verlag, Berlin, 1971. (Proceedings of Liverpool Singularities Symposium I).

[68] S. Lang. *Undergraduate analysis*. Undergraduate Texts in Mathematics. Springer-Verlag, New York, 1997.

[69] P. Lienhardt. Subdivisions of n-dimensional spaces and n-dimensional generalised maps. In *ACM Symposium on Computational Geometry*, pages 228–236. ACM Press, New York, USA, — 1989.

[70] S. Lojasiewicz. Triangulation of semianalytic sets. *Annali Della Scuola Normale de Pisa*, 3rd Series, 18:449–474, 1964.

[71] S. Lojasiewicz. Ensembles semi-analytiques. Technical Report Cours Faculté des Sciences d'Orsay, Bures-sur-Yvette, Inst. Hautes Études Sci., 1965.

[72] S. Lojasiewicz. Sur la géométrie semi- and sous-analytique. *Annales de L'Institut Fourier*, 43:1575–1595, 1993.

[73] Y. Lu. *Singularity theory and an introduction to catastrophe theory.* Universitext. Springer-Verlag (New York), 1976.

[74] M. Mantyla and R. Sulonen. Gwb: A solid modeler with euler operators. *IEEE Computer Graphics & Applications*, 2(7):17–31, 1982.

[75] W. Massey. *A basic course in algebraic topology*. Number 127 in Graduate Texts in Mathematics. Springer-Verlag (New York), 1991.

[76] H. Masuda. Topological operators and boolean operators for complex-based nonmanifold geometric models. *Computer Aided Design*, 25(2), 1993.

[77] J. Mather. *Notes on topological stability*. Lecture Notes, Harvard University. 1970.

[78] J. Mather. Stratification and mappings. In M. Peixoto, editor, *Dynamical Systems*. Academic Press (New York, 1973.

[79] J. Mather. How to stratify mappings and jet spaces. volume 535 of *Lecture Notes in Mathematics*, pages 128–176. Springer-Verlag, Berlin, 1976.

[80] M. Mazure. Geometric continuity and frenet continuity of parametric curves. Technical Report RR 846-M-1991, Laboratoire de Modélisation et Calcul - IMAG, Grenoble, France, March 1991.

[81] M. Mazure. Geometric contact for curves and surfaces. *Computer Aided Geometric Design*, 11:177–195, 1992.

[82] W. Meyer and D. Kay. A convexity structure admits but one real linearisation of dimension greater than one. *Journal of the London Mathematical Society*, 7(2):124–130, 1973.

[83] A. Middleditch. Cellular models of mixed dimension. Technical Report Internal Technical Memorandum, BRU/CAE/92:3, Department of Computer Science, Brunel University, West London, 1992.

[84] A. Middleditch and C. Reade. Improvements for the djinn api to a geometric modelling kernel. *International Journal of Shape Modeling*, 6(1):79–103, 2000.

[85] A. Middleditch, C. Reade, and A. Gomes. A formal basis for the objects of the djinn geometric modelling kernel *api*. *(Unpublished)*, 1998.

[86] A. Middleditch, C. Reade, and A. Gomes. Rationale and formal definitions for the objects of the djinn *api* to a geometric modelling kernel. *(Unpublished)*, 1998.

[87] A. Middleditch, C. Reade, and A. Gomes. Set combinations of the mixed-dimension cellular objects of the djinn api. *Computer Aided Design*, 31(11):683–694, September 1999.

[88] J. Milnor. A unique decomposition theorem for 3-manifolds. *American Journal of Mathematics*, 84:1–7, 1962.

[89] P. Moura. Logtalk 2.6 documentation. Technical Report DMI2000:1, Departamento de Matemática e Informática, Universidade da Beira Interior, Portugal, July 2000.

[90] D. Muller and F. Preparata. Finding the intersection of two convex polyhedra. *Theoretical Computer Science*, 7:217–236, 1978.

[91] M. Nakahara. *Geometry, Topology and Physics*. Graduate Student Series in Physics. Adam Hilger, IOP Publishing Ltd, 1990.

[92] C. Nash and S. Sen. *Topology and geometry for physicists*. Academic Press, Inc. (London) Ltd., 1983.

[93] P. Olver. *Equivalence, invariants and symmetry*. Cambridge University Press, Cambridge, England, 1995.

[94] A. Paoluzzi, F. Bernardini, C. Cattani, and V. Ferrucci. Dimension-independent modeling with simplicial complexes. *ACM Transactions on Graphics*, 12(1):56–102, January 1993.

[95] F. Preparata and S. Hong. Convex hulls of finite sets of points in two and three dimensions. *Communications of the ACM*, 20(2):87–93, 1977.

[96] A. Requicha. Mathematical models of rigid solid objects. Production Automation Project Tech. Memo 28, University of Rochester, 1977.

[97] A. Requicha and H. Voelcker. Boolean operations in solid modeling: Boundary evaluation and merging algorithms. *Proc. IEEE*, 73(1):30–44, January 1985.

[98] J. Roe. *Elementary analysis: the theory of calculus*. Undergraduate Texts in Mathematics. Springer-Verlag, New York, USA, 1980.

[99] J. Rossignac and M. O'Connor. Sgc: A dimension-independent model for pointsets with internal structures and incomplete boundaries. In M. Wozny, J. Turner, and K. Preiss, editors, *Geometric Modeling for Product Engineering*. IFIP, Elsevier Science Publishers B.V. (North-Holland), 1990.

[100] G. Sallee. *Incidence graphs of convex polytopes*. PhD thesis, Department of Mathematics, University of Washington, USA, 1966.

[101] A. Seidenberg. A new decision method for elementary algebra. *The Annals of Mathematics*, 2nd Series, 60(2):365–374, September 1954.

[102] V. Shapiro. Real functions for representation of rigid solids. *Computer Aided Geometric Design*, 11(2), 1994.

[103] R. Sharpe. *Differential Geometry*, volume 166 of *Graduate Texts in Mathematics*. Springer-Verlag (New-York), 1997.

[104] X. Sheng and I. Meier. Generating topological structures for surface models. *IEEE Computer Graphics & Applications*, 15(11):35–41, November 1995.

[105] M. Shiota. *Geometry of Subanalytic and Semialgebraic Sets*. Progress in Mathematics, Vol.150. Birkhauser, Boston, USA, 1997.

[106] K. Smith. *Power series from a computational point of view*. Universitext Series. Springer-Verlag, New York, 1987.

[107] R. Sriram, A. Wong, and L. He. Gnomes: an object-oriented nonmanifold geometric engine. *Computer Aided Design*, 27(11), 1995.

[108] A. Tarski. A decision method for elementary algebra and geometry. Berkeley Note, 1951.

[109] R. Thom. La stabilité topologique des applications polynomiales. *Enseignement Math.*, 8:24–33, 1962.

[110] R. Thom. Ensembles et morphisms stratifiés. *Bulletin of the American Mathematical Society*, 75:240–284, 1969.

[111] C. Thomas. The oriented homotopy type of compact 3-manifolds. *Proceedings of the London Mathematical Society*, 19(3):31–44, 1969.

[112] H. Voelcker, A. Requicha, A. Middleditch, J. Shapiro, and P. Zuckerman. Discrete part manufacturing: theory and practice. Technical Report TR-1, Production Automation Project, University of Rochester, USA, March 1974.

[113] C. Wall. Regular stratifications. In A. Dold and B. Eckman, editors, *Dynamical Systems*, volume 468 of *Lecture Notes in Mathematics*, pages 332–344. Springer-Verlag, Berlin, 1975. (Proceedings of a Symposium held at the University of Warwick 1973/1974).

[114] R. Webster. *Convexity*. Oxford Science Publications. Oxford University Press (Oxford), 1994.

[115] K. Weiler. Edge-based data structures for solid modeling in curved surface environments. *IEEE Computer Graphics & Applications*, 5(1):21–40, 1985.

[116] K. Weiler. *Topological Structures for Geometric Modeling*. PhD thesis, Rensselaer Polytechnic Institute, Troy, New York, 1986.

[117] K. Weiler. The radial edge structure: a topological representation for non-manifold geometric boundary modeling. In M. Wozny, H. McLaughlin, and J. Encarnação, editors, *Geometric Modeling for CAD Applications*, pages 3–36. Elsevier Science Publishers B.V. (North-Holland), May 1988.

[118] H. Whitney. Complexes of manifolds. *Proceedings of the National Academy of Sciences (U.S.A.)*, 33:10–11, 1947.

[119] H. Whitney. Elementary structure of real algebraic varieties. *Annals of Mthematics*, 66(3):545–556, November 1957.

[120] H. Whitney. Local properties of analytic varieties. In S. Cairns, editor, *Differential and Combinatorial Topology*, pages 205–244, Princeton, USA, 1965. Princeton University Press.

[121] H. Whitney. Tangents to an analytic variety. *The Annals of Mathematics*, 81(3):496–549, May 1965.

[122] S. Willard. *General topology*. Addison-Wesley Publishing Company, Inc., Reading, Massachusetts, USA, 1970.

[123] S. Wolfram. *Mathematica: a system for doing mathematics by computer*. Addison-Wesley Publishing Company, Inc., Reading, Massachusetts, USA, 1991.

[124] T. Wu. Considerations about a minimal set of non-manifold operators. In *IFIP W5.2 Workshop on Geometric Modeling*. International Federation for Information Processing (IFIP), Rensselaer Polytechnic Institute, Troy, New York, 1989.

[125] Y. Yamaguchi and F. Kimura. Nonmanifold topology based on coupling entities. *IEEE Computer Graphics & Applications*, 15(1), January 1995.

[126] C. Yap and C. Li. CORE library: a C/C++ library for exact computation. Technical report, Courant Institute of Mathematical Sciences, Department of Computer Science, New York University (`http://cs.nyu.edu/exact/core`), January 1999.